Copper catalyzed aerobic oxidation of hydroxamic acids to acylnitroso compounds and their trapping

DUANGDUAN CHAIYAVEIJ

Department of Chemistry

Copper catalyzed aerobic oxidation of hydroxamic acids to acylnitroso compounds and their trapping

DUANGDUAN CHAIYAVEIJ

A thesis presented to Durham University in fulfillment of the thesis requirement for the degree of Doctor of Philosophy in Chemistry

April 2013

Declaration

The work described in this thesis was carried out in the Department of Chemistry at Durham University between October 2008 and April 2013, under the supervision of Prof. Todd B. Marder and Prof. Andrew Whiting. All the work is my own, unless otherwise stated, and has not been submitted previously for a degree at this or any other university.

Statement of Copyright

Abstract

A novel *in situ* oxidation of hydroxamic acids to form the corresponding nitroso species using a copper-oxazoline complex in air was developed. The nitroso species could be trapped by a diene to give high yields of Diels-Alder adducts, with some competing ene-products with certain dienes. It was found that 10 mol% $CuCl_2$ and 20 mol% 2-ethyl-2-oxazoline in methanol under air were optimal conditions for catalyzing the oxidation of *N*-(benzyloxycarbonyl)hydroxylamine, for example, which was then trapped with various dienes to form the corresponding cycloadducts in good yields. However, this catalytic system will only works with hydroxamic acids with a heteroatom between the aryl and carbonyl group of the hydroxamic acid. It was also found that oxidation 1-hydroxy-3-phenylurea using this Cu-based oxidation system gave the best regio- and chemo-selectivity, though attempts to induce high asymmetric induction on the NDA reaction using both chiral catalysts and auxiliary approaches were unsuccessful which has implications about the rate of dissociation of the nitroso species of the copper oxidant.

Acknowledgement

First of all, I would like to thank my supervisors Prof. Todd B. Marder and Prof. Andy Whiting; I am honoured to have received their help, support and countless ideas. I highly appreciate that whenever a variety of unexpected problems arose whilst carrying out my project, I would always have them providing me with supportive guidance towards workable solutions.

To all those in the Marder and the Whiting groups both previously and at present, many thanks for all your help – especially Dr. Jon Collings, Dr. Kittiya Wongkhan, Dr. Meng Guan Tay, Dr. Andrew Crawford, Dr. Liu Chao, Dr. Marie-Helene Thibault, Dr. Bianca Bitterlich, Dr. Hazmi Tajuddin, Dr. Ricado Girling, Dr. Irene Georgiou, Dr. Hayley Charville, Dr. Alex Gehre, Garr-Layy Zhou, Adam Calow, Fahana Ferdousi and any unmentioned others.

To Mum, Dad, Grandmother, Aunt Kate, my sister Daranee, my boyfriend Narongsak, I am deeply grateful and thankful for the love, emotional support and encouragement, which are always readily offered regardless of time or distance.

This piece of work will not have been complete without analytical services, and therefore I would like to extend my gratitude to the NMR technician, Dr. Alan Kenwright; Catherine Heffernan and Ian McKeag for the 2D and high resolution NMR spectra; the HPLC staff, Dr. Aileen Congreve, for helping me to do chiral HPLC analysis; Judith Magee for the elemental analysis service; the mass spec members of staff; the brilliant glassblowers and all the department cleaners. Unforgettably, I express special thanks to Dr. Andrei Batsanov, an excellent crystallographer, for his unfaltering dedication and unfailing attempts to do all the structures that I submitted.

The last year of this PhD has challenged me with the greatest hardship I have ever encountered, but with Kim and Josh, who have brought irreplaceable joy and laughter to my life, I made my way through in good spirit. I cannot thank them enough for everything.

I have enjoyed my 9 years (!) in Durham with lots of Thai friends who have never failed to make me feel at home. In particular, I would like to thank Dr. Monsit for his help in every difficult situation; Dr. Suppachai for his kindness and for

accompanying me to anywhere I would like to go; Dr. Pisuttawan for her unwavering concern about my studying and life in general; Dr. Harit for his support and help through all encountered problems; Dr. Jitnapa for being such a dependable friend of mine; Nonthiwat, Wissarut and Chinli for their kindness in letting me stay with them for my final year; Dr. Paramita, Dr. Varodom, Dr. Sasitsaya, Dr. Suratchada, Dr. Sarocha, Dr. Pinit, Dr. Jiratchaya, Dr. Khongwit, Aniwat, Orachat, Thidarat, Wankawee, Chulachat, Pichet, Pimpunyawat, Prapaiwan, Sasiwimol, Karuntarat, Dr. Suparb, Dr. Issariya, Surasak and any unmentioned others for the happiness and cheerful times we spent together.

I would also like to extend great thanks to my sponsor, the Royal Thai Government, for giving me an opportunity under the DPST program to come here, the UK, to study and learn so many new things, to meet so many nice people and to enjoy the English weather! I am very much thankful to the OEA London for supporting me ever since the first day that I arrived the UK. I would also like to express my gratefulness to all my teachers and lecturers for the knowledge, motivation and inspiration to pursue further in the subject field.

Finally, this writing of acknowledgement cannot be complete without appreciative mentions of Carrie, Nick, Yee, Sunny, P Tum and P Ting, whose friendship filled my life in Durham with such fond memories.

List of Abbreviations

Ac - acetyl

Ar - aromatic

Bn – benzyl

Boc - *tert*-butoxycarbonyl

br - broad

Bu – butyl

Calcd – calculated

Cbz - carboxybenzyl

CG – chelating group

d – doublet

DA – Diels-Alder

DBAD - dibenzyl azodicarboxylate

dd - doublet of doublets

dba - dibenzylideneacetone

DCM - dichloromethane

DFT - density functional theory

DMAP - 4-dimethylaminopyridine

DMF – dimethylformamide

DMSO - dimethyl sulfoxide

EDG - electron donating group

EI - electron ionization

ES - electrospray

Et - ethyl

Et_2O - diethyl ether

EtOAc - ethyl acetate

EWG - electron withdrawing group

Fmoc - fluorenylmethyloxycarbonyl

FTIR - Fourier transform infrared spectroscopy

GCMS - gas chromatography mass spectrometry

HOMO - highest occupied molecular orbital

HPLC - high performance liquid chromatography

HRMS - high resolution mass spectrometry

IPA - isopropyl alcohol

IR – infrared

L - ligand

LRMS - low resolution mass spectrometry

LUMO - lowest unoccupied molecular orbital

M - molar

m - multiplet

Me - methyl

MeCN - acetonitrile

m.p. - melting point

MS - mass spectrometry

MTBE - methyl *tert-butyl* ether

MW - microwave

NDA – nitroso-Diels-Alder

NMM - *N*-methylmorpholine

NMO - *N*-methylmorpholine *N*-oxide

NMR - nuclear magnetic resonance

Ph - phenyl

Phen - phenanthroline

Pr - propyl

q - quartet

rt - room temperature

s - singlet

t - triplet

td - triplet of doublets

THF - tetrahydrofuran

TLC - thin layer chromatography

TMTU – tetramethylthiourea

Z (Cbz) - benzyloxycarbonyl

Contents

Chapter 2.

Chapter 1. Introduction

1.0 Introduction

1.1 Nitroso compounds

The nitroso functional group was first synthesized in 1874 by Baeyer,[1] that being nitroso benzene **2**. It was prepared from the reaction between diphenyl mercury **1** and nitrosyl bromide (Scheme 1).

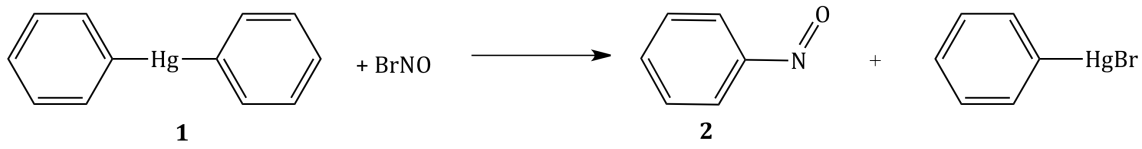

1 **2**

Scheme 1. The first nitroso compound synthesis.

Since then, the nitroso functional group has attracted attention from synthetic chemists due to its useful properties, especially for application in the synthesis of natural products.[2] They can undergo the Ehrlich-Sachs reaction,[3] nitroso-aldol reaction,[4] nitroso-Diels-Alder reaction,[1,5] ene reaction[6] and other organic processes.[7]

1.1.1 Preparation of nitroso compounds

Nitroso compounds can be prepared by several methods, depending upon the nature of the group attached to them.

1.1.1.1 Direct nitrosation

Bosch and Kochi reported a successful, direct substitution of some polymethyl-substituted benzenes **3** using nitrosonium tetrafluoroborate in acetronitrile under argon to give the nitroso arene **4** (Eq. 1.).[8]

$$\underset{\mathbf{3}}{ArH} + NO^{+} \longrightarrow \underset{\mathbf{4}}{ArNO} + H^{+} \qquad \text{(Eq. 1)}$$

Nitrosation of alkanes and cycloalkanes can be also be carried out by using a radical trapping reaction with nitric oxide.[9]

1.1.1.2 Nitroso-demetalation

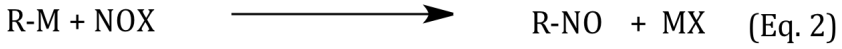

The use of nitroso-demetalation is the reaction between an organometallic compound and nitrosyl halide. The first nitroso compound, nitrosobenzene **2**, was generated by the above reaction (Eq. 2).[1] The reaction between phenylmagnesium bromide and nitrosyl chloride also gives nitroso benzene **2**.[10] Various other organometallic species studied have included: Sn,[11] Li,[12] Tl,[13] Si,[14] Al[15] and Cr.[16] These studies concluded that this is a successful reaction if the metal cation is stabilized by a leaving group .

1.1.1.3 Oxidation of hydroxamic acids

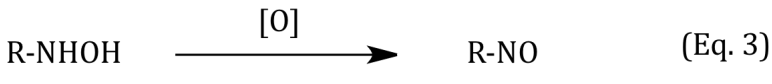

5 **6**

The oxidation of the hydroxamic acids **5** is widely used in the preparation of the corresponding nitroso compounds **6** (Eq. 3). It has been achieved under various oxidation conditions, including periodate,[17] Swern oxidation,[18] Dess-Martin periodinane,[19] lead and silver oxides,[20] transition metal-catalyzed oxidation in the presence of peroxide[21] and recently, copper-catalyzed aerobic oxidation.[22]

1.1.1.4 Oxidation of nitrile oxide

The formation of acylnitroso compounds **9** by oxidising nitrile oxides **7** using *N*-methylmorpholine-*N*-oxide (NMO) was reported by Quadrelli *et al.*[23] The electrophilic carbon of the nitrile oxide was attacked by the nucleophilic oxygen on the tertiary amine. The *N*-oxide forms a zwitterionic intermediate **8**, which gives an acyl nitroso species **7** and the tertiary amine (Scheme 2).

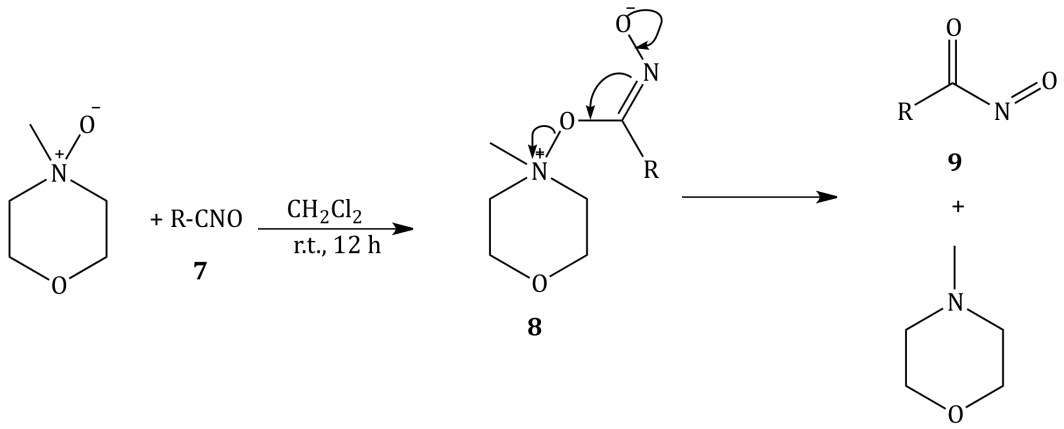

Scheme 2. Oxidation of nitrile oxide by NMO

1.1.1.5 Reduction of nitro compounds

The direct formation of nitrosobenzene from nitrobenzene was reported in 1911 by Zerewitinoff and Ostromisslensk. In their study, barium oxide was used as a reducing agent,[24] together with sodium as a source of electrons. Potassium, calcium, strontium, barium, magnesium and zinc were also used as reducing agents.[25]

The photoreduction of a ternary complex of β-cyclodextrin with a nitrophenyl ether **10** and 1-phenylethylamine under irradiation with a mercury lamp in the solid state gave >95% of corresponding nitroso compounds **11**[26] (Scheme 3).

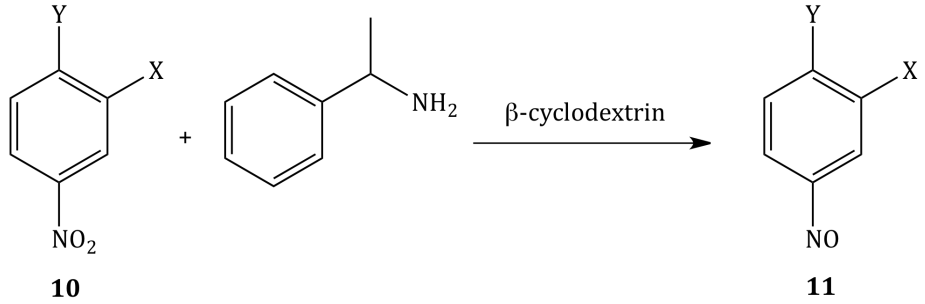

Scheme 3. Direct nitroso formation from nitrobenzene by photoreduction.

1.1.1.6 Diazo compound rearrangement

The use of diazo compounds **12** to form nitrocarbene species **13** was reported 1988 by Bannon and Williams[27] going through a facile [1,2]-oxygen shift using a rhodium(II) catalyst or upon gentle heating, to yield the acylnitroso **14** (Scheme 4).

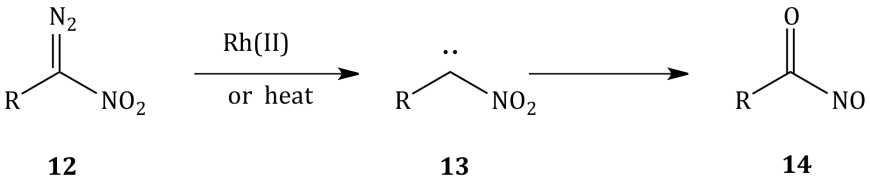

12 **13** **14**

Scheme 4. Diazo compound rearrangement route to acylnitroso species.

1.1.1.7 Cycloreversion of 9,10-dimethylantracene cycloadducts

9,10-Dimethylantracene cycloadducts **15** are well documented to undergo cycloreversion to give 9,10-dimethylanthracene and nitroso-species **16** upon heating.[28] However, it was necessary to have a trapping species present in the reaction mixture, otherwise nitrous oxide could be formed, as well as the corresponding anhydride and 9,10-dimethylantracene (Scheme 5).

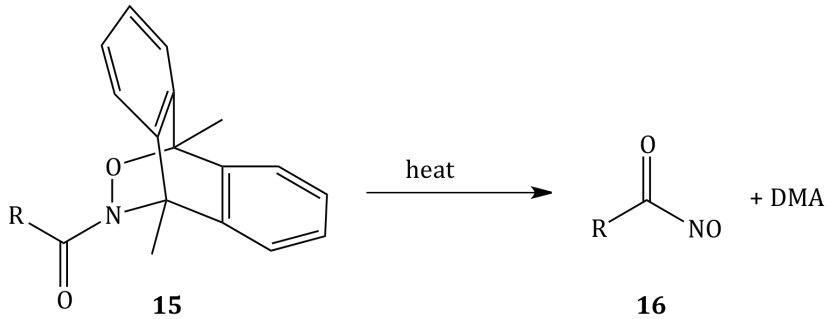

15 **16**

Scheme 5. The cycloreversible of the 9,10-dimethylantracene cycloadducts.

1.1.2 Nitroso compounds as dienophiles

Hyponitrous acid (HNO) is the simplest nitroso species known, however, due to its instability,[29] it readily forms nitrous oxide and its use as a dienophile in the nitroso-Diels-Alder reaction has been limited. Therefore, C-nitroso compounds have been employed and studied in the nitroso-Diels-Alder reaction. This has included alkylnitroso **17**, cyanonitroso **18**, α-halonitroso **19**, acetoxynitroso **20**, vinylnitroso **21**, iminonitroso **22**, arylnitroso **23**, pyridylnitroso **24**, acylnitroso **25** and nitrosoformate ester derivatives **26** (Figure 1).

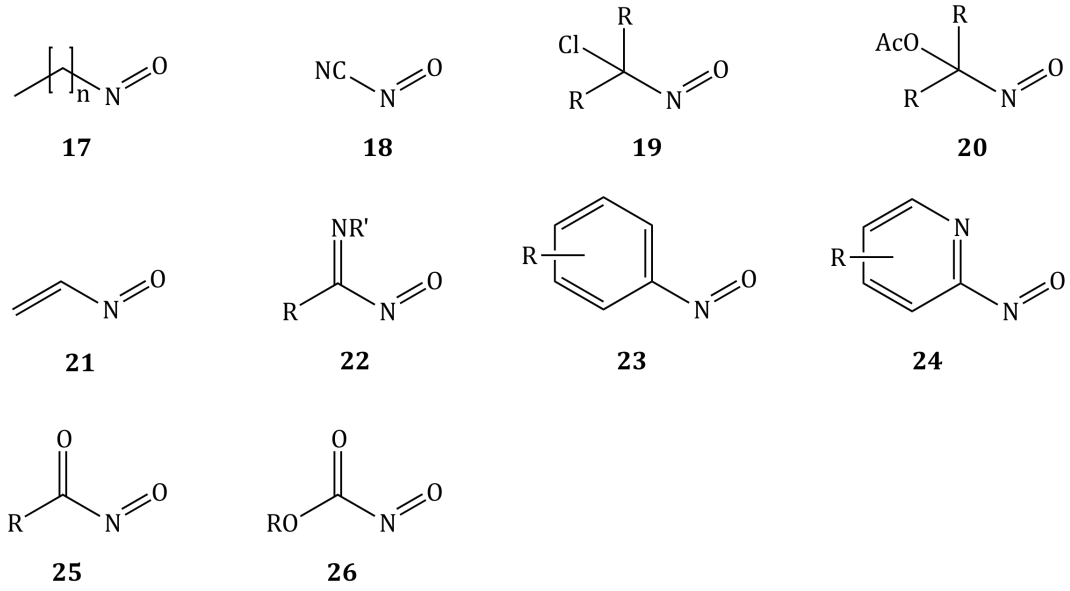

Figure 1. General structures of C-nitroso compounds.

The reactivity of these nitroso compounds as dienophiles depends upon the substituent group present. An electron-withdrawing group adjacent to the nitroso group greatly increases the rate of reaction as the LUMO energy level of the dienophile is lowered relative to the HOMO of the diene.[5, 30]

Nitroso compounds are also known to exist in equilibrium in two forms, *i.e.* a monomer and dimer species (Scheme 6).[31]

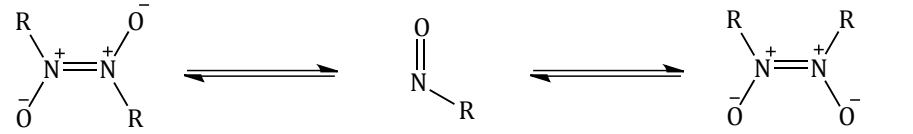

Scheme 6. Monomer-dimer equilibrium of nitroso species.

Cyanonitroso **18**, iminonitroso **22**, acylnitroso **25** and nitrosoformate esters **26** are the most reactive nitroso dienophiles used in the nitroso-Diels-Alder reaction. The latter are the most popular among all of these due to the formate group being readily removed, allowing the adducts to be used in natural product synthesis more readily.[32]

There are important effects in having a heteroatom attached to the nitroso group. Reactivity can be reduced due to resonance stabilization of the π-orbital

depending upon the heteroatom. Where the lone pair is strongly donating (Figure 2), this results in reduction of its dienophilic properties. This can be overcome by substituents where lone pair donation is prevented, as can be observed with nitroso-phosphoramide **27** and nitroso-sulfonate **28** compounds, though in these cases, σ-bond electron withdrawal still occurs resulting in a reactive, electrophilic nitroso function.[33]

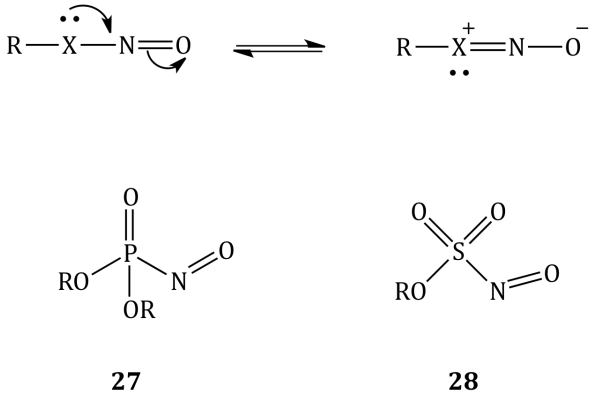

27 **28**

Figure 2. Example of resonance stabilization of hetero-nitroso compounds and σ-bond activated nitroso species.

1. 2 Nitroso-Diels-Alder reaction

The Diels–Alder (DA) reaction has been studied for nearly a century since it was first discovered by Wichterle.[34] It is one of the most useful methods for making six-membered carbocycles. A typical [4+2]-cycloaddition involves adding a diene to a dienophile to afford a six-membered ring cycloadduct. However, the diene needs to be in the s-*cis*-conformation in order to allow the π-orbitals in the diene to align with the π-orbitals in the dienophile. With the s-*trans*-conformation, which is more stable, orbital overlap is not possible with a dienophile.

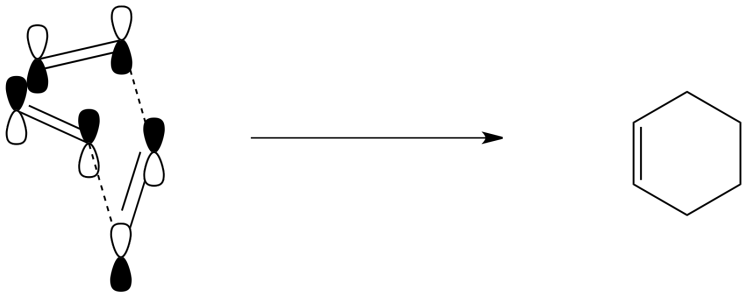

s-*cis*-conformation

Figure 3. Cisoid conformation.

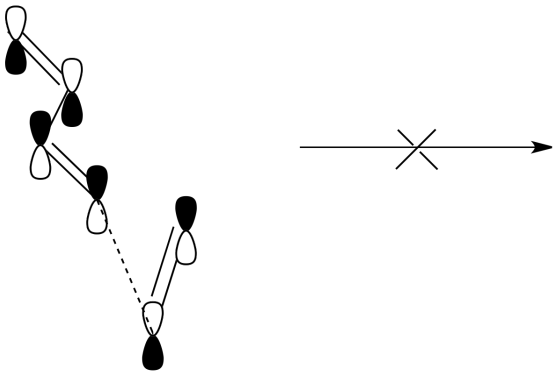

s-*trans*-conformation

Figure 4. Transoid conformation.

A concerted suprafacial [$\pi 4_s + \pi 2_s$]-cycloaddition of a diene and a dienophile is allowed according to the Woodward–Hoffmann rules.[35] This states that the rate and regiochemistry of cycloadditions are controlled by the HOMO of the diene and the LUMO of the dienophile in a normal DA reaction. An electron withdrawing group on the dienophile can lower the LUMO level whilst an electron donating group on diene can increase the HOMO level. Therefore, the rate of reaction could increase due to the dienophile being more electron-deficient and the diene being more electron-rich. An inverse electron demand DA reaction is the reaction between the LUMO of the diene and the HOMO of the dienophile. Therefore, the rate of reaction can be increased by lowering the LUMO on the diene using electron withdrawing group and the increasing HOMO on the dienophile by the use of the electron donating group. However, neither the HOMO nor LUMO has any effect on the neutral DA reaction (Scheme 7).[36]

When a Lewis acid is used to complex with an electron withdrawing group on the dienophile, the rate of reaction is increased. This is due to the amplification of the electron withdrawing effect on the dienophile in the normal DA reaction,

and on the diene in the inverse electron demand DA. As a result, the LUMO is lowered in both cases.

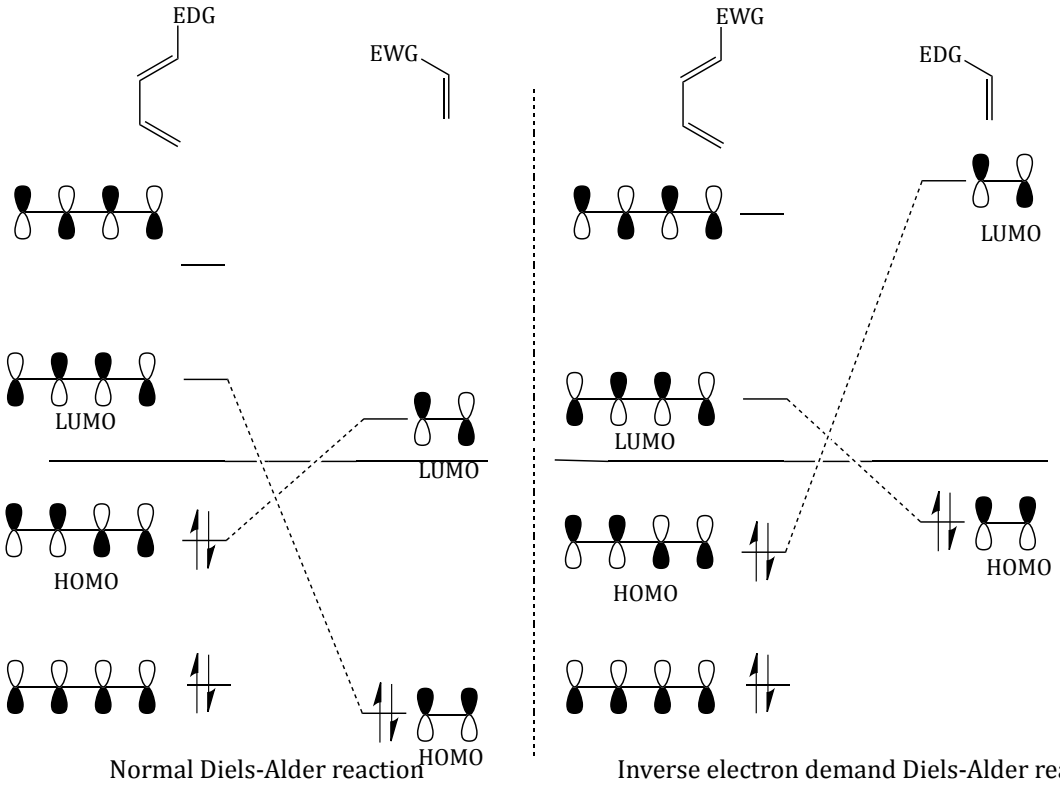

Scheme 7. The HOMO–LUMO of normal and inverse electron demand Diels–Alder reactions.

[4+2]-Cycloaddition reactions of nitroso-compounds with conjugated dienes have been studied and used as a powerful synthetic pathway to make natural products.[37,38] Nitroso-dienophiles are formed *in situ via* the oxidation of hydroxamic acid **29**. The oxidants reported include periodate,[17] Swern conditions (oxalyl chloride with DMSO)[18] and lead(IV) oxide-based oxidants,[20] which are all potentially toxic. The resulting nitroso-dienophile **30** can react with a diene *via* a hetero-DA reaction, resulting in the corresponding heterocyclic adduct **31** (Scheme 8). However, no particularly "green" catalytic systems have been developed to date.

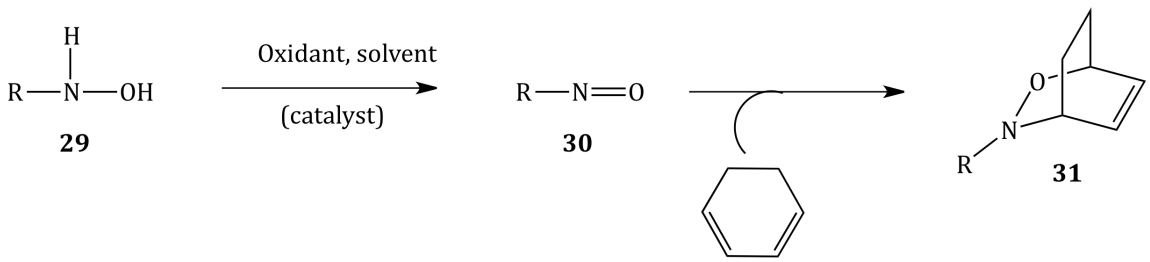

Scheme 8. [4+2]-Cycloaddition reaction of a nitroso-compound with 1,3-cyclohexadiene.

The diene used in the nitroso-Diels-Alder reaction is most often symmetric, however, with unsymmetric dienes, the regiochemistry of the product formed is uncertain. Computational studies of this particular reaction was carried out by Leach and Houk.[39] Their results showed that the nitroso-Diels-Alder reaction strongly prefers the *endo*-path, which arises from a combination of repulsion between the lone pair on the nitroso species with the electron rich diene and the interaction between the n-HOMO of the nitroso compound and the π-HOMO of the diene (Figure 5).

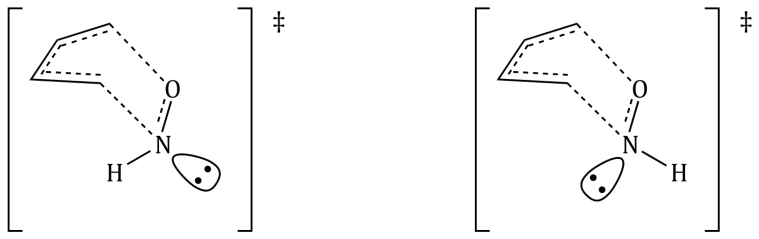

Figure 5. Transition state energies calculated for the nitroso-Diels-Alder reaction.

The regioselectivities of 1- and 2-substituted dienes were also studied. It was concluded that substitution at the 2-position of the diene **36** had a smaller effect compared with a 1-substituted diene **32**. The 1-substituted-1,3-diene, both with electron withdrawing and electron donating groups, generally gives a higher yield of proximal isomer **34** (6-substituted) than distal isomer **35** (3-substituted). Whereas 2-substituted dienes **36** give moderate selectivity for **37** over **38** (see Scheme 9).

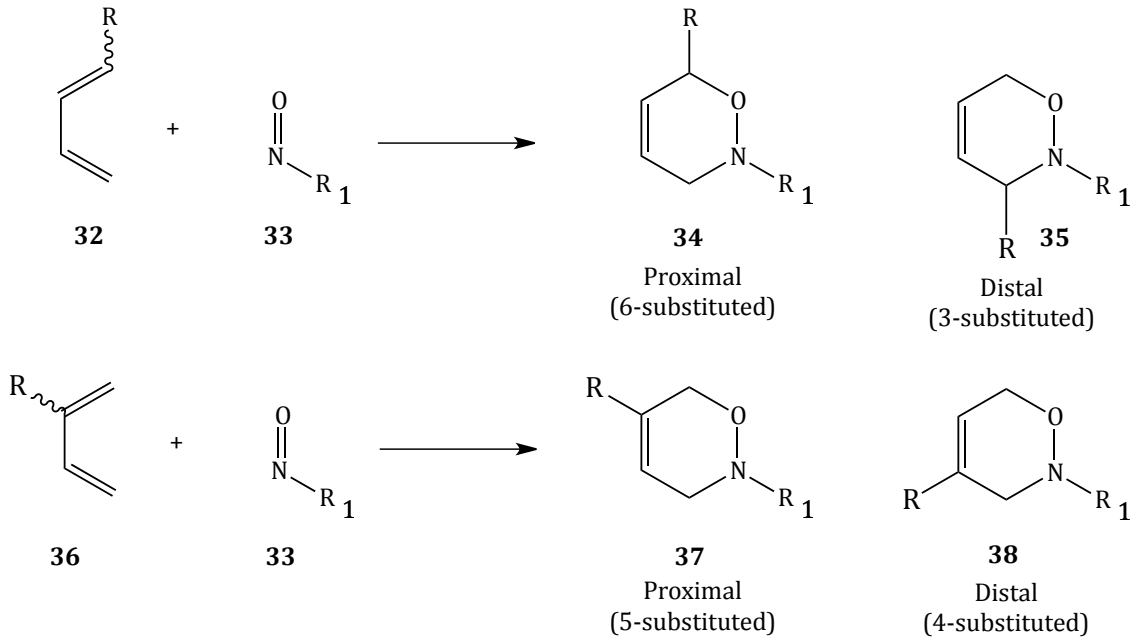

Scheme 9. The regioselectivity of 1- and 2-substituted dienes in nitroso-Diels-Alder reactions.

This study was found to be in good agreement with the experiments carried out in 1965 by Kresze and Firl.[40] It was found that unsymmetric dienes with either an electron donating **39a** or an electron withdrawing group **39b** gave the same regioisomers **41a** and **41b** respectively, with *p*-chloronitrosobenzene **40** (Scheme 10).

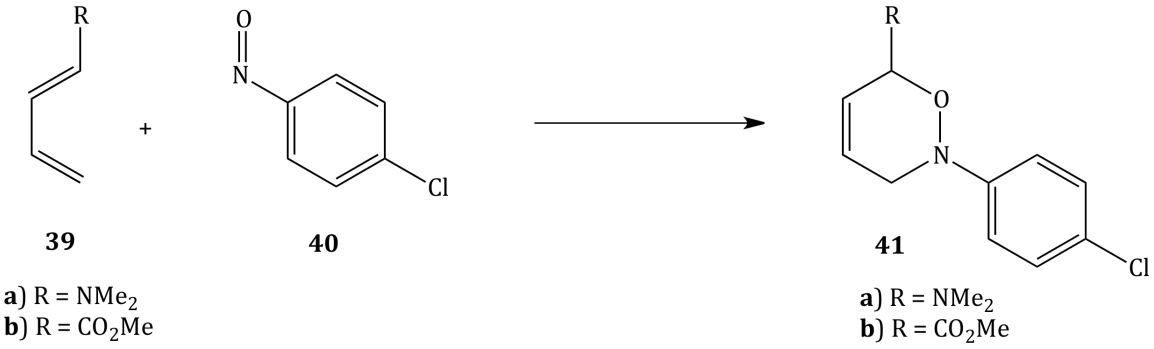

Scheme 10. The regioselectivity of the nitroso-Diels–Alder reaction with electron rich and electron deficient diene.

This result (Scheme 10) can be explained by the interaction between the HOMO of diene and LUMO of the dienophile. The C(4) of the 1-substitution diene has the

largest HOMO coefficient, which matches the largest LUMO at nitrogen of the nitroso species (the NO π* orbital)

2-Substituted dienes have the largest HOMO coefficient at C(1) resulting in the formation of a distal isomer. However, the direction of the selectivity depends upon the nature of the dienophile due to the weak directing effect of the 2-substituted diene.

1.2.1 Catalytic Nitroso-Diels-Alder Reactions

To overcome the toxicity of many oxidants used for generating nitroso compounds, Whiting *et al*.[41] and Isawa *et al*.[42] independently reported a ruthenium-catalyzed hydrogen peroxide oxidation of hydroxamic acids and subsequent hetero-Diels–Alder reaction with a diene. In Isawa's system, 10 mol% of ruthenium catalyst **46** and 4 equivalents of oxidant were required in the reaction in order to achieve good yields (Scheme 11). However, Whiting's system required only 0.1 mol% of ruthenium catalyst **43** and although this system required less catalyst, yields were poor to good (Scheme 12).

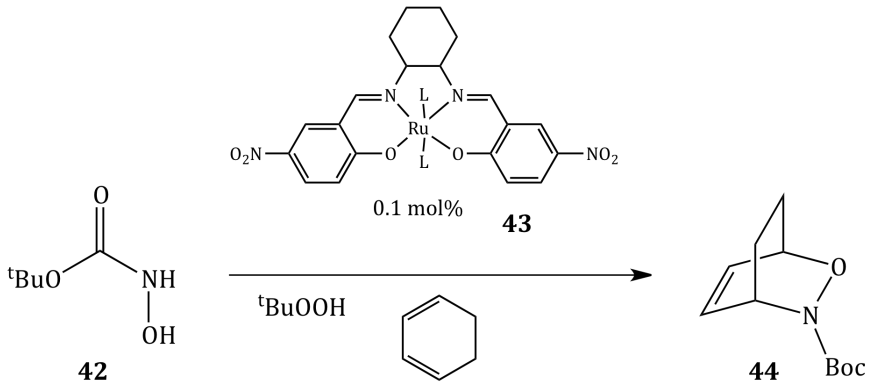

Scheme 11. Ruthenium-salen catalyzed nitroso-Diels–Alder reaction reported by Whiting *et al*.

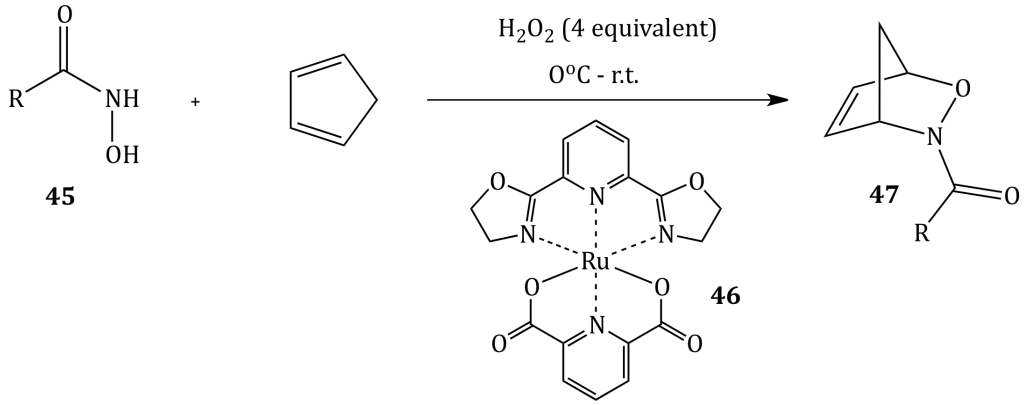

Scheme 12. Rhuthenium-pybox catalyzed nitroso-Diels–Alder reaction reported by Iwasa *et al*.

Adamo and Bruschi[43] reported the use of copper, iron and nickel with amine ligands as catalysts in the oxidation of hydroxamic acids using hydrogen peroxide. This reaction was carried out in a similar fashion to Isawa's reaction. They found that the reaction of nickel takes a longer time to complete (up to 8 days) while Cu(I), Cu(II) and Fe(III) showed high levels of activity (Scheme 13).

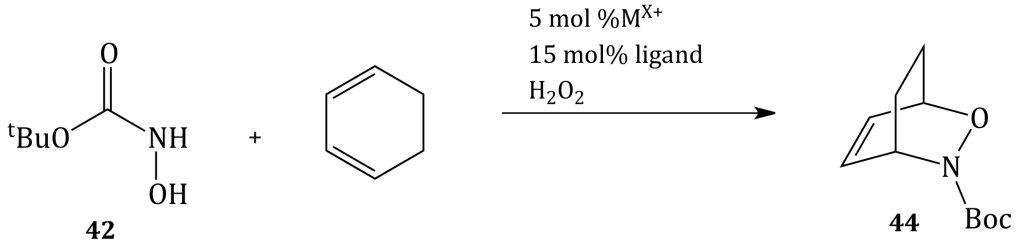

Scheme 13. Metal-catalyzed oxidation of hydroxamic acids with hydrogen peroxide reported by Amado and Bruschi.

The use of copper in the Diels–Alder reaction was first reported by Bota *et al.*[44] in 1961. In this study, cyclopentadiene and acetylene were used in the presence of $CuCl/NH_4Cl$/activated carbon catalyst to achieve the formation of 2,5-norbornadiene, however, the role of the copper catalyst was not clear.

The first copper-catalyzed nitroso–Diels–Alder reaction was first reported by Kalita and Nicholas.[45] Nitroso-compounds can be formed from the corresponding hydroxamic acids using Cu-catalysts such as $CuBr{\cdot}Me_2S$. Scheme 14 shows that when Boc-NHOH **42** was treated with 10 mol% of $CuBr.Me_2S$,

acylnitroso **48** was trapped by 1,3-cyclohexadiene to form cycloadduct **44** after 65 h in 41% yield. The efficiency of this reaction was improved dramatically by using stoichiometric quantities of oxidant such as hydrogen peroxide. The mechanism is not clear; however, a proposed mechanism starts with a Cu-induced disproportionation of Boc-NHOH **42** to form Boc-NO **48** and Boc-NH_2 **47**. Boc-NO can undergo a Diels-Alder reaction with the corresponding diene to give the cycloadduct **44**. However, in the presence of H_2O_2, Cu(I) is oxidized to Cu(II) by H_2O_2 instead of being oxidized by Boc-NHOH **42** (Scheme 15). This obviously increases the yield as there is more starting material available to form the corresponding nitroso species for the DA reaction and no disproportionation.

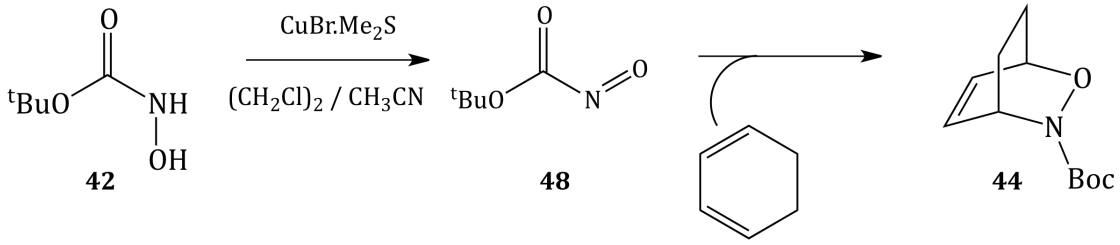

Scheme 14. CuBr·Me_2S catalyzed the oxidation of the hydroxamic acid.

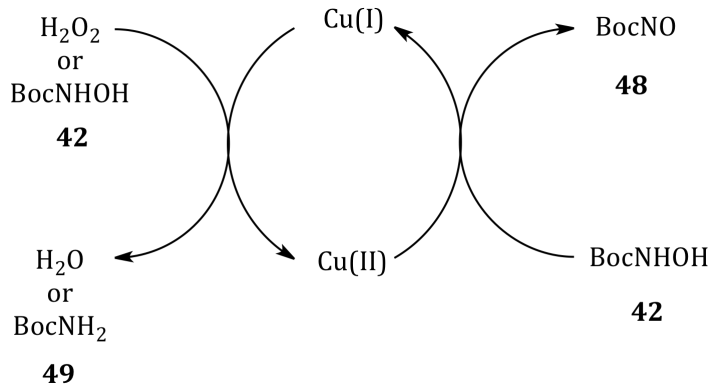

Scheme 15. A proposed mechanism of Cu-catalyzed nitroso-Diels-Alder reaction.

Tusun and Lu[46] reported the use of 0.1 mol% of dirhodium(II) caprolactamate **50** with *tert*-butyl hydroperoxide for catalyzing the *in situ* oxidative formation of acylnitroso **48** from hydroxamic acid **42** at room temperature. The acylnitroso **48** was trapped by a diene to form the corresponding cycloadduct product **44** with moderate to high yield (Scheme 16).

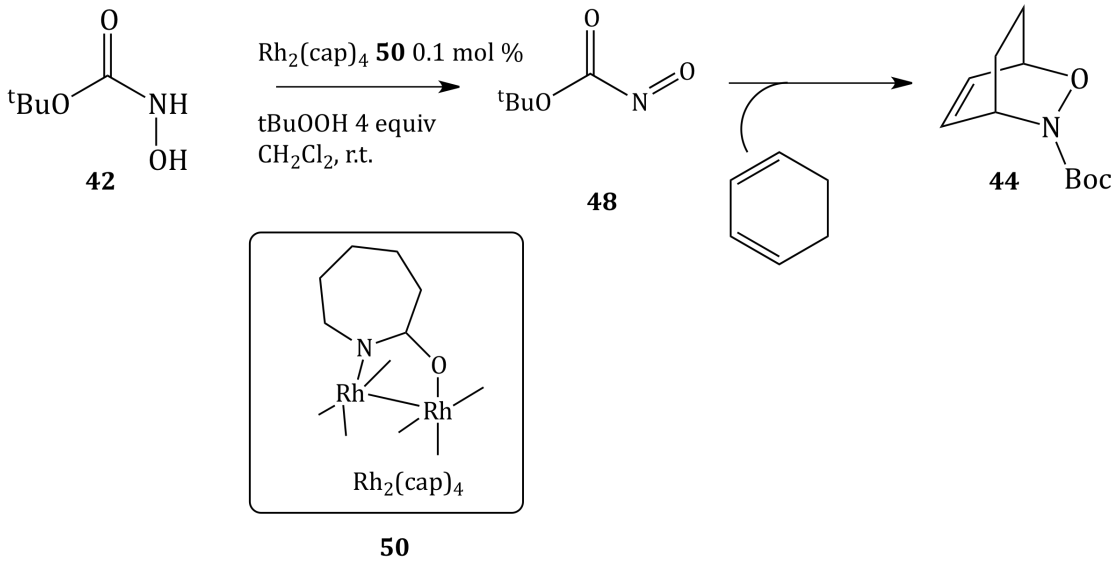

Scheme 16. Dirhodium(II) caprolactamate catalyzed in situ oxidative of hydroxamic acid reported by Tusun and Lu.

1.2.2 Asymmetric nitroso-Diels-Alder reactions

A catalytic asymmetric nitroso-Diels-Alder reaction using antibody 309-1G7 was reported in 1995 by Pandit *et al.,*[47] by reacting the nitroso compound **51** with unsymmetric diene **52**. The product **53** was obtained with >95% regioisomeric control and 82% *ee* of the cycloadduct (Scheme 17).

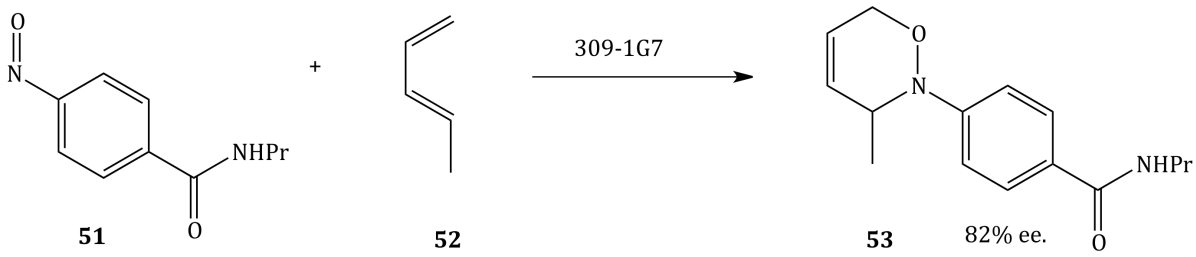

Scheme 17. Antibody 309-1G7 catalyzed the nitroso-Diels-Alder reaction.

Evans *et al.*[48] investigated the use of chiral bis(oxazoline)copper(II) complexes **56** to catalyze the enantioselective hetero–Diels–Alder reaction of α,β–unsaturated carbonyl compounds **54** with electron rich alkenes **55** resulting in cycloadduct **57** (Scheme 18). The high level of enantioselectivity was claimed to be due to the coordination of the substrate to the chiral bis(oxazoline)copper(II) catalysts to form chiral complexes **58** (Figure 6)**.**[49]

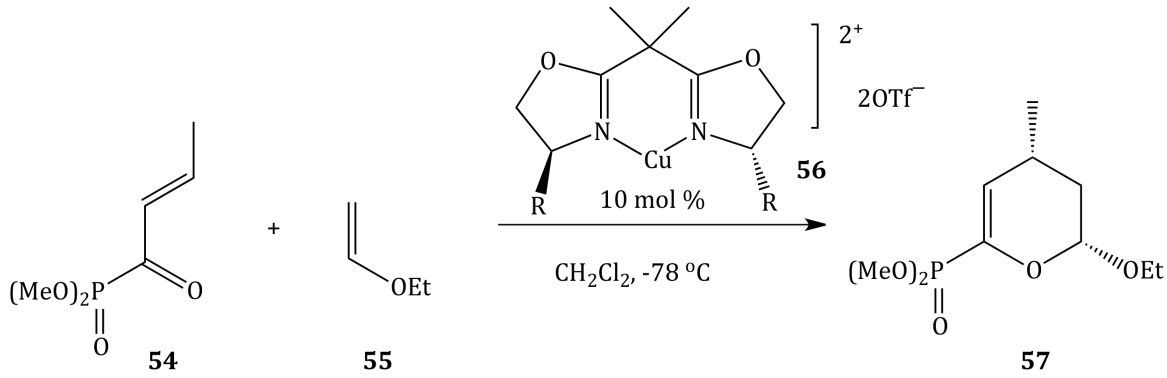

Scheme 18. Chiral bis(oxazoline)copper(II) catalyzed enantioselective hetero–Diels–Alder reaction.

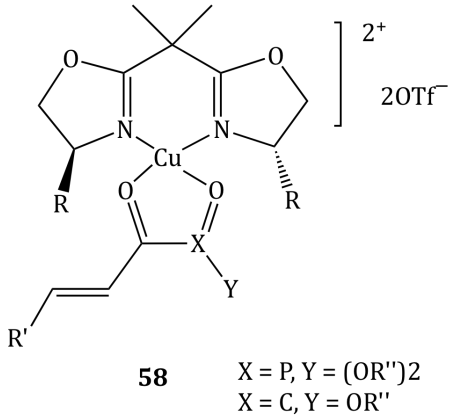

Figure 6. Chiral bis(oxazoline) copper(II) complexes **58**.

There have been a number of attempts to perform enantioselective nitroso–Diels–Alder reactions. In 2003 Watkinson and Whiting *et al.*[50] employed an enantiomerically pure ligand **59** (Figure 7) and $CuCl_2$ in this reaction. However, no enantioselectivity was detected. It was concluded from these results that the dissociation of the nitroso-compound from the chiral metal complex occured before the [4+2]-cycloaddition. The difficulties of enatioselective nitroso–Diels–Alder reactions of nitroso compounds could be due to the fact that nitroso compounds exist in a monomer-azodioxide dimer equilibrium.[31]

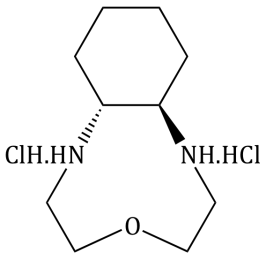

59

Figure 7. Ligand **59**.

In 2004, however, Yamamoto *et al.*[51] achieved an enantioselective nitroso–Diels–Alder reaction, using 2-nitrosopyridine derivative **61** reacting with dienes **60** in the presence of copper(I) with chiral ligands **63** or **64**. As a result, this gave the corresponding cycloadducts **62** with good enatiomeric excesses (up to 99%) (Scheme 19).

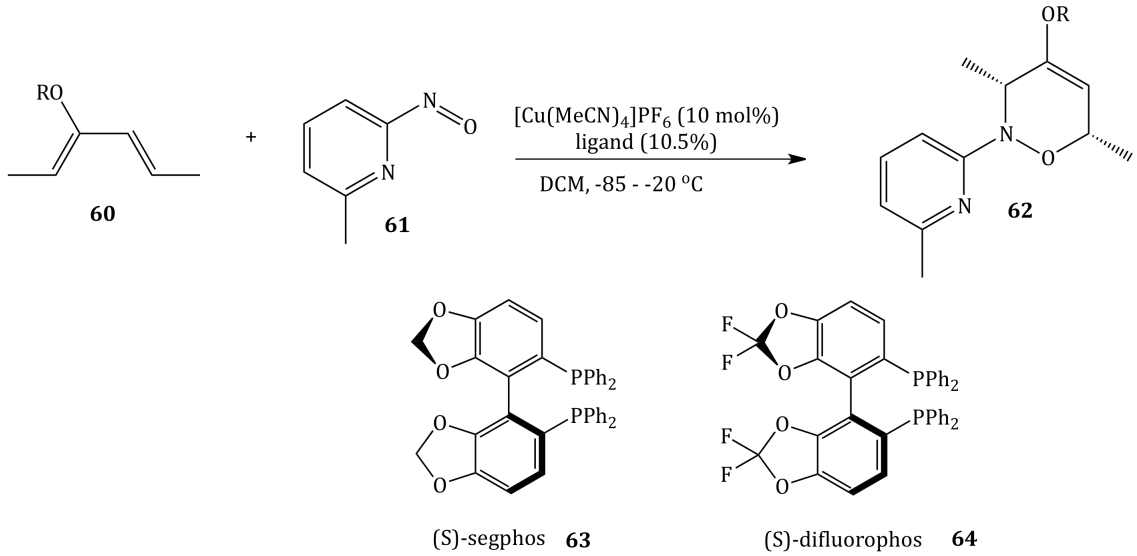

Scheme 19. Enantioselective nitroso–Diels–Alder reaction reported by Yamamoto.

Stüder *et al.*[52] reported the enantioselective nitroso–Diels–Alder reaction of 2-nitrosopyridine **65** with various dienes using $[CuPF_6(MeCN)_4]$/Walphos-CF_3 **66** as catalyst. This gave the corresponding cycloadducts **67a** and **67b**, in quantitative yield and with good to excellent enatioselectivities (up to 99% yield and 93% *ee*) (Scheme 20). However, due to the sensitivity of the catalyst, the reactions needed to be carried in the absence of air and moisture. The reason for the high enantioselectivity of 2-nitrosopyridine is due to its ability to form a plausible

chelate intermediate **68** (Figure 8), which was proposed to explain the configuration of the resulting stereogenic centres.[51]

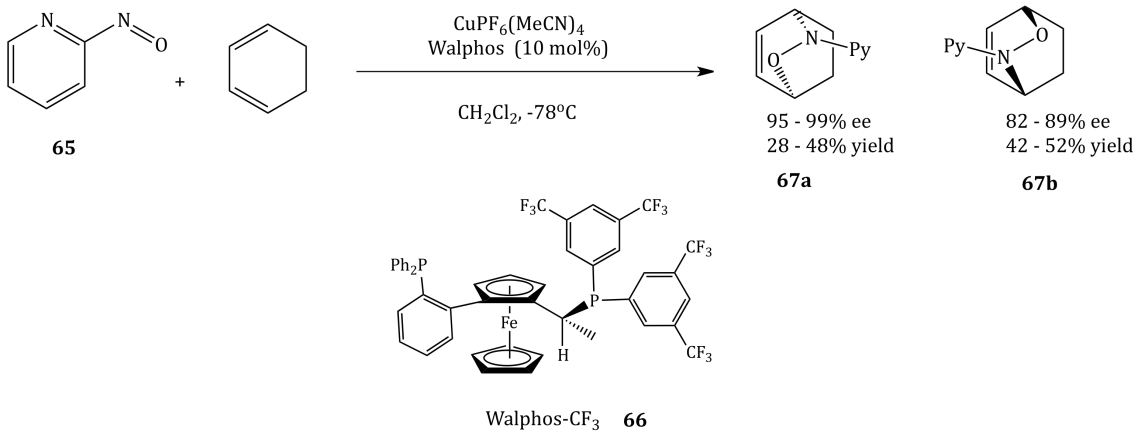

Scheme 20. Enantioselective nitroso–Diels–Alder reaction of 2-nitrosopyridine **65** using $[CuPF_6(MeCN)_4]$/Walphos-CF_3 **66** catalyst.

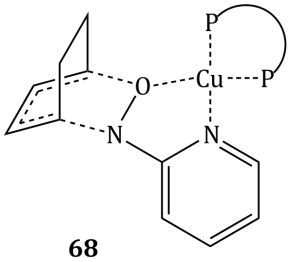

Figure 8. A plausible chelate intermediate **68** for the reaction shown in Scheme 20**.**

1.2.3 Nitroso-Diels-Alder adducts in modern organic synthesis

The nitroso-Diels-Alder has proved to be very useful in modern organic synthesis due to the attractive building block nature of the cycloadducts. These types of cycloadducts have been attractive in total synthesis because the N-O bond can be easily cleaved *via* reduction giving an alcohol and amine with a *syn*-orientation.[53] They can also undergo ring contraction to form the corresponding pyrroles.[54] There are several reports of the application of the nitroso-Diels-Alder reaction in the total synthesis of natural products. This review will focus on work from 2008 onwards.

In 2008, Stüder *et al.* reported the total synthesis of (+)-*trans*-dihydronarciclasine **71**, which is a biologically active natural product of the

Amaryllidaceae group,[55] and has potential antitumor and antiviral properties. The enantioselective, regiodivergent Diels–Alder reaction of diene **69** and 2-nitrosopyridine **65** using 10 mol % of $[CuPF_6(MeCN)_4]$/Walphos-CF_3 **66** as catalyst**,** gave the cycloadducts **70a** and **70b** (Scheme 21). The cycloadduct **70a** was then used as the precursor for the next steps, which gave the desired target product **71** at the final step (Scheme 22).

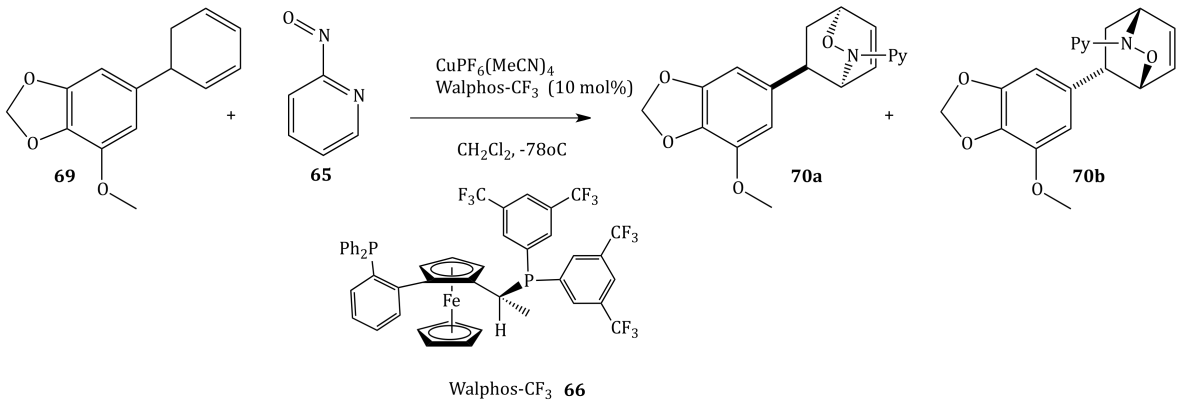

Scheme 21. The enantioselective regiodivergent Diels–Alder reaction reported by Stüder *et al.*

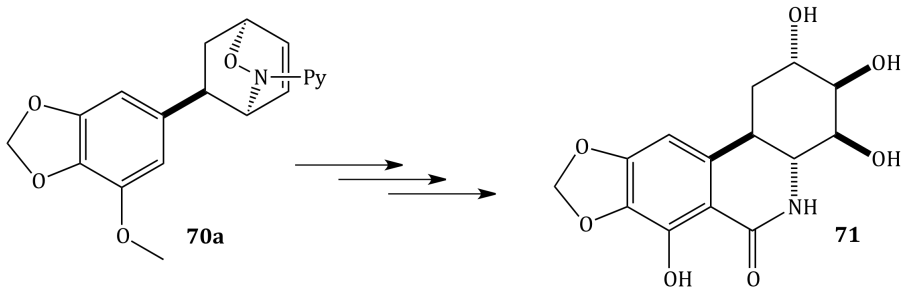

Scheme 22. The synthesis pathway of (+)-*trans*-dihydronarciclasine **71.**

A year later, the same group reported the use of this system in the synthesis of (-)-peracetylated conduramine A-1 **74**, which belongs to biologically active molecules, the amioconduritols.[56] The best diastereoselectivity and enantioselectivity was achieved using the reaction of diene **72** with 2-nitrosopyridine **65** using the same catalytic system of $[CuPF_6(MeCN)_4]$/Walphos-CF_3 **66** to yield the desired product **73** with 99% yield, d.r. > 99:1 and 93% *ee* (Scheme 23).

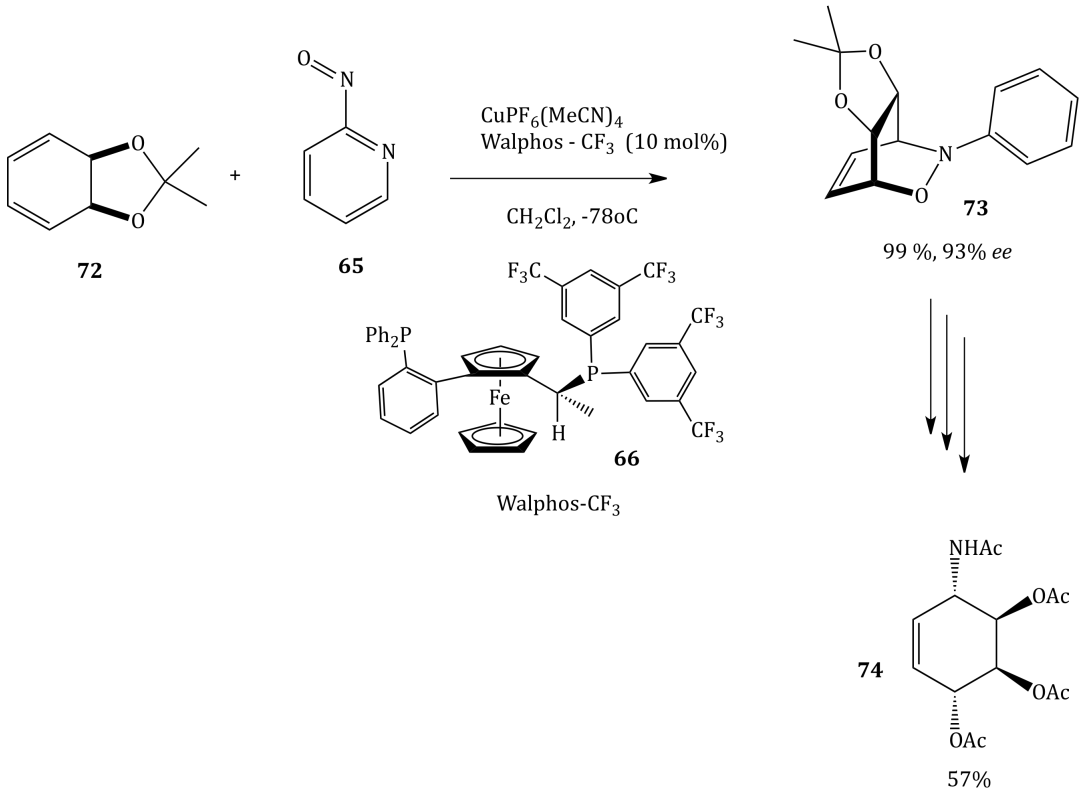

Scheme 23. Synthesis of (-)-peracetylated conduramine A-1 **74** *via* cycloadduct **73** intermediate.

Miller *et al.* reported the use of an acylnitroso Diels–Alder reaction in the diastereoselective synthesis of spironorasisteromycin **77** in 2009, which has potential due to biological activities such as anticancer, antibacterial and antiviral agents.[57] The first step involved the reaction of *tert*-butyl-*N*-hydroxycarbamate **42** using $NaIO_4$ as oxidant to form the corresponding nitroso species **48**, followed by [4+2]-cycloaddition with *N*-Cbz-protected spirocyclic diene **75**, which gave a 61% yield of cycloadduct product **76**. This intermediate underwent several reaction steps to obtain the desired product **77** (Scheme 24).

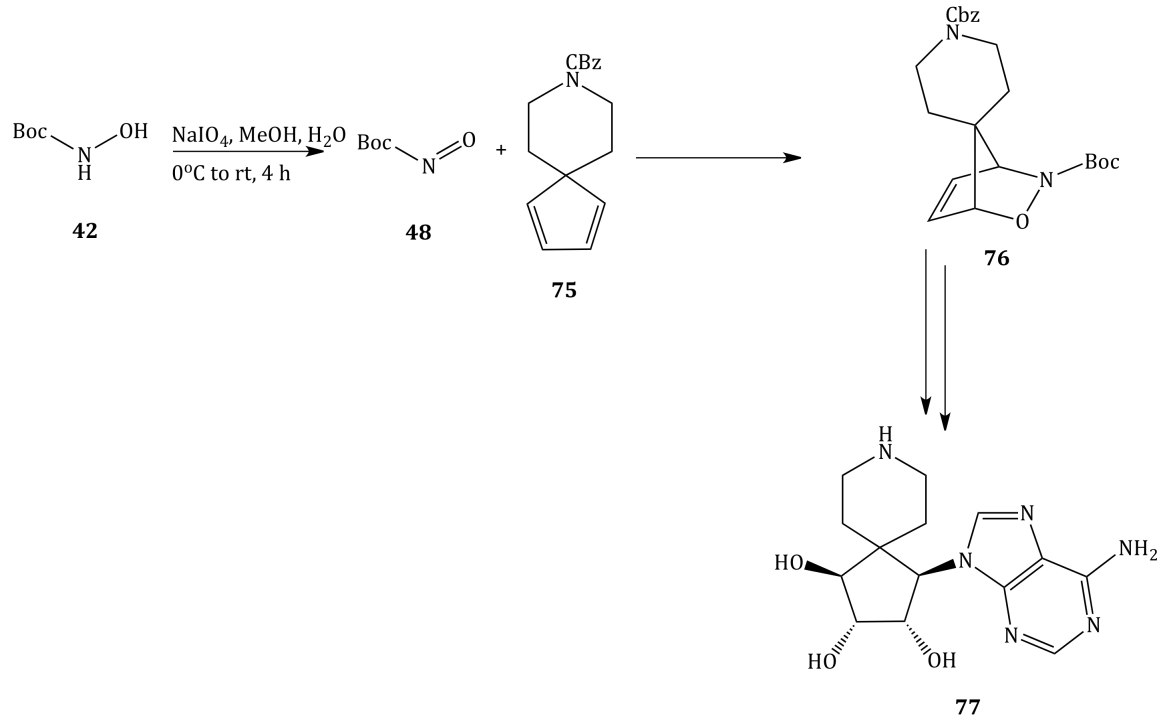

42 **48** **75** **76** **77**

Scheme 24. The disterioselective synthesis of spironorasisteromycin **77.**

In the same year, ergosterol **81** was synthesised by the same group, which also has anticancer properties. This compound was prepared by reacting acylnitroso or heterocyclenitroso compounds of type **79**, with diene **78** to give the corresponding cycloadduct **80**, which was subjected to N-O bond reduction to give the product **81** (Scheme 25).[58]

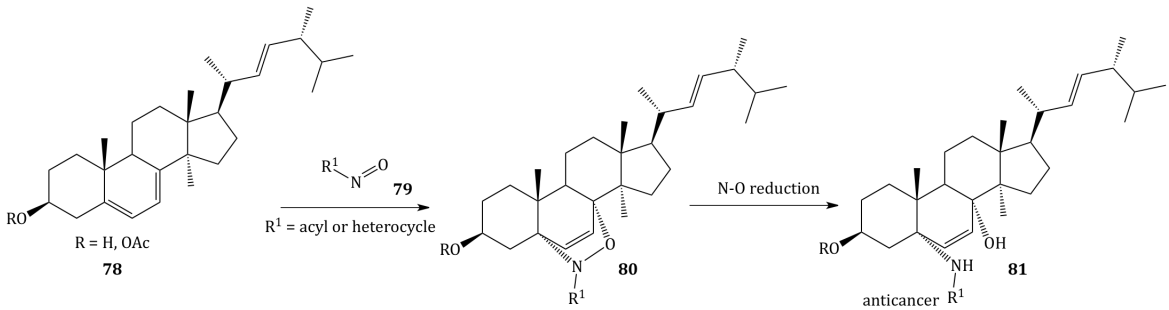

Scheme 25. The synthesis of ergosterol **81**

Marchand-Brynaert *et al.* published the use of the nitroso-Diels–Alder reaction of 1-phosphono-1,3-butadienes **82** with various nitroso compounds to access amino-phosphonic derivatives **85**, which showed promising activities in agricultural and medicinal areas.[59] The phosphono group attached to the diene at the 1-position

played an important role in the regioselectivity, and as a result, gave the proximal isomer. They concluded that aryl nitroso compounds were suitable for reacting with 1-phosphono-1,3-butadienes because they were stable at high temperature, while the acyl and α-chloro nitroso compounds were too reactive and were prone to degradation. The reactions of the arylnitroso **83** and 1-phosphono-1,3-butadiene **82** was carried out at 100 °C under microwave heating for an hour to yield up to 95% of **84**. The cycloadduct **84** was used in further reactions, to give rise to the desired aminophosphonic product **85** (Scheme 26).

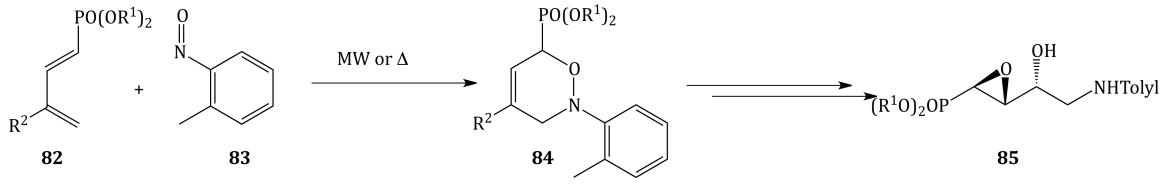

Scheme 26. Aminophosphonic derivatives **85** synthesis via the nitroso-Diels – Alder reaction.

Kouklovsky and Vincent synthesized racemic 8-epihalosaline **89** and porantheridine **90** *via* the nitroso-Diels–Alder reaction. This was achieved by reacting the nitroso compound **86** with cyclopentadiene to give the corresponding cycloadduct **87**, which was then treated with Grubb's II metathesis catalyst in the presence of an external alkene in order to induce ring-opening methathesis (ROM) followed by ring-closing methathesis (RCM), cross methathesis (CM) and ring-rearrangement metathesis gave rise to isoxazolopyridinones.[60] These were used as precursors for the next few steps to achieve the synthesis of the alkaloids **89** and **90** (Scheme 27).

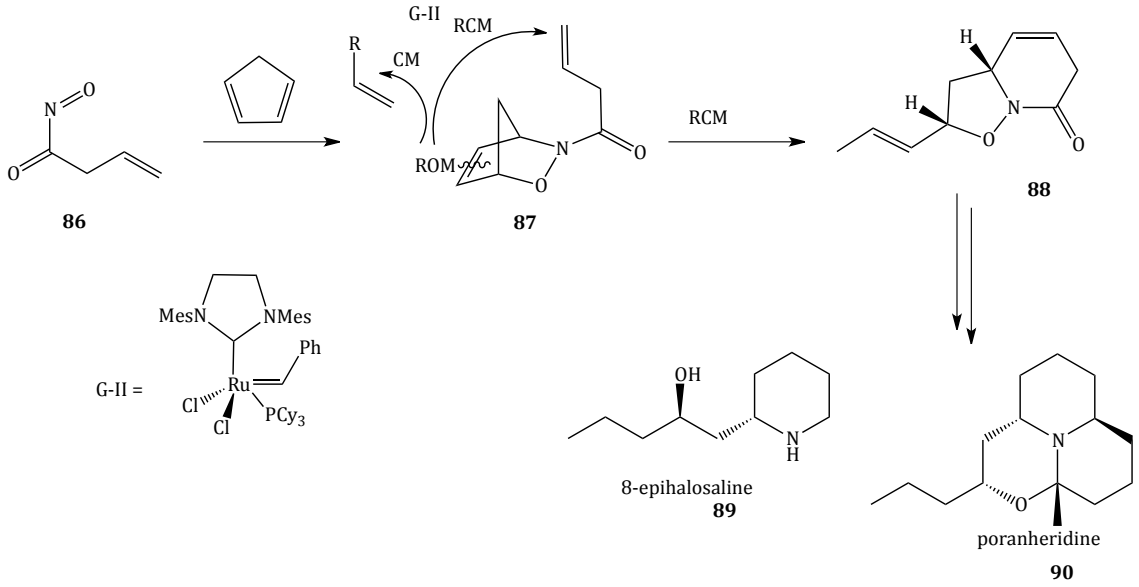

Scheme 27. The synthesis of 8-epihalosaline **89** and porantheridine **90**.

1.3 Hyrdoxamic acids synthesis

Hydroxamic acids were discovered in 1869 by Lossen.[61] They became popular in the 1980s due to their properties in biomedical applications such as antibiotics, antiasthmatics *etc.*;[62] metal ligands and in synthesis.[63] Various methods of hydroxamic acid synthesis have been reported. This report will focus on the methods that have been widely used in synthesis.

1.3.1 Synthesis of hydroxamic acids from aldehyde

Angeli and Rimini reported the reaction of aldehyde **91** and *N*-hydroxybenzenesulfonamide **92** in the presence of a base to give hydroxamic acids **93** in good to fair yield (Scheme 28).[64]

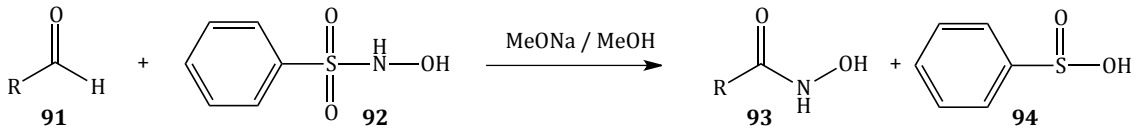

Scheme 28. The synthesis of hydroxamic acid from aldehyde.

Unfortunately, the side-product of this reaction was the sulfinic acid **94**, which caused difficulties in the purification process. To overcome this problem,

Porcheddu and Giacomelli reported the use of solid supported *N*-hydroxy-benzenesulfonamide **95** as a source of NHOH. This method gave good to excellent yields and purities by simple filtration and evaporation (Scheme 29).[65]

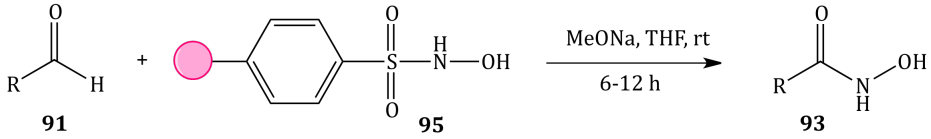

91 **95** **93**

Scheme 29. The synthesis of hydroxamic acid from aldehyde using solid supported N-hydroxybenzenesulfonamide **95**

1.3.2 Synthesis of hydroxamic acids from an ester

The reaction of ester **96** with hydroxylamine hydrochloride in the presence of alkali has been used as an important reaction for hydroxamic acid synthesis. The reaction can be carried out at 0 °C to room temperature for 4 to 12 hours, giving moderate to good yields (Scheme 30).[66]

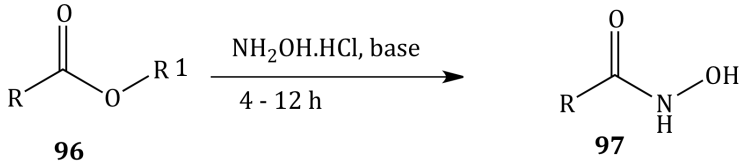

96 **97**

Scheme 30. The synthesis of hydroxamic acids from esters.

Massaro *et al*. reported the use of microwave irradiation to reduce the reaction time to 6 minutes. It is noteworthy that this method was employed with enantiomerically pure esters, which retained their stereochemistry.[67]

1.3.3 Synthesis of hydroxamic acid from acid chloride

An acid chloride **98** was readily reacted with hydroxylamine in the presence of base (Scheme 31).[68]

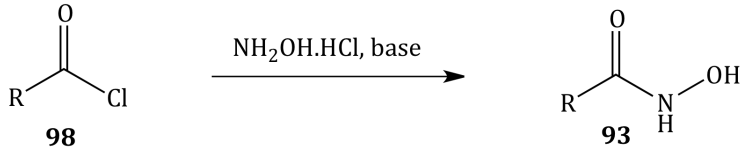

98 **93**

Scheme 31. The synthesis of hydroxamic acid from an acid chloride.

However, this method could not be applied to *N*-protected α-amino acids except those with Fmoc protecting groups. Babu *et al*. demonstrated the reaction of Fmoc–amino acid chlorides **99** with hydroxylamine hydrochloride in the presence of magnesium oxide to give Fmoc-protected amino acid hydroxamate **100** in good yields and purity (Scheme 32).[69]

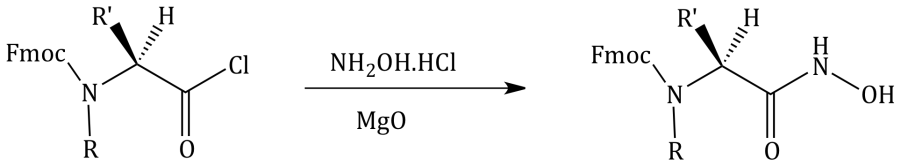

99 **100**

Scheme 32. Fmoc protected amino acid hydroxamate **100** synthesis.

1.3.4 Synthesis of hydroxamic acid from carboxylic acid

Although the reaction of esters and acid chlorides with hydroxylamine is the most economic method for preparing hydoxamic acids, the limitation of this reaction is the pH that needs to be used, *i.e.* basic conditions (pH>10). Therefore, it could not be applied to any base sensitive groups. Reddy *et al.* suggested a method to overcome this issue by reacting a carboxylic acid **101** with ethyl chloroformate to form mixed anhydride **102**, followed by reaction with hydroxylamine under neutral conditions (Scheme 33).[70]

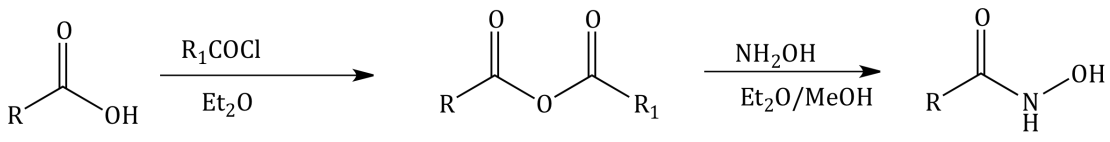

101 **102** **93**

Scheme 33. The hydroxamic acid synthesis from carboxylic acid.

However, the use of ethyl chloroformate as a carboxylic acid activator has a disadvantage due to its irritant vapour. Giacomelli *et al*. reported a one-pot hydoxamic acid reaction of a carboxylic acid with hydroxylamine hydrochloride in the presence of 2,4,6-trichloro[1,3,5]triazine (cyanuric chloride) and DMAP as catalyst at room temperature. This reaction was shown to be successful for the

synthesis of enantiomerically pure carboxylic acids and *N*-protected amino acids. Surprisingly, this was done without deprotection, even with the less stable Boc-*N*-protected group (Scheme 34).[71]

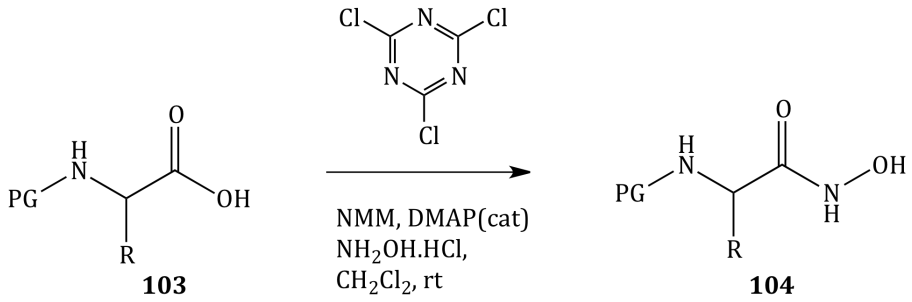

103 **104**

Scheme 34. One-pot synthesis of hydroxamic acid from carboxylix acid.

1.3.5 *N*-hydroxy urea synthesis.

N-Hydroxy ureas **106** were originally synthesized by acylation of an amine with phosgene or triphosgene to yield carbamoyl chloride or isocyanate **105**, followed by the reaction with hydroxyalamine to give the corresponding *N*-hydroxy ureas.[72] However, phosgene is very toxic, therefore, isocyanates are better to use as starting materials (Scheme 35).[73]

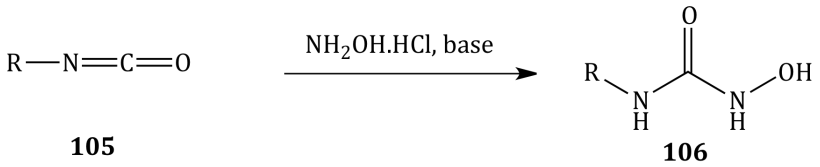

105 **106**

Scheme 35. *N*-hydroxy ureas synthesis from isocyanate.

Muñoz *et al*. suggested a preparative method for the *N*-hydroxy ureas **106** by reacting carbamoyl azides **107** with hydroxylamine under basic conditions (Scheme 36).[74]

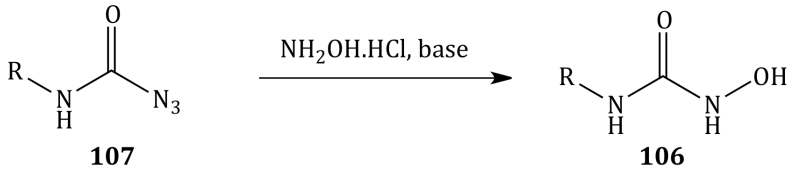

107 **106**

Scheme 36. *N*-hydroxy ureas synthesis from carbamoyl azides.

1.4 Copper-catalyzed aerobic oxidation

The chemistry of Cu(I)-dioxygen **109** adduct is of great interest due to its properties as a mild oxidant. Cu(I) **108** reacts with O_2 to form Cu(II)-peroxo species **109**, which can bind in two different positions; either end-on (μ-1,2-) or side on (μ-η^2-η^2) position. The binding site on the copper depends upon the nature of the ligands. A Cu(II)-peroxo species could readily oxidise a variety of substrates to form the corresponding 2-electron product and (LnCu(II)-OH)$_2$ species **110** (Scheme 37).[75]

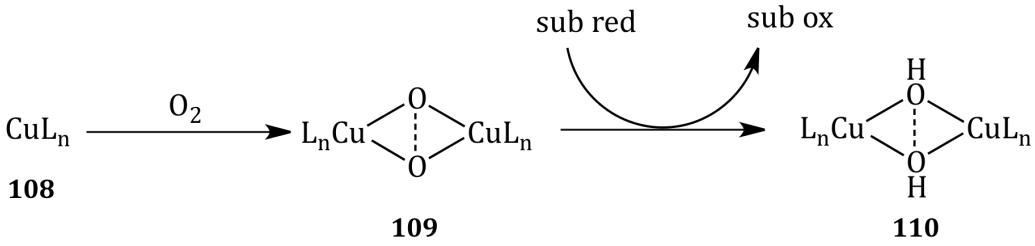

108 **109** **110**

Scheme 37. The formation of Cu(I)-dioxygen **109** adduct.

Makó *et al*. reported the use of Cu(I)Cl/1,10-phenantholine (5 mol%) and di-*tert*-butyl azodicarboxylate (5 mol%) with *N*-methylimidazole (7 mol%), which acted as the additive in the oxidation of primary alcohol **111** to aldehyde **112** in good yields (Scheme 38). [76]

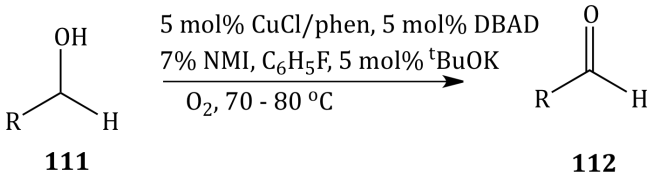

111 **112**

Scheme 38. Oxidation of primary alcohols to aldehydes using copper(I) catalyst.

Zhang and Jiao reported the use of copper(I) bromide (6 mol%) with pyridine (18 mol%) as a catalyst in the dehydrogenative coupling of anilines **113** and **114**. This

gave rise to an aromatic azo-compound **115** using oxygen in air as the oxidant. This reaction was carried out in toluene at 60 ^{0}C for 20 hours, which gave a yield of 96% for the symmetric azo-compounds and up to 73% for asymmetric azo-compounds (Scheme 39).[77]

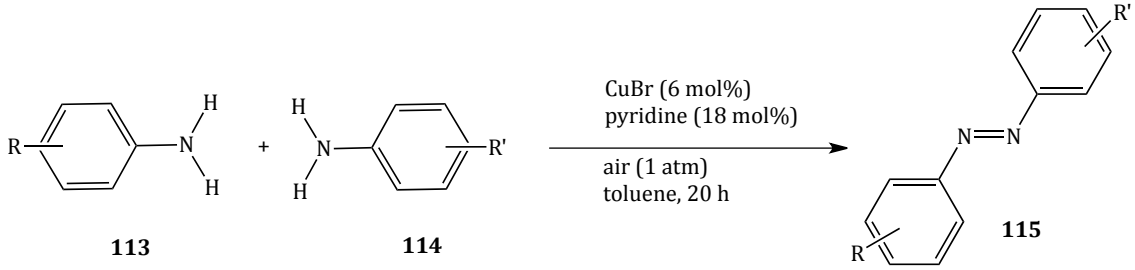

Scheme 39. The dehydrogenative coupling of anilines to aromatic azo compound.

They conducted two experiments using Cu(I)Br and Cu(II)Br$_2$ under nitrogen to see whether oxygen was the real oxidant, but both reactions were unsuccessful. Therefore, they postulated that O_2 was acting as an initiator that triggered the catalytic process, as well as being an oxidant (Scheme 40).

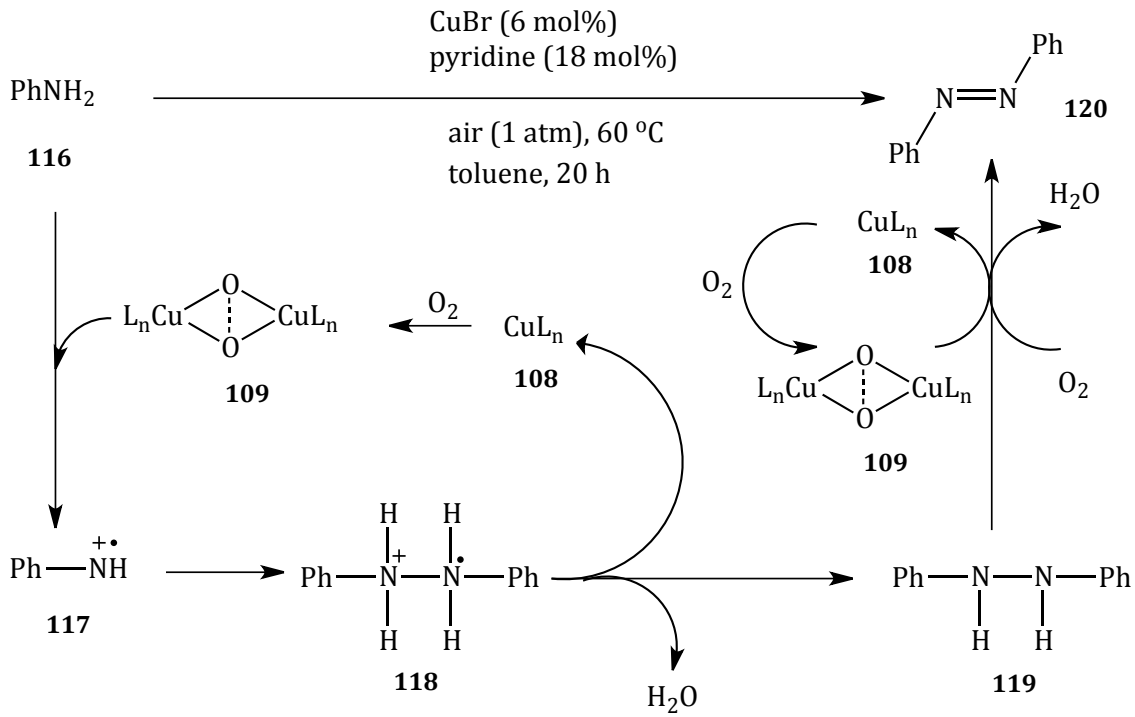

Scheme 40. A plausible mechanism of dehydrogenative coupling of anilines to azo-compounds.

A plausible mechanism involves a reaction which starts by the chelation of pyridine to Cu(I), then oxidation by O_2 to form the active catalyst species μ-η^2-η^2 peroxo complex **109**. The copper species then achieves single-electron oxidation of aniline **116** to form intermediate **117**, followed by coupling with another aniline to form a three-electron σ-bond species **118**. The loss of two protons and one electron gives hydrazine **119** formation, which was further oxidised to yield the azo-compounds **120** and regenerate the active catalyst species.

Ho and Lau reported the use of $CuCl_2.H_2O$ as a catalyst in the amination of alkenes **121** and ketones by phenylhydroxylamine **122**, which gave good regioselectivity of allylamines **123** with moderate yields (Scheme 41).[22]

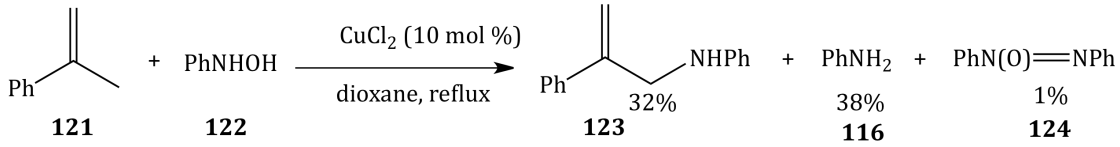

Scheme 41. The amination of alkenes by phenylhydroxylamine.

The Cu(II)-catalyzed oxidation of phenylhydroxylamine **122** was the first step in the catalytic process to form nitroso benzene **2**, followed by reaction with the alkene to give an allylhydoxylamine **125**. This species was then reduced by Cu(I) to form allylamine **126** (Scheme 42). Presumably, the reaction proceeds by an ene-reaction mechanism for the reaction of PhNO with propene.

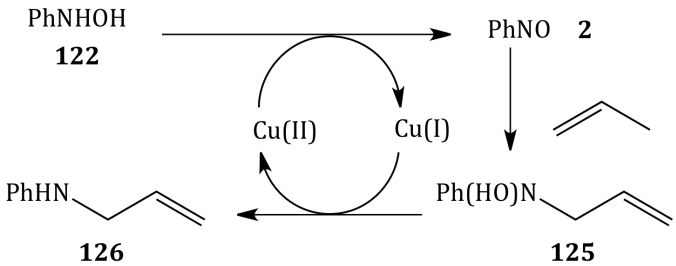

Scheme 42. A plausible mechanism for allylamine formation.

Accoring to the study of Ho and Lau, they could form phenylnitroso **2** by reacting 2 mole equivalent of $CuCl_2.H_2O$ with phenylhydroxylamine **122** at room temperature in dioxane for 3 minutes to give 70% of nitroso benzene **2** was formed with 10%

phenylamine **116** and 10% azoxybenzene as side-products. They suggested that nitroso compounds could be formed, as shown in the Eq 4.

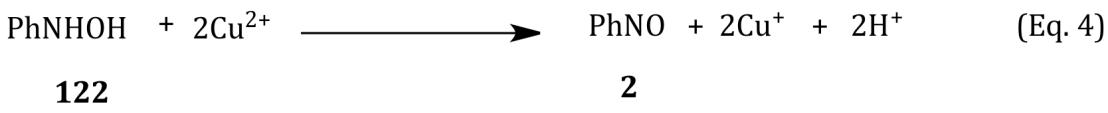

(Eq. 4)

The Eq. 5 illustrates that an amine is formed by the deoxygenation of phenylhydroxylamine by Cu(I) catalysis.

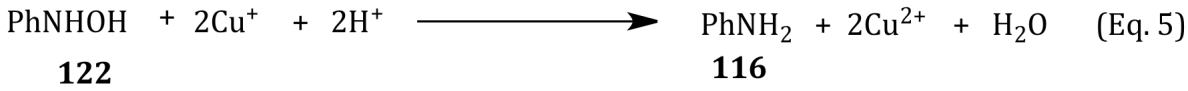

(Eq. 5)

The overall reaction is shown in Eq. 6.

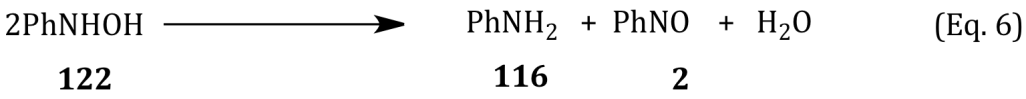

(Eq. 6)

Under certain thermal conditions, the disproportionation of phenylhydroxylamine can occur. However, when copper was present, the rate of reaction was much higher.

The azoxybenzene **124** was formed by the reaction of the nitroso benzene **2** and phenylamine species **116** (Eq. 7).

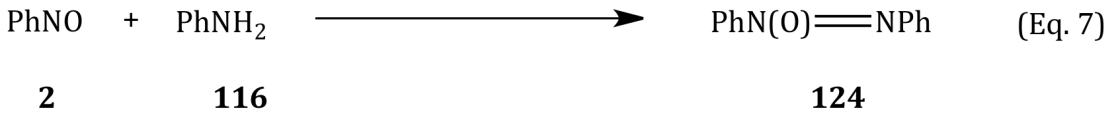

(Eq. 7)

Read de Alaniz *et al*. reported the use of Cu(I)Cl in acylnitroso ene reactions in 2011. The reaction was carried out using 5 mol% CuCl and 1.25 mol% pyridine in THF to achieve aerobic-oxidation of hydroxamic acids to the corresponding nitroso species, which readily reacted with an alkene to form ene-products. Both

intramolecular (Scheme 43) and intermolecular (Scheme 44) reactions took place to give moderate to high yields.[78]

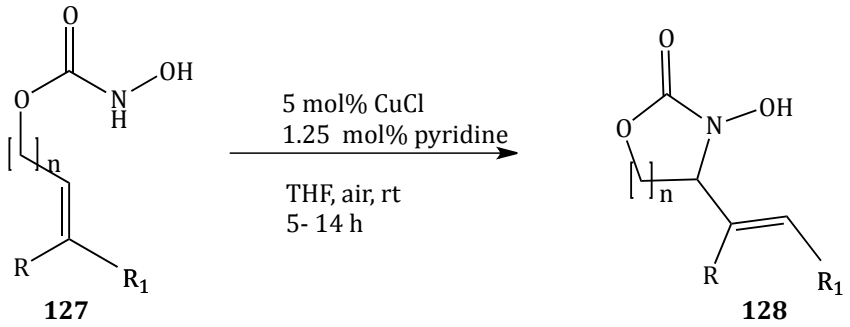

127 **128**

Scheme 43. Intramolecular ene-reaction involving an aryl nitroso species.

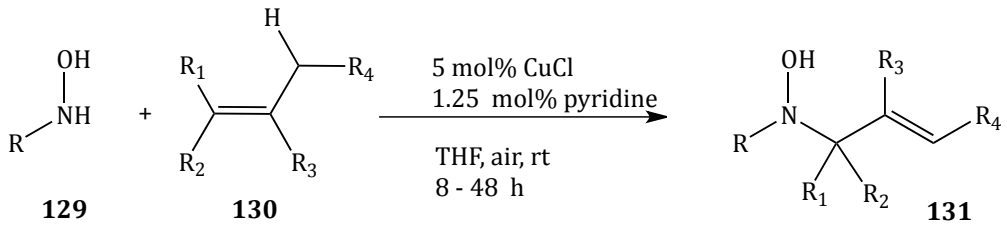

129 **130** **131**

Scheme 44. Intermolecular ene-reaction involving an aryl nitroso species.

A year later, they reported a similar catalytic system for the nitroso-Diels-Alder reaction, however, higher catalyst loading of 20% CuCl and 5 mol% pyridine was required to oxidize the hydroxamic acids **129** to the corresponding nitroso compounds, which were trapped by diene **132** to form the cycloadducts **133** (Scheme 45). The yields varied from moderate to high, which depended upon the hydroxamic acid. This procedure worked best for the corresponding hydroxamic acid forming nitrosoformate, nitrosoformamide and acylnitroso derivatives.[79]

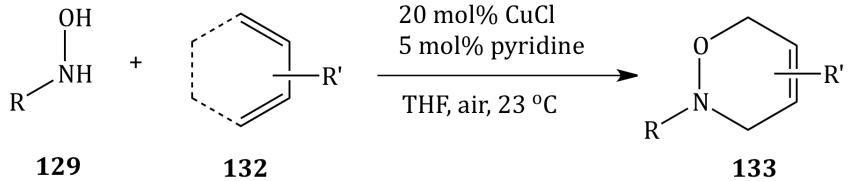

129 **132** **133**

Scheme 45. Aerobic oxidative nitroso-Diels–Alder reaction.

For a number of years, studies in the Whiting group have involved: a) developing new, greener oxidative methods for the generation of nitroso species;[80] b) demonstrating the first efficient, catalytic asymmetric arylnitroso DA reaction; and c) application of the adducts in the synthesis of bioactive compounds. To date, no highly enantioselective reaction of acylnitroso compounds has been reported, though the Whiting group has reported up to 15% e.e. using *R*-PROPHOS and $RuCl_2(PPh_3)_3$ (Scheme 46). Hence, the development of an enantiomerically benign, highly efficient catalytic asymmetric version is highly attractive.

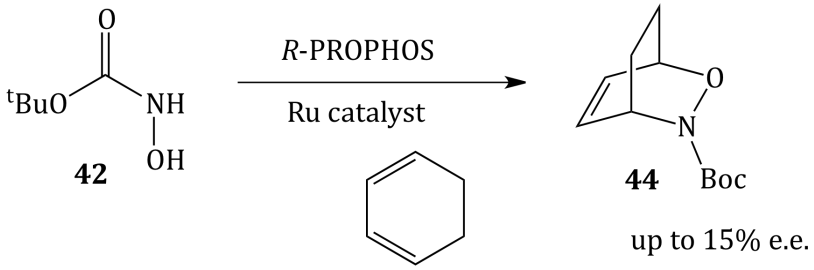

Scheme 46. Acylnitroso DA reaction using *R*-PROPHOS and Ru catalyst to achieve up to 15% e.e

Chapter 2. Results and discussion

2.0 Results and discussion

2.1 Introduction

Recently, chiral thiourea oxazolines have drawn the attention of synthetic chemists as they appear to be important ligands for several transition metal-catalyzed reactions.[81] In particular, palladium-thiourea oxazoline complexes have been reported as new catalysts in synthesis due to their properties of air and moisture stability. They are resistant to oxidation, which means they can be used in oxidative catalytic reactions. These complexes were synthesized and characterized in collaboration between the Marder and Yang groups[81] and they used these complexes in the chiral synthesis of bis(methoxycarbonylation) products, i.e. from the oxidative carbonylation of terminal olefins to give > 90% yields and up to 84% *ees*.

From some very preliminary previous studies from the Whiting group, the oxidation of hydroxamic acid **138** to nitroso-species **139** was claimed to have been achieved, which then reacted with 1,3-cyclohexadiene to form cycloadduct **140** at room temperature (see below). It was also claimed (by Ilyashenko) that using 1 mol% of a palladium catalysts with thiourea-oxazoline chiral ligands **141** - **144**, (Scheme 47) resulted in a very low yield but high enantioselectivities (up to 98% *ee*). However, for these highly preliminary studies, only a very small amount of catalyst was available and therefore, the reactions were carried out on an exceptionally small scale. The questions were therefore, whether these results could: 1) be reproduced on a larger scale; and 2) be demonstrated to indeed derive cycloadducts of type **140** with high asymmetric induction.

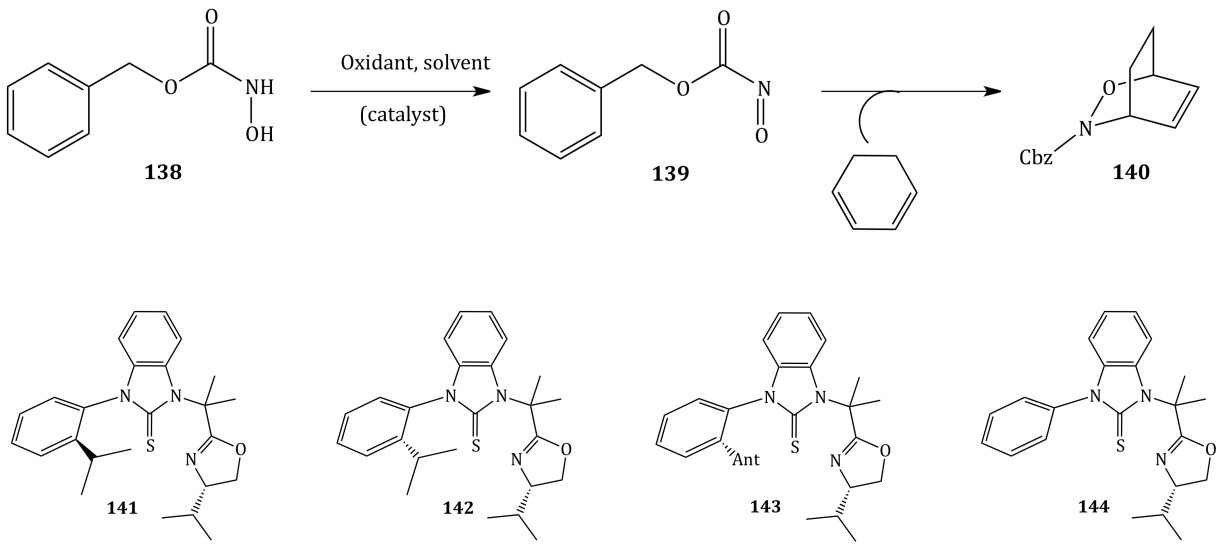

Scheme 47. The nitroso-Diels-Alder reaction using palladium catalysts with thiourea-oxazoline ligands.

2.2 Preliminary Studies

With the questions in mind from the preliminary results shown in Scheme 47, the initial aims of this project were therefore to repeat this type of reaction and determine if the results were reliable, whether they could be scaled up and whether they could be applied to other substrates, and hence in the asymmetric synthesis of chiral, bioactive compounds. The starting point in this project was therefore re-examining the reaction shown in Scheme **47** in an attempt to improve the yield of the cycloadduct **140** by increasing the catalyst loading to 5 – 10%, using both oxygen and air. These reactions were also carried out together with the addition of copper to assist in any oxidation process, and with copper alone to check on the effect of palladium *versus* copper as catalysts. The results are shown in the Table 1 with the comparable periodate-based reaction also reported.

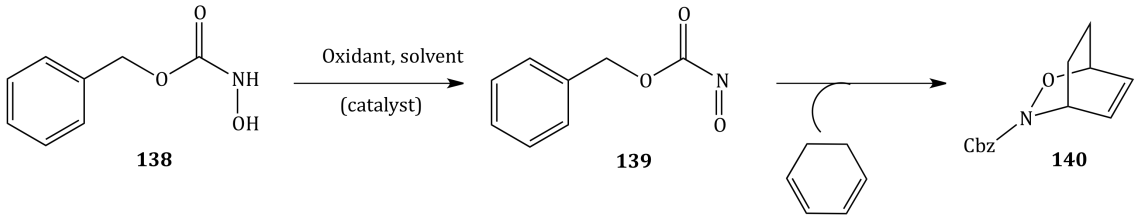

138 139 140

Table 1. The reaction of hydroxamic acid **138** with 1,3-cyclohexadiene with various catalyst systems based on palladium and copper.

Entry	Catalyst (mol%)	Co catalyst (mol%)	Oxidant	Solvent	Yield %
1	-	-	$NaIO_4$	MeOH	70
2	Pd-**141**(1)	-	O_2	MeOH	0
3	Pd-**141** (1)	-	Air	MeOH	0
4	Pd-**141** (5)	-	Air	MeOH	0
5	Pd-**141** (10)	-	Air	MeOH	0
6	Pd-**141** (1)	CuI (2)	Air	MeOH	20
7	Pd-**141** (5)	CuI (5)	O_2	MeOH	39
8	Pd-**141** (5)	CuI (10)	O_2	MeOH	42
9	Pd-**141** (1)	CuI (2)	O_2	MeOH /Et_3N	58
10	CuI (10)	-	O_2	MeOH	77

Table 1 shows the results of a catalytic study of Pd-**141** complexes in the model reaction (Scheme 47) carried out in order to confirm that the reaction of *N*-(benzyloxy-carbonyl)hydroxylamine **138** and 1,3-cyclohexadiene can actually take place through nitroso generation. The oxidation of the hydroxamic acid **138** using the $NaIO_4$ as the oxidant in the presence of 1,3-cyclohexadiene in methanol was conducted initially. The reaction was complete in 4 hours giving 70% isolated yield (Entry 1, Table 1). The cycloadduct product **140** was confirmed by NMR. The reason for using 1,3-cyclohexadiene in the model reaction was because it is commercially available, easy to handle and does not dimerize at room temperature, unlike cyclopentadiene.

Upon the premixing 1 mol% of Pd-**141** in methanol for 5 minutes, the colour of the solution was yellow. After adding *N*-(benzyloxycarbonyl) hydroxylamine **138** and 1,3-cyclohexadiene, the colour stayed the same. After 7 days, the mixture turned black but there was no desired product spot on the TLC. The black colour of the catalyst suggested the formation of Pd(0) colloid. This catalyst is moisture and air stable, therefore, the reduction of the Pd(II) complex could take place either by reduction from hydroxamic acid **138** or 1,3-cyclohexadiene. Entries 2 and 3, Table 1 were carried out at room temperature under O_2 and air respectively. However, there was no reaction even with 5 and 10 mol% catalyst loadings (Entries 4 and 5, Table 1). From the study of using Pd-**141** complexes catalyst in the enatioselective bis(methoxycarbonylation)s of terminal olefins under mild conditions,[81] it was found that a copper salt was important in this reaction. Therefore, the addition of 2 mol% CuI as a co-catalyst in the reaction with 1 mol% of Pd-**141** (Entry 6, Table 1) was carried out in methanol at room temperature. The desired product spot appeared on the TLC after 1 day and the reaction was complete in 4 days, giving the product **140** in 20% yield. Increasing the catalyst and co-catalyst loading helped to increase the yield of the cycloadduct product (Entries 7 and 8, Table 1). Adding Et_3N as base helped to increase the yield further to 58% using the same reaction timescale. However, there were some unidentified impurities on the TLC and in the NMR spectrum (Entry 9, Table 1). The use of CuI as catalyst alone in the model reaction was also carried out using 10 mol% CuI in methanol; the cycloadduct spot appeared on the TLC after 1 day and the reaction finished in 4 days giving 77% isolated yield of product **140** (Entry 10, Table 1). This reaction confirmed that copper plays a major role in the catalytic cycle in the oxidation of hydroxamic acid **138** to nitroso species and that the Pd complexes are unreactive.

Ru-based catalysts have been reported to catalyze oxidative nitroso dienophile formation, especially using Ru-pybox complexes as catalyst and ^tBuOOH or H_2O_2 as co-oxidant.[41,42] Therefore, experiments were carried out using 1 mol% $RuCl_3$ and 2 mol% ligand [tetramethylthiourea (TMTU) or 2-ethyl-2-oxazoline or **141**] using ^tBuOOH as co-oxidant in DCM at room temperature for 96 hours in the reaction shown in Scheme 47. The results are summarized in Table 2 and show that the reaction did not proceed under aerobic conditions (Entries 1, 2 and 3,

Table 2) showing that ruthenium was not able to accomplish aerobic oxidations of the type desired, and hence, copper-based oxidants look like the most promising for further development.

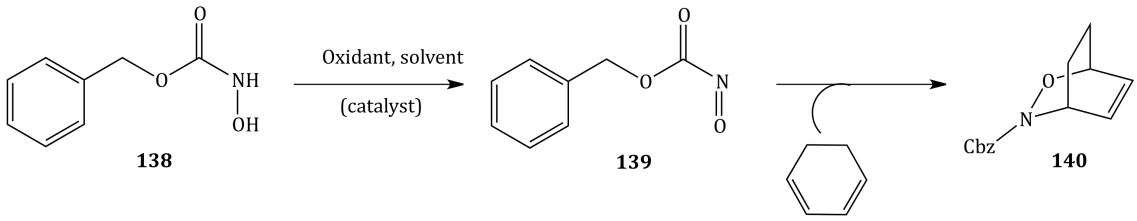

Table 2. $RuCl_3$ with thiourea and oxazoline catalysts in the model reaction, as in Scheme 47.

Entry	Catalyst (mol%)	Time	Yield %
1	$RuCl_3$(1)/TMTU (2)	96 h	0
2	$RuCl_3$(1)/2-ethyl-2-oxazoline (2)	96 h	0
3	$RuCl_3$(1)/**141** (2)	96 h	0

2.3. Copper salt screening

From the results reported in Table 1 showing that copper salts could mediate the require hydroxamic acid oxidation in air, copper salt screening reactions with different solvents were conducted using: CuI; $CuCl_2$; $CuBr_2$; and $Cu(OAc)_2$ in methanol, toluene, acetonitrile, THF, a mixed solvent system of methanol:toluene (1:4) and chloroform in the absence of any additional ligands. The results are shown in Table 3.

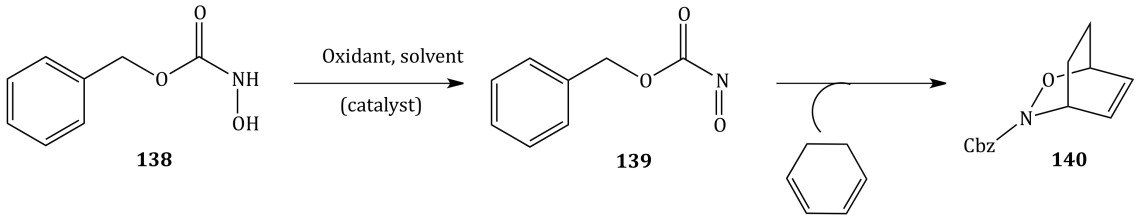

138 **139** **140**

Table 3. Screening of both copper salts and solvents for the oxidation of **138**, trapping with 1,3-cyclohexadiene to give **140**.

Entry	Catalyst (mol%)	Time*	Solvent	Yield %#
1	CuI (5)	4 d	MeOH	32
2	$CuCl_2$ (5)	15 h	MeOH	47
3	$CuBr_2$ (5)	15 h	MeOH	40
4	$Cu(OAc)_2$ (5)	5 d	MeOH	21
5	CuI (5)	6 d	Toluene	35
6	$CuCl_2$ (5)	4 d	Toluene	50
7	$CuBr_2$ (5)	4 d	Toluene	44
8	$Cu(OAc)_2$ (5)	7 d	Toluene	23
9	CuI (5)	2 d	MeCN	10
10	$CuCl_2$ (5)	22 h	MeCN	27
11	$CuBr_2$ (5)	2 d	MeCN	21
12	$Cu(OAc)_2$ (5)	2 d	MeCN	5
13	CuI (5)	26 h	THF	20
14	$CuCl_2$ (5)	26 h	THF	28
15	$CuBr_2$ (5)	26 h	THF	25
16	$Cu(OAc)_2$ (5)	26 h	THF	11
17	CuI (5)	20 h	MeOH/Toluene 1:4	72
18	$CuCl_2$ (5)	15 h	MeOH/Toluene 1:4	75
19	$CuBr_2$ (5)	20 h	MeOH/Toluene 1:4	69
20	$Cu(OAc)_2$ (5)	4 d	MeOH/Toluene 1:4	50
21	CuI (5)	21 h	$CHCl_3$	70
22	$CuCl_2$ (5)	15 h	$CHCl_3$	77
23	$CuBr_2$ (5)	21 h	$CHCl_3$	68
24	$Cu(OAc)_2$ (5)	3 d	$CHCl_3$	52

*Time = reaction time (as defined by 100% consumption of hydroxamic acid by TLC analysis).

Yield = isolated yield after SiO_2 chromatography.

The reactions outlined in Entries 1-4, Table 3 were carried out in methanol. After mixing CuI with methanol, the solution was colourless, but upon the addition of the diene and hydroxamic acid, the mixture turned a milky colour due to the diene not dissolving fully in the methanol. The mixture turned colourless when the reaction was completed after 4 days (Entry 1, Table 3), though only low yields of the adducts (32%) was obtained. For Entry 2 (Table 3), after dissolving the $CuCl_2$ in methanol, the colour changed to yellow-green. Addition of the diene and hydroxamic acid changed the reaction mixture colour to a cloudy-pale yellow. The reaction completed in 15 hours with 47% isolated yield and the colour changed back to the yellow-green of $CuCl_2$. This colour change showed that the reaction seemed to be self-indicating. For Entry 3 (Table 3), the colour of $CuBr_2$ in methanol was yellow and the colour changed to a cloudy-pale yellow when the diene and hydroxamic acid were added. The reaction was completed in 15 hours with 40% isolated yield and the mixture changed back to the starting colour. For Entry 4 (Table 3), when dissolving $Cu(OAc)_2$ in methanol, the colour of the solution was pale blue. Addition of diene and hydroxamic acid changed the colour to a cloudy-yellow-green. The reaction was completed in 5 days the lowest isolated yields was obtained, being 21%.

When the copper salt screenings were conducted using toluene as solvent, they gave a similar trend to the methanol reactions, but the solubility of the copper salts was very low and hence, the reaction times were the longest among all the solvents that were used (Entries 5 – 8, Table 3), with reaction times up to 7 days. The isolated yield of the cycloadduct products was low to moderate (23-50%). $CuCl_2$ gave the highest yield, followed by $CuBr_2$, CuI and $Cu(OAc)_2$. In acetonitrile solvent, the copper salts were readily dissolved and different colours were produced in the different solvents, except for CuI, which gave a colourless solution in all solvents. The $CuCl_2$-based mixtures gave yellow solutions, in all cases which darkened upon the addition of the diene and hydroxamic acid. The reaction was complete in 22 hours and the colour changed back to the original colour of yellow giving 27% isolated yield (Entry 10, Table 3). $CuBr_2$ mixtures were dark green, which turned jade green upon adding the starting materials. The reaction was

stirred and completed in 2 days and the colour of the mixture changed to brownish green giving 21% isolated yield (Entry 11, Table 3). $Cu(OAC)_2$ in acetronitrile was blue and this changed to yellow-green after the staring materials were added. The completion of the reaction took 2 days with the lowest isolated yield of 2% (Entry 12, Table 3). By using THF as solvent (Entries 13-16, Table 3), all the reactions were completed in 26 hours. The isolated yields were low (11 – 28%), however. From these results, it can be summarized that methanol gave the shortest reaction times among all the solvents, with generally good copper salt solubility. Toluene gave the best isolated yield among the four solvent systems but the copper solubility was the lowest and solubilisation appeared to be the slow part of the reaction. Therefore, the mixed solvent system of methanol and toluene (1:4) were conducted (Entries 17-20, Table 3). The isolated yields of the cycloadduct product were improved in all cases (up to 75%). The reaction times for CuI and $Cu(OAc)_2$ were also improved compared with both single solvent systems. The $CuCl_2$ reaction time was 15 hours, which was the same as the reaction time in methanol. However, the $CuBr_2$ catalyst in the mixed solvent system was slower than the reaction in methanol. Although the chlorinated solvent was not the ideal solvent for this system because even with a trace can damage chiral HPLC column supports, chloroform-d was used as the NMR solvent and the copper salts were screened in chloroform (Entries 21–24, Table 3). The $CuCl_2$ reaction time could be monitored as the colour changed from green to yellow and then back to green when the reaction completed (15 hours), which was the fastest among them all the reactions. It also gave the highest isolated yield of the cycloadduct product (77%). The CuI and $CuBr_2$ reactions were completed in 21 hours with 70% and 68% isolated yields respectively.

Overall, $CuCl_2$ was the best copper catalyst in the model reaction. $CuCl_2$ in MeOH/toluene (1:4, v/v) gave the second best yield of 75%. With only MeOH, even though the reaction was fast, there was a side-product formed. A problem with using toluene as the only solvent was the solubility of the hydroxamic acid, which caused the reaction to be slower. With a combination of the two solvents, we can overcome this problem to some extent.

2.4 Ligand screening

2.4.1 Chiral thiourea oxazoline ligand screening

The effect of $CuCl_2$ with thiourea-oxazoline ligands **141** - **144** in the model reaction (Scheme 47) in MeOH/toluene (1:4, v/v) was next examined in air in order to probe the effect of these ligand systems, if any. This solvent system was chosen because the cycloadduct product **140** could then be directly examined using chiral HPLC to check if there was any asymmetric induction. The results of this study are reported in Table 4.

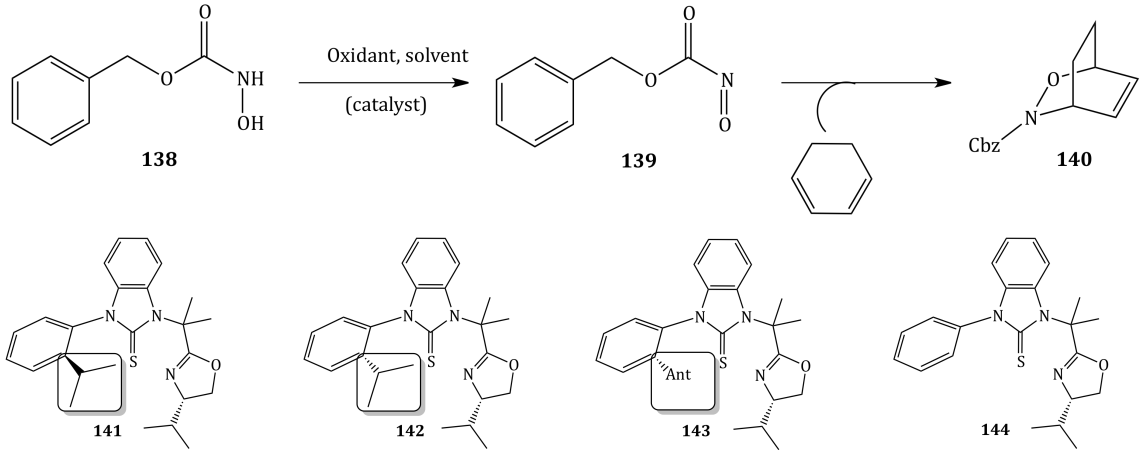

138 139 140

141 142 143 144

Table 4. $CuCl_2$ with thiourea-oxazoline ligands in the model reaction (Scheme 47) carried out in toluene-MeOH in air.

Entry	Catalyst (mol%)	Time	Yield of 140 % (*ee*)
1	$CuCl_2$(5)	15 h	75 (0)
2	$CuCl_2$(5) **141** (5)	10 h	81 (0)
3	$CuCl_2$(5) **142** (5)	18 h	70 (0)
4	$CuCl_2$(1) **143** (1)	15 h	75 (0)
5	$CuCl_2$(5) **144** (5)	24 h	77 (0)

Entry 1, Table 4 is the standard reaction with 5 mol% $CuCl_2$ without any ligand. The reaction was completed in 15 hours with 75% isolated yield. Therefore, 5 mol% thiourea-oxazoline ligand **141** with 5 mol% $CuCl_2$ was tested (Entry 2, Table 4) and upon the mixing of the copper salt with ligand, the colour was yellow and the mixture turned colourless upon the additional of diene and hydroxamic acid. The reaction was completed in 10 hours, confirmed by the TLC. This reaction was very easily purified by flash column chromatrography. The cycloadduct product **140** obtained was very pure and crystallized. The crystal structure was confirmed by the X-ray diffraction techniques (Figure 9).

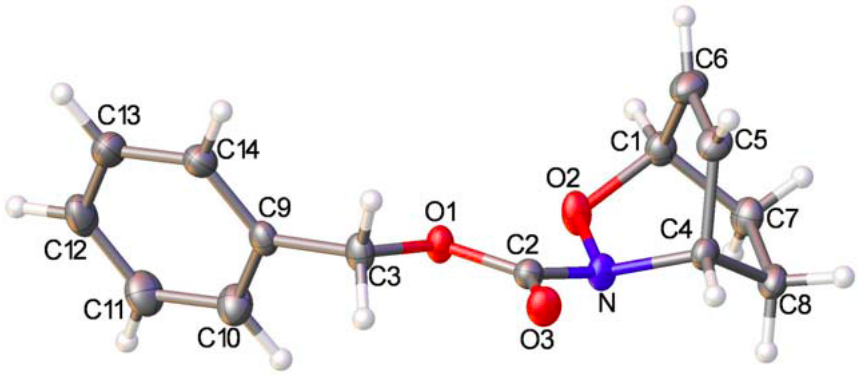

Figure 9. X-ray crystal structure of **140** from Entry 2, Table 4.

Ligand **142** is an atropoisomer of the ligand **141**, which was also used as a ligand in the standard reaction (Scheme 47). These atropoisomers differ in the conformation of the ^{i}Pr substituent on the phenyl ring. Use of 5 mol% thiourea oxazoline ligand **142** with 5 mol% $CuCl_2$ as catalyst in the model reaction took longer to complete (18 hours) and lower yield (70%) compared to $CuCl_2$-**141** system (Entry 3, Table 4). Ligand **143** has the anthracene substituent on the phenyl ring and with only 1 mol% of this ligand and 1 mol% $CuCl_2$ could be used due to the small quantity of this ligand that was supplied. The reaction time of this reaction was 15 hours and which gave 75% isolated yield of the cycloadduct product **140** (Entry 4, Table 4). The last entry in Table 5 used 5 mol% $CuCl_2$ and 5 mol% ligand **144**; a ligand which has no substituent on the phenyl ring. The reaction was completed in 24 hours giving 77% isolated yield. From this table, it can be concluded that the thiourea-oxazoline ligands **141** and **143** can help to improve the rate of the reaction compared to the $CuCl_2$ with no ligand added,

whereas **142** and **144** lowered the reaction rate marginally. However, these reactions were easily purified and gave high purity cycloadduct product **140** with a simple purification technique. Unfortunately, in all cases, there was no asymmetric induction, and therefore, in order to understand the catalytic properties of the catalyst system in more detail, the next set of experiments were conducted using both tetramethylthiourea (tmtu) and 2-ethyl-2-oxazoline as ligands separately in the model reaction as in Scheme 47. The results are shown in Table 5.

2.4.2 Thiorea and oxazoline ligand screening

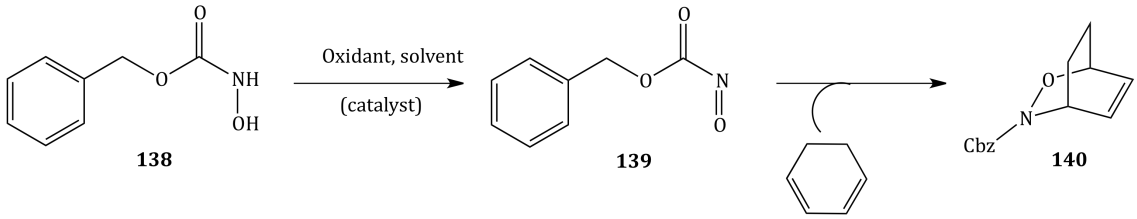

138 **139** **140**

Table 5. The reaction of hydroxamic acid **138** with 1,3-cyclohexadiene using 10 mol% $CuCl_2$ in methanol with various ligands to give **140**.

Entry	Ligand (mol%)	Time (h)	Yield %	*ee*
1	-	15	48	0
2	TMTU (10)	15	60	0
3	TMTU (20)	15	55	0
4	2-ethyl-2-oxazoline (10)	15	53	0
5	2-ethyl-2-oxazoline (20)	3	86	0
6	TMTU (10), 2-ethyl-2-oxazoline (10)	15	68	0
7	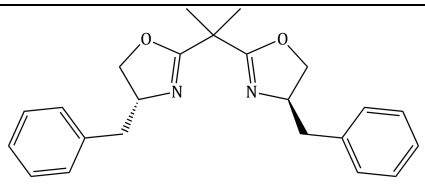 **145** (10)	2	70	0

Entry 1 (Table 5) is a reaction, which is a control reaction using 10 mol% $CuCl_2$ with no ligand present in the reaction mixture. The reaction completed in 15 hours, giving compound **140** in 48%. For Entries 2 and 3 (Table 5),

tetramethylthiourea (TMTU) was employed as ligand (10 and 20 mol% respectively). These reactions also completed in 15 hours, which was the same reaction time as with no ligand present. The isolated yields of these reactions were slightly increased (60 and 55% respectively). For Entry 4 (Table 5), the use of 10 mol% 2-ethyl-2-oxazoline in the standard reaction was carried out. The reaction completed in 15 hours, giving in cycloadduct **140** in 53%. Increasing the 2-ethyl-2-oxazoline ligand to 20 mol% helped to increase the yield (86%) and speeded up the reaction to give completion in 3 hours (Entry 5, Table 5). in Entry 6 (Table 5), 10 mol% TMTU and 10 mol% 2-ethyl-2-oxazoline were both used as ligands and the reaction completed in 15 hours giving cycloadduct **140** in 68%. It can be concluded that the optimal reaction conditions were achieved in the presence of the 20 mol% oxazoline ligand and 10 mol% $CuCl_2$, which gave the shortest reaction time with the highest yield and the product **140** was obtained most readily in a clean state. It can also be concluded that thiourea has no major bebeficial effect upon this reaction, and generally, there were no side-products formed in the reactions either. These results represent a new methodology which results in fewer complications in product purification and presents no hazards due to the toxicity of the oxidant.[4,5]

After having established that the Cu-oxazoline catalyst system works well, chiral bis-oxazolines were tested with 1:1 copper/ligand ratio, i.e. the same as that found to be optimal for the ration of the copper:ligand ration in Table 5, Entry 5. It was found that this system, involving $CuCl_2$, in methanol with ligand **145** proceeded even faster (2 hours) that using two equivalents of the mono-oxazoline (Entry 7, Table 5). However, there was still no enantioelectivity according to chiral HPLC, even though an enantiomerically pure bis-oxazoline **145** was employed.

Determination of enantiomeric excess

The enantiomeric excess of cycloadduct **140** was determined by HPLC using a Chiralcel OD column using IPA/hexane, 1:9 v/v. However, there were no *ee*s found in any cases in either Table 4 or 5. With these results, it might be concluded that the dissociation of the nitroso compound from the metal oxidation catalyst (copper-oxazoline system) is fast and takes place before the hetero-DA reaction can occur.

2.5 Methodology testing with various dienes

2.5.1 Reactions in chloroform

Even though the use of 10 mol% $CuCl_2$ and 20 mol% 2-ethyl-2-oxazoline catalyst system did not give any enantioselectivity, it worked well in term of reaction rate and giving clean product with the model reaction of *N*-(benzyloxy-carbonyl)hydroxylamine **138** and 1,3-cyclohexadiene giving good yields. Therefore, the reaction of *N*-(benzyloxy-carbonyl)hydroxylamine **138** with various dienes was tested in chloroform. The results are shown in Table 6 and Eq. 8.

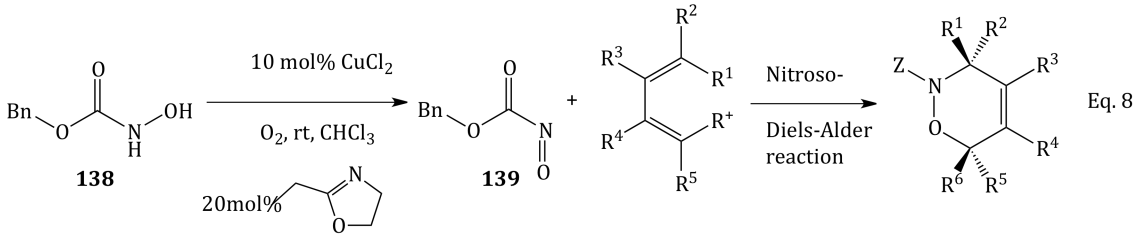

Eq. 8

Table 6. Reaction of *N*-(benzyloxy-carbonyl)hydroxylamine **138** with various dienes in chloroform using the copper-oxazoline catalyst and air system.

Entry	Diene	Product	Time	Yields %
1		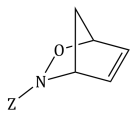 **146**	4 h	99
2		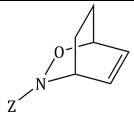 **140**	3 h	86
3		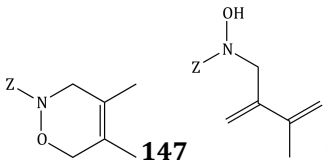 **147** **148**	24 h	86 (ratio of **147**: **148** = 7:1)
4	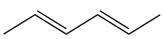	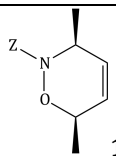 **149**	5 h	83
5		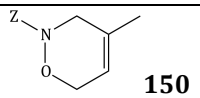 **150** 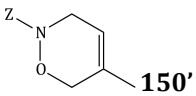 **150'** 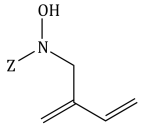 **151**	24 h	73 (ratio of **150** and **150'** : **151** = 9:1 and **150**:**150'** = 2:1)

6	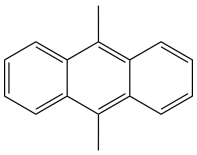	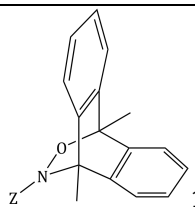 **152**	24 h	86
7	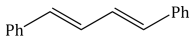	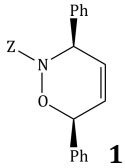 **153**	24 h	74
8		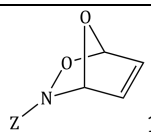 **154**	72 h	0
9		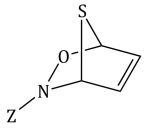 **155**	72 h	0
10	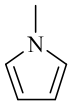	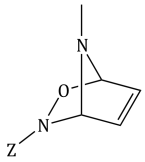 **156**	72 h	0

Entry 1 (Table 6) shows the reaction of the hydroxamic acid **138** with freshly cracked cyclopentadiene. The colour of the copper-ligand complex in chloroform was initially dark green, which changed to yellow upon adding the hydroxamic acid **138** and diene. The reaction was stirred at the room temperature and the completion time was 4 hours, which was confirmed by the disappearance of the starting material spot on the TLC and the colour of the reaction mixture also changing back to dark green. This confirmed again the self-indicating nature of the reaction. The reaction product was purified by flash silica gel chromatography to yield 99% of the cycloadduct product **146**. The structure of **146** was confirmed by ^{1}H and ^{13}C NMR (Figures 10 and 11).

Figure 10 shows the ^{1}H NMR spectrum of the cycloadduct **146**. The peaks at 1.71 and 1.98 ppm are the protons at the CH_2 group of the bicyclic system. The peaks in the region of 5.02- 5.21 ppm have integrals for 4 protons, two of which correspond to the protons of the CH group at the bridge and the rest are the protons of the CH_2 of the benzyl group. The peak at 6.35 ppm belongs to the two protons on the alkene.

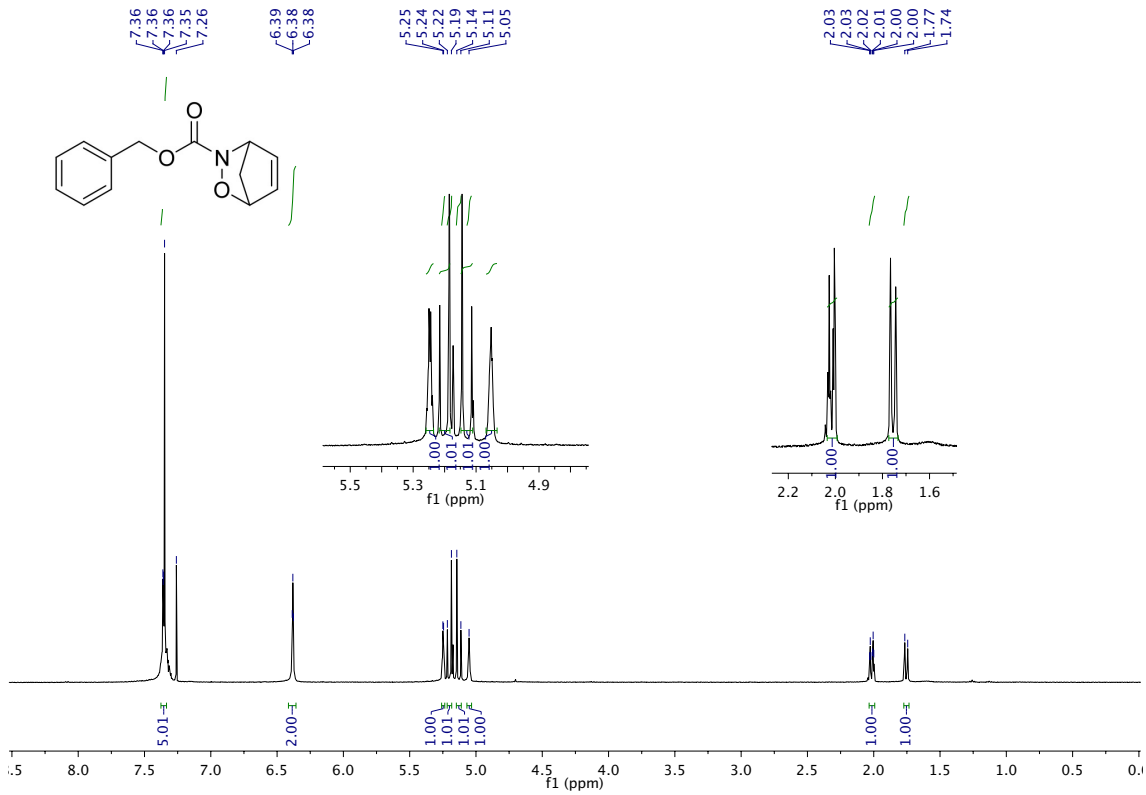

Figure 10. ^{1}H NMR of the cycloadduct **146.**

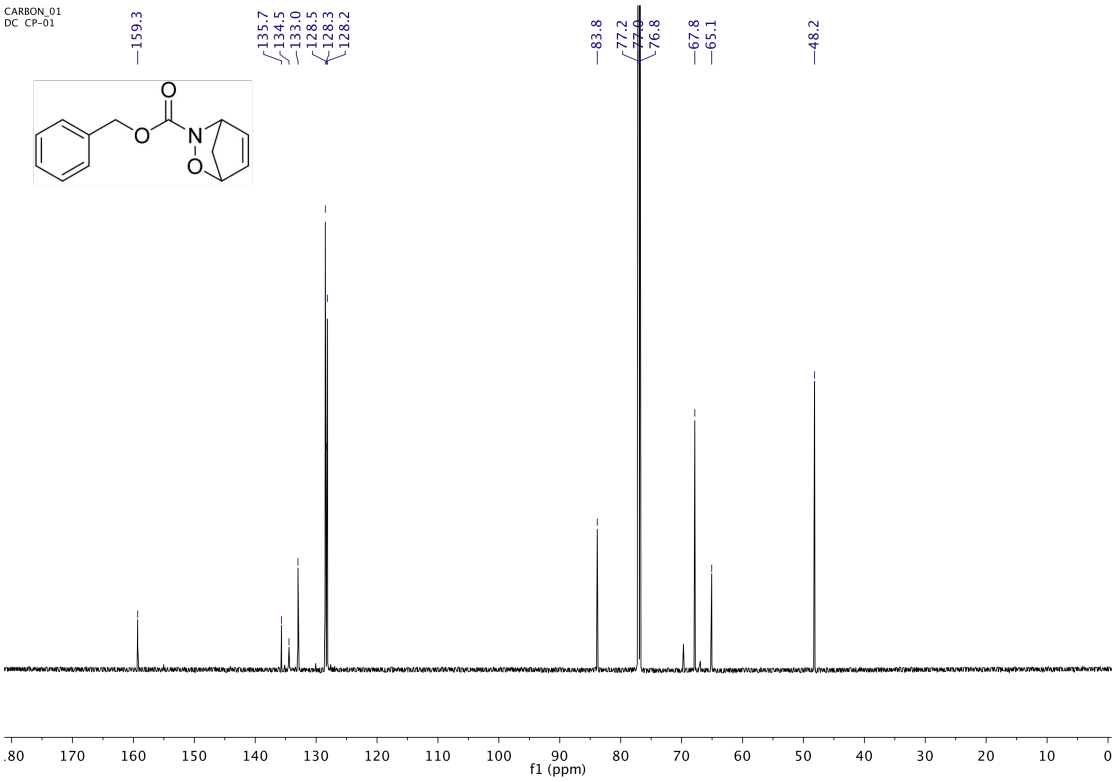

Figure 11. ^{13}C NMR of cycloadduct **146.**

Figure 11 shows the ^{13}C NMR spectrum of cycloadduct **146**. The peak at 48.2 ppm is the CH_2 group of the bicyclic system. The peak at 65.1 ppm corresponds to CH_2 of the benzyl group. Peaks 67.8 and 83.8 ppm correspond to the CH adjacent to N and

O respectively. Three peaks at 128.2, 128.3 and 128.5 ppm are the carbons in the ring and a peak at 133.0 ppm is the *ipso*-carbon. Two peaks at 134.5 and 135.7 ppm are alkene carbons. The peak at 159.3 ppm is the carbonyl carbon. All the analytical data match with the literature.[17c]

Entry 2 (Table 6) was the standard reaction discussed previously, *i.e*. using 1,3-cyclohexadiene as in Scheme 47, which was repeated for comparison. This result agreed with the previous result from Entry 5, Table 5. For the reaction of the hydroxamic acid **138** with 2,3-dimethyl-1,3-butadiene, however, there was a competing ene-reaction as well as the nitroso-Diels-Alder reaction (Entry 3, Table 6) resulting in a mixture of **147** and **148**. This occurred because 2,3-dimethyl-1,3-butadiene contains both alkene π-bonds and allylic σ-bonds, which can react with the nitroso-group to form the ene-product as in Scheme 48.

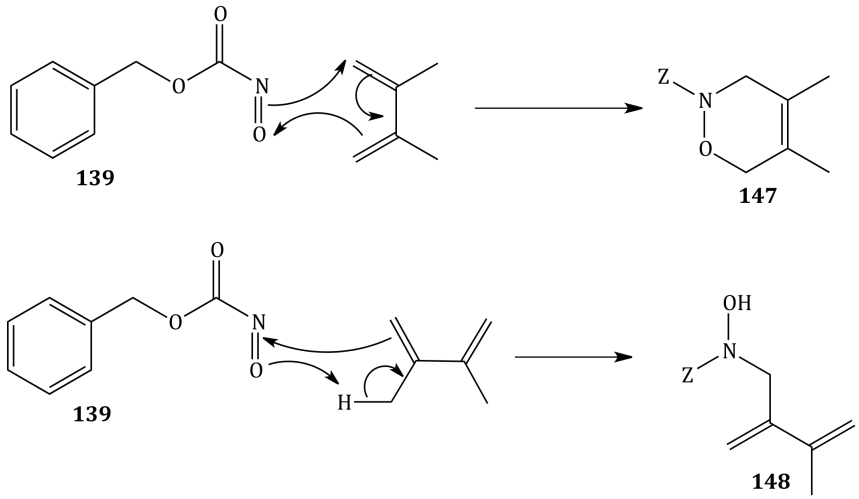

Scheme 48. The competing reactions of nitroso species **139** with 2,3-dimethyl-1,3-butadiene.

The reaction was completed in 24 hours with an overall yield of 86% after flash silica gel chromatography. The ratio of the cycloadduct **147** to ene-product **148** was 7:1 by the integration of the signals at δ 1.66 and 1.58 (CH_3 signals for **147)** *versus* the signal at δ 1.92 (CH_3 for **148**) (see Figure 12). After further purification by column chromatography, the ene-product could not be separated out in a pure enough state to do further analysis. The cycloadduct **147** was, however, isolated in 75% yield as a pure compound.

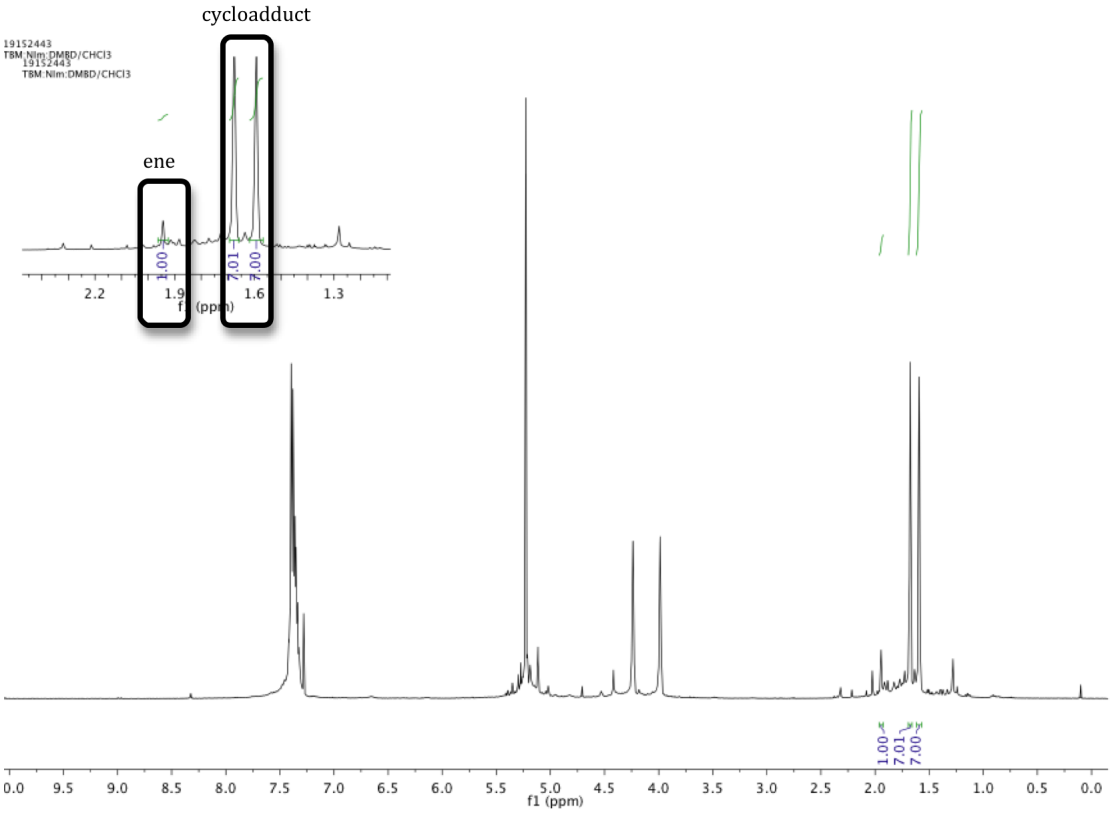

Figure 12. The crude ^{1}H NMR spectrum of the reaction of Z-hydroxamic acid **138** with 2,3-dimethyl-1,3-butadiene from Entry 3, Table 6 under oxidative conditions

The reaction of the Z-hydroxamic acid **138** with 2,4-hexadiene was also conducted (Entry 4, Table 6) and even though this diene has alkene π-bonds and allylic σ-bonds, no ene side-product was observed. The reaction was completed in 5 hours to give cycloadduct **149** with in a high isolated yield of 83%.

In contrast, Entry 5 (Table 6) shows the reaction of the Z-hydroxamic acid **138** with isoprene. The nitroso species **139** was generated as usual and then trapped by the isoprene (Scheme 49). The reaction was completed within 24 hours yielding regioisomeric cycloadducts **150** and **150'** and ene-product **151**. The ratio of cycloadducts to ene product was 9:1, and the ratio of cycloadduct **150** to **150'** was 2:1. The ratio of **150** to **150'** to **151** was determined from the crude product by ^{1}H NMR (Figure 13) using the signals at δ 4.10 to 4.02 (CH_2 resonances in **150** and **150'** respectively) to 4.70 (CH_2 in **151**). The overall yield was 81%, however, after column chromatography, only cycloadducts **150** and **150'** were separated out together in 73% isolated yield. The regioselectivity study reported by Leach and

Houk[39] stated that the direction of the selectivity depends upon the nature of the dienophile due to the weak directing effect of the 2-substituent of the diene.

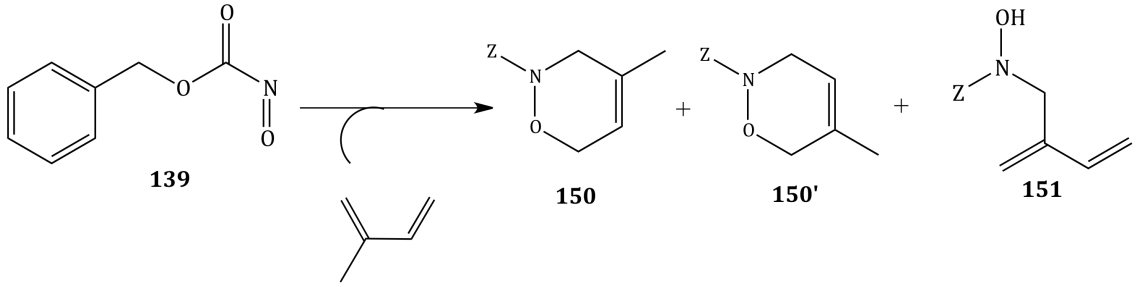

Scheme 49. The reaction of the nitroso species **139** with isoprene.

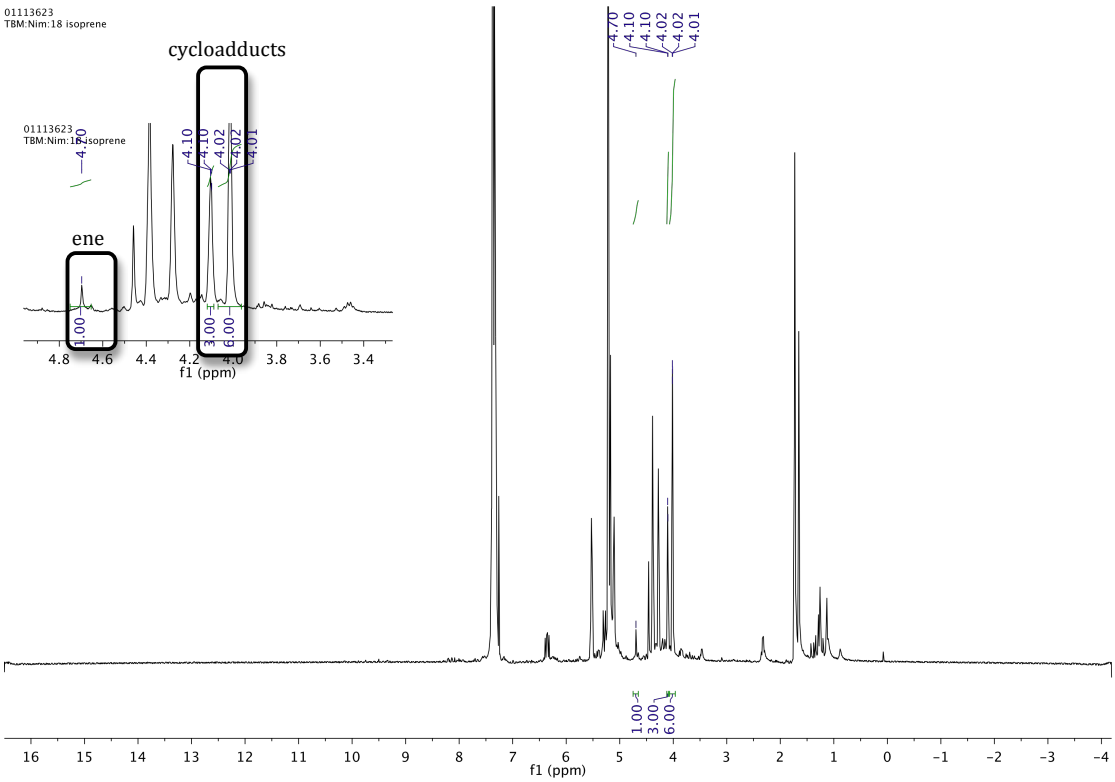

Figure 13. The crude ^{1}H NMR spectrum of the ene and cycloadducts product between Z-hydroxamic acid **138** with isoprene (Entry 5, Table 6).

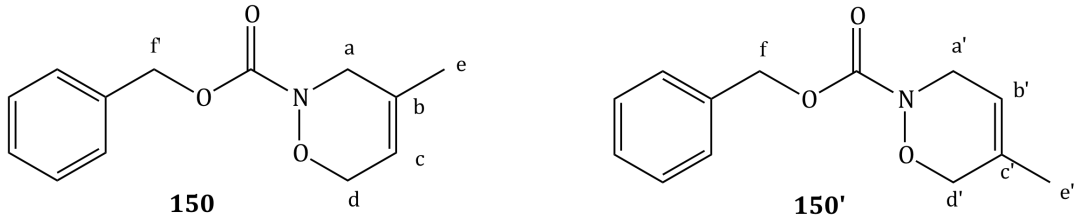

Figure 14. The two regioisomer cycloadducts from the reaction of **138** with isoprene under oxidative conditions.

The assignment of the peaks for the two regioisomers of **150** and **150'** (Figure 14) can be obtained from the ^{1}H NMR, and 2D NMR techniques of COSY, HSQC and HMBC NMR spectrum (see Figure 15).

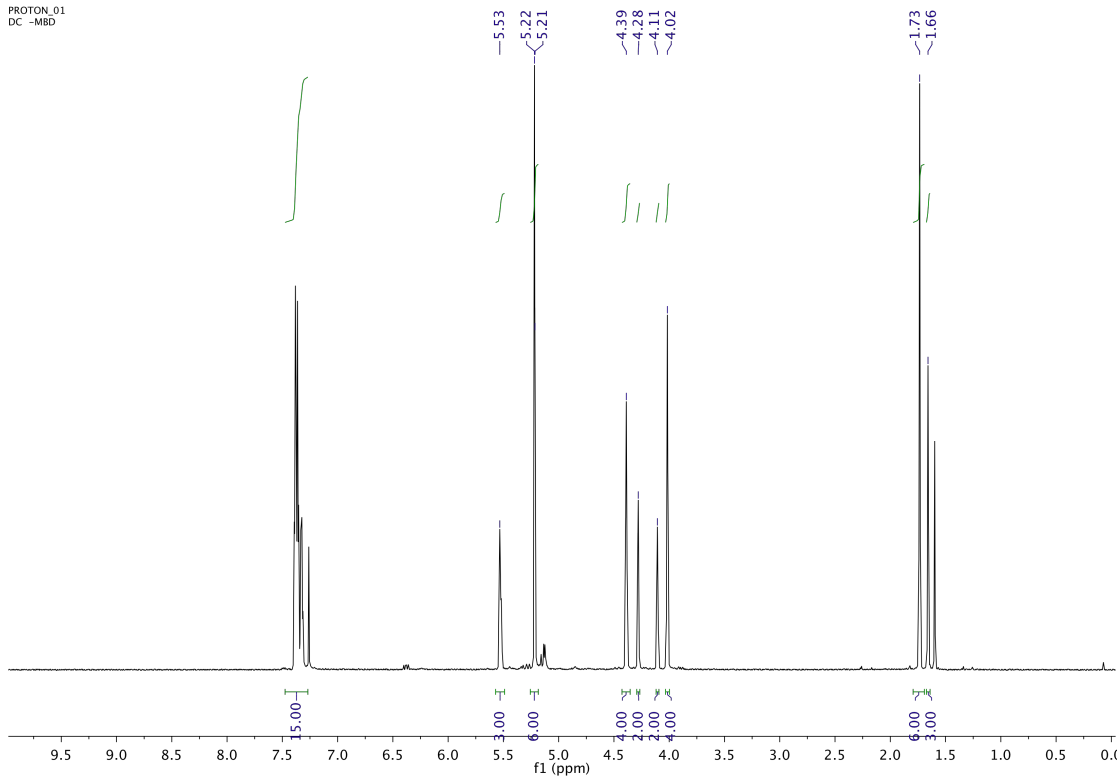

Figure 15. ^{1}H NMR of **150** and **150'** after purification by silica gel chromatography.

From the ^{1}H NMR of **150** and **150'** shown in Figure 15, there are two sets of peaks in the non-aromatic region (*i.e.* at 166 and 1.73 ppm) which can be assigned to the CH_3 groups of He and He'. The four peaks in the 4.50-4.00 ppm region can be assigned to the CH_2 proton signals of Ha, Ha', Hd and Hd' and the peak at 5.22 ppm

can be assigned to the CH_2 of the benzyl group (Hf and Hf'). The ene protons of c and b' appeared at 5.53 ppm (see Figure 15). However, this information was not sufficient to distinguish the two regioisomers **150** and **150'**, therefore, 2D NMR spectra were required for a more detailed analysis.

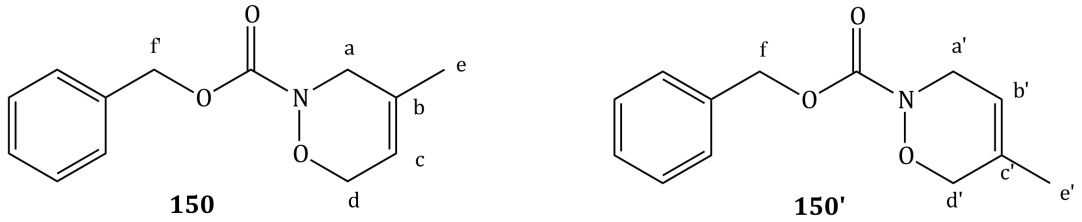

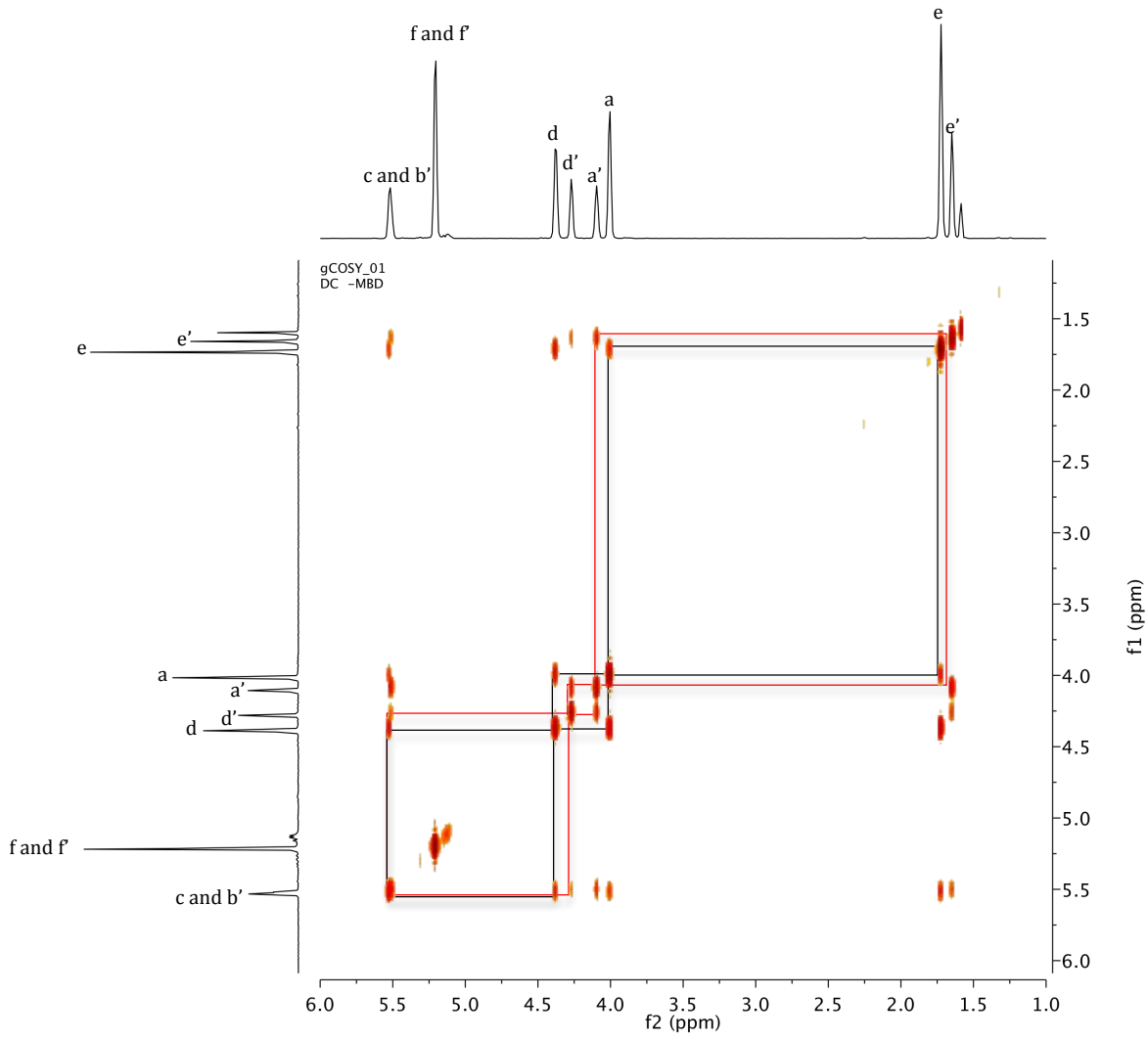

Figure 16. COSY NMR of the mixture of regioisomers **150** and **150'**.

The COSY NMR for the mixture of **150** and **150'** is shown in Figure 16 which confirmed the correlation of the protons and also allowed the classification of the two sets of protons. From the fact that the proton next to oxygen will shift to lower

field than the one next to nitrogen, therefore, the CH_2 protons next to oxygen was assigned at 4.39 ppm (major) and 4.28 ppm (minor), and the CH_2 proton next to nitrogen at 4.02 ppm (major) and 4.11 ppm (minor). The major regioisomer has the non-aromatic peaks at 1.73 (He), 4.02 (Ha), 4.39 (Hd), 5.22 (Hf) and 5.53 (Hc) ppm. The minor regioisomer has 1.66 (He'), 4.11 (Ha'), 4.28 (Hd'), 5.21 (Hf') and 5.53 (Hb') ppm. The peaks at 5.21 and 5.22 ppm do not correlate with any of protons in the non-aromatic region, which could be confirmed to be the Hf and Hf' protons.

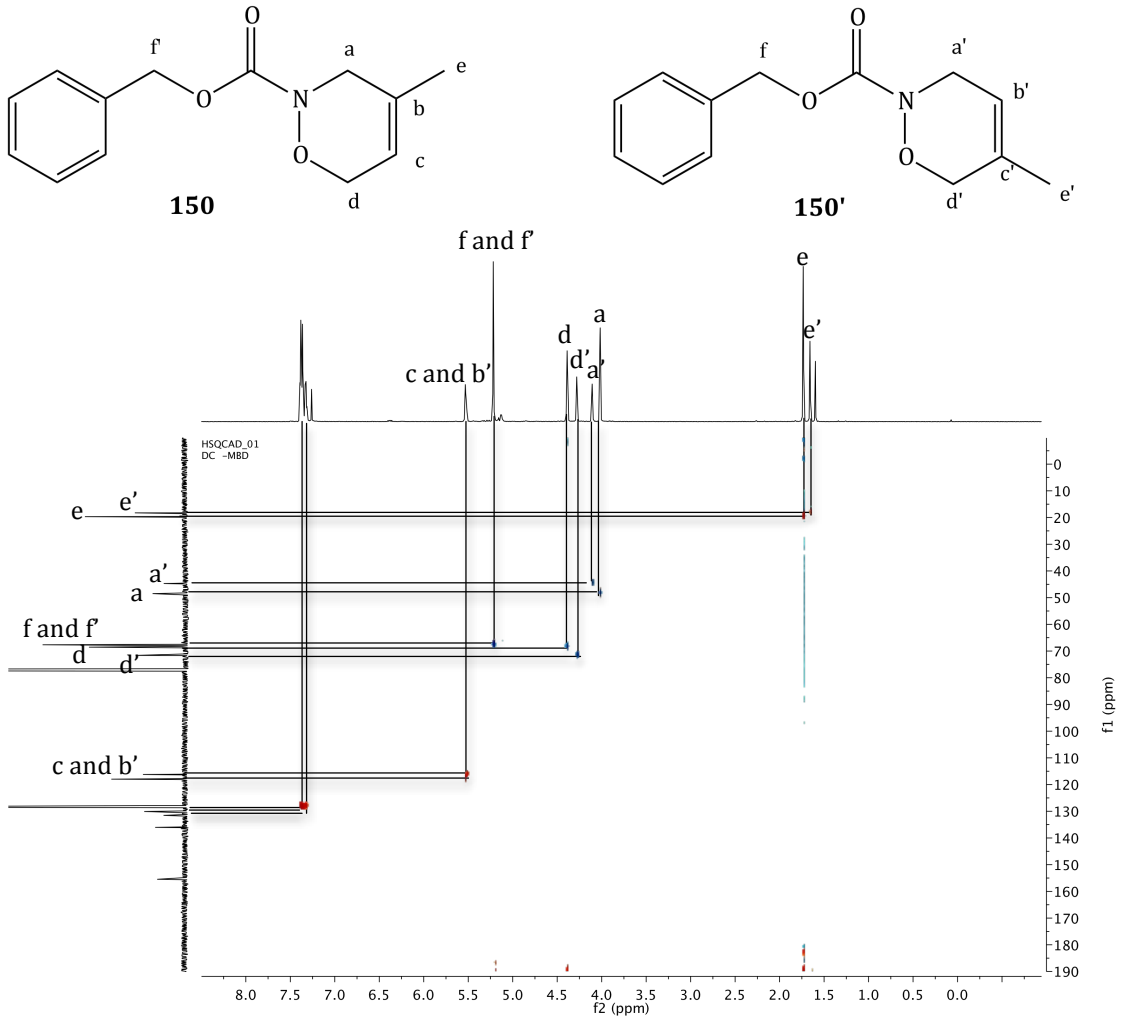

Figure 17. HSQC NMR of **150** and **150'**.

From all the information from the ^{1}H NMR and ^{13}C NMR spectra, all the signals could be assigned using the HSQC NMR spectra (Figure 17). The signals due to the protons attached to different carbons were considered, which allowed the differentiation of the carbon peaks of each regioisomer. The major regioisomer has

peaks at 19.7 (Ce), 48.5 (Ca), 67.7 (Cf), 68.5 (Cd) and 118.0 (Cb and Cc) ppm. The minor regioisomer has peaks at 18.2 (Ce'), 44.8 (Ca'), 67.7 (Cf'), 71.6 (Cd') and 116.3 (Cb' and Cc') ppm. Even though all the peaks can be assigned, which regioisomer is the major product was still unsolved, therefore, the HMBC NMR was employed (Figure 18).

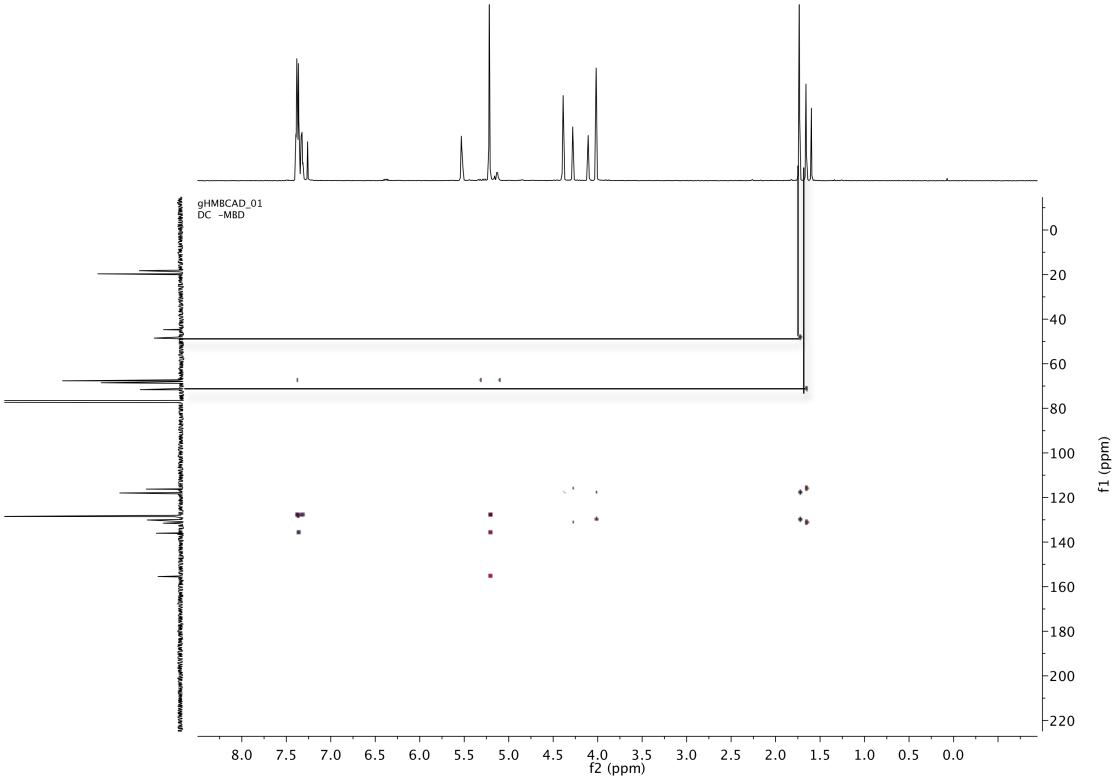

Figure 18. HMBC NMR of **150** and **150'**.

The long-range correlation spectrum shown in Figure 18 shows that the major peak due to the CH_3 protons (He) correlated to the carbon peak at 48.5 ppm, which corresponds to the CH_2 carbon next to nitrogen in the ring. The minor CH_3 peak correlated to the carbon peak at 71.6 ppm, which is the peak of CH_2 carbon next to oxygen. From these sources of information, the two regioisomers were assigned. The major regioisomer was **150** and the minor regioisomer was **150'**.

The reaction of *in situ* generated nitroso species **139** with 9,10-dimethylantracene under the Cu-oxazoline catalytic conditions was then tested

(Entry 6, Table 6). The reaction completed in 24 hours and it was noteworthy because this reaction was fluorescent under UV light at the beginning. However, when the reaction completed, the fluorescence disappeared due to the reduced conjugation in the cycloadduct **152**. Upon completion and work up, the product was isolated in an impressive yield of 86%. The cycloadduct **152** was pure and crystallized upon isolation to give crystals suitable for single crystal X-ray diffraction analysis. The X-ray structure confirmed the connectivity and is as shown in Figure 19.

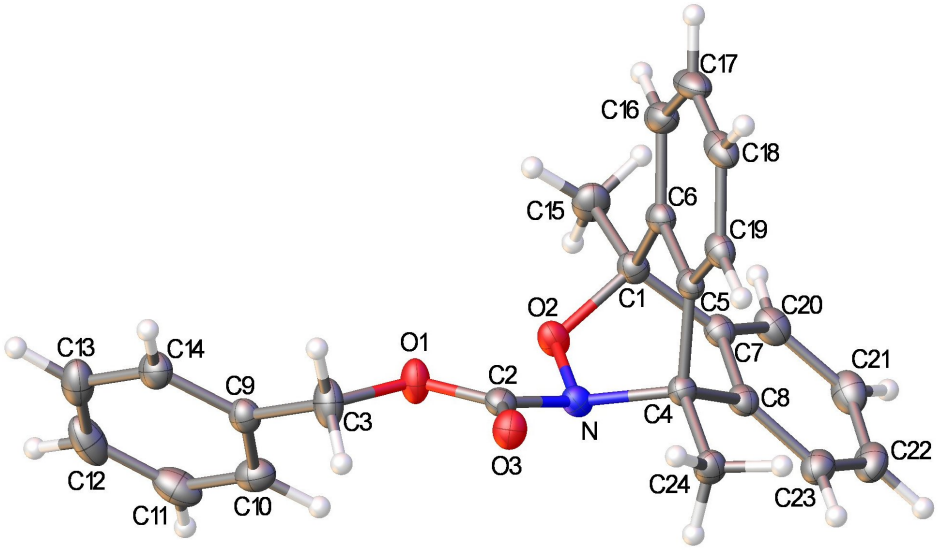

Figure 19. Crystal structure of cycloadduct **152**.

The reaction of the Z-hydroxamic acid **138** with 2,3-diphenyl-1,3-butadiene was conducted with this oxidative catalytic system (Entry 7, Table 6). In this system, the diene was not volatile and was therefore difficult to separate from the cycloadduct product. In order to circumvent this problem, an excess of the hydroxamic acid **138** (1.2 equivalents) was employed. The reaction was then completed in 24 hours, yielding cycloadduct **153** as a colourless viscous oil in 74% isolated yield after purification.

Furan, thiophene and *N*-methylpyrrole were also used as dienes in this copper-based oxidation system, as shown in Entries 8-10, Table 6. However, there was no desired cycloadduct product observed even after 72 hours, even when all the hydroxamic acid **138** spot disappeared according to TLC and the reaction mixture changed to a black colour. This suggested that decomposition of the

nitroso species was occurring rather than reaction with the dienes. The rate of reaction of the nitroso species (after it was generated by the copper catalyst) must be lower than the rate of decomposition (Scheme 50) or that the cycloaddition occurs but this could be reversible. Hence, the reason for these unsuccessful systems is still unclear, it could be explained by the gap between the HOMO and LUMO of the diene and dienophile, which may be too large for efficient formation of the required Diels-Alder transition state allowing decomposition of the acyl nitroso species, or the reaction is indeed too reversible and eventually dienophile decomposition consumes the nitroso species.

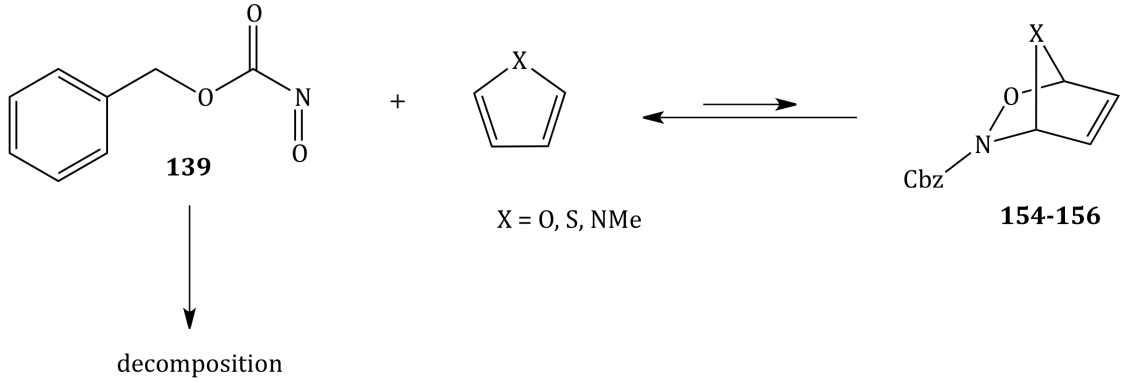

Scheme 50. Reaction pathway of nitroso compound **139** with furan, thiophene and *N*-methylpyrrole.

2.5.2 Reaction in methanol

In order to examine the effect of solvent polarity and H-bonding upon the reaction, we decided to compare the reactions carried out in methanol with those run in chloroform. Because the use of chloroform as a solvent is less desirable, being environmentally unfriendly, methanol was used as the solvent in a repeat of the earlier experiments. The results are shown in Table 7 and Eq. 9.

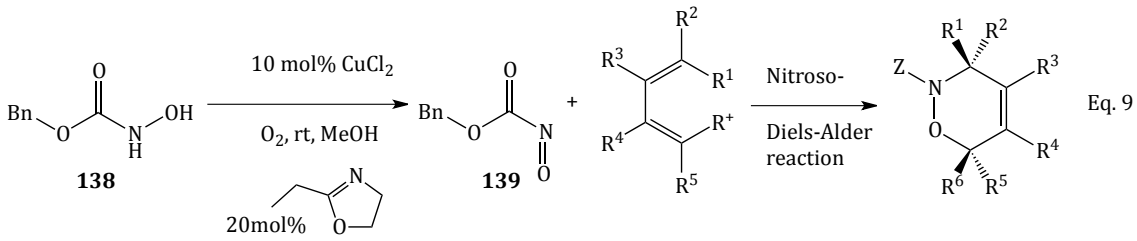

Eq. 9

Table 7. Reaction of Z-hydroxamic acid **138** with various dienes in methanol using oxidative copper-oxazoline catalyst. .

Entry	Diene	Product	Time	Yields %
1		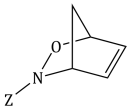 **146**	3 h	97
2		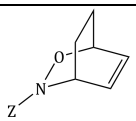 **140**	3 h	92
3		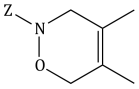 **147** 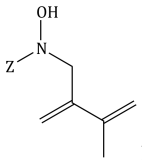 **148**	2 h	83 (ratio of **147**: **148** = 5:1)
4	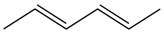	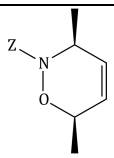 **149**	2 h	97
5		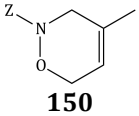 **150** 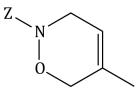 **150'** 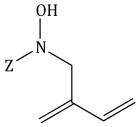 **151**	8 h	79 (ratio of **150** and **150'** : **151** = 8.5:1 and **150**:**150'** = 2:1)
6	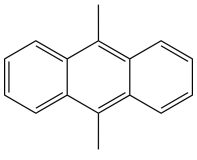	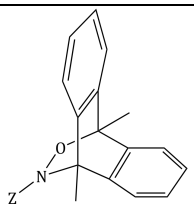 **152**	10 h	88

7	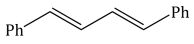	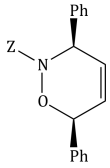 **153**	18 h	79
8		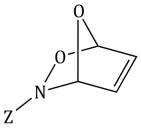 **154**	72 h	0
9		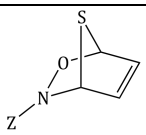 **155**	72 h	0
10	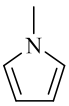	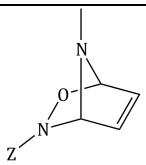 **156**	72 h	0

The result of the reaction of Z-hydroxamic acid **138** with freshly cracked cyclopentadiene is shown in Entry 1, Table 7. The reaction time in methanol was one hour shorter than in chloroform and the isolated yield of **146** was slightly lower (only 2% less) but was still high (97%). Entry 2 (Table 7) shows the reaction of the Z-hydroxamic acid **138** with 1,3-cyclohexadiene. The reaction time was the same as the reaction in chloroform but the isolated yield of **140** was improved by 6% (from 86% to 92%) and there was a major improvement in the reaction time of Z-hydroxamic acid **138** with 2,3-dimethyl-1,3-butadiene, as shown in Entry 3, Table 7, from 24 hours in chloroform to 2 hours in methanol. However, the ratio between the cycloaduct **147** and the ene-product **148** was lower at 5:1 (compared to 7:1 in chloroform). The reason for this lower ratio is still unclear, however, it may due to the rate of the nitroso generation in this system; the faster the generation rate, the better the ene can compete with the NDA. However, the ene product could not be separated using silica gel column chromatography, only the cycloadduct was obtained in 83% isolated yield as a pure product. The reaction between Z-hydroxamic acid **138** and 2,4-hexadiene (Entry 4, Table 7) showed an improvement in the isolated yield of **149** compared to the reaction in chloroform (from 83% to 97%) and the reaction time was also reduced from five to two hours.

The reaction of Z-hydroxamic acid **138** and isoprene to yield cycloadducts **150**, **150'** and eneproduct **151** is shown in Entry 5, Table 7. The reaction time was three times shorter than the reaction in chloroform and the yield was slightly higher (6%). The ratio between the cycloadducts and ene-product was slightly lower (9:1 in chloroform *versus* 8.5:1 in methanol) but the ratio between the cycloadducts **150** and **150'** stayed the same (*i.e* 2:1 respectively). This suggested that the solvent and/or the rate of the nitroso generation does not have any major effect on the regioselectivity for this system. The reaction in methanol of Z-hydroxamic acid and 9,10-dimethylantracene (Entry 6, Table 7) to give **152** was also improved, in terms of the reaction time from 24 to 10 hours and isolated yield from 86% to 88%. Entry 7, Table 7 shows that the cycloadduct **153** was isolated in 79% with the reaction time of 18 hours from the reaction of Z-hydroxamic acid **138** with 1,4-diphenylbutadiene. The reactions of Z-hydroxamic acid with furan, thiophene and *N*-methylpyrrole were also conducted, however, none of the desired cycloadducts were observed in any cases. These observations reactions are similar to the reactions in chloroform and confirm either the lack of reactivity of the nitroso species with these dienes, or that the addition is indeed reversible.

Overall, the reaction of Z-hydroxamic acid **138** with various dienes in methanol can proceed faster than in chloroform and with higher isolated yields. This may be explained by the improved solubility of the Z-hydroxamic acid **138** and $CuCl_2$ in methanol, which is better than in chloroform, therefore, there is faster nitroso generation which is readily trapped by the dienes before it can either dimerize, decompose or react with the solvent. From Entry 3, Table 6 and Entry 3, Table 7, it can be seen that by changing the reaction solvent, the ratio between the cycloadduct and ene-product changed. Hence, a set of solvent screening experiments for the reaction between Z-hydroxamic acid **138** and 2,3 dimethyl-1,3-butadiene using copper-oxazoline catalytic system was conducted and the results are shown in Table 8.

2.6 Solvent effects on the rate of NDA *versus* ene-reaction

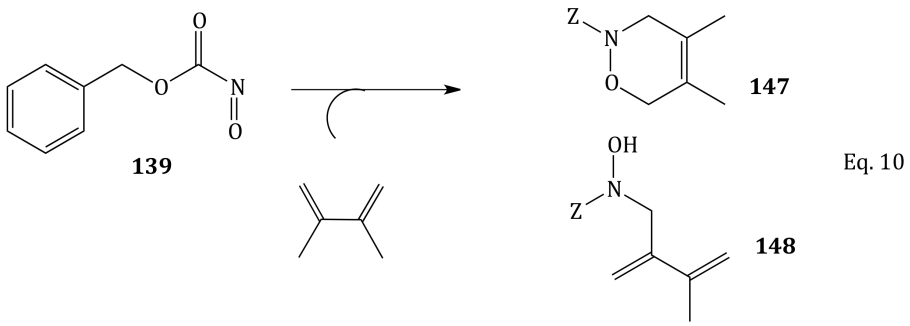

Eq. 10

Table 8. The solvent screening of the reaction of Z-hydroxamic acid **138** and 2,3 dimethyl-1,3-butadiene.

Entry	Solvent	Time (h)	Ratio **147**:**148**	Yield %
1	MeOH	2	5:1	84
2	MTBE	20	15:1	85
3	MeCN	144	25:1	80
4	EtOH	7	4:1	83
5	EtOAc	7	4:1	81
6	IPA	48	13:1	89
7	MTHF	20	12:1	88
8	Toluene	4	12:1	82
9	4:1 Toluene/MeOH	3	5:1	82
10	Chloroform	3	7:1	82

Table 8 shows the results of the solvent screening which focused on the ratio between the cycloadduct **147** and ene-product **148**. Entry 1 (Table 8) shows the reaction in methanol, which has the highest polarity among all the solvents used in this table. The reaction completed in 2 hours, giving 84% overall yield and was the fastest reaction, giving a 5:1 ratio of **147**:**148**, which matched Entry 3 (Table 7). MTBE, which is a good solvent for microwave reactions, was tested in Entry 2

(Table 8). This reaction completed in 20 hours and gave a **147**:**148** ratio of 15:1, in 85% overall yield. Acetonitrile, which is known to form complexes with copper was also tested,[82] resulted in the the slowest reaction (144 hours). However, it also gave the best ratio of **147**:**148**, *i.e.* of 25:1. This long reaction time and yet high chemoselectivity may be explained by the fact that acetonitile can chelate with the copper to form complexes and this complexation may compete with the 2-ethyl-2-oxazoline ligand, which is the active catalyst species. Therefore, the rate of acylnitroso generation may become slow. The rate of NDA reaction is probably higher than the rate of the ene-reaction and hence, with a low concentration of the acylnitroso compound, it can be more efficiently trapped by the diene, and only a small amount undergoes ene-reaction. Both ethanol and ethyl acetate gave very similar results, even though ethanol is more polar that ethyl acetate (Entry 4 and 5, Table 8). These two reactions completed in 7 hours, giving a 4:1 ratio of **147**:**148**. In the high polarity solvent isopropanol (Entry 6, Table 8), the reaction rate was surprisingly low (48 hours for complete reaction) but the ratio of the two products (NDA to ene) was good (13:1) giving 89% overall yield. 2-Methyltetrahydrofuran was also tested in Entry 7 (Table 8) being a widely used green solvent. The reaction time was 20 hours with the chemoselectivity ratio of 12:1 and giving an 88% overall yield. Even though the solubility of the hydroxamic acid **138** in toluene was not good, the reaction was complete in 4 hours with an 82% overall yield and 12:1 ratio of **147**:**148** (Entry 8, Table 8). Due to the solubility issues of the hydroxamic acid **138** in toluene, the mixed solvent of toluene:methanol (4:1) was employed in the Entry 9 (Table 8). The reaction was faster than pure toluene, however, the ratio between **147**:**148** decreased from 12:1 to 5:1, which is the same ratio as that carried out in pure methanol. The reaction in chloroform was also tested and the result matched the earlier experiment (see Entry 3, Table 6).

From Table 8 it can be concluded that the reaction of Z-hydroxamic acid **138** with 2,3-dimethyl-1,3-butadiene in various solvents gave overall yields from 80-89% with different ratios of cycloadduct to ene-product. The solvent that gave the highest ratio of the NDA adduct was acetonitrile, whereas MTBE, IPA, toluene and MTHF gave good chemoselectivities. Chloroform, methanol, toluene:methanol (4:1), ethanol and ethyl acetate gave lower selectivity. In general, the longer the reaction time, the better the chemoselectivity in term of NDA *versus* ene-reaction.

2.7 Effect of chiral ligand on the NDA reaction

Success in the use of copper with the achiral oxazoline ligand system in the oxidation of the Z-hydroxamic acid **138** to give the acylnitroso species **139**, which was trapped by the various dienes was now established, hence, the use of chiral ligands in this reaction was conducted. The results are shown in the Table 9 and Eq. 11.

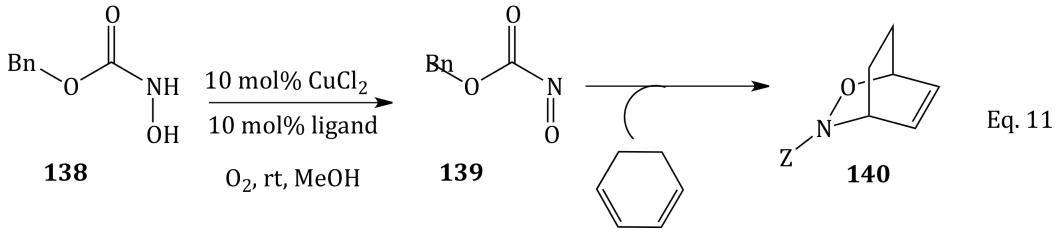

138 **139** **140** Eq. 11

Table 9. Reaction of hydroxamic acid **138** with 1,3-cyclohexadiene using chiral ligands.

Entry	Ligand	Time (h)	Yield %	*ee*
1	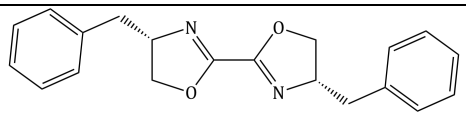 **157**	2	98	0
2	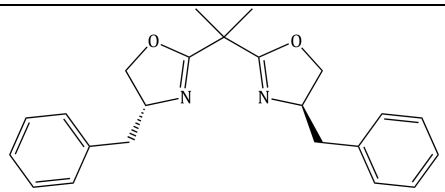 **145**	2	99	0
3	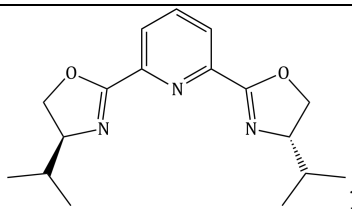 **158**	2	96	0

The use of 10 mol% chiral bisoxazoline ligand **157** with 10 mol% $CuCl_2$ in the model reaction of Z-hydroxamic acid **138** and 1,3-cyclohexadiene was conducted. The result is shown in Entry 1 (Table 9). The reaction was stirred at room temperature, the colour of the pre-mixed copper-ligand complex was green and turned pale yellow upon adding the Z-hydroxamic acid **138**. This indicated a

change in oxidation state of the copper. The reaction completed in 2 hours and after purification, the isolated yield was high (98%). However, there was no *ee* observed as determined by HPLC using a Chiralcel OD column using IPA/hexane, 1:9 v/v. Entry 2 (Table 9) shows the model reaction with 10 mol% chiral bisoxazoline ligand **145** with 10 mol% $CuCl_2$. The reaction completed in 2 hours again, giving 99% isolated yield. and again, there was no *ee* observed in this case. The use of 10 mol% pybox ligand **158** with 10 mol% $CuCl_2$ in the same reaction was also tested. The result shown in Entry 3 (Table 9) shows that the reaction completed in 2 hours and the cycloadduct **140** was isolated in 96% though with no *ee* after chiral HPLC.

From these results, even when pure chiral ligands were used in the model reaction, there was no *ee* observed which suggests that dissociation of the nitroso dienophile from copper after it is generated is fast and it does not stay bound to the copper so that it can be trapped by the diene.

2.8 Hydroxamic acid synthesis

After establishing that the copper-oxazoline catalyzed oxidation NDA reaction worked well, but did not give any enantioselectivity, we can speculate that this is due to the rapid dissociation of the nitroso dienophile from the metal. Therefore, the hypothesis of having a nitroso species that can chelate to copper after the oxidation may help to increase the enantioselectivity. Hence, we decided to examine different hydroxamic acids, which after the oxidation, might chelate to copper, as shown by species such as **159** or **160** (Figure 20) and hence, might provide a method by which we could control the enantioselectivity. We therefore examined the synthesis of the hydroxamic acids shown in Figure 21.

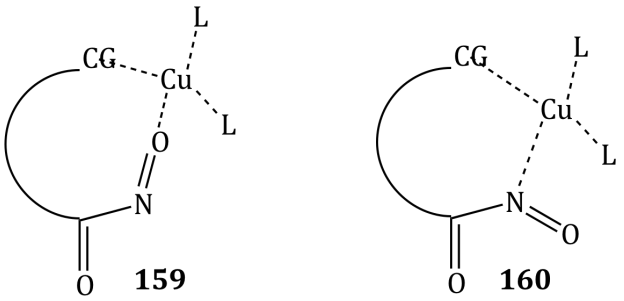

CG =chelating group

Figure 20. Proposed chelation model structures of hydroxamic acids that might chelate to copper.

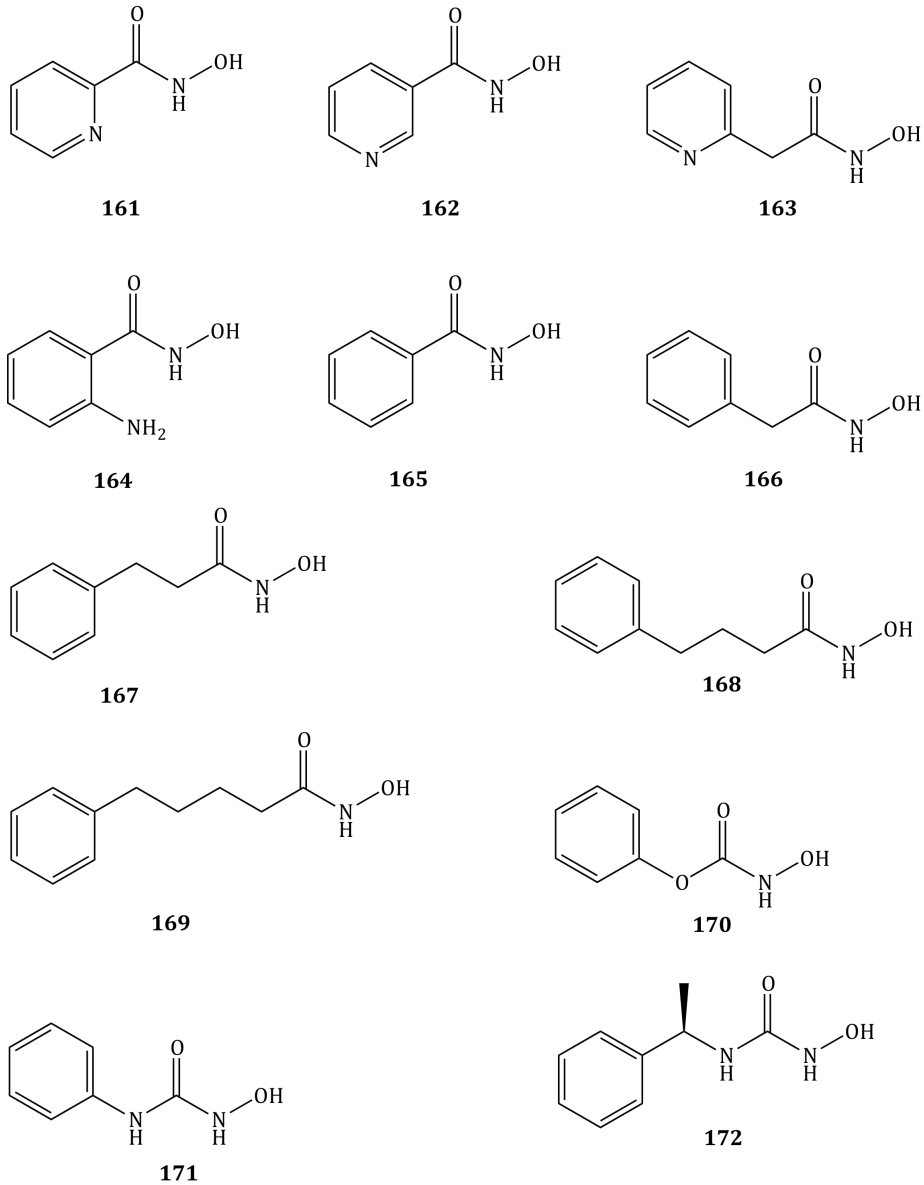

Figure 21. Examples of possible hydroxamic acids for use in acylnitroso generation.

The hydroxamic acids shown in Figure 21 were synthesized according to the literature.[66-73] There are three different methods that have been used for the hydroxamic acid syntheses, depending upon the availability of the starting materials. The simplest synthesis method is the reaction of an ester or acid chloride with hydroxylamine hydrochloride and sodium hydroxide (Scheme 51). The reaction was stirred for 4 hours and completion of the reaction was confirmed by TLC. The mixture was then acidified and most of the hydroxamic acid usually precipitated out directly from the reaction, giving the hydroxamic acids **161**-**167** and **170**.

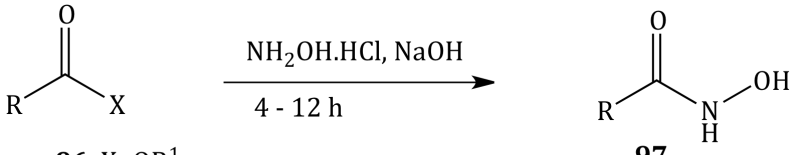

96, X=OR[1]
98, X=Cl

97

Scheme 51. Hydroxamic acid synthesis from simple aliphatic ester.

Compound **161**, which is a 2-pyridinehydroxamic acid and contains the pyridine ring as a chelating group for copper, which, we surmised that it may help in the chiral selectivity as it could form either 5- or 6-membered ring chelates by acting as a bidentate ligand. Compound **162** is an isomer of **161**, with the carbonyl group on the 3-position and this compound could only chelate as a monodentate ligand. Structure **163** was synthesized with a CH_2 group attached to the 2-position and next to the carbonyl group. The aim of this compound was to prove the chelation position on the nitroso group, based on the hypothesis that if it chelated on N, chiral selectivity should be observed. On the other hand, if there was no enantiomeric excess, the chelation would likely be on O or no chelation on the nitroso group occurs at all. Compound **164** has the NH_2 on the phenyl ring in the 2-position, next to the carbonyl hydroxamic acid group. This NH_2 could chelate to copper to help to lock the nitroso species in place, which could then be trapped by the diene. The phenyl carbonyl hydroxamic acid species were also synthesized with a C_nH_{2n} chain, where n = 0-4 away from the ring (**165** – **169**).

Compound **168** did not have an ester derivative commercially available as a starting material, only the 4-phenylbutyric acid compound was available.

Therefore, an alternative procedure needed to be used. There are two synthetic pathways reported that could be used to synthesize **168**: One is converting the acid to the corresponding ester and then following the procedure in Scheme 51; and the other employs a one pot synthesis using the acid as a starting material using DMAP as catalyst with NMM, cyanuric chloride and hydroxylamine hydrochloride. When this was carried out, the reaction completed in 24 hours (Scheme 52), however, the yield was low (25%) and it was difficult to separate the desired product from the other impurities. Moreover, the cyanuric acid was difficult to work with because the vapour is irritating.

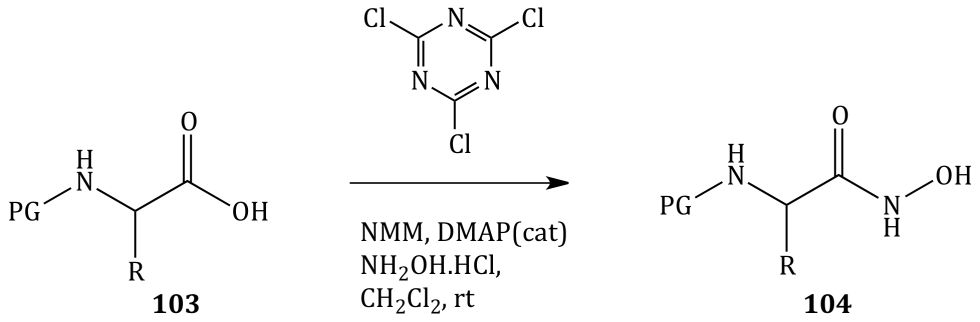

103 **104**

Scheme 52. Hydroxamic acid **104** synthesis using an acid as starting material.

Compound **169** was synthesized by the first pathway using the procedure shown in Scheme 53. The reaction involved the esterification of 5-phenylvaleric acid with methanol using hydrogen chloride gas generated by dropping 36% HCl into 98% H_2SO_4. The reaction was completed in 15 minutes,and the ester was used without any further purification. Sodium hydroxide and hydroxylamine hydrochloride solution were then added dropwise in the same fashion as the Scheme 51, which provided **169** in 67% isolated yield.

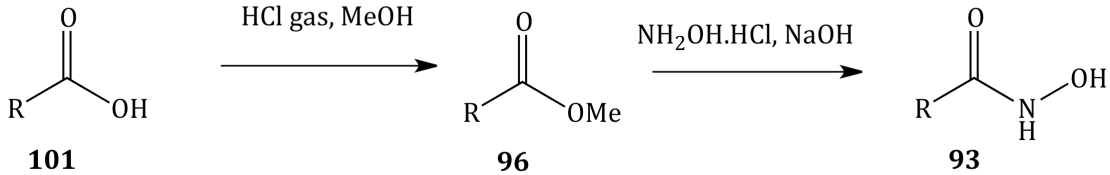

101 **96** **93**

Scheme 53. Hydroxamic acid synthesis via estrification followed by hydroxylamination.

The phenyl hydroxycarbamate **170**, which has an O next to the phenyl ring, was employed in order to study the effect of the heteroatom next to the carbonyl hydroxamic acid group in the copper-oxazoline oxidation system. This compound **170** was synthesized by reacting phenyl chloroformate with sodium hydroxide and hydroxylamine hydrochloride. The reaction completed in 4 hours, giving 59 % isolated yield hydroxamic acid **170.** The 1-hydroxy-3-phenylurea **171** and (*S*)-1-hydroxy-3-(1-phenylethyl)urea **172**, both of which contain nitrogen heteroatom next to the hydroxamic acid group, were synthesized from the isocyanate with sodium hydroxide and hydroxylamine hydrochloride (Scheme 54). The reactions both completed in 3 hours to give 52% and 49% of **171** and **172** respectively. Compound **171** was recrystalized from diethyl ether to give a crystal suitable for single crystal X-ray analysis. The X-ray crystal structure is shown in Figure 22.

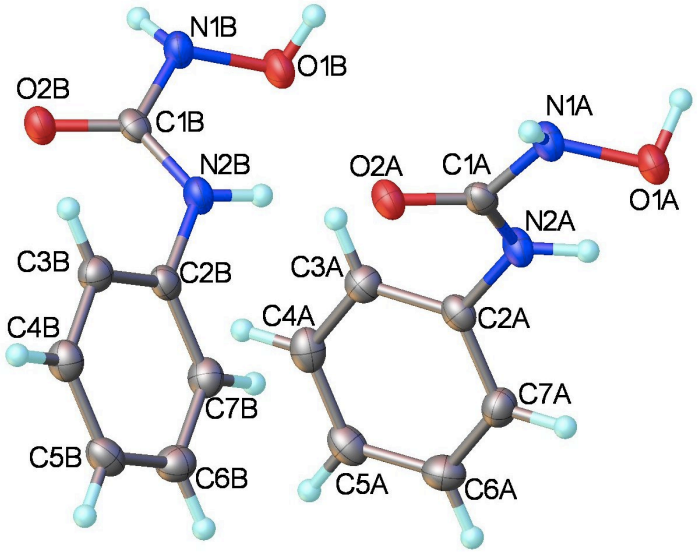

Figure 22. X-ray crystal structure of hydroxamic acid **171**.

Compound **172** is a chiral compound, which was synthesized based on the hypothesis that if the chiral hydroxamic acid was used as a starting material, with a chiral ligand system, it would be interesting to see if was capable of controlling the absolute stereochemistry of the NDA product, and it would be possible to probe both the use of a chiral dienophile, together with a chiral catalyst to investigate whether there was any interaction between the two (see below).

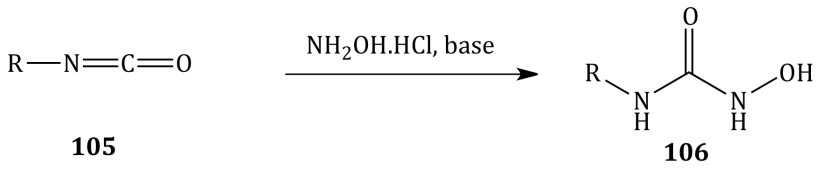

Scheme 54. Hydroxy urea synthesis from an isocyanate.

Compound **172** was synthesized by the same method as in Scheme 54, however, in this reaction there was a side-product **172s** (Figure 21) formed by the reaction of the hydroxamic acid **172** with excess isocyanate (see Scheme 55).[74] Compound **172** was recrystalized from diethyl ether to give a crystals suitable for single crystal X-ray analysis. The X-ray crystal structure is shown in Figure 23.

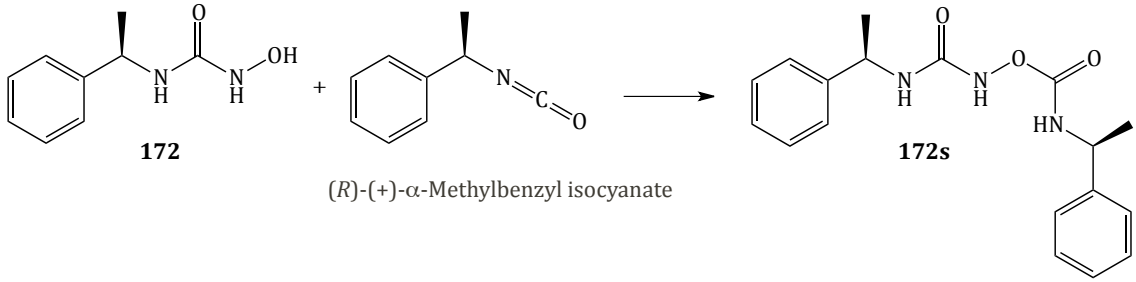

Scheme 55. The reaction of hydroxamic acid **172** with the iscyanate forming compound **172s**.

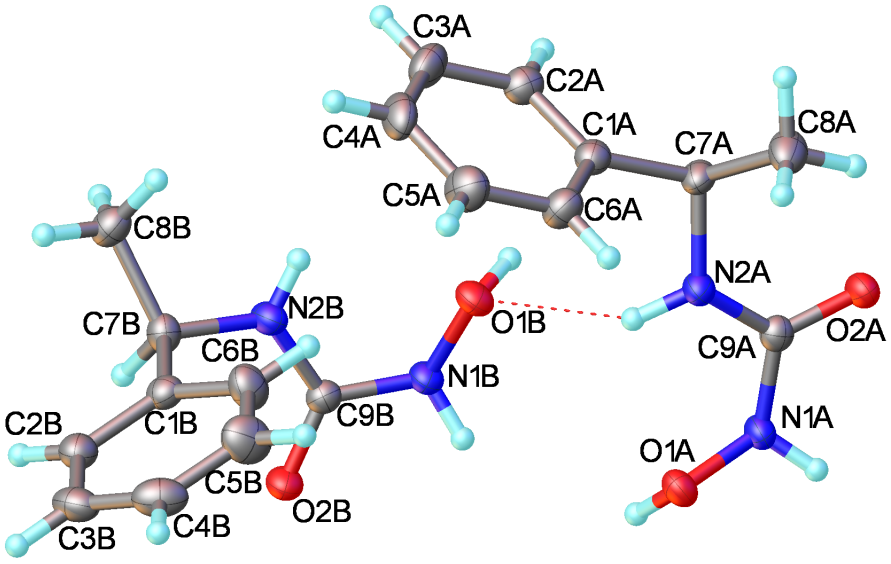

Figure 23. X-ray crystal structure of hydroxamic acid **172**.

Figure 23 shows the X-ray crystal structure of hydroxamic acid **172**, which shows hydrogen bonding between the OH and NH of the urea groups. It also shows the two conformations that these type of system can adopt, one with the C=O *s-trans* to the CH_3 group and the other with the C=O *s-cis* to the CH_3 group. Interestingly, it is between these two conformations that the hydrogen bonding occurs, suggesting that the energy difference between these is relatively minimal and that facile interconversion occurs during crystalization.

2.9 NDA reaction of hydroxamic acids with 1,3-cyclohexadiene using $NaIO_4$ as oxidant

Having prepared all the hydroxamic acids **161** – **172**, they were tested for their ability to undergo the NDA reaction, and initially this was carried out by using $NaIO_4$ as the oxidant. Trapping was carried out with 1,3-cychohexadiene and the results are shown in Table 10 and Eq. 12..

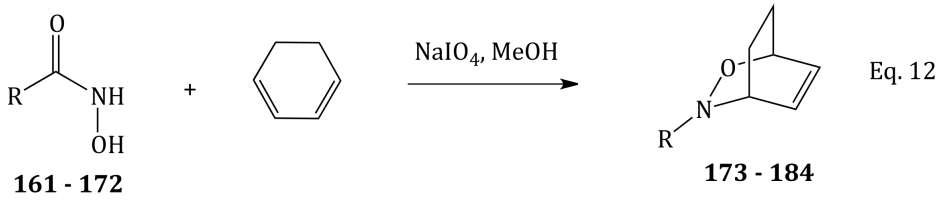

161 - 172 **173 - 184** Eq. 12

Table 10. Reaction of different hydroxamic acids with 1,3-cyclohexadiene using $NaIO_4$ as the oxidant.

Entry	Hydroxamic acid	Product	Time (h)	Yield %
1	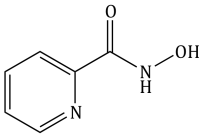 **161**	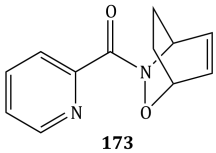 **173**	4	42
2	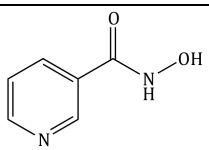 **162**	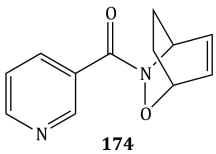 **174**	4	31

3	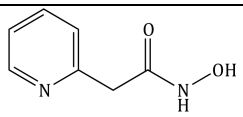 **163**	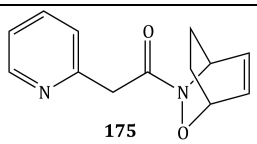 **175**	4	0
4	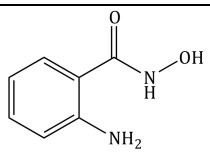 **164**	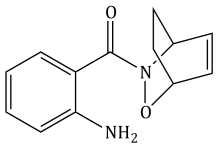 **176**	4	0
5	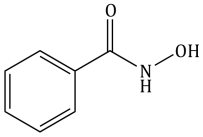 **165**	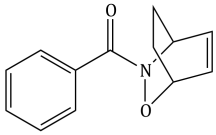 **177**	4	53
6	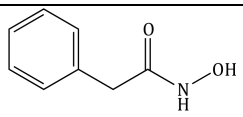 **166**	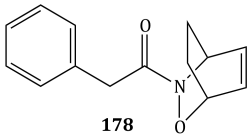 **178**	4	48
7	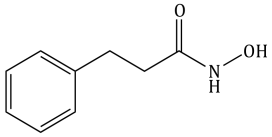 **167**	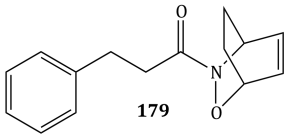 **179**	4	49
8	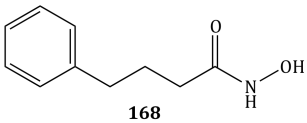 **168**	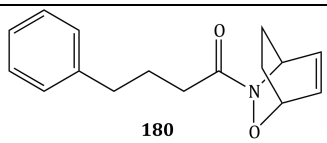 **180**	4	32
9	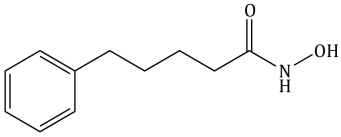 **169**	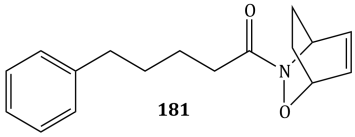 **181**	4	38
10	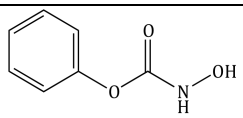 **170**	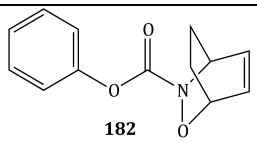 **182**	2	51
11	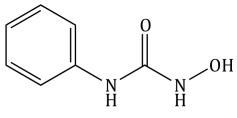 **171**	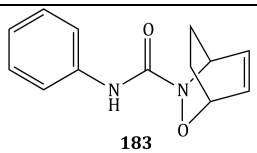 **183**	2	49
12	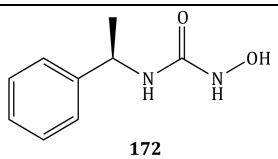 **172**	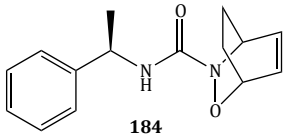 **184**	2	42

Entries 1 and 2 (Table 10) show the reactions of hydroxamic acids **161** and **162**, which contained a pyridine ring in the structure. Both reactions completed in 4 hours and upon the mixing the reagents, both reactions turned yellow and the colour got darker when the reaction completed. The products **173** and **174** were isolated as off-white solids with low to moderate yields. For compounds **163** and **164**, however, there was no cycloadduct **175** or **176** observed even after 4 hours and the colour of the mixture changed from yellow to dark brown (Entry 4, Table 10). This suggested decomposition of the starting material or nitroso species rather than reaction with the diene (Entries 3 and 4, Table 10). Entries 5 – 9 (Table 10) show the reactions between the acyl hydroxamic acids (each of which have C_nH_{2n} chains attached to the ring) with 1,3-cyclohexadiene. All these reactions also all completed in 4 hours and compounds **177** and **178** were isolated as off-white solids, which after recrytalization gave suitable crystals for the X-ray analysis. The X-ray structures of both compounds are shown in Figure 24.

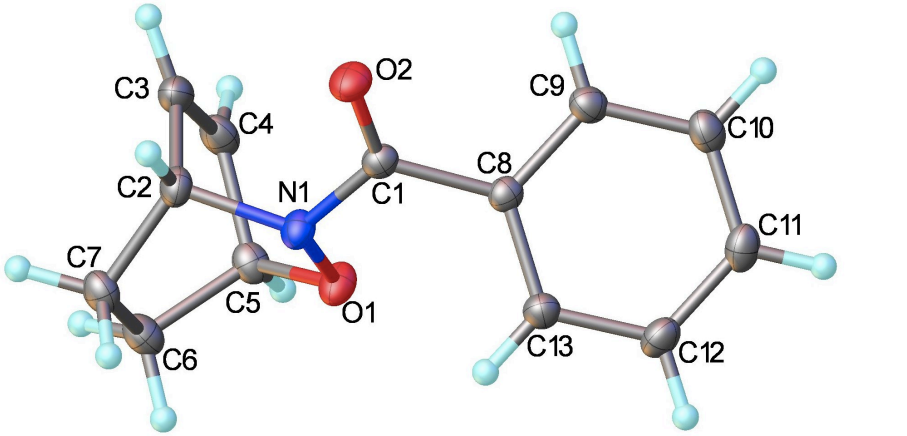

177

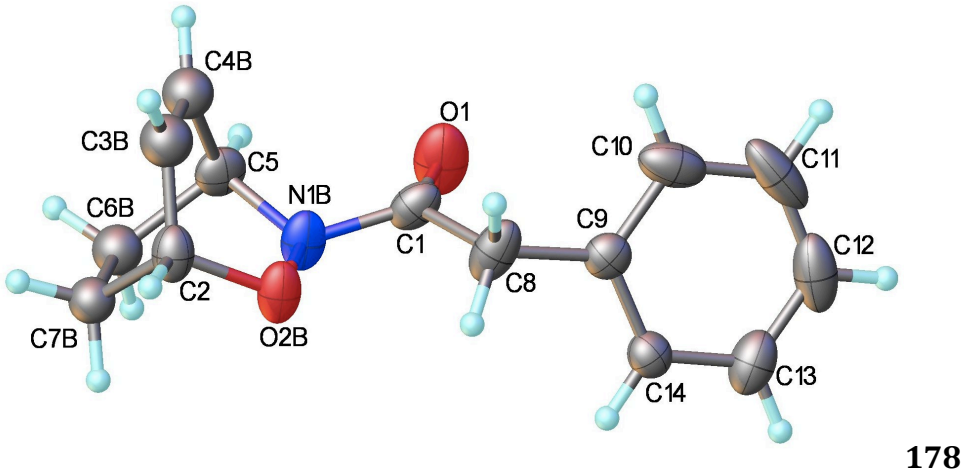

178

Figure 24. X-ray crystal structures of cycloadducts **177** and **178**.

In both these structures, we can observe the co-planarity of the amide system, and a high degree of similarity to the previous acylnitroso cycloadducts reported previously (*vide supra*).

Compounds **179** – **181** were, however, isolated as viscous oils, rather than solids as with **177** and **178** perhaps indicating that the further the hydroxamic acid group is placed from the aryl ring, there is more conformational flexibility of the side-chain and, therefore, the preferred state changes from solid to liquid.

In order to see the effect of the heteroatom between the phenyl ring and the hydroxamic acid group, cycloadduct **182** was synthesized from the reaction of 1,3-cyclohexadiene and hydroxamic acid **170**, which contains an oxygen as the connecting heteroatom. The product, a white solid, was isolated in 51% yield (Entry 10, Table 10). The corresponding nitrogen heteroatom version was also tested *i.e.* **171**, which also gave a white solid cycloadduct **183** in 49% isolated yield (Entry 11, Table 10).

Entry 12 (Table 10) shows a reaction of 1,3-cyclohexadiene with the hydroxamic acid **172**, which has a chiral centre in between the phenyl ring and the urea group. This reaction was completed in 4 hours giving a white solid product with 49% yield. Hence, there is very little difference in reaction efficiency between oxy and aza substituted acylnitroso species generated from **170** or **171**. The benzylic urea system, however, does appear to be slightly less reactive, which though potentially a steric effect, is more likely an electronic effect, comparing the aniline urea system **171** with the benzylic amine system **172**.

From all the results in Table 10, it can be concluded that for most of the new hydroxamic acids (apart from hydroxamic acids **163** and **164**), can react with 1,3-cyclohexadiene to form cycloadduct with moderate to low yields. The lack of reactivity of **164** is likely not due to the lack of oxidation; the starting material was consumed. More likely, it stems from a nitroso decomposition reaction, either by reaction with the solvent or aniline oxidation by producing the dark reaction mixture typical of azo-oxides and related species.

2.10 NDA reaction of hydroxamic acids with 2,3-dimethyl-1,3-butadiene using $NaIO_4$ as oxidant

The reaction of these hydroxamic acids with 2,3-dimethyl-1,3-butadiene was also conducted, the purpose being to see the chemoselectivity between the NDA *versus* ene-reaction. The results are shown in Table 11 and Eq. 13.

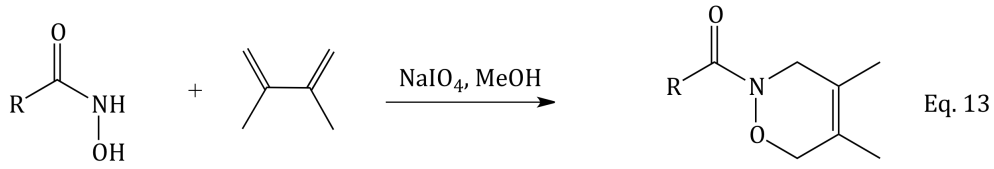

Eq. 13

161 - 172 **185 - 196**

Table 11. Reaction of hydroxamic acids with 2,3-dimethyl-1,3-butadiene using $NaIO_4$ as the oxidant

Entry	Hydroxamic acid	Product	Yield%
1	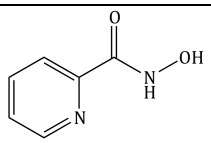 **161**	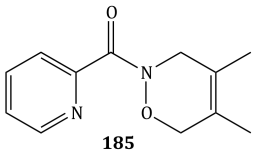 **185**	21
2	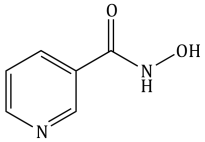 **162**	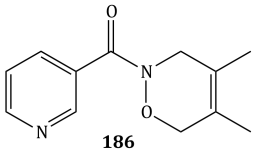 **186**	18
3	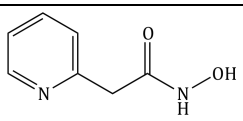 **163**	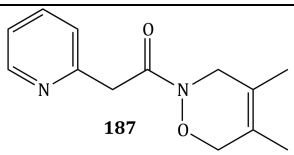 **187**	0
4	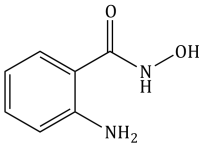 **164**	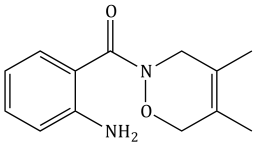 **188**	0
5	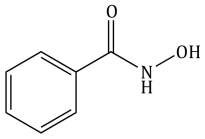 **165**	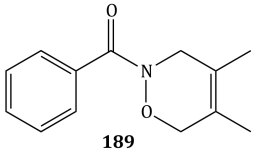 **189**	46

6	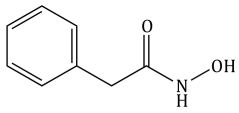 **166**	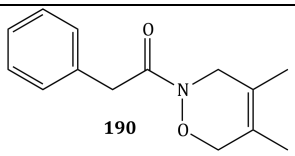 **190**	42
7	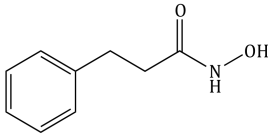 **167**	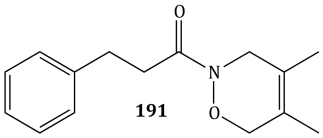 **191**	37
8	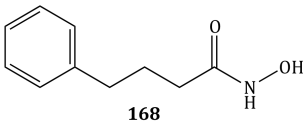 **168**	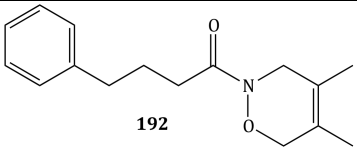 **192**	40
9	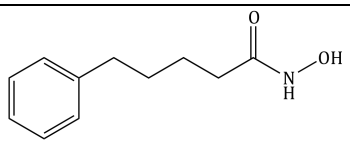 **169**	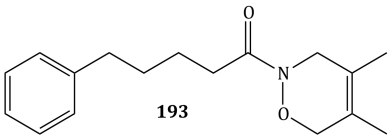 **193**	41
10	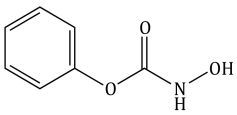 **170**	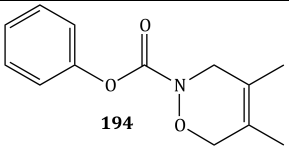 **194**	47
11	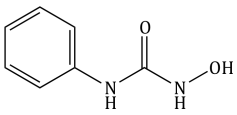 **171**	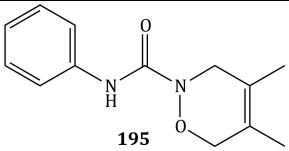 **195**	45
12	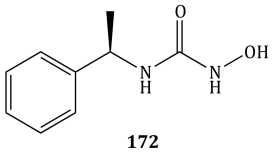 **172**	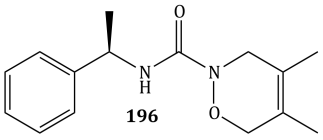 **196**	13

Entries 1 and 2 (Table 11) show the reaction of the hydroxamic acid **161** and **162** which contain a pyridine ring in 2- and 3-position respectively, with 2,3-dimethyl-1,3-butadiene. All reactions finished in 2 hours, giving cycloadducts **185** and **186** as off-white solids in low yields. The cycloadduct **185** was recrystalized from diethyl ether to give a crystal suitable for the X-ray crystal analysis. The structure is shown in Figure 25.

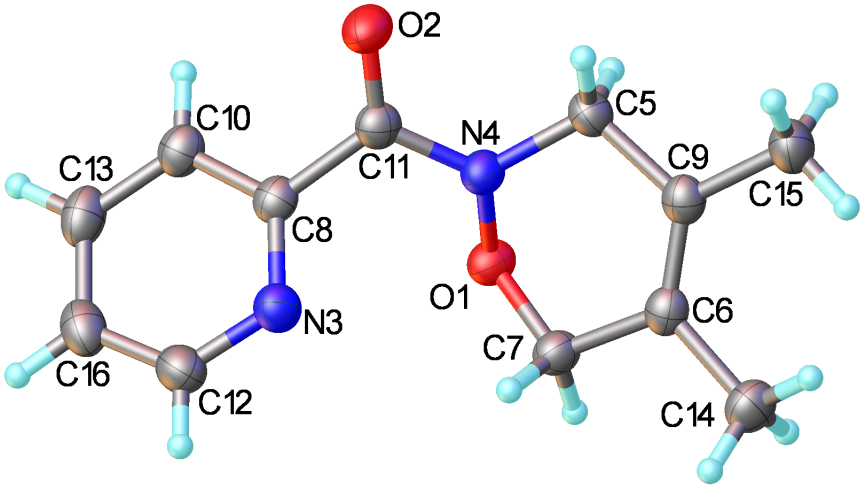

Figure 25. X-ray crystal structures of **cycloadduct 185.**

From the X-ray structure of cycloadduct **177** shown in Figure 25, it can be seen that the C-N bond of the pyridine ring and C-N bond in cycloadduct is in an s-*trans* position relative to both the C-N and N-O bonds.

Entry 3 (Table 11) shows the unsuccessful reaction of the hydroxamic acid **163** with 2,3-dimethyl-1,3-butadiene. The reaction was stirred and monitored by TLC and the starting material was consumed in 2 hours, however, no cycloadduct **187** was observed. The black sticky oil obtained did not give any useful information by ^{1}H NMR and this suggested decomposition of the nitroso species, as mentioned for Entry 3, Table 10.

Entry 4 (Table 11) shows the reaction between the hydroxamic acid **164** with 2,3-dimethyl-1,3-butadiene. Upon the mixing, the mixture colour was yellow and after 4 hours, the TLC showed that the starting material spot had disappeared. However, there was no desired product formed, only one long stripe could be seen, indicating of compete decomposition. The result of the oxidation of hydroxamic acid **165**, however, to form the corresponding nitroso species and then trapping by 2,3-dimethyl-1,3-butadiene is shown in Entry 5 (Table 11). The cycloadduct **189** was obtained as a white solid in 46% isolated yield. Surprisingly, there no ene product observed in the NMR, only unidentified impurities present in the crude product. This suggested that some decomposition of the nitroso species had occurred before it could be trapped by the diene. Entries 6-9 (Table 11) all worked in a very similar fashion but the cycloadducts of these reactions were colourless, viscous oils and isolated in moderate yields. In all of these oxidations, methyl

carbamate side-products were also separated, most likely as a result of methanolysis after the hydroxamic acid was oxidized to form the reactive nitroso species. The acylnitroso species can react with methanol to form the corresponding methyl carbamate with loss of HNO (see Scheme 56). The reason for proposing this reaction scheme, rather than direct methanolysis of the hydroxamic acid, is because the hydroxamic acid group is stable in methanol whereas acyl nitroso species are known to react readily with mild nucleophiles.[83]

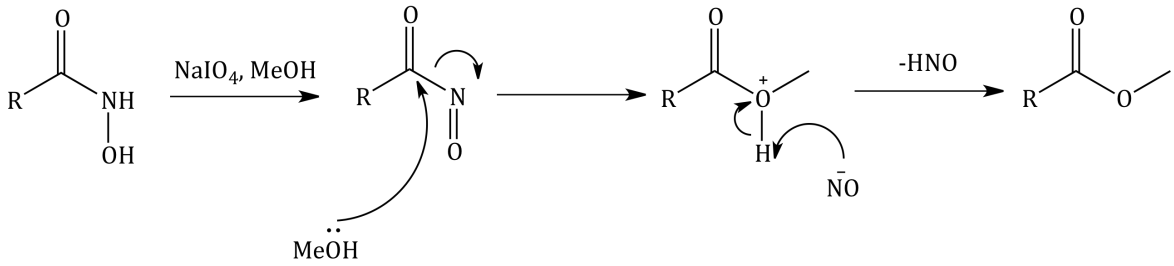

Scheme 56. Methanolysis mechanism for an acylnitroso compound after oxidation of the of hydroxamic acid.

Entry 10 (Table 11) shows the reaction of hydroxamic acid **170**, which contains an oxygen as the heteroatom. The reaction completed in 4 hours and the product **194** was obtained as a white solid in 47% yield. Again, surprisingly, there was no ene product observed and no evidence of methanolysis product present in the crude ^{1}H NMR spectrum. Compound **195** was obtained in a similar fashion in a yield of 45% and again, there was no ene-product and methanolysis product observed in the crude ^{1}H NMR spectrum, only unidentified impurities. This suggested that in these two cases, there was no decomposition of the acylnitroso species or methanolysis, and the ene-reaction could not compete with the NDA reaction.

Entry 12 (Table 11) shows the reaction of the chiral hydroxamic acid **172** with 2,3-dimethyl-1,3-butadiene. The reaction completed in 4 hours giving cycloadduct **196** as colourless oil in low yield (13%). However, the purification of this crude reaction product was difficult due to the presence of impurities, which were not identifiable.

2.11 NDA reaction of hydroxamic acids with 1,3-cyclohexadiene using Cu-oxazoline catalyst

From the results shown in Table 11, we can draw the conclusions that the different hydroxamic acids are readily oxidized to acylnitroso species, which can undergo NDA reactions efficiently. Therefore, we decided to conduct similar experiments by reacting these hydroxamic acids with 1,3-cyclohexadiene using 10 mol% $CuCl_2$ and 20 mol% 2-ethyl-2-oxazoline in methanol oxidation system, rather than periodate. The results are shown in Table 12 and Eq. 14.

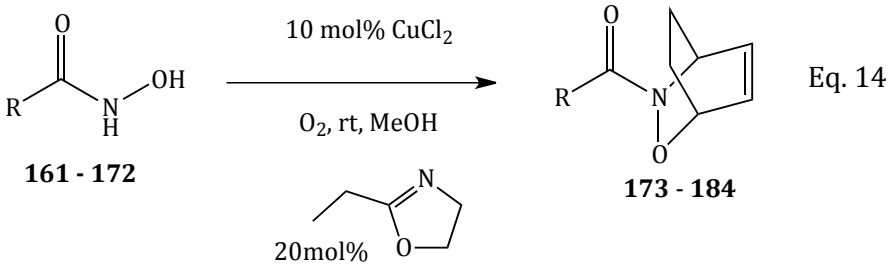

Eq. 14

Table 12. Reaction of hydroxamic acids with 1,3-cyclohexadiene using 10 mol% $CuCl_2$ and 20 mol% 2-ethyl-2-oxazoline as oxidation catalyst system.

Entry	Hydroxamic acid	Product	Yield %
1	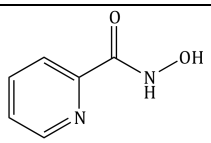 **161**	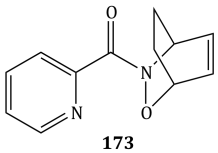 **173**	0
2	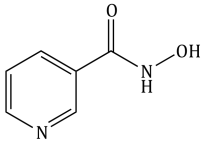 **162**	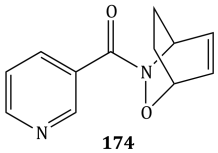 **174**	0
3	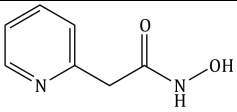 **163**	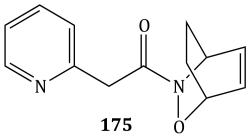 **175**	0
4	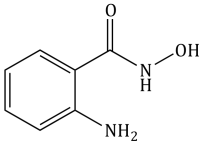 **164**	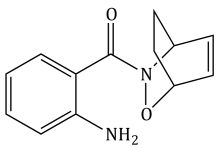 **176**	0

5	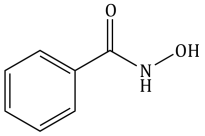 **165**	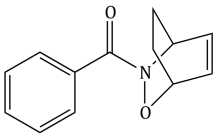 **177**	0
6	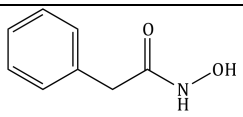 **166**	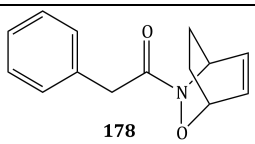 **178**	0
7	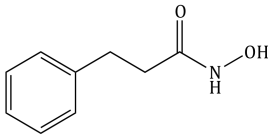 **167**	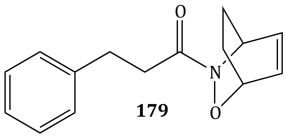 **179**	0
8	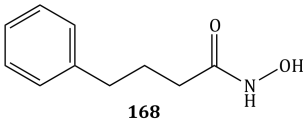 **168**	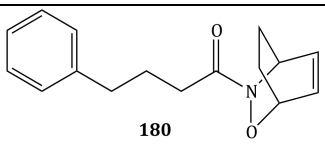 **180**	0
9	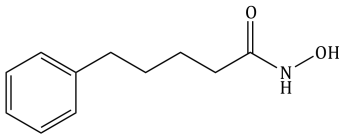 **169**	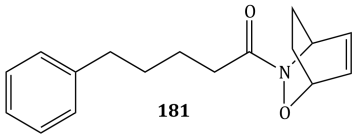 **181**	0
10	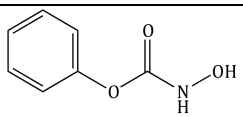 **170**	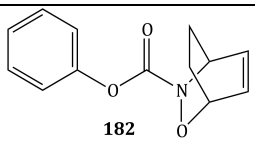 **182**	98
11	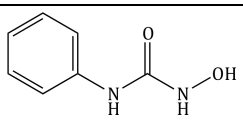 **171**	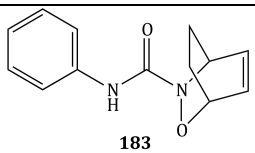 **183**	98
12	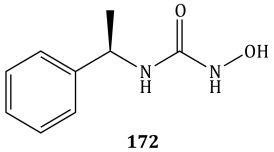 **172**	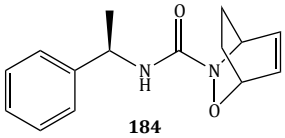 **184**	97

Entry 1 (Table 12) shows the reaction of 2-pyridinehydroxamic acid **161** with 1,3-cyclohexadiene using the Cu-oxazoline catalytic oxidation system. Upon adding the 2-ethy-2-oxazoline to the yellow solution of $CuCl_2$, the colour changed to green. However, after adding **161**, a turquoise precipitate was formed and the reaction did not proceed even after longer reaction times. For example, there was no desired cycloadduct **173** formed even after 4 days and even the addition of H_2O_2

failed to produce any reaction. The turquoise precipitate suggested that there was strong chelation between copper and **161**, which agrees with the work reported by Lisowski et al.[84] Indeed, they reacted a copper salt with **161** in methanol, which gave a metallacrown structure as shown in Figure 26, with a copper to hydroxamic acid ratio of 5:4.

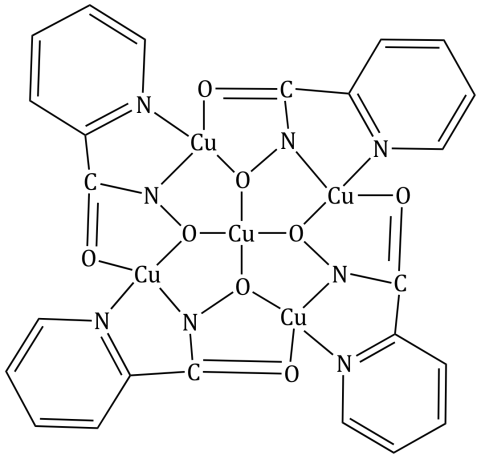

Figure 26. Copper-2-pyridinehydroxamic acid metallacrown complex.

Entry 2 (Table 12) shows the reaction of 3-pyridinehydroxamic acid **162**, which because the hydroxamic acid group is in the 3-position, cannot form bidentate chelation complexes with copper. However, even in this case there was no product **174** formed and there was a green precipitate, which formed slowly over 4 hours. The addition of hydrogen peroxide also did not help the reaction to proceed. Moreover, increasing the temperature to 40 ^{o}C or heating the reaction under reflux conditions did not make the reaction proceed. The green precipitate formation again suggested that strong chelation between the pyridine ring and copper was occurring.

Entry 3 (Table 4) shows the reaction between hydroxamic acid **163** and 1,3-cyclohexadiene. The reaction was stirred and monitored by TLC, however, there was no desired cycloadduct **175** formed even after 72 hours. However, a green precipitate was again observed, which did not dissolve in any organic solvent. Also, the addition of hydrogen peroxide and heating at 40 ^{o}C again failed to show any product spot by TLC. When the reaction of hydroxamic acid **164** with cyclohexadiene with the copper-oxazoline system was conducted (Entry 4, Table

12), there was no cycloadduct **176** formed, as with the previous reactions (*e.g.* Entry 4, Table 10). The reaction colour did change to dark brown and the starting material disappeared by TLC, which confirmed the consumption of the hydroxamic acid and most likely through acylnitroso decomposition.

Entries 5-9 (Table 12) show the reactions of 1,3-cycloheadiene with the hydroxamic acids with the C_nH_{2n} (n = 0-4) chains between the phenyl ring and hydroxamic acid group, and again using the copper-oxazoline and air system as catalyst. The reaction mixtures were stirred and monitored by TLC, however, there were no cycloadducts formed in any of these reactions. Even when hydrogen peroxide was added with heating under reflux was employed, the reactions still did not proceed. Interestingly, the reaction mixtures stayed the same green colour even after 72 hours, which reinforced that there was no oxidation taking place.

The hydroxamic acid **170**, which contains an oxygen heteroatom between the carbonyl group and phenyl ring, was tested with cyclohexadiene in the same air and copper-oxazoline conditions (Entry 10, Table 12). Upon mixing the copper with the oxazoline ligand, the colour of the mixture was green, it then changed to yellow upon the addition of the hydroxamic acid **170**. The reaction completed after 2 hours and gave the cycloadduct **182** in high yield (98%). After slow recrystalization of the compound **182**, a single crystal which was suitable for the X-ray crystal analysis was obtained. The structure of this cycloadduct **182** was confirmed and is shown in Figure 27.

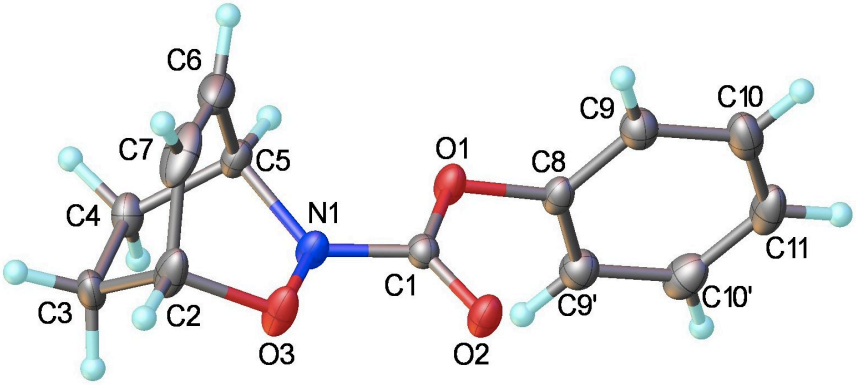

Figure 27. X-ray crystal structure of cycloadduct **182**.

The crystal structure of compound **182** shows co-planarity of the C=O and N-O bonds. However, and in contrast to structures such as **178** (*vide supra*), an s-*cis* conformation is preferred of the C-O double bond to the N-O bond and the O-phenyl ring has to rotate from sterically clashing with the carbonyl group.

Compound **171**, which contains the corresponding nitrogen as the heteroatom in the same position compared with Entry 10 (Table 12), was employed under the same conditions (Entry 11, Table 12). This reaction proceeded in a similar fashion to compound **170**, but the reaction time was twice as long (4 hours). The isolated yield of the white solid product cycloadduct **183** was 98% again. After recrystalization, a single crystal was obtained and was analyzed using X-ray diffraction analysis. The structure of this cycloadduct **183** is shown in Figure 28.

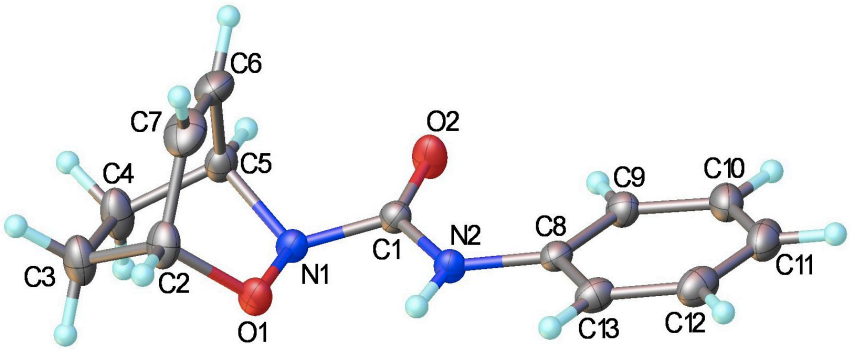

Figure 28. X-ray crystal structure of cycloadduct **183**.

Interestingly, the preferred conformation of the C=O to N-O bonds swaps back to an s-trans arrangement, compared with Fig. 27. This arrangement appears to be less sterically encumbered and more conjugated compared to Figure 24 (compound **182**). In that case, the phenyl ring is not fully co-planar with the carbamate moiety. However, in **183** (Figure 28), the s-*trans* conformation of the urea C=O to N-O bond of the cycloadduct, places the aniline-derived N-H and phenyl ring in a vertually co-planar and 'extended' conformation.

The reaction of chiral hydroxamic acid **172** with 1,3-cyclohexadiene under the model conditions was then conducted (Entry 12, Table 12). This reaction completed in 4 hours as well, yielding cycloadduct **184** in an excellent 97% yield.

The cycloadduct was analyzed by chiral HPLC and ^{1}H NMR. However, there was no diastereocontrol and a 1:1 mixture of distereoisomers was obtained.

From the results in Table 12, it can be concluded that in the copper-oxazoline catalytic intermolecular NDA reaction, the heteroatom between the phenyl ring and hydroxamic group seems to be necessary for the oxidation of the hydroxamic acid to acylnitroso to take place. Why this might be the case is not clear, but presumably it is an electronic effect that affects the ease of oxidation of hydroxamic acid.

2.12 The study of the reaction of compound 170 with various dienes.

The hydroxamic acids **170** and **171** were then tested with various dienes using the copper-oxazoline catalytic oxidation system that has been established. The results are shown in Tables 13 and 14 respectively.

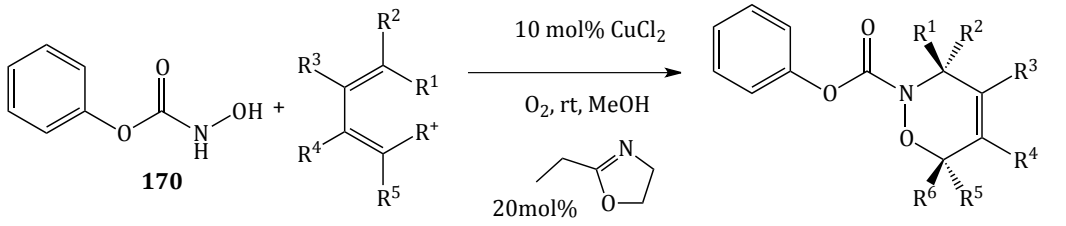

Eq. 15

Table 13. The reaction of hydroxamic acid **170** with various dienes according to Eq. 15.

Entry	Diene	Product	Time (h)	Yield %
1		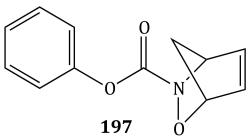 **197**	2	99
2		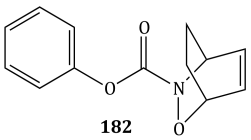 **182**	2	98

3		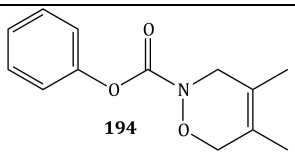 **194** 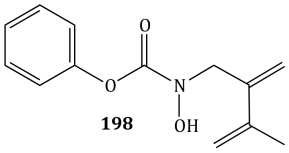 **198**	3	95 (ratio of **194**:**198** 6:1
4		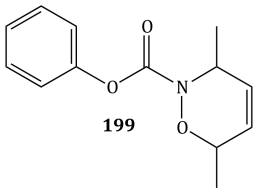 **199**	3	93
5		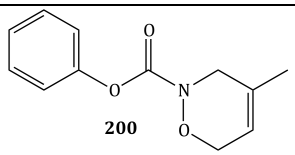 **200** 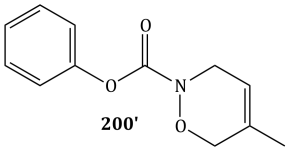 **200'** 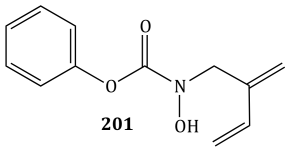 **201**	3.5	90 (**200** and **200'** : **201** = 3:1 and **200**:**200'** = 1.79:1)
6	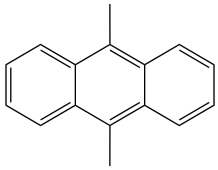	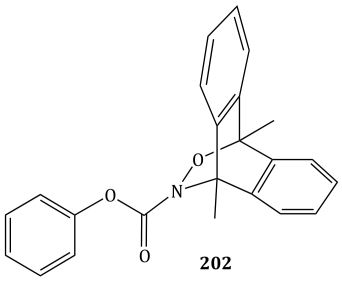 **202**	24	80
7	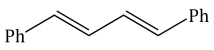	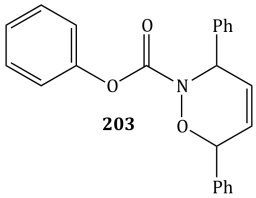 **203**	24	82

8	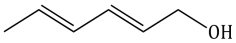	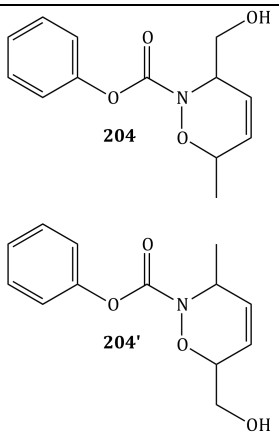	1.5	93 (ratio of **204**:**204'** 1:1)

Entry 1 (Table 13) shows the reaction of hydroxamic acid **170** with freshly cracked cyclopentadiene using 10 mol% $CuCl_2$ and 20 mol% 2-ethyl-2-oxazoline in methanol. The copper-oxazoline solution was dark green, which suddenly changed to pale yellow upon the adding of hydroxamic acid and turned back to the original colour when the reaction completed after 2 hours. The cycloadduct **197** was isolated as a white solid, which formed crystals suitable for single crystal X-ray analysis from diethyl ether, as shown in Figure 29.

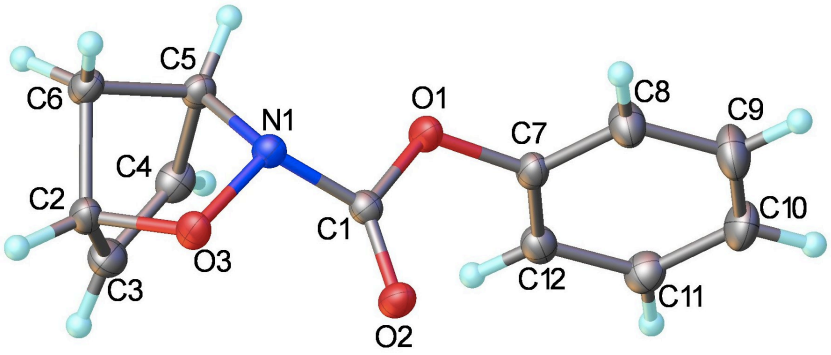

Figure 29. X-ray crystal structure of cycloadduct **197**.

Figure 29 shows the conformation of the compound **197**, which shows an s-cis conformation of the C-O double bond to the N-O bond, which agrees with the conformation observed in compound **182**.

The result of the oxidation of hydroxamic acid **170** to form the acylnitroso species, which was then trapped by 1,3-cyclohexadiene is shown in Entry 2 (Table 13). This result agrees with the previous reaction in Entry 10, Table 12. The result of copper-oxazoline catalyzed oxidation of compound **170** to form the acylnitroso

intermediate, which was then reacted with 2,3-dimethyl-1,3-butadiene, is shown in Entry 3 (Table 13). The reaction was completed in 3 hours and again, it was self-indicated by the colour changes. After work up, a colourless oil was obtained which characterized by ^{1}H NMR, and which indicated that two compounds were present in the crude product. This included two cycloadducts **194** and ene product **198**, in a 6:1 ratio. The overall yield was an excellent 95%. After silica gel column chromatography, the cycloadduct **194** was separated and was pure enough to do a full analysis. The ene fraction contained other unidentified impurities, which could not be separated.

The reaction of hydroxamic acid **170** with 2,4-hexadiene under these catalytic conditions completed in 3 hours. There was no ene-product observed; only cycloadduct **199** was obtained as colourless oil in 93% isolated yield (Entry 4, Table 13). The result of the NDA reaction of the acylnitroso species, which was formed from the Cu-oxidation of the hydroxamic acid **170,** with isoprene is shown in Entry 5 (Table 13). This reaction completed in 3.5 hours and there were 3 products observed in the crude ^{1}H NMR spectrum; cycloadducts **200** and **200'** and the ene product **201**. The ratio of the cycloadducts **200** and **200'** to the ene-product **201** was 3:1, and the ratio between **200** and **200'** was 1.79:1. These cycloadducts were inseparable by chromatography, therefore, the assignment of these two regioisomers was achieved using 2D NMR techniques, as mentioned previously. The ene-product **201**, however, could not be separated pure enough to do further analysis.

The reaction of compound **170** with 9,10-dimethylantacene in the Cu-oxazoline catalytic conditions was also conducted and the result is shown in Entry 6 (Table 13). This reaction completed in 24 hours and was monitored by TLC by the disappearance of the starting material or by the fluorescent properties of the diene. The cycloadduct **202** has no fluorescence under UV light due to the reduced conjugation. The cycloadduct **202** was obtained as a colourless oil in 80% yield. Entry 7 (Table 13) shows the result of the reaction of hydroxamic acid **170** with 1,4-diphenyl-1,3-butadiene under the model catalyst conditions. The reaction completed in 24 hours yielding cycloadduct **203** as colourless oil in 82%. Entry 8 (Table 13) demonstrates the reaction of hydroxamic acid **170** with the asymmetric diene, 2,4-hexadien-1-ol, under the model conditions. The reaction completed in

1.5 hours giving the cycloadducts **204** and **204'** according to the crude ^{1}H NMR spectrum, which also showed that no ene-product was formed. The ratio between these two cycloadducts was 1:1, surprisingly. However, these two regioisomers could not be separated from one another by chromatography. Therefore, the proton and carbon spectra for each regioisomer could not be easily assigned. In addition the 2D NMR spectra did not give any useful information in this case. However, the assignment of **204** and **204'** was possible after the similar systems **212** and **212'** were assigned. More details will be discussed later in this thesis.

From the results shown in Table 13, it can be concluded that the hydroxamic acid **170** with an oxygen heteroatom between the phenyl ring and the hydroxamic acid group can react readily with various dienes under the Cu-oxazoline catalytic system, giving good yields of products, though the levels of either regiocontrol in the NDA reaction or chemoselectivity between the NDA and ene reaction were not particularly impressive.

2.13 The study of the reaction of compound 171 with various dienes.

In order to further confirm the effects of heteroatoms between the phenyl ring and the hydroxamic acid group, experiments using the hydroxamic acid **171**, which contains a nitrogen heteroatom, with various dienes were conducted. The results are shown in Table 14 and Eq. 16.

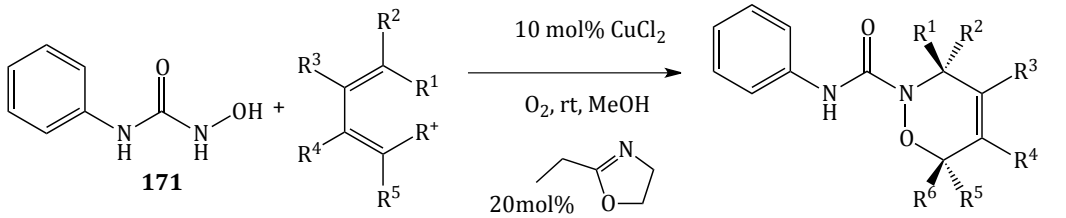

Eq. 16

Table 14. The reaction of hydroxamic acid **171** with various dienes according to Eq. 16.

Entry	Diene	Product	Time (h)	Yield %
1		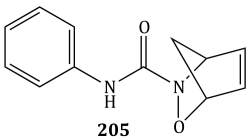 205	4	96

2		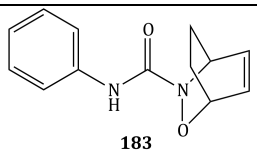 **183**	4	98
3		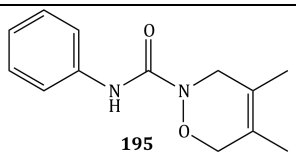 **195** 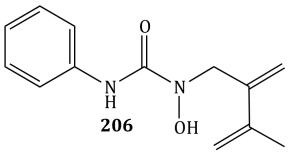 **206**	6	90 (ratio of **195**:**206** = 9:1)
4	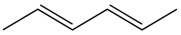	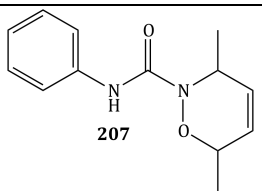 **207**	4	97
5		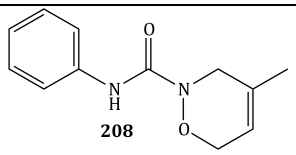 **208** 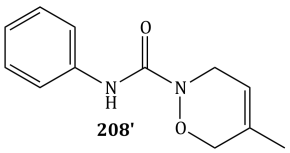 **208'** 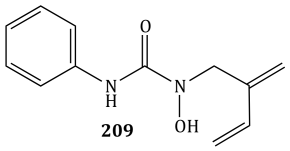 **209**	6	95 (**208** and **208'** : **209** = 9:1 and **208**:**208'** = 4.45:1)
6	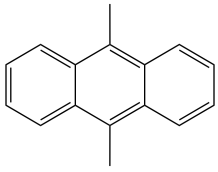	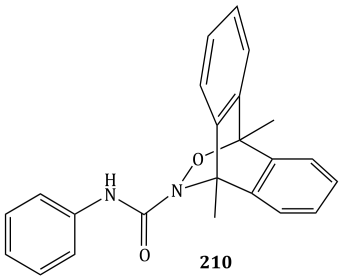 **210**	48	10* the starting material recovery

7	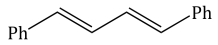	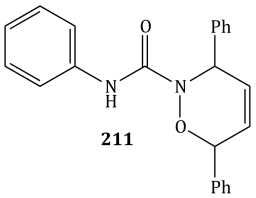 **211**	48	30* after purified the diphenylbutadidne shows on the NMR
8	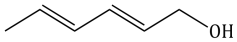	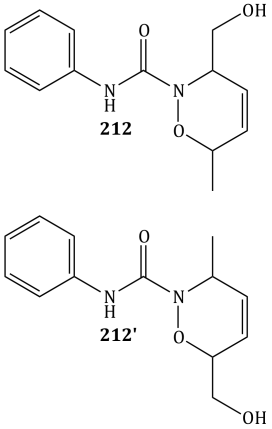 **212** **212'**	3	90 (ratio of **212**:**212'** = 1.5:1)

Entry 1 (Table 14) shows the result of the reaction between freshly cracked cyclopentadiene with hydroxamic acid **171**, using the Cu-oxazoline catalytic system in methanol. This reaction was monitored by the colour change and was also confirmed by TLC. It completed in 4 hours, yielding cycloadduct **205** as a white solid in an efficient 96%. The similar experiment of the hydroxamic acid **171** with 1,3-cyclohexadiene under the same conditions also gave a high isolated yield of the cycloadduct **183** (Entry 2, Table 14), which agreed with the result reported in Entry 11, Table 12.

The nitroso-Diels-Alder *versus* ene reaction was studied using the compound **170** with 2,3-dimethyl-1,3-butadiene under the standard conditions. The reaction completed in 6 hours and after the flash chromatography, the crude product was analyzed by ^{1}H NMR, showing that it contained two compounds: cycloadduct **195** and ene-product **206**. The ratio between cycloadduct **195** and ene product **206** was 9:1, which is the best chemoselectivity observed, especially compared to the reaction of the hydroxamic acid with oxygen heteroatom product, *i.e*. **170** (cycloadduct:ene ratio = 6:1). The reason for the improved selectivity is still unknown, however, one possibility is that the nitrogen heteroatom, which is less electronegative than oxygen, makes the nitroso group less electrophilic.

Therefore, the preferred pathway is the NDA reaction, compared to the ene reaction. Whether this is indeed the reason requires further investigation and especially using theoretical studies. The crude product was purified by chromatography to yield the pure cycloaduuct **195**, which after recrystalization gave a crystal suitable for single crystal X-ray diffraction analysis. The structure is shown in Figure 30. The ene product, however, could not be separated in a pure enough state to do further analysis.

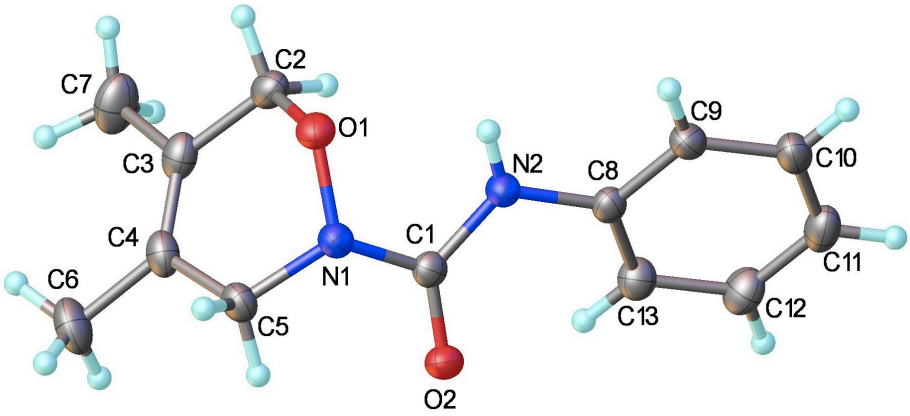

Figure 30. X-ray crystal structure of cycloadduct **195**.

Compound **195**, as with the previous urea-like NDA adducts, shows a preference for an s-trans conformation of N-O to C=O arrangement. Also as before, this allows the urea N-H function to be co-planar with the benzene group.

The reaction of hydroxamic acid **171** with 2,4-hexadiene, which has methyl groups in the 1- and 4-positions, using the model reaction, was studied. The reaction completed in 4 hours with only cycloaduuct **207** being observed in the crude product ^{1}H NMR spectrum. After the purification, a colourless oil was obtained in 97% isolated yield (Entry 4, Table 14).

Entry 5 (Table 14) shows the result of the reaction between hydroxamic acid **171** with isoprene under the copper(II)-catalyzed conditions. The reaction completed in 6 hours, with 3 products being shown by ^{1}H NMR. The products consisted of cycloadducts **208** and **208'**, and ene product **209**, with a combined the yield of 95%. The ratio of cycloadducts to ene-product was 9:1, which is the highest observed and far better than the oxygen heteroatom version (3:1) (Entry 5, Table 13). The ratio between the two cycloadducts **208** and **208'** was 4.45:1, which again is better than the oxygen heteroatom containing system. After

purification by silica gel chromatography, the cycloadducts were separated from the ene-product. However, the separation of the two cycloadducts was not possible due to them having the same rf. The ene product **209**, as with the others, could not be separated in a pure enough state to characterize it fully.

Entries 6 and 7 (Table 14) show the reaction between the hydroxamic acid **171** with 9,10-dimethylantracene and 1,4-diphenyl-1,3-butadiene, respectively, under the model conditions. These reactions were stirred and monitored for 48 hours, however, the reactions did not go to completion. The crude ^{1}H NMRs of both cycloadducts **210** and **211** showed that the desired products were formed, however, after purification of both cycloadducts, diene starting material was still present in the ^{1}H NMR spectra. Even repeating the column chromatography several times did not give pure enough product to be characterized. This suggested that the cycloadducts were undergoing cyclo-reversion upon standing, to give back the dienes and nitroso species, which then decompose leaving the diene.

Entry 8 (Table 14) shows the reaction of the asymmetric diene, 2,4-hexadien-1-ol, with hydroxamic acid **171**. The reaction completed in 3 hours giving a 90% yield of cycloadducts **212** and **212'** with a ratio of 1.5:1. Although this is not a major level of regiocontrol, it is an improvement compared to Entry 8, Table 12, which was only 1:1. This ratio can be obtained from the integral of the NH proton in the crude ^{1}H NMR spectrum shown in Figure 31. The structures of **212** and **212'** are shown in Figure 32.

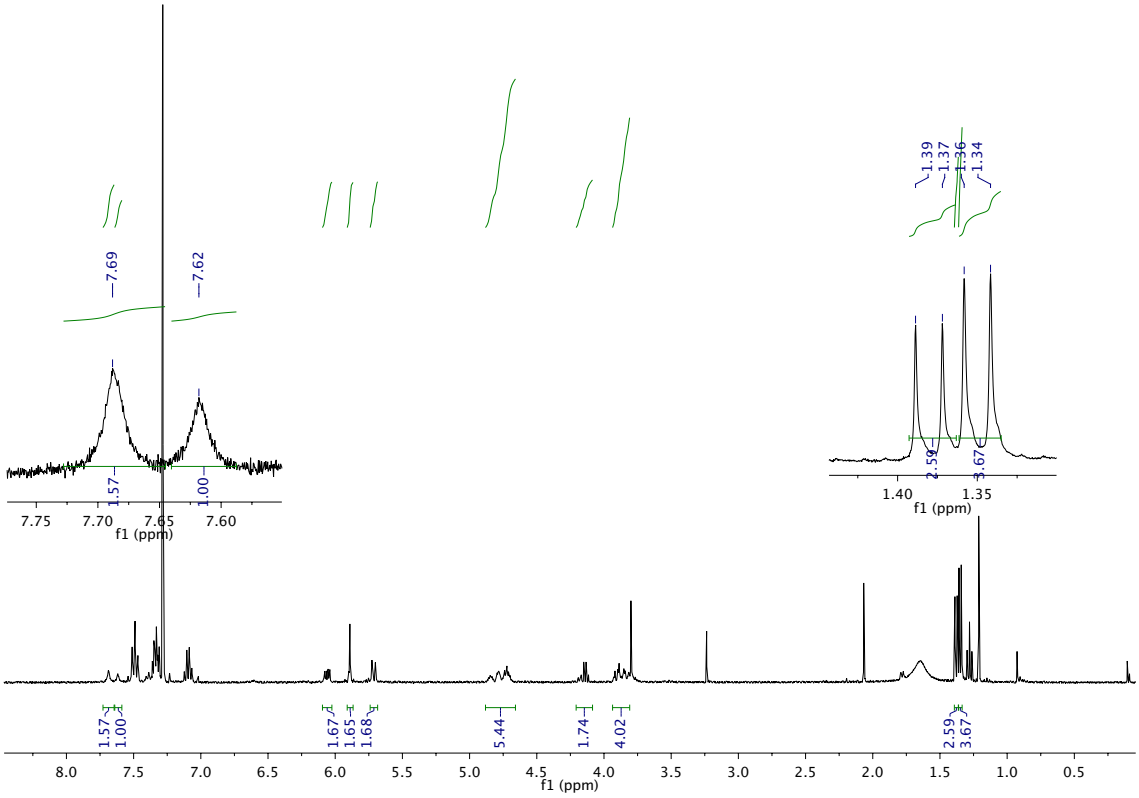

Figure 31. Crude ^{1}H NMR of the cycloadduct **212** and **212'**.

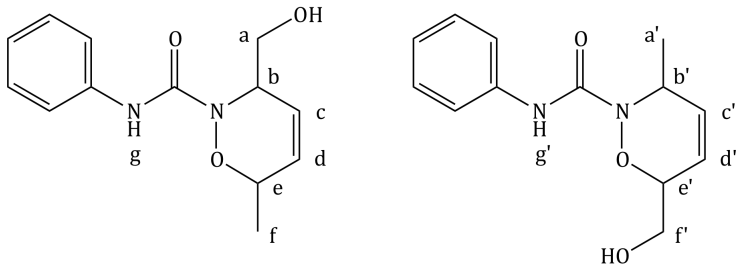

Figure 32. The structure of cycloadduct **212** and **212'**.

The two cycoadducts **212** and **212'** have very similar R_F values, however, this mixture was purified and analyzed by the COSY, NOESY, HSQC and HMBC NMR techniques, along with ^{1}H NMR and ^{13}C NMR. The ^{1}H NMR and ^{13}C NMR of the purified cycloadducts are shown in Figure 33.

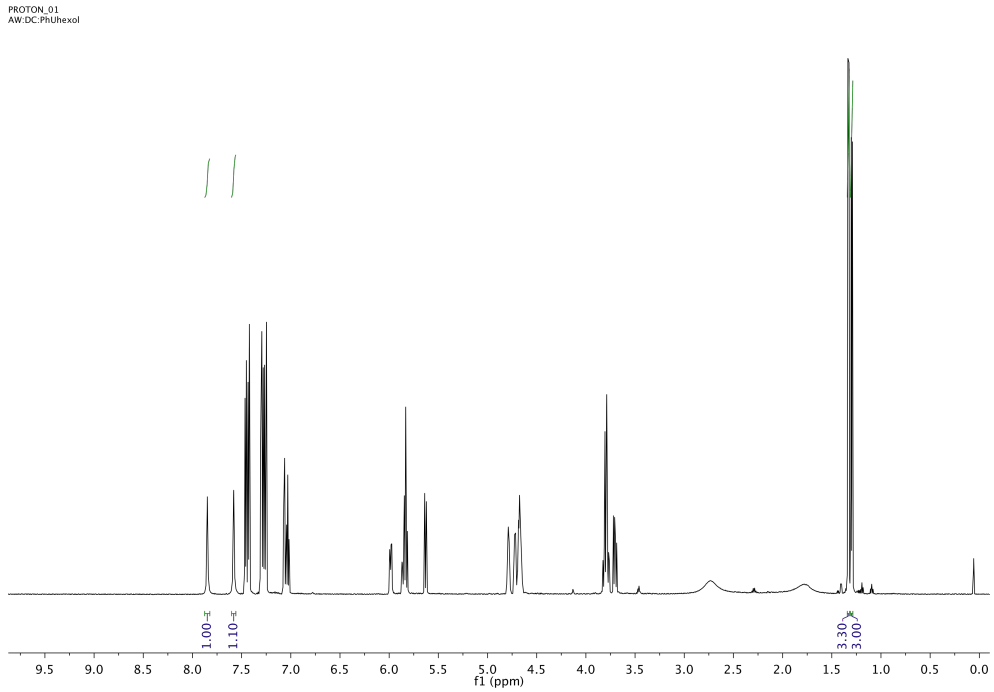

^{1}H NMR

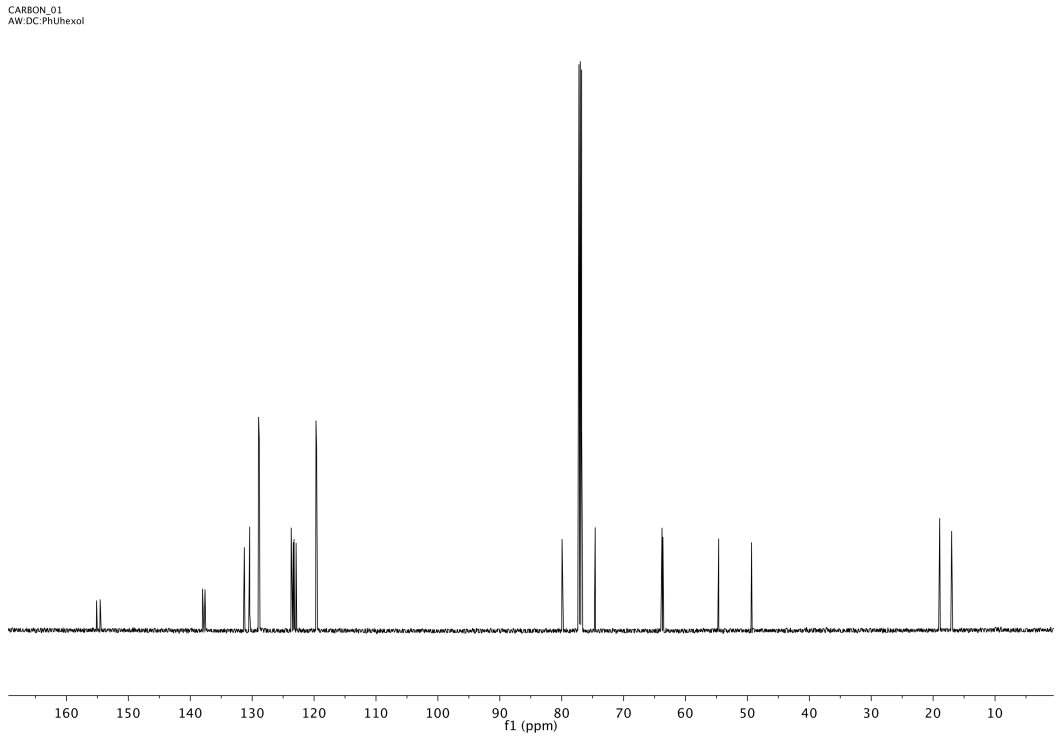

^{13}C NMR

Figure 33. ^{1}H and ^{13}C NMR of the mixture of cycloadducts **212** and **212'**.

Figure 33 shows, that after purification by chromatography, the product consisted of only two regioisomers and with a reduced ratio of 1:1.1 in this column fraction. COSY (Figure 34) showed the correlation of the methyl group f and a' to the CH

group of b, b', e and e'. Protons b and e' correlated with the CH_2 protons a and f' respectively. The protons b, b', e and e' also correlated to the alkene protons of c, c', d and d'. One regioisomer had the alkene proton signals well separated, while the other had them close together.

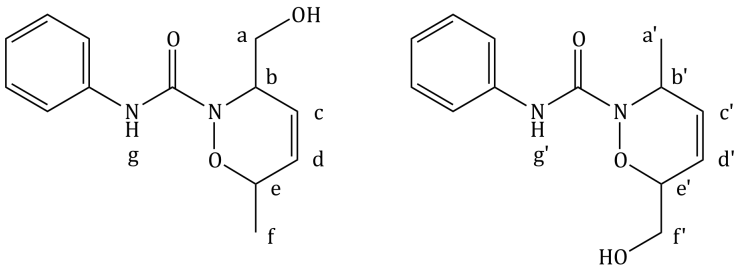

212 and **212'**

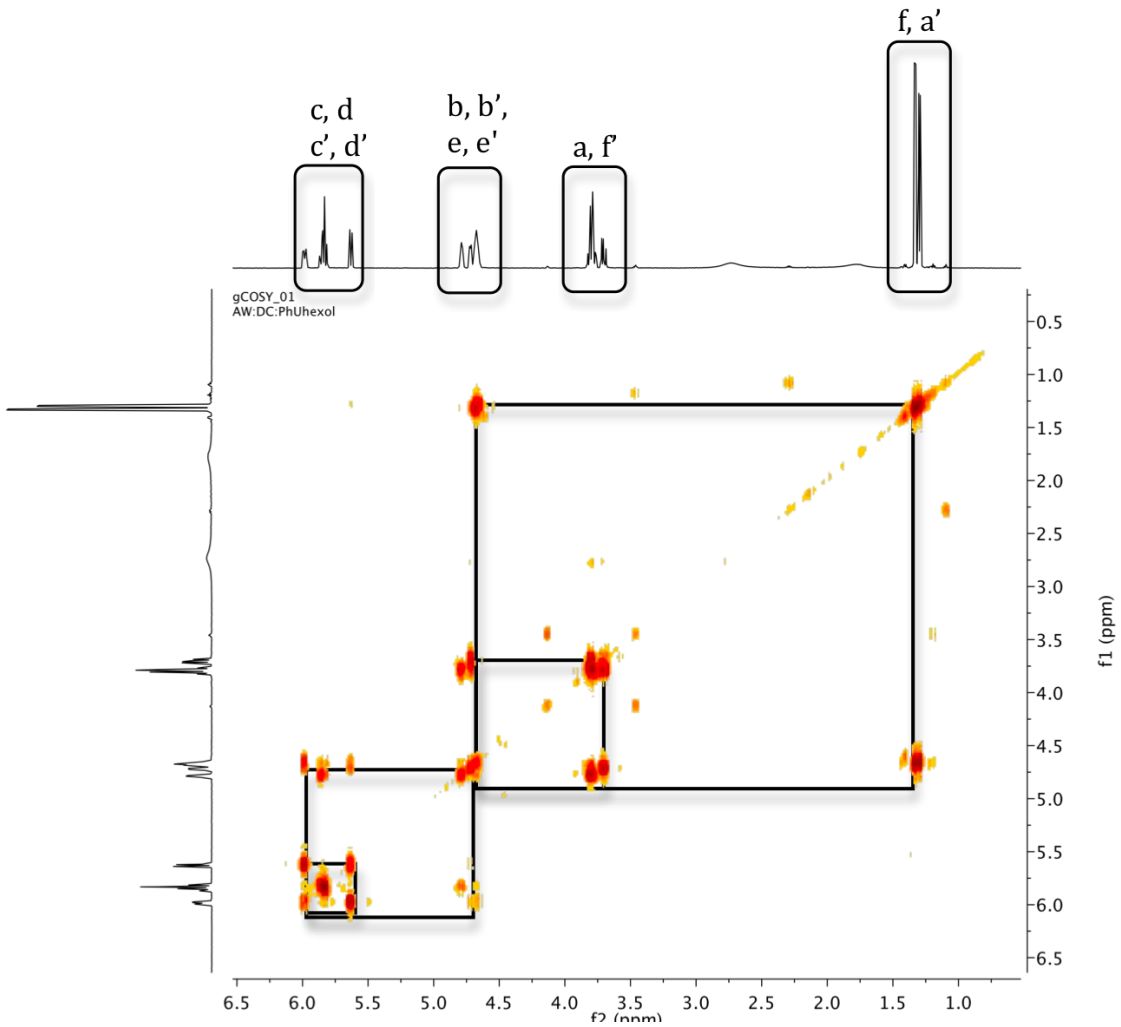

Figure 34. COSY NMR of cycloadducts **212** and **212'**.

The NOESY of this mixture of two regioisomers **212** and **212'**, however, did not give any useful information for the assignment of these compounds. Therefore, separation of the two cycloadducts was attempted again. Even though these two could not be separated completely, the best separation was from a fraction with the majority component being one regioisomer. This sample was then characterized by the 2D NMR to give useful information in the long-range correlation. The NOESY of this sample showed (Figure 35) a correlation between the NH proton to the CH_3 group and the CH proton. Therefore, the peak at 4.62 ppm belongs to the CH group next to the CH_3. This confirms that the regioisomer that was separated out in this sample was **212'**. From the NOESY spectrum, the structure was confirmed as shown in Figure 36.

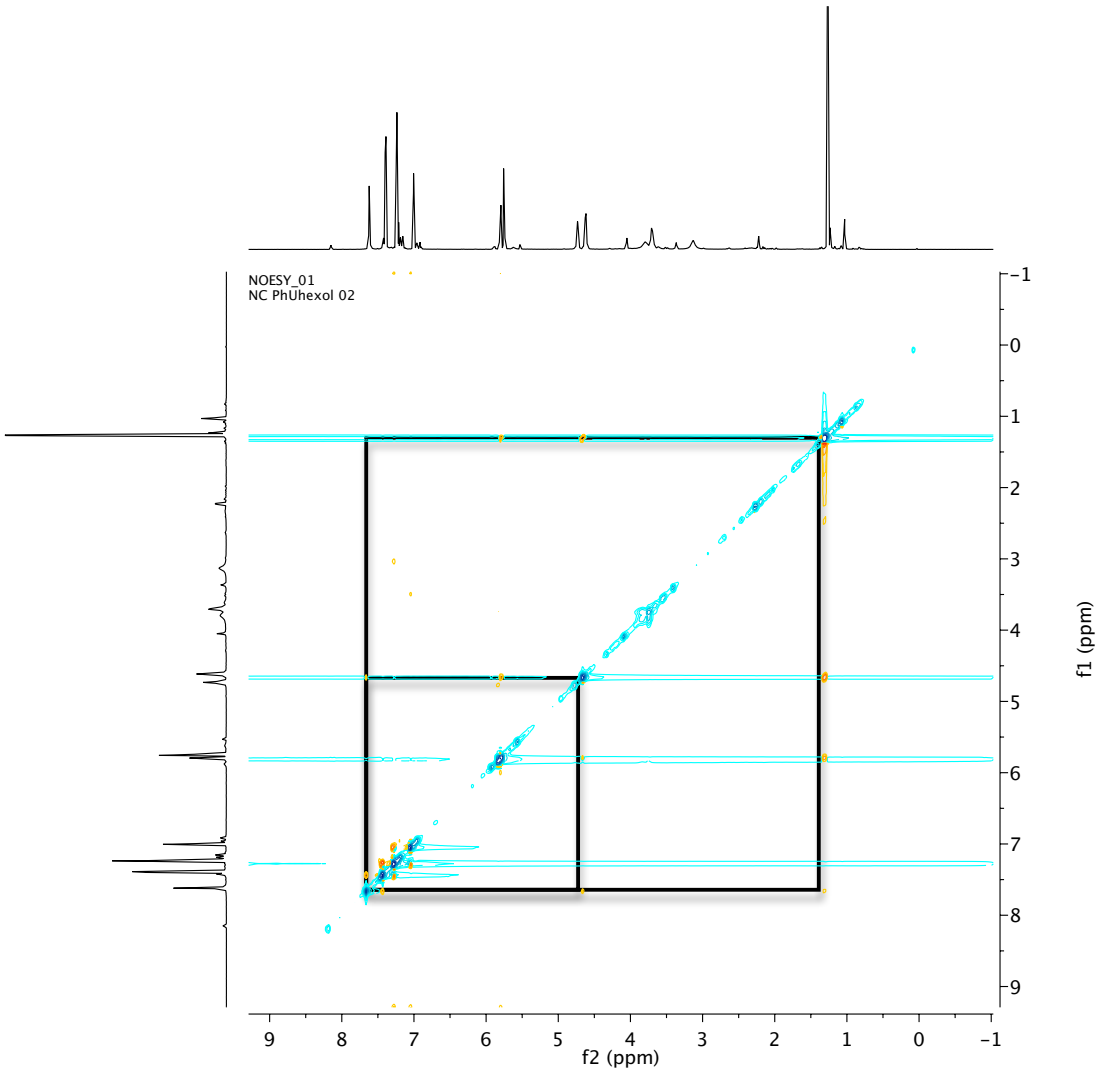

Figure 35. NOESY of cycloadduct **212'.**

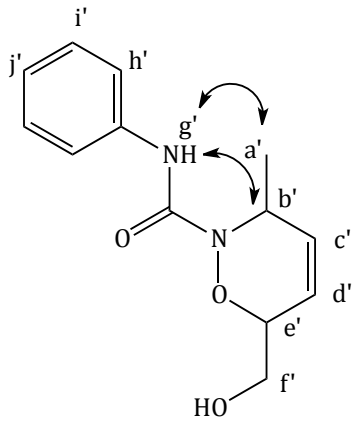

Figure 36. Compound **212'** structure as determined by NOESY.

After the a', b' and g' H's were assigned, the COSY NMR was further analyzed (Figure 37), which allowed the assignment of the peaks in the non-aromatic region. The peak at 1.26 ppm corresponds to the proton at the a' position; that at 3.71 ppm corresponds to f'; that at 4.62 ppm corresponds to b'; that at 4.73 ppm corresponds to e'; that at 5.75 ppm corresponds to c'; and that at 5.80 ppm corresponds to d'. From this information, it is possible to assign the carbon NMR of this compound by the HSQC NMR shown in Figure 38.

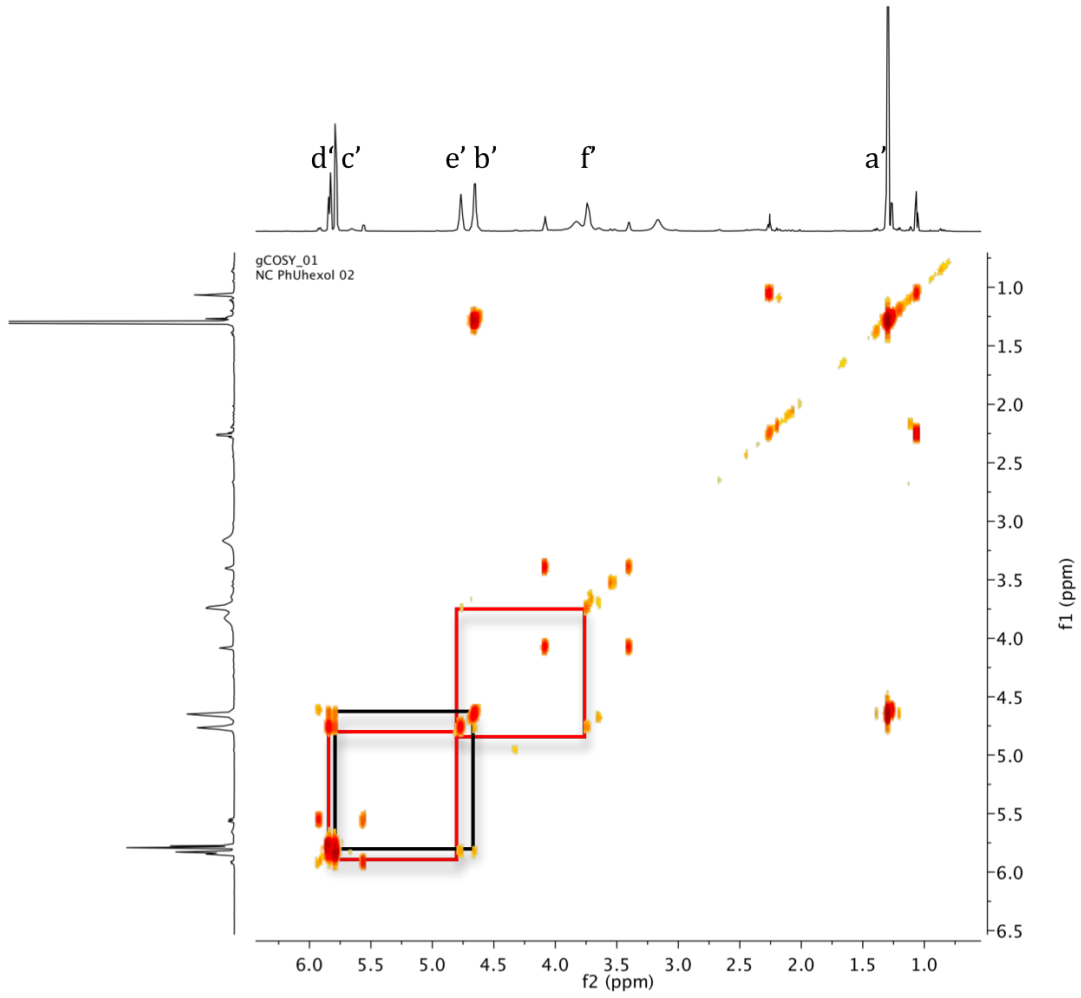

Figure 37. COSY NMR of **212'.**

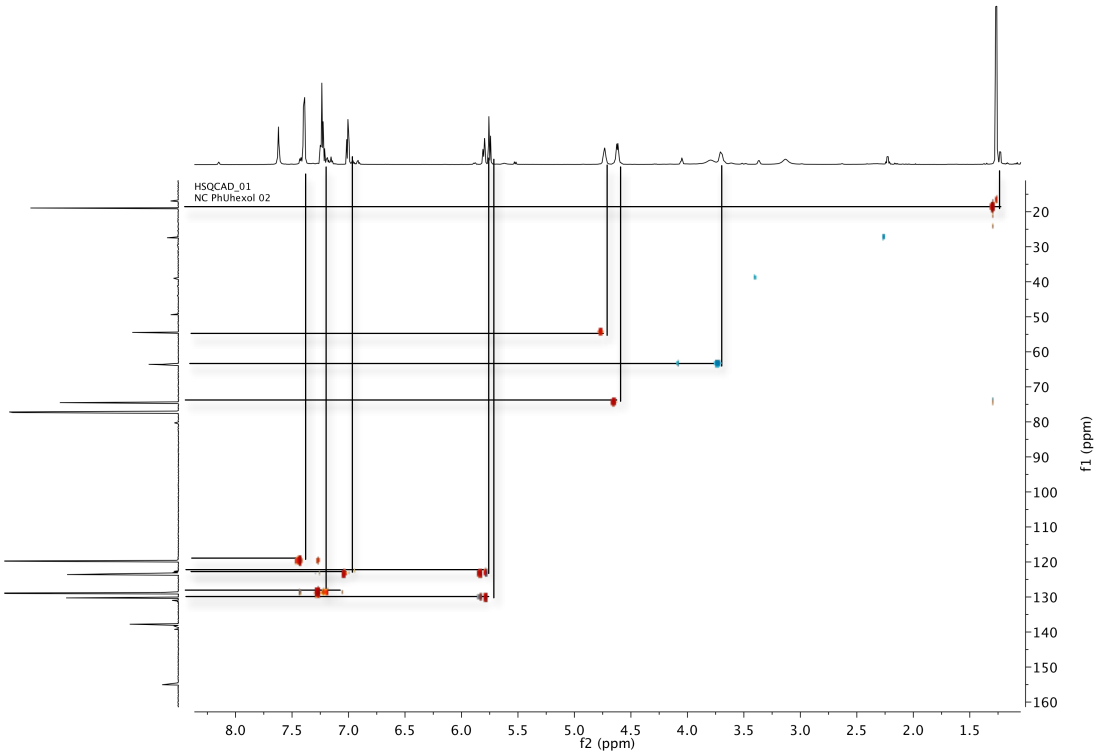

Figure 38. HSQC NMR of **212'.**

The HSQC correlation between the protons and carbons of this compound ensured the confirmation of the position of the carbons. For the CH (e') next to oxygen in the cycloadduct **212'**, the carbon peak appeared at 74.5 ppm, which was at lower field than the CH (b') next to nitrogen (54.5 ppm). This information is very useful in order to assign the structure of this and other compounds. All the cycloadducts that had been synthesized and characterized previously, the assignment of them based on the theory that carbons next to the oxygen would shift to lower field than carbons next to the nitrogen. However, there was not enough information to prove this until compounds **212** and **212'** were characterized. All the carbons connected to protons were assigned, however, the *ipso* and carbonyl carbons could not be assigned by this HSQC analysis, therefore, HMBC NMR was performed. The result is shown in Figure 39.

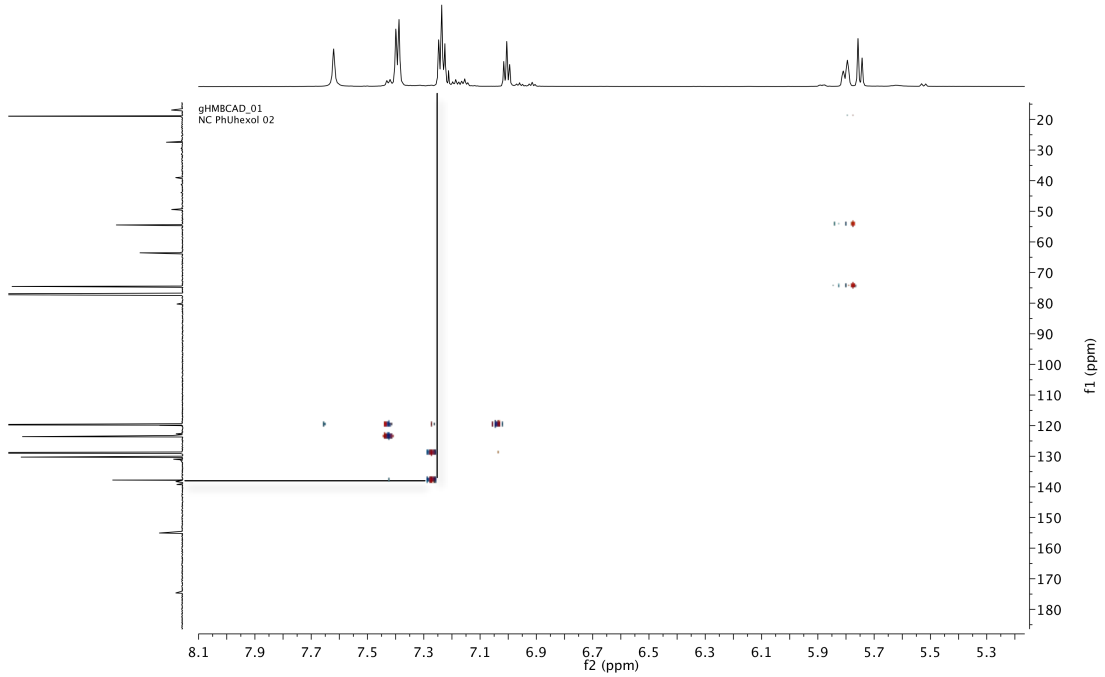

Figure 39. HMBC NMR of compound **212'**

The HMBC (Figure 39) shows the long-range correlation of the aromatic proton of the *ipso*-carbon at 137.8 ppm, therefore, the peak at 155.1 ppm corresponds to the carbonyl carbon. After the *ipso*-carbon was assigned, this then allowed the assignment of the protons in the aromatic region. The peak at 7.23 ppm corresponds to the two protons at the h' position, 7.40 ppm, which corresponds to the two protons at i, and, that at 7.00 ppm corresponds to one proton at j. After all the proton and carbon peaks for compound **212'** were assigned, the rest of the peaks in Figure 30 had to belong to compound **212**, which could also be assigned using the same logic. With all the information obtained from the NMR spectra, the regioselectivity of the reaction could be confirmed as compound **212** being the major regioisomer over compound **212'** (1.5:1).

2.14 Asymmetric synthesis attempt

2.14.1 Chiral ligand in reaction of compound 171 with 1,3-cyclohexadiene

Hydroxamic acid **171**, with the nitrogen heteroatom between the phenyl ring and hydroxamic acid group, has the potential to be chelated to the copper in a milder fashion than the nitrogen on pyridine ring as with compounds **161**-**163**. The

proposed chelation is shown in Figure 40, possibly occurring as shown in either structures A or B. Such chelation might result in chiral selectivity in the NDA system using chiral copper-oxazoline catalytic systems. Therefore, experiments using the hydroxamic acid **171** as the starting material were conducted under copper-chiral ligand conditions. The results are shown in Table 15 and Eq. 17.

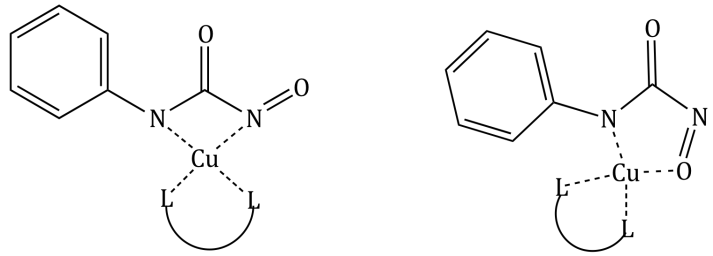

Figure 40. Proposed chelation of nitroso compounds derived from hydroxamic acid **171** with copper-ligand systems.

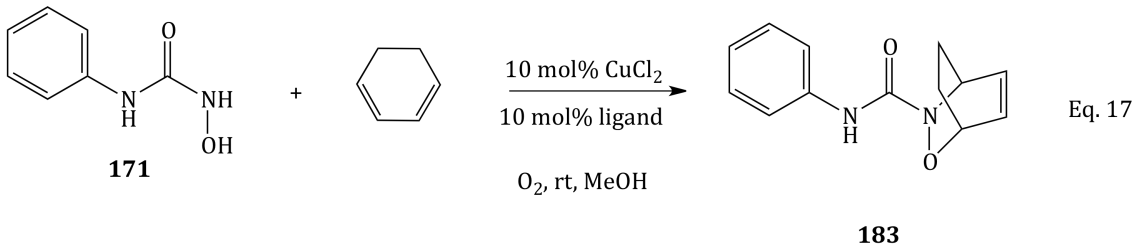

Table 15. The reaction of hydroxamic acid **171** with 1,3-cyclohexadiene using $CuCl_2$ and chiral ligand .

Entry	Ligand	Time (h)	Yield % of **183**	*ee* of **183**
1	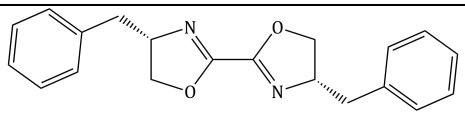 **157**	4	95	0
2	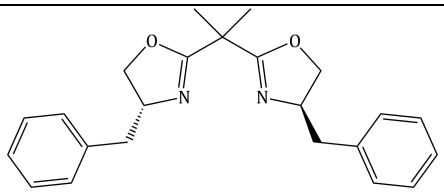 **145**	3	98	0

3	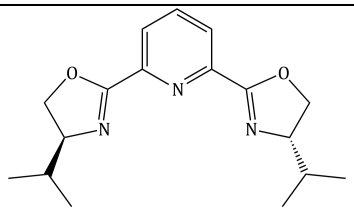 **158**	4	96	0

Entry 1 (Table 15), shows the result of the reaction between hydroxamic acid **171** with 1,3-cyclohexadiene using 10 mol% $CuCl_2$ and 10 mol% 2,2′-bis[(4*S*)-4-benzyl-2-oxazoline] **157**. The reaction completed in 4 hours, yielding the cycloadduct **183** in 95%. The white crystalline solid cycloadduct **183** was analyzed by chiral HPLC using an OD chiral HPLC column, using 6.5:3.5 hexane :IPA. However, there was no asymmetric induction observed.

For the Entry 2 (Table 15), the same experiment was carried out with 10mol% $CuCl_2$and 10 mol% (+)-2,2′-isopropylidenebis[(4*R*)-4-benzyl-2-oxazoline] **145**. The reaction completed in 3 hours, which was an hour faster than the achiral oxazoline (Entry 2, Table 14) showing that bidentate ligands speed up the reaction. The isolated yield of this reaction was 98%, however, there was no *ee* observed after the cycloadduct **183** as determined by chiral HPLC.

The pybox ligand **158** was also used as a chiral ligand in this reaction system (Entry 3, Table 15). The reaction completed in 4 hours, giving 96% isolated yield of product **183**, which was then analyzed by the chiral HPLC. This again showed that the racemic product was obtained.

From all the results shown in Table 15, it was clear that there was no enantioselectivity produced, even though pure chiral ligands were employed in this aerobic oxidation, copper-catalyzed system. The reactions were clean and fast, which shows that the acylnitroso compound did not chelate to the copper during the NDA step of the reaction, however, the oxidation reaction was improved compared with the monodentate ligand system.

2.14.2 Chiral ligand in reaction of compound 172 with 1,3-cyclohexadiene

Reactions of chiral hydroxamic acid **172** with 1,3-cyclohexadiene using $CuCl_2$ and the different chiral ligands was also studied. This study was based on the

assumption that if a chiral hydroxamic acid was used, the product would be obtained as a mixture of diastereoisomers capable of showing double diastereo-selectivity[86] due to additional interaction of the chiral auxiliary and the Cu-ligand chirality. This was intended as a final method of proving the coordination, or otherwise, of the nitroso dienophile to the Cu catalyst used also for the oxidation. The results of this study are shown in Table 16 and Eq. 18.

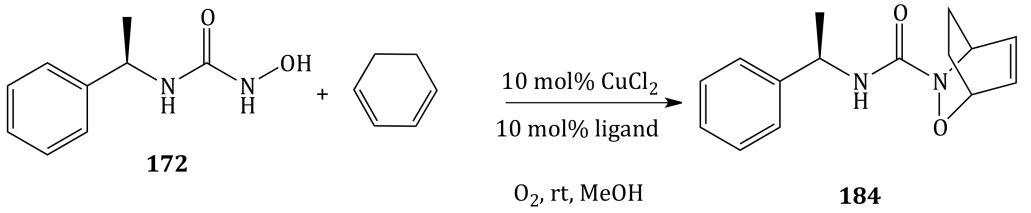

172 **184** Eq. 18

Table 16. The reaction of chiral hydroxamic acid **172** with 1,3-cyclohexadiene using $CuCl_2$ and chiral ligand.

Entry	Ligand	Time (h)	Yield (%)	*d.e.* (%)
1	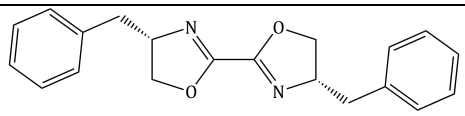 **157**	2	98	13
2	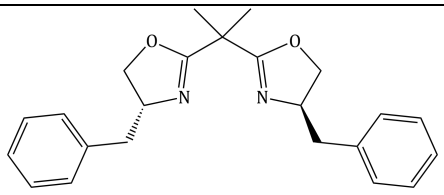 **145**	2	99	13
3	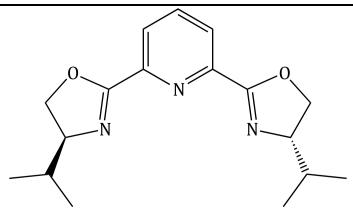 **158**	2	98	13
4	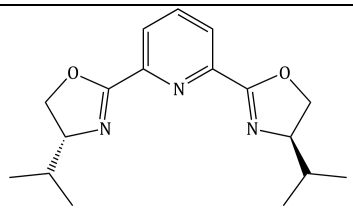 **213**	2	99	13

Entry 1, Table 16 shows the result of the reaction of chiral hydroxamic acid **172** with 1,3-cyclohexadiene with 10 mol% $CuCl_2$ and chiral bis-oxazoline ligand **157**. The reaction completed in 2 hours, which was half the time of the reaction using 2-ethyl-2-oxazoline as a ligand (Entry 12, Table 12). The white solid cycloadduct **184** was obtained in 98% isolated yield and was analyzed by chiral HPLC using the same OD column which was used to separate both possible the related enantiomers. However, there was only low asymmetric control observed in this reaction and shown by a *de* of 13% (i.e. a ration of 1.3:1 for the two diastereoisomers). When chiral ligand **145** was also employed in this study (Entry 2, Table 16), the reaction completed in 2 hours giving compound **184** in 99%. This pure compound was again analyzed by the chiral HPLC but again showed low *de* (13%). Entry 3 (Table 16) shows the effect of the ligand **158** on the same reaction, since this ligand helped the reaction to proceed and complete in 2 hours also, yielding the cycloadduct in 98%. However, there was still low *de* observed after chiral HPLC analysis was performed, which was notably the same 13% The cycloadduct **184** was also recrystalized by a slow evaporation technique using diethyl ether to give crystals suitable for the single crystal X-ray diffraction analysis. The result is shown in Figure 41.

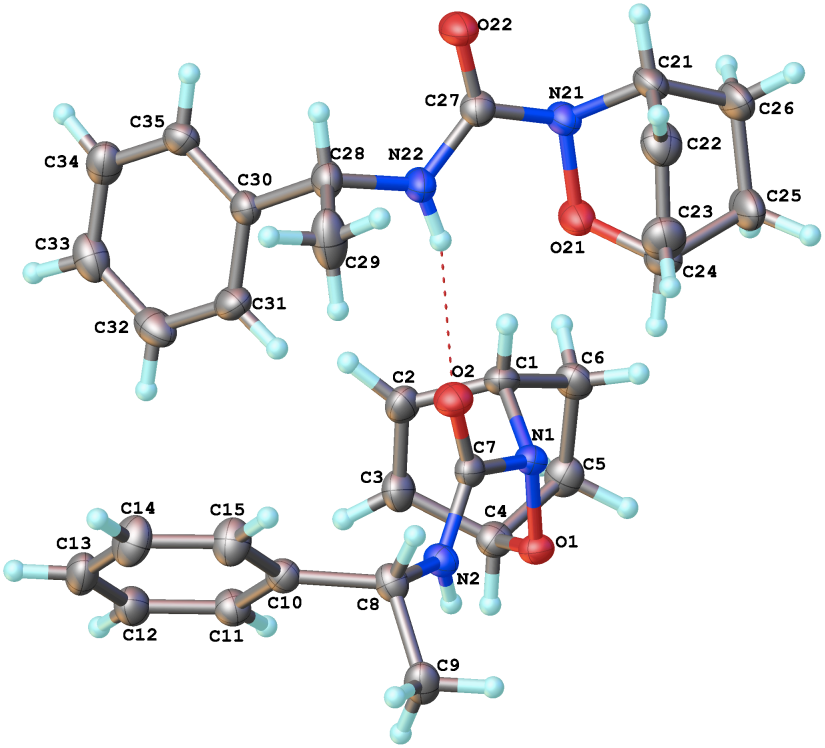

Figure 41. X-ray structure of cycloadduct **184**.

Figure 41 shows the X-ray structure of cycloadduct **184**, which confirmed that the product was a 1.3:1 mixture of diastereoisomers, using the enatiomerically pure starting material and chiral Cu ligands were used in the reaction. This confirms that there must be rapid dissociation of the acylnitroso compound of the Cu before it can be trapped by the diene, resulting in no major stereocontrol effects. Entry 4 (Table 16) shows the result of the reaction of chiral hydroxamic acid **172** with 1,3-cyclohexadiene with 10 mol% $CuCl_2$ and chiral pybox ligand **213**, which is the opposite absolute stereochemistry ligand to the ligand **158**. The reaction completed in 2 hours giving cycloadduct **184** in 99%. However, there was still only the same low de observed (13%). This experiment confirmed therefore that there was no double diastereocontrol in this system and essentially proves that there was no chelation between the copper complex and nitroso-species during the NDA reaction.

2.15 Chemoselectivity of hydroxamic acid.

From the study of the reaction of the different hydroxamic acids and 2,3-dimethyl-1,3-butadiene under the copper-oxazoline catalytic system, the results show that the ratio between the NDA and ene reaction depends upon the nature of the hydroxamic acid. The highest ratio of NDA:ene reaction that can be obtained so far was obtained from using hydroxamic acid **171** (9:1). These studies also show that the stronger electron withdrawing group attached to the NHOH function, the better the NDA reaction, presumably due to the lower LUMO of the nitroso species.[5,30] This assumes that with the stronger EWG next to the NHOH group, the ratio between the NDA and ene reaction is increased. In order to prove this, the hydroxamic acid **172**, which contained stronger electron withdrawing groups than compund **171** was tested. The result, as expected, shows that there was no ene product observed, only the desired cycloadduct **196** was obtained in 99%.

2.16 Conclusions

From the work shown in this thesis, the following conclusions can be drawn: 1) that the copper-oxazoline complex is an excellent catalyst for the arerobic oxidation of acyl hydroxamic acid to generate the corresponding acyl nitroso species; 2) that this system can only be used with the hydroxamic acid containing a hetero-atom between the aryl and carbonyl group; 3) that the nitroso species generated *in situ* can be trapped by most dienes resulting in the corresponding cycloadducts; 4) the yield of the products were variable from high to moderate, depending upon the reaction time because there was decomposition of the nitroso species competing with the NDA reaction. The longer the trapping time (slower NDA reaction), the lower the yield generally; 5) when using diene containing both alkene π-bonds and allylic σ-bonds, which can react with the nitroso-group to form the ene-product, the solvent plays a major role in the chemoselectivity. Acetonitrile gave the longest reaction time but the best result in the chemoselectivity; 6) the chemoselectivity of this system depends upon the reactivity of the hydroxamic acid - the higher the reactivity, the lower the chemoselectivity. Overall this catalytic aerobic oxidation is a particularly efficient, mild, clean, simple and environmentally benign for generating acyl nitroso species *in situ* and trapping them via a NDA reaction.

2.17 Future Work

The oxidation of the hydroxamic acids under the copper-oxazoline and air system to form the corresponding nitroso species and then trapping them using a diene was accomplished. However, the asymmetric synthesis of the NDA reaction adducts failed. Therefore, computational work on the NDA reaction is needed in order to find out the likely mechanism(s) operating in the reaction, which would allow us to understand the nature of the reaction between the nitroso species and the diene. This will lead to the catalytic design for an asymmetric synthesis perhaps in future.

The catalytic aerobic oxidation of the hydroxamic acids is clean and simple, therefore, it can be used in the natural product synthesis of alkaloids. This *in situ* oxidation of the hydroxamic acids has an advantage over the nitroso species

because it is more stable. Some examples of this system were employed by the Shea group, who showed the utility of this reaction in intra-molecular NDA. They also tested this methodology with a hydrazide to form the corresponding azo-compound and the trapped by the diene. This leads to the future work of studying the oxidation of hydrazides to form the azo compounds and their applications.

Chapter 3. Experimental

3.0 Experimental

General

All reactions were performed in the presence of air, unless otherwise stated. All reagents were purchased from Aldrich and TCI and were used as received without further purification unless otherwise stated. Solvents (AR grade) were used as received. Thiourea-oxazoline ligands were prepared by the group of Professor Yang of Peking University as reported in the literature.[81] ^{1}H NMR and $^{13}C\{^{1}H\}$ spectra were recorded using Bruker Avance 400 operating at 400 MHz for ^{1}H NMR and ^{13}C NMR at 101 MHz, Varian VNMRS 700 operating at 700 MHz for ^{1}H NMR and ^{13}C NMR at 176 MHz, or for ^{1}H NMR recorded at 500 MHz using a Bruker DRX 500 spectrometer or at 600 MHz using an Advance 600 spectrometer, with corresponding ^{13}C NMR at 125 MHz using a Bruker DRX 500 spectrometer or at 150 MHz using an Advance 600 spectrometer. $CDCl_3$ and DMSO-d_6 was used as the solvent for all NMR samples. ^{1}H NMR chemical shifts are reported with reference to TMS using residual proton on non deuterated solvent ($CDCl_3$: 7.26 ppm) whereas ^{13}C NMR spectra are reported with reference to TMS using the carbon signals of the deuterated solvent ($CDCl_3$: 77.23 ppm) Elemental analysis was performed using an Exeter Analytical E440 machine by departmental service at Durham University. All chromatography was carried out using silica gel (Silica gel LC60A 40-63 μm), which obtained from Fluorochem. The removal of solvent was performed on a rotary evaporator under vacuum. IR spectra were recorded on a Perkin-Elmer 1615 FTRIR spectrometer. Melting points were determined using an Electrothermal melting point apparatus and are uncorrected. Low resolution mass spectrometry was carried out on a Waters TQD equipped with Acquity UPLC and an electrospray ion source, and high resolution mass spectrometry was carried out on a Waters LCT Premier XE equipped with Acquity UPLC and a lock-mass electrospray ion source.

3.1 Palladium catalyst screening

Entry 1, Table 1

N-(Benzyloxycarbonyl)hydroxylamine (210 mg, 1.26 mmol) dissolved in methanol (10 mL) was added dropwise to a mixture of 1,3-cyclohexadiene (150 mg, 1.87

mmol), sodium periodate (269 mg, 1.26 mmol) and methanol (20 mL) at room temperature. The reaction mixture was stirred for 4 hours and monitored by TLC. Then the solvent was removed in *vacuo*. and the crude product was purified by silica gel chromatography (6:1 v/v, hexane/EtOAc) to obtain the product as a white solid. Product yield: 216 mg (70%); m.p. 84-86 °C; ^{1}H NMR (400 MHz, $CDCl_3$) δ 7.45 – 7.28 (m, 5H), 6.67 – 6.46 (m, 2H), 5.24 – 5.17 (m, 1H), 5.13 (d, *J* = 12.3 Hz, 1H), 4.82 (dt, *J* = 7.9, 2.8 Hz, 1H), 4.76 (ddd, *J* = 5.5, 3.8, 1.8 Hz, 1H), 2.26 – 2.17 (m, 1H), 2.12 (ddt, *J* = 12.4, 9.0, 3.1 Hz, 1H), 1.53 – 1.44 (m, 1H), 1.42 – 1.34 (m, 1H); ^{13}C{^{1}H} NMR (101 MHz, $CDCl_3$) δ 158.1, 136.0, 132.0, 131.6, 128.5, 128.2, 128.1, 71.0, 67.7, 50.2, 23.5, 20.6; FTIR (thin film) *inter alia* 1698, 1265, 1049, 744, 696 cm^{-1}; LRMS (ESI+) m/z 268.1 (M+ + Na); HRMS (ESI+) m/z Calcd for $C_{14}H_{15}NO_3Na$ 268.0950 found 268.0928; Anal. Calcd for $C_{14}H_{15}NO_3$: C 68.55, H 6.16, N 5.71, found: C 68.59, H, 6.22, N 5.60[17c]

GP 1: *General procedure for the nitroso-Diels-Alder reaction forming benzyl 2-oxa-3-azabicyclo[2.2.2]oct-5-ene-3-carboxylate* ***140***

1,3-Cyclohexadiene (5 equivalents) and catalyst were added to a microwave tube followed by toluene (4 mL). *N*-(Benzyloxycarbonyl)hydroxylamine in methanol (1 mL) was added and the resulting solution was stirred at room temperature and monitored by TLC. The completion of the reaction was confirmed by the disappearance of the starting material spot by TLC. The solvents were removed under reduced pressure and the crude product purified by silica gel chromatography (hexane: ethyl acetate, 6:1 v/v as the eluent) to give the product **140** as a white solid.

Entry 6, Table 1

According to **GP1**: *N*-(Benzyloxycarbonyl)hydroxylamine (91 mg, 0.54 mmol), 1,3-cyclohexadiene (60 mg, 0.75 mmol), PdL2up (4 mg, 0.007 mmol) and CuI (2 mg, 0.011 mmol). The reaction was stirred for 2 days and a white solid product was obtained. Product **140** yield: 27 mg (20%).

Entry 7, Table 1

According to **GP1**: *N*-(Benzyloxycarbonyl)hydroxylamine (57 mg, 0.34mmol) 1,3-cyclohexadiene (97 mg, 1.21 mmol), PdL2up (10 mg, 0.02 mmol) and CuI (3 mg, 0.02 mmol). The tube was sealed and O_2 gas was injected to the mixture. The reaction was stirred for 2 days. The product **140** was obtained in a yield of 33 mg (39%).

Entry 8, Table 1

According to **GP1**: *N*-(Benzyloxycarbonyl)hydroxylamine (57 mg, 0.34 mmol) 1,3-cyclohexadiene (100 mg, 1.25 mmol), PdL2up (10 mg, 0.02 mmol) and CuI (7 mg, 0.03 mmol). The tube was sealed and O_2 gas was injected into the reaction mixture. The reaction was stirred for 2 days. Product **140** yield: 35 mg (42%).

Entry 9, Table 1

According to **GP1**: *N*-(Benzyloxycarbonyl)hydroxylamine (57 mg, 0.34 mmol) 1,3-cyclohexadiene (137 mg, 1.71 mmol), PdL2up (2 mg, 0.004 mmol), CuI (1 mg, 0.007 mmol) and Et_3N (1 mL). The tube was sealed and O_2 gas was injected into the reaction mixture. The reaction was stirred for 2 days. Product **140** yield: 49 mg (58%).

Entry 10, Table 1

According to **GP1**: *N*-(Benzyloxycarbonyl)hydroxylamine (68 mg, 0.41 mmol), 1,3-cyclohexadiene (100 mg, 1.25 mmol) and CuI (8 mg, 0.04 mmol). The tube was sealed and O_2 gas was injected into the reaction mixture. The reaction was stirred for 2 days. Product **140** yield: 77 mg (77%).

3.2 Copper salts and solvents screening

GP 2:*General procedure for the nitroso-Diels-Alder reaction forming Benzyl 2-oxa-3-azabicyclo[2.2.2]oct-5-ene-3-carboxylate **140***

1,3-Cyclohexadiene was added to a microwave tube, which contained the catalyst (5 mol%) in the solvent(s) (5 mL). *N*-(Benzyloxycarbonyl)hydroxylamine was added to the solution. The resulting solution was stirred and monitored by TLC. The completion of the reaction was confirmed by the disappearance of the starting

material spot on the TLC. The solvent(s) was removed under reduced pressure. The crude product was purified by silica gel column chromatography (hexane/EtOAc, 6:1 v/v, as the eluent) to obtain the product of white solid.

Entry 1, Table 3

According to **GP2**: *N*-(Benzyloxycarbonyl)hydroxylamine (56 mg, 0.33 mmol) 1,3-cyclohexadiene (134 mg, 1.66 mmol) and CuI (3 mg, 0.02 mmol) in MeOH. The reaction was stirred for 4 days. Product **140** yield: 26 mg (32%).

Entry 2, Table 3

According to **GP2**: *N*-(Benzyloxycarbonyl)hydroxylamine (57 mg, 0.34 mmol) 1,3-cyclohexadiene (137 mg, 1.71 mmol) and $CuCl_2$ (2 mg, 0.02 mmol) in MeOH The reaction was stirred for 15 hours. Product **140** yield: 40 mg (47%).

Entry 3, Table 3

According to **GP2**: *N*-(Benzyloxycarbonyl)hydroxylamine (56 mg, 0.33 mmol) 1,3-cyclohexadiene (134 mg, 1.66 mmol) and $CuBr_2$ (4 mg, 0.02 mmol) in MeOH. The reaction was stirred for 15 hours. Product **140** yield: 33 mg (40%).

Entry 4, Table 3

According to **GP2**: *N*-(Benzyloxycarbonyl)hydroxylamine (55 mg, 0.33 mmol) 1,3-cyclohexadiene (131 mg, 1.64 mmol) and $Cu(OAc)_2$ (3 mg, 0.02 mmol) in MeOH. The reaction was stirred for 5 days. Product **140** yield: 17 mg (21%).

Entry 5, Table 3

According to **GP2**: *N*-(Benzyloxycarbonyl)hydroxylamine (55 mg, 0.33 mmol), 1,3-cyclohexadiene (132 mg, 1.64 mmol) and CuI (3 mg, 0.02 mmol) in toluene. The reaction was stirred for 6 days. Product **140** yield: 28 mg (35%).

Entry 6, Table 3

According to **GP2**: *N*-(Benzyloxycarbonyl)hydroxylamine (54 mg, 0.32 mmol), 1,3-cyclohexadiene (130 mg, 1.61 mmol) and $CuCl_2$ (2 mg, 0.02 mmol) in toluene. The reaction was stirred for 4 days. Product **140** yield: 40 mg (50%).

Entry 7, Table 3

According to **GP2**: *N*-(Benzyloxycarbonyl)hydroxylamine (55 mg, 0.33 mmol), 1,3-cyclohexadiene (132 mg, 1.64 mmol) and $CuBr_2$ (4 mg, 0.02 mmol) in toluene. The reaction was stirred for 4 days. Product **140** yield: 36 mg (44%).

Entry 8, Table 3

According to **GP2**: *N*-(Benzyloxycarbonyl)hydroxylamine (56 mg, 0.34 mmol), 1,3-cyclohexadiene (135 mg, 1.68 mmol) and $Cu(OAc)_2$ (3 mg, 0.02 mmol) in toluene. The reaction was stirred for 7 days. Product **140** yield: 19 mg (23%).

Entry 9, Table 3

According to **GP2**: *N*-(Benzyloxycarbonyl)hydroxylamine (56 mg, 0.33 mmol), 1,3-cyclohexadiene (133 mg, 1.66 mmol) and CuI (3 mg, 0.02 mmol) in MeCN. The reaction was stirred for 2 days. Product **140** yield: 8 mg (10%).

Entry 10, Table 3

According to **GP2**: *N*-(Benzyloxycarbonyl)hydroxylamine (57 mg, 0.34 mmol), 1,3-cyclohexadiene (136 mg, 1.69 mmol) and $CuCl_2$ (2 mg, 0.02 mmol) in MeCN. The reaction was stirred for 22 hours. Product **140** yield: 22 mg (27%).

Entry 11, Table 3

According to **GP2**: *N*-(Benzyloxycarbonyl)hydroxylamine (55 mg, 0.33 mmol), 1,3-cyclohexadiene (132 mg, 1.64 mmol) and $CuBr_2$ (4 mg, 0.02 mmol) in MeCN. The reaction was stirred for 2 days. Product **140** yield: 17 mg (21%).

Entry 12, Table 3

According to **GP2**: *N*-(Benzyloxycarbonyl)hydroxylamine (57 mg, 0.34 mmol), 1,3-cyclohexadiene (136 mg, 1.69 mmol) and $Cu(OAc)_2$ (3 mg, 0.02 mmol) in MeCN. The reaction was stirred for 2 days. Product **140** yield: 4 mg (5%).

Entry 13, Table 3

According to **GP2**: *N*-(Benzyloxycarbonyl)hydroxylamine (56 mg, 0.34 mmol),

1,3-cyclohexadiene (135 mg, 1.68 mmol) and CuI (3 mg, 0.02 mmol) in THF. The reaction was stirred for 26 hours. Product **140** yield: 17 mg (20%).

Entry 14, Table 3

According to **GP2**: *N*-(Benzyloxycarbonyl)hydroxylamine (55 mg, 0.33 mmol), 1,3-cyclohexadiene (131 mg, 1.63 mmol) and $CuCl_2$ (2 mg, 0.02 mmol) in THF. The reaction was stirred for 26 hours. Product **140** yield: 22 mg (28%).

Entry 15, Table 3

According to **GP2**: *N*-(Benzyloxycarbonyl)hydroxylamine (57 mg, 0.34 mmol), 1,3-cyclohexadiene (135 mg, 1.69 mmol) and $CuBr_2$ (4 mg, 0.02 mmol) in THF. The reaction was stirred for 26 hours. Product **140** yield: 21 mg (25%).

Entry 16, Table 3

According to **GP2**: *N*-(Benzyloxycarbonyl)hydroxylamine (55 mg, 0.33 mmol), 1,3-cyclohexadiene (131 mg, 1.64 mmol) and $Cu(OAc)_2$ (3 mg, 0.02 mmol) in THF. The reaction was stirred for 26 hours. Product **140** yield: 9 mg (11%).

Entry 17, Table 3

According to **GP2**: *N*-(Benzyloxycarbonyl)hydroxylamine (57 mg, 0.34 mmol), 1,3-cyclohexadiene (137 mg, 1.70 mmol) and CuI (3 mg, 0.02 mmol) in MeOH/toluene (1:4 v/v). The reaction was stirred for 20 hours. Product **140** yield: 60 mg (72%).

Entry 18, Table 3

According to **GP2**: *N*-(Benzyloxycarbonyl)hydroxylamine (58 mg, 0.35 mmol), 1,3-cyclohexadiene (139 mg, 1.73 mmol) and $CuCl_2$ (2 mg, 0.02 mmol) in MeOH/toluene (1:4 v/v). The reaction was stirred for 15 hours. Product **140** yield: 64 mg (75%)

Entry 19, Table 3

According to **GP2**: *N*-(Benzyloxycarbonyl)hydroxylamine (59 mg, 0.35 mmol),

1,3-cyclohexadiene (142 mg, 1.77 mmol) and $CuBr_2$ (4 mg, 0.02 mmol) in MeOH/toluene (1:4 v/v). The reaction was stirred for 20 hours. Product **140** yield: 60 mg (69%)

Entry 20, Table 3

According to **GP2**: *N*-(Benzyloxycarbonyl)hydroxylamine (59 mg, 0.35 mmol), 1,3-cyclohexadiene (141 mg, 1.76 mmol) and $Cu(OAc)_2$ (3 mg, 0.02 mmol) in MeOH/toluene (1:4 v/v). The reaction was stirred for 4 days. Product **140** yield: 43 mg (50%).

Entry 21, Table 3

According to **GP2**: *N*-(Benzyloxycarbonyl)hydroxylamine (57 mg, 0.34 mmol), 1,3-cyclohexadiene (137 mg, 1.70 mmol) and CuI (3 mg, 0.02 mmol) in chloroform. The reaction was stirred for 4 days. Product **140** yield: 59 mg (70%).

Entry 22, Table 3

According to **GP2**: *N*-(Benzyloxycarbonyl)hydroxylamine (55 mg, 0.33 mmol), 1,3-cyclohexadiene (132 mg, 1.70 mmol) and $CuCl_2$ (2 mg, 0.02 mmol) in chloroform. The reaction was stirred for 15 hours. Product **140** yield: 62 mg (77%).

Entry 23, Table 3

According to **GP2**: *N*-(Benzyloxycarbonyl)hydroxylamine (50 mg, 0.30 mmol), 1,3-cyclohexadiene (120 mg, 1.50 mmol) and $CuBr_2$ (3 mg, 0.02 mmol) in chloroform. The reaction was stirred for 15 hours. Product **140** yield : 50 mg (68%).

Entry 24, Table 3

According to **GP2**: *N*-(Benzyloxycarbonyl)hydroxylamine (54 mg, 0.32 mmol), 1,3-cyclohexadiene (129 mg, 1.62 mmol) and $Cu(OAc)_2$ (3 mg, 0.02 mmol) in chloroform. The reaction was stirred for 5 days. Product **140** yield: 41 mg (52%).

3.3 Thiourea oxazoline ligands screening

Entry 1, Table 4

According to **GP1**: *N*-(Benzyloxycarbonyl)hydroxylamine (127 mg, 0.76 mmol) 1,3-cyclohexadiene (305 mg, 3.80 mmol) and $CuCl_2$ (5 mg, 0.04 mmol). The reaction was stirred for 2 days. Product **140** yield: 140 mg (75%).

Entry 2, Table 4

According to **GP1**: *N*-(Benzyloxycarbonyl)hydroxylamine (120 mg, 0.72 mmol), 1,3-cyclohexadiene (287 mg, 3.58 mmol), $CuCl_2$ (5 mg, 0.04 mmol) and L2up (15 mg, 0.04 mmol). The reaction was stirred for 2 days. Product **140** yield: 142 mg (81%).

Entry 3, Table 4

According to **GP1**: *N*-(Benzyloxycarbonyl)hydroxylamine (138 mg, 0.83 mmol), 1,3-cyclohexadiene (331 mg, 4.13 mmol), $CuCl_2$ (6 mg, 0.04 mmol) and L2down (17 mg, 0.04 mmol). The reaction was stirred for 2 days. Product **140** yield: 142 mg (70%).

Entry 4, Table 4

According to **GP1**: *N*-(Benzyloxycarbonyl)hydroxylamine (125 mg, 0.75 mmol), 1,3-cyclohexadiene (300 mg, 3.74 mmol), $CuCl_2$ (1 mg, 0.007 mmol) and L11down (4 mg, 0.007 mmol). The reaction was stirred for 2 days. Product **140** yield: 138 mg (75%).

Entry 5, Table 4

According to **GP1**: *N*-(Benzyloxycarbonyl)hydroxylamine (110 mg, 0.66 mmol), 1,3-cyclohexadiene (264 mg, 3.30 mmol), $CuCl_2$ (4 mg, 0.03 mmol) and L6 (13 mg, 0.03 mmol). The reaction was stirred for 2 days. Product **140** yield: 125 mg (77%). The enantiomeric excess of cycloadduct **140** was determined by HPLC using Chiralcel OD column, 254 nm UV detector, IPA/hexane, 1:9 v/v, produce peaks at retention times of 14.09 and 18.05 minutes.

3.4 Reaction of *N*-(benzyloxycarbonyl)-hydroxylamine with 1,3-cyclohexadiene using different Cu-ligand(s) catalyst

GP 3: *General procedure for the nitroso-Diels-Alder reaction forming benzyl 2-oxa-3-azabicyclo[2.2.2]oct-5-ene-3-carboxylate **140** using different ligands*

1,3-Cyclohexadiene was added to a microwave tube, which contained the $CuCl_2$ (10 mol%) and ligand in the chloroform (5 mL). *N*-(Benzyloxycarbonyl)-hydroxylamine was added to the solution. The resulting solution was stirred and monitored by TLC. The completion of the reaction was confirmed by the disappearance of the starting material spot on the TLC. The solvent was removed under reduced pressure. The crude product was purified by silica gel column chromatography (hexane/EtOAc, 6:1 v/v, as the eluent) to obtain the product as a white solid.

Entry 1, Table 5

According to **GP3**: *N*-(Benzyloxycarbonyl)hydroxylamine (101 mg, 0.60 mmol), 1,3-cyclohexadiene (242 mg, 3.02 mmol) and $CuCl_2$ (8 mg, 0.06 mmol). The reaction was stirred for 24 hours. Product **140** yield: 71 mg (48%).

Entry 2, Table 5

According to **GP3**: *N*-(Benzyloxycarbonyl)hydroxylamine (104 mg, 0.62 mmol), 1,3-cyclohexadiene (249mg, 3.10 mmol), $CuCl_2$ (8 mg, 0.06 mmol) and tetramethylthiourea (8 mg, 0.06 mmol). The reaction was stirred for 15 hours. Product **140** yield: 91 mg (60%).

Entry 3, Table 5

According to **GP3**: *N*-(Benzyloxycarbonyl)hydroxylamine (102 mg, 0.61 mmol), 1,3-cyclohexadiene (244 mg, 3.05 mmol), $CuCl_2$ (8 mg, 0.06 mmol) and tetramethylthiourea (16 mg, 0.12 mmol). The reaction was stirred for 15 hours. Product **140** yield: 82 mg (55%).

Entry 4, Table 5

According to **GP3**: *N*-(Benzyloxycarbonyl)hydroxylamine (103 mg, 0.62 mmol), 1,3-cyclohexadiene (247 mg, 3.08 mmol), $CuCl_2$ (8 mg, 0.06 mmol) and 2-ethyl-2-oxazoline (6 mg, 0.06 mmol). The reaction was stirred for 15 hours. Product **140** yield: 80 mg (53%).

Entry 5, Table 5

According to **GP3**: *N*-(Benzyloxycarbonyl)hydroxylamine (104 mg, 0.62 mmol), 1,3-cyclohexadiene (249 mg, 3.10 mmol), $CuCl_2$ (8 mg, 0.06 mmol) and 2-ethyl-2-oxazoline (12 mg, 0.12 mmol). The reaction was stirred for 3 hours. Product **140** yield: 110 mg (72%).

Entry 6, Table 5

According to **GP3**: *N*-(Benzyloxycarbonyl)hydroxylamine (102 mg, 0.61 mmol), 1,3-cyclohexadiene (245 mg, 3.05 mmol), $CuCl_2$ (8 mg, 0.06 mmol), tetramethylthiourea (8 mg, 0.06 mmol) and 2-ethyl-2-oxazoline (6 mg, 0.06 mmol). The reaction was stirred for 15 hours. Product **140** yield: 102 mg (68%).

Entry 7, Table 5

According to **GP3**: *N*-(Benzyloxycarbonyl)hydroxylamine (61 mg, 0.37 mmol), 1,3-cyclohexadiene (123 mg, 1.53 mmol), $CuCl_2$ (5 mg, 0.04 mmol), and *(+)*-2,2′-Isopropylidenebis[(4R)-4-benzyl-2-oxazoline] **145** (13 mg, 0.04 mmol). The reaction was stirred for 2 hours. Product **140** yield: 63 mg (70%).

3.5 The reaction of *N*-(benzyloxycarbonyl)hydroxylamine 138 with various dienes

3.5.1 Reaction in chloroform

GP 4: *General procedure for the in situ nitroso-generation-Diels-Alder reaction using N-(benzyloxycarbonyl)hydroxylamine **138** with various dienes in chloroform*

To a $CHCl_3$ (5 ml) solution of the appropriate diene, $CuCl_2$ and ligand (2-ethyl-2-oxazoline) was added *N*-(benzyloxycarbonyl)hydroxylamine. The resulting

solution was stirred at room temperature in air and was monitored by TLC. The completion of the reaction was confirmed by the disappearance of the starting material. The solvent was removed by evaporation and the crude product was purified by silica gel chromatography (hexane: ethyl acetate, 6:1 v/v, as eluent).

Entry 1, Table 6

1-(2-Oxa-3-azabicyclo[2.2.1]hept-5-en-3-yl)-2-phenylethanone **146**

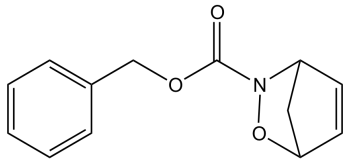

According to **GP4**: Using *N*-(benzyloxycarbonyl)hydroxylamine (135 mg, 0.81 mmol), freshly cracked cyclopentadiene (64 mg, 0.97 mmol), $CuCl_2$ (11 mg, 0.08 mmol) and 2-ethyl-2-oxazoline (16 mg, 0.16 mmol), the reaction was stirred for 4 h giving **146** as a white solid (185 mg, 99%); m.p. 76-78 °C (lit. 58-60 °C). ^{1}H NMR (400 MHz, $CDCl_3$) δ 7.37 – 7.32 (m, 5H), 6.36 (t, *J* = 1.9 Hz, 2H), 5.24 – 5.21 (m, 1H), 5.18 (d, *J* = 12.2 Hz, 1H), 5.11 (d, *J* = 12.2 Hz, 1H), 5.03 (dd, *J* = 2.2, 1.0 Hz, 1H), 1.99 (d, *J* = 8.7 Hz, 1H), 1.75 – 1.71 (m, 1H); ^{13}C{^{1}H} NMR (101 MHz, $CDCl_3$) δ 159.30, 135.7, 134.5, 133.0, 128.5, 128.3, 128.1, 83.8, 67.8, 65.1, 48.2; FTIR (thin film) *inter alia* 1737, 1702, 1333, 1269, 1176, 1088, 843, 731, 696 cm^{-1}; LRMS (ESI+) m/z 254.2 (M+ + Na); HRMS (ESI+) m/z Calcd for $C_{13}H_{13}NO_3Na$ 254.0817 found 254.0809.[17c]

Entry 2, Table 6

1-((1*R*,4*S*)-2-Oxa-3-azabicyclo[2.2.2]oct-5-en-3-yl)-2-phenylethanone **140**

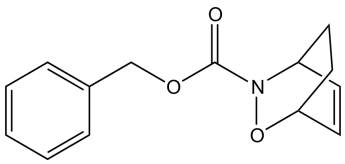

According to **GP4**: Using *N*-(benzyloxycarbonyl)hydroxylamine (129 mg, 0.77 mmol), 1,3-cyclohexadiene (77 mg, 0.96 mmol), $CuCl_2$ (10 mg, 0.08 mmol) and 2-ethyl-2-oxazoline (15 mg, 0.15 mmol), the reaction was stirred for 3 h, giving **140** as a white solid (163 mg, 86%); m.p. 84-86 °C; ^{1}H NMR (400 MHz, $CDCl_3$) δ 7.45 – 7.28 (m, 5H), 6.67 – 6.46 (m, 2H), 5.24 – 5.17 (m, 1H), 5.13 (d, *J* = 12.3 Hz, 1H), 4.82

(dt, *J* = 7.9, 2.8 Hz, 1H), 4.76 (ddd, *J* = 5.5, 3.8, 1.8 Hz, 1H), 2.26 – 2.17 (m, 1H), 2.12 (ddt, *J* = 12.4, 9.0, 3.1 Hz, 1H), 1.53 – 1.44 (m, 1H), 1.42 – 1.34 (m, 1H); $^{13}C\{^{1}H\}$ NMR (101 MHz, $CDCl_3$) δ 158.1, 136.0, 132.0, 131.6, 128.5, 128.2, 128.1, 71.0, 67.7, 50.2, 23.5, 20.6; FTIR (thin film) *inter alia* 1698, 1265, 1049, 744, 696 cm^{-1}; LRMS (ESI+) m/z 268.1 (M+ + Na); HRMS (ESI+) m/z Calcd for $C_{14}H_{15}NO_3Na$ 268.0950 found 268.0928.

Entry 3, Table 6

1-(4,5-Dimethyl-3,6-dihydro-2*H*-1,2-oxazin-2-yl)-2-phenylethanone **147**

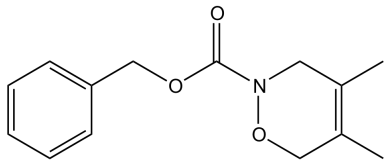

According to **GP4**: Using *N*-(benzyloxycarbonyl)hydroxylamine (135 mg, 0.81 mmol), 2,3-dimethyl-1,3-butadiene (80 mg, 0.97 mmol), $CuCl_2$ (11 mg, 0.08 mmol) and 2-ethyl-2-oxazoline (16 mg, 0.16 mmol), the reaction was stirred for 24 h. The ratio of **147** to **148** was determined on the crude product by ^{1}H NMR using the signals at δ 1.66 and 1.58 (CH_3 signals for **147**) *versus* the signal at δ 1.92 (CH_3 for **148**), and the signals at δ 3.97 and 4.22 (each CH_2 in **147**) versus the signals δ 4.39 (CH_2 in **148**)**.** Purification of the crude product gave **147** as a colourless oil (150 mg, 75%). The ratio of **147**:**148** = 7:1: ^{1}H NMR (400 MHz, $CDCl_3$) δ 7.40 – 7.32 (m, 5H), 5.21 (s, 2H), 4.22 (d, *J* = 1 Hz, 2H), 3.97 (dd, *J* = 2, 1 Hz, 2H), 1.66 (dd, *J* = 2, 1 Hz, 3H), 1.58 (dd, *J* = 2, 1 Hz, 3H); $^{13}C\{^{1}H\}$ NMR (101 MHz, $CDCl_3$) δ 155.5, 136.1, 128.5, 128.2, 128.1, 123.1, 121.8, 71.6, 67.6, 48.4, 15.2, 13.8; FTIR (thin film) *inter alia* 1709 (C=O), 1216, 1087, 752, 696 cm^{-1}; LRMS (ESI+) m/z 270.2 (M+ + Na); HRMS (ESI+) m/z Calcd for $C_{14}H_{17}NO_3Na$ 270.1106 found 270.1107.

Entry 4, Table 6

1-(3,6-Dimethyl-3,6-dihydro-2*H*-1,2-oxazin-2-yl)-2-phenylethanone **149**

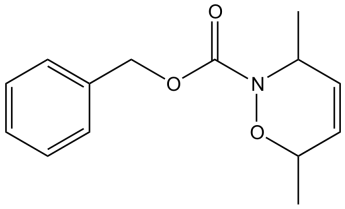

According to **GP4**: Using *N*-(benzyloxycarbonyl)hydroxylamine (144 mg, 0.86

mmol), 2,4-hexadiene (69 mg, 1.04 mmol), $CuCl_2$ (12 mg, 0.09 mmol) and 2-ethyl-2-oxazoline (17 mg, 0.17 mmol), the reaction was stirred for 5 h, giving **149** (177 mg, 83%). ^{1}H NMR (400 MHz, $CDCl_3$) δ 7.42 – 7.28 (m, 5H), 5.77 (ddt, *J* = 8.8, 4.4, 2.2 Hz, 1H), 5.69 – 5.64 (m, 1H), 5.28 – 5.23 (m, 1H), 5.17 (d, *J* = 12.4 Hz, 1H), 4.64 (d, *J* = 6.0 Hz, 1H), 4.49 (ddd, *J* = 8.5, 4.2, 2.0 Hz, 1H), 1.34 – 1.29 (m, 3H), 1.27 (d, *J* = 6.7 Hz, 3H); ^{13}C{^{1}H} NMR (101 MHz, $CDCl_3$) δ 154.7, 136.3, 128.8, 128.5, 128.1, 127.9, 127.7, 73.9, 67.3, 50.1, 18.8, 18.2; FTIR (thin film) *inter alia* 1698 (C=O), 1202, 1286, 1113, 1064, 751, 696 cm^{-1}; LRMS (ESI+) m/z 270.9 (M+ + Na); HRMS (ESI+) m/z Calcd for $C_{14}H_{17}NO_3Na$ 270.1106 found 270.1086.

Entry 5, Table 6

1-(4-Methyl-3,6-dihydro-2*H*-1,2-oxazin-2-yl)-2-phenylethanone **150** and 1-(5-methyl-3,6-dihydro-2*H*-1,2-oxazin-2-yl)-2-phenylethanone **150'**

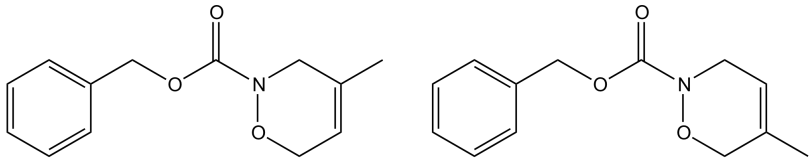

According to **GP4**: Using *N*-(benzyloxycarbonyl)hydroxylamine (140 mg, 0.837 mmol), isoprene (68.5 mg, 1.00 mmol), $CuCl_2$ (11 mg, 0.08 mmol) and 2-ethyl-2-oxazoline (17 mg, 0.17 mmol), the reaction was stirred for 24 h. The ratio of **150** to **150'** to **151** was determined on the crude product by ^{1}H NMR using the signals at δ 1.74 to 1.66 (CH_3 resonances in **150** and **150'** respectively) to 4.70 (CH_2 in **151).** Purification of the crude product gave **150** and **150'** as a viscous oil (143 mg, 73%). The ratio of **150**:**150'** = 2:1 and ratio of **150** and **150'**:**151** = 9:1;

150: ^{1}H NMR (400 MHz, $CDCl_3$) δ 7.43 – 7.32 (m, 5H), 5.57 – 5.54(m, 1H), 5.24 (s, 2H), 4.41 (td, *J* = 4.5, 2.2 Hz, 2H), 4.04 (td, *J* = 3.3, 2.4 Hz, 2H), 1.80 – 1.72 (m, 3H); ^{13}C{^{1}H} NMR (101 MHz, $CDCl_3$) δ 155.5, 136.1, 130.1, 128.5, 128.2, 128.1, 118.0, 68.5, 67.7, 48.5, 19.7.

150': ^{1}H NMR (400 MHz, $CDCl_3$) δ 7.45 – 7.30 (m, 5H), 5.54-5.52 (m, 1H), 5.23 (s, 2H), 4.33 – 4.28 (m, 2H), 4.16 – 4.10 (m, 2H), 1.70-1.66 (m, 3H); ^{13}C{^{1}H} NMR (101 MHz, $CDCl_3$) δ 155.5, 136.1, 131.6, 128.5, 128.2, 128.1, 116.3, 71.6, 67.7, 44.8, 18.2; FTIR (thin film) *inter alia* 1706 (C=O), 1214, 1097, 751, 696 cm^{-1}; LRMS (ESI+) m/z 256.5 (M+ + Na); HRMS (ESI+) m/z Calcd for $C_{13}H_{15}NO_3Na$ 256.0950 found 256.0959.

Entry 6, Table 6

1-((9*s*,10*s*)-9,10-Dimethyl-9,10-dihydro-9,10-(epoxyimino)anthracen-11-yl)-2-phenylethanone **152**

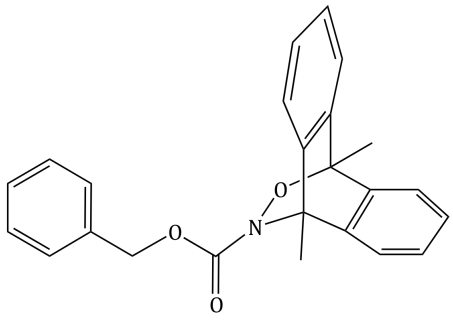

According to **GP4**: Using *N*-(benzyloxycarbonyl)hydroxylamine (65 mg, 0.39 mmol), 9,10-dimethylanthracene (67 mg, 0.32 mmol), $CuCl_2$ (5 mg, 0.04 mmol) and 2-ethyl-2-oxazoline (8 mg, 0.08 mmol), the reaction was stirred for 24 h, giving **152** as a white solid (124 mg, 86%); m.p. 133- 134 °C (lit. 132 – 134 °C).[17c] ^{1}H NMR (400 MHz, $CDCl_3$) δ 7.49 – 7.45 (m, 2H), 7.42 – 7.39 (m, 2H), 7.29 – 7.26 (m, 4H), 7.26-7.22 (m 3H), 7.01 – 6.95 (m, 2H), 5.00 (s, 2H), 2.63 (s, 3H), 2.27 (s, 3H); ^{13}C{^{1}H} NMR (101 MHz, $CDCl_3$) δ 159.6, 141.8, 140.5, 136.2, 128.2, 127.6, 127.2, 127.2, 127.0, 121.5, 120.7, 79.1, 67.1, 64.0, 16.5, 15.0; FTIR (thin film) *inter alia* 1698, 1278, 1258, 752, 696 cm^{-1}; LRMS (ESI+) m/z 394.1 (M+ + Na); HRMS (ESI+) m/z Calcd for $C_{24}H_{21}NO_3Na$ 394.1419 found 394.1425.

Entry 7, Table 6

1-(3,6-Diphenyl-3,6-dihydro-2*H*-1,2-oxazin-2-yl)-2-phenylethanone **153**

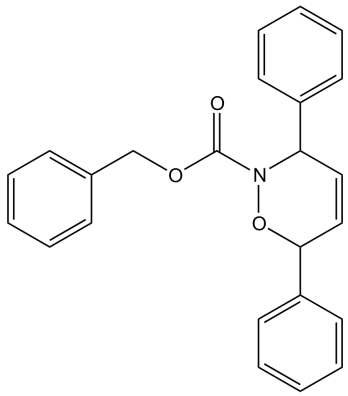

According to **GP4**: Using *N*-(benzyloxycarbonyl)hydroxylamine (128 mg, 0.77 mmol), 1,4-diphenyl-1,3-butadiene (132 mg, 0.64 mmol), $CuCl_2$ (10 mg, 0.08 mmol) and 2-ethyl-2-oxazoline (15 mg, 0.15 mmol), the reaction was stirred for 24 h, giving **153** as a colourless oil (211 mg, 74%); ^{1}H NMR (400 MHz, $CDCl_3$) δ 7.55 –

7.32 (m, 15H), 6.18 – 6.13 (m, 1H), 6.11 – 6.06 (m, 1H), 5.66 (s, 1H), 5.61 (s, 1H), 5.32 (d, *J* = 12.4 Hz, 1H), 5.18 (d, *J* = 12.4 Hz, 1H); $^{13}C\{^{1}H\}$ NMR (101 MHz, $CDCl_3$) δ 154.8, 138.7, 137.0, 136.2, 129.0, 128.7, 128.6, 128.5, 128.2, 128.1, 128.0, 128.0, 127.9, 127.7, 126.0, 79.7, 67.6, 57.1; FTIR (thin film) *inter alia* 1698 (C=O), 1272, 1091, 750, 720, 695; LRMS (ESI+) m/z 394.2 (M+ + Na); HRMS (ESI+) m/z Calcd for $C_{24}H_{21}NO_3Na$ 394.1419 found 394.1416.

3.5.2 Reaction in methanol

GP5: *General procedure for the in situ nitroso-generation-Diels-Alder reaction using N-(benzyloxycarbonyl)hydroxylamine **138** with various dienes in methanol*

To a MeOH (5 ml) solution of the appropriate diene, 10 mol% $CuCl_2$ and 20 mol% 2-ethyl-2-oxazoline was added *N*-(benzyloxycarbonyl)hydroxylamine**.** The resulting solution was stirred at room temperature in air and was monitored by TLC. The completion of the reaction was confirmed by the disappearance of the starting material. The solvent was removed by evaporation and the crude product was purified by silica gel chromatography (hexane: ethyl acetate, 6:1 v/v, as eluent).

Entry 1, Table 7

According to **GP5**: *N*-(Benzyloxycarbonyl)hydroxylamine (132 mg, 0.79 mmol), 1.2 equivalent of cyclopentadiene (63 mg, 0.95 mmol), $CuCl_2$ (11 mg, 0.08 mmol) and 2-ethyl-2-oxazoline (16 mg, 0.16 mmol). The reaction was stirred for 3 hours. Product **146** yield: 177 mg (97%).

Entry 2, Table 7

According to **GP5**: *N*-(Benzyloxycarbonyl)hydroxylamine (137mg, 0.82 mmol), 1.2 equivalent of 1,3-cyclohexadiene (79 mg, 0.99 mmol), $CuCl_2$ (11 mg, 0.08 mmol) and 2-ethyl-2-oxazoline (16 mg, 0.16 mmol). The reaction was stirred for 3 hours. Product **140** yield: 185 mg (92%).

Entry 3, Table 7

According to **GP5**: *N*-(Benzyloxycarbonyl)hydroxylamine (129 mg, 0.77 mmol), 1.2 equivalent of 2,3-dimethyl-1,3-butadiene (76 mg, 0.93 mmol), $CuCl_2$ (10 mg, 0.08

mmol) and 2-ethyl-2-oxazoline (15 mg, 0.15 mmol). The reaction was stirred for 2 hours. The ratio of **147**:**148** = 5:1. Total product yield: 158 mg (83%).

Entry 4, Table 7

According to **GP5**: *N*-(Benzyloxycarbonyl)hydroxylamine (134 mg, 0.80 mmol), 1.2 equivalent of 2,4-hexadiene (79 mg, 0.96 mmol), $CuCl_2$ (11 mg, 0.08 mmol) and 2-ethyl-2-oxazoline (16 mg, 0.16 mmol). The reaction was stirred for 2 hours. Product **149** yield: 192 mg (97%).

Entry 5, Table 7

According to **GP5**: *N*-(Benzyloxycarbonyl)hydroxylamine (140 mg, 0.84 mmol), 1.2 equivalent of isoprene (69 mg, 1.00 mmol), $CuCl_2$ (11 mg, 0.08 mmol) and 2-ethyl-2-oxazoline (17 mg, 0.17 mmol). The reaction was stirred for 8 hours. The ratio of cycloadduct **150**, **150'** to ene **151** was 8.5:1 and the ratio of **150**:**150'** was 2:1. Total product yield: 155 mg (79%).

Entry 6, Table 7

According to **GP5**: *N*-(Benzyloxycarbonyl)hydroxylamine (55 mg, 0.33 mmol), 9,10-dimethyl anthracene (57 mg, 0.28 mmol), $CuCl_2$ (4 mg, 0.03 mmol) and 2-ethyl-2-oxazoline (7 mg, 0.07 mmol). The reaction was stirred for 10 hours. Product **152** yield: 90 mg (88%).

Entry 7, Table 7

According to **GP5**: *N*-(Benzyloxycarbonyl)hydroxylamine (104 mg, 0.62 mmol), 1,4-diphenyl-1,3-butadiene(107 mg, 0.52 mmol), $CuCl_2$ (8 mg, 0.06 mmol) and 2-ethyl-2-oxazoline (12 mg, 0.12 mmol). The reaction was stirred for 18 hours. Product **153** yield: 152 mg (79%).

3.6 Solvent effect of the nitroso-Diels-Alder *versus* ene reaction

GP6: *General procedure for the nitroso-Diels-Alder reaction forming benzyl 2-oxa-3-azabicyclo[2.2.2]oct-5-ene-3-carboxylate **146** in various solvent*

N-(Benzyloxycarbonyl)hydroxylamine dissolved in solvent (10 mL) was added dropwise to a solution of 2,3-dimethyl-1,3-butadiene (2 equivalents), 10% $CuCl_2$ and 20% 2-ethyl-2-oxazoline in 20 mL of solvent at room temperature. The reaction mixture was stirred and monitored by TLC. The solvent was removed under vacuum. The crude product was purified by silica gel chromatography (6:1 v/v, hexane/EtOAc) to obtain the product.

Entry 1, Table 8 MeOH as a solvent

According to **GP6**: *N*-(Benzyloxycarbonyl)hydroxylamine(101 mg, 0.60 mmol), 2,3-dimethyl-1,3-butadiene (96 mg, 1.20 mmol), $CuCl_2$ (8 mg, 0.06 mmol) and 2-ethyl-2-oxazoline (12 mg, 0.12 mmol) the reaction was stirred for 2 h. The ratio of **147**:**148** = 5:1. Total product yield: 125 mg (84%).

Entry 2, Table 8 MTBE as a solvent

According to **GP6**: *N*-(Benzyloxycarbonyl)hydroxylamine (103 mg, 0.62 mmol), 2,3-dimethyl-1,3-butadiene (98 mg, 1.23 mmol), $CuCl_2$ (8 mg, 0.06 mmol) and 2-ethyl-2-oxazoline (12 mg, 0.12 mmol) the reaction was stirred for 20 h. The ratio of **147**:**148** = 15:1. Total product yield: 130 mg (85%).

Entry 3, Table 8 MeCN as a solvent

According to **GP6**: *N*-(Benzyloxycarbonyl)hydroxylamine (108 mg, 0.65 mmol), 2,3-dimethyl-1,3-butadiene (104 mg, 1.30 mmol), $CuCl_2$ (9 mg, 0.07 mmol) and 2-ethyl-2-oxazoline (13 mg, 0.13 mmol) the reaction was stirred for 144 h. The ratio of **147**:**148** = 25:1. Total product yield: 128 mg (80%).

Entry 4, Table 8 EtOH as a solvent

According to **GP6**: *N*-(Benzyloxycarbonyl)hydroxylamine (105 mg, 0.63 mmol), 2,3-dimethyl-1,3-butadiene (101 mg, 1.26 mmol), $CuCl_2$ (9 mg, 0.06 mmol) and 2-ethyl-2-oxazoline (13 mg, 0.13 mmol) the reaction was stirred for 7 h. The ratio of **147**:**148** = 4:1. Total product yield: 130 mg (83%).

Entry 5, Table 8 EtOAc as a solvent

According to **GP6**: *N*-(Benzyloxycarbonyl)hydroxylamine (117 mg, 0.70 mmol), 2,3-dimethyl-1,3-butadiene (112 mg, 1.40 mmol), $CuCl_2$ (9 mg, 0.07 mmol) and 2-ethyl-2-oxazoline (14 mg, 0.14 mmol) the reaction was stirred for 7 h. The ratio of **147**:**148** = 4:1. Total product yield: 141 mg (81%).

Entry 6, Table 8 IPA as a solvent

According to **GP6**: *N*-(Benzyloxycarbonyl)hydroxylamine (102 mg, 0.61 mmol), 2,3-dimethyl-1,3-butadiene (98 mg, 1.22 mmol), $CuCl_2$ (8 mg, 0.06 mmol) and 2-ethyl-2-oxazoline (12 mg, 0.12 mmol) the reaction was stirred for 48 h. The ratio of **147**:**148** = 13:1. Total product yield: 135 mg (89%).

Entry 7, Table 8 2Methyl-THF as a solvent

According to **GP6**: *N*-(Benzyloxycarbonyl)hydroxylamine (107 mg, 0.64 mmol), 2,3-dimethyl-1,3-butadiene (103 mg, 1.28 mmol), $CuCl_2$ (9 mg, 0.06 mmol) and 2-ethyl-2-oxazoline (13 mg, 0.13 mmol) the reaction was stirred for 20 h. The ratio of **147**:**148** = 12:1. Total product yield: 140 mg (88%).

Entry 8, Table 8 Toluene as a solvent

According to **GP6**: *N*-(Benzyloxycarbonyl)hydroxylamine (107 mg, 0.64 mmol), 2,3-dimethyl-1,3-butadiene (102 mg, 1.28 mmol), $CuCl_2$ (9 mg, 0.06 mmol) and 2-ethyl-2-oxazoline (13 mg, 0.13 mmol) the reaction was stirred for 4 h. The ratio of **147**:**148** = 12:1. Total product yield: 129 mg (82%).

Entry 9, Table 8 4:1 Toluene/MeOH as a solvent

According to **GP6**: *N*-(Benzyloxycarbonyl)hydroxylamine (113 mg, 0.68 mmol), 2,3-dimethyl-1,3-butadiene (108 mg, 1.35 mmol), $CuCl_2$ (9 mg, 0.07 mmol) and 2-ethyl-2-oxazoline (13 mg, 0.14 mmol) the reaction was stirred for 3 h. The ratio of **147**:**148** = 5:1. Total product yield: 137 mg (82%).

Entry 10, Table 8 Chloroform as a solvent

According to **GP6**: *N*-(Benzyloxycarbonyl)hydroxylamine (116 mg, 0.69 mmol), 2,3-dimethyl-1,3-butadiene (111 mg, 1.38 mmol), $CuCl_2$ (9 mg, 0.07 mmol) and 2-

ethyl-2-oxazoline (14 mg, 0.14 mmol) the reaction was stirred for 3 h. The ratio of **147**:**148** = 7:1. Total product yield: 121 mg (82%).

3.7 Chiral oxazoline ligand screening

***GP7** : General procedure for 10% $CuCl_2$ and chiral ligand catalytic system*

To a methanol (5 ml) solution of the 1,3-cyclohexadiene, 10% $CuCl_2$ and 10% ligand was added hydroxamic acid**.** The resulting solution was stirred at room temperature in air and was monitored by TLC. The completion of the reaction was confirmed by the disappearance of the starting material. The solvent was removed by evaporation and the crude product was purified by silica gel chromatography (hexane: ethyl acetate, 6:1 v/v, as eluent).

Entry 1, Table 9

According to **GP7**: *N*-(Benzyloxycarbonyl)hydroxylamine (55 mg, 0.33 mmol), 1,3-cyclohexadiene (48 mg, 0.60 mmol), $CuCl_2$ (4 mg, 0.03 mmol) and 2,2′-bis[(4*S*)-4-benzyl-2-oxazoline] **157** (12 mg, 0.03 mmol). The reaction was completed in 2 hours to yield the product **140** as a white solid (74 mg, 98%).

Entry 2, Table 9

According to **GP7**: *N*-(Benzyloxycarbonyl)hydroxylamine (57 mg, 0.34 mmol), 1,3-cyclohexadiene (54 mg, 0.68 mmol), $CuCl_2$ (4 mg, 0.03 mmol) and (+)-2,2′-isopropylidenebis[(4*R*)-4-benzyl-2-oxazoline] **145** (11 mg, 0.03 mmol). The reaction was completed in 2 hours to yield the product **140** as a white solid (77 mg, 99%).

Entry 3, Table 9

According to **GP7**: *N*-(Benzyloxycarbonyl)hydroxylamine (50 mg, 0.30 mmol), 1,3-cyclohexadiene (48 mg, 0.60 mmol), $CuCl_2$ (4 mg, 0.03 mmol) and 2,6-bis[(4*S*)-(−)-isopropyl-2-oxazolin-2-yl]pyridine **158** (9 mg, 0.03 mmol). The reaction was completed in 2 hours to yield the product **140** as a white solid (66 mg, 96%). The enantiomeric excess of cycloadduct **140** was determined by HPLC using Chiralcel OD column, 254 nm UV detector, IPA:hexane, 1:9 v/v, produced peaks at retention time 14.09 and 18.05 minutes.

3.8 Hydroxamic acids synthesis

GP8: *General procedure of hydroxamic acid synthesis:*

Four equivalents of sodium hydroxide were dissolved in water followed by two equivalents of hydroxylamine hydrochloride. Then this solution was added dropwise to the appropriate ester in methanol. The reaction was stirred at room temperature for 4 hours and monitored by TLC. When the reaction finished, the solution was acidified with 5% HCl to pH 5.5. The solvent was removed in vacuum to yield a mixture of product and sodium chloride, which then redissolved in methanol. The sodium chloride was removed by filtration. The methanol was removed in vacuum to give the corresponding product, which then recrystallised from hot water to give the pure product.

2-Pyridinehydroxamic acid 161

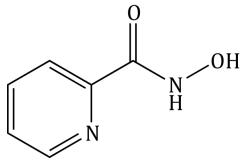

According to **GP8**: Ethyl-2-picolinate (5.00 g, 33 mmol) in 100 ml of methanol, sodium hydroxide (5.29 g, 132 mmol), hydroxylamine hydrochloride (4.60 g, 66 mmol) in 100 ml of water. The product **161** was isolated as a white solid (3.00 g, 66%); m.p. 119 – 120 °C; ^{1}H NMR (400 MHz, DMSO-d_6) δ 11.46 (s, 1H), 9.24 (s, 1H), 8.63 (dt, *J* = 4.8, 1.3 Hz, 1H), 8.04 – 7.97 (m, 2H), 7.64 – 7.57 (m, 1H); ^{13}C{^{1}H} NMR (101 MHz, DMSO-d_6) δ 162.2, 151.0, 149.4, 138.5, 127.2, 122.7.; FTIR (thin film) *inter alia* 3264 (broad), 2778 (broad), 1662 (C=O), 1592, 1570, 1516, 1475, 1177, 1030, 816; LRMS (ESI-) m/z 161.4 (M^+ Na); HRMS (ESI+) m/z Calcd for $C_6H_6N_2O_2Na$ 161.0327 found 161.0323.

3-Pyridinehydroxamic acid 162

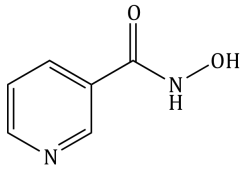

According to **GP8**: Ethyl nicotinate (5.00 g, 33 mmol) in 100 ml of methanol, sodium hydroxide (5.29 g, 132 mmol), hydroxylamine hydrochloride (4.60 g, 66 mmol) in 100 ml of water. The product **162** was isolated as a white solid (2.70 g, 59%): m.p. 160 – 161 °C; ^{1}H NMR (400 MHz, DMSO-d_6) δ 11.37 (s, 1H), 9.59 – 8.99 (m, 1H), 8.89 (dt, *J* = 20.8, 10.4 Hz, 1H), 8.74 – 8.61 (m, 1H), 8.18 – 8.00 (m, 1H), 7.49 (ddd, *J* = 7.9, 4.8, 0.8 Hz, 1H); ^{13}C{^{1}H} NMR (101 MHz, DMSO-d_6) δ 162.9, 152.3, 148.3, 135.1, 128.9, 124.0; FTIR (thin film) *inter alia* 1634 (C=O), 1594, 1495, 1472, 1422, 1305, 1024, 700; LRMS (ESI-) m/z 137.1 (M^+ -H); HRMS (ESI-) m/z Calcd for $C_6H_5N_2O_2$ 137.0351 found 137.0332.

***N*-Hydroxy-2-(pyridin-2-yl)acetamide 163**

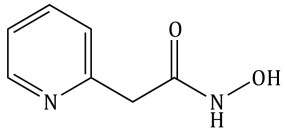

According to **GP8**: Ethyl 2-pyridylacetate (2.00 g, 12.1 mmol) in 50ml of methanol, sodium hydroxide (1.94 g, 48.4 mmol), hydroxylamine hydrochloride (1.68 g, 24.2 mmol) in 50 ml of water. The product **163** was isolated as a white solid (0.93g, 50%): m.p. 159 – 161 °C; ^{1}H NMR (600 MHz, DMSO-d_6) δ 10.93 (s, 1H), 8.97 (s, 1H), 8.57 (d, *J* = 4.3 Hz, 1H), 7.96 (dd, *J* = 7.6, 6.4 Hz, 1H), 7.52 (d, *J* = 7.8 Hz, 1H), 7.47 – 7.41 (m, 1H), 3.64 (s, 2H); ^{13}C{^{1}H} NMR (151 MHz, DMSO-d_6) δ 165.3, 154.5, 146.7, 139.1, 124.9, 122.8, 40.5; FTIR (thin film) *inter alia* 1677 (C=O), 1645, 1600, 1546, 1442, 1044, 1012, 797, 764, 616; LRMS (ESI+) m/z 175.4 (M^+ Na); HRMS (ESI+) m/z Calcd for $C_7H_8N_2O_2Na$ 175.0483 found 175.0473.

2-Amino-*N*-hydroxybenzamide 164

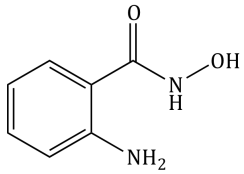

According to **GP8**: Methyl 2-aminobenzoate (10.00 g, 66.2 mmol) in 200 ml of methanol, sodium hydroxide (10.60 g, 265 mmol), hydroxylamine hydrochloride (9.20 g, 132 mmol) in 200 ml of water. The product **164** was isolated as a pale yellow solid (6.10 g, 60%): m.p. 143-145 °C; ^{1}H NMR (400 MHz, DMSO-d_6) δ 10.91 (s, 1H), 8.89 (s, 1H), 7.30 (dd, *J* = 13.1, 6.5 Hz, 1H), 7.12 (ddd, *J* = 8.5, 7.2, 1.5 Hz, 1H), 6.69 (dd, *J* = 8.2, 1.0 Hz, 1H), 6.51 – 6.44 (m, 1H), 6.22 (s, 2H); ^{13}C{^{1}H} NMR (101 MHz, DMSO-d_6) δ 166.8, 149.2, 131.5, 127.5, 116.2, 114.7, 113.2; FTIR (thin film) *inter alia* 3163, 2950, 2856, 1618, 1560, 1493, 1449, 1348, 1249, 1021, 741, 671; LRMS (ESI+) m/z 175.1 (M^+ +Na); HRMS (ESI+) m/z Calcd for $C_7H_8N_2O_2Na$ 175.0483 found 175.0473.

***N*-Hydroxybenzamide 165**

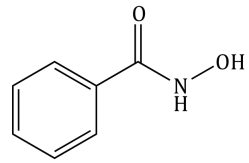

According to **GP8**: Methylbenzoate (5.30 g, 38.9 mmol) in 100 ml of methanol, sodium hydroxide (6.23 g, 156 mmol), hydroxylamine hydrochloride (5.41 g, 77.9 mmol) in 100 ml of water. The product **165** was isolated as a white solid (3.4 g, 64%); m.p. 121 – 123 °C; ^{1}H NMR (400 MHz, DMSO-d_6) δ 11.22 (s, 1H), 9.05 (s, 1H), 7.82 – 7.68 (m, 2H), 7.54 – 7.48 (m, 1H), 7.48 – 7.36 (m, 2H); ^{13}C{^{1}H} NMR (101 MHz, DMSO-d_6) δ 164.7, 133.3, 131.6, 128.8, 127.3; FTIR (thin film) *inter alia* 3292, 3062, 2746, 1644, 1602, 1557, 1490, 1316, 1163, 1022, 897, 787, 689; LRMS (ESI+) m/z 138.2 (M^+ +H); HRMS (ESI+) m/z Calcd for $C_7H_8NO_2$ 138.0555 found 138.055.

***N*-Hydroxy-2-phenylacetamide 166**

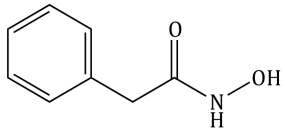

According to **GP8**: Methylphenylacetate (10.2 g, 67.9 mmol) in 200 ml of methanol, sodium hydroxide (10.9 g, 272 mmol), hydroxylamine hydrochloride (9.4 g, 135 mmol) in 200 ml of water. The product **166** was isolated as an off-white solid (5.6 g, 54%); m.p. 139–142°C; ^{1}H NMR (400 MHz, DMSO-d_6) δ 10.67 (s, 1H), 8.84 (s, 1H), 7.32 – 7.19 (m, 5H), 3.28 (s, 2H); ^{13}C{^{1}H} NMR (101 MHz, DMSO-d_6) δ 167.0, 136.1, 128.9, 128.1, 126.4, 39.4; FTIR (thin film) *inter alia* 3186, 3002, 2902, 1631 (C=O), 1548, 1495, 1455, 1054, 978, 715; LRMS (ESI-) m/z 150.2 (M^+ -H); HRMS (ESI+) m/z Calcd for $C_8H_8NO_2$ 150.0555 found 150.0555.

***N*-Hydroxy-3-phenylpropanamide 167**

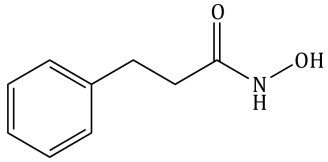

According to **GP8**: Ethylhydrocinnamate (9.4 g, 52.7 mmol) in 200 ml of methanol, sodium hydroxide (8.4 g, 210 mmol), hydroxylamine hydrochloride (7.3 g, 105 mmol) in 200 ml of water. The product **167** was isolated as a white solid (4.9 g, 56%); m.p. 75 – 77 °C; ^{1}H NMR (400 MHz, $CDCl_3$) δ 9.20 (s, 2H), 7.25 – 7.20 (m, 2H), 7.18 – 7.10 (m, 3H), 2.87 (t, *J* = 8 Hz, 2H), 2.38 (t, *J* = 8 Hz, 2H); ^{13}C{^{1}H} NMR (101 MHz, $CDCl_3$) δ 171.1, 140.2, 128.6, 128.3, 126.4, 34.6, 31.3; FTIR (thin film) *inter alia* 3296, 3062, 2782, 1662 (C=O), 1626, 1557, 1496, 1455, 1062, 995, 695; LRMS (ESI+) m/z 188.2 (M^+ +Na); HRMS (ESI+) m/z Calcd for $C_9H_{11}NO_2Na$ 188.0687 found 188.0689.

***N*-Hydroxy-4-phenylbutanamide 168**

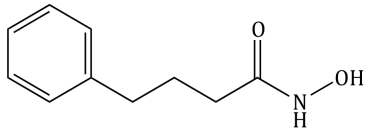

4-Phenylbutyric acid (7.4 g, 45.1 mmol), NMM (5.0 g, 50.5 mmol), DMAP (0.06 g, 0.05 mmol) and hydroxylamine hydrochloride (3.5 g, 50.5 mmol) were dissolved in 150 ml of DCM in 250 ml round bottom flask. The mixture was stirred and cooled to 0° C. Then cyanuric chloride (2.5 g, 15.0 mmol) was added to the solution and the mixture was warmed to room temperature. The reaction was stirred for 24 hours. After completion, the solution was filtered through Celite, then washed with 45 ml of 1 M HCl (3X). The organic layer was separated and dried over $MgSO_4$. The solvent was evaporated in vacuum to yield a white solid product, which was then purified by siliga gel column chromatography (EtOAc as eluent) to give product **168** (2.00 g, 25%); m.p. 71 – 74 °C; ^{1}H NMR (400 MHz, DMSO-d_6) δ 10.36 (s, 1H), 8.71 (s, 1H), 7.28 – 7.23 (m, 2H), 7.18 – 7.14 (m, 3H), 2.54 (t, *J* = 8.0 Hz, 2H), 1.95 (t, *J* = 8.0 Hz, 2H), 1.82 – 1.71 (m, 2H); ^{13}C{^{1}H} NMR (101 MHz, DMSO-d_6) δ 168.8, 141.6, 128.3, 128.3, 125.7, 34.6, 31.8, 27.0; FTIR (thin film) *inter alia* 3170, 3024, 2908, 1622 (C=O), 1542, 1495, 1459, 1065, 1016, 742, 694; LRMS (ESI+) m/z 202.2 (M^+ +Na); HRMS (ESI+) m/z Calcd for $C_{10}H_{13}NO_2Na$ 202.0844 found 202.0849.

***N*-Hydroxy-5-phenylpentanamide 169**

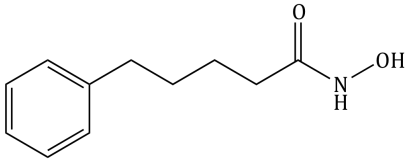

Hydrogen chloride gas generated from dropping 36% HCl into 98% H_2SO_4 was bubbled into a solution of 5-phenylvaleric acid (5.0 g, 28.1 mmol) in 150 ml of methanol at room temperature for 15 minutes. Then sodium hydroxide (4.5 g, 112 mmol), hydroxylamine hydrochloride (3.9 g, 56.2 mmol) in 100 ml of water was added dropwise to the solution. The reaction was stirred for 24 hours and then acidified to pH 5.5 using 10% HCl. The solvents were removed under vacuum. The

residue was redissolved in methanol and the sodium chloride was removed by filtration. The solvent then removed to yield a yellow oil, which was recrystalised from ether to yield a white solid product **169** (3.60 g, 67%); m.p. 68 – 71 °C; ^{1}H NMR (400 MHz, DMSO-d_6) δ 10.32 (s, 1H), 8.67 (s, 1H), 7.27 (t, *J* = 7.5 Hz, 2H), 7.20 – 7.14 (m, 3H) 2.56 (t, *J* = 6.7 Hz, 2H), 1.97 (t, *J* = 6.8 Hz, 2H), 1.63 – 1.39 (m, 4H); ^{13}C{^{1}H} NMR (101 MHz, DMSO-d_6) δ 169.0, 142.0, 128.2, 128.2, 125.6, 34.8, 32.1, 30.5, 24.8; FTIR (thin film) *inter alia* 3186, 3038, 2910, 1618 (C=O), 1434, 1085, 992, 962, 749, 698; LRMS (ESI+) m/z 216.2 (M^+ +Na); HRMS (ESI+) m/z Calcd for $C_{11}H_{15}NO_2Na$ 216.1000 found 216.1007.

Phenyl hydroxycarbamate 170

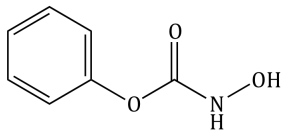

A solution of phenyl chloroformate (5.32 g, 34.0 mmol) in ether was added dropwise in 30 minutes to a stirred solution of hydroxylamide hydrochloride (2.36 g, 34.0 mmol) and potassium cabonate (5.17 g, 37.4 mmol) in 30 ml of ether and 5 ml of water at 5 °C. After the addition, the reaction was stirred at room temperature for 4 hours. The organic layer was separated and dried over $MgSO_4$. The solvent was evaporated *in vacuo* to yield a white solid product **170** (3.10 g, 59%); m.p. 98 – 101 °C; ^{1}H NMR (400 MHz, DMSO-d_6) δ 10.33 (s, 1H), 9.08 (s, 1H), 7.42 – 7.36 (m, 2H), 7.25 – 7.19 (m, 1H), 7.13 – 7.07 (m, 2H), ^{13}C{^{1}H} NMR (101 MHz, DMSO-d_6) δ 155.5, 150.7, 129.4, 125.1, 121.5; FTIR (thin film) *inter alia* 3299, 1687 (C=O), 1511, 1492, 1284, 1201, 1105, 795, 687; LRMS (ESI+) m/z 176.1 (M^+ +Na); HRMS (ESI+) m/z Calcd for $C_7H_7NO_3Na$ 176.0324 found 176.0333.

1-Hydroxy-3-phenylurea 171

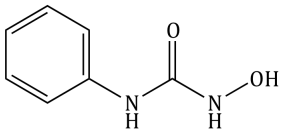

A solution of phenylisocyanate (4.00 g, 33.6 mmol) in 10 ml of DCM was added dropwise over 30 minutes to a solution of sodium hydroxide (1.34 g, 33.6 mmol) and hydroxylamine hydrochloride (2.33 g, 33.6 mmol) in 5 ml of water and 60 ml of DCM at 0 °C. After the addition, the reaction was warmed up to the room temperature and stirred for 3 hours to yield a white solid. The reaction was washed by 20 ml of water and 20 ml of DCM. The precipitate was filtered out recrystalised in ethyl acetate to give the product **171** as a white solid (2.53 g, 50 %); m.p. 148 – 150 °C; ^{1}H NMR (400 MHz, DMSO-d_6) δ 8.96 (s, 1H), 8.81 (s, 1H), 8.75 (s, 1H), 7.59 (d, *J* = 8.5 Hz, 2H), 7.23 (t, *J* = 7.9 Hz, 2H), 6.95 (t, *J* = 7.3 Hz, 1H); ^{13}C{^{1}H} NMR (101 MHz, DMSO-d_6) δ 159.0, 139.8, 128.9, 122.6, 119.6; FTIR (thin film) *inter alia* 3221, 2951, 2894, 1630, 1595, 1537, 1501, 1449, 1074, 755, 688 cm^{-1}; LRMS (ESI+) m/z 175.1 (M^+ +Na); HRMS (ESI+) m/z Calcd for $C_7H_8N_2O_2Na$ 175.0483 found 175.0483.

(*S*)-1-Hydroxy-3-(1-phenylethyl)urea 172

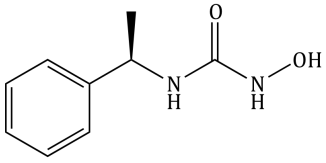

and

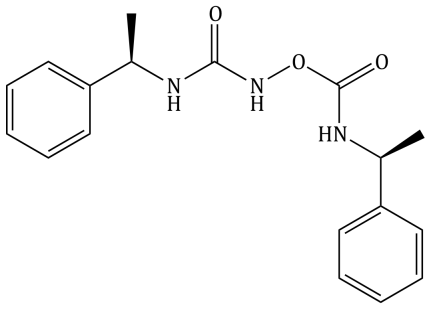

A solution of (*S*)-(1-isocyanatoethyl)benzene (1.00 g, 6.79 mmol) in 10 ml of DCM was added dropwise over 30 minutes to a solution of sodium hydroxide (0.27 g, 6.79 mmol) and hydroxylamine hydrochloride (0.47 g, 6.79 mmol) in 1 ml of water and 20 ml of DCM at 0 °C. After the addition, the reaction was warmed up to the room temperature and stirred for 3 hours. The reaction was washed by 20 ml of water and 20 ml of DCM. The organic phase was separated and dry over $MgSO_4$. The removal of solvent give a colourless oil which then was separated by column

chromatography (ethyl acetate as eluent) to yield 0.60 g (49%) of product **172**; m.p. 106-108 °C ; ^{1}H NMR (400 MHz, DMSO-d_6) δ 8.67 (d, *J* = 0.8 Hz, 1H), 8.40 (s, 1H), 7.42 – 7.34 (m, 4H), 7.30 – 7.24 (m, 1H), 7.00 (d, *J* = 8.7 Hz, 1H), 4.94- 4.86 (m, 1H), 1.45 (d, *J* = 7.1 Hz, 3H); ^{13}C{^{1}H} NMR (101 MHz, DMSO-d_6) δ 161.0, 145.8, 128.6, 126.9, 126.5, 48.6, 23.1; FTIR (thin film) *inter alia* 3311, 2931, 1649 (C=O), 1514, 766, 698 cm^{-1}; LRMS (ESI+) m/z 203.5 (M^+ +Na); HRMS (ESI+) m/z Calcd for $C_9H_{12}N_2O_2Na$ 203.0796 found 203.0796 and orange oil side product (0.31 g) which is 1-[{[(1S)-1-phenylethyl]carbamoyl})amino]-N-[(1R)-1-phenylethyl]formamide **172s**; ^{1}H NMR (400 MHz, $CDCl_3$) δ 9.30 (s, 1H), 7.32 – 7.08 (m, 12H), 4.87 (s, 2H), 1.45 (s, 6H); ^{13}C{^{1}H} NMR (101 MHz, $CDCl_3$) δ 153.1, 142.0, 127.7, 126.4, 124.9, 49.2, 21.7; FTIR (thin film) *inter alia* 3270, 3029, 2971, 1691 (C=O), 1658 (C=O), 1491, 1209, 696 cm^{-1}; LRMS (ESI+) m/z 350.7 (M^+ +Na); HRMS (ESI+) m/z Calcd for $C_{18}H_{21}N_3O_3Na$ 350. 1481 found 350.1472.

3.9 Acyl cycloaducts synthesis using sodium periodate

***GP9**: General procedure of acyl cycloaducts using sodium periodate*

Hydroxamic acid dissolved in methanol (10 mL) was added dropwise to a solution of diene, sodium periodate in methanol (20 mL) at room temperature. The reaction mixture was stirred for 4 hours and monitored by TLC. Then the solvent was removed under vacuum. The crude product was purified by silica gel chromatography (6:1 v/v, hexane/EtOAc) to obtain the product.

3.9.1 Reaction of hydroxamic acids with 1,3-cyclohexadiene

Entry 1, Table 10: 2-Oxa-3-azabicyclo[2.2.2]oct-5-en-3-yl(pyridin-2-yl) methanone **173**

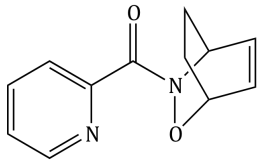

According to **GP9**: 2-Pyridinehydroxamic acid (0.27 g, 2.0 mmol),1,3-cyclohexadiene (0.31 mg, 3.9 mmol), sodium periodate (0.42 g, 2.0 mmol) The

reaction mixture was stirred for 4 hours to give a white solid product **173** (177 mg, 42%); m.p. 110 – 112 °C; ^{1}H NMR (400 MHz, $CDCl_3$) δ 8.77 – 8.50 (m, 1H), 8.00 – 7.57 (m, 2H), 7.49 – 7.29 (m, 1H), 6.89 – 6.41 (m, 2H), 5.66 – 5.37 (m, 1H), 5.06 – 4.67 (s, 1H), 2.50 – 2.18 (m, 2H), 1.67 – 1.40 (m, 2H); ^{13}C{^{1}H} NMR (101 MHz, $CDCl_3$) δ 162.1, 152.4, 148.1, 137.1, 132.0, 131.1, 125.2, 124.8, 71.8, 51.6, 23.4, 22.0; FTIR (thin film) *inter alia* 2933, 1632 (C=O), 1566, 954, 748, 710, 668 cm^{-1}; LRMS (ESI+) m/z 239.5 (M^+ +Na); HRMS (ESI+) m/z Calcd for $C_{12}H_{12}N_2O_2Na$ 239.0796 found 239.0814.

Entry 2, Table 10: 2-Oxa-3azabicyclo[2.2.2]oct-5-en-3-yl(pyridin-3-yl)methanone **174**

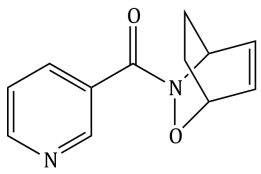

According to **GP9**: 3-Pyridinehydroxamic acid (143 mg, 1.03 mmol), 1,3-cyclohexadiene (166 mg, 2.06 mmol), sodium periodate (221 mg, 1.03 mmol). The reaction mixture was stirred for 4 hours. The product **174** was obtained as an off-white solid (69 mg, 31 %); m.p. 105 – 107 °C; ^{1}H NMR (400 MHz, $CDCl_3$) δ 8.92 (s, 1H), 8.64 (d, *J* = 3.4 Hz, 1H), 7.99 (s, 1H), 7.30 (dd, *J* = 14.7, 7.8 Hz, 1H), 6.73 (s, 1H), 6.54 (s, 1H), 5.43 (s, 1H), 4.78 (s, 1H), 2.37 – 2.17 (m, 2H), 1.56 (p, *J* = 11.2 Hz, 2H); ^{13}C{^{1}H} NMR (101 MHz, $CDCl_3$) δ 166.1, 151.4, 150.1, 136.5, 133.3, 131.7, 129.9, 122.7, 72.3, 47.1, 23.5, 20.9; FTIR (thin film) *inter alia* 1639 (C=O), 1586, 1387, 924, 882, 824, 735, 699 cm^{-1}; LRMS (ESI+) m/z 217.1 (M^+ +H); HRMS (ESI+) m/z Calcd for $C_{12}H_{13}N_2O_2$ 217.0977 found 217.0993.

Entry 5, Table 10: 2-Oxa-3-azabicyclo[2.2.2]oct-5-en-3-yl(phenyl)metha-none **177**

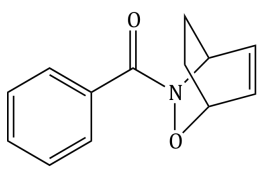

According to **GP9**: *N*-Hydroxybenzamide (594 mg, 4.33 mmol), 1,3-cyclohexadiene (694 mg, 8.66 mmol), sodium periodate (927 mg, 4.33 mmol). The reaction

mixture was stirred for 4 hours. The product **177** was obtained as an off-white solid (317 mg, 53%); m.p. 111 – 114 °C; ^{1}H NMR (400 MHz, $CDCl_3$) δ 7.64 (s, 2H), 7.46 – 7.33 (m, 3H), 6.66 (br, 1H), 6.54 (s, 1H), 5.38 (br, 1H), 4.79 (s, 1H), 2.36 – 2.18 (m, 2H), 1.58 – 1.45 (m, 2H); ^{13}C{^{1}H} NMR (101 MHz, $CDCl_3$) δ 168.9, 134.4, 132.8, 131.8, 130.7, 128.5, 128.0, 71.9, 47.4, 23.5, 21.2; FTIR (thin film) *inter alia* 1638 (C=O), 929, 881, 788, 726, 703 cm^{-1}; LRMS (ESI+) m/z 216.2 (M^+ + H); HRMS (ESI+) m/z Calcd for $C_{13}H_{14}NO_2$ 216.1025 found 216.1037.

Entry 6, Table 10: 2-Oxa-3-azabicyclo[2.2.2]oct-5-en-3-yl)-2-phenyl-ethanone **178**

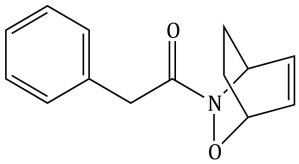

According to **GP9**: *N*-Hydroxy-2-phenylacetamide (290 mg, 1.92 mmol), 1,3-cyclohexadiene (307 mg, 3.84 mmol), sodium periodate (410 mg, 1.92 mmol). The reaction mixture was stirred for 4 hours. The product **178** was obtained as an off-white solid (275 mg, 48 %); m.p. 74 -76 °C; ^{1}H NMR (400 MHz, $CDCl_3$) δ 7.37 – 7.19 (m, 5H), 6.66 – 6.56 (m, 1H), 6.50 – 6.42 (m, 1H), 5.33 – 5.22 (m, 1H), 4.80 – 4.70 (m, 1H), 3.70 – 3.57 (m, 2H), 2.17 – 1.99 (m, 2H), 1.50 – 1.39 (m, 2H); ^{13}C{^{1}H} NMR (101 MHz, $CDCl_3$) δ 170.5, 134.8, 132.9, 131.3, 129.5, 128.2, 126.5, 71.9, 46.6, 40.1, 23.4, 21.0; FTIR (thin film) *inter alia* 1640 (C=O), 1412, 1086, 955, 900, 828, 734, 698 cm^{-1}; LRMS (ESI+) m/z 252.3 (M^+ + Na); HRMS (ESI+) m/z Calcd for $C_{14}H_{15}NO_2$ Na 252.1000 found 252.1010.

Entry 7, Table 10: 2-Oxa-3-azabicyclo[2.2.2]oct-5-en-3-yl)-3-phenylpropan-1-one **179**

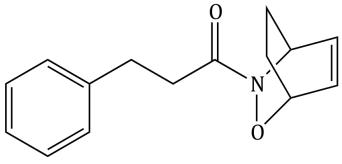

According to **GP9**: *N*-Hydroxy-3-phenylpropanamide (171 mg, 1.03 mmol), 1,3-cyclohexadiene (166 mg, 2.06 mmol), sodium periodate (221 mg, 1.03 mmol). The reaction mixture was stirred for 4 hours. The product **179** was obtained as

colourless oil (123 mg, 49 %); ^{1}H NMR (400 MHz, $CDCl_3$) δ 7.30 – 7.26 (m, 2H), 7.24 – 7.18 (m, 3H), 6.69 – 6.59 (m, 1H), 6.53 – 6.48 (m, 1H), 5.30 (s, 1H), 4.74 (s, 1H), 2.91 (t, *J* = 8.0 Hz, 2H), 2.70 – 2.62 (m, 1H), 2.59 – 2.51 (m, 1H), 2.19 – 2.12 (m, 1H), 2.12 – 2.05 (m, 1H), 1.52 – 1.45 (m, 2H); ^{13}C{^{1}H} NMR (101 MHz, $CDCl_3$) δ 171.1, 140.4, 132.0, 130.3, 127.4, 127.3, 124.9, 70.8, 45.4, 33.9, 29.3, 22.5, 20.1; FTIR (thin film) *inter alia* 1644 (C=O), 1453, 1166, 954, 902, 748, 699 cm^{-1}; LRMS (ESI+) m/z 266.3 (M^+ + Na); HRMS (ESI+) m/z Calcd for $C_{15}H_{17}NO_2$ Na 266.1157 found 266.1169.

Entry 8, Table 10: 2-Oxa-3-azabicyclo[2.2.2]oct-5-en-3-yl)-4-phenylbutan-1-one **180**

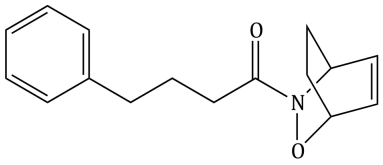

According to **GP9**: *N*-Hydroxy-4-phenylbutanamide (153 mg, 0.85 mmol), 1,3-cyclohexadiene (137 mg, 1.70 mmol), sodium periodate (183 mg, 0.85 mmol). The reaction mixture was stirred for 4 hours. The product **180** was obtained as colourless oil (70 mg, 32 %); ^{1}H NMR (400 MHz, $CDCl_3$) δ 7.24 – 7.16 (m, 2H), 7.14 – 7.06 (m, 3H), 6.55 (t, *J* = 6.6 Hz, 1H), 6.42 (t, *J* = 6.6 Hz, 1H), 5.20 (s, 1H), 4.66 (s, 1H), 2.60 – 2.51 (m, 2H), 2.31 – 2.17 (m, 2H), 2.13 – 1.94 (m, 2H), 1.88 – 1.77 (m, 2H), 1.47 – 1.35 (m, 2H); ^{13}C{^{1}H} NMR (101 MHz, $CDCl_3$) δ 171.9, 141.0, 132.1, 130.2, 127.5, 127.3, 124.8, 70.8, 45.4, 34.4, 31.7, 24.8, 22.6, 20.1; FTIR (thin film) *inter alia* 1644 (C=O), 1453, 955, 902, 833, 746, 699 cm^{-1}; LRMS (ESI+) m/z 280.3 (M^+ + Na); HRMS (ESI+) m/z Calcd for $C_{16}H_{19}NO_2$ Na 280.1313 found 280.1314.

Entry 9, Table 10: 2-Oxa-3-azabicyclo[2.2.2]oct-5-en-3-yl)-5-phenylpentan -1-one **181**

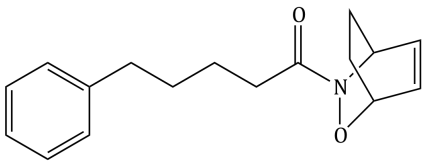

According to **GP9**: *N*-Hydroxy-5-phenylpentanamide (225 mg, 1.16 mmol), 1,3-cyclohexadiene (187 mg, 2.32 mmol), sodium periodate (249 mg, 1.16 mmol). The

reaction mixture was stirred for 4 hours. The product **181** was obtained as colourless oil (120 mg, 38 %); ^{1}H NMR (400 MHz, $CDCl_3$) δ 7.30 – 7.26 (m, 2H), 7.21 – 7.17 (m, 3H), 6.63 (t, *J* = 6.7 Hz, 1H), 6.52 – 6.47 (m, 1H), 5.29 (s, 1H), 4.75 (s, 1H), 2.63 (t, *J* = 7.2 Hz, 2H), 2.39 – 2.27 (m, 2H), 2.23 – 2.16 (m, 1H), 2.12 – 2.07 (m, 1H), 1.68 – 1.60 (m, 4H), 1.53 – 1.47 (m, 2H); ^{13}C{^{1}H} NMR (101 MHz, $CDCl_3$) δ 173.2, 142.5, 133.1, 131.2, 128.4, 128.2, 125.6, 71.7, 46.4, 35.7, 33.0, 31.1, 23.9, 23.6, 21.1; FTIR (thin film) *inter alia* 1648 (C=O), 1452, 1166, 956, 901, 834, 746, 698 cm^{-1}; LRMS (ESI+) m/z 294.3 (M^+ + Na); HRMS (ESI+) m/z Calcd for $C_{17}H_{21}NO_2$ Na 294.1470 found 294.1468.

Entry 10, Table 10: Phenyl-2-oxa-3-azabicyclo[2.2.2]oct-5-ene-3-carboxylate **182**

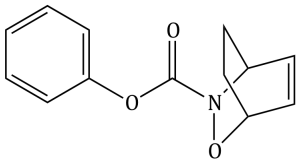

According to **GP9**: Phenyl hydroxycarbamate (128 mg, 0.83 mmol), 1,3-cyclohexadiene (134 mg, 1.68 mmol), sodium periodate (179 mg, 0.83 mmol). The reaction mixture was stirred for 2 hours. The product **182** was obtained as a white solid (99 mg, 51 %); m.p. 127 – 129 °C; ^{1}H NMR (400 MHz, $CDCl_3$) δ 7.37 – 7.28 (m, 2H), 7.21 – 7.15 (m, 1H), 7.14 – 7.06 (m, 2H), 6.73 – 6.64 (m, 1H), 6.63 – 6.57 (m, 1H), 4.99 – 4.90 (m, 1H), 4.88 – 4.80 (m, 1H), 2.31 – 2.17 (m, 2H), 1.59 – 1.52 (m, 1H), 1.48 – 1.40 (m, 1H); ^{13}C{^{1}H} NMR (101 MHz, $CDCl_3$) δ 155.9, 150.9, 132.0, 131.8, 129.3, 125.6, 121.5, 71.4, 50.3, 23.4, 20.7; FTIR (thin film) *inter alia* 1716 (C=O), 1389, 1196, 1067, 994, 750, 691 cm^{-1}; LRMS (ESI+) m/z 254.2 (M^+ + Na); HRMS (ESI+) m/z Calcd for $C_{13}H_{13}NO_3Na$ 254.0793 found 254.0800.

Entry 11, Table 10: *N*-Phenyl-2-oxa-3-azabicyclo[2.2.2]oct-5-ene-3-carboxamide **183**

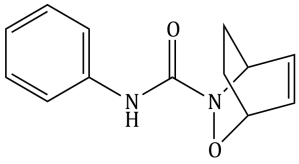

According to **GP9**: 1-Hydroxy-3-phenylurea (131 mg, 0.86 mmol), 1,3-cyclohexadiene (138 mg, 1.72 mmol), sodium periodate (184 mg, 0.86 mmol). The

reaction mixture was stirred for 2 hours. The product **183** was obtained as a white solid (97 mg, 49%); m.p. 102 – 104 °C; ^{1}H NMR (400 MHz, $CDCl_3$) δ 7.63 (s, 1H), 7.44 (dd, *J* = 8.6, 1.0 Hz, 2H), 7.28 (dd, *J* = 10.9, 5.4 Hz, 2H), 7.10 – 7.01 (m, 1H), 6.62 – 6.56 (m, 1H), 6.55 – 6.47 (m, 1H), 5.06 – 4.98 (m, 1H), 4.83 – 4.75 (m, 1H), 2.25 – 2.13 (m, 2H), 1.61 – 1.53 (m, 1H), 1.43 – 1.36 (m, 1H); ^{13}C{^{1}H} NMR (101 MHz, $CDCl_3$) δ 159.3, 137.7, 132.7, 130.4, 128.9, 123.5, 119.3, 71.2, 50.0, 23.9, 20.0; FTIR (thin film) *inter alia* 1667 (C=O), 1594, 1531, 1445, 1228, 907, 767, 701 cm^{-1}; LRMS (ESI+) m/z 253.2 (M^+ + Na); HRMS (ESI+) m/z Calcd for $C_{13}H_{14}N_2O_2Na$ 253.0953 found 253.0958.

Entry 12, Table 10: *N*-((*R*)-1-Phenylethyl)-2-oxa-3-azabicyclo[2.2.2]oct-5-ene-3-carboxamide **184**

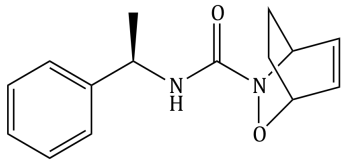

According to **GP9**: (*S*)-1-Hydroxy-3-(1-phenylethyl)urea (125 mg, 0.70 mmol), 1,3-cyclohexadiene (112 mg, 1.39 mmol), sodium periodate (149 mg, 0.70 mmol). The reaction mixture was stirred for 2 hours. The product **184** was obtained as a white solid (76 mg, 42%); m.p. 92 - 94 °C; ^{1}H NMR (700 MHz, $CDCl_3$) δ 7.33 – 7.22 (m, 3H), 7.22 – 7.17 (m, 2H), 6.54 – 6.40 (m, 2H), 5.99 (dd, *J* = 22.7, 7.1 Hz, 1H), 4.96 – 4.84 (m, 2H), 4.64 (d, *J* = 2.1 Hz, 1H), 2.16 – 2.03 (m, 2H), 1.52 – 1.45 (m, 1H), 1.41 (dd, *J* = 12.6, 6.9 Hz, 3H), 1.34 – 1.28 (m, 1H); ^{13}C{^{1}H} NMR (176 MHz, $CDCl_3$) δ 161.5, 161.4, 143.7, 143.5, 132.2, 132.1, 130.2, 130.2, 128.5, 128.4, 127.1, 127.0, 126.0, 125.9, 70.5, 50.3, 50.1, 49.1, 49.1, 23.9, 23.9, 22.4, 22.3, 20.1, 20.0. FTIR (thin film) *inter alia*; 1651, 1515, 1494, 1230, 906, 766, 699, 667 cm^{-1}; LRMS (ESI+) m/z 281.2 (M^+ + Na); HRMS (ESI+) m/z Calcd for $C_{15}H_{18}N_2O_2Na$ 281.1266found 281.1268.

3.9.2 Reaction of hydroxamic acids with 2,3-dimethyl-1,3-butadiene

Entry 1, Table 11: (4,5-Dimethyl-3,6-dihydro-2*H*-1,2-oxazin-2-yl)(pyridin-2-yl)methanone **185**

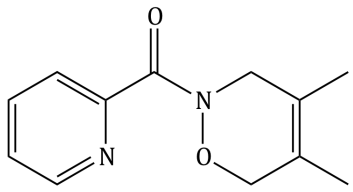

According to **GP9**: 2-Pyridinehydroxamic acid (109 mg, 0.79 mmol), 2,3-dimethyl-1,3-butadiene (130 mg, 1.58 mmol), sodium periodate (169 g, 0.79 mmol). The reaction mixture was stirred for 4 hours. The product **185** was obtained as an off-white solid (36 mg, 21%); m.p. 85-87 °C; ^{1}H NMR (400 MHz, $CDCl_3$) δ 8.63 (d, *J* = 4.5 Hz, 1H), 7.78 (td, *J* = 7.8, 1.4 Hz, 1H), 7.61 (s, 1H), 7.38 – 7.33 (m, 1H), 4.24 (s, 4H), 1.70 (s, 3H), 1.60 (d, *J* = 0.8 Hz, 3H); ^{13}C{^{1}H} NMR (101 MHz, $CDCl_3$) δ 153.0, 148.8, 136.5, 124.8, 123.1, 121.3, 73.2, 45.5, 15.3, 13.8; FTIR (thin film) *inter alia*; 1638, 1447, 1415, 1228, 1191, 1024, 993, 806, 748, 690 cm^{-1}; LRMS (ESI+) m/z 219.3 ($M^+ + H^+$); HRMS (ESI+) m/z Calcd for $C_{12}H_{15}N_2O_2$ 219.1134 found 219.1150.

Entry 2, Table 11: (4,5-Dimethyl-3,6-dihydro-2*H*-1,2-oxazin-2-yl)(pyridin-3-yl)methanone **186**

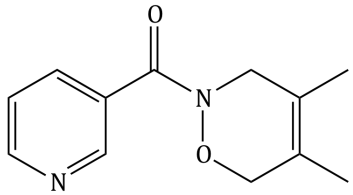

According to **GP9**: 3-Pyridinehydroxamic acid (152 mg, 1.10 mmol), 2,3-dimethyl-1,3-butadiene (181 mg, 2.20 mmol), sodium periodate (235 g, 1.10 mmol). The reaction mixture was stirred for 2 hours. The product **186** was obtained as an off-white solid (43 mg, 18%); m.p. 89-91 °C; ^{1}H NMR (400 MHz, $CDCl_3$) δ 8.96 (d, *J* = 1.5 Hz, 1H), 8.68 (dd, *J* = 4.9, 1.7 Hz, 1H), 8.03 (dt, *J* = 7.9, 1.9 Hz, 1H), 7.36 (ddd, *J* = 7.9, 4.9, 0.9 Hz, 1H), 4.20 (s, 2H), 4.13 (s, 2H), 1.73 (d, *J* = 0.8 Hz, 3H), 1.59 (dd, *J* =

1.8, 0.9 Hz, 3H); $^{13}C\{^{1}H\}$ NMR (101 MHz, $CDCl_3$) δ 166.9, 151.5, 149.6, 136.4, 129.5, 123.0, 122.5, 121.7, 73.0, 46.1, 15.4, 13.7; FTIR (thin film) *inter alia*; 1640, 1415, 1230, 1021, 826, 729, 697 cm^{-1}; LRMS (ESI+) m/z 241.1 (M^+ + Na); HRMS (ESI+) m/z Calcd for $C_{12}H_{14}N_2O_2Na$ 241.0953 found 241.0964.

Entry 5, Table 11: (4,5-Dimethyl-3,6-dihydro-2*H*-1,2-oxazin-2-yl)(phenyl) methanone **189**

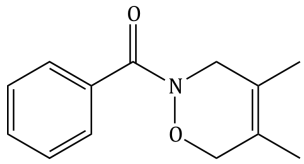

According to **GP9**: *N*-hydroxybenzamide (152 mg, 1.14 mmol), 2,3-dimethyl-1,3-butadiene (186 mg, 2.28 mmol), sodium periodate (243 mg, 1.14 mmol). The product **189** was obtained as a white solid (113 mg, 46 %); m.p. 62 - 64 °C; ^{1}H NMR (400 MHz, $CDCl_3$) δ 7.72 – 7.65 (m, 2H), 7.49 – 7.44 (m, 1H), 7.43 – 7.38 (m, 2H), 4.18 (s, 2H), 4.14 (s, 2H), 1.71 (s, 3H), 1.59 (dd, *J* = 1.8, 0.9 Hz, 3H); $^{13}C\{^{1}H\}$ NMR (101 MHz, $CDCl_3$) δ 169.5, 133.8, 130.8, 128.5, 127.9, 122.7, 121.9, 72.8, 46.6,15.4, 13.7; FTIR (thin film) *inter alia* 1640 (C=O), 1398, 1222, 1029, 796, 719, 696 cm^{-1}; LRMS (ESI+) m/z 240.2 (M^+ + Na); HRMS (ESI+) m/z Calcd for $C_{13}H_{15}NO_2$ Na 240.1000 found 240.0097.

Entry 6, Table 11:1-(4,5-Dimethyl-3,6-dihydro-2*H*-1,2-oxazin-2-yl)-2-phenylethanone **190**

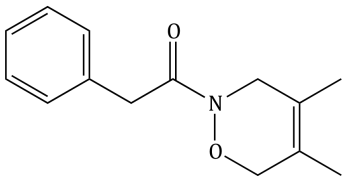

According to **GP9**: *N*-hydroxy-2-phenylacetamide (164 mg, 1.09 mmol), 2,3-dimethyl-1,3-butadiene (179 mg, 2.18 mmol), sodium periodate (233 mg, 1.09 mmol). The product **190** was obtained as colourless oil (105 mg, 42 %); ^{1}H NMR (400 MHz, $CDCl_3$) δ 7.38 – 7.26 (m, 4H), 7.26 – 7.21 (m, 1H), 4.03 (s, 4H), 3.79 (s, 2H), 1.66 (s, 3H), 1.59 – 1.51 (m, 3H); $^{13}C\{^{1}H\}$ NMR (101 MHz, $CDCl_3$) δ 169.9,

135.1, 129.3, 128.5, 126.7, 122.5, 121.8, 73.0, 45.2, 39.7, 15.3, 13.7; FTIR (thin film) *inter alia* 1652 (C=O), 1434, 1223, 711, 694 cm^{-1}; LRMS (ESI+) m/z 254.3 (M^+ + Na); HRMS (ESI+) m/z Calcd for $C_{14}H_{17}NO_2$ Na 254.1157 found 254.1136.

Entry 7, Table 11:1-(4,5-Dimethyl-3,6-dihydro-2*H*-1,2-oxazin-2-yl)-3-phenylpropan-1-one **191**

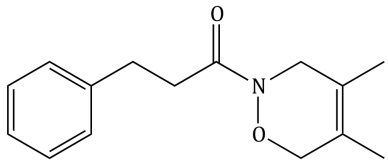

According to **GP9**: *N*-hydroxy-3-phenylpropanamide (131 mg, 0.80 mmol), 2,3-dimethyl-1,3-butadiene (131 mg, 1.59 mmol), sodium periodate (170 mg, 0.80 mmol). The product **191** was obtained as colourless oil (72 mg, 37%); ^{1}H NMR (400 MHz, $CDCl_3$) δ 7.32 – 7.26 (m, 2H), 7.25 – 7.17 (m, 3H), 4.08 (s, 2H), 4.04 (s, 2H), 3.00 – 2.95 (m, 2H), 2.82 – 2.71 (m, 2H), 1.67 (s, 3H), 1.58 – 1.54 (m, 3H); ^{13}C{^{1}H} NMR (101 MHz, $CDCl_3$) δ 170.3, 140.44, 127.5, 127.5, 125.1, 121.5, 121.0, 72.0, 44.0, 32.9, 29.8, 14.3, 12.8; FTIR (thin film) *inter alia* 1651 (C=O), 1440, 1212, 750, 699 cm^{-1}; LRMS (ESI+) m/z 268.3 (M^+ + Na); HRMS (ESI+) m/z Calcd for $C_{15}H_{19}NO_2$ Na 268.1313 found 268.1296.

Entry 8, Table 11: 1-(4,5-Dimethyl-3,6-dihydro-2*H*-1,2-oxazin-2-yl)-4-phenylbutan-1-one **192**

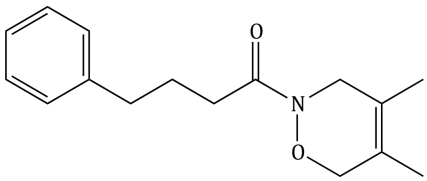

According to **GP9**: *N*-hydroxy-4-phenylbutanamide (137 mg, 0.77 mmol), 2,3-dimethyl-1,3-butadiene (126 mg, 1.54 mmol), sodium periodate (164 mg, 0.77 mmol). The product **192** was obtained as colourless oil (80 mg, 40 %); ^{1}H NMR (400 MHz, $CDCl_3$) δ 7.30 – 7.26 (m, 2H), 7.23 – 7.16 (m, 3H), 4.16 (s, 2H), 4.02 (s, 2H), 2.72 – 2.66 (m, 2H), 2.47 (t, *J* = 7.5 Hz, 2H), 2.03 – 1.95 (m, 2H), 1.68 (d, *J* = 0.8 Hz, 3H), 1.59 (d, *J* = 0.9 Hz, 3H); ^{13}C{^{1}H} NMR (101 MHz, $CDCl_3$) δ 171.9, 141.8,

128.5, 128.3, 125.8, 122.5, 122.1, 72.9, 45.0, 35.4, 31.4, 26.1, 15.3, 13.8; FTIR (thin film) *inter alia* 1654 (C=O), 1439, 1216, 749, 699 cm^{-1}; LRMS (ESI+) m/z 282.3 (M^+ + Na); HRMS (ESI+) m/z Calcd for $C_{16}H_{21}NO_2$ 282.1470 Na found 282.1472.

Entry 9, Table 11: 1-(4,5-Dimethyl-3,6-dihydro-2*H*-1,2-oxazin-2-yl)-5-phenylpentan-1-one **193**

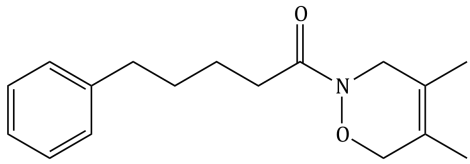

According to **GP9**: *N*-hydroxy-5-phenylpentanamide (149 mg, 0.77 mmol), 2,3-dimethyl-1,3-butadiene (126 mg, 1.54 mmol), sodium periodate (164 mg, 0.77 mmol). The product **193** was obtained as colourless oil (86 mg, 41 %); ^{1}H NMR (400 MHz, $CDCl_3$) δ 7.29 – 7.24 (m, 2H), 7.24 – 7.13 (m, 3H), 4.17 (s, 2H), 4.02 (s, 2H), 2.65 (t, *J* = 7.1 Hz, 2H), 2.46 (d, *J* = 6.4 Hz, 2H), 1.73 – 1.64 (m, 7H), 1.59 (d, *J* = 0.9 Hz, 3H); ^{13}C{^{1}H} NMR (101 MHz, $CDCl_3$) δ 172.1, 142.4, 128.4,128.3, 125.7, 122.5,122.10, 72.9, 45.0, 35.7, 32.0, 31.2, 24.4, 15.3, 13.8; FTIR (thin film) *inter alia* 1655 (C=O), 1435, 1212, 748, 699 cm^{-1}; LRMS (ESI+) m/z 296.3 (M^+ + Na); HRMS (ESI+) m/z Calcd for $C_{17}H_{23}NO_2$ Na 296.1626 found 296.1629 .

Entry 10, Table 11: Phenyl-4,5-dimethyl-3,6-dihydro-2*H*-1,2-oxazine-2-carboxylate **194**

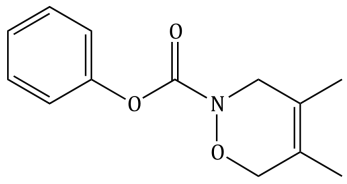

According to **GP9**: Phenyl hydroxycarbamate (133 mg, 0.87 mmol), 2,3-dimethyl-1,3-butadiene (143 mg, 1.74 mmol), sodium periodate (186 mg, 0.87 mmol). The product **194** was obtained as colourless oil (95.4 mg, 47%); ^{1}H NMR (400 MHz, $CDCl_3$) δ 7.40 – 7.34 (m, 2H), 7.24 – 7.19 (m, 1H), 7.19 – 7.13 (m, 2H), 4.34 (s, 2H), 4.09 (s, 2H), 1.73 – 1.69 (m, 3H), 1.66 – 1.59 (m, 3H); ^{13}C{^{1}H} NMR (101 MHz,

$CDCl_3$) δ 153.6, 150.9, 129.3, 125.6, 123.2, 121.8, 121.6, 72.0, 48.4, 15.2, 13.9; FTIR (thin film) *inter alia* 1720 (C=O), 1388, 1356, 1202, 1162, 1068, 755, 726, 688 cm^{-1}; LRMS (ESI+) m/z 256.2 (M^+ + Na); HRMS (ESI+) m/z Calcd for $C_{13}H_{15}NO_3Na$ 256.0950 found 256.0955.

Entry 11, Table 11: 4,5-Dimethyl-*N*-phenyl-3,6-dihydro-2*H*-1,2-oxazine-2-carboxamide **195**

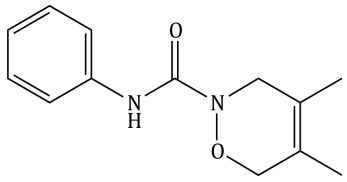

According to **GP9**: 1-Hydroxy-3-phenylurea (138 mg, 0.91 mmol), 2,3-dimethyl-1,3-butadiene (149 mg, 1.81 mmol), sodium periodate (194 mg, 0.91 mmol). The product **195** was obtained as a white solid (95 mg, 45%); m.p. 99-102 °C; ^{1}H NMR (400 MHz, $CDCl_3$) δ 7.66 (s, 1H), 7.46 (dd, *J* = 19.3, 8.2 Hz, 2H), 7.31 (t, *J* = 7.9 Hz, 2H), 7.06 (t, *J* = 7.4 Hz, 1H), 4.29 (t, *J* = 9.9 Hz, 2H), 3.97 (t, *J* = 10.1 Hz, 2H), 1.78 – 1.68 (m, 3H), 1.63 – 1.61 (m, 3H); ^{13}C{^{1}H} NMR (101 MHz, $CDCl_3$) δ 155.5, 138.0, 129.0, 123.4, 122.6, 119.3, 119.3, 72.5, 47.7, 15.5, 13.7; FTIR (thin film) *inter alia* 1652 (C=O), 1594, 1527, 1446, 1435, 1221, 758, 731, 692 cm^{-1}; LRMS (ESI+) m/z 255.3 (M^+ + Na); HRMS (ESI+) m/z Calcd for $C_{13}H_{16}N_2O_2Na$ 255.1109 found 255.1121.

Entry 12, Table 11: (*R*)-4,5-Dimethyl-*N*-(1-phenylethyl)-3,6-dihydro-2*H*-1,2-oxazine-2-carboxamide **196**

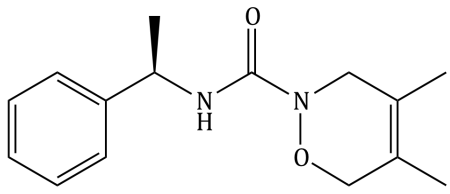

(*S*)-1-Hydroxy-3-(1-phenylethyl)urea (98 mg, 0.54 mmol), 2,3-dimethyl-1,3-butadiene (89 mg, 1.09 mmol), sodium periodate (116 mg, 0.54 mmol). The product **196** was obtained as a colourless oil (18 mg, 13 %); ^{1}H NMR (400 MHz,

$CDCl_3$) δ 7.39 – 7.30 (m, 4H), 7.29 – 7.22 (m, 1H), 5.99 (d, *J* = 8.0 Hz, 1H), 5.07 – 4.98 (m, 1H), 4.25 – 4.15 (m, 2H), 3.87 (dt, *J* = 19.8, 9.9 Hz, 2H), 1.71 – 1.64 (m, 3H), 1.61 – 1.56 (m, 3H), 1.52 (d, *J* = 6.9 Hz, 3H); $^{13}C\{^1H\}$ NMR (101 MHz, $CDCl_3$) δ 157.8, 143.9, 128.6, 128.6, 127.2, 126.1, 122.7, 122.6, 72.0, 49.2, 48.2, 22.5, 15.5, 13.7; FTIR (thin film) *inter alia* 3308 (NH), 1652 (C=O), 1510, 1209, 1026, 762, 699 cm^{-1}; LRMS (ESI+) m/z 261.1 (M^+ + H); HRMS (ESI+) m/z Calcd for $C_{15}H_{21}N_2O_2$ 261.1603 found 261.1619.

3.10 Reaction of hydroxamic acids with 1,3-cyclohexadiene using 10 mol% $CuCl_2$ and 20 mol% of 2-ethyl-2-oxazoline in methanol

***GP10**: General procedure of copper-oxazoline catalyzed oxidation of hydroxamic acids*

To a MeOH (5 ml) solution of 1.2 equivalent 1,3-cyclohexadiene, 10 mol% $CuCl_2$ and 20 mol% 2-ethyl-2-oxazoline was added hydroxamic acid**.** The resulting solution was stirred at room temperature in air and was monitored by TLC. The completion of the reaction was confirmed by the disappearance of the starting material. The solvent was removed by evaporation and the crude product was purified by silica gel chromatography (hexane:ethyl acetate, 6:1 v/v, as eluent).

Entry 10, Table 12: (1*R*,4*S*)-Phenyl-2-oxa-3-azabicyclo[2.2.2]oct-5-ene-3-carboxylate **182**

According to **GP10**: Phenyl hydroxycarbamate (103 mg, 0.67 mmol), 1,3-cyclohexadiene (66 mg, 0.80 mmol), $CuCl_2$ (9 mg, 0.07 mmol) and 2-ethyl-2-oxazoline (13 mg, 0.13 mmol), the reaction completed in 2 h giving **182** (152 mg, 98 %) as a white solid.

Entry 11, Table 12: (1*R*,4*S*)-*N*-Phenyl-2-oxa-3-azabicyclo[2.2.2]oct-5-ene-3-carboxamide **183**

According to **GP10**: 1-Hydroxy-3-phenylurea (105 mg, 0.69 mmol), 1,3-cyclohexadiene (68 mg, 0.83 mmol), $CuCl_2$ (9 mg, 0.07 mmol) and 2-ethyl-2-

oxazoline (14 mg, 0.14 mmol), the reaction completed in 4 h giving **183** (156 mg, 98%) as a white solid.

Entry 12, Table 12: *N*-((*R*)-1-Phenylethyl)-2-oxa-3-azabicyclo[2.2.2]oct-5-ene-3-carboxamide **184**

According to **GP10**: (*S*)-1-Hydroxy-3-(1-phenylethyl)urea (99 mg, 0.55 mmol), 1,3-cyclohexadiene (53 mg, 0.66 mmol), $CuCl_2$ (7 mg, 0.05 mmol) and 2-ethyl-2-oxazoline (11 mg, 0.11 mmol), the reaction completed in 4 h giving **184** (141 mg, 97%) as a white solid.

3.11 Reaction of phenyl hydroxycarbamate 170 with various dienes.

GP11*: General procedure of copper-oxazoline catalyzed oxidation of phenyl hydroxycarbamate* ***170***

To a MeOH (5 ml) solution of diene (1.2 equivalent for Entry 1-5 and 0.83 equivalent for Entry 5-6), 10 mol% $CuCl_2$ and 20 mol% 2-ethyl-2-oxazoline was added phenyl hydroxycarbamate **170.** The resulting solution was stirred at room temperature in air and was monitored by TLC. The completion of the reaction was confirmed by the disappearance of the starting material. The solvent was removed by evaporation and the crude product was purified by silica gel chromatography (hexane:ethyl acetate, 6:1 v/v, as eluent).

Entry 1, Table 13: Phenyl 2-oxa-3-azabicyclo[2.2.1]hept-5-ene-3-carboxylate **197**

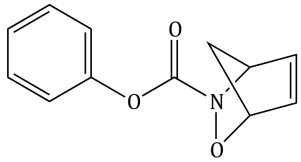

According to **GP11**: Using phenyl hydroxycarbamate (162 mg, 1.06 mmol), freshly cracked cyclopentadiene (84 mg, 1.27 mmol), $CuCl_2$ (14 mg, 0.11 mmol) and 2-ethyl-2-oxazoline (21 mg, 0.21 mmol), the reaction was stirred for 2 h giving **197** (228 mg, 99%) as a white solid; m.p. 113 – 114 °C; ^{1}H NMR (400 MHz, $CDCl_3$) δ 7.39

– 7.33 (m, 2H), 7.24 – 7.19 (m, 1H), 7.14 – 7.08 (m, 2H), 6.61 (dt, *J* = 5.5, 1.9 Hz, 1H), 6.52 – 6.47 (m, 1H), 5.35 (d, *J* = 1.4 Hz, 1H), 5.21 (s, 1H), 2.12 (dt, *J* = 8.8, 1.9 Hz, 1H), 1.86 (d, *J* = 8.8 Hz, 1H); $^{13}C\{^{1}H\}$ NMR (101 MHz, $CDCl_3$) δ 156.4, 149.7, 133.6, 132.4, 128.4, 124.8, 120.4, 83.3, 64.4, 47.4; FTIR (thin film) *inter alia* 1749 (C=O), 1587, 1489, 1332, 1271, 1192, 1181, 770, 746, 691 cm^{-1}; LRMS (ESI+) m/z 240.2 (M^+ + Na); HRMS (ESI+) m/z Calcd for $C_{12}H_{11}NO_3Na$ 240.0637 found 240.0650.

Entry 2, Table 13: (1*R*,4*S*)-Phenyl 2-oxa-3-azabicyclo[2.2.2]oct-5-ene-3-carboxylate **182**

According to **GP11**: Using phenyl hydroxycarbamate (158 mg, 1.03 mmol), 1,3-cyclohexadiene (99 mg, 1.24 mmol), $CuCl_2$ (14 mg, 0.11 mmol) and 2-ethyl-2-oxazoline (21 mg, 0.21 mmol), the reaction was stirred for 2 h giving **182** (234 mg, 98 %) as a white solid.

Entry 3, Table 13: Phenyl 4,5-dimethyl-3,6-dihydro-2*H*-1,2-oxazine-2-carboxylate **194**

According to **GP11**: Using phenyl hydroxycarbamate (173 mg, 1.13 mmol), 2,3-dimethyl-1,3-butadiene (111 mg, 1.36 mmol), $CuCl_2$ (15 mg, 0.11 mmol) and 2-ethyl-2-oxazoline (22 mg, 0.22 mmol), the reaction was stirred for 3 h giving **194** (250 mg, 95%) in colourless oil. The ratio of **194**:**198** is 6:1.

Entry 4, Table 13: Phenyl 3,6-dimethyl-3,6-dihydro-2*H*-1,2-oxazine-2-carboxylate **199**

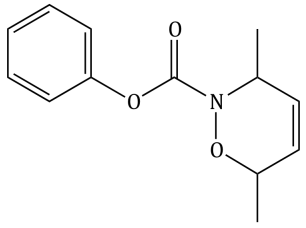

According to **GP11**: Using phenyl hydroxycarbamate (131 mg, 0.86 mmol), 2,4-hexadiene (84 mg, 1.03 mmol), $CuCl_2$ (12 mg, 0.09 mmol) and 2-ethyl-2-oxazoline (17 mg, 0.17 mmol), the reaction was stirred for 3 h giving **199** (185 mg, 93%) as a colourless oil; ^{1}H NMR (400 MHz, $CDCl_3$) δ 7.39 – 7.35 (m, 2H), 7.22 (dd, *J* = 10.6, 4.3 Hz, 1H), 7.18 – 7.14 (m, 2H), 5.84 (ddd, *J* = 10.2, 4.3, 2.1 Hz, 1H), 5.79 – 5.71 (m, 1H), 4.85 – 4.73 (m, 1H), 4.64 – 4.57 (m, 1H), 1.42 (d, *J* = 6.7 Hz, 3H), 1.33 (d, *J* = 6.7

Hz, 3H); $^{13}C\{^{1}H\}$ NMR (101 MHz, $CDCl_3$) δ 152.8, 150.8, 129.2, 128.6, 127.5, 125.4, 121.5, 74.3, 50.2, 18.7, 18.1; FTIR (thin film) *inter alia* 1715 (C=O), 1366, 1189, 1037, 748, 725, 689 cm^{-1}; LRMS (ESI+) m/z 256.3 (M^+ + Na); HRMS (ESI+) m/z Calcd for $C_{13}H_{15}NO_3Na$ 256.0950 found 256.0926.

Entry 5, Table 13: Phenyl 4-methyl-3,6-dihydro-2*H*-1,2-oxazine-2-carboxylate **200** and phenyl 5-methyl-3,6-dihydro-2*H*-1,2-oxazine-2-carboxylate **200'**

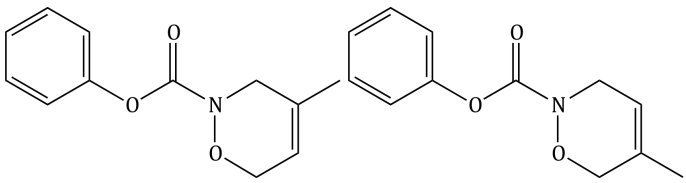

According to **GP11**: Using phenyl hydroxycarbamate (142 mg, 0.93 mmol), isoprene (70 mg, 1.11 mmol), $CuCl_2$ (12 mg, 0.09 mmol) and 2-ethyl-2-oxazoline (18 mg, 0.18 mmol), the reaction was stirred for 3.5 h giving **200/200'** (183 mg, 90 %) as a colourless oil. The ratio of **200** and **200'**:**201** = 3:1 and the ratio of **200**:**200'** = 1.79:1;

200: ^{1}H NMR (400 MHz, $CDCl_3$) δ 7.40 – 7.35 (m, 2H), 7.25 – 7.20 (m, 1H), 7.19 – 7.14 (m, 2H), 5.64 – 5.60 (m, 1H), 4.54 – 4.47 (m, 2H), 4.18 – 4.09 (m, 2H), 1.81 – 1.75 (m, 3H); $^{13}C\{^{1}H\}$ NMR (101 MHz, $CDCl_3$) δ 150.8, 129.4, 125.7, 121.6, 121.6, 118.0, 116.2, 68.9, 48.5, 19.9.

200': ^{1}H NMR (400 MHz, $CDCl_3$) δ 7.41 – 7.34 (m, 2H), 7.25 – 7.19 (m, 1H), 7.19 – 7.13 (m, 2H), 5.60 – 5.57 (m, 1H), 4.42 – 4.37 (m, 2H), 4.26 – 4.20 (m, 2H), 1.74 – 1.70 (m, 3H); $^{13}C\{^{1}H\}$ NMR (101 MHz, $CDCl_3$) δ 153.6, 131.6, 130.1, 125.7, 121.6, 118.0, 115.3, 72.0, 44.8, 18.3; FTIR (thin film) *inter alia* 1717 (C=O), 1383, 1200, 1163, 1070, 752, 688 cm^{-1}; LRMS (ESI+) m/z 242.2 (M^+ + Na); HRMS (ESI+) m/z Calcd for $C_{12}H_{13}NO_3Na$ 242.0793 found 242.0771.

Entry 6, Table 13: (9*S*,10*S*)-Phenyl-9,10-dimethyl-9,10-dihydro-9,10-(epoxy-imino)-anthracene-11-carboxylate **202**

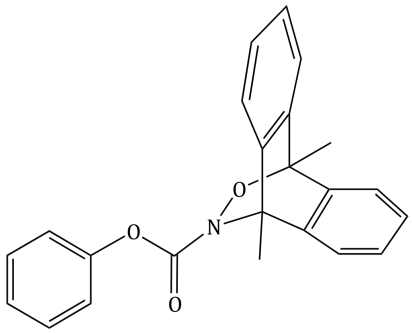

According to **GP11**: Using phenyl hydroxycarbamate (39 mg, 0.25 mmol), 9,10-dimethylanthracene (47 mg, 0.23 mmol), $CuCl_2$ (3 mg, 0.03 mmol) and 2-ethyl-2-oxazoline (5 mg, 0.05 mmol), the reaction was stirred for 24 h giving **202** (70 mg, 80%) in colourless oil; ^{1}H NMR (400 MHz, $CDCl_3$) δ 7.57 – 7.52 (m, 2H), 7.49 – 7.45 (m, 2H), 7.38 – 7.32 (m, 4H), 7.29 – 7.25 (m, 2H), 7.17 – 7.14 (m, 1H), 6.78 – 6.69 (m, 2H), 2.67 (d, *J* = 13.8 Hz, 3H), 2.34 (s, 3H); $^{13}C\{^{1}H\}$ NMR (101 MHz, $CDCl_3$) δ 158.1, 150.8, 141.6, 140.4, 129.2, 127.4, 125.6, 121.6, 121.6, 120.8, 79.7, 64.5, 16.4, 15.0; FTIR (thin film) *inter alia* 1725 (C=O), 1274, 1229, 1194, 1016, 741, 688 cm^{-1}; LRMS (ESI+) m/z 380.2 (M^+ + Na); HRMS (ESI+) m/z $C_{23}H_{19}NO_3Na$ 380.1263 found 380.1257.

Entry 7, Table 13: Phenyl 3,6-diphenyl-3,6-dihydro-2*H*-1,2-oxazine-2-carboxylate **203**

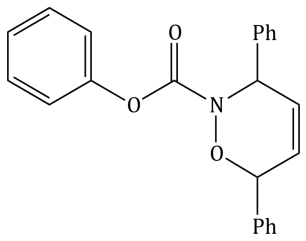

According to **GP11**: Using phenyl hydroxycarbamate (92 mg, 0.60 mmol), 1,4-diphenyl-1,3-butadiene (111 mg, 0.54 mmol), $CuCl_2$ (8 mg, 0.06 mmol) and 2-ethyl-2-oxazoline (12 mg, 0.12 mmol), the reaction was stirred for 24 h giving **203** (172 mg, 82%); m.p. 144 – 147 °C; ^{1}H NMR (400 MHz, $CDCl_3$) δ 7.61 – 7.57 (m, 2H), 7.50 – 7.46 (m, 2H), 7.44 – 7.34 (m, 8H), 7.24 – 7.20 (m, 1H), 7.15 (d, *J* = 7.6 Hz, 2H), 6.25 – 6.15 (m, 2H), 5.81 – 5.73 (m, 2H); $^{13}C\{^{1}H\}$ NMR (101 MHz, $CDCl_3$) δ 188.5,

153.1, 150.9, 138.4, 136.8, 129.3, 129.2, 128.8, 128.7, 128.2, 128.1, 127.9, 125.9, 125.7, 121.7, 80.3, 77.2; FTIR (thin film) *inter alia* 1716 (C=O), 1360, 1272, 1194, 868, 747, 726, 689 cm^{-1}; LRMS (ESI+) m/z 380.2 (M^+ + Na); HRMS (ESI+) m/z Calcd for $C_{23}H_{19}NO_3Na$ 380.1263 found 380.1227.

Entry 8, Table 13: Phenyl-3-(hydroxymethyl)-6-methyl-3,6-dihydro-2*H*-1,2-oxazine-2-carboxylate **204** and phenyl 6-(hydroxymethyl)-3-methyl-3,6-dihydro-2*H*-1,2-oxazine -2-carboxylate **204'**

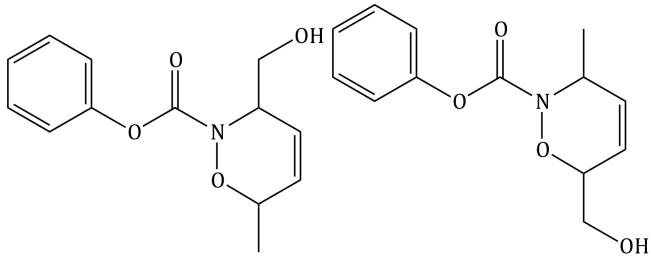

According to **GP11**: Using phenyl hydroxycarbamate (140 mg, 0.91 mmol), 2,4-hexadiene-1-ol (90 mg, 0.91mmol), $CuCl_2$ (12 mg, 0.09 mmol) and 2-ethyl-2-oxazoline (18 mg, 0.18 mmol), the reaction was stirred for 3 h giving **204/204'** (210 mg, 93 %) in yellow oil. The ratio of **204**:**204'** = 1:1;

204: ^{1}H NMR (400 MHz, $CDCl_3$) δ 7.46 – 7.34 (m, 2H), 7.28 – 7.21 (m, 1H), 7.21 – 7.11 (m, 2H), 6.06 – 6.02 (m, 1H) , 5.87 – 5.83 (m, 1H) , 4.63 – 4.56 (m, 1H) , 4.55 – 4.45 (m, 2H), 4.11 (dd, *J* = 7.2, 2.3 Hz, 1H) , 1.94 (s, 1H), 1.53 (d, *J* = 7.0 Hz, 3H); $^{13}C\{^1H\}$ NMR (101 MHz, $CDCl_3$) δ 153.1, 150.8, 131.26, 129.4, 125.7, 123.0, 121.6, 75.89, 65.6, 63.52, 50.5, 21.0

204': ^{1}H NMR (400 MHz, $CDCl_3$) δ 7.46 – 7.34 (m, 2H), 7.28 – 7.21 (m, 1H), 7.21 – 7.11 (m, 2H) , 6.02 – 5.97 (m, 1H), 5.79 (dt, *J* = 10.3, 1.5 Hz, 1H) , 4.86 – 4.80 (m, 1H) , 4.71 – 4.63 (m, 1H) , 3.86 (dd, *J* = 12.5, 3.0 Hz, 1H), 3.75 (dd, *J* = 12.4, 6.3 Hz, 1H), 2.45 (br, 1H), 1.45 (d, *J* = 6.7 Hz, 3H); $^{13}C\{^1H\}$ NMR (101 MHz, $CDCl_3$) δ 153.1, 150.8, 130.1, 129.4, 125.7, 123.8, 121.6, 79.3, 63.6, 50.8, 18.3; FTIR (thin film) *inter alia* 1715 (C=O), 1369, 1312, 1188, 1164, 1065, 749, 689 cm^{-1}; LRMS (ESI+) m/z 272.3 (M^+ + Na); HRMS (ESI+) m/z Calcd for $C_{13}H_{15}NO_4Na$ 272.0899 found 272.0907.

3.12 Reaction of 1-hydroxy-3-phenylurea 171 with various dienes.

GP12**: General procedure of copper-oxazoline catalyzed oxidation of 1-hydroxy-3-phenylurea **171

To a MeOH (5 ml) solution of diene (1.2 equivalent for Entry 1-5 and 0.83 equivalent for Entry 5-6), 10 mol% $CuCl_2$ and 20 mol% 2-ethyl-2-oxazoline was added 1-hydroxy-3-phenylurea **171.** The resulting solution was stirred at room temperature in air and was monitored by TLC. The completion of the reaction was confirmed by the disappearance of the starting material. The solvent was removed by evaporation and the crude product was purified by silica gel chromatography (hexane:ethyl acetate, 6:1 v/v, as eluent).

Entry 1, Table 14: *N*-Phenyl-2-oxa-3-azabicyclo[2.2.1]hept-5-ene-3-carboxamide **205**

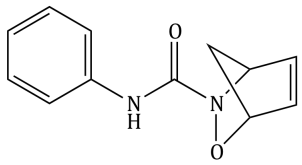

According to **GP12**: Using 1-hydroxy-3-phenylurea (182 mg, 1.20 mmol), freshly cracked cyclopentadiene (95 mg, 1.44 mmol), $CuCl_2$ (16 mg, 0.12 mmol) and 2-ethyl-2-oxazoline (24 mg, 0.24 mmol), the reaction was stirred for 4 h giving **205** (249 mg, 96 %) as a white solid; m.p. 108 -112 °C; ^{1}H NMR (400 MHz, $CDCl_3$) δ 7.48 (t, *J* = 16.2 Hz, 1H), 7.42 (dt, *J* = 8.7, 1.7 Hz, 2H), 7.31 – 7.26 (m, 2H), 7.08 – 7.03 (m, 1H), 6.52 (dt, *J* = 5.5, 1.9 Hz, 1H), 6.39 (ddd, *J* = 5.6, 2.3, 1.6 Hz, 1H), 2.08 (dt, *J* = 8.8, 1.9 Hz, 1H), 1.83 (d, *J* = 8.8 Hz, 1H); ^{13}C{^{1}H} NMR (101 MHz, $CDCl_3$) δ 159.7, 137.4, 135.6, 132.0, 129.0, 123.8, 119.3, 84.4, 65.2, 48.7. FTIR (thin film) *inter alia* 1660 (C=O), 1596, 1522, 1448, 1338, 753, 690 cm^{-1}; LRMS (ESI+) m/z 270.2 (M^+ + Na); HRMS (ESI+) m/z Calcd for $C_{12}H_{12}N_2O_2Na$ 239.0796 found 239.0782.

Entry 2, Table 14: (1*R*,4*S*)-*N*-Phenyl-2-oxa-3-azabicyclo[2.2.2]oct-5-ene-3-carboxamide **183**

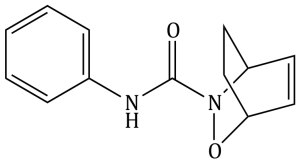

According to **GP12**: Using 1-hydroxy-3-phenylurea (150 mg, 0.98 mmol), 1,3-cyclohexadiene (95 mg, 1.18 mmol), $CuCl_2$ (13 mg, 0.098 mmol) and 2-ethyl-2-oxazoline (19 mg, 0.19 mmol), the reaction was stirred for 4 h giving **183** (222 mg, 98%) as a white solid; m.p. 102 – 104 °C; ^{1}H NMR (400 MHz, $CDCl_3$) δ 7.63 (s, 1H), 7.44 (dd, *J* = 8.6, 1.0 Hz, 2H), 7.28 (dd, *J* = 10.9, 5.4 Hz, 2H), 7.10 – 7.01 (m, 1H), 6.62 – 6.56 (m, 1H), 6.55 – 6.47 (m, 1H), 5.06 – 4.98 (m, 1H), 4.83 – 4.75 (m, 1H), 2.25 – 2.13 (m, 2H), 1.61 – 1.53 (m, 1H), 1.43 – 1.36 (m, 1H); ^{13}C{^{1}H} NMR (101 MHz, $CDCl_3$) δ 159.3, 137.7, 132.7, 130.4, 128.9, 123.5, 119.3, 71.2, 50.0, 23.9, 20.0; FTIR (thin film) *inter alia* 1667 (C=O), 1594, 1531, 1445, 1228, 907, 767, 701 cm^{-1}; LRMS (ESI+) m/z 253.2 (M^+ + Na); HRMS (ESI+) m/z Calcd for $C_{13}H_{14}N_2O_2Na$ 253.0953 found 253.0958.

Entry 3, Table 14: 4,5-Dimethyl-*N*-phenyl-3,6-dihydro-2*H*-1,2-oxazine-2-carboxamide **195**

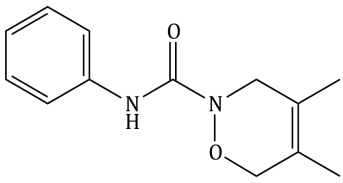

According to **GP12**: Using 1-hydroxy-3-phenylurea (186 mg, 1.22 mmol), 2,3-dimethyl-1,3-butadiene (125 mg, 1.47 mmol), $CuCl_2$ (16 mg, 0.12 mmol) and 2-ethyl-2-oxazoline (24 mg, 0.24 mmol), the reaction was stirred for 6 h giving **195** (255 mg, 90 %) as a white solid. The ratio of **195**:**206** = 9:1; m.p. 99-102 °C; ^{1}H NMR (400 MHz, $CDCl_3$) δ 7.66 (s, 1H), 7.46 (dd, *J* = 19.3, 8.2 Hz, 2H), 7.31 (t, *J* = 7.9 Hz, 2H), 7.06 (t, *J* = 7.4 Hz, 1H), 4.29 (t, *J* = 9.9 Hz, 2H), 3.97 (t, *J* = 10.1 Hz, 2H), 1.78 – 1.68 (m, 3H), 1.63 – 1.61 (m, 3H); ^{13}C{^{1}H} NMR (101 MHz, $CDCl_3$) δ 155.5, 138.0, 129.0, 123.4, 122.6, 119.3, 119.3, 72.5, 47.7, 15.5, 13.7; FTIR (thin film) *inter alia* 1652 (C=O), 1594, 1527, 1446, 1435, 1221, 758, 731, 692 cm^{-1}; LRMS (ESI+) m/z

255.3 (M^+ + Na); HRMS (ESI+) m/z Calcd for $C_{13}H_{16}N_2O_2Na$ 255.1109 found 255.1121.

Entry 4, Table 14: 3,6-Dimethyl-*N*-phenyl-3,6-dihydro-2*H*-1,2-oxazine-2-carboxamide **207**

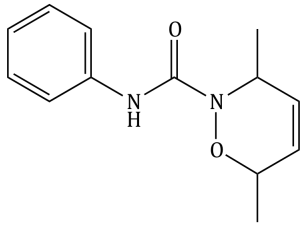

According to **GP12**: Using 1-hydroxy-3-phenylurea (120 mg, 0.79 mmol), 2,4-hexadiene (78 mg, 0.95 mmol), $CuCl_2$ (11 mg, 0.08 mmol) and 2-ethyl-2-oxazoline (16 mg, 0.16 mmol). The reaction was stirred for 4 h giving **207** (177 mg, 97%) as colourless oil; ^{1}H NMR (400 MHz, $CDCl_3$) δ 7.60 (s, 1H), 7.49 (d, *J* = 8.6, 2H), 7.34 – 7.27 (m, 3H), 7.09 – 7.02 (m, 2H), 5.91 – 5.85 (m, 1H), 5.75 – 5.67 (m, 1H), 4.74 – 4.59 (m, 2H), 1.34 (d, *J* = 6.7 Hz, 3H), 1.30 (d, *J* = 6.7 Hz, 3H); ^{13}C{^{1}H} NMR (101 MHz, $CDCl_3$) δ 154.4, 138.1, 128.9, 128.6, 128.1, 123.2, 119.3, 75.2, 49.0, 19.0, 16.9; FTIR (thin film) *inter alia* 1669 (C=O), 1649, 1594, 1522, 1444, 1231, 751, 727, 692 cm^{-1}; LRMS (ESI+) m/z 233.2 (M^+ + H); HRMS (ESI+) m/z Calcd for $C_{13}H_{17}N_2O_2$ 233.1290 found 233.1315.

Entry 5, Table 14: 4-Methyl-*N*-phenyl-3,6-dihydro-2*H*-1,2-oxazine-2-carboxamide **208** and 5-methyl-*N*-phenyl-3,6-dihydro-2*H*-1,2-oxazine-2-carboxamide **208'**

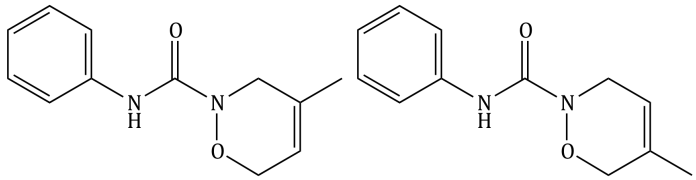

Using 1-hydroxy-3-phenylurea (140 mg, 0.92 mmol), isoprene (75 mg, 1.10 mmol), $CuCl_2$ (12 mg, 0.092 mmol) and 2-ethyl-2-oxazoline (18 mg, 0.18 mmol), the reaction was stirred for 6 h giving **208/208'** (191 mg, 95%) as a white solid. The ratio of **208**:**208'** = 4.45:1 and the ratio of **208** and **208'**:**209** = 9:1; m.p. 69 – 72 °C; **208:** ^{1}H NMR (400 MHz, $CDCl_3$) δ 7.68 (s, 1H), 7.48 (dt, *J* = 8.8, 1.7 Hz, 2H), 7.31 (tq, *J* = 5.8, 1.9 Hz, 2H), 7.11 – 7.02 (m, 1H), 5.55 (ddt, *J* = 4.5, 3.0, 1.6 Hz, 1H), 4.47 (dp, *J* = 4.3, 2.1 Hz, 2H), 4.02 (d, *J* = 0.8 Hz, 2H), 1.82 – 1.77 (m, 3H); ^{13}C{^{1}H} NMR (101 MHz, $CDCl_3$) δ 155.5, 138.0, 131.0, 129.0, 123.4, 119.3, 117.5, 69.4, 47.8, 19.9.

208': ^{1}H NMR (400 MHz, $CDCl_3$) δ 7.68 (s, 1H), 7.48 (dt, *J* = 8.8, 1.7 Hz, 2H), 7.31 (tq, *J* = 5.8, 1.9 Hz, 2H), 7.10 – 7.03 (m, 1H), 5.61 (dd, *J* = 3.3, 1.7 Hz, 1H), 4.36 (d, *J* = 0.7 Hz, 2H), 4.10 (dd, *J* = 3.4, 2.1 Hz, 2H), 1.71 (d, *J* = 1.5 Hz, 3H); ^{13}C{^{1}H} NMR (101 MHz, $CDCl_3$) δ 155.6, 137.9, 131.1, 129.0, 123.4, 119.3, 117.0, 72.5, 44.0, 18.2; FTIR (thin film) *inter alia* 1644 (C=O), 1593, 1514, 1447, 1215, 751, 725, 689 cm^{-1}; LRMS (ESI+) m/z 241.3 (M^+ + Na); HRMS (ESI+) m/z Calcd for $C_{12}H_{14}N_2O_2Na$ 241.0953 found 241.0940.

Entry 6, Table 14: **210**

According to **GP12**: Using 1-hydroxy-3-phenylurea (37 mg, 0.24 mmol), 9,10-dimethylanthracene (45 mg, 0.22 mmol), $CuCl_2$ (3 mg, 0.02 mmol) and 2-ethyl-2-oxazoline (5 mg, 0.05 mmol), the reaction was stirred for 48 h giving **4h** (9 mg, 10%)

Entry 7, Table 14: *N*,3,6-Triphenyl-3,6-dihydro-2*H*-1,2-oxazine-2-carboxamide **211**

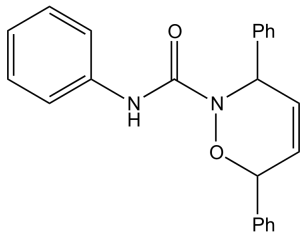

According to **GP12**: Using 1-hydroxy-3-phenylurea (79 mg, 0.52 mmol), 1,4-diphenyl-1,3-butadiene (96 mg, 0.47 mmol), $CuCl_2$ (7 mg, 0.05 mmol) and 2-ethyl-2-oxazoline (10 mg, 0.10 mmol), the reaction was stirred for 48 h **211** (50 mg, 30 %) as colourless oil; ^{1}H NMR (400 MHz, $CDCl_3$) δ 7.64 – 7.58 (m, 3H), 7.55 – 7.49 (m, 4H), 7.34 – 7.31 (m, 4H), 7.14 – 7.02 (m, 4H), 6.72 (s, 1H), 6.29 – 6.18 (m, 1H), 6.15 – 6.08 (m, 1H), 5.92 – 5.83 (m, 1H), 5.74 – 5.67 (m, 1H); ^{13}C{^{1}H} NMR (101 MHz, $CDCl_3$) δ 153.8, 138.5, 137.9, 136.9, 129.5, 129.0, 128.9, 128.5, 128.3, 128.1, 128.0, 127.5, 126.9, 123.4, 119.4, 81.3, 55.7; FTIR (thin film) *inter alia* 1710 (C=O), 1599, 1526, 1500, 1446, 1314,1225, 1068, 752, 723, 691 cm^{-1}; LRMS (ESI+) m/z 379.3 (M^+ + Na); HRMS (ESI+) m/z Calcd for $C_{23}H_{20}N_2O_2Na$ 379.1422 found 379.1428.

Entry 8, Table 14: 6-(Hydroxymethyl)-3-methyl-*N*-phenyl-3,6-dihydro-2*H*-1,2-oxa -zine-2-carboxamide **212** and 3-(hydroxymethyl)-6-methyl-*N*-phenyl-3,6-dihydro-2*H*-1,2-oxazine-2-carboxamide **212'**

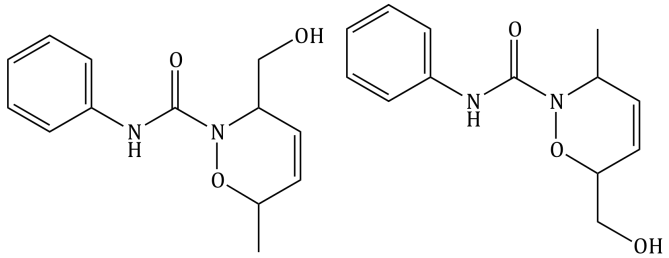

According to **GP12**: Using 1-hydroxy-3-phenylurea (70 mg, 0.46 mmol), 2,4-Hexadien-1-ol (45 mg, 0.46 mmol), $CuCl_2$ (7 mg, 0.05 mmol) and 2-ethyl-2-oxazoline (9 mg, 0.09 mmol). The reaction was stirred for 3 h giving **212/212'** (103 mg, 90%) as colourless oil. The ratio of **212**:**212'** = 1.5:1;

212: ^{1}H NMR (400 MHz, $CDCl_3$) δ 7.88 (s, 1H), 7.52 – 7.43 (m, 2H), 7.36 – 7.29 (m, 2H), 7.13 – 7.03 (m, 1H), 6.02 (ddd, *J* = 10.2, 4.6, 2.3 Hz, 1H), 5.66 (dt, *J* = 10.2, 1.5 Hz, 1H), 4.70 (ddd, *J* = 11.0, 5.5, 3.4 Hz, 2H), , 3.89 – 3.82 (m, 2H), 2.42 (br, 1H), , 1.26 (d, *J* = 6.6 Hz, 3H); ^{13}C{^{1}H} NMR (151 MHz, $CDCl_3$) δ 154.6, 137.6, 130.4 (ene), 129.0, 123.7, 123.2(ene), 119.7, 74.5, 63.8, 54.6, 18.9;

212': ^{1}H NMR (400 MHz, $CDCl_3$) δ 7.67 (s, 1H), 7.44 (d, *J* = 8.0 Hz, 2H), 7.28 (t, *J* = 7.7 Hz, 2H), 7.05 (t, *J* = 7.4 Hz, 1H), 5.85 (d, *J* = 10.6 Hz, 1H), 5.80 (d, *J* = 10.3 Hz, 1H), 4.78 (s, 1H), 4.67 (dd, *J* = 12.6, 6.2 Hz, 1H), 3.84 (s, 1H), 3.76 (s, 1H), 3.18 (s, 1H), 1.31 (d, *J* = 6.7 Hz, 3H); ^{13}C{^{1}H} NMR (151 MHz, $CDCl_3$) δ 155.1, 138.0, 131.3 (ene), 128.9, 123.4, 122.9 (ene), 119.6, 80.0, 63.7, 49.3, 17.0; FTIR (thin film) *inter alia* 1707 (C=O), 1600, 1534, 1501, 1446, 1314, 1224, 1067, 753, 724, 691 cm^{-1}; LRMS (ESI+) m/z 271.2 (M^+ + Na); HRMS (ESI+) m/z Calcd for $C_{13}H_{16}N_2O_3Na$ 271.1083 found 271.1069.

3.13 Reaction of 1-hydroxy-3-phenylurea 171 and 1,3-cyclohexadiene using 10% $CuCl_2$ and chiral ligand

***GP13**: General procedure for 10%$CuCl_2$ and chiral ligand catalytic system*

To a methanol (5 ml) solution of the 1,3-cyclohexadiene, 10% $CuCl_2$ and 10% ligand was added hydroxamic acid**.** The resulting solution was stirred at room temperature in air and was monitored by TLC. The completion of the reaction was confirmed by the disappearance of the starting material. The solvent was removed by evaporation and the crude product was purified by silica gel chromatography (hexane: ethyl acetate, 6:1 v/v, as eluent).

Entry 1, Table 15

According to **GP13**: 1-Hydroxy-3-phenylurea (94 mg, 0.62 mmol), 1,3-cyclohexadiene (101 mg, 1.24 mmol), $CuCl_2$ (8 mg, 0.06 mmol) and 2,2′-bis[(4*S*)-4-benzyl-2-oxazoline] (20 mg, 0.06 mmol). The reaction was finished in 4 hours to yield the white solid product **171** (135 mg, 95%).

Entry 2, Table 15

According to **GP13**: 1-Hydroxy-3-phenylurea (47 mg, 0.31mmol), 1,3-cyclohexadiene (50 mg, 0.62 mmol), $CuCl_2$ (4 mg, 0.03 mmol) and (+)-2,2′-isopropylidenebis[(4*R*)-4-benzyl-2-oxazoline] (11 mg, 0.03 mmol). The reaction was completed in 3 hours to yield the white solid product **171** (69 mg, 98%).

Entry 3, Table 15

According to **GP13**: 1-Hydroxy-3-phenylurea (36 mg, 0.24 mmol), 1,3-cyclohexadiene (38 mg, 0.48 mmol), $CuCl_2$ (3 mg, 0.04 mmol) and 2,6-bis[(4*S*)-(−)-isopropyl-2-oxazolin-2-yl]pyridine (7 mg, 0.04 mmol). The reaction was completed in 4 hours to yield the white solid product **171** (53 mg, 96 %). The enantiomeric excess of cycloadduct **183** was determined by HPLC using Chiralcel OD column, 254 nm UV detector, IPA/hexane, 3.5:6.5 v/v, giving peaks at retention times 9.06 and 19.90 minutes.

3.14 Reaction of (*S*)-1-Hydroxy-3-(1-phenylethyl)urea 172 and 1,3-cyclohexadiene using 10% $CuCl_2$ and chiral ligand

Entry 1, Table 16

According to **GP13**: (*S*)-1-Hydroxy-3-(1-phenylethyl)urea (97 mg, 0.54 mmol), 1,3-cyclohexadiene (86 mg, 1.08 mmol), $CuCl_2$ (7 mg, 0.05 mmol) and 2,2′-bis[(4*S*)-4-benzyl-2-oxazoline] (17 mg, 0.05 mmol). The reaction completed in 2 hours to yield the white solid product **172** (136 mg, 98%).

Entry 2, Table 16

According to **GP13**: (*S*)-1-Hydroxy-3-(1-phenylethyl)urea (94 mg, 0.52 mmol), 1,3-cyclohexadiene (83 mg, 1.04 mmol), $CuCl_2$ (7 mg, 0.05 mmol) and (+)-2,2′-isopropylidene-bis[(4*R*)-4-benzyl-2-oxazoline] (19 mg, 0.05 mmol). The reaction completed in 2 hours to yield the white solid product **172** (133 mg, 99%).

Entry 3, Table 16

According to **GP13**: (*S*)-1-Hydroxy-3-(1-phenylethyl)urea (71 mg, 0.39 mmol), 1,3-cyclohexadiene (63 mg, 0.78 mmol), $CuCl_2$ (5 mg, 0.04 mmol) and 2,6-bis[(4*S*)-(−)-isopropyl-2-oxazolin-2-yl]pyridine (12 mg, 0.04 mmol). The reaction completed in 2 hours to yield the white solid product **172** (99 mg, 98%).

Entry 4, Table 16

According to **GP13**: (*S*)-1-Hydroxy-3-(1-phenylethyl)urea (82 mg, 0.46 mmol), 1,3-cyclohexadiene (73 mg, 0.92 mmol), $CuCl_2$ (6 mg, 0.05 mmol) and 2,6-bis[(4*R*)-(−)-isopropyl-2-oxazolin-2-yl]pyridine (14 mg, 0.05 mmol). The reaction completed in 2 hours to yield the white solid product **172** (116 mg, 99%).

3.15 Reaction of (*S*)-1-Hydroxy-3-(1-phenylethyl)urea 172 and 2,3-dimethyl-1,3-butadiene using 10% $CuCl_2$ and 20% 2-ethyl-2-oxazoline

(*R*)-4,5-Dimethyl-*N*-(1-phenylethyl)-3,6-dihydro-2*H*-1,2-oxazine-2-carboxamide **196**

To a MeOH (5 ml) solution of 2,3-dimethyl-1,3-butadiene (58 mg, 0.71 mmol), $CuCl_2$ (5 mg, 0.04 mmol) and 2-ethyl-2-oxazoline (7 mg, 0.07 mmol) was added (*S*)-1-Hydroxy-3-(1-phenylethyl)urea (64 mg, 0.36 mmol)**.** The resulting solution was stirred at room temperature in air and was monitored by TLC. The reaction completed in 6 hours. The solvent was removed by evaporation and the crude product was purified by silica gel chromatography (hexane:ethyl acetate, 6:1 v/v, as eluent). The product **196** was obtained as a colourless oil (92 mg, 99%).

Chapter 4. References

References

1. A. Baeyer, *Ber. Dtsch. Chem. Ges*, **1874**, *7*, 1638.
2. S.M. Weinreb, R. R. Staib, *Tetrahedron* **1982**, *38*, 3087.
3. P. Ehrlich, F. Sachs, *Ber. Dtsch. Chem. Ges*, **1899**, *32*, 3341.
4. N. Momiyama, H. Yamamoto, *J. Am. Chem. Soc*. **2005**, *127*, 1080.
5. G.W. Kirby, *Chem. Soc. Rev*, **1977**, *6*, 1.
6. W. Adam, O. Krebs, *Chem. Rev.* **2003**, *103*, 4131.
7. H. Yamamoto, M. Kawasaki, *Bull. Chem. Soc. Jpn*. **2007**, *80*, 595.
8. E. Bosch, J.K. Kochi *J. Org. Chem* **1994**, *59*, 5573.
9. E. Müller, H. Metzger, D. Fries, U. Heuschkel, K. Witte, E. Waidelich, G. Schmid *Angew. Chem.* **1959**, *71*, 229.
10. a)B. Oddo. *Gazz. Chim. Ital*. **1911**, 39, 659.; b) W. L. Waters, P. G. Marsh *J. Org. Chem.* **1975**, *40*, 3344.
11. a) J.C. Motte, H.G. Viehe, *Chimia* **1975**, *29*, 515.; b) E. H.Bartlett, C. Eaborn, D. R. M. Walton, *J. Chem. Soc*. **1970**, 1717.
12. J. M. Kauffman, J. Green, M. S. Cohen, M. M. Fein, E. L. Cottrill, *J. Am. Chem. Soc.* **1964**, *86*, 4210.
13. E. C.Taylor, R. H. Danforth, A. McKillop, *J. Org. Chem*. **1973**, *38,* 2088.
14. L. Birkofer, M. Franz, *Chem. Ber.* **1971**, *104*, 3062.
15. P. W. K. Flanagan, *Chem. Abstr*. **1965**, *63*, 17899e.
16. M. Herberhold, L. Haumaier, *Angew. Chem., Int. Ed. Engl.* **1984**, *23*, 521.
17. a)V.Tolman, J. Hanus, P. Sedmera, *Collect. Czech. Chem. Commun.* **1947,** *12,* 292.; b) C. A. Miller, R.A. Batey, *Org. Lett.* **2004**, *6*, 699.; c) G. W. Kirby, H. McGuigan, J. W. M. Machinnon, D. McLean and R. P.Sharma, *J. Chem. Soc., Perkin Trans. 1***, 1985**, 1437.
18. S. Aoyagi, R. Tanaka, M. Naruse, C. Kibayashi, *J. Org. Chem.* **1998**, *63*, 8397.
19. N. E. Jenkins, R. W. Ware, Jr., R. N. Atkinson, S. B. King, *Synth. Commun*. **2000**, *30*, 947.
20. L. H. Dao, J. M. Dust, D. Mackay, K. N. Watson, *Can. J. Chem*. **1979**, *57*, 1712.
21. a) K. R. Flower, A. P. Lightfoot, H. Wan, A. Whiting, *Chem. Commun.* **2001**, 1812.; b) S. Iwasa, K. Tajima, S. Tsushima, H. Nishiyama, *Tetrahedron Lett.*

2001, *42*, 5897.; c) S. Iwasa, A. Fakhruddin, Y. Tsukamoto, M. Kameyama, H. Nishiyama, *Tetrahedron Lett.* **2002**, *43*, 6159.

22. C.-M. Ho, T.-C. Lau, *New J. Chem.* **2000,** *24*, 859.
23. . Quadrelli, M. Mella, A. G. Invernizzi, P. Caramella, *Tetrahedron* **1999**, *55*, 10497.
24. T. Zerewitinoff, I. Ostromisslensky, *Ber.* **1911**, *44*, 2402.
25. S. Kobayashi, Y. Aoyama, Japan Patent 4329, Sept. 9, 1953; *Chem. Abstr*. **1953**, *49*, 4712h.
26. M. Mir, J. Marquet, E. Cayo´ n, *Tetrahedron Lett.* **1992**, *33*, 7053.
27. P. E. O Bannon, D. P. William, *Tetrahedron Lett.* **1988**, *29*, 5719.
28. J. E. T. Corrie, G. W. Kirby, J. W. M. Mackinnon, *J. Chem. Soc. Perkin Trans. 1* **1985**, 883.
29. F. Fringuelli, A. Taticchi, *Dienes in the Diets-Alder Reactions;* **1990**, Wiley, New Y ork.
30. L. Bollans, J. Bacsa, J. A. Iggo, G. A. Morris, A. V. Stachulski, *Org. Biomol. Chem*, **2009**, *7*, 4531.
31. R. R. Holmes, R. P. Bayer, L. A. Errede, H. R. Davis, A. W. Wiesenfeld, P. M. Bergman and D. L. Nicholas, *J. Org. Chem*., **1965**, *30*, 3837.
32. A. Ak, S. Prudent, D. LeNouen, A. Defoin, C. Tarnus, *Bioorg. Med. Chem. Lett.* **2010**, *20*, 7410.
33. a) R. W. Ware, Jr., S. B. King, *J. Org. Chem*. **2000**, *65*, 8725.; b) K. K. Singal, B. Singh, B. Raj, *Synth. Commun.* **1993**, *23*, 107.
34. O. Wichterle, Collect. *Czech. Chem. Commun*. **1947**, *12*, 292.
35. J. J. Vollmer, K. L. Servis, *J. Chem. Educ.* **1970**, *47*, 491.
36. R. Sustmann, *Pure Appl. Chem*. **1974**, 40, 569.
37. T. Sato, S. Aoyagi, C. Kibayashi, *Org. Lett.* **2003**, *5*, 3839.
38. L. Zhu, R. Lauchli, M. Loo, K. J. Shea, *Org. Lett.* **2007**, *9*, 2269.
39. A. G. Leach, K. N. Houk, *J. Org. Chem.* **2001**, *66*, 5192.
40. G. Kresze, J. Firl, *Tetrahedron Lett*. **1965**, 1163.
41. K. R. Flower, A. P. Lightfoot, H. Wan, A. Whiting, *J. Chem. Soc., Perkin Trans. 1* **2002**, 2058.
42. S. Iwasa, A. Fakhruddin, Y. Tsukamoto, M. Kameyama, H. Nishiyama, *Tetrahedron Lett*. **2002**, *43*, 6159.

43. M. F. A. Adamo, S. Bruschi, *J. Org. Chem*., **2007**, *72*, 2666.
44. T. Bota, C. Bucur, I. Drimus, L. Stănescu, D. Sändulescu, *Rev. Chim. (Bucharest, Rom.)* **1961**, *12*, 503.
45. B. Kalita, K. M. Nicholas, *Tetrahedron Lett.* **2005**, *46*, 1451.
46. X. Tusun, C. – D. Lu, *Synlett*. **2012**, 23, 1801.
47. A. A. P. Meekel, M. Resmini, U. K. Pandit, *J. Chem. Soc., Chem. Commun.* **1995**, 571.
48. D. A. Evans, J. S. Johnson, C. S. Burgey, K. R. Campos, *Tetrahedron Lett.* **1999**, 2879.
49. D. A. Evans, S. J. Miller, T. Lectka, P. von Matt, *J. Am. Chem. Soc.* **1999**, *121,* 7559.
50. S. Pulacchini, K. F. Sibbons, K. Shastri, M. Motevalli, M. Watkinson, H. Wan, A. Whiting, A. P. Lightfoot, *J. Chem. Soc., Dalton Trans.* **2003**, 2043.
51. Y. Yamamoto, H. Yamammoto, *J. Am. Chem. Soc*. **2004**, 126, 4128.
52. C. K. Jana, A. Studer, *Angew. Chem. Int. Ed*. **2007**, 46, 6542.
53. Y. Watanabe, H. Iida, C. Kibayashi, *J. Org. Chem*., **1989**, *54*, 4088.
54. G. Calvet, N. Blanchard, C. Kouklovsky, *Synthesis*, **2005**, 3346.
55. C. K. Jana, A. Studer, *Chem. Eur. J*. **2008**, *14*, 6326.
56. C. K. Jana, S. Grimme, A. Studer *Chem. Eur. J*, **2009**, *15*, 9078.
57. W. Lin, K. G. Virga, K.-H. Kim, J. Zajicek, D. Mendel, M. J. Miller *J. Org, Chem.* **2009**, *74*, 5941.
58. B. Yang, P. A. Miller, U. Mollmann, M. J. Miller *Org. Lett*. **2009**, *11*, 2828.
59. J.-C. Monbaliu, B. Tinant, J. Marchand-Brynaert, *J. Org. Chem*. **2010**, *75*, 5478.
60. P. Sancibrao, D. Karila, C. Kouklovsky, G. Vincent , *J. Org. Chem*. **2010**, *75*, 4333.
61. H. Lossen, *Liebigs Ann Chem.* **1869**, *150*, 314.
62. E. M. F. Muri, M. J. Nieto, R. D. Sindelar, J. S. Williamson, *Curr. Med. Chem*. **2002**, *9*, 1631.
63. A. J. Stemmler, J. W. Kampf, M. L. Kirk, B. H. Atasi and V. L. Pecoraro, *Inorg. Chem.,* **1999**, *38***,** 2807.
64. a) A. Angeli, *Gazz. Chim. Ital.* **1896**, *26*, 17.; b) E. Rimini, *Gazz. Chim. Ital.* **1901**, *31*, 84.
65. A. Porcheddu, G. Giacomelli *J. Org. Chem*.**2006**, *71*, 7057.

66. J. P. Devlin, W. D. Ollis, J. E. J. Thorpe, *J. Chem. Soc., Perkin Trans. 1* **1975**, 846.
67. A. Massaro, A. Mordini, G. Reginato, F. Russo and M. Taddei, *Synthesis* **2007**,3201.
68. A. O. Stewart, D. W. Brooks, *J. Org. Chem.* **1992**, *57*, 5020.
69. G.-R. Vasanthakumar and V. V. S. Babu, *Tetrahedron Lett.* **2003***, 44***,** 4099.
70. A. S. Reddy, M. S. Kumar and G. R. Reddy, *Tetrahedron Lett.* **2000***, 41***,** 6285.
71. G. Giacomelli, A. Porcheddu, M. Salaris, *Org. Lett.* **2003***, 5***,** 2715.
72. S. Uesato, Y. Hashimoto, M. Nishino, Y. Nagaoka, H. Kuwajima, *Chem. Pharm. Bull.* **2002**, *50*, 1280.
73. G. Clifton, S. R. Bryant, C. G. Skinner, *J. Med. Chem*. **1970**, *13*, 377.
74. J. Paz, C. Pérez-Balado, B. Iglesias, L. Muñoz, *J. Org. Chem*. **2010**, *75*, 8039.
75. a) S. Itoh, M. Taki, H. Nakao, P. L. Holland, W. B. Tolman, L. Que Jr., S. Fukazumi, *Angew. Chem. Int. Ed.* **2000**, 39, 398.; b) C. X. Zhang, H.-C. Liang, E. Kim, S. Kaderli, C. D. Incarvito, A. D. Zuberbühler, A. L. Rheingold, K. D. Karlin, *J. Am. Chem. Soc.* **2003**, 125, 634.
76. I. E. Markó, A. Gautier, R. Dumeunier, K. Doda, F. Philippart, S. M. Brown, C. J. Urch, *Angew. Chem. Int. Ed.* **2004**, *43*, 1588.
77. C. Zhang, N. Jiao, *Angew. Chem. Int. Ed*. **2010**, *49*, 6174.
78. C. P. Frazier, J. R. Engelking, J. Read de Alaniz, *J. Am. Chem. Soc.* **2011**, *133*, 10430.
79. C. P. Frazier, A. Bugarin, J. R. Engelking, J. Read de Alaniz, *Org. Lett.* **2012**, *14*, 3620.
80. a) J. A. K. Howard, G. Ilyashenko, H. Sparks, A. Whiting, *Dalton Trans.*, **2007**, 2108.; b) J. A. K. Howard, G. Ilyashenko, H. A. Sparkes, A. Whiting,a, A. R. Wright, *Adv. Synth. Catal.* **2008**, *350*, 869.
81. a) B. Liang, J. Liu, Y. X. Gao, K. Wongkhan, D. X. Shu, Y. Lan, A. Li, A. S. Batsanov, J. A. K. Howard, T. B. Marder, J. H. Chen, Z. Yang, *Organometallics* **2007** 26, 4756.; b) Y.-X. Gao, L. Chang, H. Shi, B. Liang, K. Wongkhan, D. Chaiyaveij, A.S. Batsanov, T. B. Marder, C.-C. Li, Z. Yang,a, Y. Huang, *Adv. Synth. Catal.* **2010**, *352*, 1955.
82. H.-C. Liang, E. Kim, C. D. Incarvito, A. L. Rheingold, K. D. Karlin, *Inorg. Chem.* **2002**, 41, 2209.
83. P. Zuman, B. Shah, *Chem. Rev*. **1994**, *94*, 1621.

84. S. H. Seda, J. Janczak , J. Lisowski *Inorg. Chim. Acta* **2006,** *359,* 1055–1063.
85. A. Defoin, M. Joubert, J.-M. Heuchel, C. Strehler, J. Streith, *Synthesis* **2000**, 12, 1719.
86. E. L. Eliel, S. H. Wilen, L. N. Mander, *Stereochemistry of Organic Compounds.*, Wiley, New York, **1994**.

Appendix

Benzyl 2-oxa-3-azabicyclo[2.2.2]oct-5-ene-3-carboxylate **140**

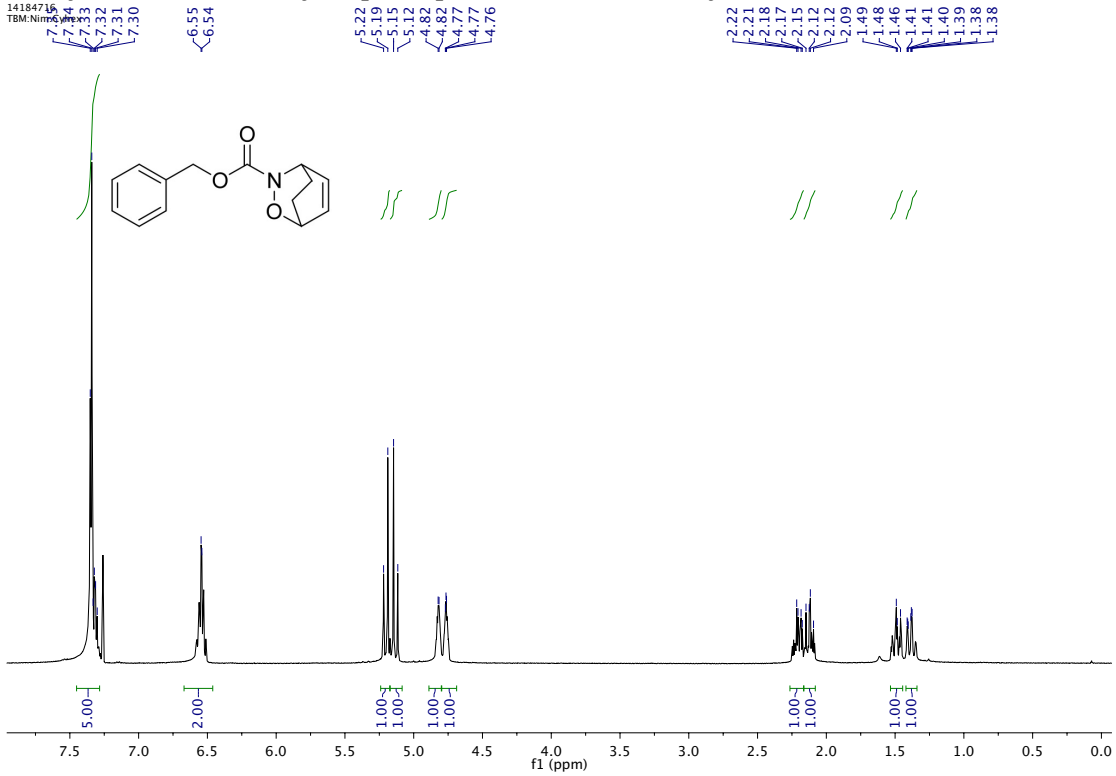

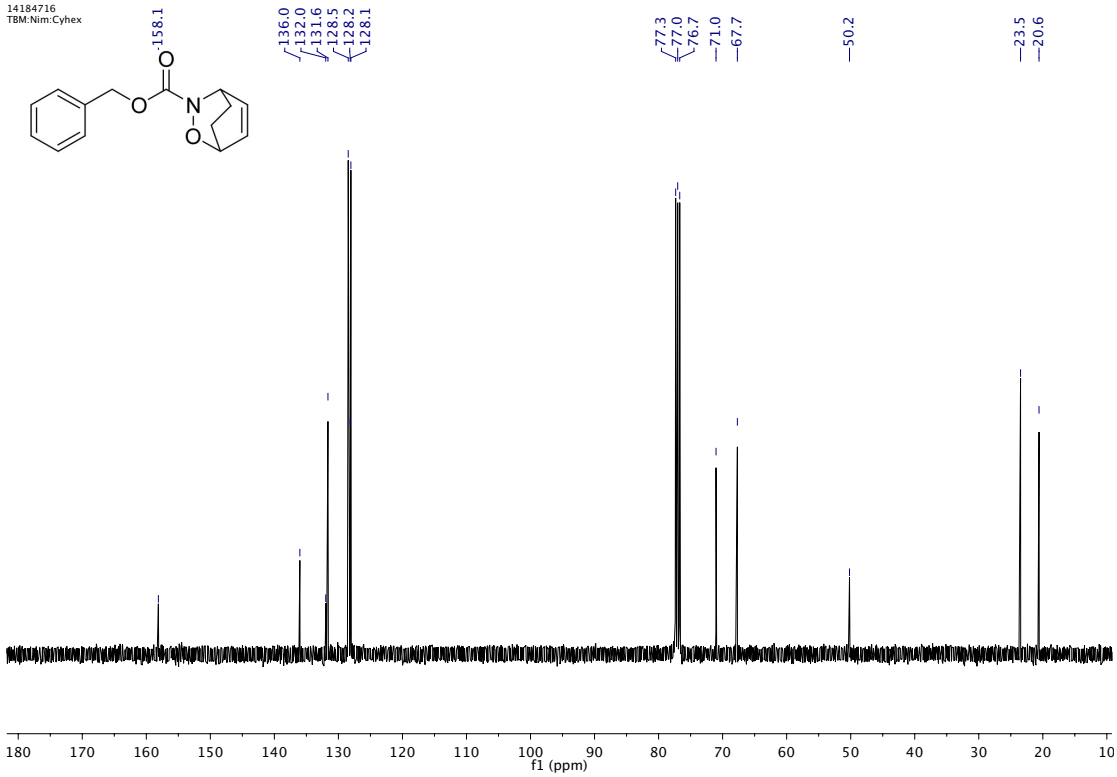

1-(2-Oxa-3-azabicyclo[2.2.1]hept-5-en-3-yl)-2-phenylethanone **146**

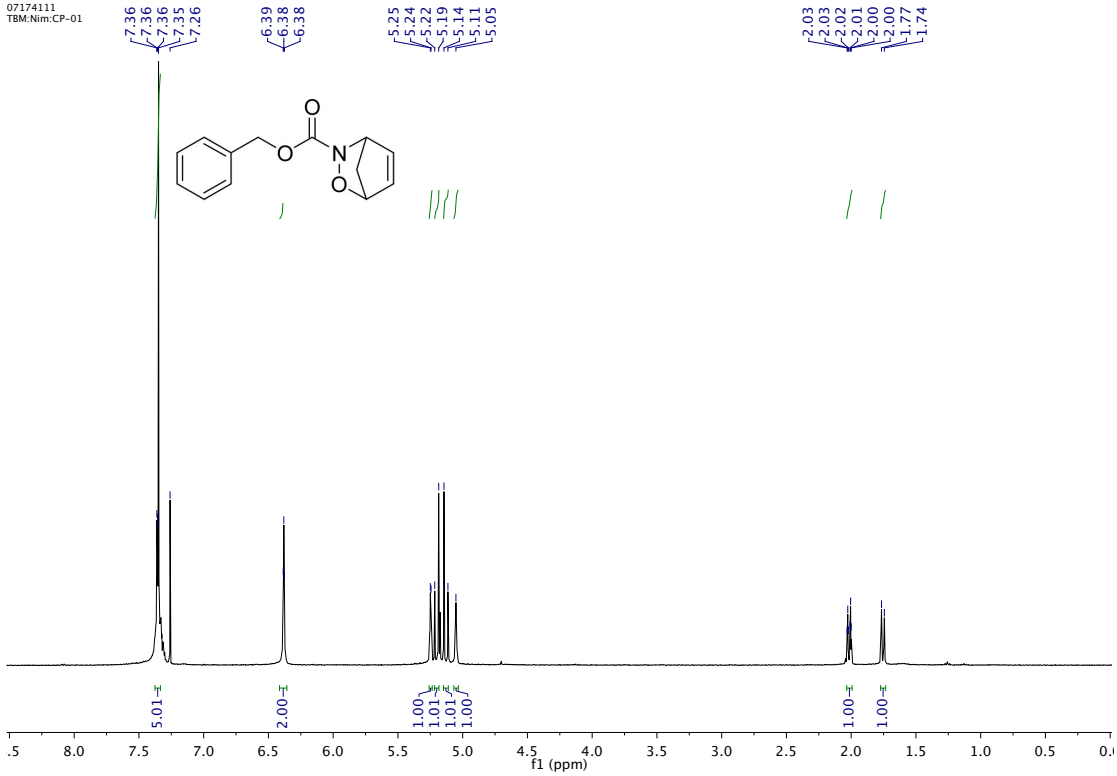

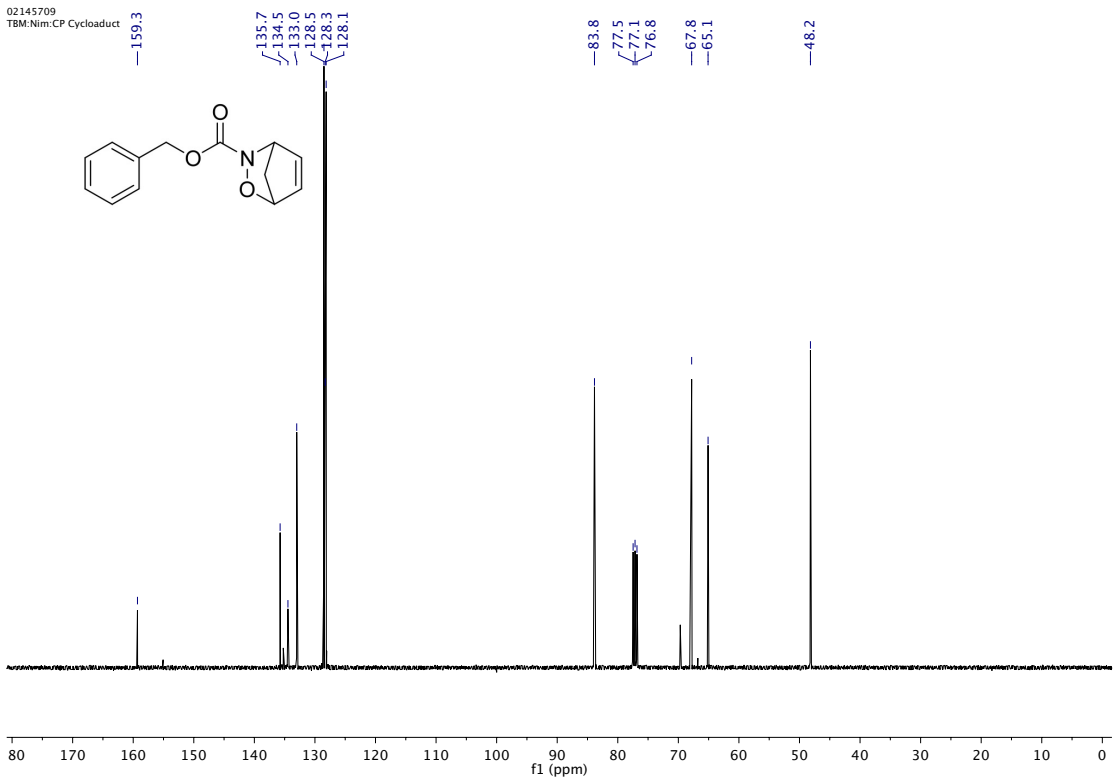

1-(4,5-Dimethyl-3,6-dihydro-2*H*-1,2-oxazin-2-yl)-2-phenylethanone **147**

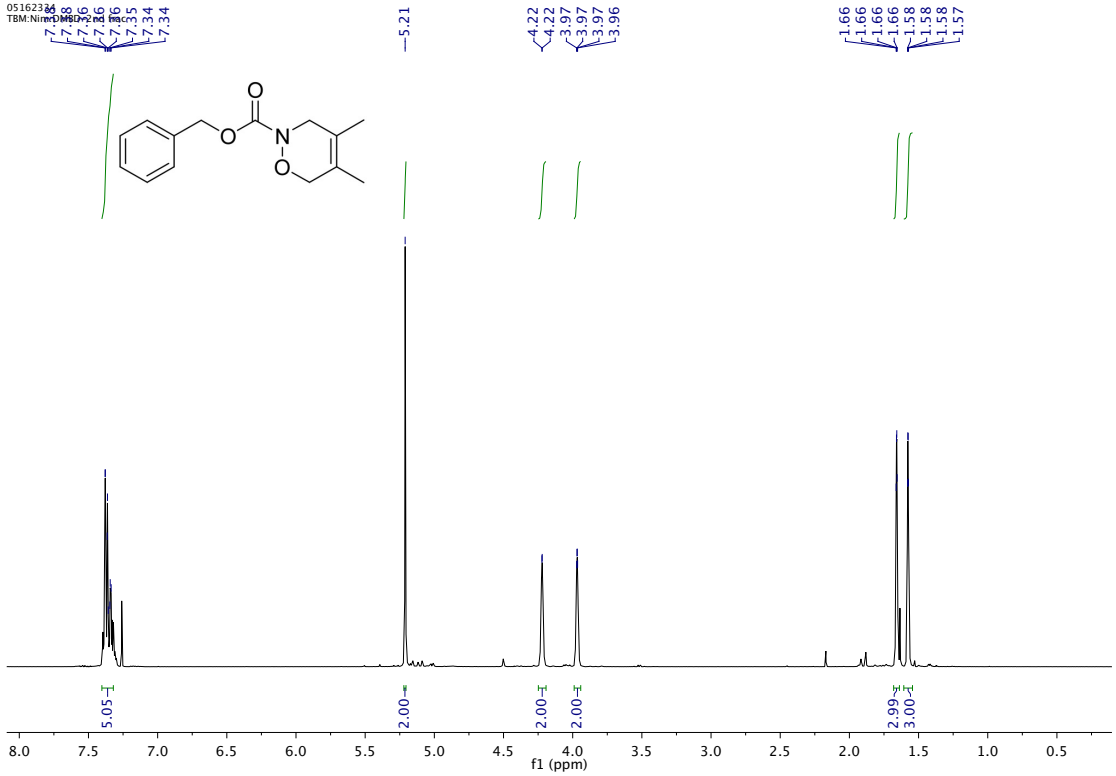

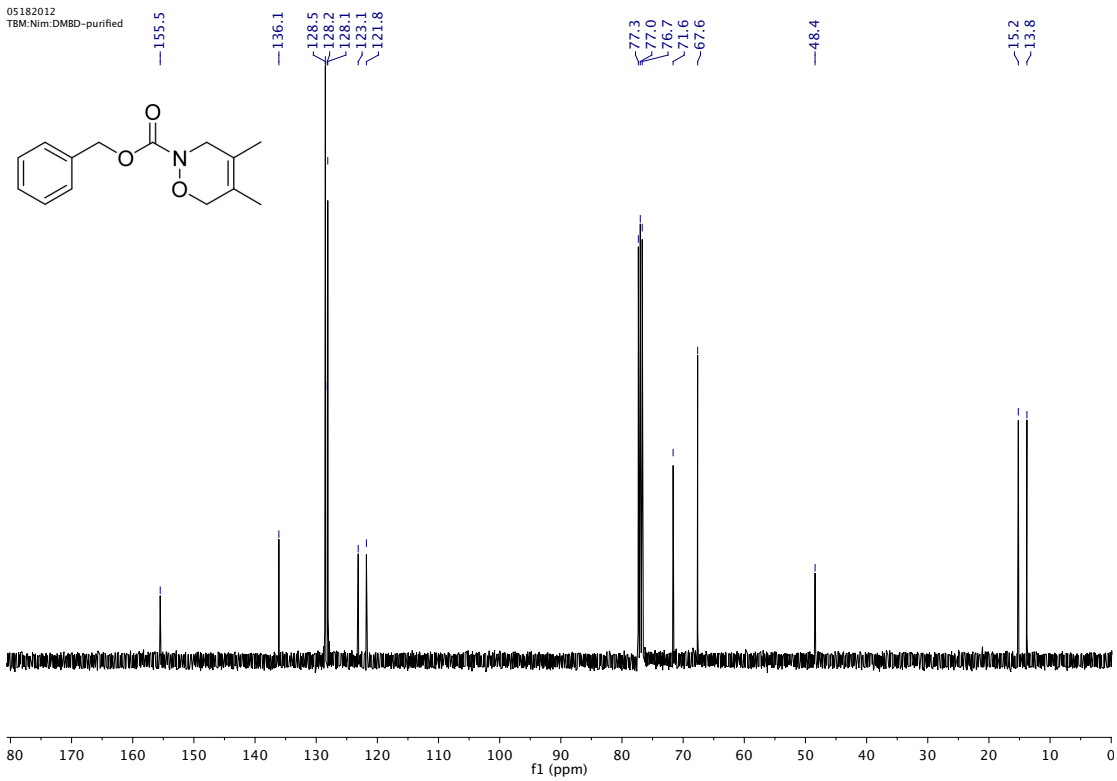

1-(3,6-Dimethyl-3,6-dihydro-2*H*-1,2-oxazin-2-yl)-2-phenylethanone **149**

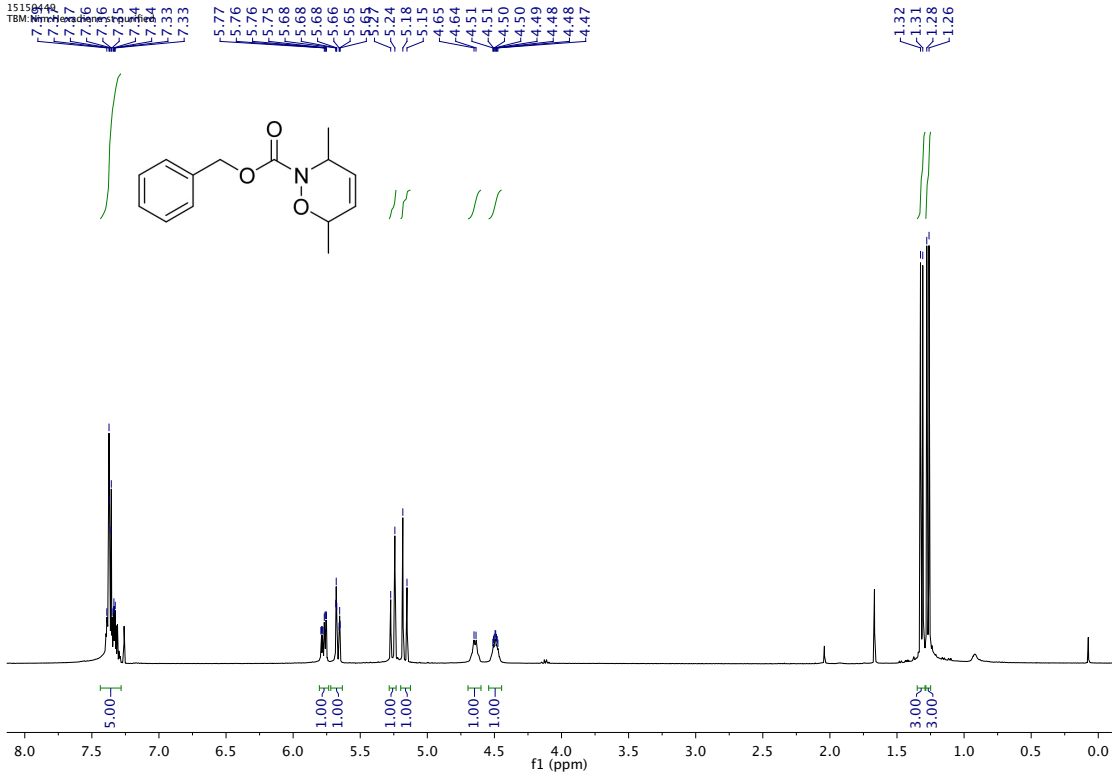

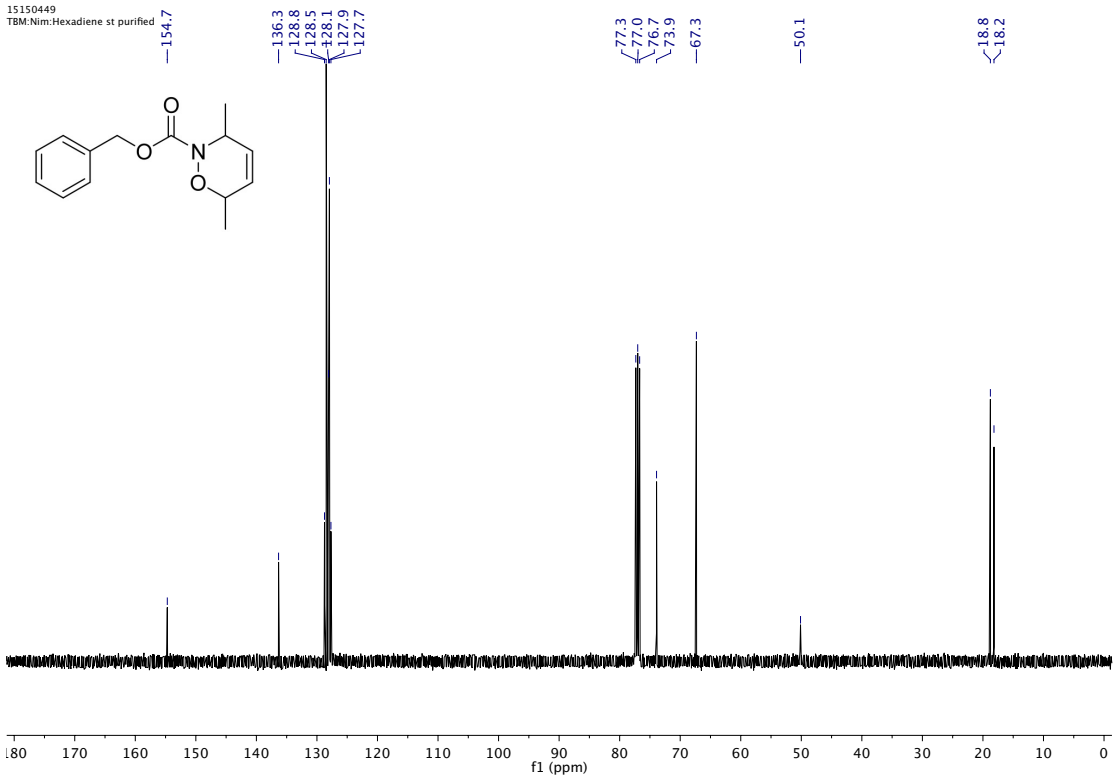

1-(4-Methyl-3,6-dihydro-2*H*-1,2-oxazin-2-yl)-2-phenylethanone **150** and 1-(5-methyl-3,6-dihydro-2*H*-1,2-oxazin-2-yl)-2-phenylethanone **150'**

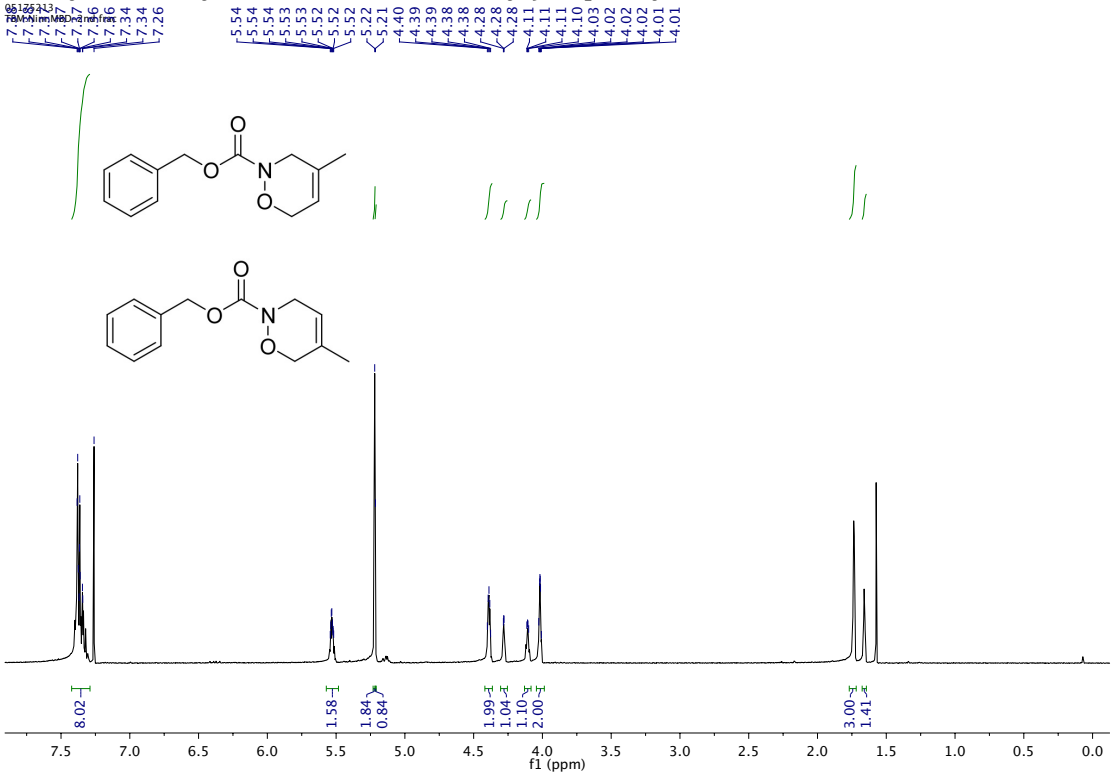

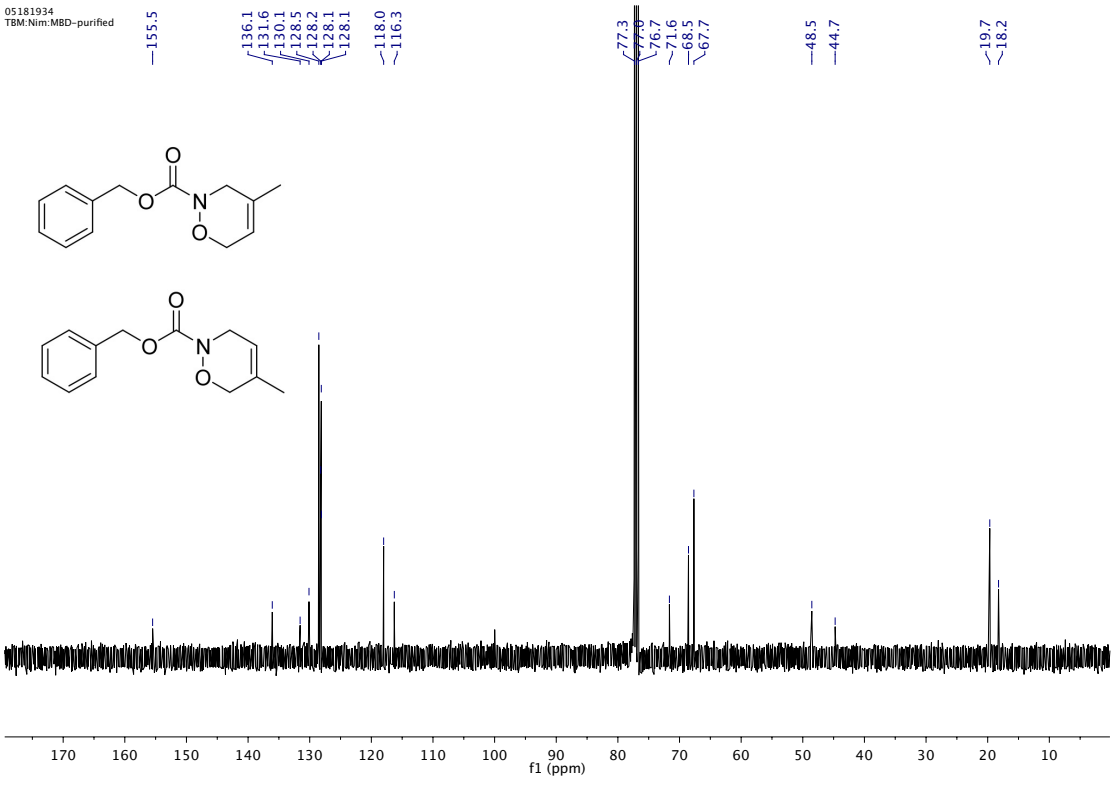

1-((9*s*,10*s*)-9,10-Dimethyl-9,10-dihydro-9,10-(epoxyimino)anthracen-11-yl)-2-phenylethanone **152**

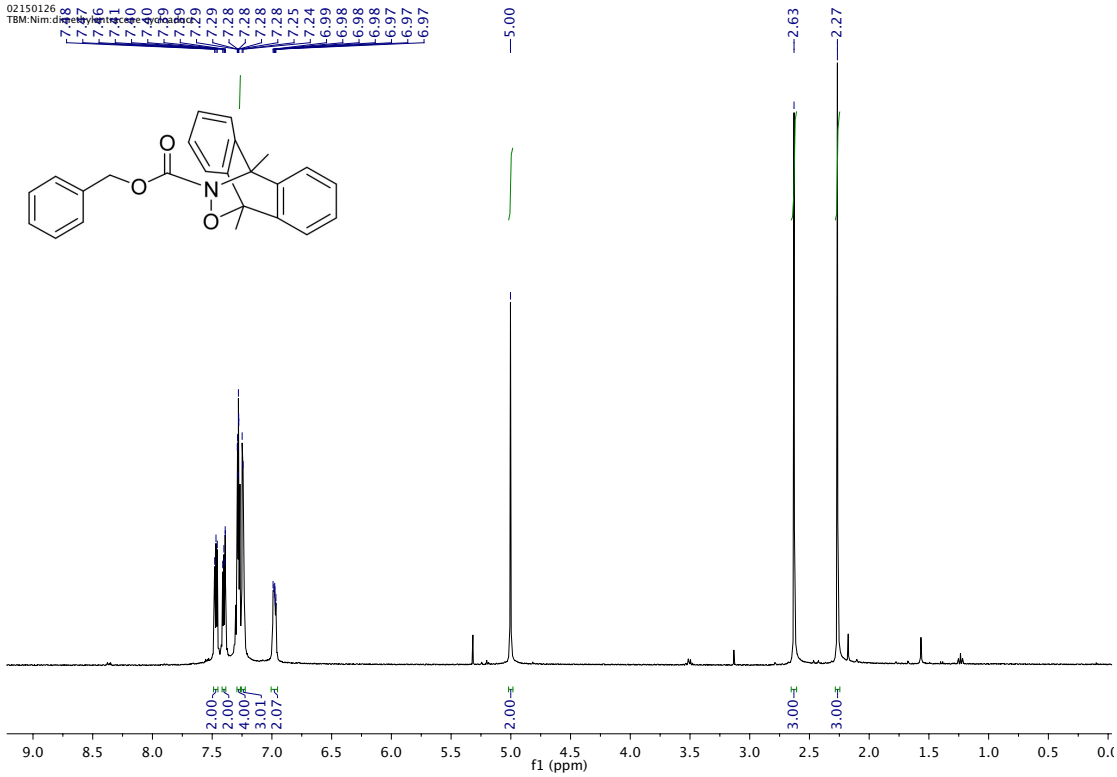

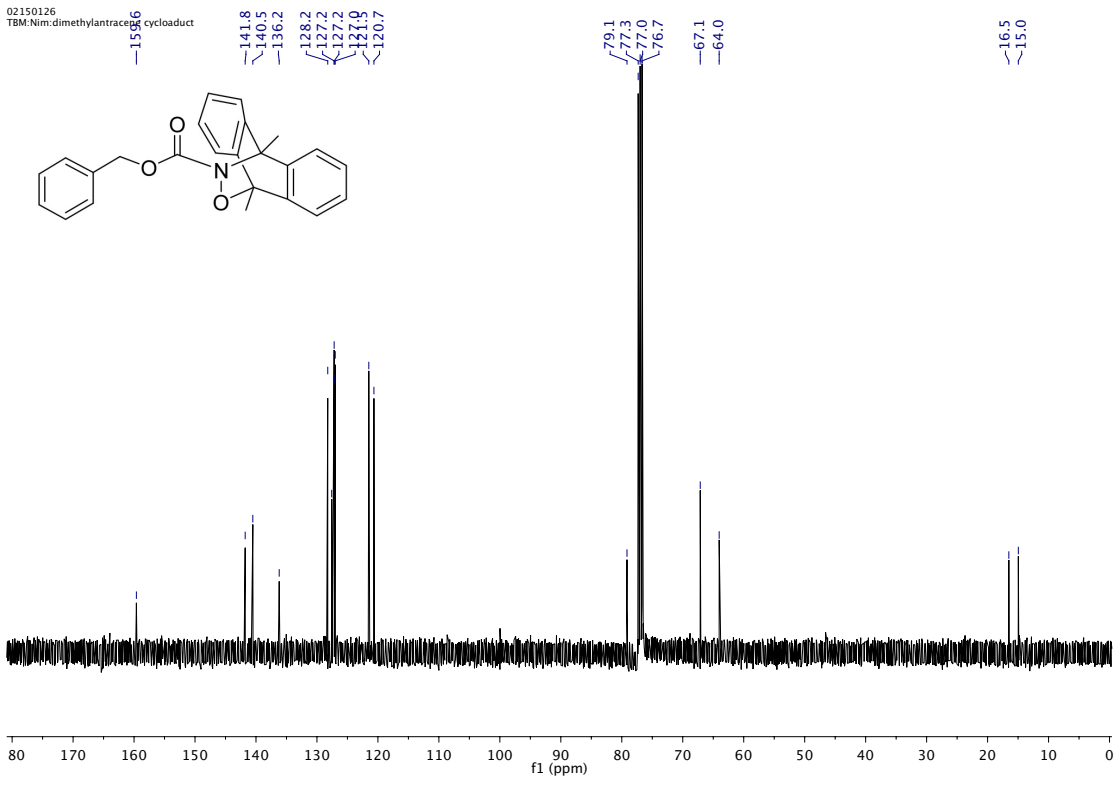

1-(3,6-Diphenyl-3,6-dihydro-2*H*-1,2-oxazin-2-yl)-2-phenylethanone **153**

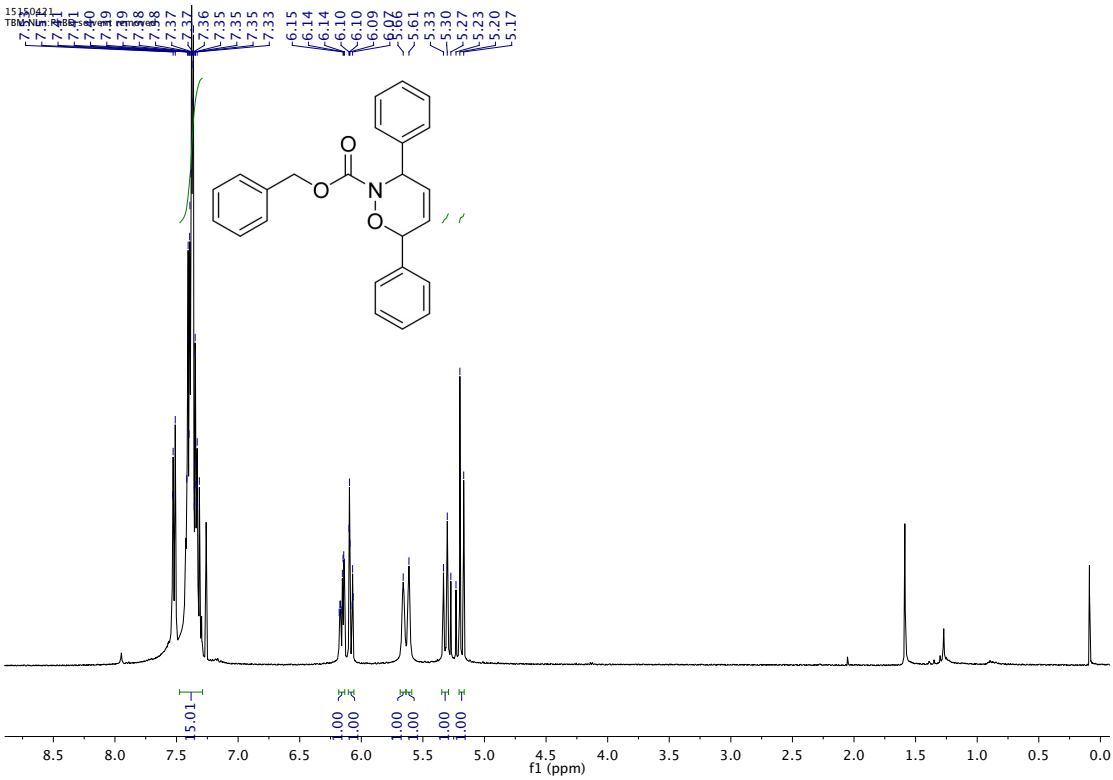

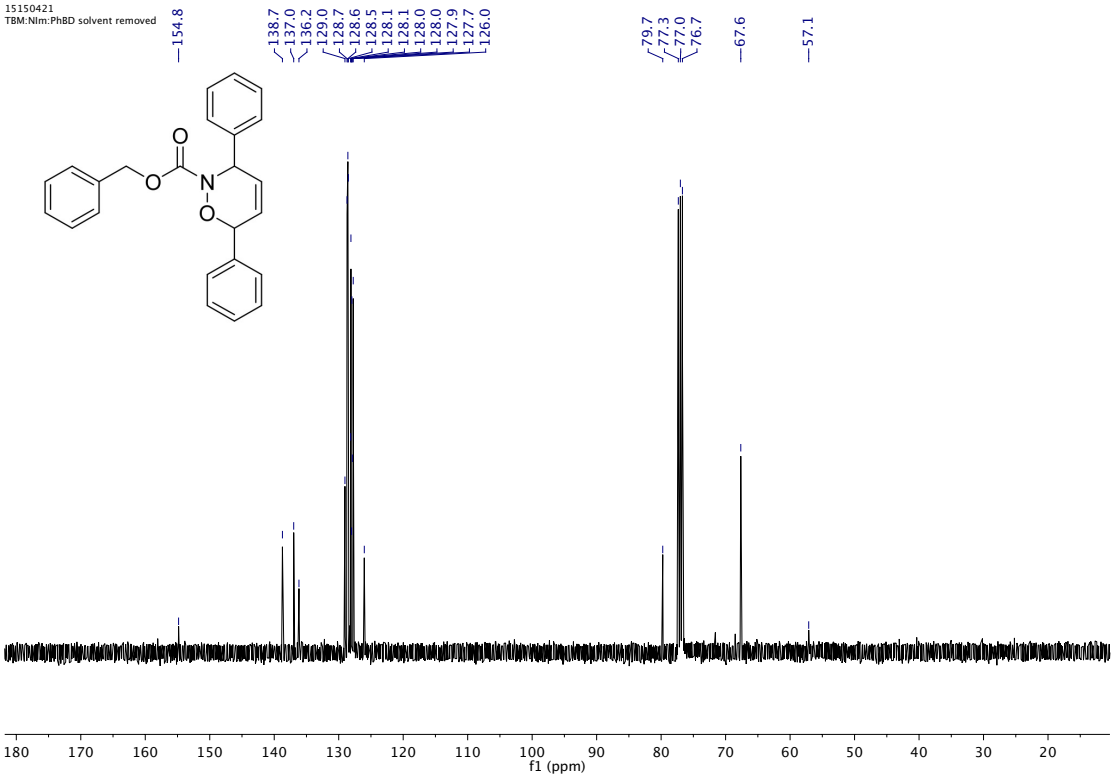

2-Pyridinehydroxamic acid **161**

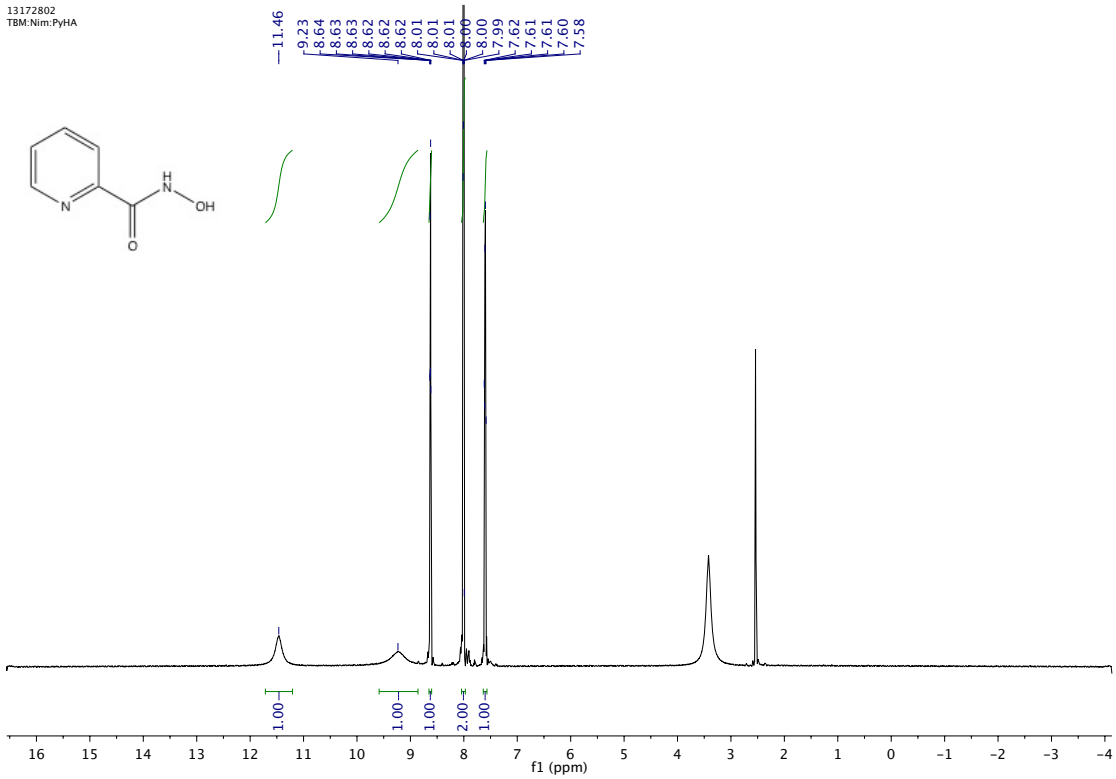

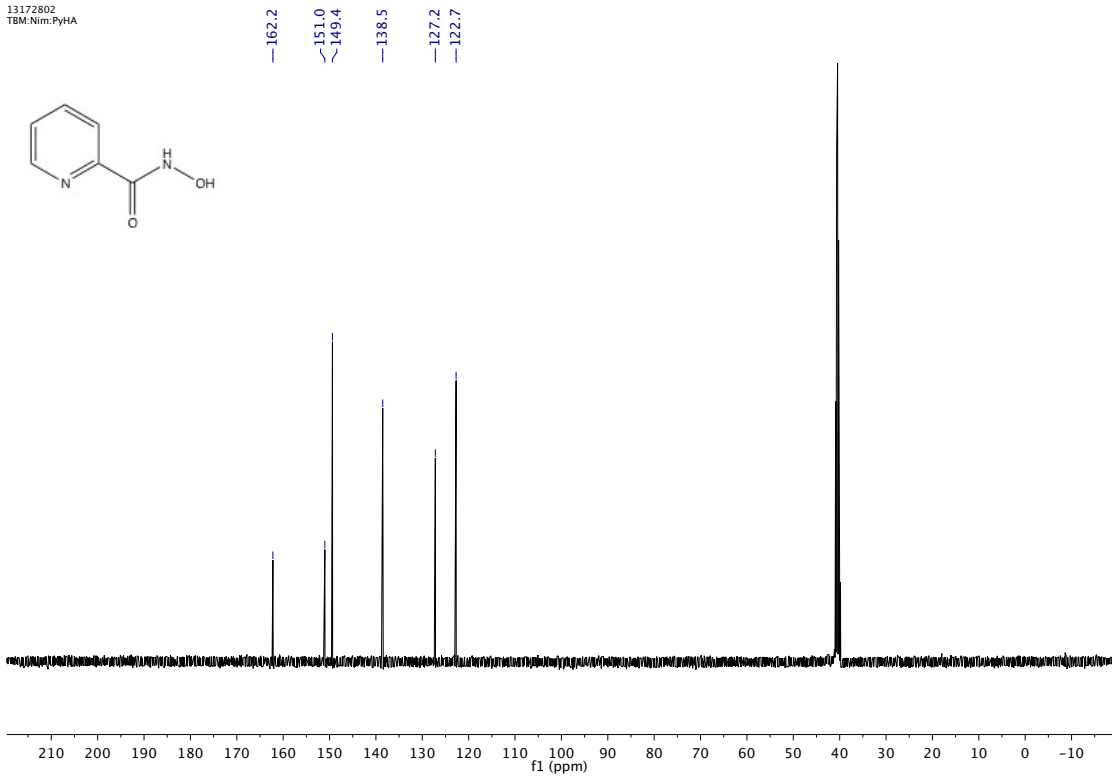

3-Pyridinehydroxamic acid **162**

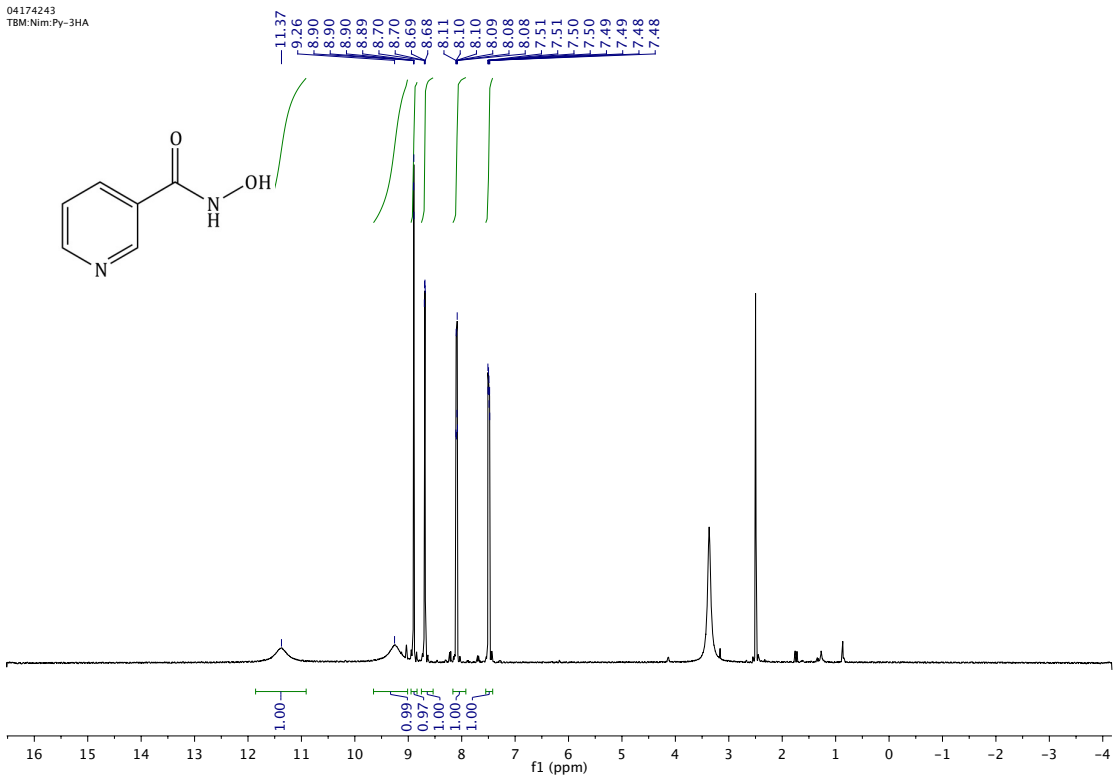

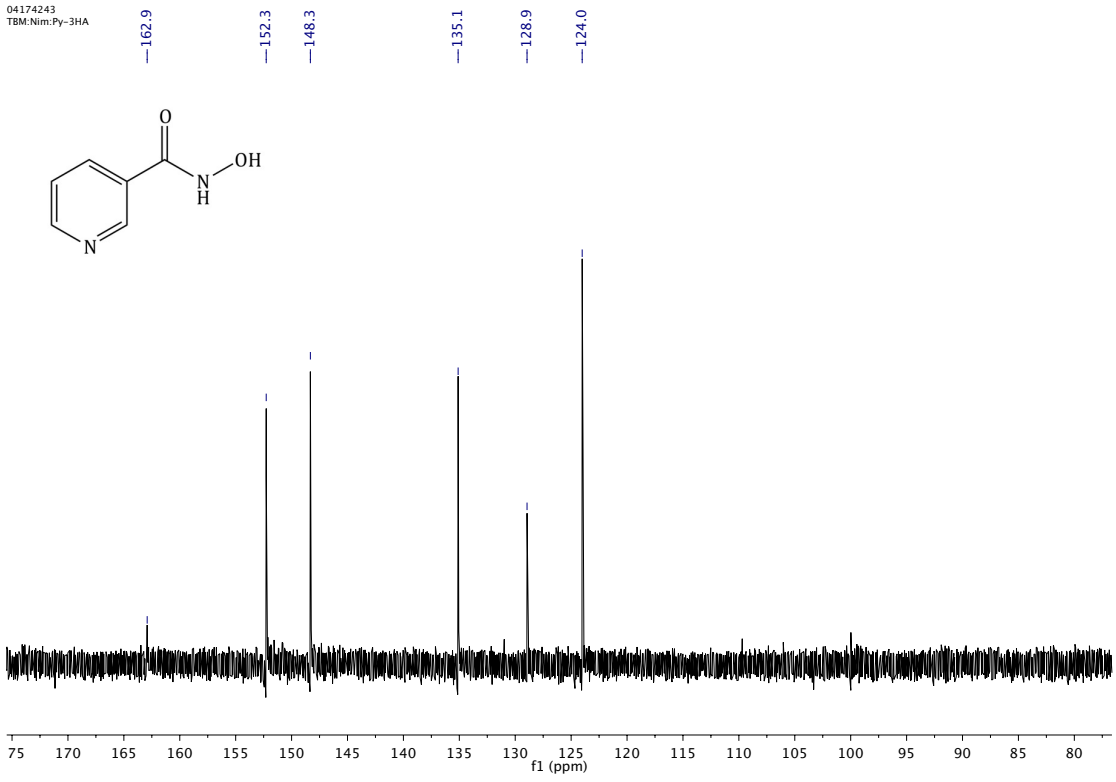

N-Hydroxy-2-(pyridin-2-yl)acetamide **163**

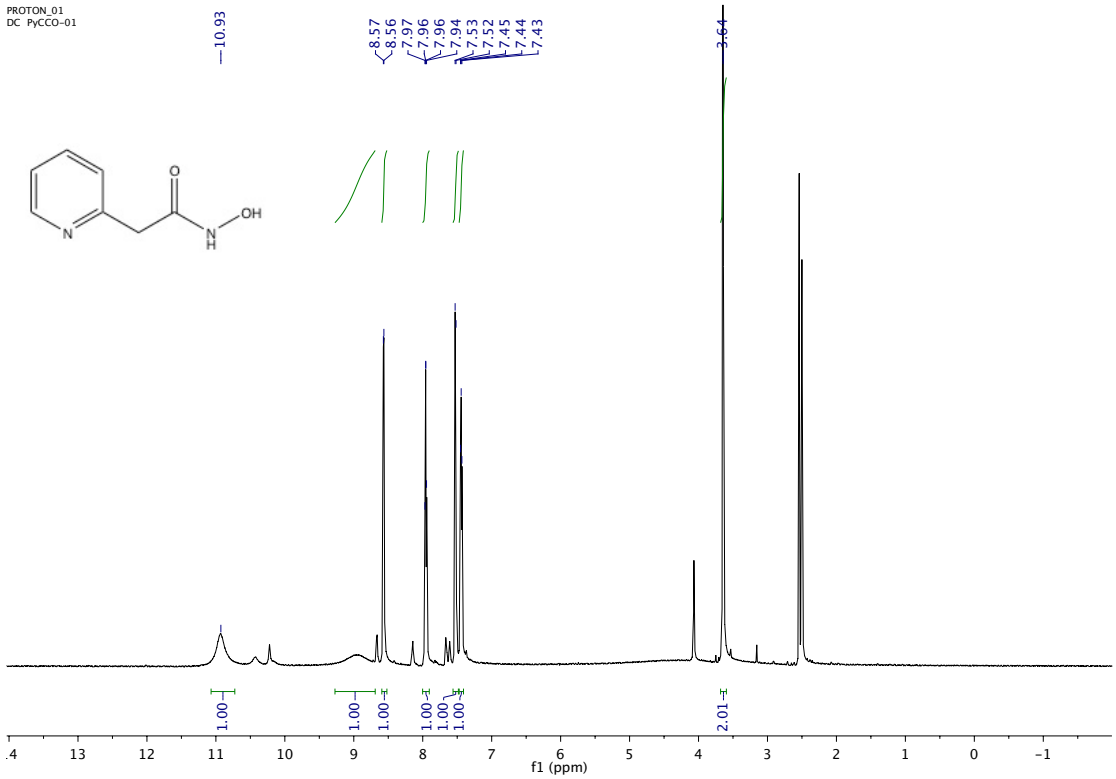

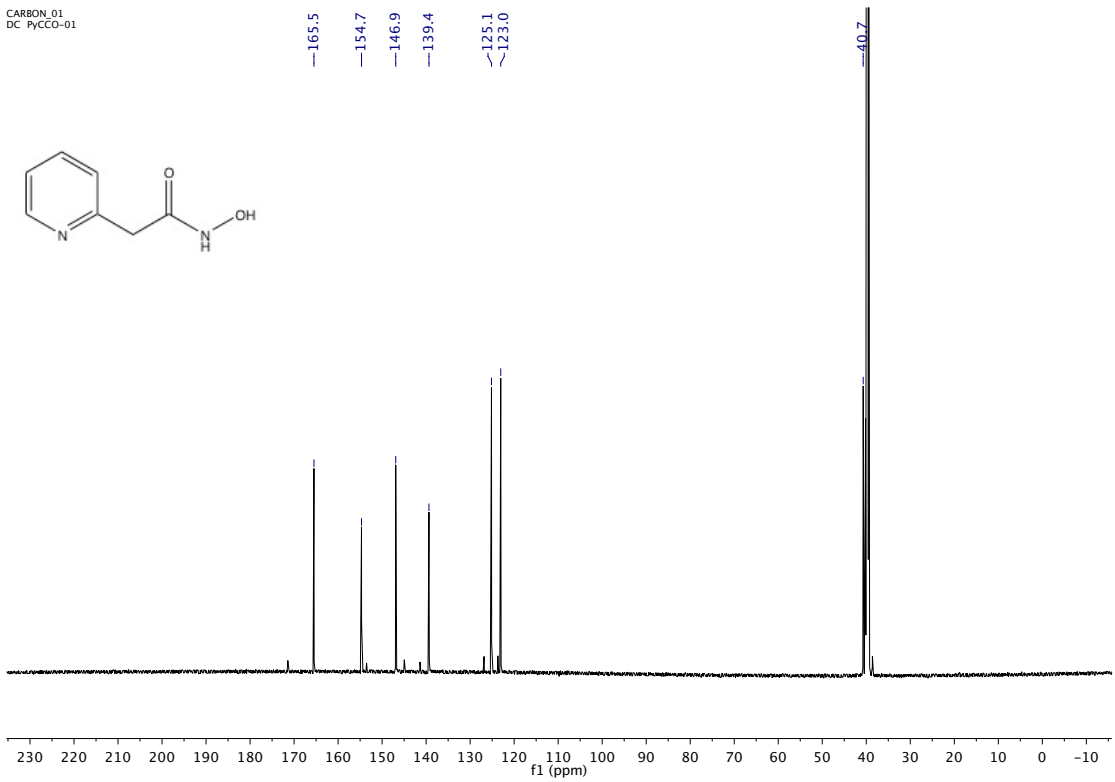

2-Amino-*N*-hydroxybenzamide **164**

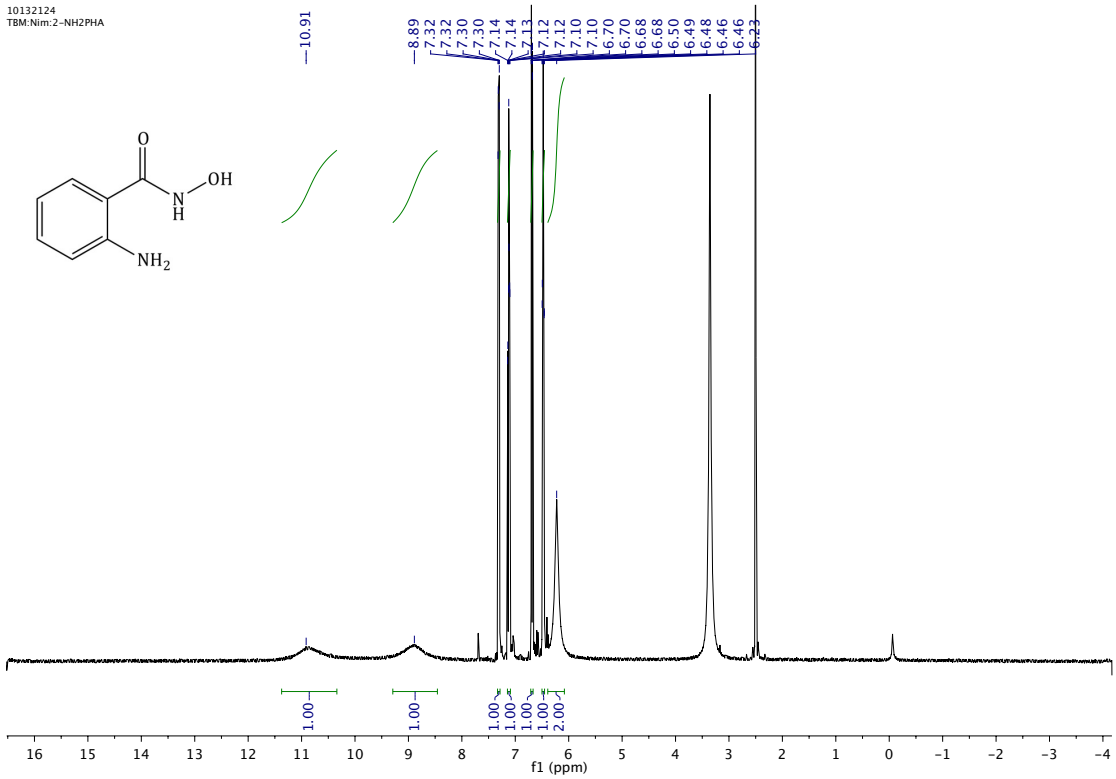

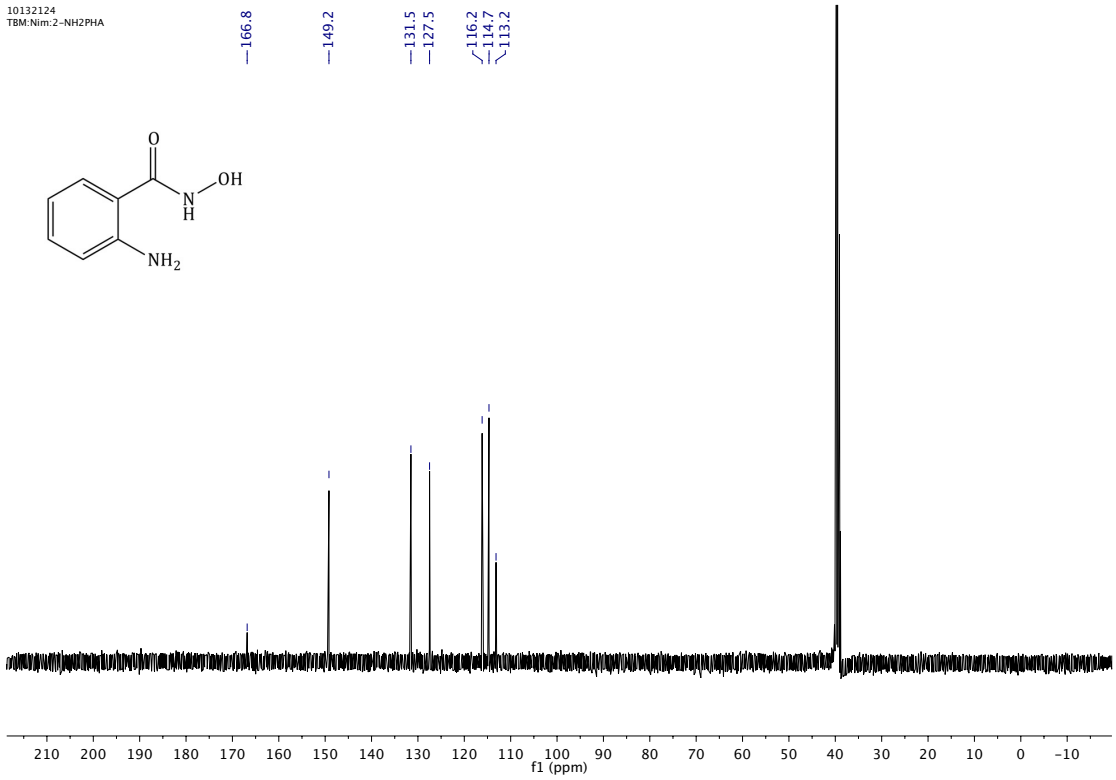

N-Hydroxybenzamide **165**

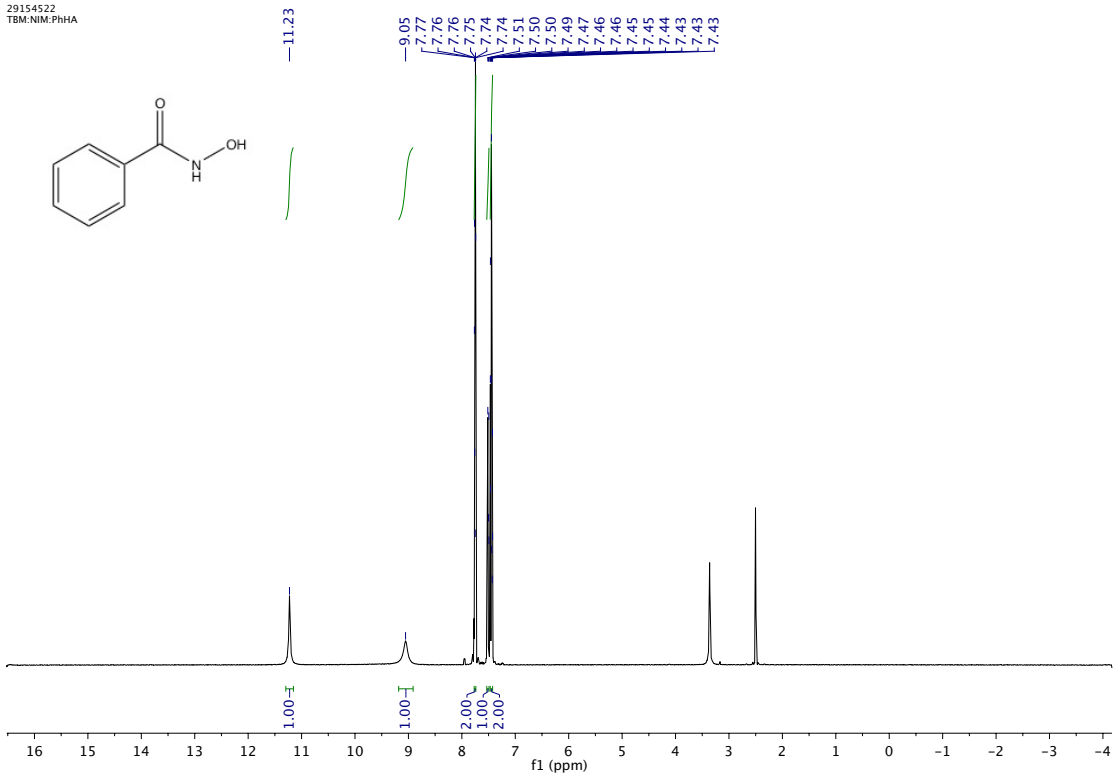

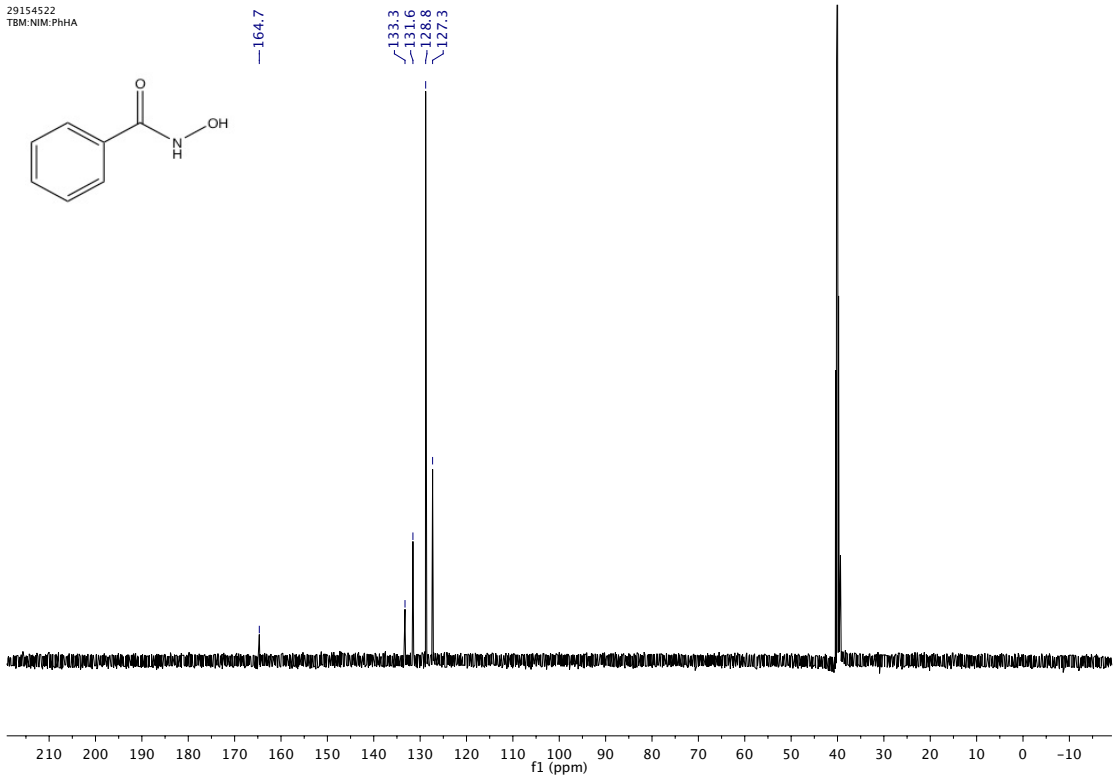

N-Hydroxy-2-phenylacetamide **166**

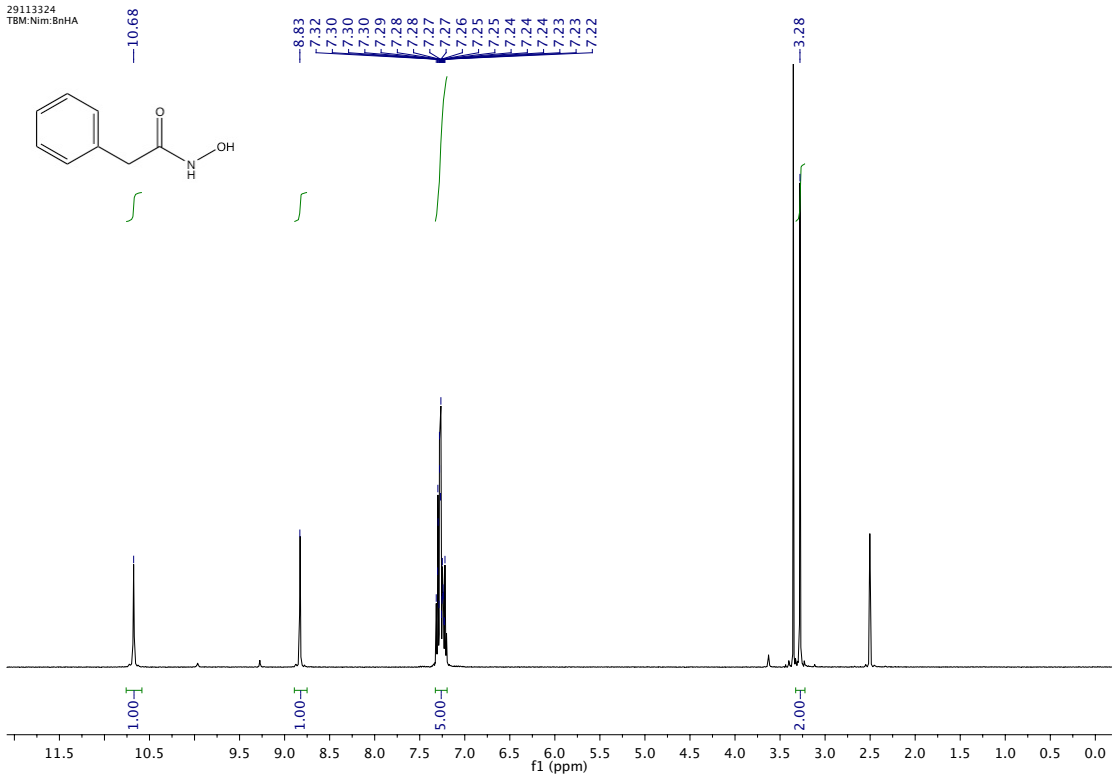

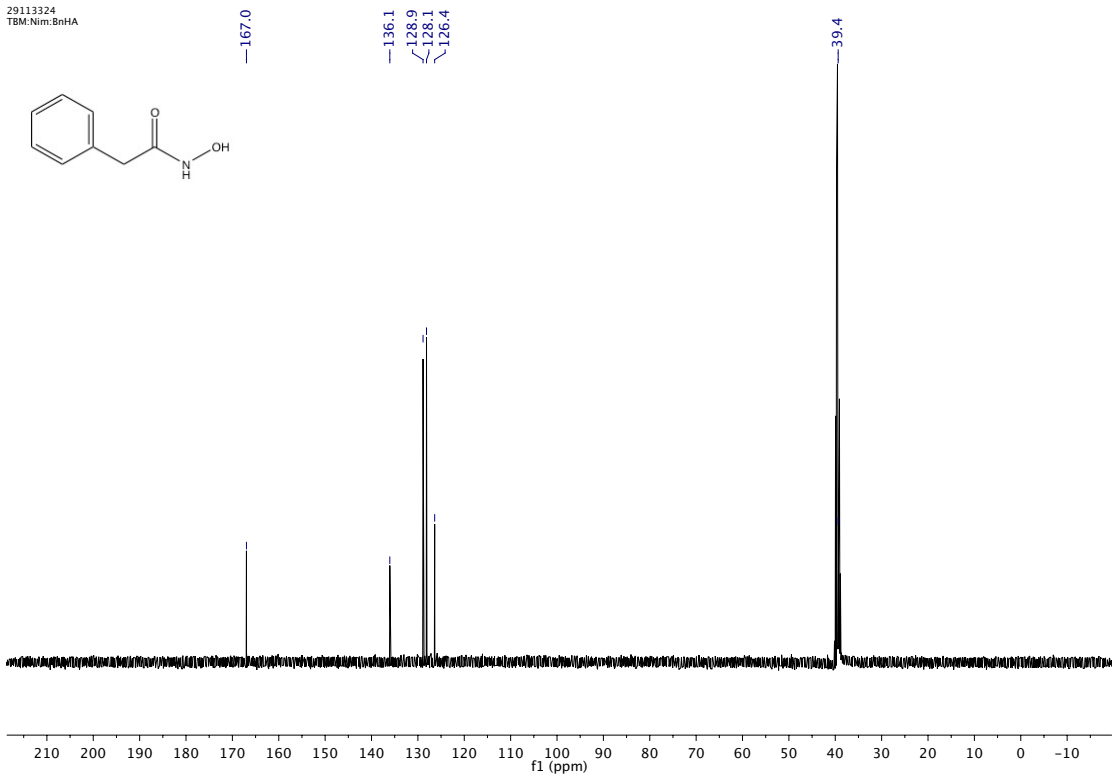

N-Hydroxy-3-phenylpropanamide **167**

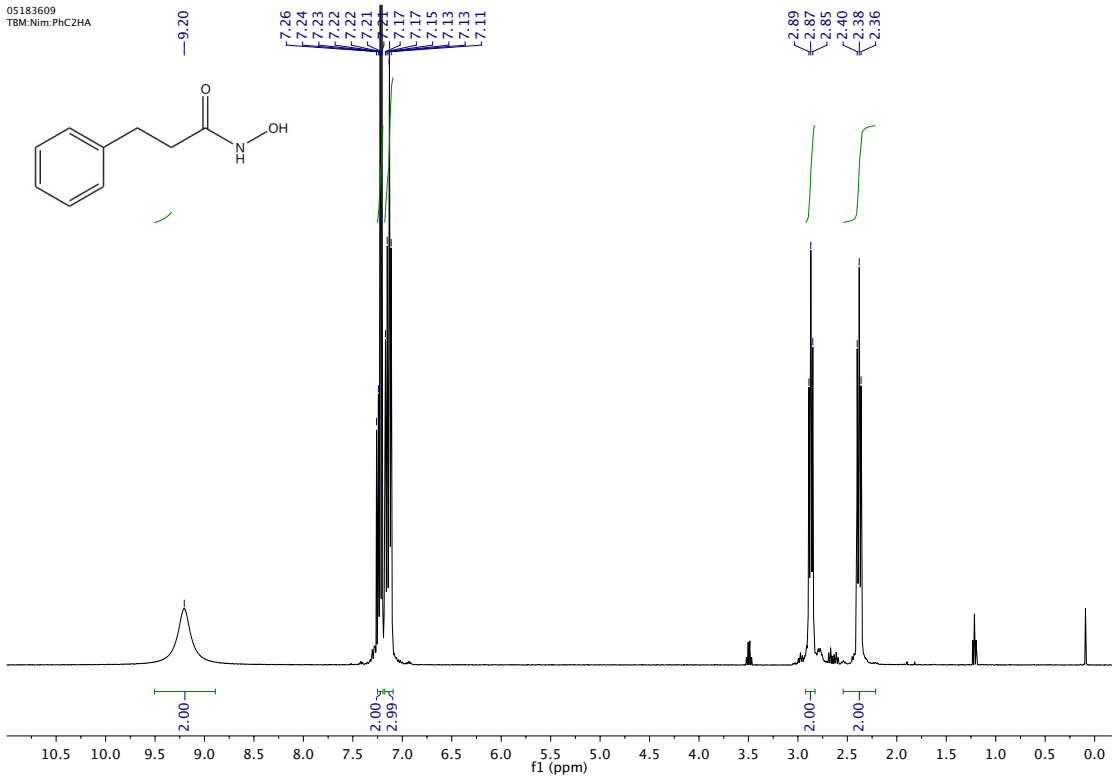

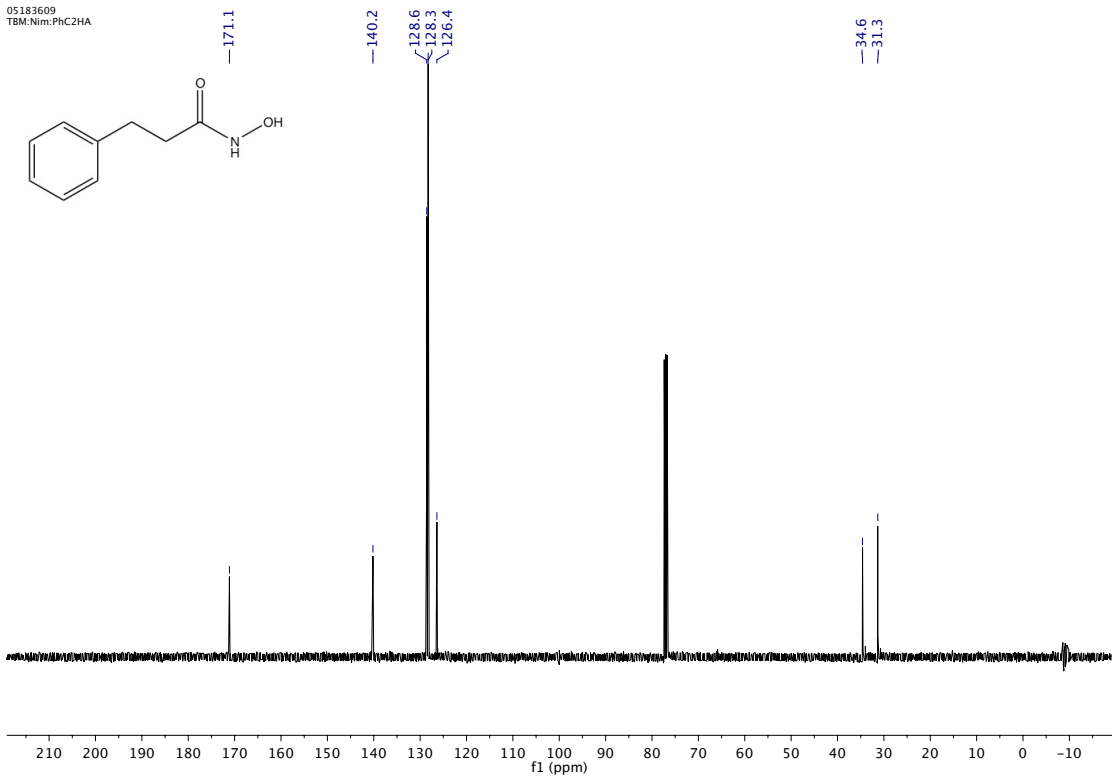

N-Hydroxy-4-phenylbutanamide **168**

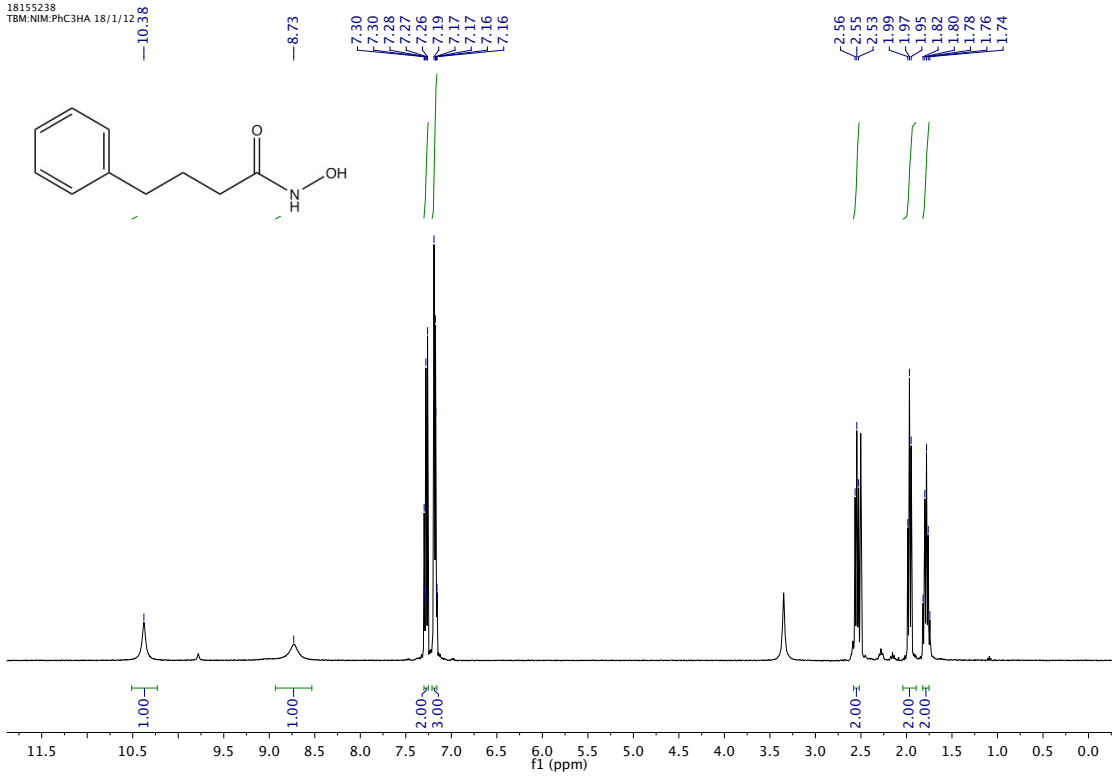

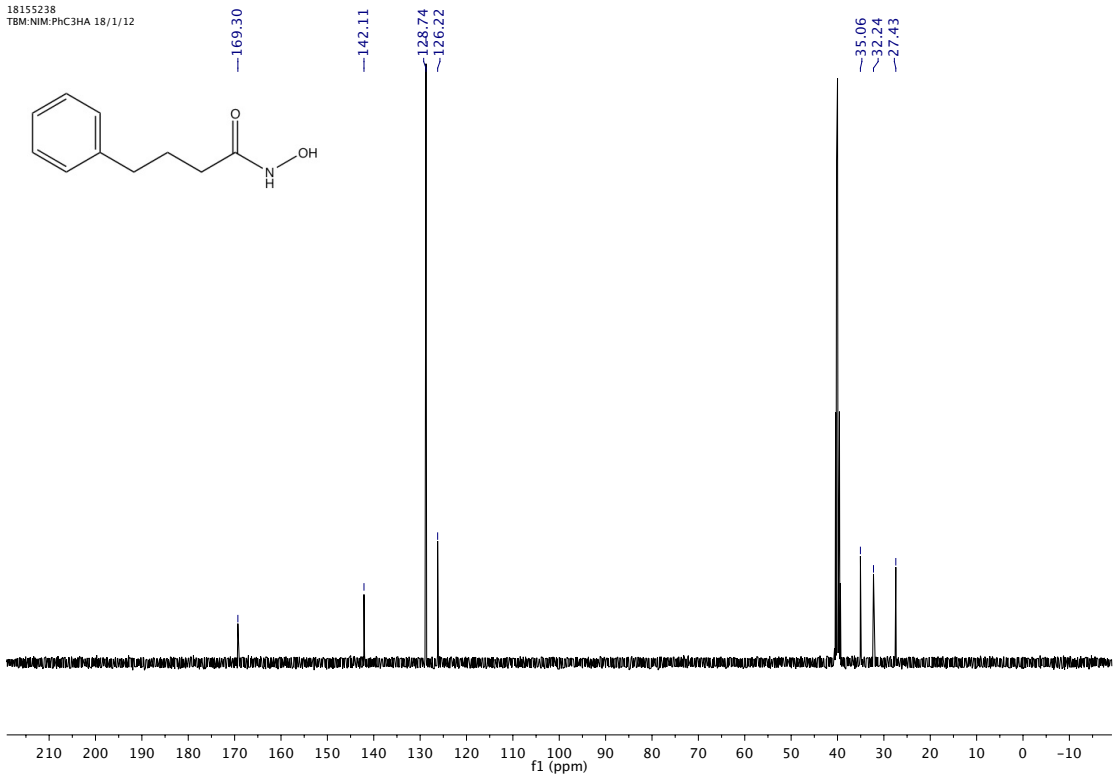

N-Hydroxy-5-phenylpentanamide **169**

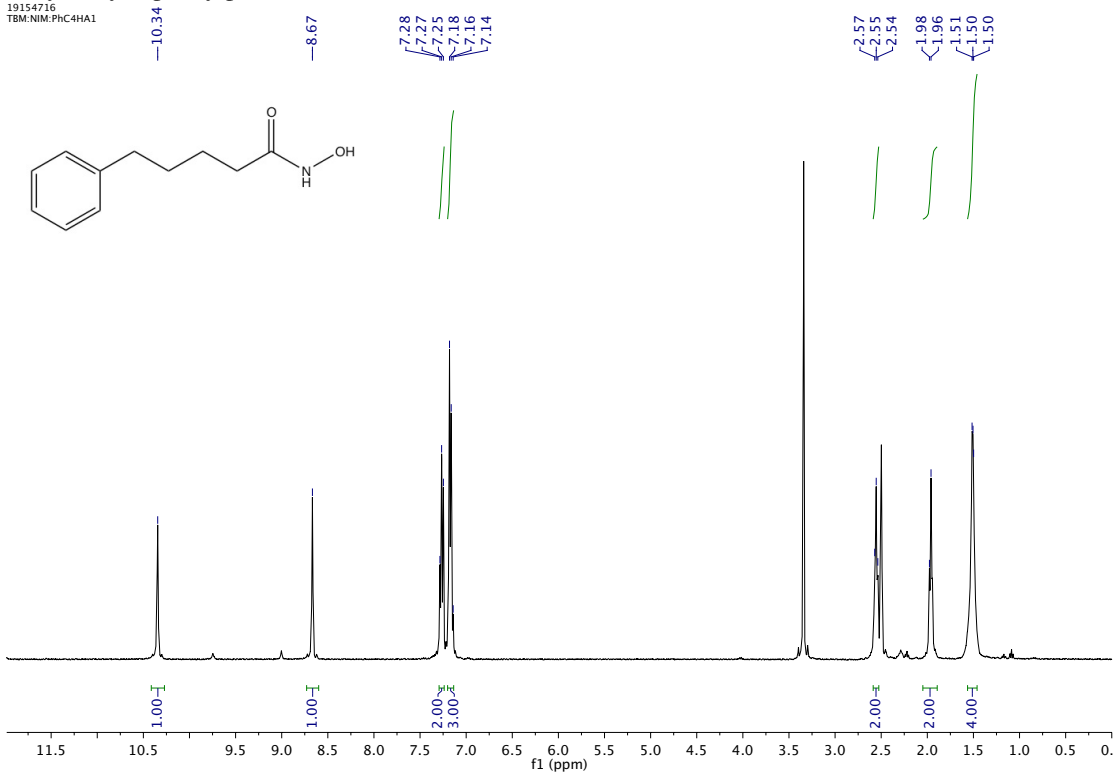

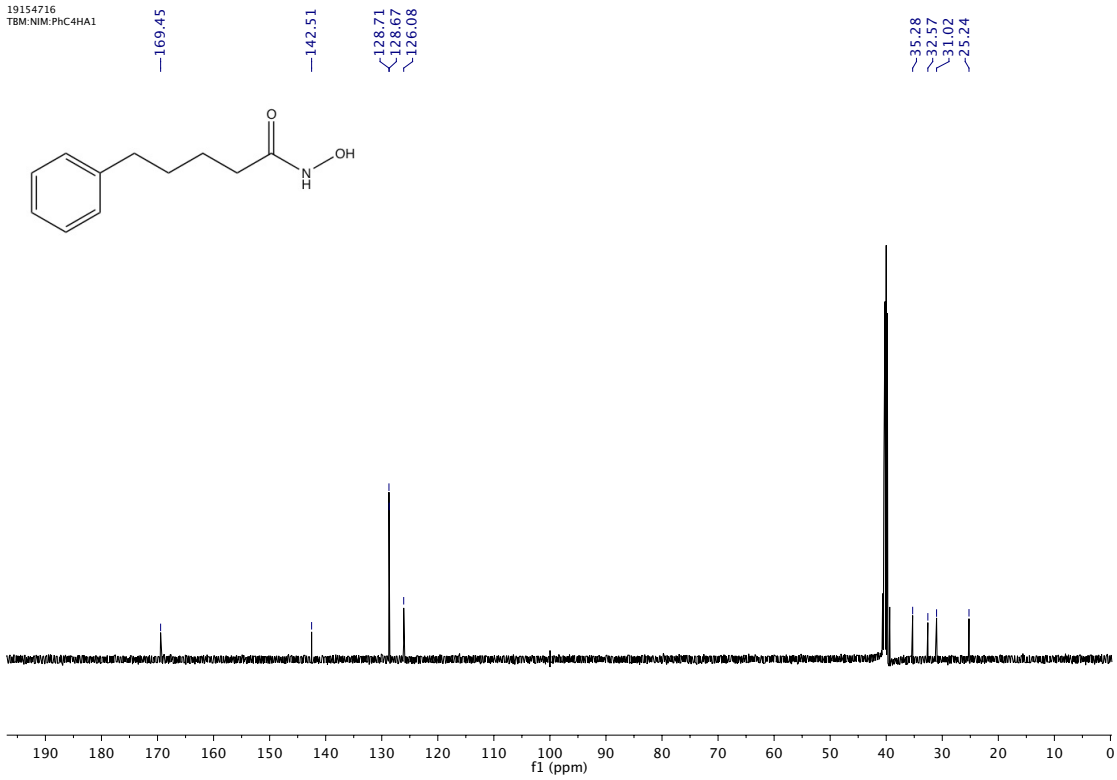

Phenyl hydroxycarbamate **170**

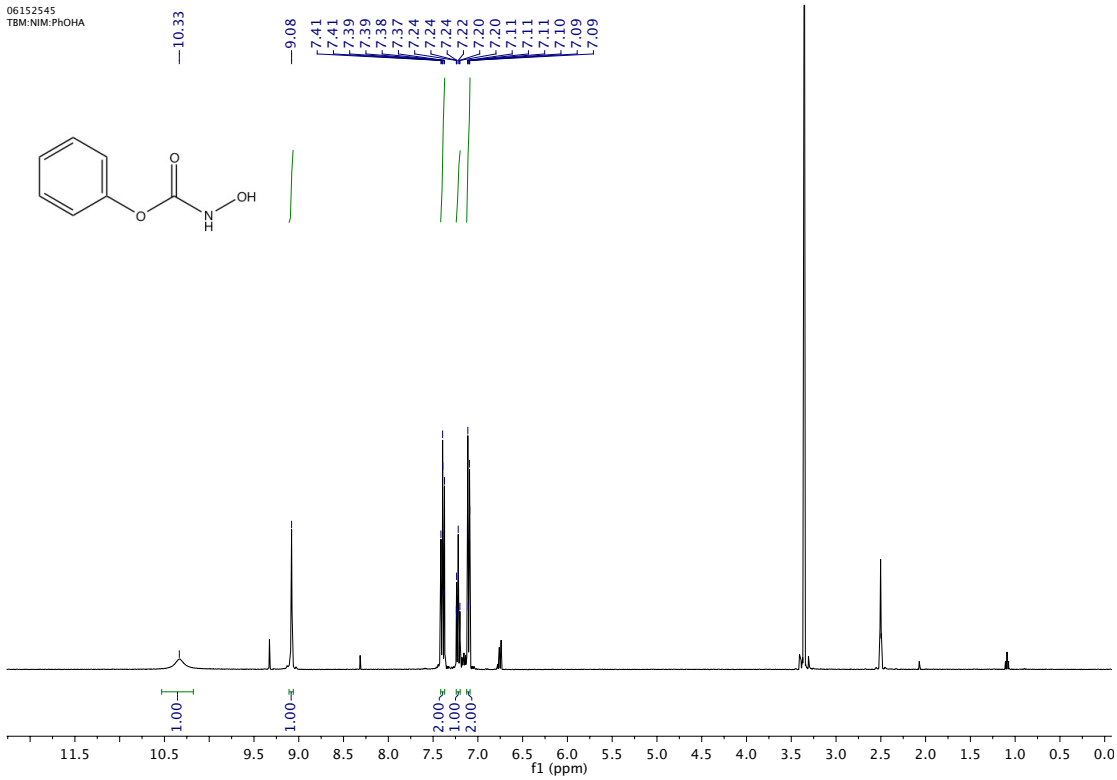

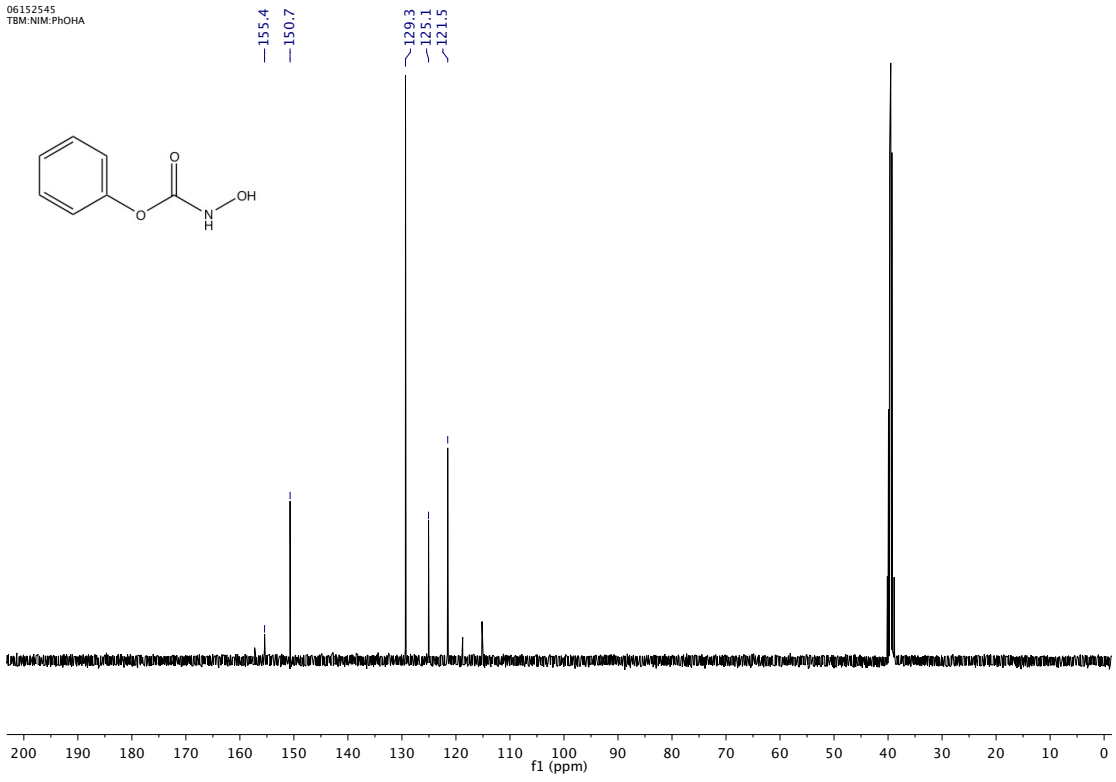

1-Hydroxy-3-phenylurea **171**

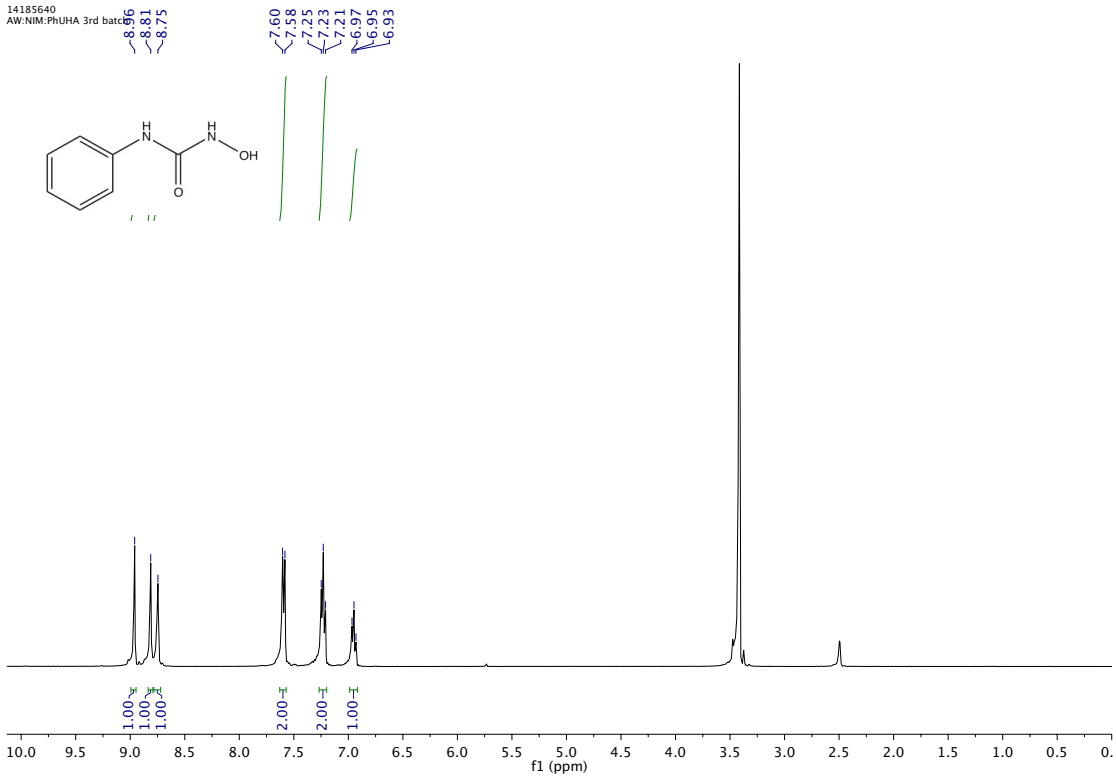

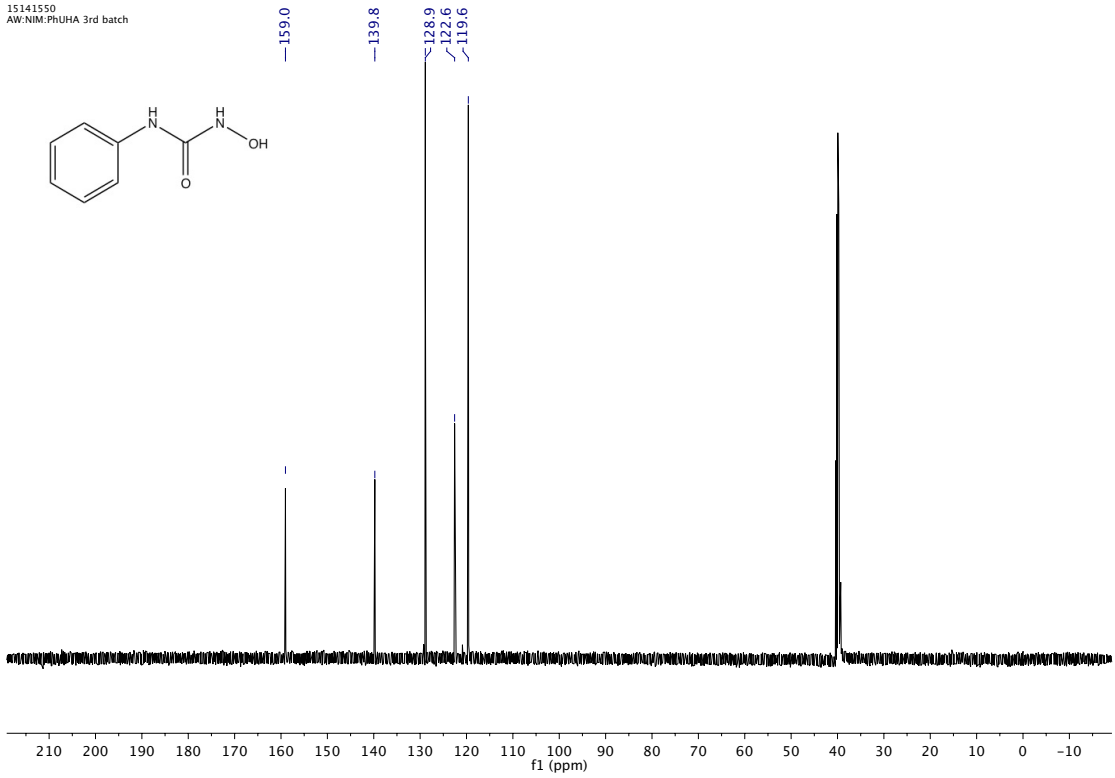

(*S*)-1-Hydroxy-3-(1-phenylethyl)urea **172**

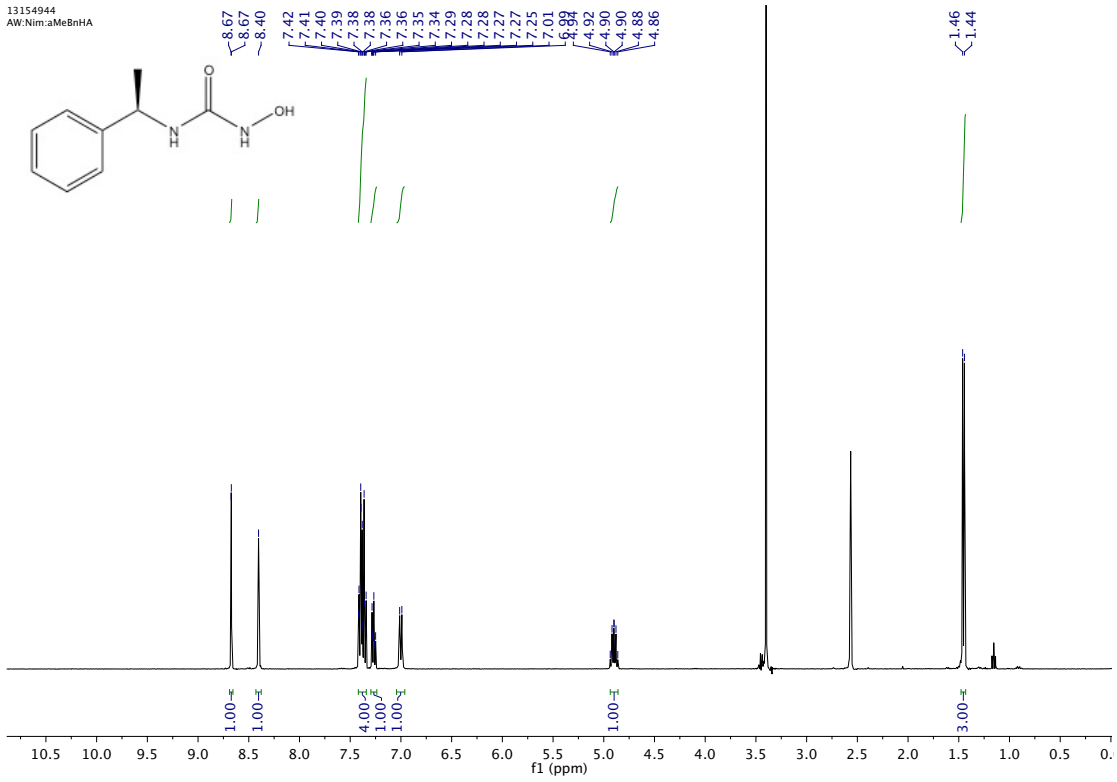

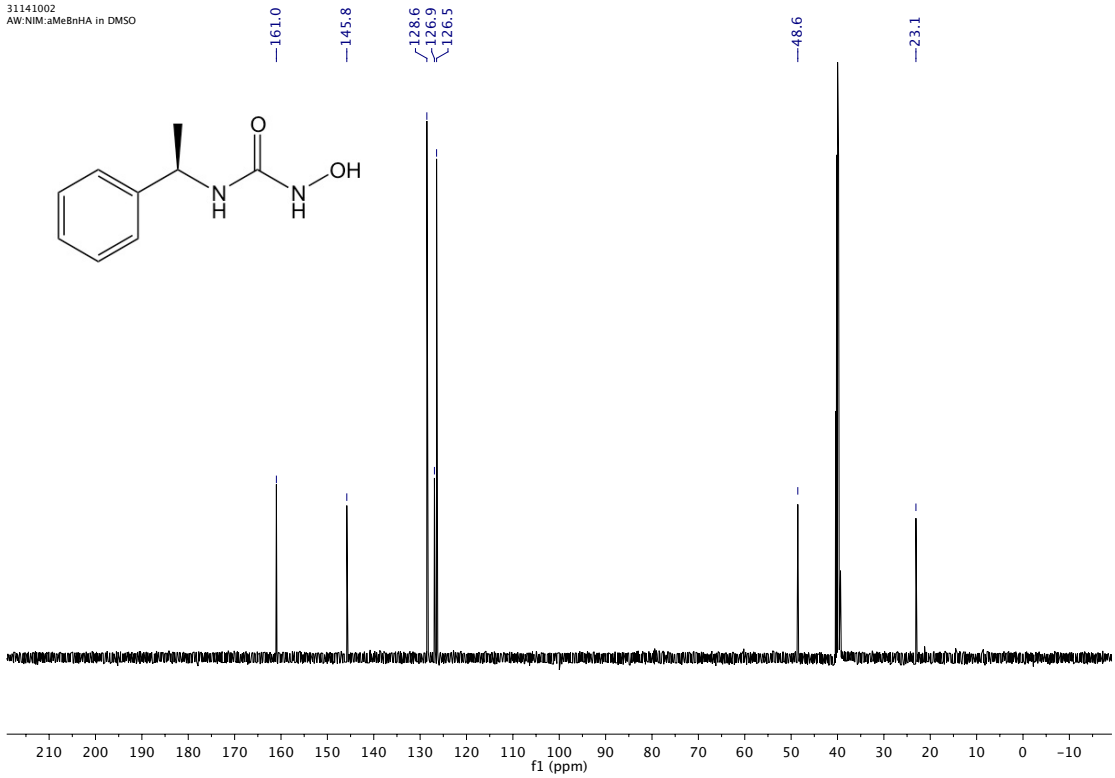

1-[{[(1S)-1-phenylethyl]carbamoyl})amino]-N-[(1R)-1-phenylethyl]formamide

172s

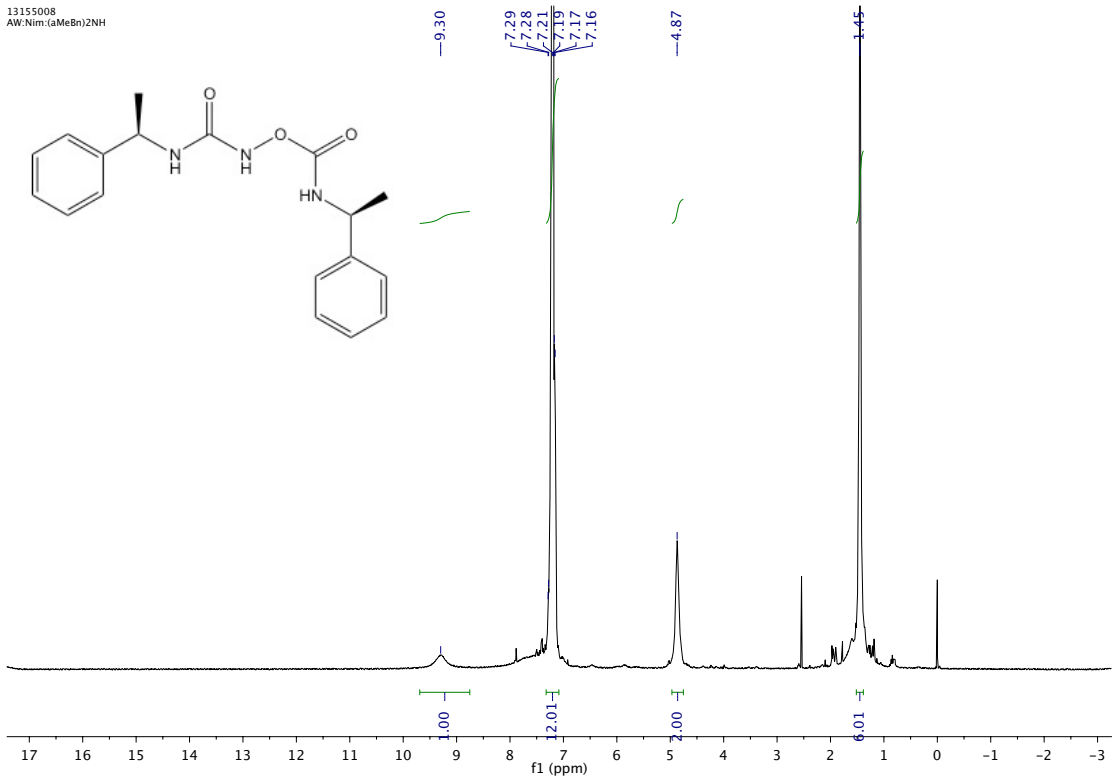

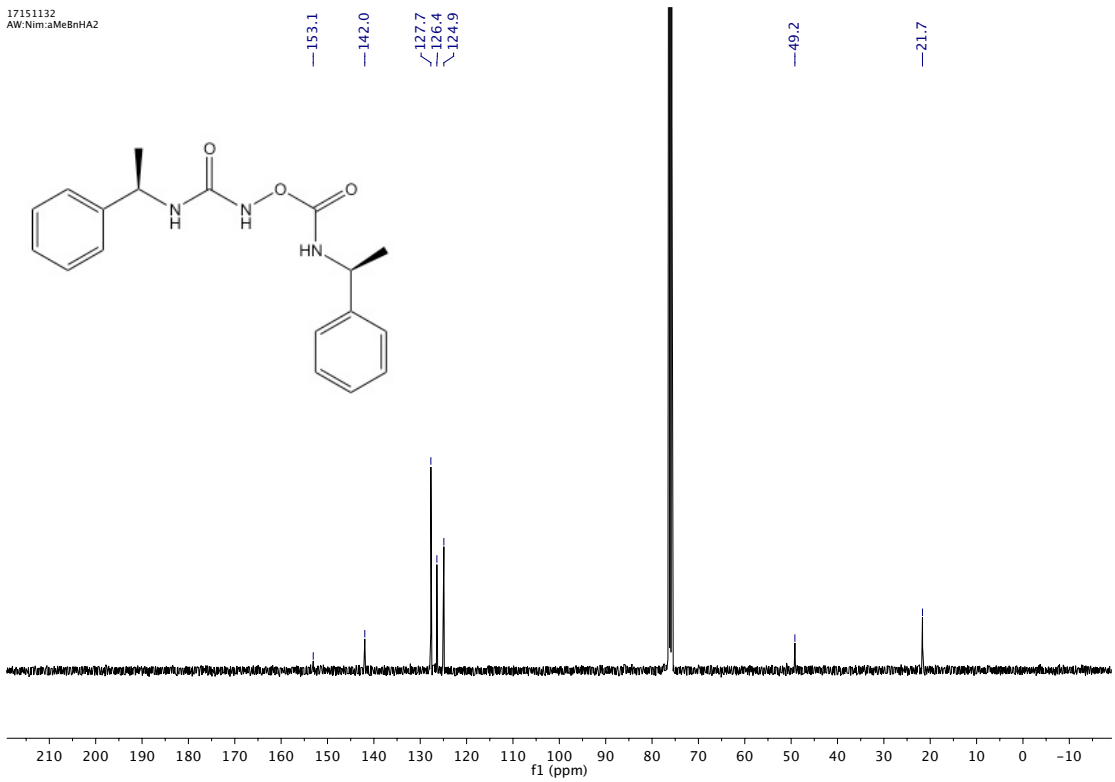

2-Oxa-3-azabicyclo[2.2.2]oct-5-en-3-yl(pyridin-2-yl) methanone **173**

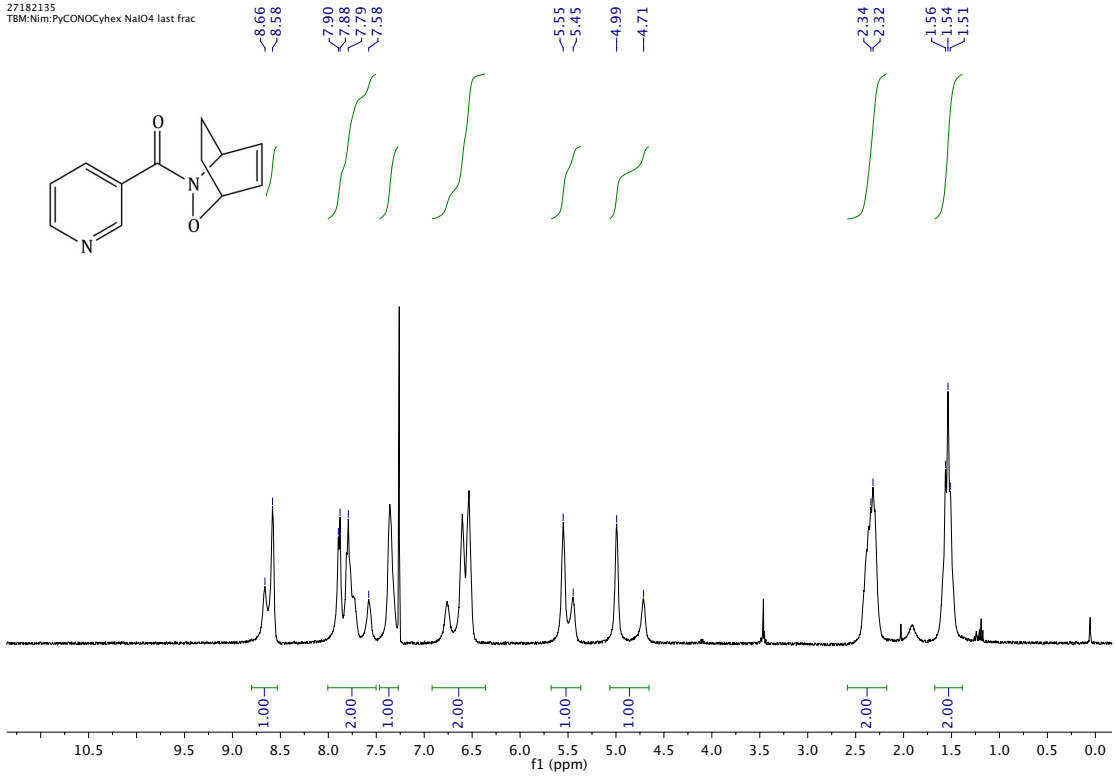

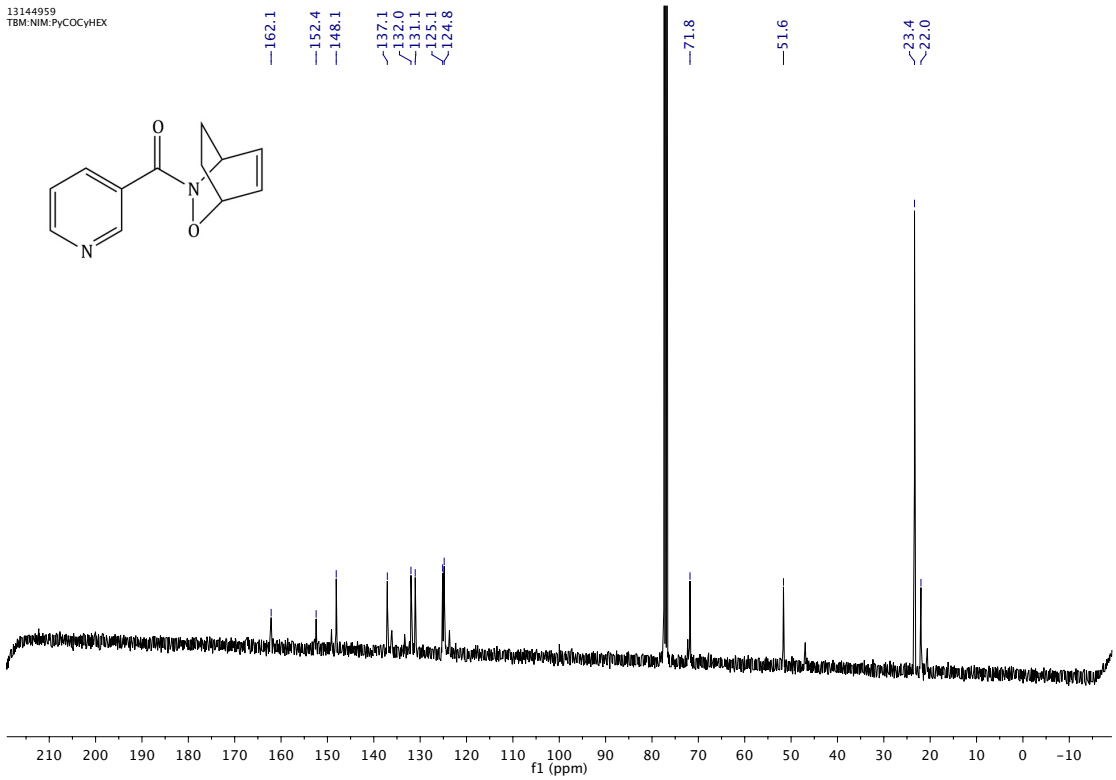

2-Oxa-3azabicyclo[2.2.2]oct-5-en-3-yl(pyridin-3-yl)methanone **174**

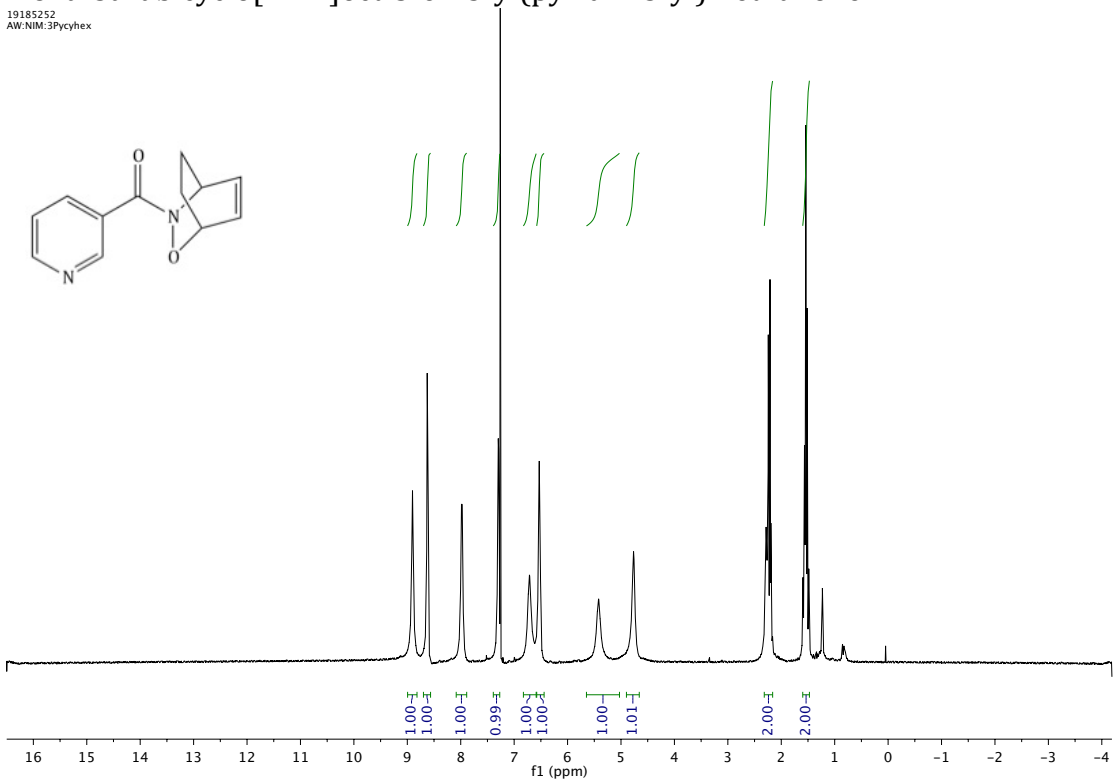

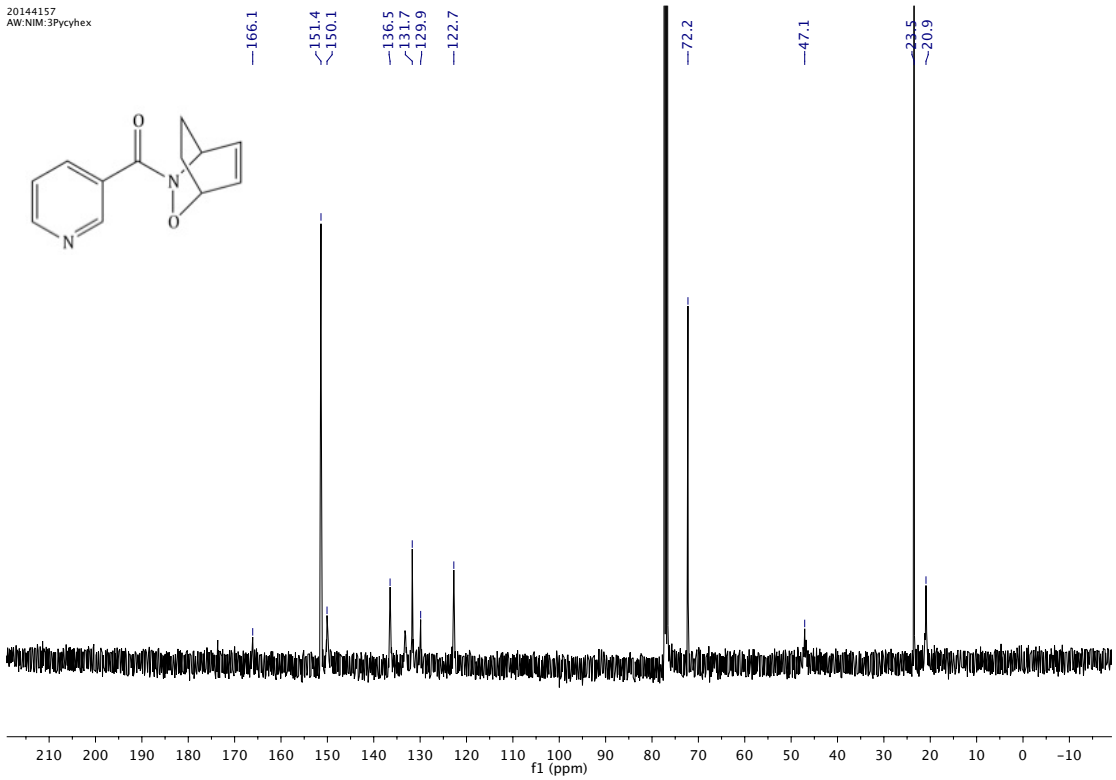

2-Oxa-3-azabicyclo[2.2.2]oct-5-en-3-yl(phenyl)metha-none **177**

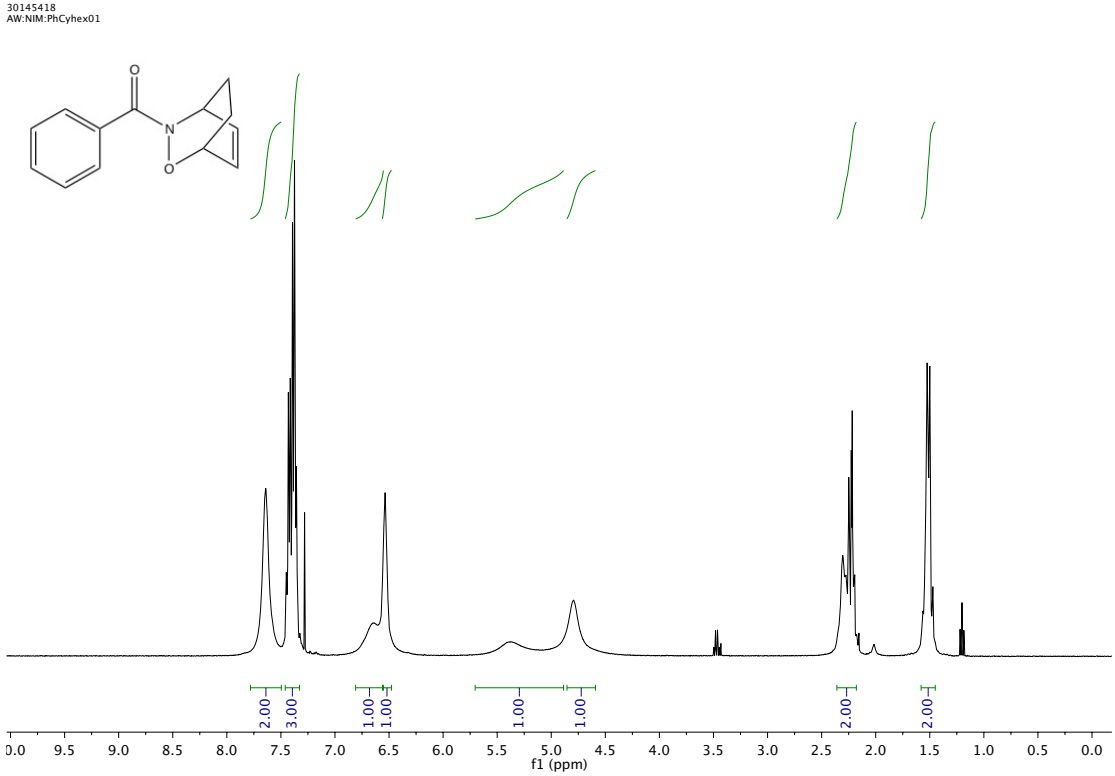

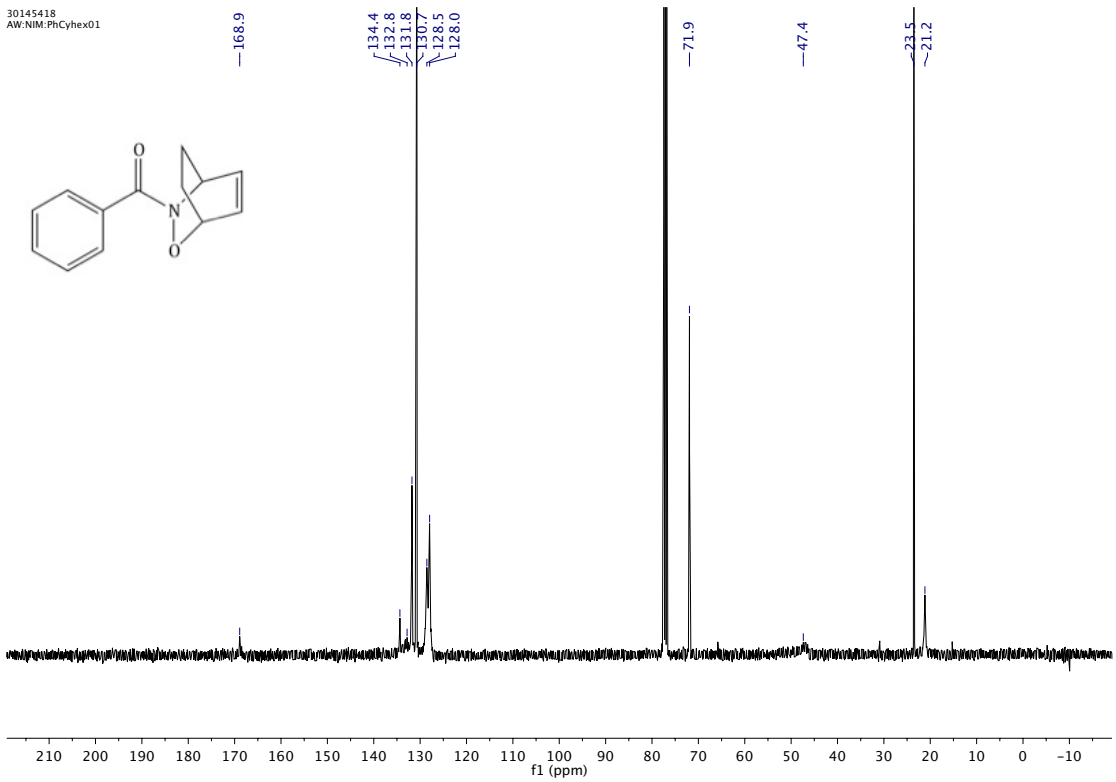

2-Oxa-3-azabicyclo[2.2.2]oct-5-en-3-yl)-2-phenyl-ethanone **178**

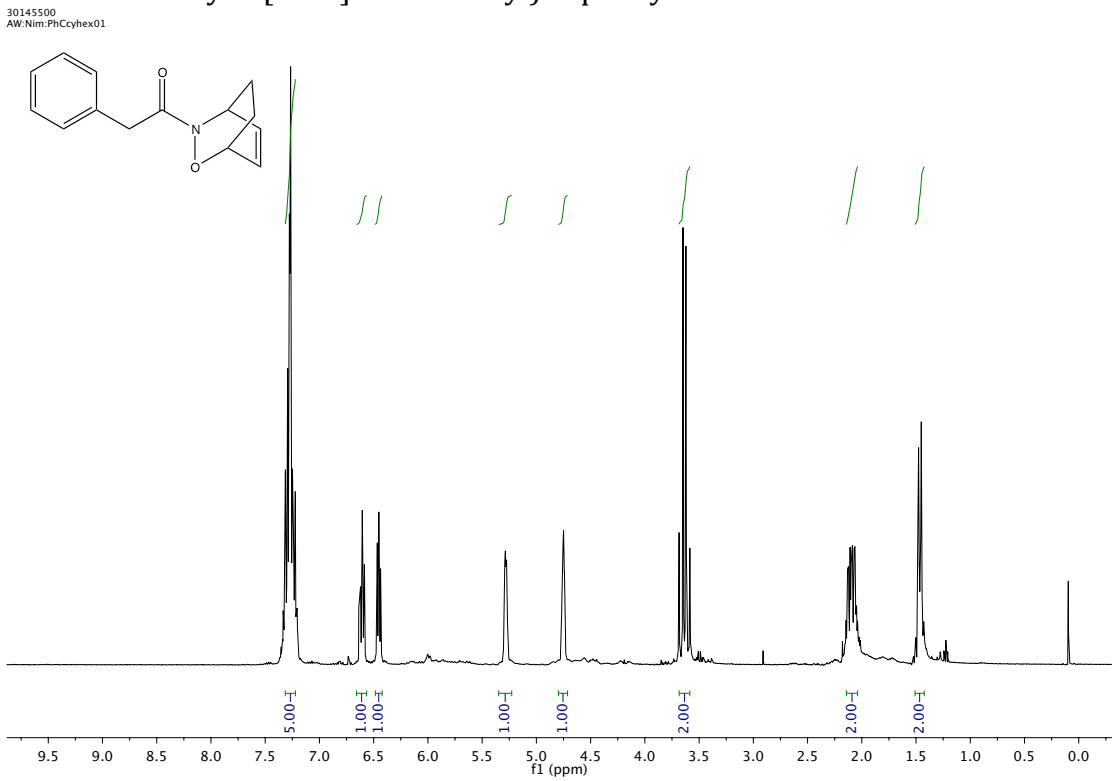

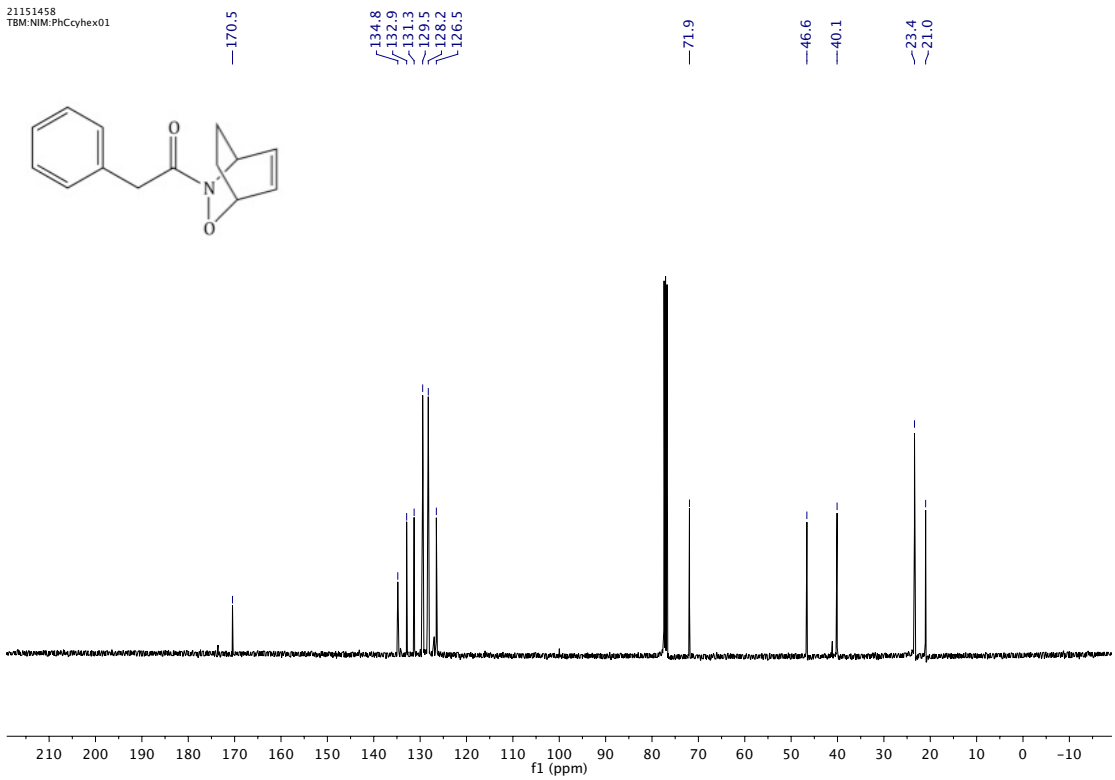

2-Oxa-3-azabicyclo[2.2.2]oct-5-en-3-yl)-3-phenylpropan-1-one **179**

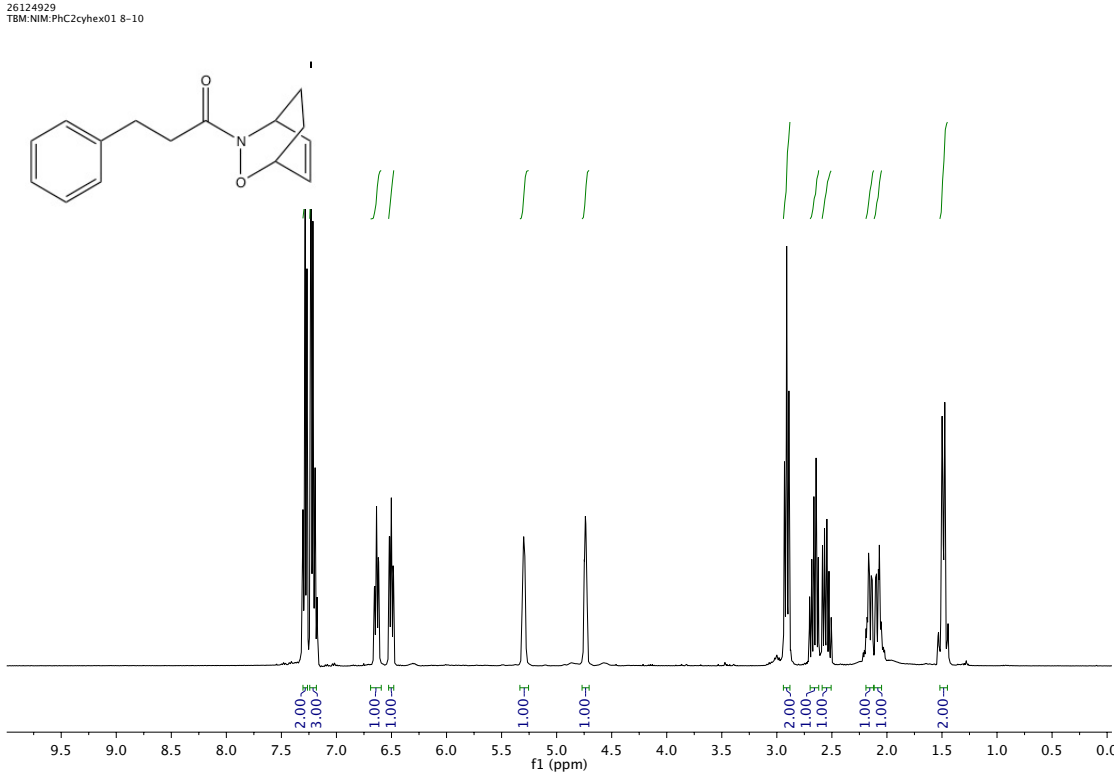

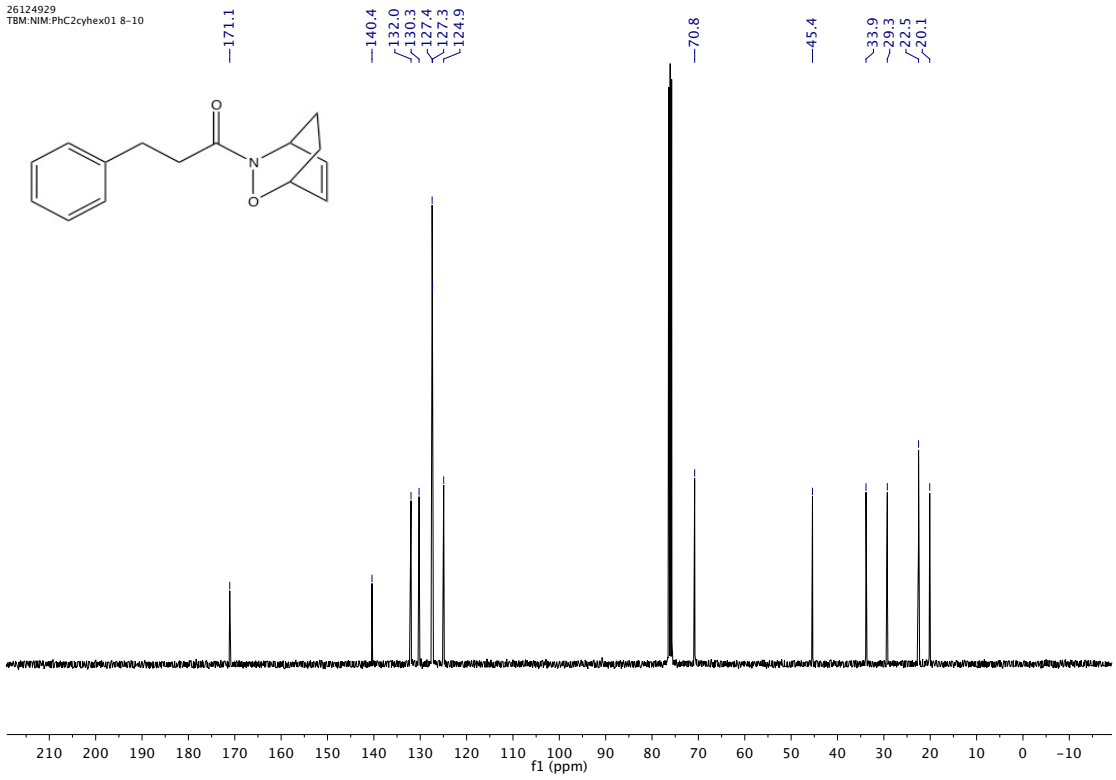

2-Oxa-3-azabicyclo[2.2.2]oct-5-en-3-yl)-4-phenylbutan-1-one **180**

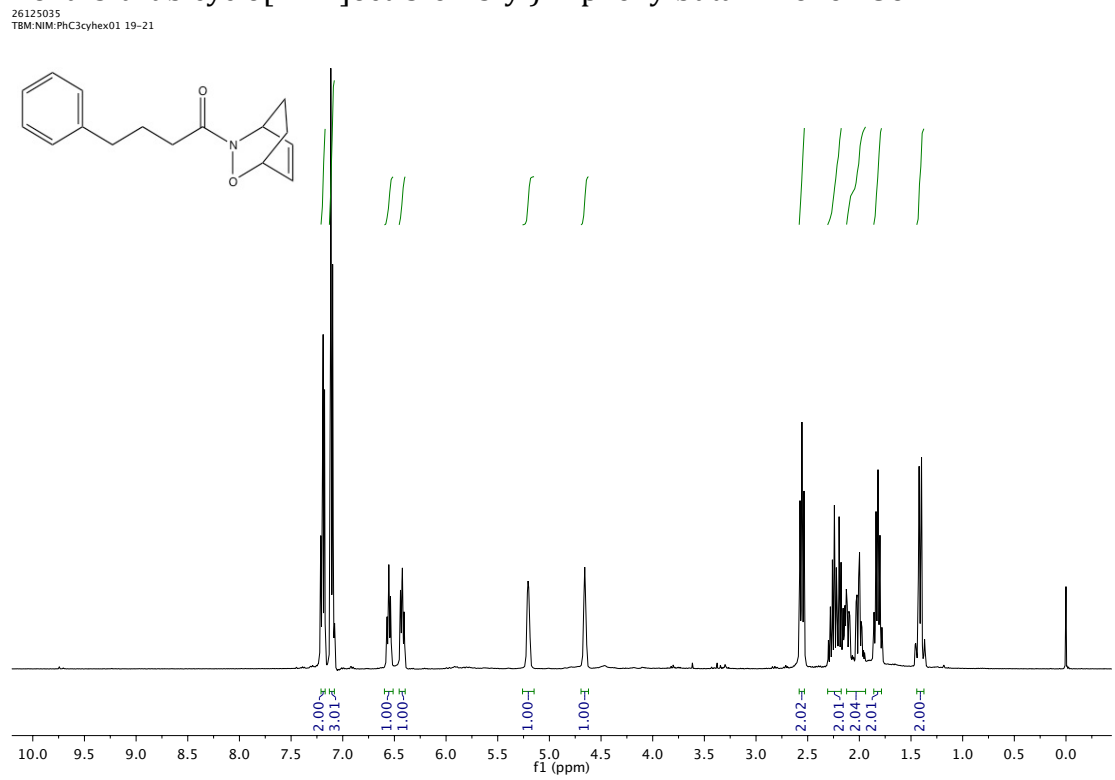

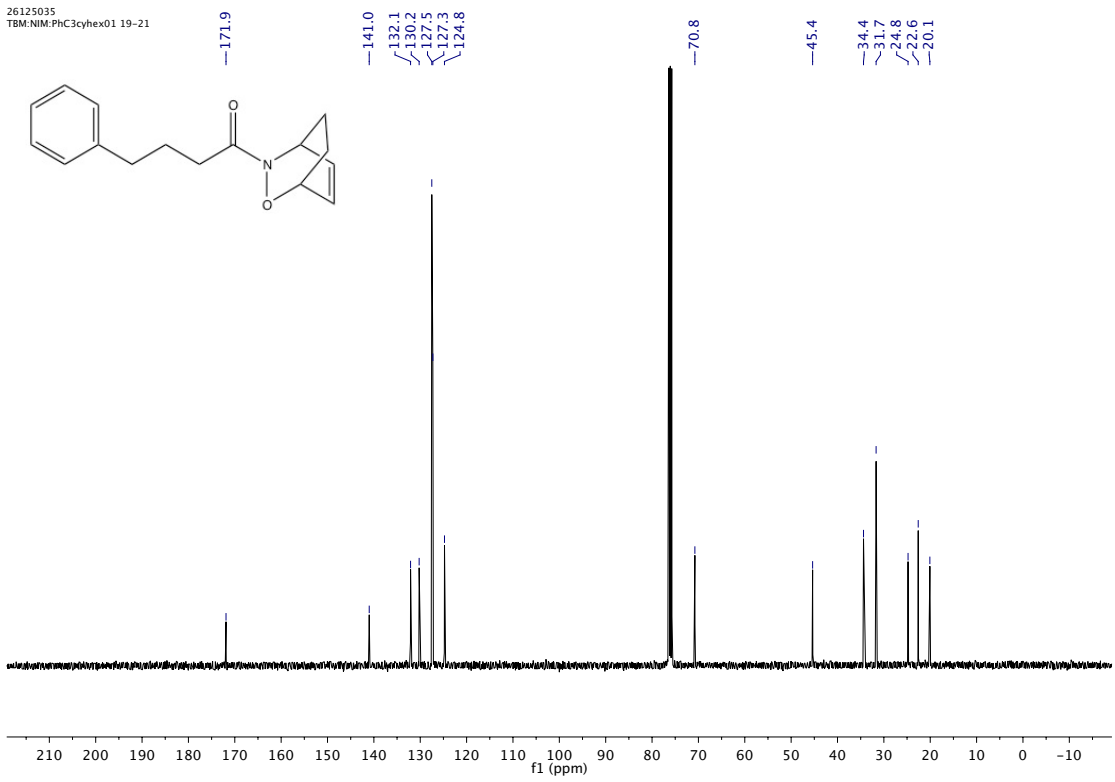

2-Oxa-3-azabicyclo[2.2.2]oct-5-en-3-yl)-5-phenylpentan -1-one **181**

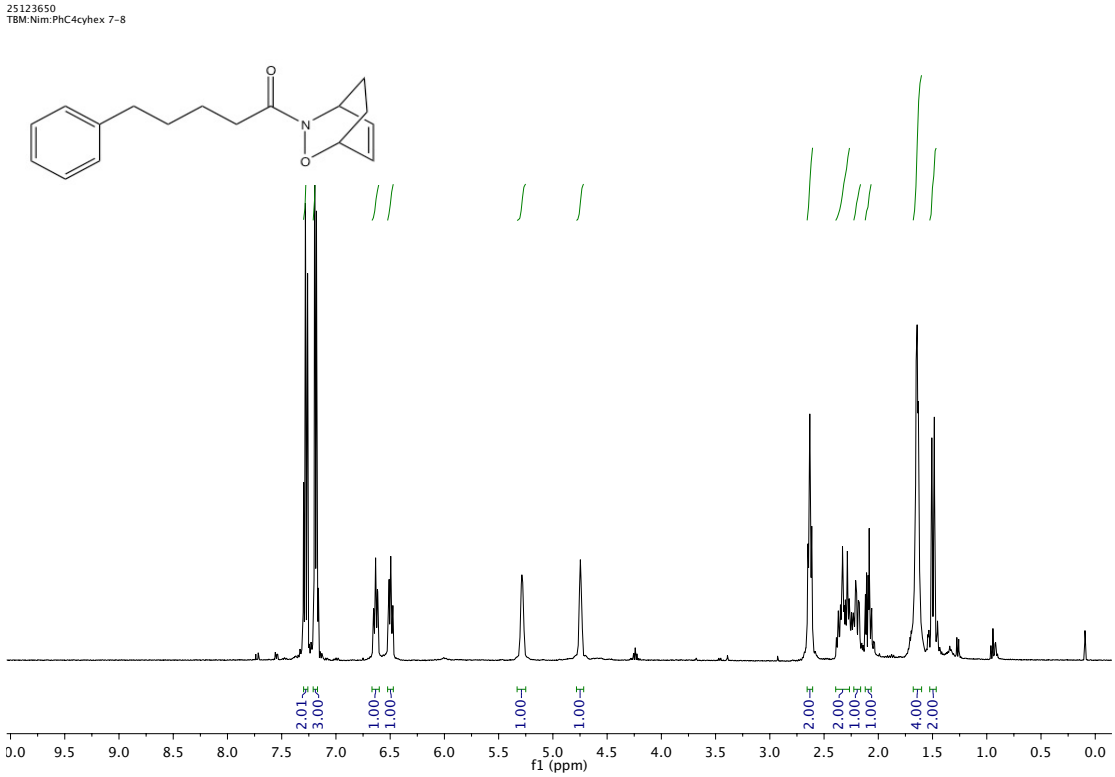

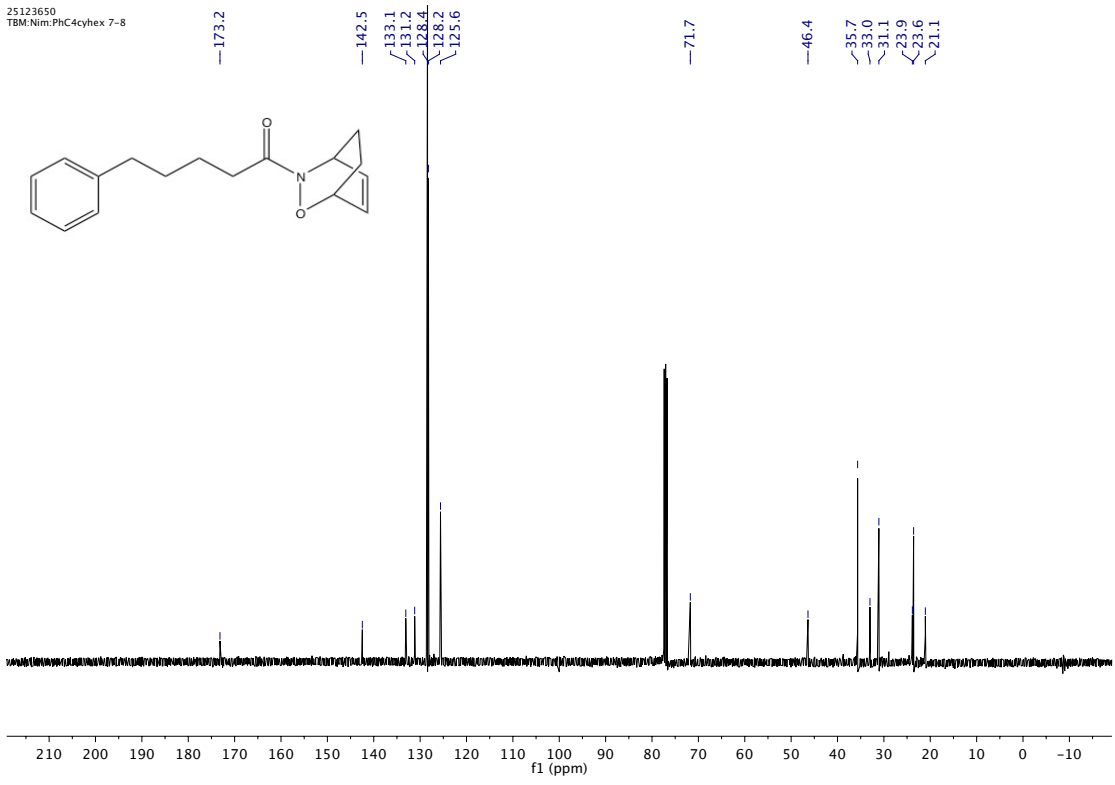

Phenyl-2-oxa-3-azabicyclo[2.2.2]oct-5-ene-3-carboxylate **182**

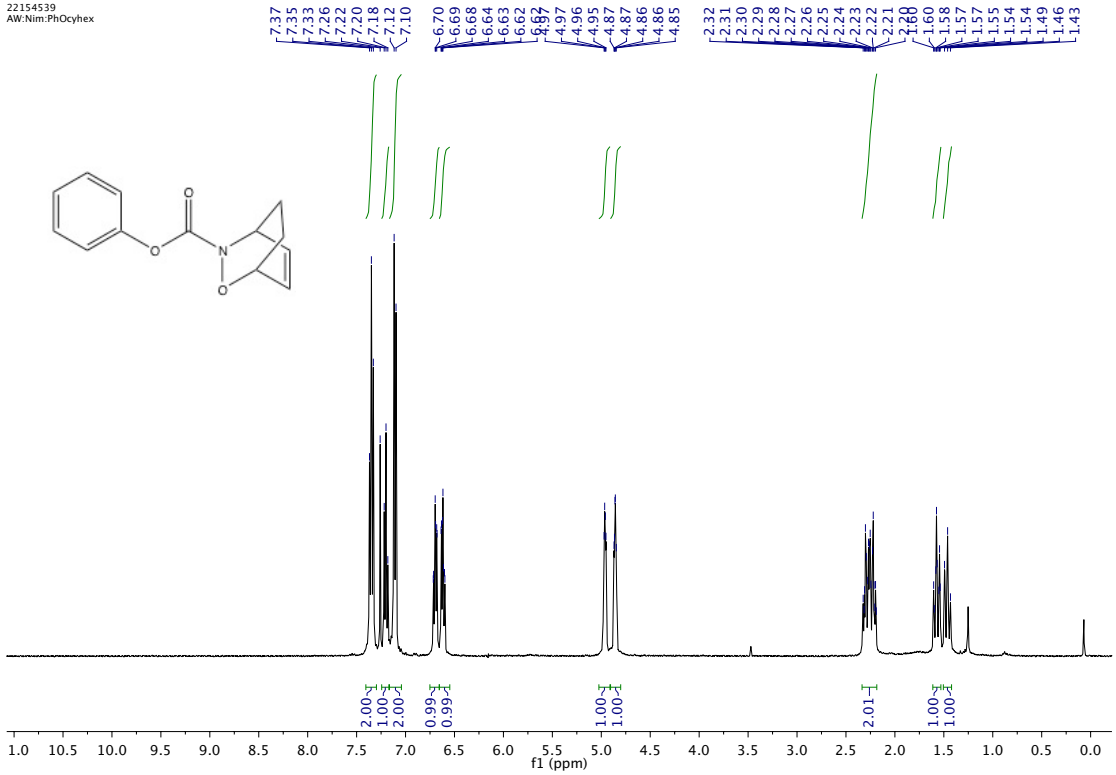

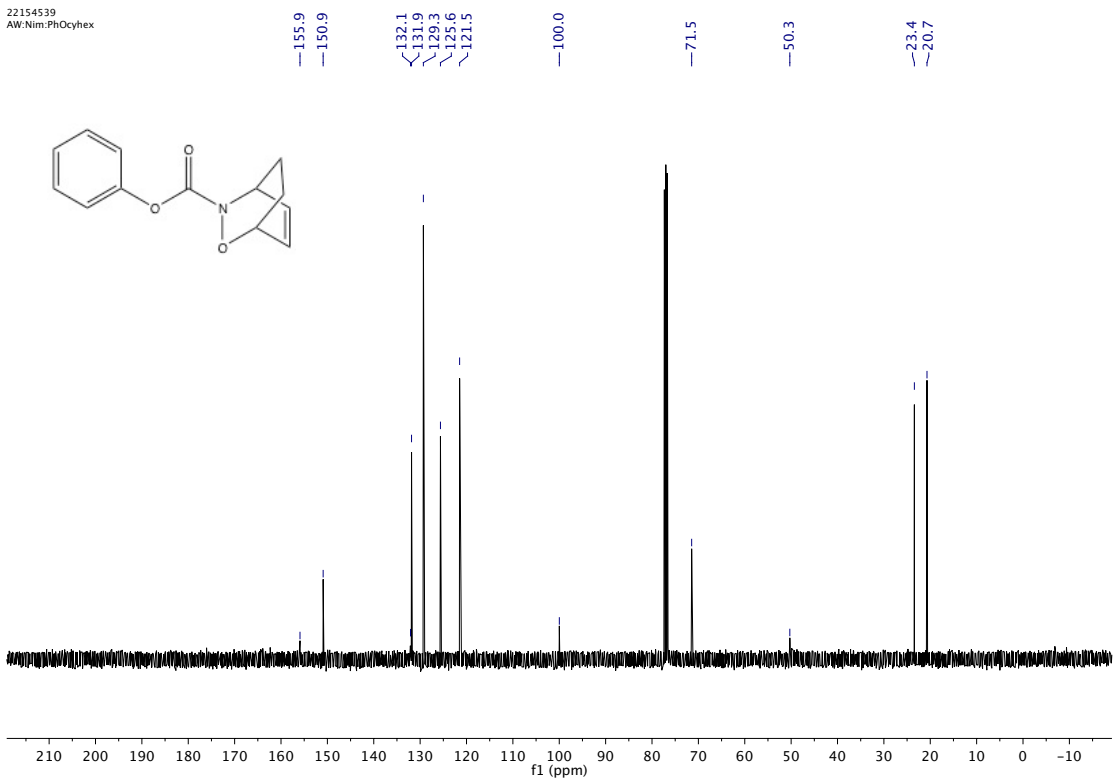

N-Phenyl-2-oxa-3-azabicyclo[2.2.2]oct-5-ene-3-carboxamide **183**

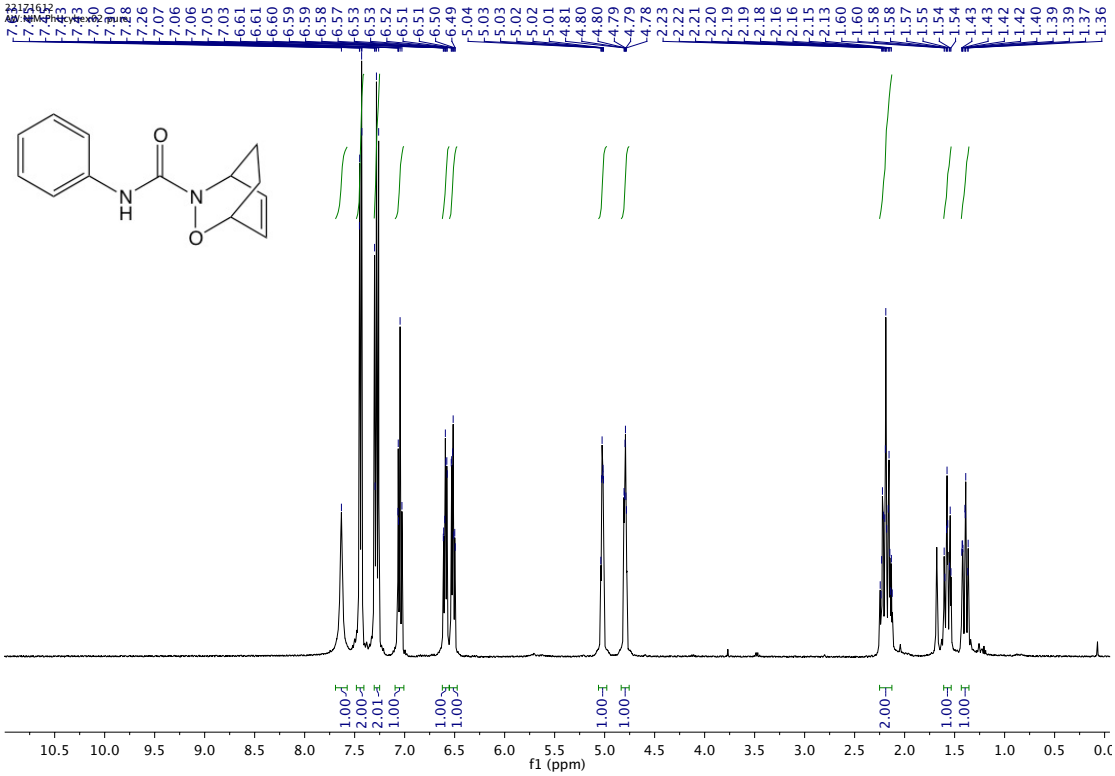

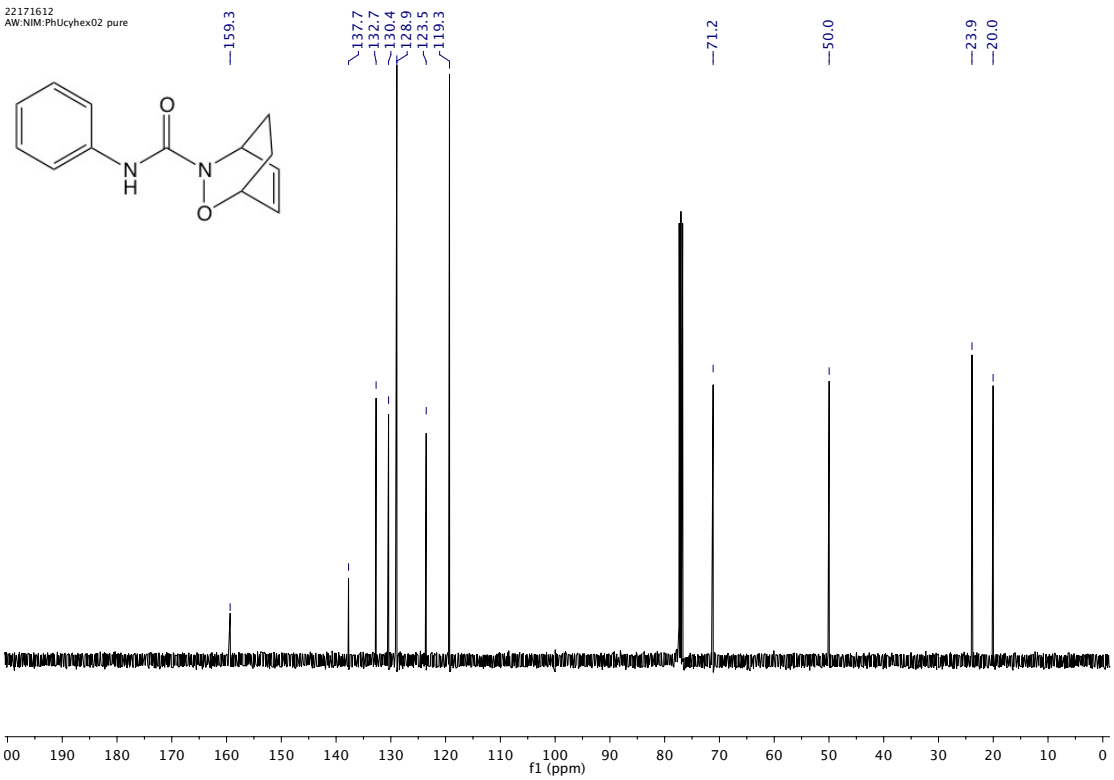

N-((*R*)-1-Phenylethyl)-2-oxa-3-azabicyclo[2.2.2]oct-5-ene-3-carboxamide **184**

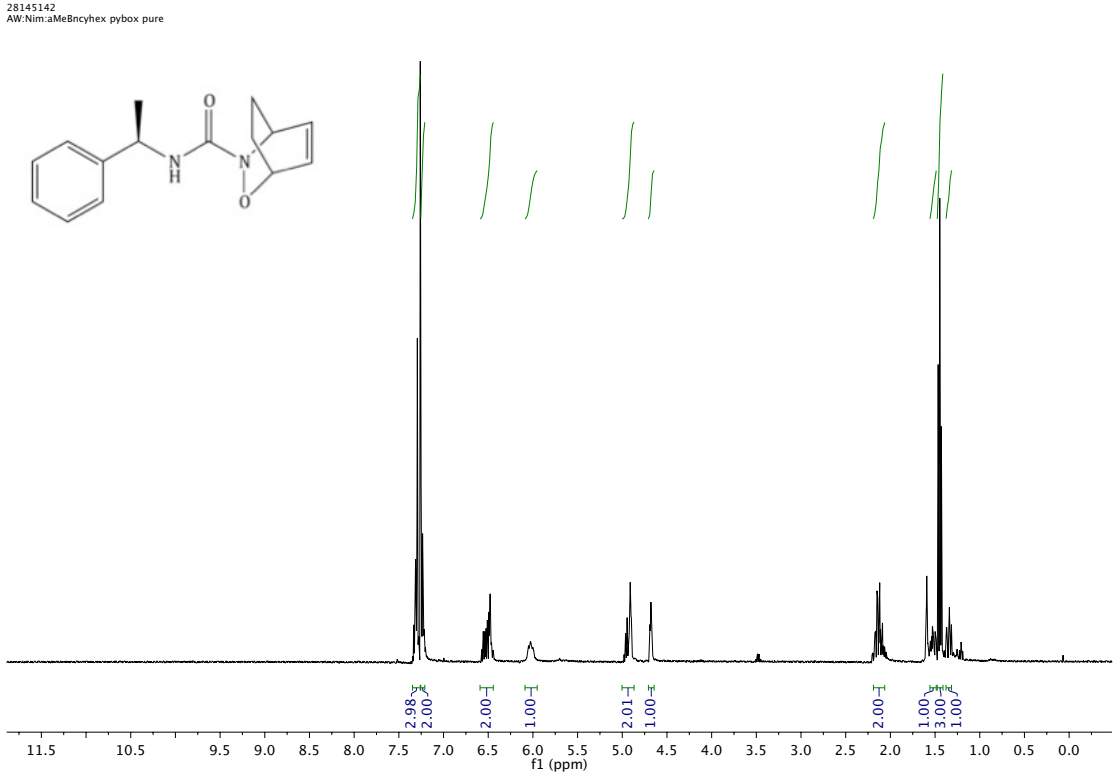

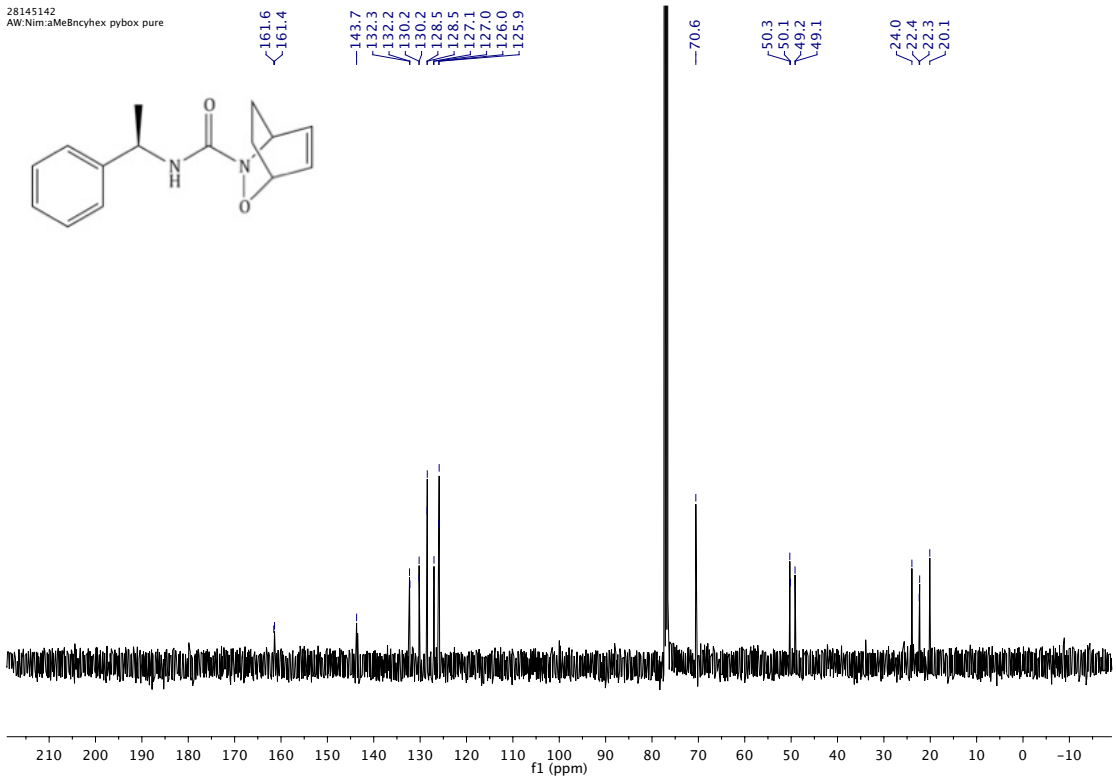

(4,5-Dimethyl-3,6-dihydro-2*H*-1,2-oxazin-2-yl)(pyridin-2-yl)methanone **185**

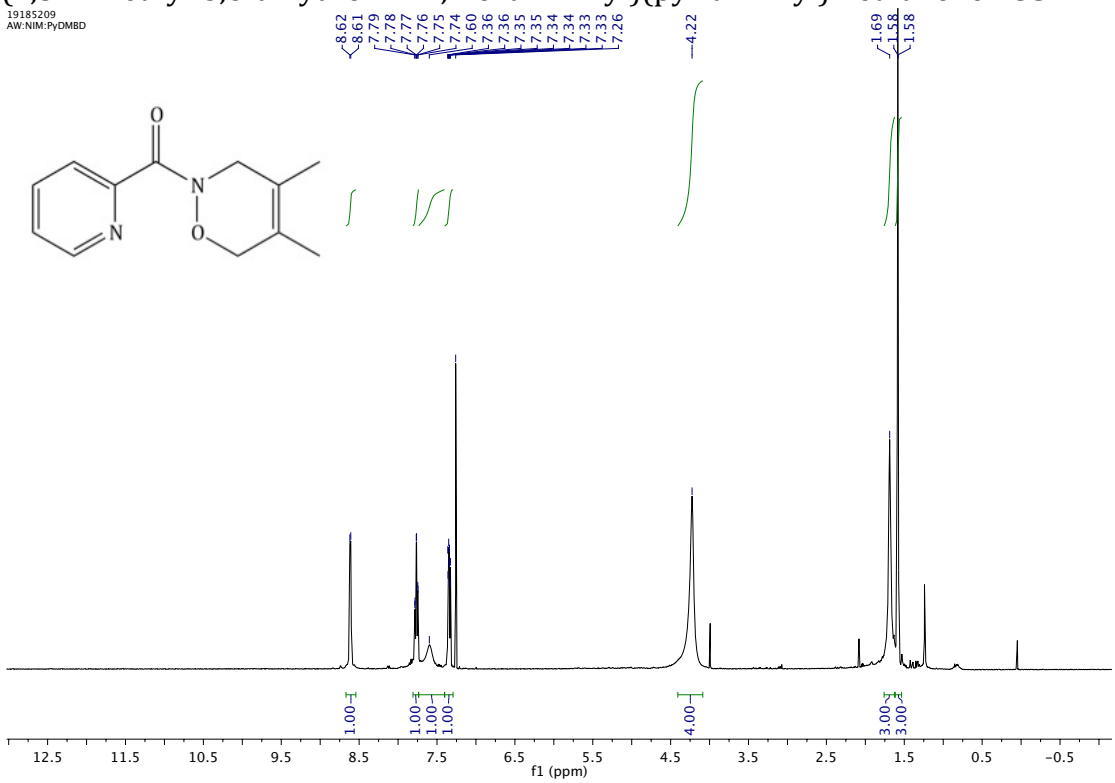

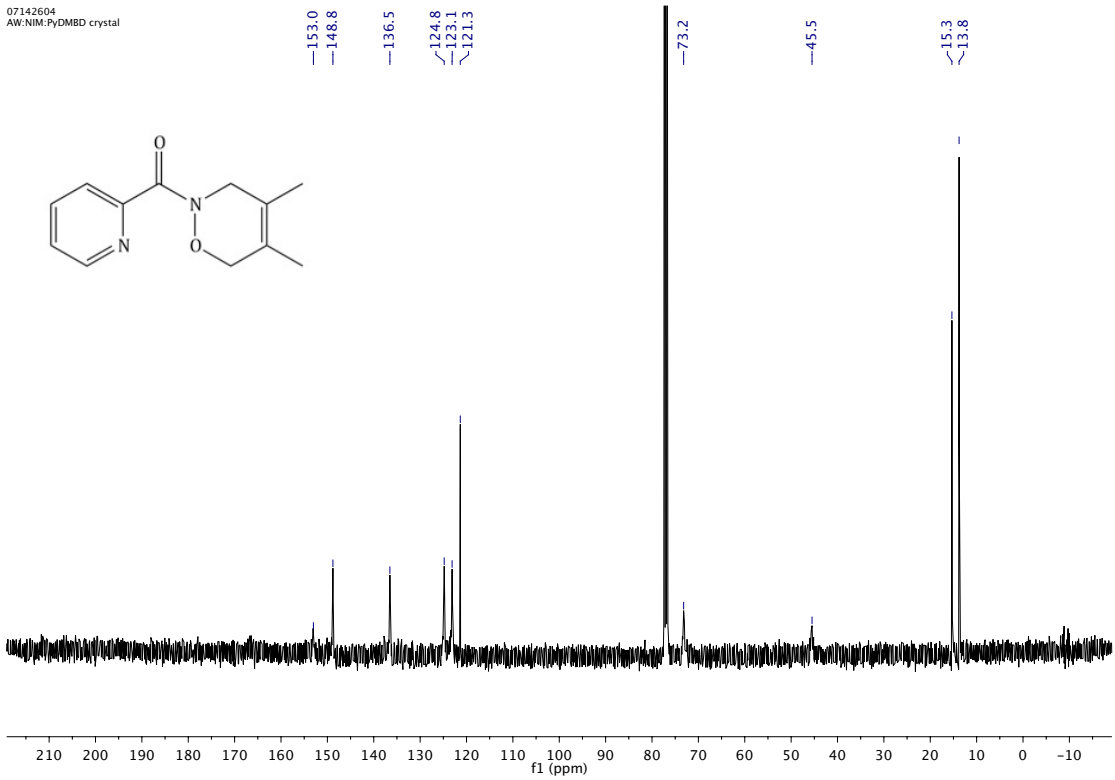

(4,5-Dimethyl-3,6-dihydro-2*H*-1,2-oxazin-2-yl)(pyridin-3-yl)methanone **186**

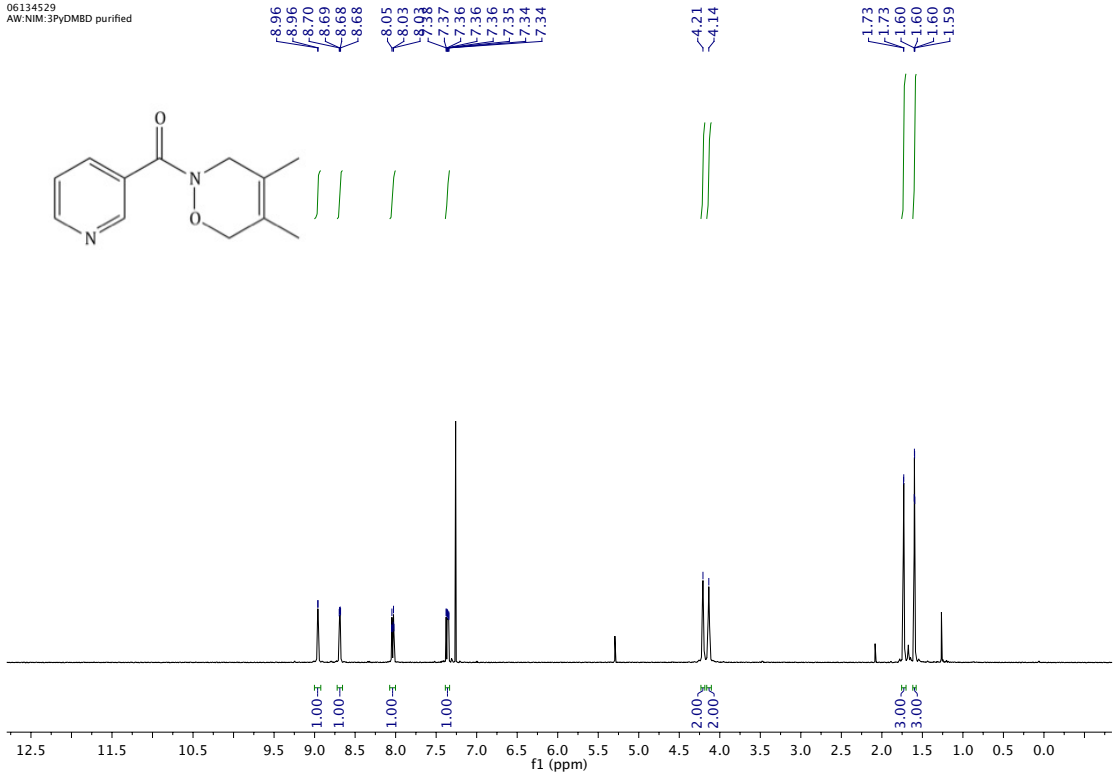

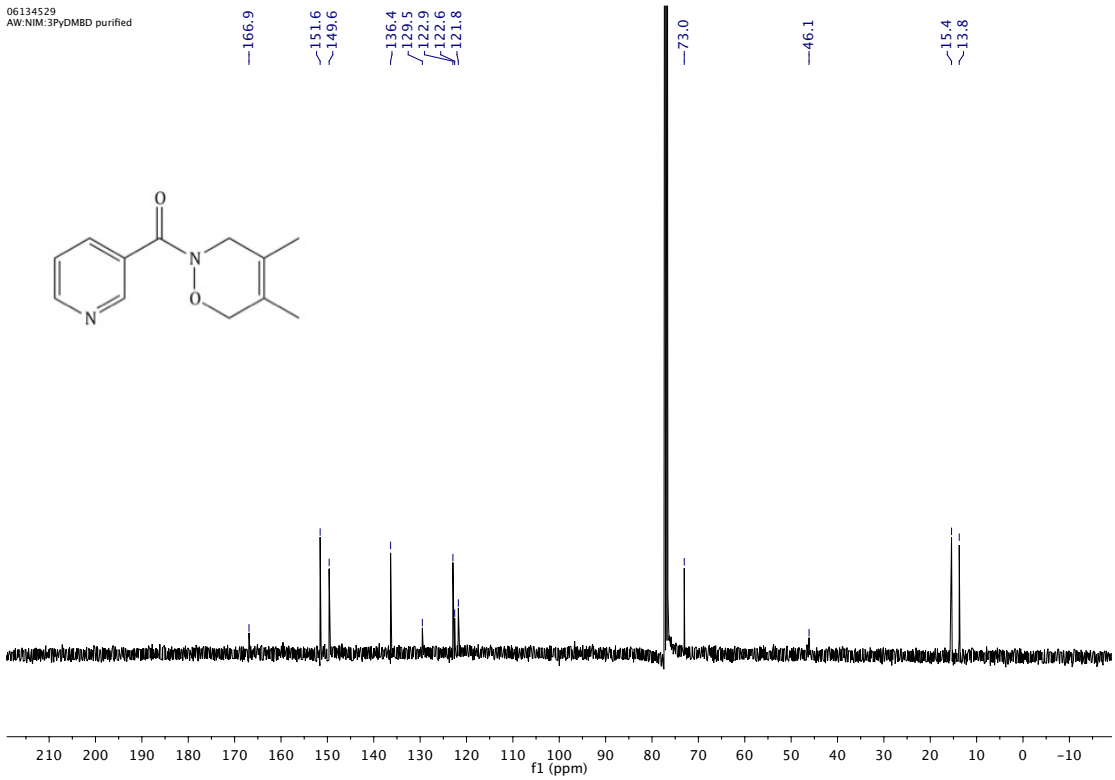

(4,5-Dimethyl-3,6-dihydro-2*H*-1,2-oxazin-2-yl)(phenyl) metha-none **189**

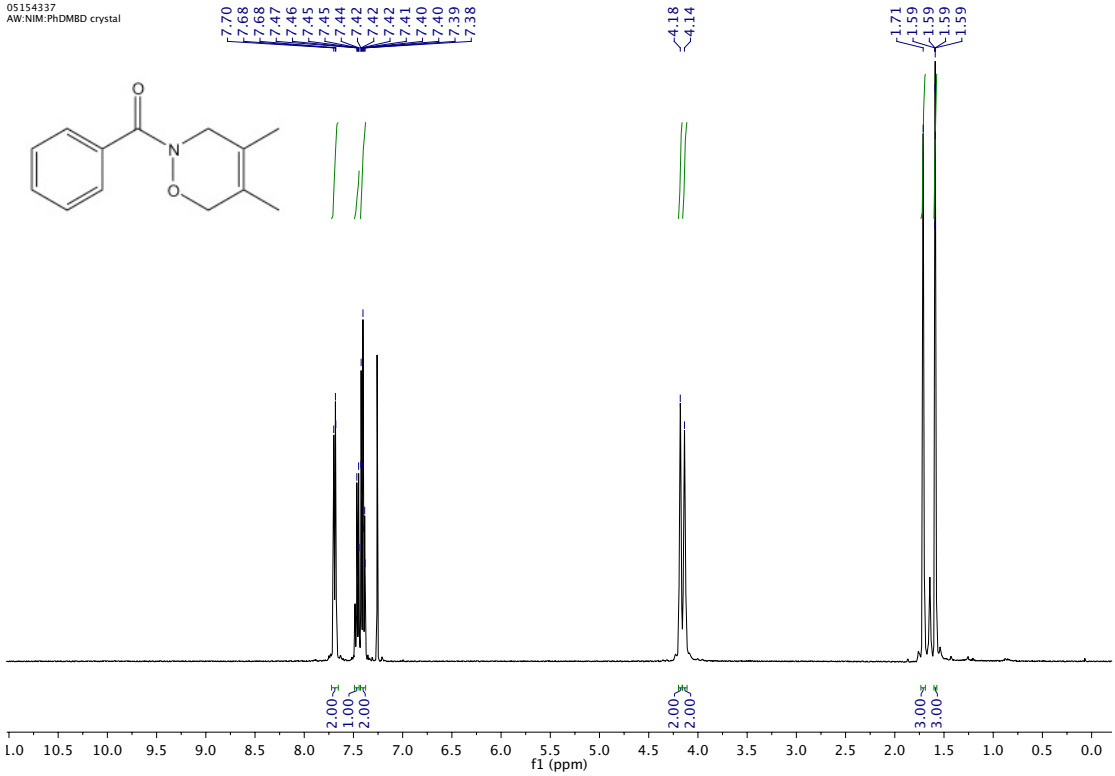

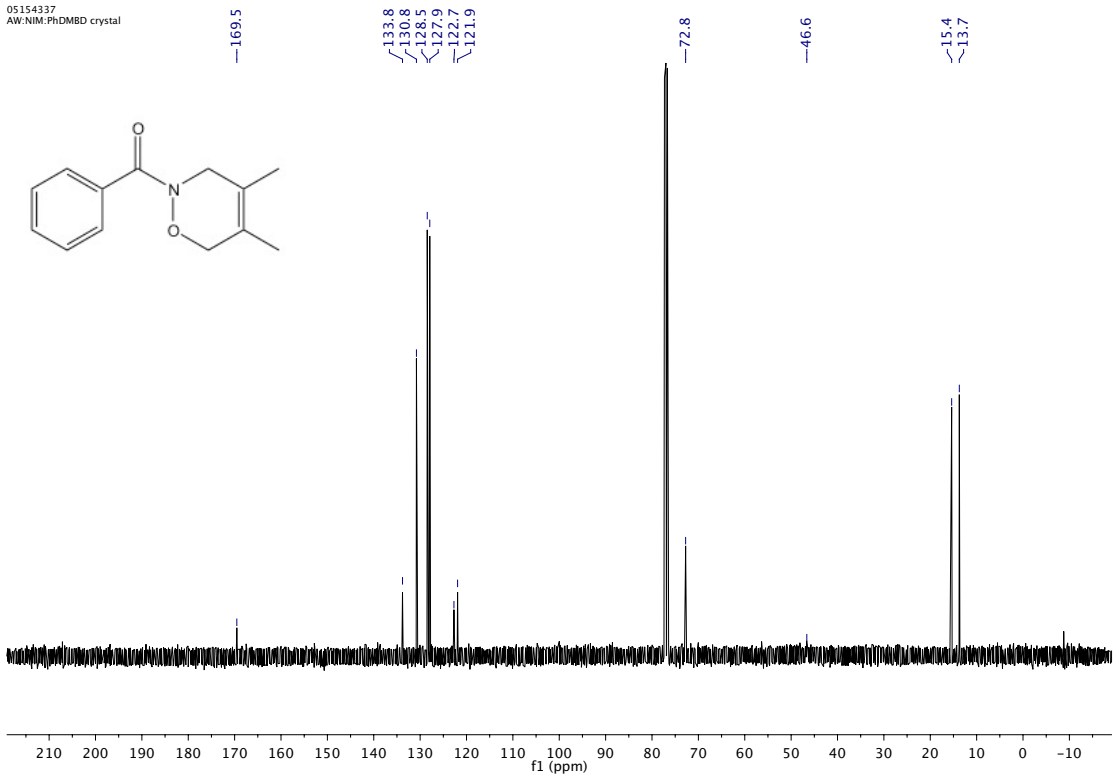

1-(4,5-Dimethyl-3,6-dihydro-2*H*-1,2-oxazin-2-yl)-2-phenyletha-none **190**

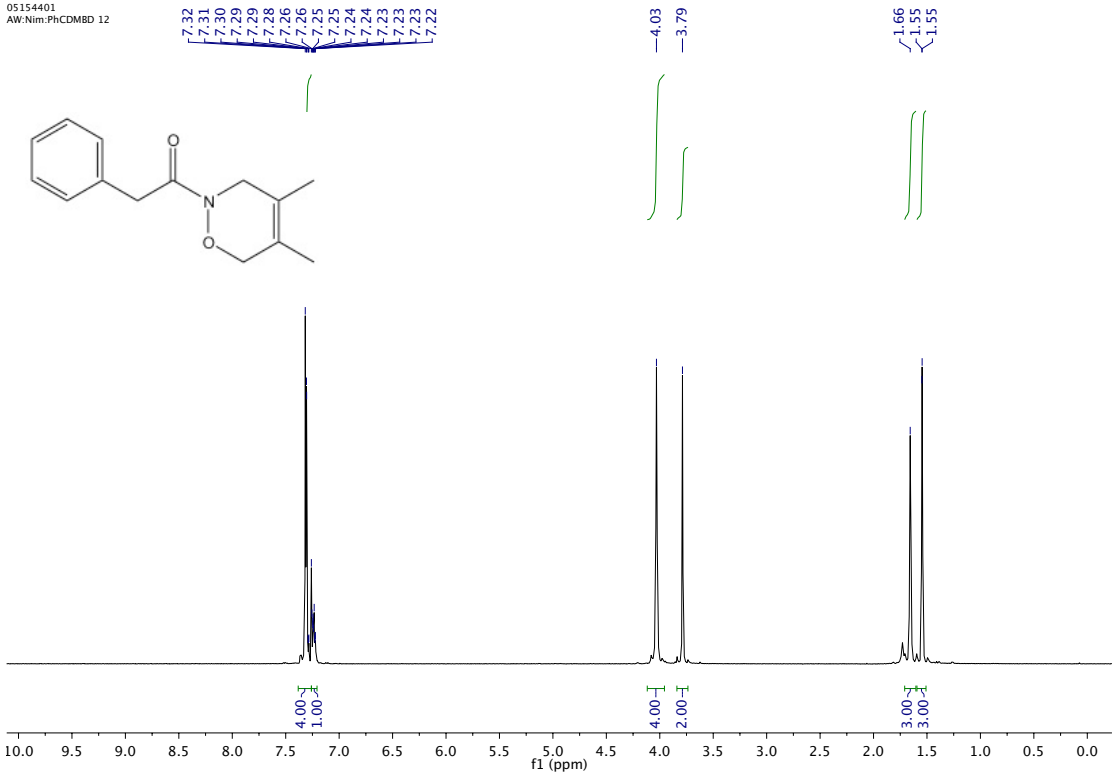

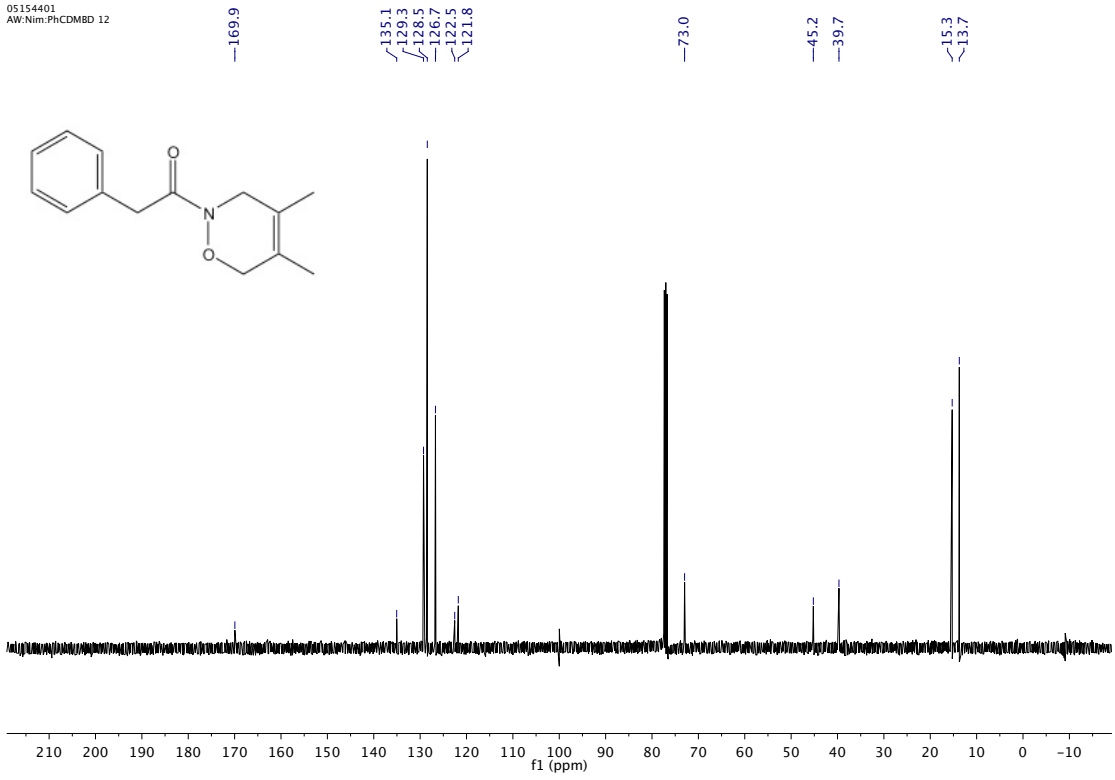

1-(4,5-Dimethyl-3,6-dihydro-2*H*-1,2-oxazin-2-yl)-3-phenylpro-pan-1-one **191**

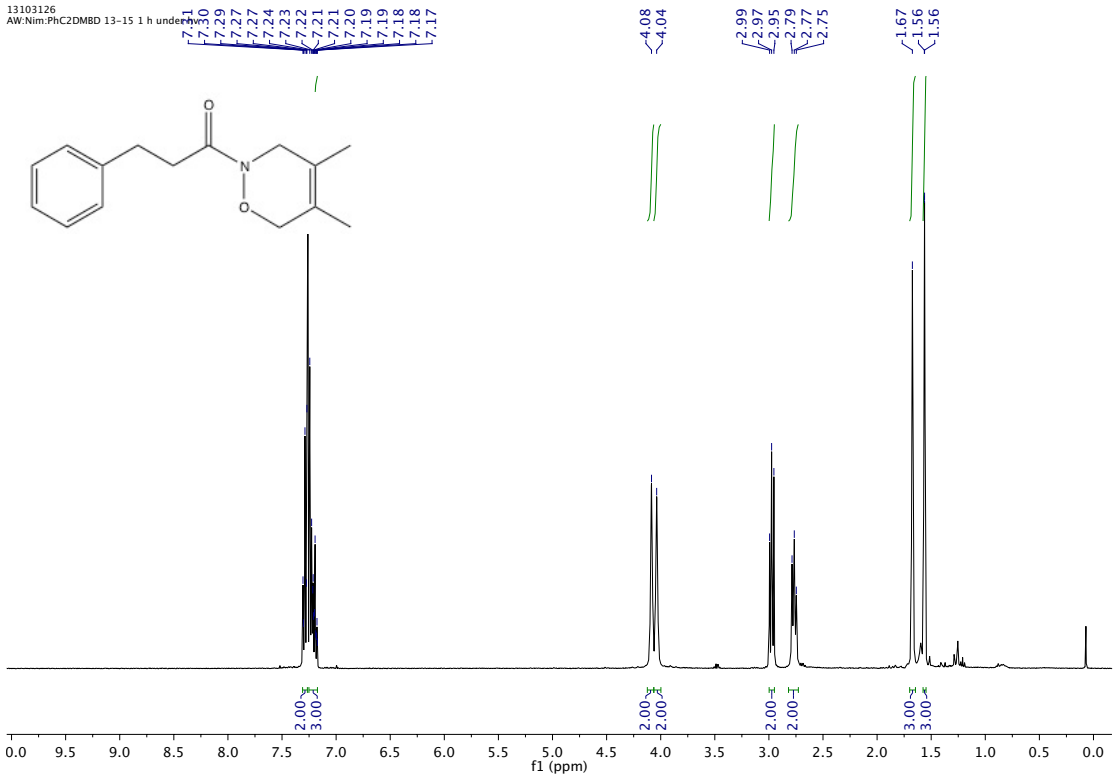

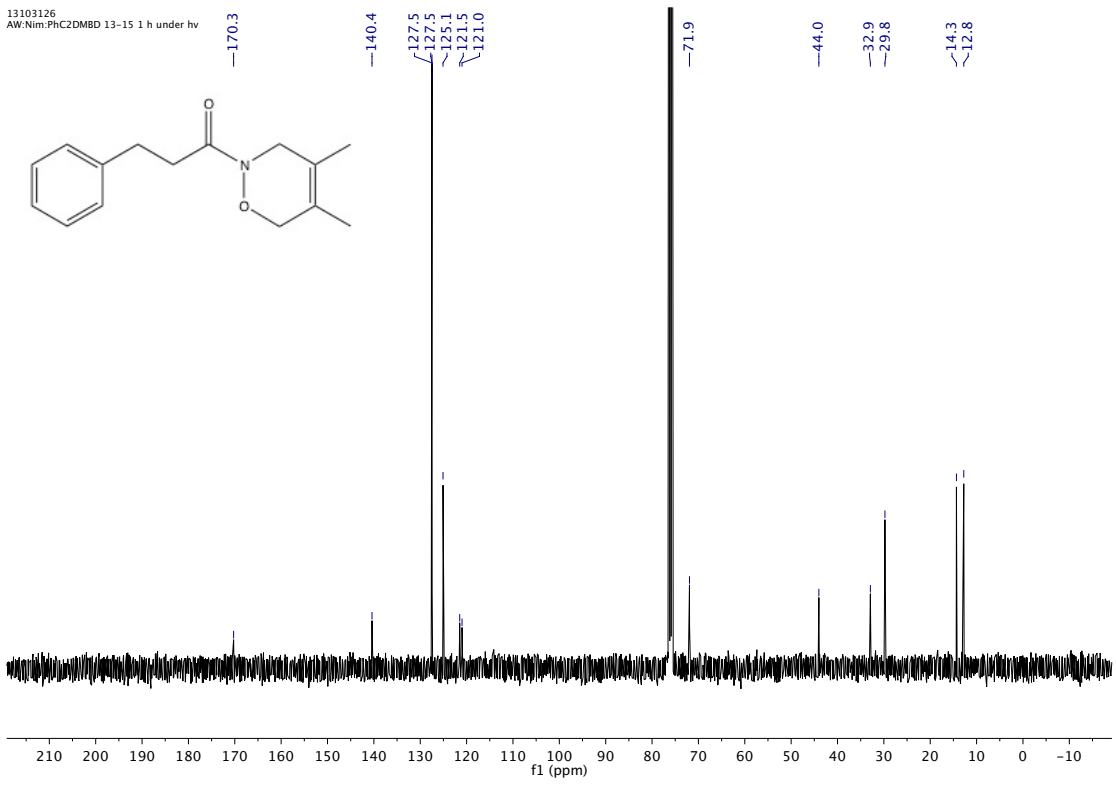

1-(4,5-Dimethyl-3,6-dihydro-2*H*-1,2-oxazin-2-yl)-4-phenylbu-tan-1-one **192**

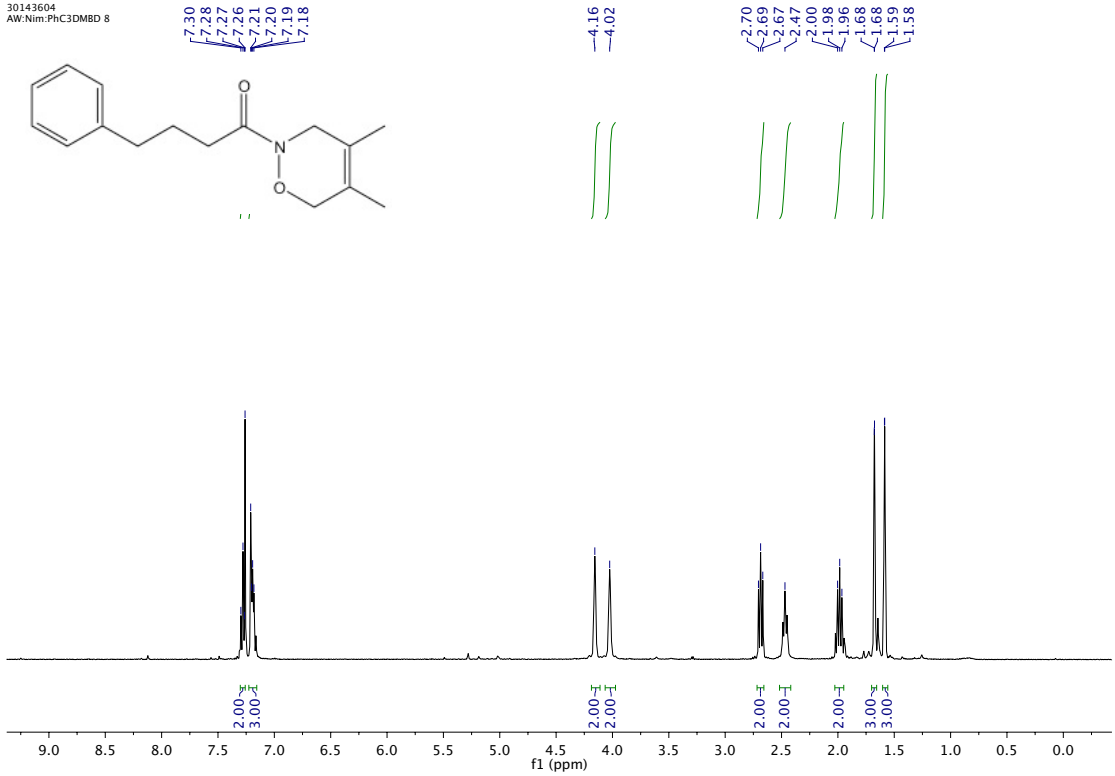

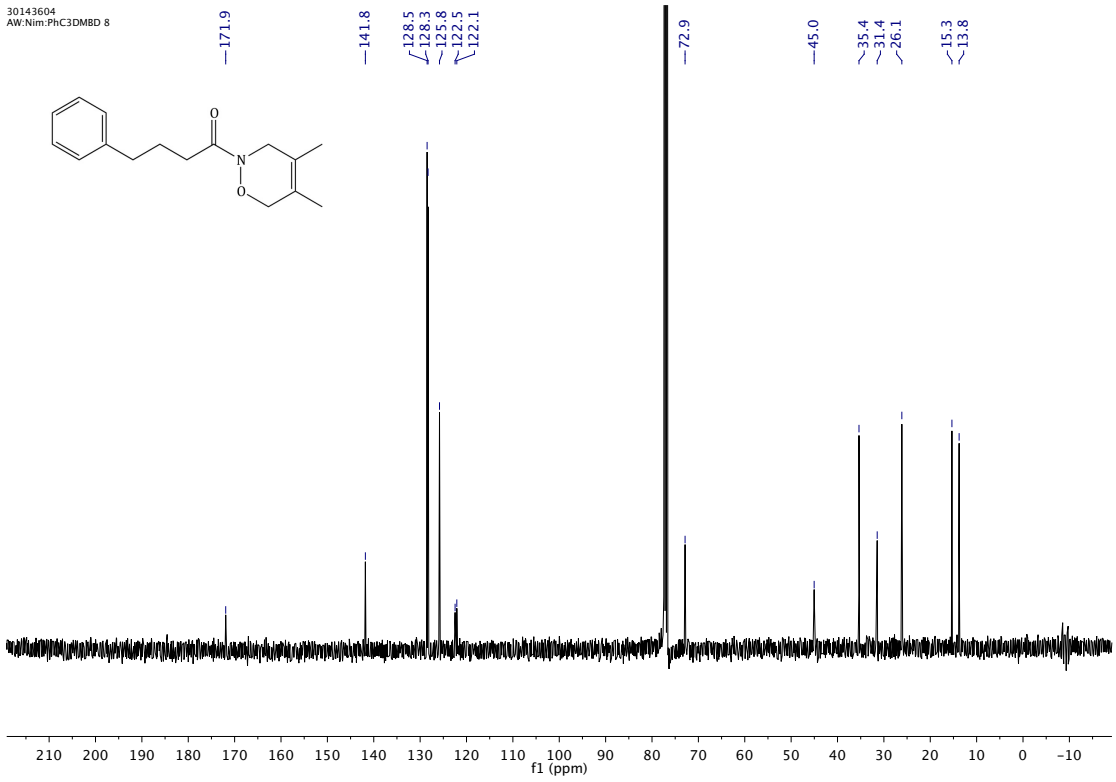

1-(4,5-Dimethyl-3,6-dihydro-2*H*-1,2-oxazin-2-yl)-5-phenylpen-tan-1-one **193**

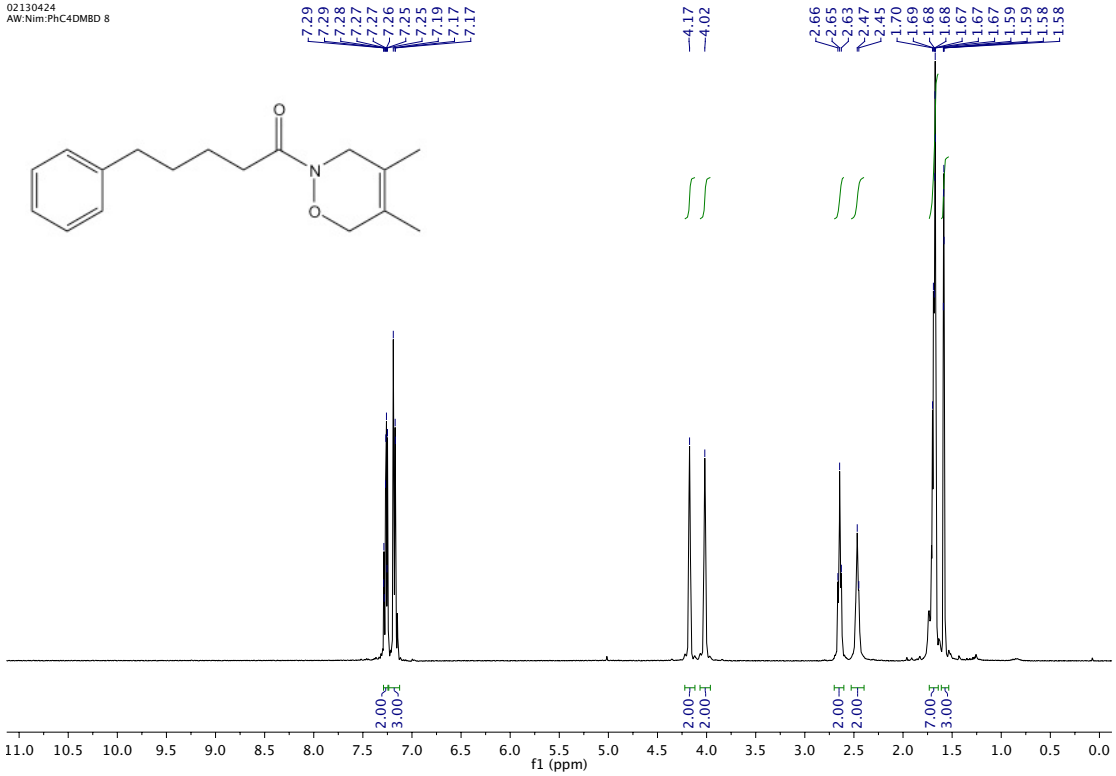

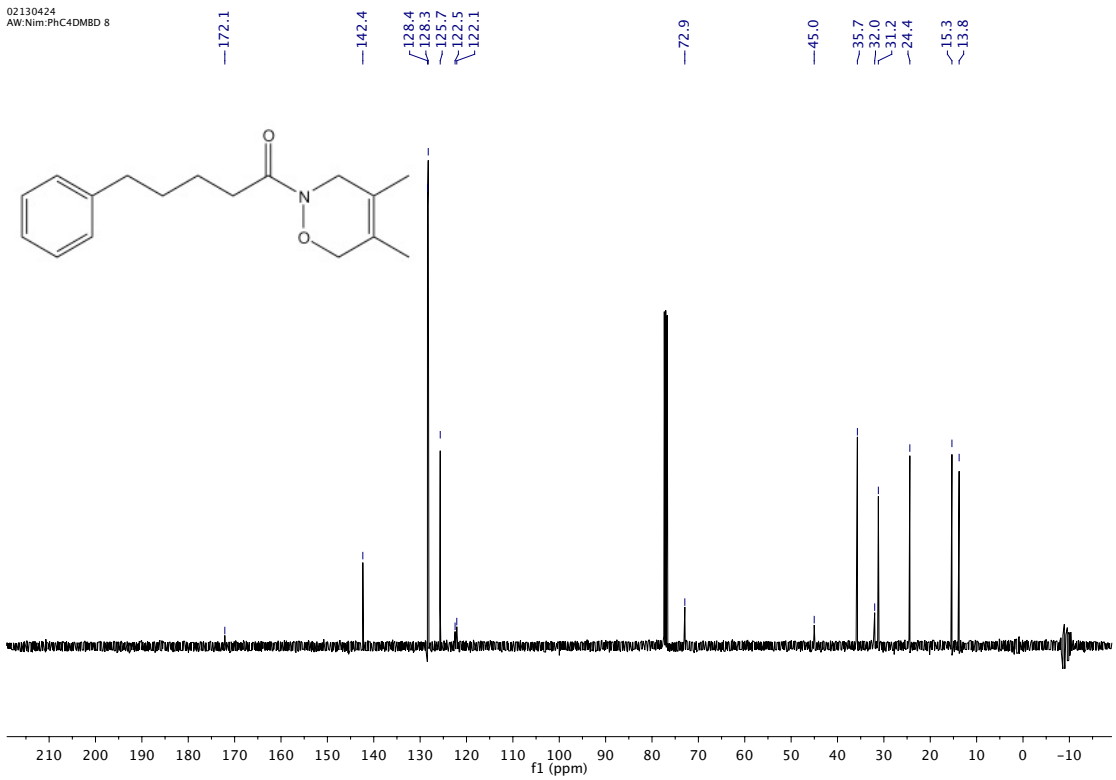

Phenyl-4,5-dimethyl-3,6-dihydro-2*H*-1,2-oxazine-2-carboxy-late **194**

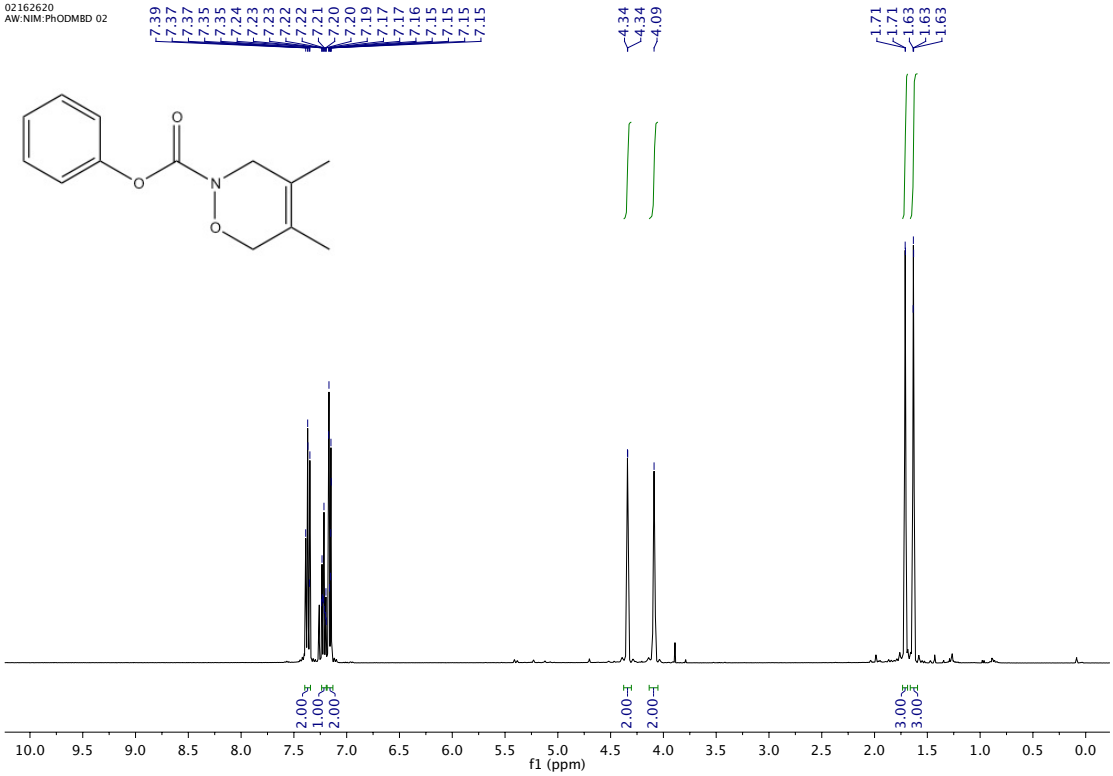

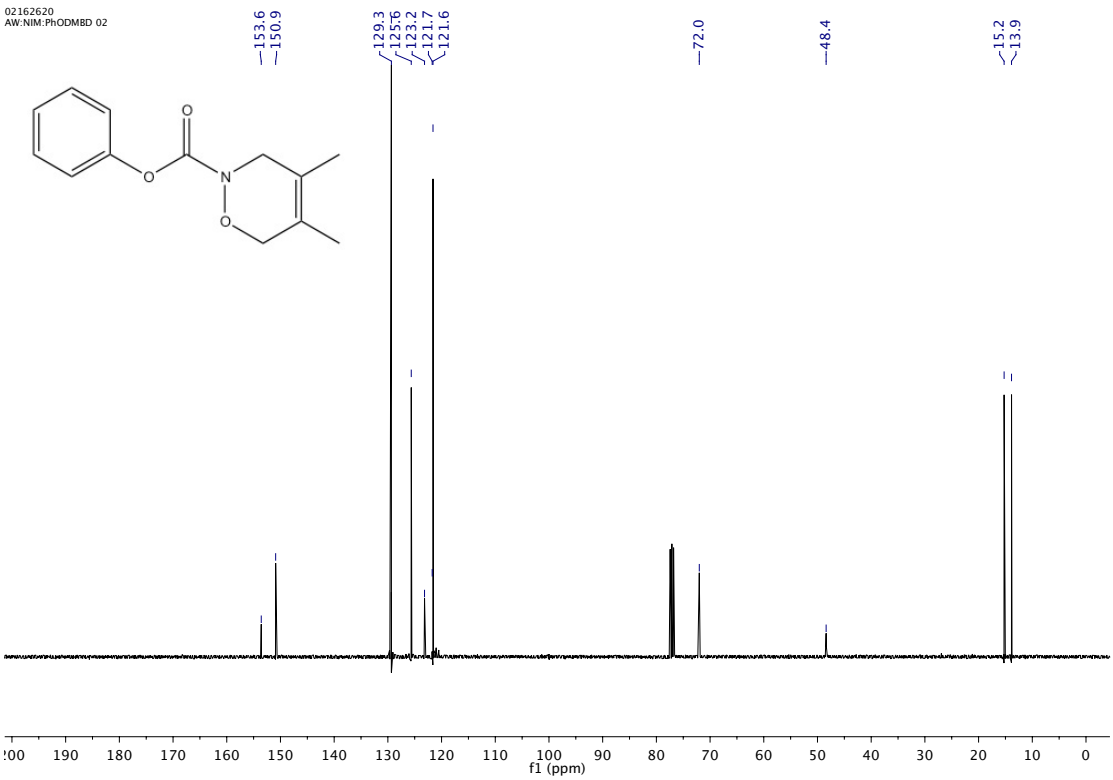

4,5-Dimethyl-*N*-phenyl-3,6-dihydro-2*H*-1,2-oxazine-2-carbox-amide **195**

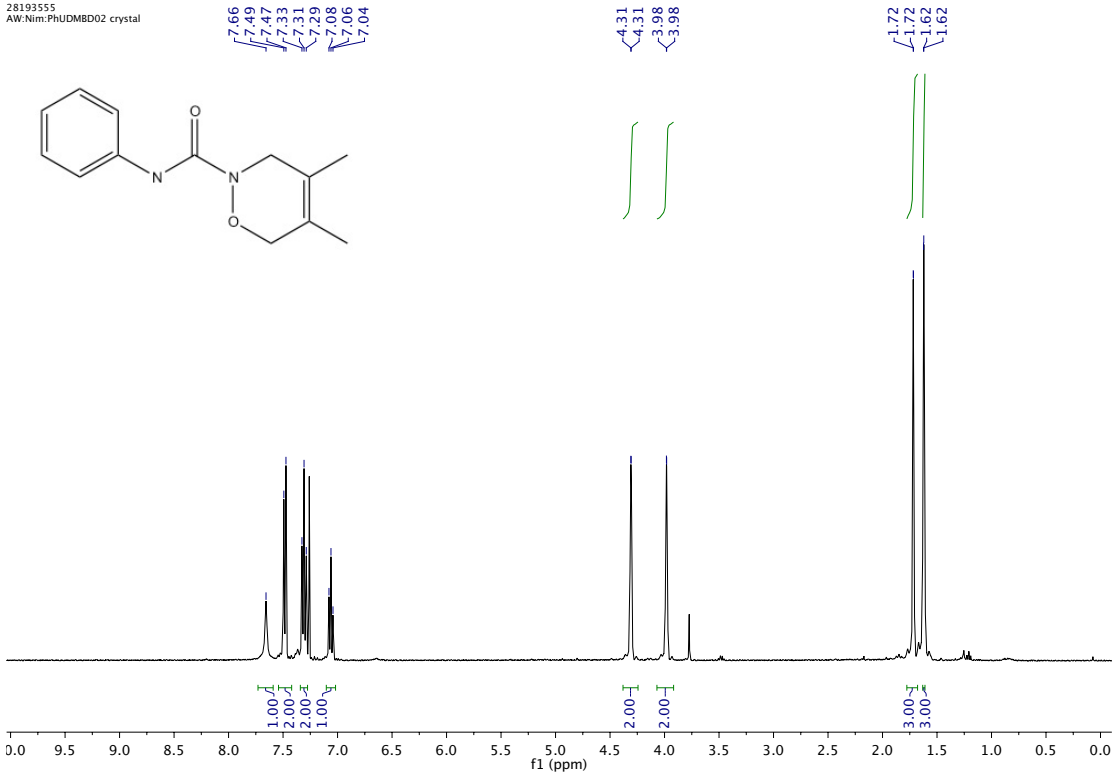

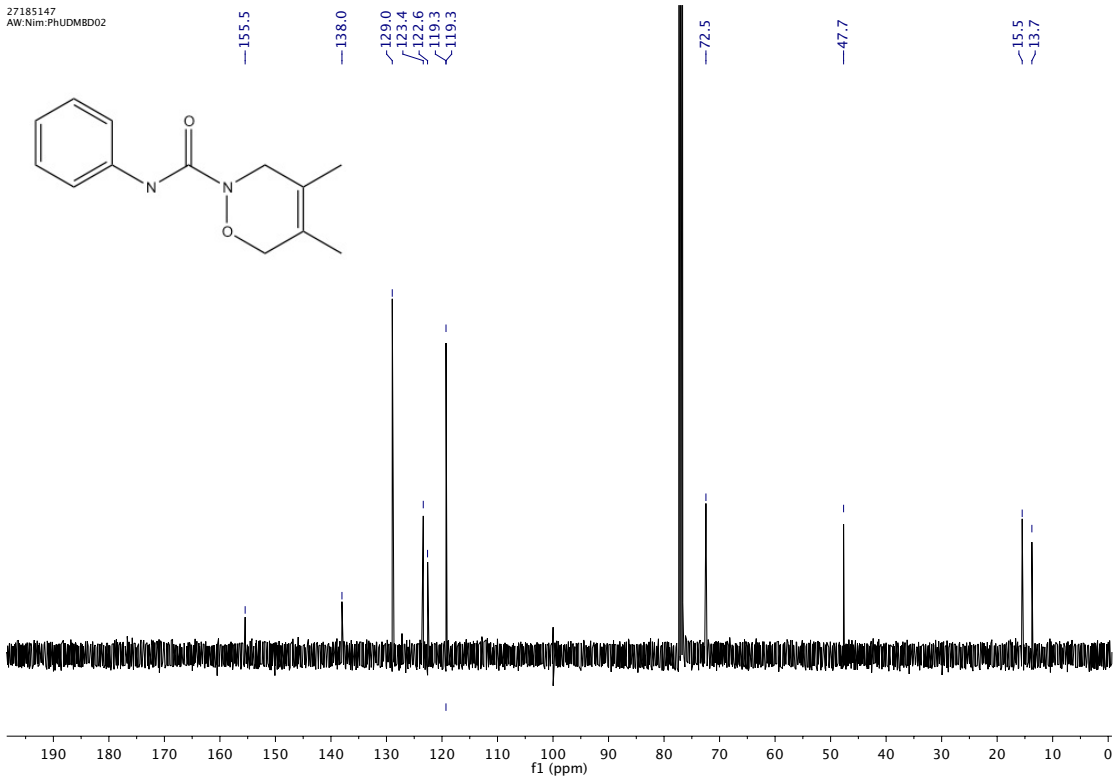

(*R*)-4,5-Dimethyl-*N*-(1-phenylethyl)-3,6-dihydro-2*H*-1,2-oxazine-2-carboxamide

196

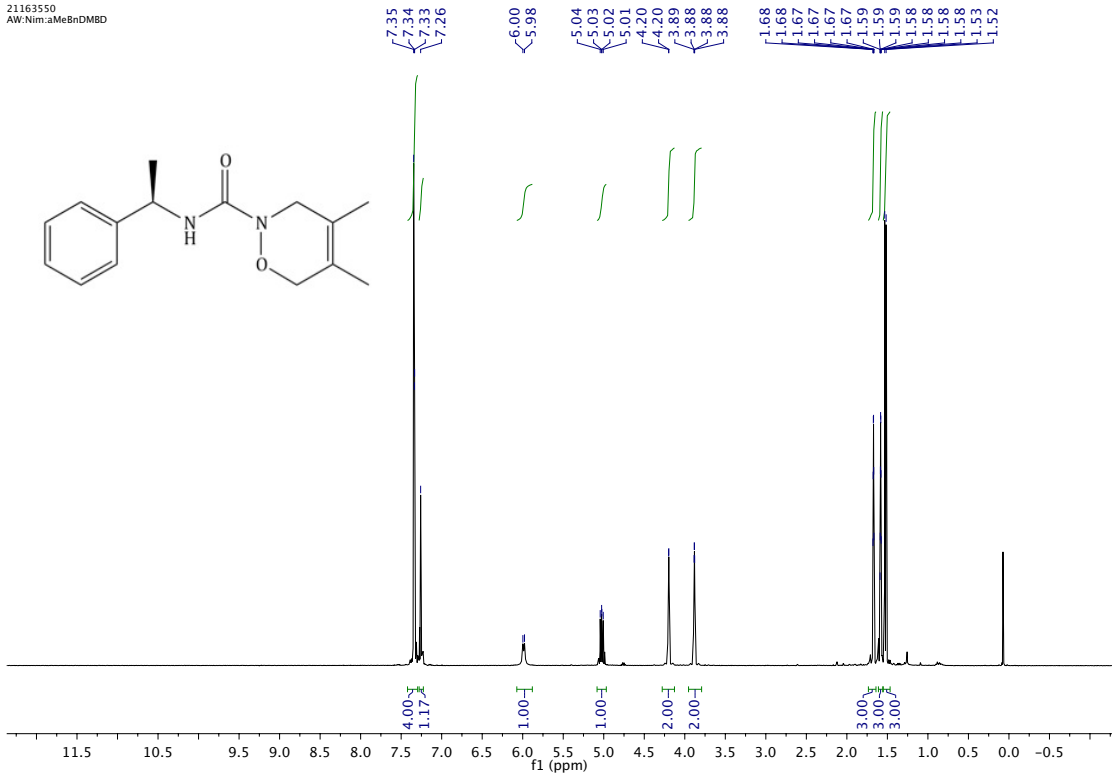

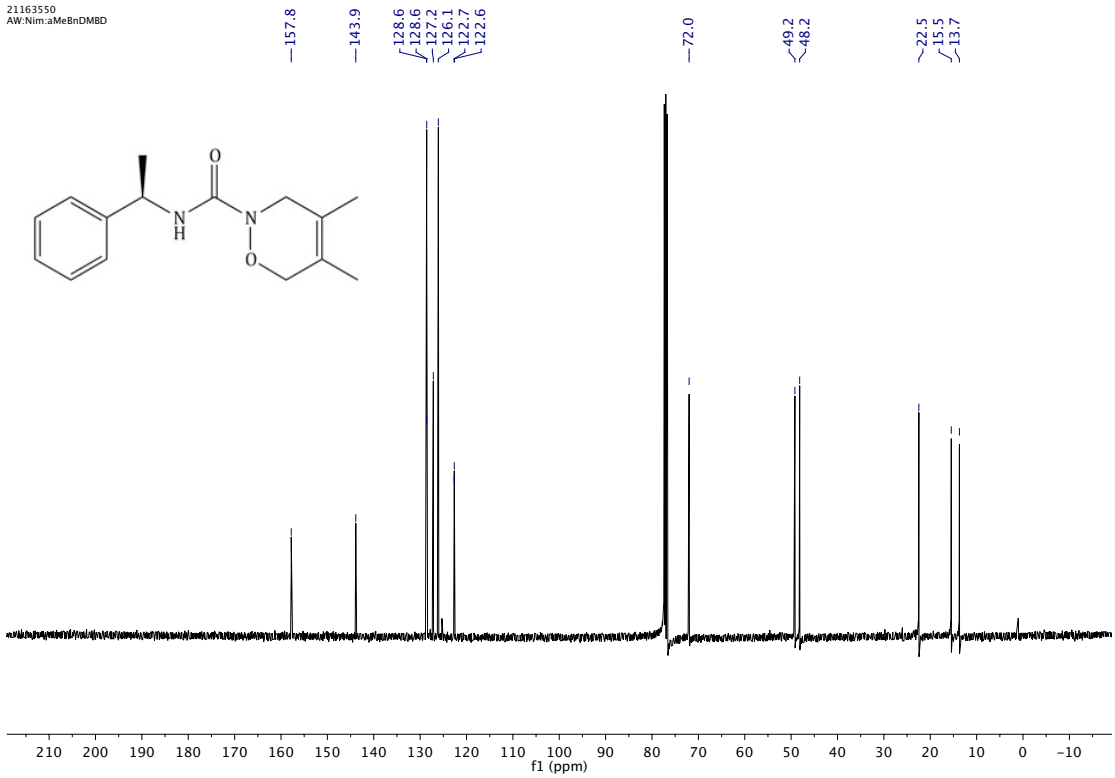

Phenyl 2-oxa-3-azabicyclo[2.2.1]hept-5-ene-3-carboxylate **197**

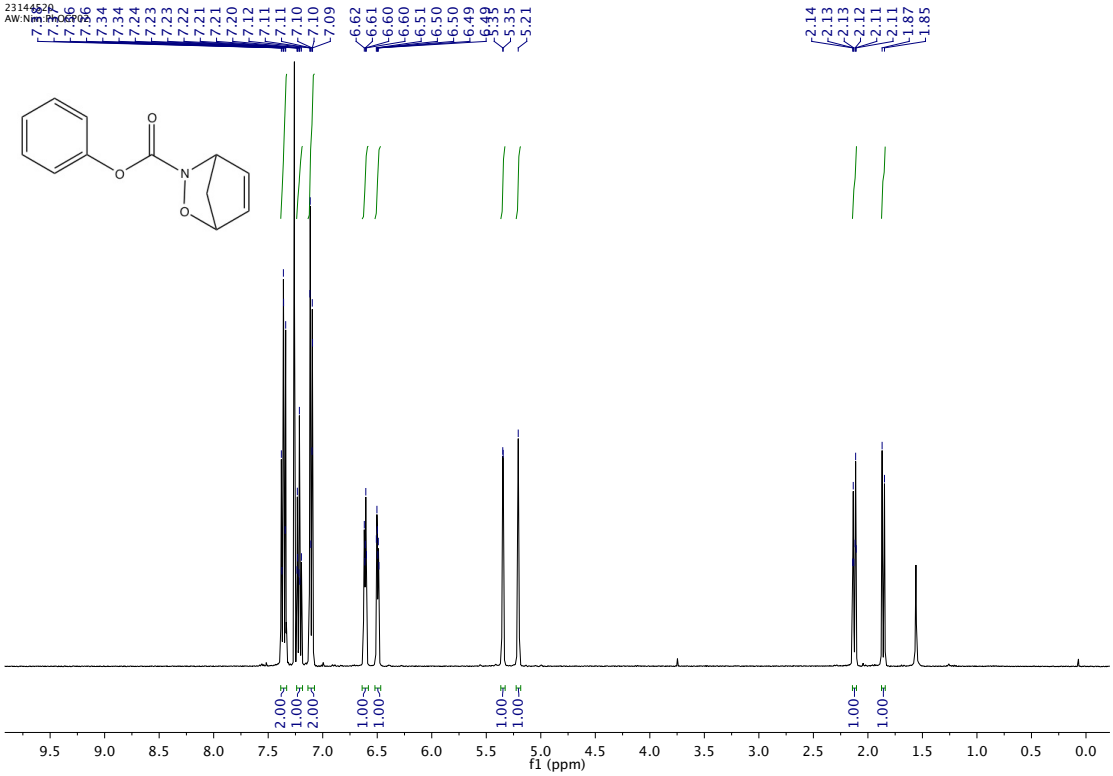

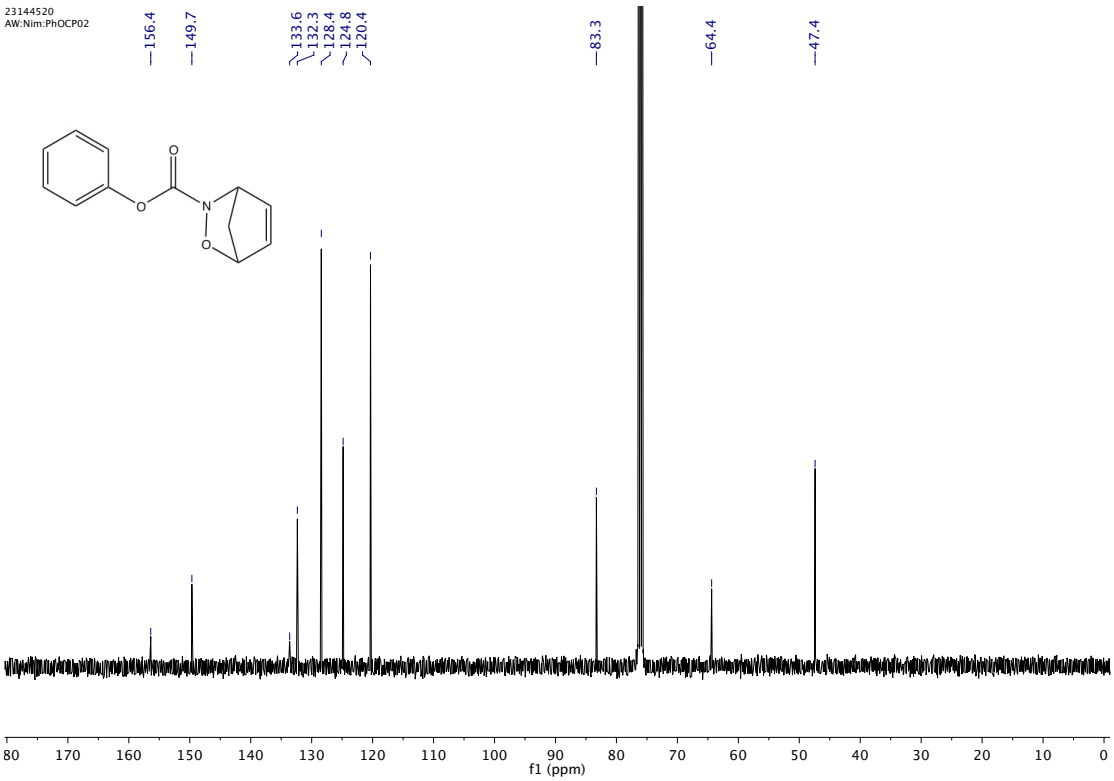

Phenyl 3,6-dimethyl-3,6-dihydro-2*H*-1,2-oxazine-2-carboxylate **199**

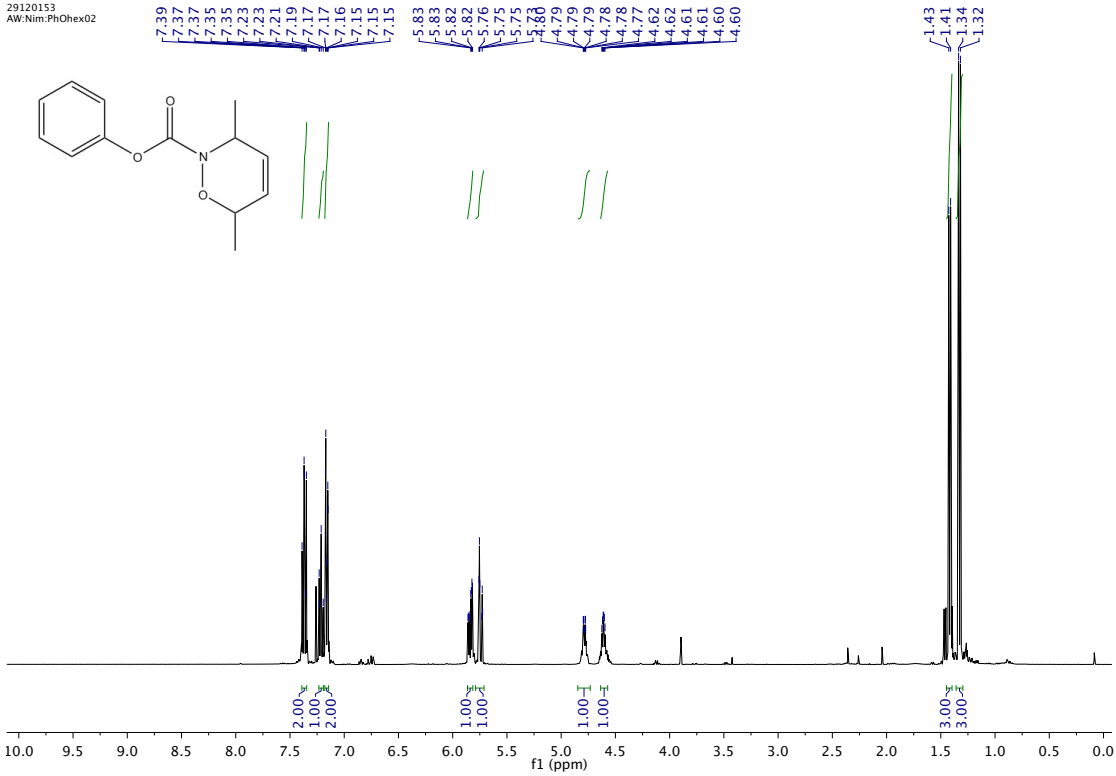

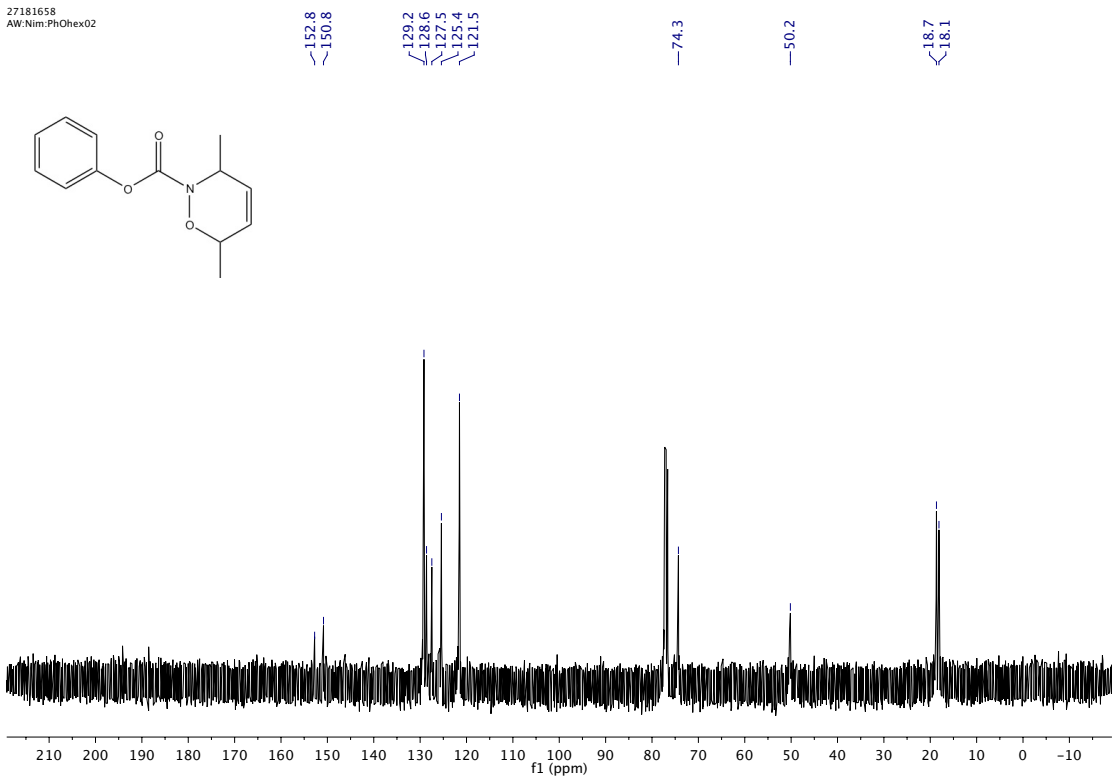

Phenyl 4-methyl-3,6-dihydro-2*H*-1,2-oxazine-2-carboxylate **200** and phenyl 5-methyl-3,6-dihydro-2*H*-1,2-oxazine-2-carboxylate **200'**

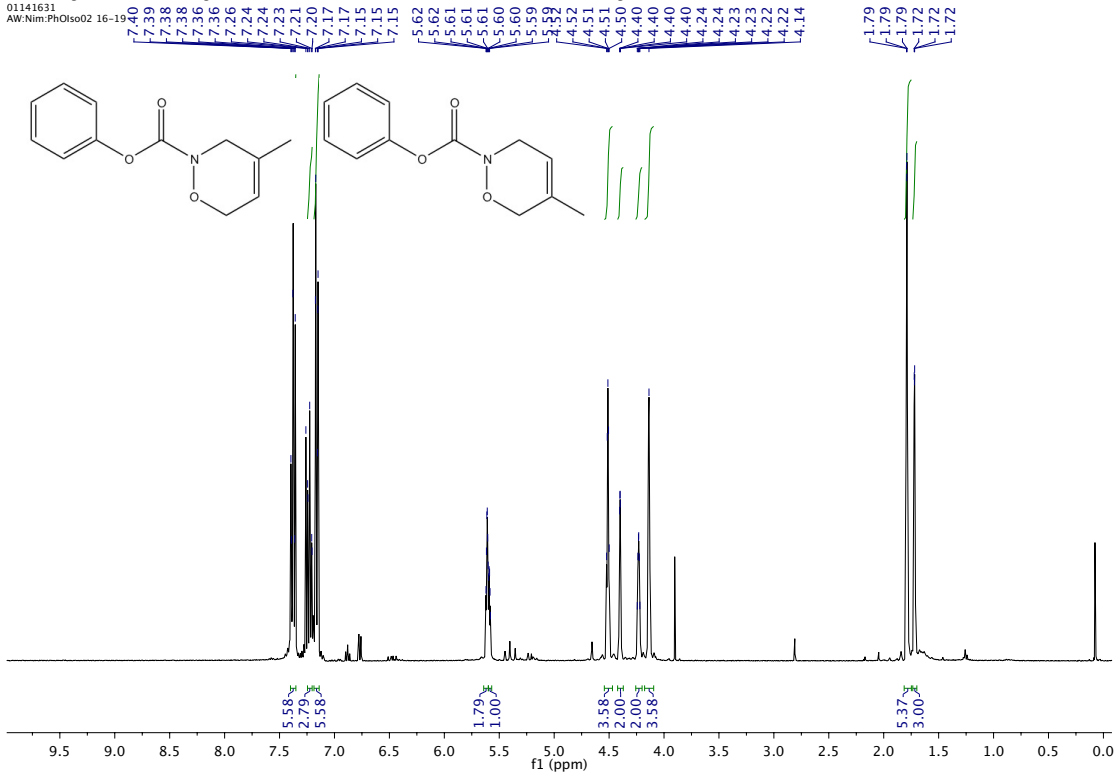

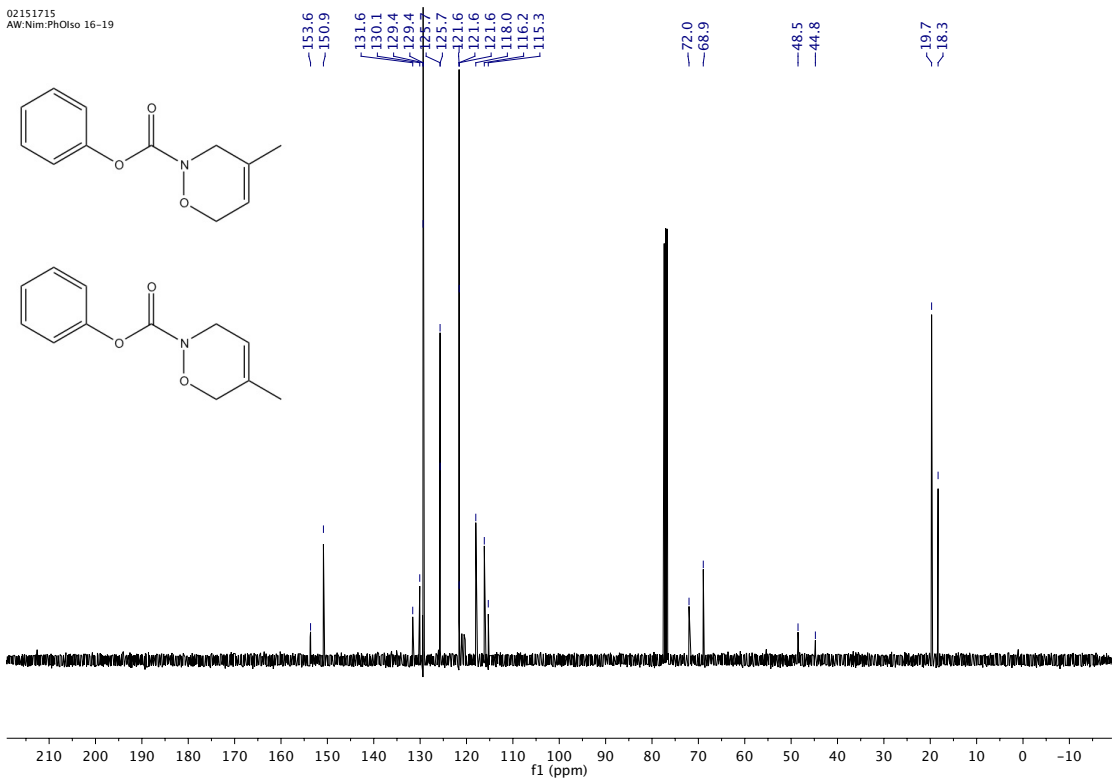

(9*S*,10*S*)-Phenyl-9,10-dimethyl-9,10-dihydro-9,10-(epoxy-imino)-anthracene-11-carboxylate **202**

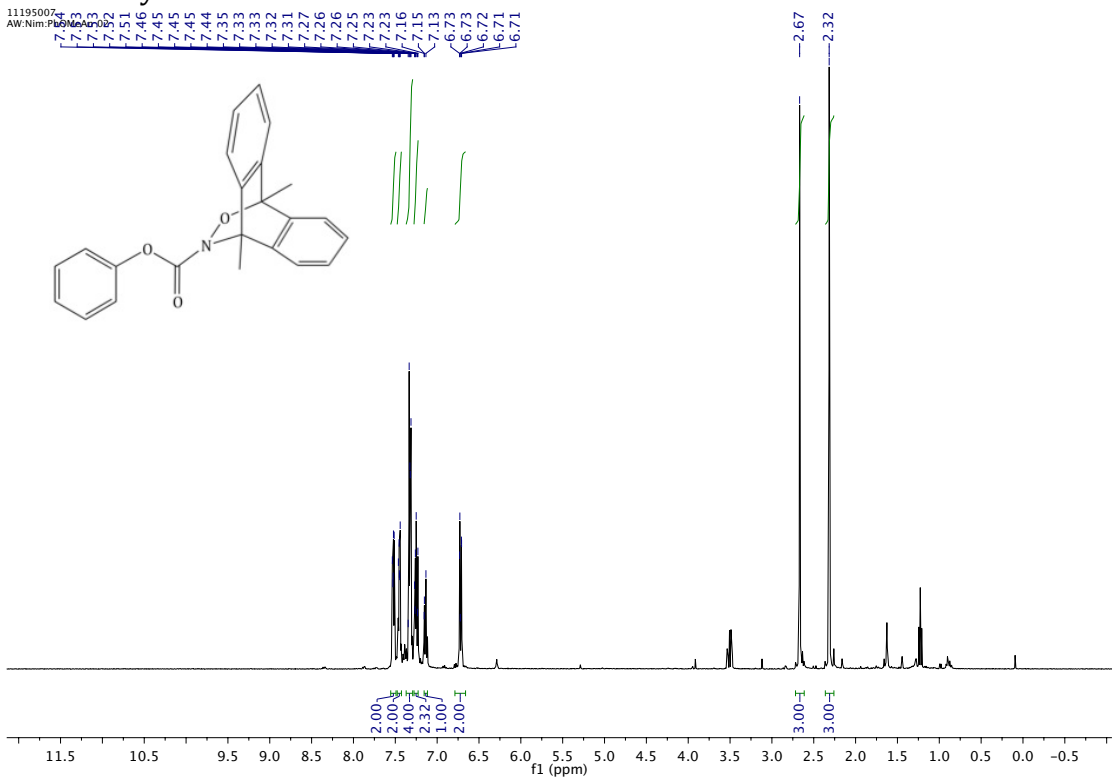

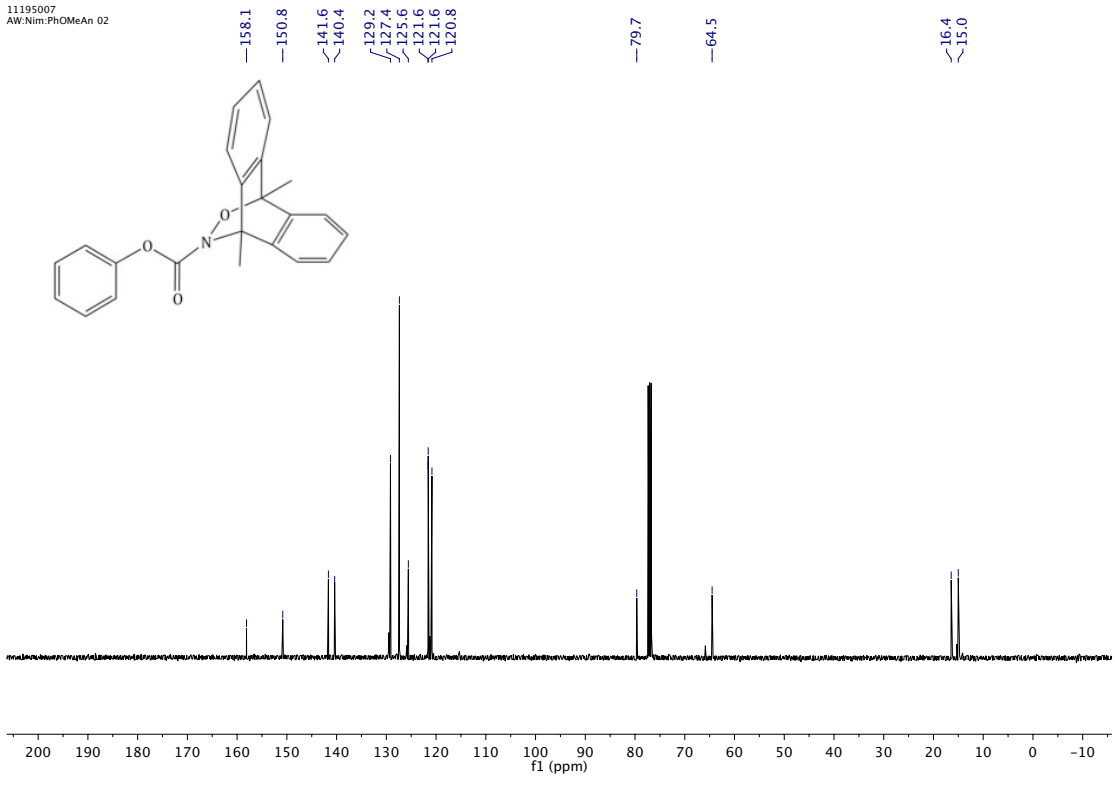

Phenyl 3,6-diphenyl-3,6-dihydro-2*H*-1,2-oxazine-2-carboxylate **203**

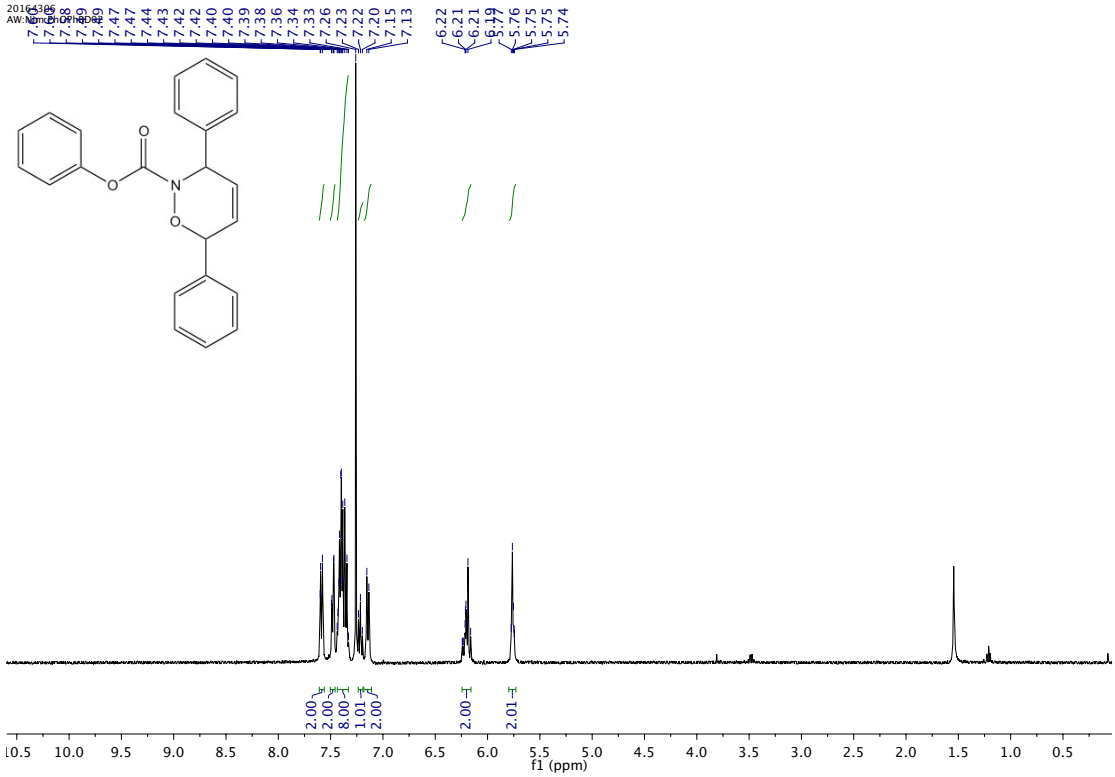

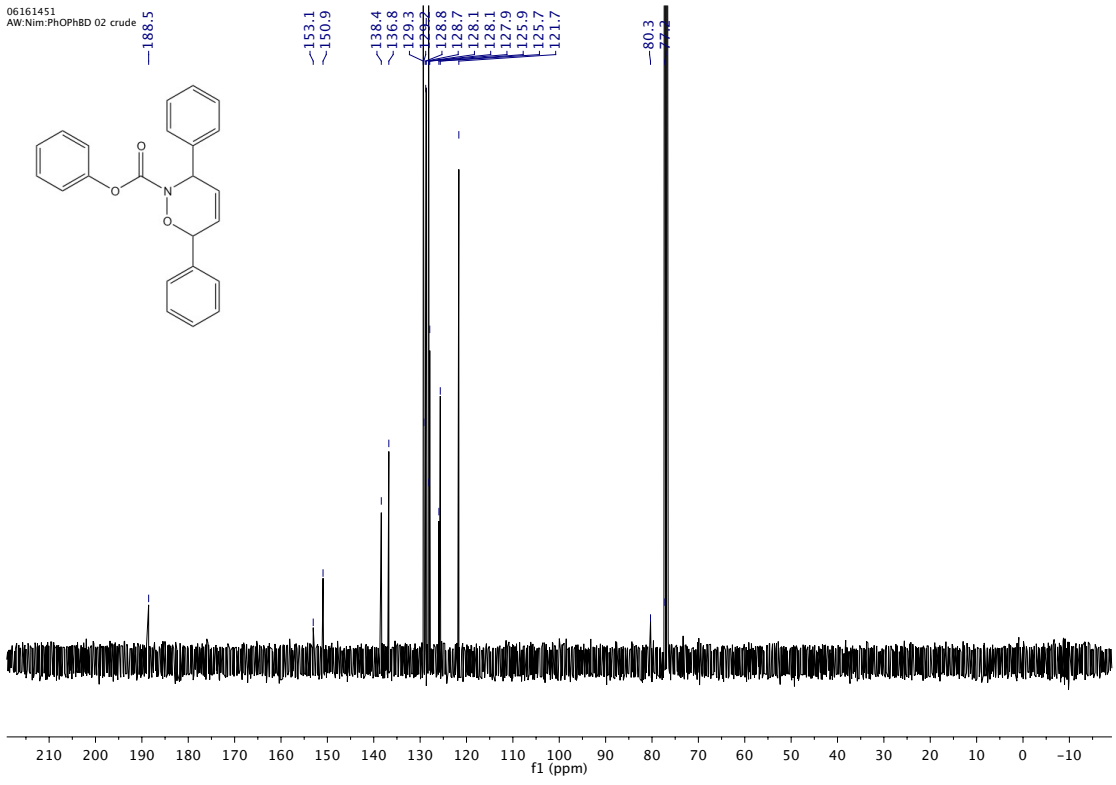

Phenyl-3-(hydroxymethyl)-6-methyl-3,6-dihydro-2*H*-1,2-oxa-zine-2-carboxylate **204** and phenyl 6-(hydroxymethyl)-3-methyl-3,6-dihydro-2*H*-1,2-oxazine -2-carboxylate **204'**

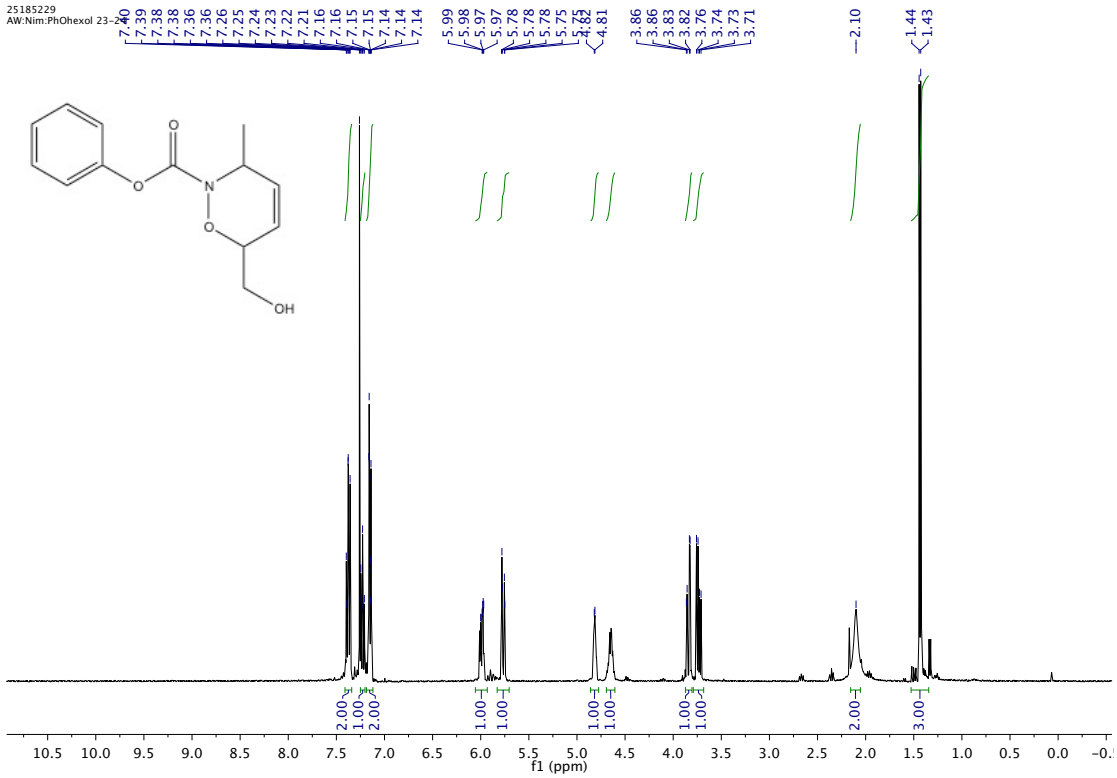

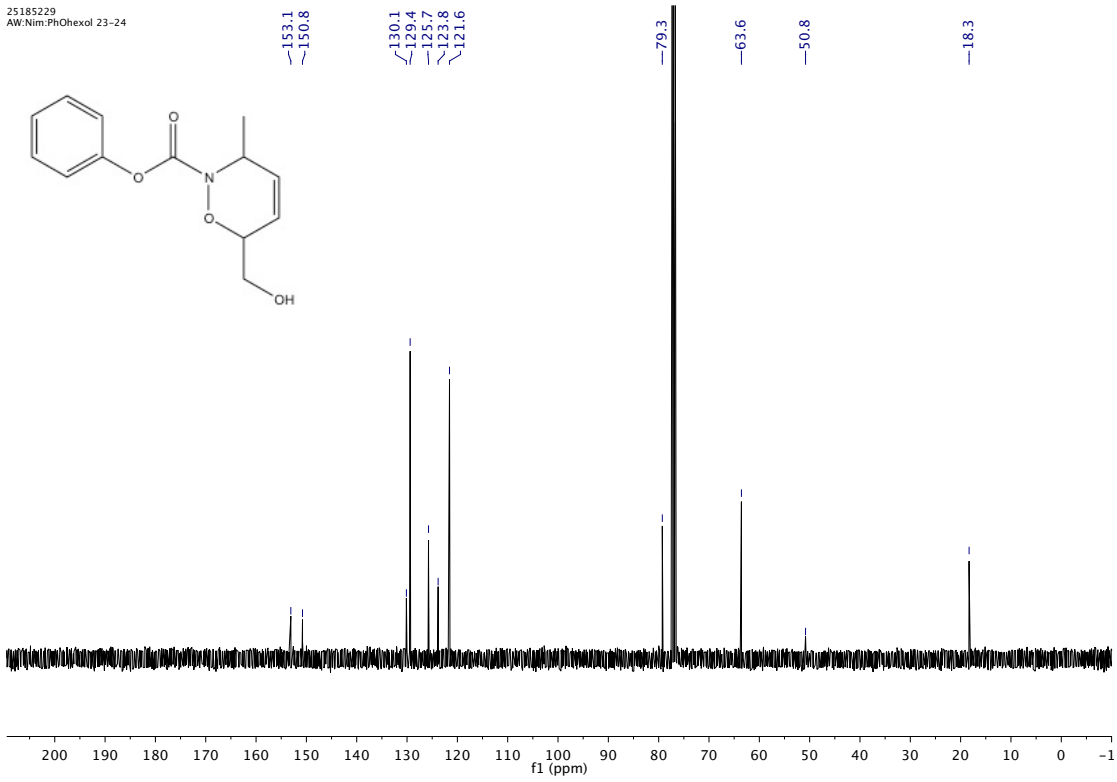

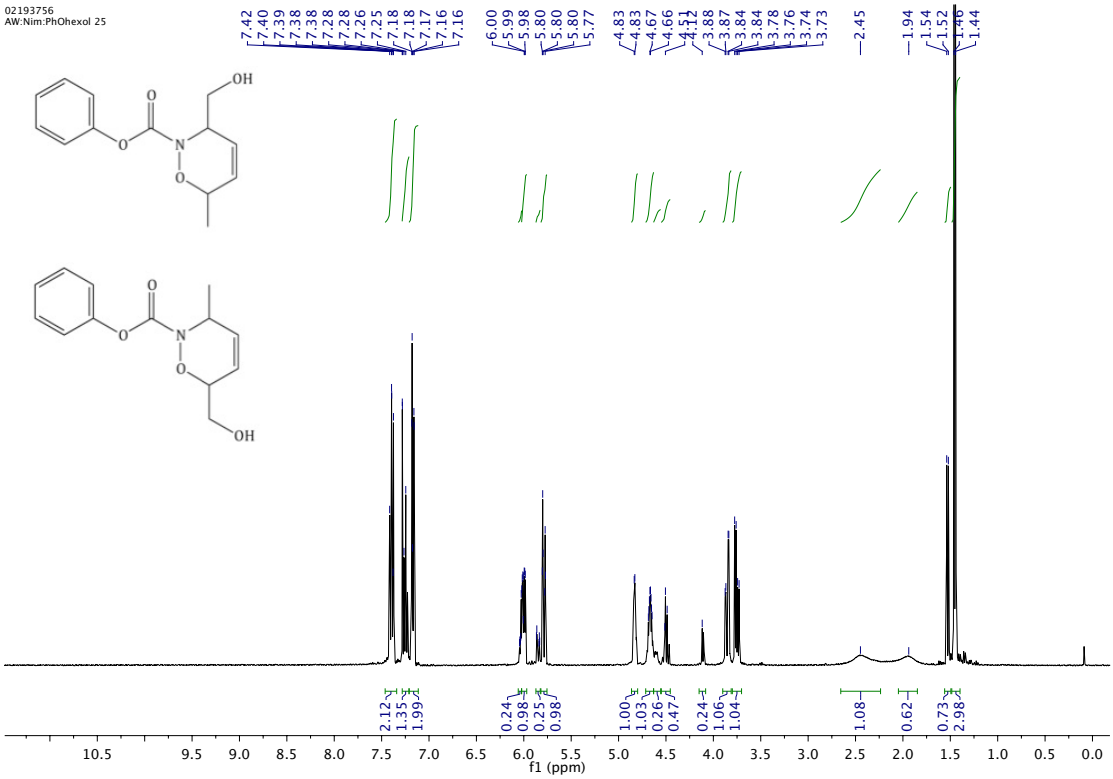
02193756
AW:Nim:PhOhexol 25
7.42
7.40
7.39
7.38
7.38
7.28
7.28
7.26
7.25
7.18
7.17
7.16
7.16
6.00
5.99
5.98
5.80
5.80
5.80
5.77
4.83
4.83
4.67
4.66
4.51
4.12
3.88
3.87
3.84
3.84
3.78
3.76
3.74
3.73
2.45
1.94
1.54
1.52
1.46
1.44
OH
OH
2.12
1.35
1.99
0.24
0.98
0.25
0.98
1.00
1.03
0.26
0.47
0.24
1.06
1.04
1.08
0.62
0.73
2.98
f1 (ppm)

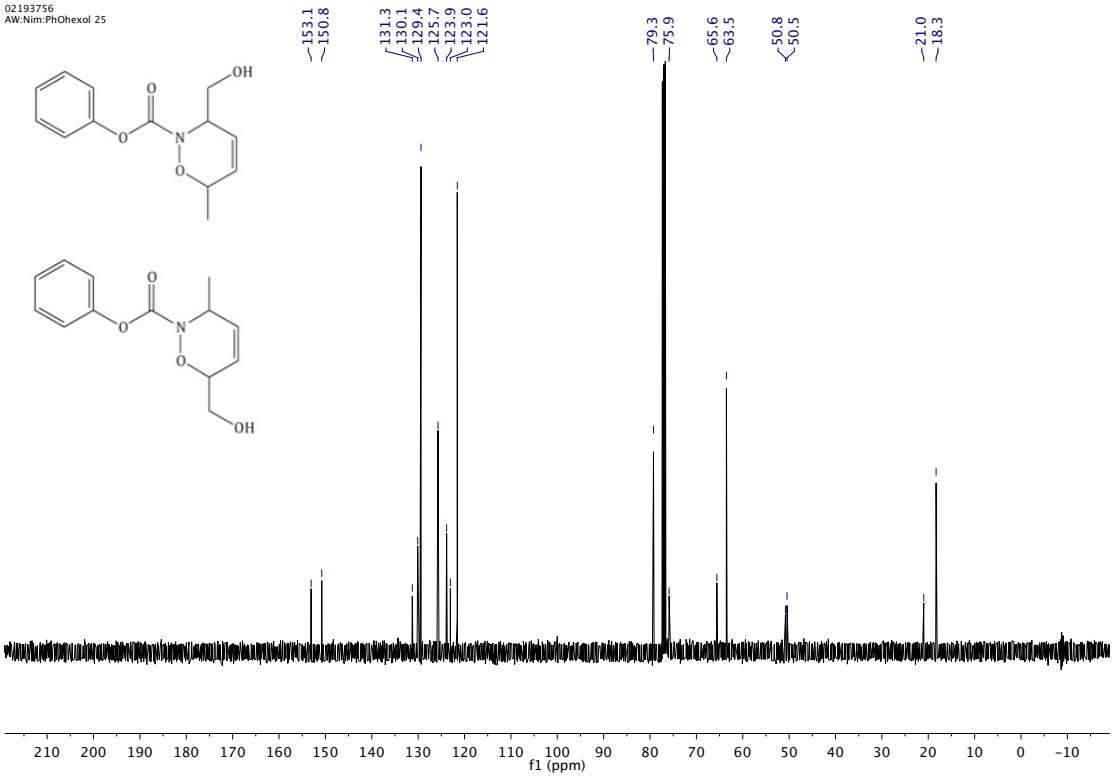
02193756
AW:Nim:PhOhexol 25
153.1
150.8
131.3
130.1
129.4
125.7
123.9
123.0
121.6
79.3
75.9
65.6
63.5
50.8
50.5
21.0
18.3
OH
OH
f1 (ppm)

N-Phenyl-2-oxa-3-azabicyclo[2.2.1]hept-5-ene-3-carboxamide **205**

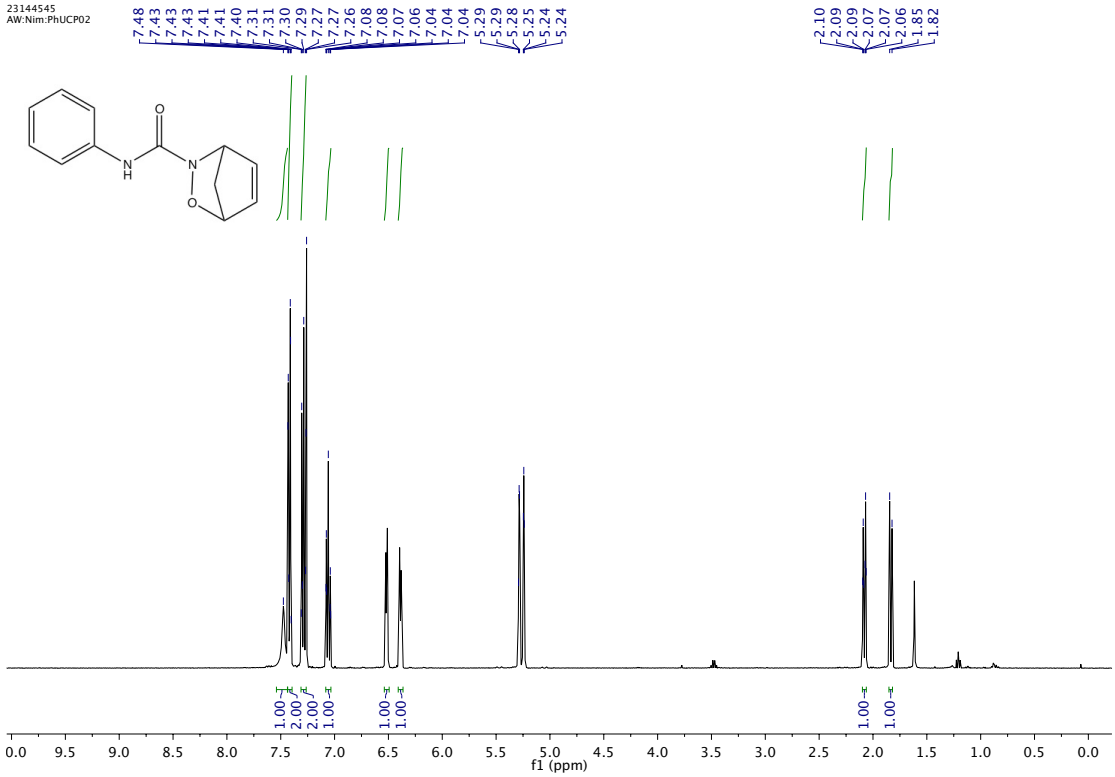

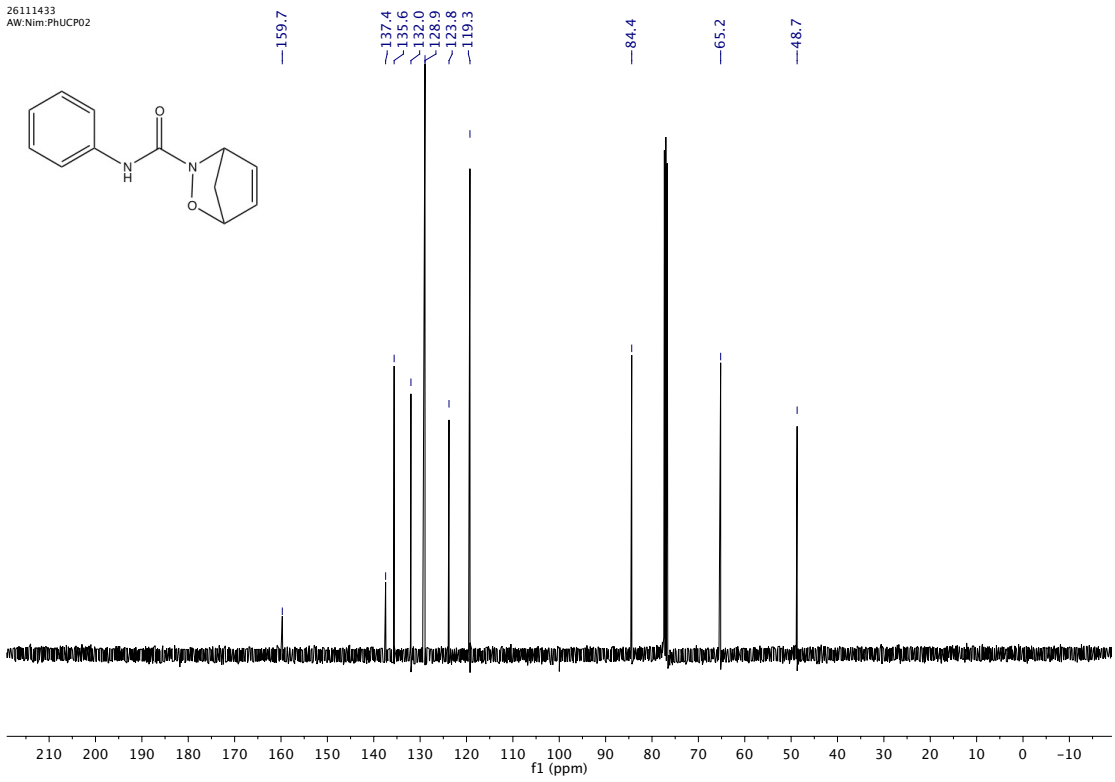

3,6-Dimethyl-*N*-phenyl-3,6-dihydro-2*H*-1,2-oxazine-2-carboxamide **207**

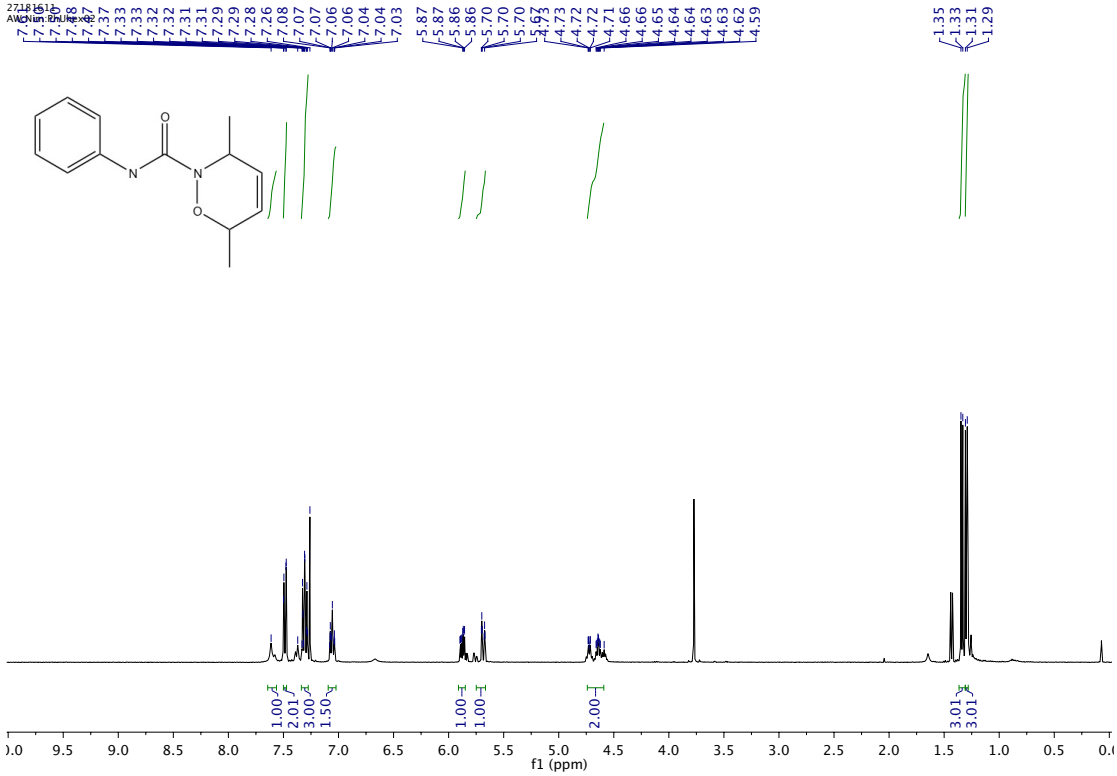

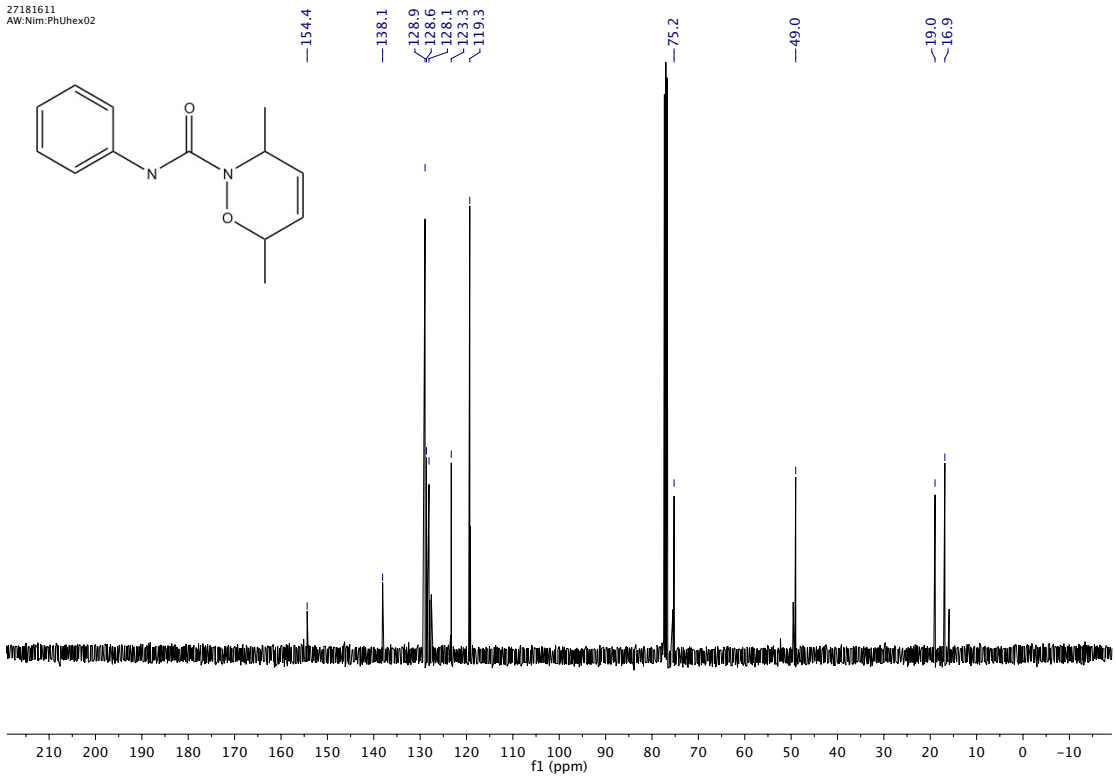

4-Methyl-*N*-phenyl-3,6-dihydro-2*H*-1,2-oxazine-2-carboxamide **208** and 5-methyl-*N*-phenyl-3,6-dihydro-2*H*-1,2-oxazine-2-carboxamide **208'**

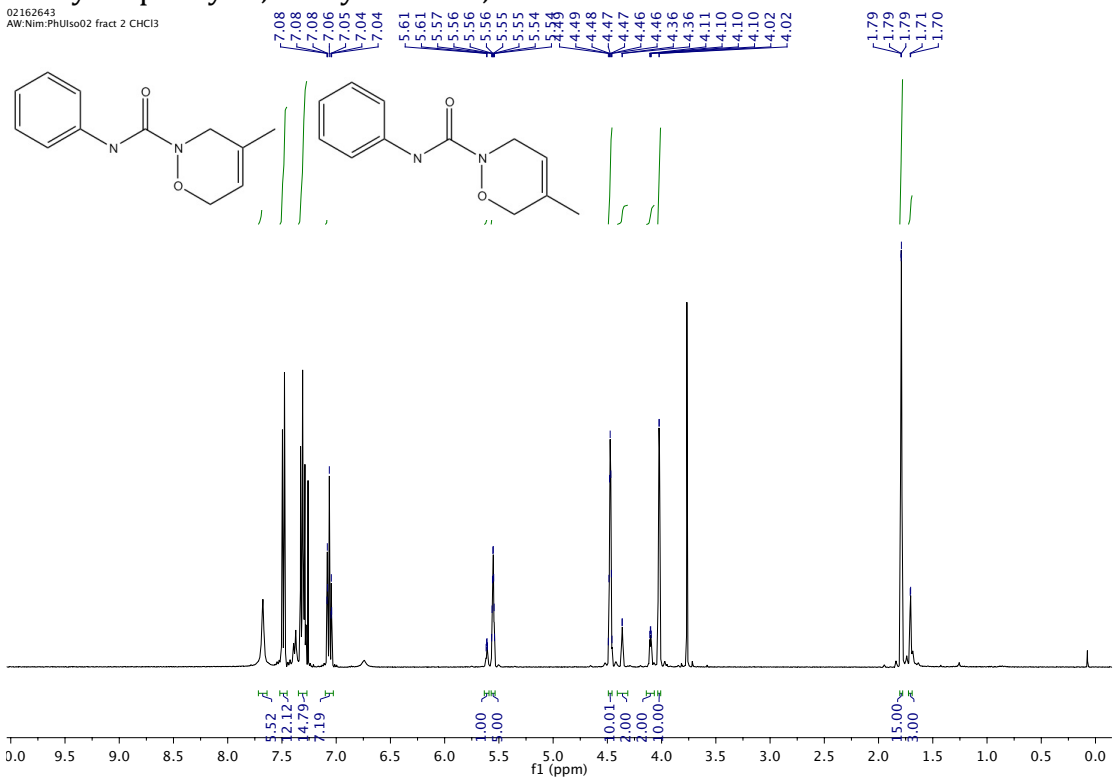

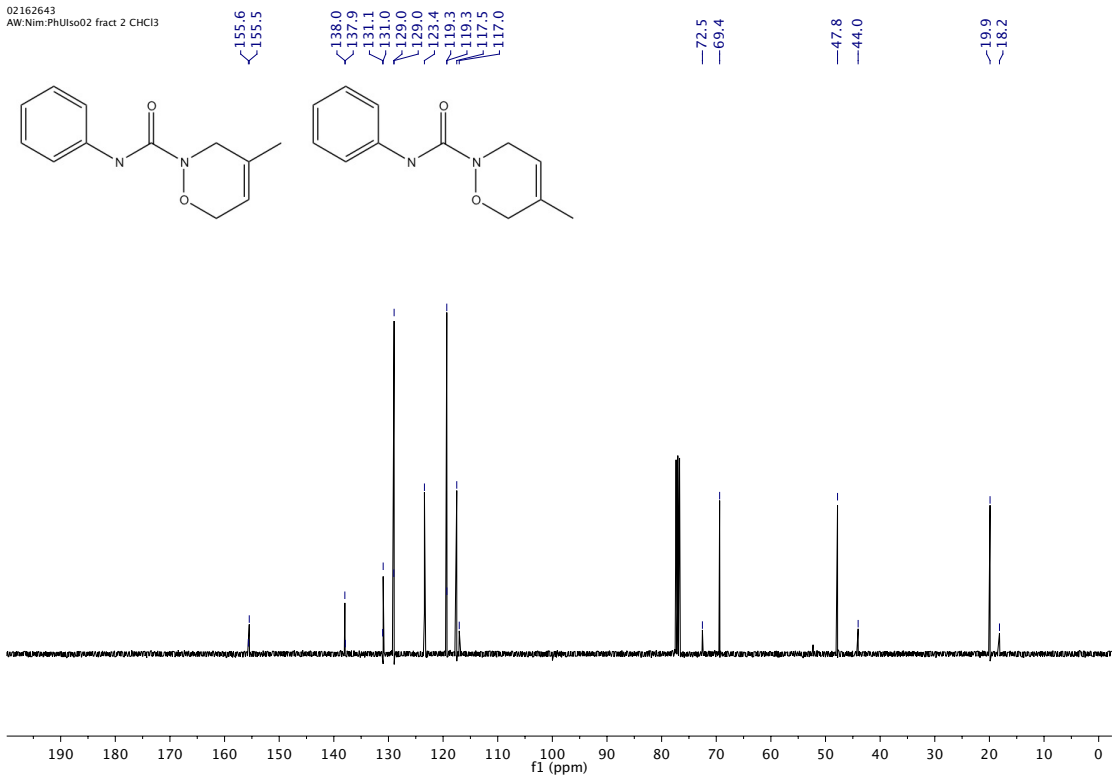

N,3,6-Triphenyl-3,6-dihydro-2*H*-1,2-oxazine-2-carboxamide **211**

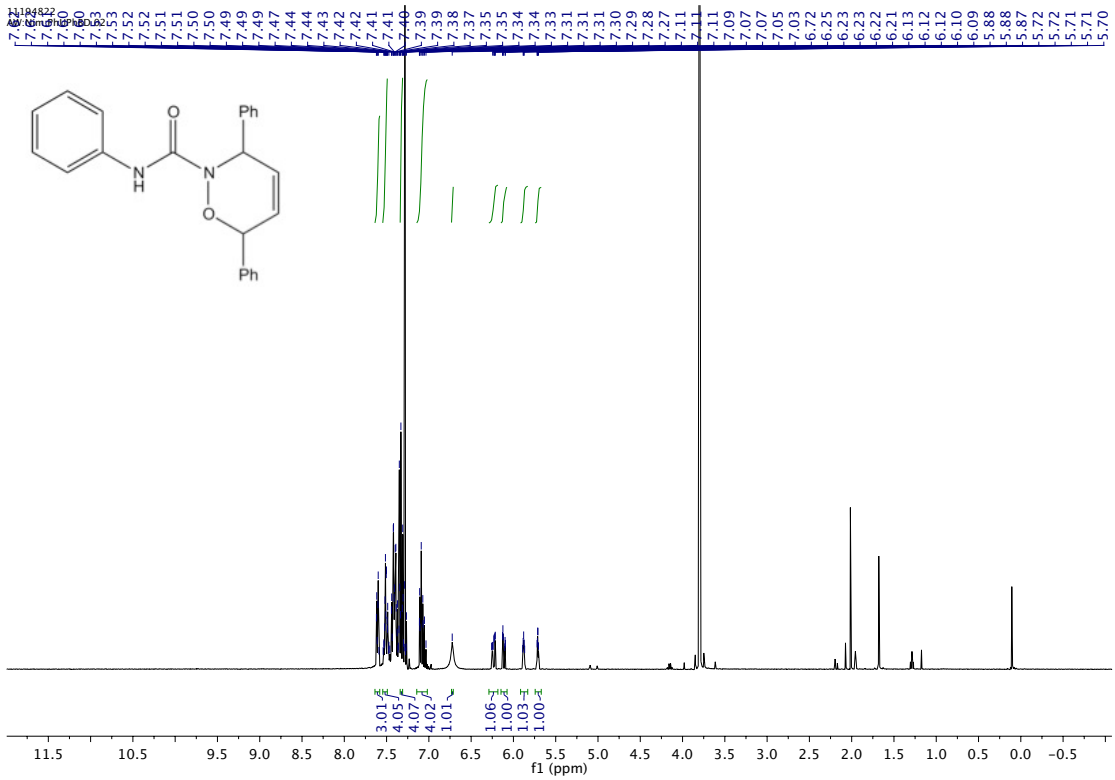

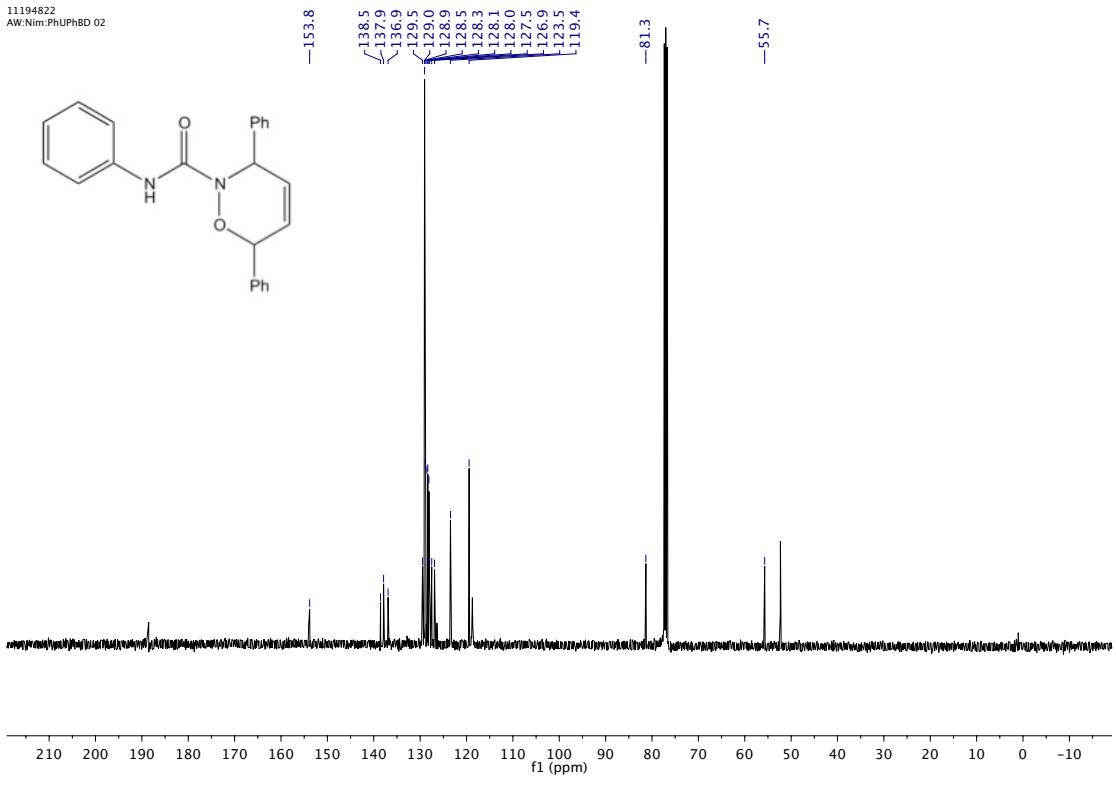

6-(Hydroxymethyl)-3-methyl-*N*-phenyl-3,6-dihydro-2*H*-1,2-oxa -zine-2-carboxamide **212** and 3-(hydroxymethyl)-6-methyl-*N*-phenyl-3,6-dihydro-2*H*-1,2-oxazine-2-carboxamide **212'**

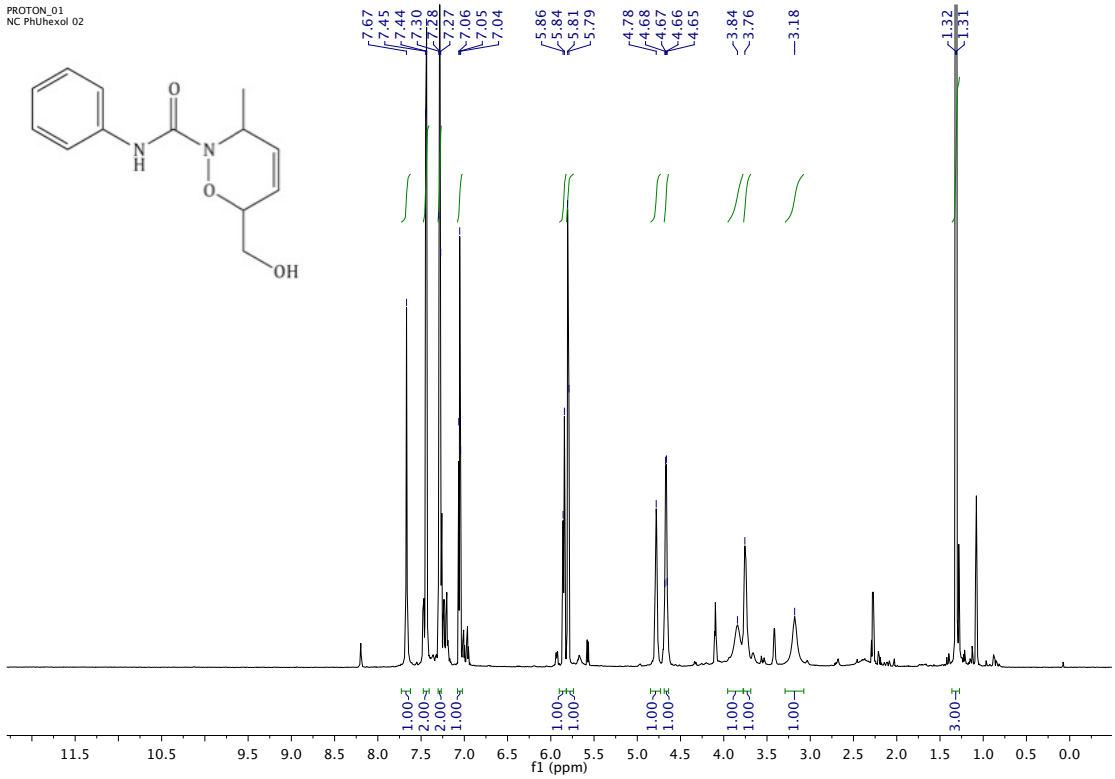

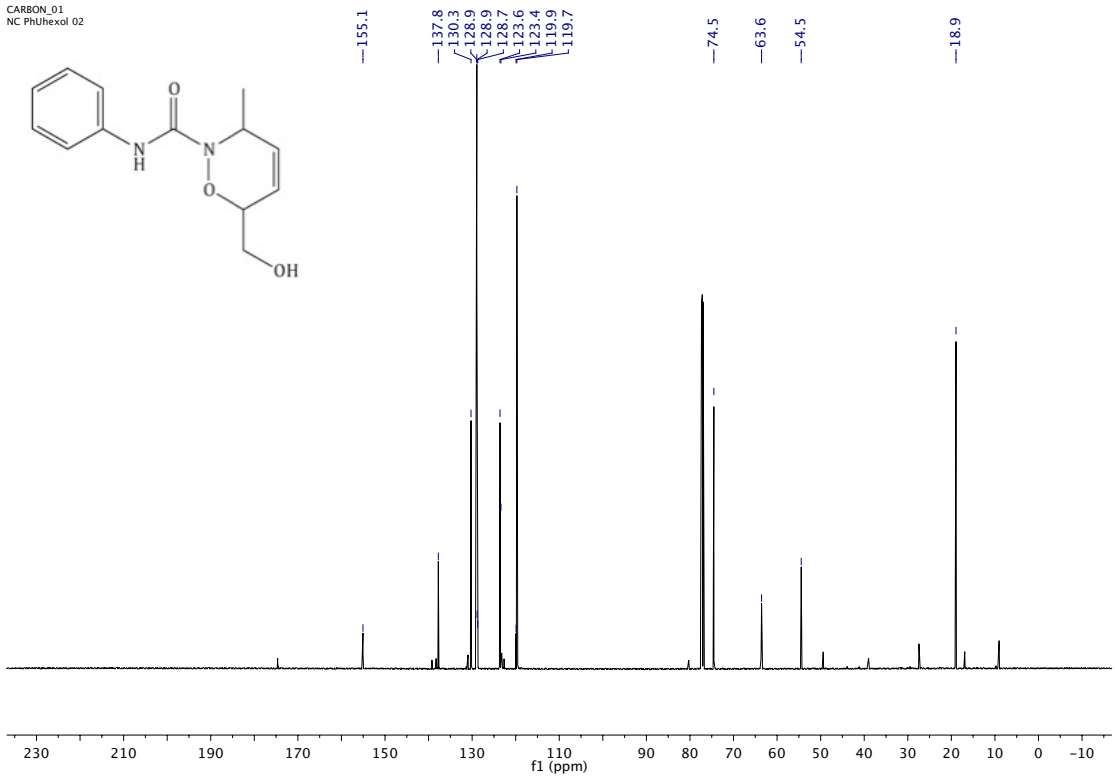

1-((1*R*,4*S*)-2-Oxa-3-azabicyclo[2.2.2]oct-5-en-3-yl)-2-phenylethanone **140**
09srv331

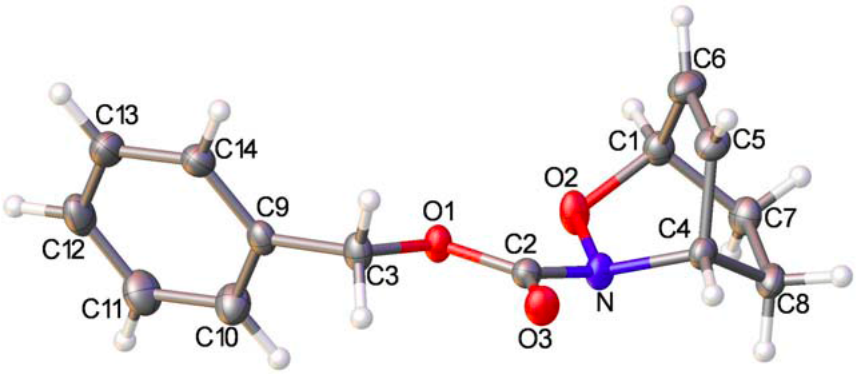

Table 1 Crystal data and structure refinement for 09srv331

Identification code	09srv331
Empirical formula	$C_{14}H_{15}NO_3$
Formula weight	245.27
Temperature/K	120.0
Crystal system	Triclinic
Space group	P-1
a/Å, b/Å, c/Å	6.0126(3), 10.4102(5), 10.6716(5)
α/°, β/°, γ/°	65.453(6), 88.454(6), 84.712(7)
Volume/Å^3	604.96(5)
Z	2
ρ_{calc}mg/mm^3	1.346
m/mm^{-1}	0.095
F(000)	260
Crystal size/mm^3	0.52 × 0.33 × 0.31
Theta range for data collection	2.10 to 30.00°
Index ranges	-8 ≤ h ≤ 8, -14 ≤ k ≤ 14, -15 ≤ l ≤ 15
Reflections collected	11016
Independent reflections	3525[R(int) = 0.0483]
Data/restraints/parameters	3525/0/223
Goodness-of-fit on F^2	1.062
Final R indexes [I>2σ (I)]	R_1 = 0.0407, wR_2 = 0.1122
Final R indexes [all data]	R_1 = 0.0436, wR_2 = 0.1154
Largest diff. peak/hole / e Å^{-3}	0.444/-0.201

Table 2 Atomic Coordinates (Å×10^4) and Equivalent Isotropic Displacement Parameters (Å^2×10^3) for 09srv331. U_{eq} is defined as 1/3 of of the trace of the orthogonalised U_{IJ} tensor.

Atom	*x*	*y*	*z*	U(eq)
O1	3590(11)	4154.8(6)	2706(7)	21.22(15)
O2	6763.6(12)	4004.2(6)	4260.1(7)	24.46(16)
O3	3963.9(12)	1802.9(7)	3220.7(7)	25.17(16)
N3	6536.7(13)	2770.2(7)	4004.3(8)	20.49(16)
C1	7487.8(15)	3565.9(9)	5693.7(9)	22.12(18)
C4	7160(14)	1429.4(8)	5231.7(9)	19.97(17)
C5	5704.5(16)	1431.3(10)	6404.5(10)	24.71(19)

C6	5869.1(17)	2611.3(11)	6636.5(11)	29.7(2)
C7	9784.3(15)	2758.4(10)	5866.5(10)	23.97(18)
C8	9591.7(15)	1476.1(10)	5558.4(10)	24.44(19)
C9	4582.5(14)	2833.5(9)	3321.8(9)	18.7(17)
C10	1608.1(16)	4263.8(9)	1893.2(9)	22.74(18)
C11	984.6(15)	5809.6(9)	1037.9(9)	20.91(18)
C12	2447.7(17)	6623.1(11)	52.9(11)	30(2)
C13	1839(2)	8046.2(11)	-767.7(12)	34.5(2)
C14	-237(2)	8660.7(10)	-612.6(10)	32.1(2)
C15	-1710.1(19)	7856.1(11)	354(11)	31.7(2)
C16	-1094.4(17)	6429.3(10)	1183.1(10)	25.99(19)

Table 3 Anisotropic Displacement Parameters ($Å^2×10^3$) for 09srv331. The Anisotropic displacement factor exponent takes the form: $-2π^2[h^2a^{*2}U_{11}+...+2hka×b×U_{12}]$

Atom	U_{11}	U_{22}	U_{33}	U_{23}	U_{13}	U_{12}
O1	25.4(3)	15.3(3)	22.2(3)	-7.1(2)	-6.9(2)	0.9(2)
O2	31.8(3)	12.9(3)	26.2(3)	-4.7(2)	-9(3)	-3.5(2)
O3	31.2(4)	17(3)	28.2(3)	-10(3)	-4(3)	-2.8(2)
N3	23.3(4)	13.1(3)	22.7(3)	-4.9(3)	-3.3(3)	-1.5(2)
C1	25.4(4)	18(4)	22.9(4)	-8.6(3)	-2.1(3)	-0.3(3)
C4	22.1(4)	13.7(3)	21(4)	-4.5(3)	-0.1(3)	0.6(3)
C5	22.5(4)	21.4(4)	27(4)	-6.8(3)	5.6(3)	-3.7(3)
C6	28.3(5)	26.3(5)	30.3(5)	-8.8(4)	7.9(4)	1.2(4)
C7	21.2(4)	23.4(4)	27.2(4)	-10.1(3)	-3.8(3)	-2(3)
C8	19.3(4)	25.9(4)	22.8(4)	-5.7(3)	-0.3(3)	2.7(3)
C9	21.7(4)	15.9(3)	17.6(3)	-6.2(3)	0.8(3)	-0.9(3)
C10	26(4)	18.6(4)	22.5(4)	-7.1(3)	-7.4(3)	-1.2(3)
C11	25.9(4)	19(4)	17.5(4)	-7.1(3)	-4.8(3)	-1.1(3)
C12	27(5)	26.4(5)	30.3(5)	-5.7(4)	0.3(4)	-2.5(4)
C13	40.2(6)	25.7(5)	29.4(5)	-2.6(4)	1.9(4)	-7.4(4)
C14	48.9(6)	20(4)	22.9(4)	-5(3)	-5.5(4)	1.7(4)
C15	40.4(6)	25.9(5)	26.3(5)	-10.5(4)	-0.3(4)	7.5(4)
C16	32.5(5)	23.5(4)	20.5(4)	-8.3(3)	1.8(3)	0.7(3)

Table 4 Bond Lengths for 09srv331.

Atom	Atom	Length/Å	Atom	Atom	Length/Å
O1	C9	1.3411(10)	C4	C8	1.5220(13)
O1	C10	1.4609(10)	C5	C6	1.3625(14)
O2	N3	1.4383(9)	C7	C8	1.5161(13)
O2	C1	1.4689(11)	C10	C11	1.5001(12)
O3	C9	1.2137(10)	C11	C16	1.3881(13)
N3	C9	1.3811(11)	C11	C12	1.3942(13)
N3	C4	1.4885(11)	C12	C13	1.3911(14)
C1	C6	1.4972(13)	C13	C14	1.3871(17)
C1	C7	1.5226(13)	C14	C15	1.3856(16)
C4	C5	1.5083(13)	C15	C16	1.3966(13)

Table 5 Bond Angles for 09srv331.

Atom	Atom	Atom	Angle/°	Atom	Atom	Atom	Angle/°
C9	O1	C10	113.73(7)	C7	C8	C4	108.79(7)
N3	O2	C1	109.64(6)	O3	C9	O1	124.90(8)
C9	N3	O2	113.92(7)	O3	C9	N3	122.12(8)
C9	N3	C4	116.70(7)	O1	C9	N3	112.75(7)
O2	N3	C4	112.21(7)	O1	C10	C11	107.41(7)
O2	C1	C6	109.09(7)	C16	C11	C12	119.38(8)
O2	C1	C7	107.30(7)	C16	C11	C10	120.15(8)
C6	C1	C7	109.71(7)	C12	C11	C10	120.41(8)
N3	C4	C5	107.58(7)	C13	C12	C11	120.33(10)
N3	C4	C8	106.14(7)	C14	C13	C12	119.99(10)
C5	C4	C8	109.87(8)	C15	C14	C13	120.05(9)
C6	C5	C4	111.79(8)	C14	C15	C16	119.96(10)
C5	C6	C1	112.48(8)	C11	C16	C15	120.28(9)
C8	C7	C1	108.71(7)				

Table 6 Hydrogen Atom Coordinates (Å×10⁴) and Isotropic Displacement Parameters (Å²×10³) for 09srv331.

Atom	*x*	*y*	*z*	U(eq)
H1	7490(2)	4457(14)	5776(14)	24(3)
H4	6940(2)	668(14)	4960(14)	26(3)
H5	4690(3)	746(19)	6823(18)	52(5)
H6	5040(3)	2880(19)	7270(19)	54(5)
H7A	10870(3)	3370(2)	5320(2)	58(5)
H7B	10350(3)	2510(18)	6774(19)	51(5)
H8A	10500(3)	1465(17)	4806(17)	43(4)
H8B	10130(3)	548(19)	6318(19)	51(4)
H10B	430(2)	3810(14)	2545(15)	28(3)
H10A	1980(2)	3756(14)	1312(14)	28(3)
H12	3940(3)	6176(16)	-34(16)	41(4)
H13	2910(3)	8581(18)	-1443(18)	50(4)
H14	-690(3)	9667(17)	-1191(18)	46(4)
H15	-3230(3)	8310(19)	448(18)	51(4)
H16	-2150(2)	5853(16)	1912(16)	37(4)

Experimental

Single crystals of $C_{14}H_{15}NO_3$ **[09srv331]** were recrystallised from **[solvents]** mounted in inert oil and transferred to the cold gas stream of the diffractometer.

Crystal structure determination of [09srv331]

Crystal Data. $C_{14}H_{15}NO_3$, M =245.27, Triclinic, a = 6.0126(3) Å, b = 10.4102(5) Å, c = 10.6716(5) Å, α = 65.453(6)°, β = 88.454(6)°, γ = 84.712(7)°, U = 604.96(5) Å^3, T = 120.0, space group P-1 (no. 2), Z = 2, μ(Mo-Kα) = 0.095, 11016 reflections measured, 3525 unique (R_{int} = 0.0483) which were used in all calculations. The final $wR(F_2)$ was 0.1154 (all data).

This report has been created with Olex2, compiled on Sep 30 2009 11:08:49. Please let us know if there are any errors or if you would like to have additional featrues.

1-((9*s*,10*s*)-9,10-Dimethyl-9,10-dihydro-9,10-(epoxyimino)anthracen-11-yl)-2-phenylethanone **152**

10srv180

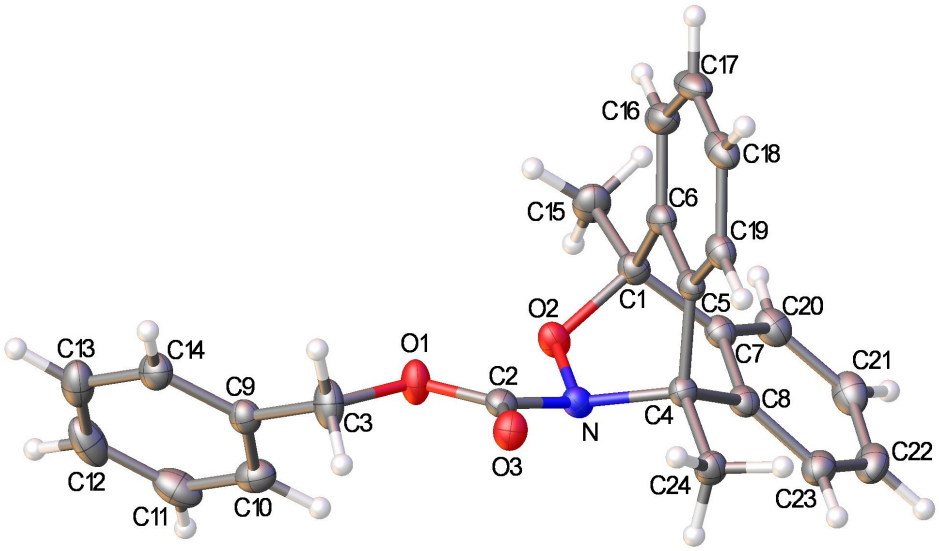

Table 1: Crystal data and structure refinement for 10srv180

Identification code	10srv180
Empirical formula	$C_{24}H_{21}NO_3$
Formula weight	371.42
Temperature / K	120
Crystal system	monoclinic
Space group	$P2_1/c$
a / Å, b / Å, c / Å	8.3176(3), 16.6568(4), 13.6584(4)
α/°, β/°, γ/°	90.00, 90.566(7), 90.00
Volume / Å^3	1892.21(10)
Z	4
ρ_{calc} / mg mm^{-3}	1.304
μ / mm^{-1}	0.086
F(000)	784
Crystal size / mm^3	0.6 × 0.08 × 0.07
2Θ range for data collection	4.9 to 55°
Index ranges	-10 ≤ h ≤ 10, -21 ≤ k ≤ 21, -17 ≤ l ≤ 17
Reflections collected	21447
Independent reflections	4332[R(int) = 0.0309]
Data/restraints/parameters	4332/0/337
Goodness-of-fit on F^2	1.024
Final R indexes [I>2σ (I)]	R_1 = 0.0390, wR_2 = 0.0968
Final R indexes [all data]	R_1 = 0.0503, wR_2 = 0.1061
Largest diff. peak/hole / e Å^{-3}	0.306/-0.192

Table 2 Fractional Atomic Coordinates (×10⁴) and Equivalent Isotropic Displacement Parameters (Å²×10³) for 10srv180. U_{eq} is defined as 1/3 of of the trace of the orthogonalised U_{IJ} tensor.

Atom	*x*	*y*	*z*	U(eq)
O1	2546.9(12)	5651.1(5)	1919.8(7)	28.0(2)
O2	3689.7(10)	4331.4(5)	1528.8(6)	22.5(2)
O3	2523.4(11)	5447.7(5)	3551.8(6)	25.3(2)
N	3002.6(12)	4405.2(6)	2489.2(7)	19.2(2)
C1	5154.4(15)	3822.5(7)	1539.9(9)	21.7(3)
C2	2736.0(14)	5207.1(7)	2726.7(9)	20.0(2)
C3	1882(2)	6448.2(8)	2075.1(10)	30.9(3)
C4	3766.2(14)	3839.2(7)	3225.2(8)	18.7(2)
C5	5517.3(14)	4103.7(7)	3278.9(9)	19.2(2)
C6	6246.4(14)	4115.3(7)	2355.9(9)	20.7(2)
C7	4554.0(15)	2999.6(7)	1831.9(9)	20.9(2)
C8	3740.2(14)	3017.4(7)	2724.1(9)	20.2(2)
C9	1123.7(15)	6704.5(8)	1122.9(9)	22.5(3)
C10	101.5(16)	6187.5(9)	607.9(10)	28.3(3)
C11	-605.3(18)	6435.7(10)	-265.2(11)	35.9(3)
C12	-300.1(19)	7194.4(10)	-632.2(11)	37.9(4)
C13	703.1(19)	7708.6(9)	-125.1(11)	33.7(3)
C14	1412.6(16)	7465.4(8)	753.8(10)	26.0(3)
C15	5798.1(18)	3897.5(9)	516(1)	28.9(3)
C16	7837.3(16)	4356.2(8)	2267.7(11)	26.7(3)
C17	8689.6(16)	4582.6(8)	3107.8(11)	29.7(3)
C18	7971.6(16)	4572.2(8)	4013.3(11)	27.6(3)
C19	6367.3(15)	4337.1(7)	4108.7(10)	22.5(3)
C20	4719.2(16)	2285.7(8)	1320.7(10)	26.3(3)
C21	4054.2(17)	1587.3(8)	1704.2(11)	30.1(3)
C22	3219.7(17)	1608.5(8)	2574.7(11)	30.1(3)
C23	3052.1(16)	2326.1(8)	3094.7(10)	25.8(3)
C24	2867.2(16)	3832.7(8)	4183.9(9)	23.2(3)

Table 3 Anisotropic Displacement Parameters (Å²×10³) for 10srv180. The Anisotropic displacement factor exponent takes the form: $-2\pi^2[h^2a^{*2}U_{11}+...+2hka\times b\times U_{12}]$

Atom	U_{11}	U_{22}	U_{33}	U_{23}	U_{13}	U_{12}
O1	39.9(5)	21.5(5)	22.4(5)	2.1(4)	0.5(4)	9.0(4)
O2	24.7(4)	25.9(5)	16.9(4)	0.2(3)	1.1(3)	5.9(4)
O3	32.0(5)	22.6(4)	21.1(5)	-1.6(4)	-1.0(4)	1.1(4)
N	19.2(5)	22.0(5)	16.3(5)	-0.7(4)	0.4(4)	2.4(4)
C1	21.3(6)	22.2(6)	21.5(6)	-1.3(5)	1.6(5)	2.6(5)
C2	16.3(5)	22.1(6)	21.6(6)	0.1(5)	-2.1(4)	-0.6(4)
C3	46.8(9)	20.3(6)	25.6(7)	-1.4(5)	-5.9(6)	8.7(6)
C4	19.0(6)	18.8(6)	18.2(6)	0.6(4)	-1.1(4)	1.0(4)
C5	18.0(6)	15.4(5)	24.4(6)	-0.2(4)	-1.3(4)	2.0(4)

C6	20.0(6)	17.1(5)	24.8(6)	-0.6(5)	0.7(5)	1.9(4)
C7	20.1(6)	20.7(6)	21.8(6)	-1.9(5)	-3.5(5)	1.2(5)
C8	18.5(6)	20.3(6)	21.8(6)	-1.0(5)	-4.1(4)	-0.2(4)
C9	24.0(6)	22.1(6)	21.4(6)	-1.1(5)	0.9(5)	3.6(5)
C10	26.0(7)	27.2(7)	31.9(7)	-4.4(6)	4.1(5)	-2.8(5)
C11	24.8(7)	46.6(9)	36.1(8)	-14.5(7)	-5.4(6)	3.3(6)
C12	40.2(8)	47.8(9)	25.5(7)	-3.3(6)	-7.3(6)	19.6(7)
C13	43.7(8)	29.0(7)	28.6(7)	3.9(6)	2.8(6)	11.4(6)
C14	28.5(7)	21.6(6)	28.0(7)	-1.6(5)	0.6(5)	2.5(5)
C15	33.3(7)	31.1(7)	22.3(6)	-0.5(5)	6.8(5)	3.4(6)
C16	21.7(6)	22.1(6)	36.5(8)	0.7(5)	4.7(5)	1.1(5)
C17	16.8(6)	24.2(6)	48.2(9)	-2.1(6)	-1.2(6)	-1.2(5)
C18	23.4(6)	20.8(6)	38.4(8)	-5.6(5)	-8.8(6)	1.9(5)
C19	23.4(6)	18.1(6)	25.9(6)	-2.4(5)	-3.8(5)	3.3(5)
C20	26.5(6)	27.1(7)	25.1(7)	-5.2(5)	-4.5(5)	3.0(5)
C21	34.3(7)	21.3(6)	34.3(7)	-6.5(6)	-8.4(6)	2.2(5)
C22	32.9(7)	20.7(6)	36.5(8)	1.2(6)	-6.2(6)	-4.2(5)
C23	25.9(6)	23.5(6)	27.9(7)	1.2(5)	-2.6(5)	-2.9(5)
C24	25.2(6)	23.6(6)	20.7(6)	1.7(5)	2.4(5)	1.2(5)

Table 4 Bond Lengths for 10srv180.

Atom	Atom	Length/Å	Atom	Atom	Length/Å
O1	C2	1.3352(15)	C6	C16	1.3892(17)
O1	C3	1.4548(16)	C7	C8	1.4001(17)
O2	N	1.4413(13)	C7	C20	1.3865(17)
O2	C1	1.4841(14)	C8	C23	1.3839(18)
O3	C2	1.2106(15)	C9	C10	1.3955(18)
N	C2	1.3928(15)	C9	C14	1.3860(18)
N	C4	1.5133(15)	C10	C11	1.387(2)
C1	C6	1.5117(17)	C11	C12	1.384(2)
C1	C7	1.5136(17)	C12	C13	1.378(2)
C1	C15	1.5075(18)	C13	C14	1.393(2)
C3	C9	1.5016(18)	C16	C17	1.395(2)
C4	C5	1.5227(16)	C17	C18	1.379(2)
C4	C8	1.5306(17)	C18	C19	1.3980(19)
C4	C24	1.5144(17)	C20	C21	1.393(2)
C5	C6	1.4044(17)	C21	C22	1.383(2)
C5	C19	1.3855(17)	C22	C23	1.3980(19)

Table 5 Bond Angles for 10srv180.

Atom	Atom	Atom	Angle/°	Atom	Atom	Atom	Angle/°
C2	O1	C3	115.28(10)	C16	C6	C1	126.52(12)
N	O2	C1	111.85(8)	C16	C6	C5	120.13(12)
O2	N	C4	112.57(8)	C8	C7	C1	111.95(10)
C2	N	O2	111.06(9)	C20	C7	C1	127.54(12)
C2	N	C4	120.62(10)	C20	C7	C8	120.50(12)
O2	C1	C6	108.09(9)	C7	C8	C4	113.78(10)

O2	C1	C7	104.30(9)	C23	C8	C4	125.79(11)
O2	C1	C15	104.02(10)	C23	C8	C7	120.39(12)
C6	C1	C7	107.17(10)	C10	C9	C3	120.64(12)
C15	C1	C6	116.16(11)	C14	C9	C3	120.14(12)
C15	C1	C7	116.14(11)	C14	C9	C10	119.21(12)
O1	C2	N	110.89(10)	C11	C10	C9	120.01(13)
O3	C2	O1	124.61(11)	C12	C11	C10	120.39(14)
O3	C2	N	124.01(11)	C13	C12	C11	119.85(14)
O1	C3	C9	106.87(10)	C12	C13	C14	120.13(14)
N	C4	C5	104.29(9)	C9	C14	C13	120.40(13)
N	C4	C8	104.84(9)	C6	C16	C17	118.92(13)
N	C4	C24	111.80(10)	C18	C17	C16	120.89(12)
C5	C4	C8	106.83(9)	C17	C18	C19	120.62(12)
C24	C4	C5	116.14(10)	C5	C19	C18	118.83(12)
C24	C4	C8	112.04(10)	C7	C20	C21	119.04(13)
C6	C5	C4	112.46(10)	C22	C21	C20	120.44(12)
C19	C5	C4	126.92(11)	C21	C22	C23	120.79(13)
C19	C5	C6	120.59(11)	C8	C23	C22	118.81(13)
C5	C6	C1	113.31(10)				

Table 6 Hydrogen Atom Coordinates (Å×10⁴) and Isotropic Displacement Parameters (Å²×10³) for 10srv180.

Atom	*x*	*y*	*z*	U(eq)
H3A	1090.0(2)	6428(11)	2638(13)	43(5)
H3B	2760.0(2)	6809(10)	2276(12)	37(4)
H10	-100.0(2)	5642(10)	870(12)	37(4)
H11	-1290.0(2)	6077(11)	-614(13)	45(5)
H12	-780.0(2)	7367(11)	-1234(13)	45(5)
H13	950.0(2)	8241(12)	-390(13)	50(5)
H14	2110.0(2)	7833(10)	1121(12)	33(4)
H15A	4970.0(2)	3712(10)	33(12)	35(4)
H15B	6730.0(2)	3548(10)	447(12)	38(4)
H15C	6090.0(2)	4467(10)	382(12)	37(4)
H16	8332(18)	4358(9)	1627(11)	26(4)
H17	9800.0(2)	4749(10)	3057(11)	35(4)
H18	8574(19)	4725(9)	4599(11)	29(4)
H19	5839(19)	4328(9)	4766(12)	29(4)
H20	5331(19)	2276(9)	713(12)	30(4)
H21	4170.0(2)	1079(10)	1364(12)	34(4)
H22	2750.0(2)	1127(10)	2824(12)	33(4)
H23	2476(19)	2321(9)	3716(12)	31(4)
H24A	1690.0(2)	3729(10)	4061(11)	30(4)
H24B	3267(18)	3386(9)	4590(11)	26(4)
H24C	2989(19)	4348(10)	4548(12)	31(4)

Experimental

Single crystals of $C_{24}H_{21}NO_3$ **[10srv180]** were recrystallised from

[solvents] mounted in inert oil and transferred to the cold gas stream of the diffractometer.

Crystal structure determination of [10srv180]

Crystal Data. $C_{24}H_{21}NO_3$, M =371.42, monoclinic, a = 8.3176(3) Å, b = 16.6568(4) Å, c = 13.6584(4) Å, β = 90.566(7)°, U = 1892.21(10) Å^3, T = 120, space group $P2_1/c$ (no. 14), Z = 4, μ(MoKα) = 0.086, 21447 reflections measured, 4332 unique (R_{int} = 0.0309) which were used in all calculations. The final $wR(F_2)$ was 0.1061 (all data).

This report has been created with Olex2, compiled on 2011.02.15 svn.r1672.
Please let us know if there are any errors or if you would like to have additional featrues.

1-Hydroxy-3-phenylurea **171**

12srv074

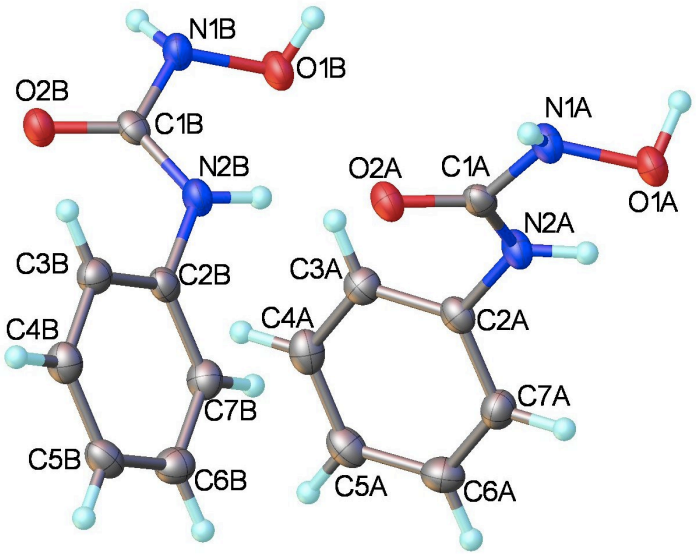

Table 1 Crystal data and structure refinement for 12srv074

Identification code	12srv074
Empirical formula	$C_7H_8N_2O_2$
Formula weight	152.15
Temperature/K	120
Crystal system	triclinic
Space group	P-1
a/Å	5.3049(4)
b/Å	5.9648(5)
c/Å	24.0989(18)
α/°	94.598(18)
β/°	90.430(18)
γ/°	110.027(16)
Volume/Å^3	713.64(10)
Z	4
ρ_{calc}mg/mm^3	1.416
m/mm^{-1}	0.106
F(000)	320.0
Crystal size/mm^3	0.26 × 0.12 × 0.06
2Θ range for data collection	1.7 to 49.98°
Index ranges	-6 ≤ h ≤ 6, -7 ≤ k ≤ 7, -28 ≤ l ≤ 28
Reflections collected	8767
Independent reflections	2514[R(int) = 0.0620]
Data/restraints/parameters	2514/0/223
Goodness-of-fit on F^2	0.995
Final R indexes [I>=2σ (I)]	R_1 = 0.0383, wR_2 = 0.0897
Final R indexes [all data]	R_1 = 0.0546, wR_2 = 0.0962
Largest diff. peak/hole / e Å^{-3}	0.18/-0.21

Table 2 Fractional Atomic Coordinates (×10⁴) and Equivalent Isotropic Displacement Parameters (Å²×10³) for 12srv074. U_{eq} is defined as 1/3 of of the trace of the orthogonalised U_{IJ} tensor.

Atom	*x*	*y*	*z*	U(eq)
O1A	12948(2)	6160(2)	4741.0(5)	27.5(3)
O2A	7984(2)	8484(2)	4401.6(5)	25.6(3)
N1A	11773(3)	7936(3)	4681.2(7)	25.0(4)
N2A	8926(3)	5227(3)	4020.5(6)	24.1(4)
C1A	9443(3)	7220(3)	4370.7(7)	21.8(4)
C2A	6537(3)	4192(3)	3680.2(7)	22.4(4)
C3A	5578(3)	5568(3)	3357.7(7)	25.2(4)
C4A	3249(3)	4497(3)	3031.2(7)	27.7(4)
C5A	1881(3)	2053(3)	3023.3(8)	28.9(4)
C6A	2876(3)	683(3)	3338.9(8)	30.2(5)
C7A	5195(3)	1744(3)	3669.3(7)	27.5(4)
O1B	8044(2)	6363(2)	256.2(5)	26.7(3)
O2B	3195(2)	8926(2)	598.7(5)	24.6(3)
N1B	6888(3)	8171(3)	318.0(7)	23.6(4)
N2B	4298(3)	5985(3)	981.8(6)	23.3(4)
C1B	4678(3)	7702(3)	627.8(7)	20.7(4)
C2B	2031(3)	5183(3)	1320.5(7)	21.7(4)
C3B	1195(3)	6788(3)	1651.0(7)	24.8(4)
C4B	-1020(3)	5933(3)	1974.2(7)	26.5(4)
C5B	-2401(3)	3484(3)	1974.9(8)	28.1(4)
C6B	-1525(3)	1916(3)	1646.1(8)	28.5(4)
C7B	672(3)	2745(3)	1318.8(7)	26.0(4)

Table 3 Anisotropic Displacement Parameters (Å²×10³) for 12srv074. The Anisotropic displacement factor exponent takes the form: -2π²[h²a*²U_{11}+...+2hka×b×U_{12}]

Atom	U_{11}	U_{22}	U_{33}	U_{23}	U_{13}	U_{12}
O1A	20.1(7)	32.1(7)	33.7(8)	3.3(6)	0.4(6)	13.3(6)
O2A	20.4(6)	30.6(7)	28.0(7)	-1.1(5)	-0.5(5)	12.4(5)
N1A	21.4(8)	28.5(9)	27.6(9)	-1.8(7)	-0.6(7)	12.7(7)
N2A	20.6(8)	27.5(8)	26.6(8)	-2.4(7)	-1.8(6)	12.7(7)
C1A	18.1(9)	26.9(10)	20.8(9)	5.9(8)	4.1(7)	7.3(7)
C2A	19.5(9)	28.3(10)	20.0(9)	-1.0(7)	1.6(7)	9.6(7)
C3A	25.7(9)	26.2(10)	23.8(10)	0.3(8)	1.3(8)	9.4(8)
C4A	30.3(10)	36.6(11)	20.6(9)	1.3(8)	0.5(8)	17.7(9)
C5A	22.9(9)	37.2(11)	25.3(10)	-2.9(9)	-1.7(8)	10.0(8)
C6A	26.5(10)	28.6(10)	31.2(11)	1.4(8)	1.5(8)	4.1(8)
C7A	29.4(10)	27.7(10)	27.7(10)	5.5(8)	0.6(8)	12.3(8)
O1B	19.9(7)	29.1(7)	34.3(8)	0.8(6)	0.8(6)	12.8(6)
O2B	20.5(6)	30.1(7)	26.5(7)	5.2(5)	1.9(5)	12.6(5)
N1B	21.4(8)	27.3(8)	26.3(9)	6.1(7)	1.8(7)	12.7(6)
N2B	20.2(8)	27.8(8)	25.6(8)	3.8(7)	2.0(6)	12.7(7)
C1B	16.0(8)	23.8(9)	20.7(9)	-2.2(8)	-3.5(7)	5.9(7)

C2B	17.9(9)	27.4(10)	21.1(9)	4.3(8)	-0.9(7)	9.1(7)
C3B	25.1(10)	24.9(10)	24.7(9)	3.0(8)	-1.0(8)	8.8(8)
C4B	28.1(10)	31.7(10)	22.8(10)	1.1(8)	2.4(8)	14.4(8)
C5B	21.8(9)	38.1(11)	24.6(10)	5.4(8)	2.2(8)	9.7(8)
C6B	28.2(10)	26.3(10)	28.1(10)	2.3(8)	-1.7(8)	6.0(8)
C7B	27.6(10)	26.9(10)	24.8(10)	-1.1(8)	-0.3(8)	12.0(8)

Table 4 Bond Lengths for 12srv074.

Atom	Atom	Length/Å	Atom	Atom	Length/Å
O1A	N1A	1.4166(17)	O1B	N1B	1.4106(18)
O2A	C1A	1.2506(19)	O2B	C1B	1.2478(18)
N1A	C1A	1.358(2)	N1B	C1B	1.354(2)
N2A	C1A	1.347(2)	N2B	C1B	1.349(2)
N2A	C2A	1.424(2)	N2B	C2B	1.423(2)
C2A	C3A	1.385(2)	C2B	C3B	1.386(2)
C2A	C7A	1.386(2)	C2B	C7B	1.384(2)
C3A	C4A	1.385(2)	C3B	C4B	1.384(2)
C4A	C5A	1.387(3)	C4B	C5B	1.392(3)
C5A	C6A	1.383(3)	C5B	C6B	1.380(2)
C6A	C7A	1.385(3)	C6B	C7B	1.381(2)

Table 5 Bond Angles for 12srv074.

Atom	Atom	Atom	Angle/°	Atom	Atom	Atom	Angle/°
C1A	N1A	O1A	115.79(14)	C1B	N1B	O1B	116.34(14)
C1A	N2A	C2A	123.94(14)	C1B	N2B	C2B	124.36(14)
O2A	C1A	N1A	119.24(15)	O2B	C1B	N1B	119.92(16)
O2A	C1A	N2A	123.82(15)	O2B	C1B	N2B	123.35(15)
N2A	C1A	N1A	116.84(15)	N2B	C1B	N1B	116.61(15)
C3A	C2A	N2A	121.46(16)	C3B	C2B	N2B	121.28(15)
C3A	C2A	C7A	120.13(16)	C7B	C2B	N2B	118.60(15)
C7A	C2A	N2A	118.41(16)	C7B	C2B	C3B	120.12(16)
C4A	C3A	C2A	119.80(17)	C4B	C3B	C2B	119.45(16)
C3A	C4A	C5A	120.35(17)	C3B	C4B	C5B	120.83(16)
C6A	C5A	C4A	119.53(17)	C6B	C5B	C4B	118.81(17)
C5A	C6A	C7A	120.45(17)	C5B	C6B	C7B	120.97(17)
C6A	C7A	C2A	119.73(17)	C6B	C7B	C2B	119.82(16)

Table 6 Hydrogen Bonds for 12srv074.

D	H	A	d(D-H)/Å	d(H-A)/Å	d(D-A)/Å	D-H-A/°
O1A	H1A	O2A[1]	0.95(2)	1.77(2)	2.7214(17)	174.4(18)
N1A	H1	O2A[2]	0.90(2)	2.03(2)	2.918(2)	166.8(18)
O1B	H1B	O2B[1]	0.89(2)	1.83(2)	2.7178(17)	175(2)
N1B	H2	O2B[3]	0.855(19)	2.07(2)	2.923(2)	172.4(16)

[1]1+X,+Y,+Z; [2]2-X,2-Y,1-Z; [3]1-X,2-Y,-Z

Table 7 Hydrogen Atom Coordinates (Å×10⁴) and Isotropic Displacement Parameters (Å²×10³) for 12srv074.

Atom	*x*	*y*	*z*	U(eq)
H1A	14700(40)	6880(40)	4608(9)	45(6)
H1	11760(40)	8840(40)	4998(9)	39(6)
H2A	9950(30)	4310(30)	4083(7)	21(5)
H3A	6514	7241	3361	30
H4A	2586	5441	2811	33
H5A	271	1324	2803	35
H6A	1964	-997	3329	36
H7A	5863	798	3888	33
H1B	9730(40)	7140(40)	383(10)	55(7)
H2	6840(30)	8900(30)	29(8)	19(5)
H2B	5270(40)	5070(30)	931(8)	30(5)
H3B	2136	8462	1655	30
H4B	-1605	7031	2199	32
H5B	-3920	2904	2198	34
H6B	-2447	241	1645	34
H7B	1248	1646	1093	31

Experimental

Single crystals of $C_7H_8N_2O_2$ **[12srv074]** were **[]**. A suitable crystal was selected and **[]** on a **Bruker SMART CCD 6000** diffractometer. The crystal was kept at 120 K during data collection. Using Olex2 [1], the structure was solved with the XS [2] structure solution program using Direct Methods and refined with the XL [3] refinement package using Least Squares minimisation.

1. O. V. Dolomanov, L. J. Bourhis, R. J. Gildea, J. A. K. Howard and H. Puschmann, OLEX2: a complete structure solution, refinement and analysis program. J. Appl. Cryst. (2009). 42, 339-341.
2. XS, G.M. Sheldrick, Acta Cryst. (2008). A64, 112-122
3. XL, G.M. Sheldrick, Acta Cryst. (2008). A64, 112-122

Crystal structure determination of [12srv074]

Crystal Data. $C_7H_8N_2O_2$, M =152.15, triclinic, a = 5.3049(4) Å, b = 5.9648(5) Å, c = 24.0989(18) Å, α = 94.598(18)°, β = 90.430(18)°, γ = 110.027(16)°, V = 713.64(10) Å^3, T = 120, space group P-1 (no. 2), Z = 4, μ(MoKα) = 0.106, 8767 reflections measured, 2514 unique (R_{int} = 0.0620) which were used in all calculations. The final wR_2 was 0.0962 (all data) and R_1 was 0.0383 (>2sigma(I)).

This report has been created with Olex2, compiled on 2011.11.01 svn.r2039. Please let us know if there are any errors or if you would like to have additional featrues.

(*S*)-1-Hydroxy-3-(1-phenylethyl)urea **172**

13srv109

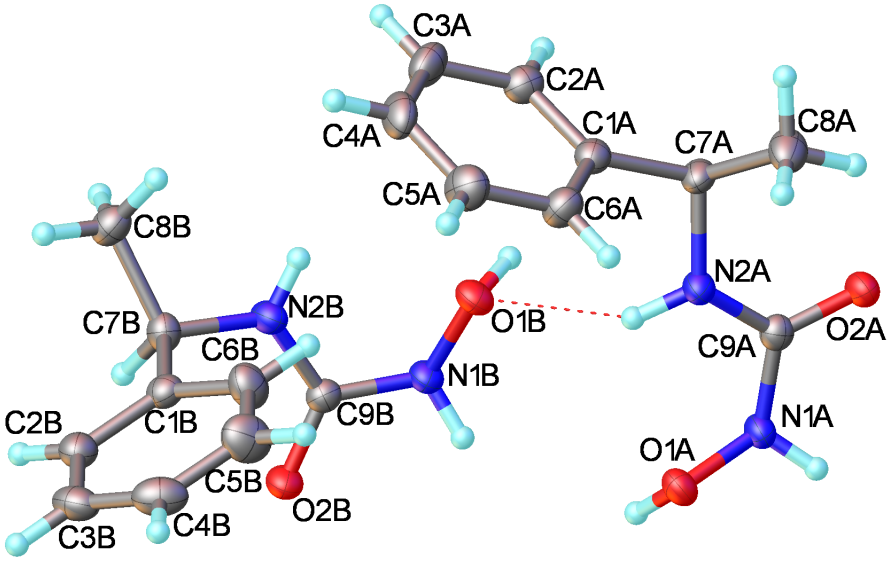

Table 1 Crystal data and structure refinement for 13srv109

Identification code	13srv109
Empirical formula	$C_9H_{12}N_2O_2$
Formula weight	180.21
Temperature/K	120
Crystal system	orthorhombic
Space group	$P2_12_12_1$
a/Å	7.2202(3)
b/Å	10.5445(5)
c/Å	25.0280(13)
α/°	90
β/°	90
γ/°	90
Volume/Å^3	1905.47(16)
Z	8
ρ_{calc}mg/mm^3	1.256
m/mm^{-1}	0.090
F(000)	768.0
Crystal size/mm^3	0.53 × 0.3 × 0.2
2Θ range for data collection	3.254 to 60.002°
Index ranges	-10 ≤ h ≤ 10, -14 ≤ k ≤ 14, -35 ≤ l ≤ 35
Reflections collected	20707
Independent reflections	5554[R(int) = 0.0363]
Data/restraints/parameters	5554/0/263
Goodness-of-fit on F^2	1.053
Final R indexes [I>=2σ (I)]	R_1 = 0.0397, wR_2 = 0.0971
Final R indexes [all data]	R_1 = 0.0506, wR_2 = 0.1035
Largest diff. peak/hole / e Å^{-3}	0.24/-0.21
Flack parameter	-1.0(5)

Table 2 Fractional Atomic Coordinates (×10⁴) and Equivalent Isotropic Displacement Parameters (Å²×10³) for 13srv109. U_{eq} is defined as 1/3 of of the trace of the orthogonalised U_{IJ} tensor.

Atom	*x*	*y*	*z*	U(eq)
O1A	10788(2)	5504.4(13)	2960.2(6)	25.4(3)
O2A	10402.7(19)	8731.9(12)	2704.3(5)	25.3(3)
N1A	10867(2)	6625.8(15)	2650.9(6)	23.1(3)
N2A	8693(2)	7413.1(15)	3240.1(6)	22.7(3)
C1A	6090(3)	7706.9(18)	3823.8(7)	22.9(4)
C2A	4204(3)	7693.9(19)	3713.6(7)	26.9(4)
C3A	2977(3)	7085(2)	4052.3(9)	33.6(5)
C4A	3612(3)	6486(2)	4507.6(9)	35.2(5)
C5A	5497(3)	6476(2)	4618.7(8)	36.0(5)
C6A	6722(3)	7086(2)	4279.7(8)	30.0(4)
C7A	7434(3)	8386.4(18)	3457.3(7)	23.4(4)
C8A	8477(3)	9442(2)	3745.2(9)	34.7(5)
C9A	9987(3)	7649.0(17)	2869.1(7)	20.8(3)
O1B	5708(2)	5324.3(12)	2948.5(6)	25.7(3)
O2B	5487.9(19)	2064.9(12)	2755.1(5)	26.2(3)
N1B	5887(2)	4179.1(14)	2659.2(6)	22.9(3)
N2B	3504(2)	3406.2(16)	3184.9(6)	24.4(3)
C1B	3719(3)	2002.9(18)	3972.5(7)	23.5(4)
C2B	3515(3)	783.4(19)	4172.1(8)	26.4(4)
C3B	4508(3)	386(2)	4616.7(8)	31.7(4)
C4B	5702(3)	1221(2)	4869.1(8)	36.8(5)
C5B	5910(4)	2435(2)	4676.3(9)	40.3(5)
C6B	4923(3)	2827(2)	4230.8(8)	32.9(4)
C7B	2575(3)	2413.4(18)	3490.9(7)	22.8(3)
C8B	661(3)	2889(2)	3661.9(8)	28.7(4)
C9B	4972(3)	3160.6(17)	2876.1(7)	21.0(3)

Table 3 Anisotropic Displacement Parameters (Å²×10³) for 13srv109. The Anisotropic displacement factor exponent takes the form: -2π²[h²a*²U_{11}+...+2hka×b×U_{12}]

Atom	U_{11}	U_{22}	U_{33}	U_{23}	U_{13}	U_{12}
O1A	29.2(7)	17.7(6)	29.3(7)	0.7(5)	0.4(6)	-0.4(6)
O2A	26.2(7)	20.7(6)	29.1(7)	3.2(5)	3.7(5)	0.7(6)
N1A	24.0(7)	18.9(7)	26.6(7)	0.3(6)	4.6(6)	-1.0(6)
N2A	22.3(7)	19.2(7)	26.5(7)	-1.3(6)	4.1(6)	-1.3(6)
C1A	22.0(8)	23.2(9)	23.5(7)	-3.3(7)	3.3(6)	0.0(7)
C2A	25.0(9)	30.1(10)	25.6(8)	-3.2(7)	-0.4(7)	-0.1(8)
C3A	22.0(9)	39.6(12)	39.3(11)	-7.4(9)	3.0(8)	-6.9(9)
C4A	36.1(11)	33.3(11)	36.3(10)	-0.6(9)	14.4(9)	-7.5(9)
C5A	38.2(12)	40.5(12)	29.4(10)	8.0(9)	4.3(9)	0.9(10)
C6A	25.0(9)	36.4(11)	28.5(9)	3.4(8)	0.4(7)	1.4(8)
C7A	20.5(8)	23.8(9)	26.0(8)	-2.3(7)	3.9(7)	0.4(7)
C8A	35.5(11)	29(1)	39.5(11)	-11.5(9)	9.9(9)	-7.8(9)

C9A	20.8(8)	21.8(8)	19.8(7)	-0.7(6)	-0.8(6)	-0.4(7)
O1B	29.1(7)	18.8(6)	29.3(7)	-2.3(5)	0.6(6)	1.3(6)
O2B	27.1(7)	20.8(6)	30.8(7)	-3.2(5)	5.5(5)	0.7(5)
N1B	24.1(8)	19.2(7)	25.5(7)	-2.6(6)	3.3(6)	-0.2(6)
N2B	25.7(8)	21.2(8)	26.3(7)	2.1(6)	6.1(6)	3.0(6)
C1B	21.4(8)	26.3(9)	22.7(8)	-0.7(7)	2.2(6)	1.5(7)
C2B	25.4(9)	24.7(9)	29.0(9)	-1.0(7)	1.5(7)	1.6(8)
C3B	36.9(11)	29.6(10)	28.5(9)	3.0(8)	4.3(8)	9.9(9)
C4B	40.4(12)	44.3(12)	25.5(9)	-4.2(8)	-4.8(9)	14.1(11)
C5B	43.5(13)	40.0(12)	37.2(11)	-8.5(9)	-12.8(9)	-1.0(11)
C6B	37.5(11)	28.1(10)	33(1)	-1.7(8)	-4.9(9)	-4.5(9)
C7B	23.9(8)	23.3(9)	21.3(7)	1.0(7)	1.1(6)	-2.5(7)
C8B	23.5(9)	36.6(11)	26.1(8)	3.2(8)	2.1(7)	1.4(9)
C9B	20.3(8)	23.3(8)	19.5(8)	0.1(6)	-0.4(6)	1.1(7)

Table 4 Bond Lengths for 13srv109.

Atom	Atom	Length/Å	Atom	Atom	Length/Å
O1A	N1A	1.414(2)	O1B	N1B	1.4140(19)
O2A	C9A	1.251(2)	O2B	C9B	1.251(2)
N1A	C9A	1.366(2)	N1B	C9B	1.373(2)
N2A	C7A	1.475(2)	N2B	C7B	1.460(2)
N2A	C9A	1.341(2)	N2B	C9B	1.337(2)
C1A	C2A	1.390(3)	C1B	C2B	1.387(3)
C1A	C6A	1.393(3)	C1B	C6B	1.389(3)
C1A	C7A	1.516(3)	C1B	C7B	1.524(3)
C2A	C3A	1.384(3)	C2B	C3B	1.389(3)
C3A	C4A	1.381(3)	C3B	C4B	1.385(3)
C4A	C5A	1.389(3)	C4B	C5B	1.377(3)
C5A	C6A	1.384(3)	C5B	C6B	1.386(3)
C7A	C8A	1.525(3)	C7B	C8B	1.531(3)

Table 5 Bond Angles for 13srv109.

Atom	Atom	Atom	Angle/°	Atom	Atom	Atom	Angle/°
C9A	N1A	O1A	115.01(14)	C9B	N1B	O1B	114.94(14)
C9A	N2A	C7A	123.76(16)	C9B	N2B	C7B	121.91(16)
C2A	C1A	C6A	118.63(18)	C2B	C1B	C6B	118.61(18)
C2A	C1A	C7A	120.81(17)	C2B	C1B	C7B	119.38(17)
C6A	C1A	C7A	120.56(17)	C6B	C1B	C7B	121.98(17)
C3A	C2A	C1A	120.68(18)	C1B	C2B	C3B	120.91(19)
C4A	C3A	C2A	120.33(19)	C4B	C3B	C2B	119.7(2)
C3A	C4A	C5A	119.6(2)	C5B	C4B	C3B	120.0(2)
C6A	C5A	C4A	120.0(2)	C4B	C5B	C6B	120.2(2)
C5A	C6A	C1A	120.76(19)	C5B	C6B	C1B	120.7(2)
N2A	C7A	C1A	106.78(15)	N2B	C7B	C1B	111.68(15)
N2A	C7A	C8A	112.22(16)	N2B	C7B	C8B	109.04(15)
C1A	C7A	C8A	112.06(15)	C1B	C7B	C8B	111.17(14)
O2A	C9A	N1A	118.54(16)	O2B	C9B	N1B	118.93(16)

O2A	C9A	N2A	124.41(16)	O2B	C9B	N2B	123.68(17)
N2A	C9A	N1A	117.03(16)	N2B	C9B	N1B	117.29(16)

Table 6 Hydrogen Bonds for 13srv109.

D	H	A	d(D-H)/Å	d(H-A)/Å	d(D-A)/Å	D-H-A/°
O1A	H01A	O2A[1]	0.88(3)	1.77(3)	2.6455(19)	174(3)
N1A	H1NA	O2B[2]	0.88(3)	1.98(3)	2.859(2)	175(2)
N2A	H2NA	O1B	0.90(3)	2.47(3)	3.166(2)	134(2)
O1B	H01B	O2B[3]	0.89(3)	1.80(3)	2.6863(19)	173(3)
N1B	H1NB	O2A[1]	0.88(3)	1.99(3)	2.868(2)	171(2)
N2B	H2NB	O1A[4]	0.89(3)	2.30(3)	3.010(2)	136(2)

[1]2-X,-1/2+Y,1/2-Z; [2]2-X,1/2+Y,1/2-Z; [3]1-X,1/2+Y,1/2-Z; [4]-1+X,+Y,+Z

Table 7 Torsion Angles for 13srv109.

A	B	C	D	Angle/°	A	B	C	D	Angle/°
O1A	N1A	C9A	O2A	160.73(16)	O1B	N1B	C9B	O2B	-158.01(17)
O1A	N1A	C9A	N2A	-20.9(2)	O1B	N1B	C9B	N2B	25.5(2)
C1A	C2A	C3A	C4A	0.4(3)	C1B	C2B	C3B	C4B	0.8(3)
C2A	C1A	C6A	C5A	-0.5(3)	C2B	C1B	C6B	C5B	0.5(3)
C2A	C1A	C7A	N2A	-117.20(19)	C2B	C1B	C7B	N2B	-152.88(17)
C2A	C1A	C7A	C8A	119.5(2)	C2B	C1B	C7B	C8B	85.1(2)
C2A	C3A	C4A	C5A	-1.3(3)	C2B	C3B	C4B	C5B	-0.5(3)
C3A	C4A	C5A	C6A	1.4(4)	C3B	C4B	C5B	C6B	0.2(4)
C4A	C5A	C6A	C1A	-0.5(3)	C4B	C5B	C6B	C1B	-0.2(4)
C6A	C1A	C2A	C3A	0.5(3)	C6B	C1B	C2B	C3B	-0.8(3)
C6A	C1A	C7A	N2A	63.0(2)	C6B	C1B	C7B	N2B	29.3(2)
C6A	C1A	C7A	C8A	-60.2(2)	C6B	C1B	C7B	C8B	-92.8(2)
C7A	N2A	C9A	O2A	7.5(3)	C7B	N2B	C9B	O2B	11.8(3)
C7A	N2A	C9A	N1A	-170.85(16)	C7B	N2B	C9B	N1B	-171.95(16)
C7A	C1A	C2A	C3A	-179.25(17)	C7B	C1B	C2B	C3B	-178.72(17)
C7A	C1A	C6A	C5A	179.30(18)	C7B	C1B	C6B	C5B	178.38(19)
C9A	N2A	C7A	C1A	174.96(16)	C9B	N2B	C7B	C1B	73.6(2)
C9A	N2A	C7A	C8A	-61.9(2)	C9B	N2B	C7B	C8B	-163.15(17)

Table 8 Hydrogen Atom Coordinates (Å×10⁴) and Isotropic Displacement Parameters (Å²×10³) for 13srv109.

Atom	*x*	*y*	*z*	U(eq)
H01A	10470(40)	4890(20)	2738(11)	38(7)
H1NA	12000(40)	6800(20)	2540(9)	29(6)
H2NA	8320(40)	6600(30)	3286(10)	38(7)
H2A	3752	8107	3402	32
H3A	1691	7079	3971	40
H4A	2764	6084	4743	42
H5A	5945	6050	4927	43
H6A	8009	7081	4359	36

H7A	6721	8768	3155	28
H81A	9171	9083	4046	43(4)
H82A	7592	10072	3879	43(4)
H83A	9339	9850	3496	43(4)
H01B	5400(40)	5890(20)	2700(11)	43(7)
H1NB	7050(40)	4010(20)	2581(10)	36(7)
H2NB	3170(40)	4210(20)	3238(10)	33(6)
H2B	2684	213	4002	32
H3B	4368	-455	4747	38
H4B	6377	955	5175	44
H5B	6733	3006	4849	48
H6B	5071	3668	4101	39
H7B	2401	1661	3253	27
H81B	793	3696	3852	37(4)
H82B	81	2263	3898	37(4)
H83B	-115	3013	3345	37(4)

Experimental

Single crystals of $C_9H_{12}N_2O_2$ **[13srv109]** were **[]**. A suitable crystal was selected and **[]** on a **Bruker SMART CCD 6000** diffractometer. The crystal was kept at 120 K during data collection. Using Olex2 [1], the structure was solved with the XS [2] structure solution program using Direct Methods and refined with the ShelXL-2012 [3] refinement package using Least Squares minimisation.

4. O. V. Dolomanov, L. J. Bourhis, R. J. Gildea, J. A. K. Howard and H. Puschmann, OLEX2: a complete structure solution, refinement and analysis program. J. Appl. Cryst. (2009). 42, 339-341.
5. XS, G.M. Sheldrick, Acta Cryst. (2008). A64, 112-122
6. SHELXL-2012, G.M. Sheldrick, Acta Cryst. (2008). A64, 112-122

Crystal structure determination of [13srv109]

Crystal Data for $C_9H_{12}N_2O_2$ (M =180.21): orthorhombic, space group $P2_12_12_1$ (no. 19), a = 7.2202(3) Å, b = 10.5445(5) Å, c = 25.0280(13) Å, V = 1905.47(16) Å^3, Z = 8, T = 120 K, μ(MoKα) = 0.090 mm^{-1}, $Dcalc$ = 1.256 g/mm^3, 20707 reflections measured (3.254 ≤ 2Θ ≤ 60.002), 5554 unique (R_{int} = 0.0363) which were used in all calculations. The final R_1 was 0.0397 (I > 2σ(I)) and wR_2 was 0.1035 (all data).

This report has been created with Olex2, compiled on Mar 21 2013 11:16:32. Please let us know if there are any errors or if you would like to have additional featrues.

2-Oxa-3-azabicyclo[2.2.2]oct-5-en-3-yl(phenyl)metha-none **177**

12srv020

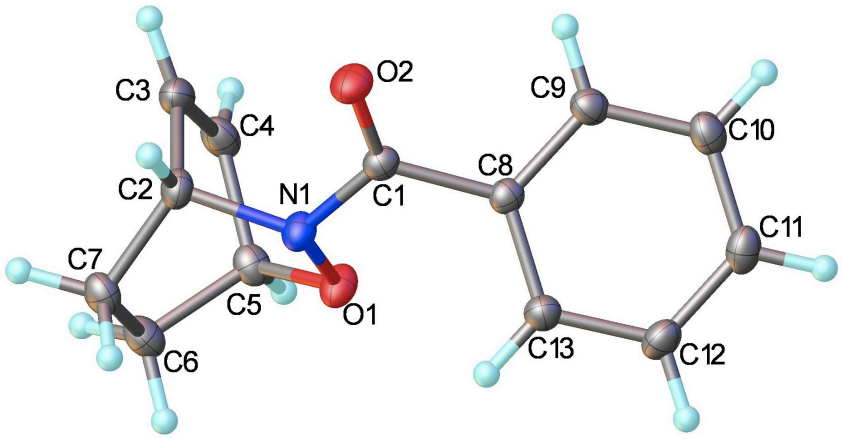

Table 1 Crystal data and structure refinement for 12srv020

Identification code	12srv020
Empirical formula	$C_{13}H_{13}NO_2$
Formula weight	215.24
Temperature/K	120
Crystal system	monoclinic
Space group	$P2_1/c$
a/Å	9.0358(9)
b/Å	10.3716(13)
c/Å	11.8962(14)
α/°	90.00
β/°	108.091(10)
γ/°	90.00
Volume/Å^3	1059.7(2)
Z	4
ρ_{calc}mg/mm^3	1.349
m/mm^{-1}	0.091
F(000)	456.0
Crystal size/mm^3	0.4 × 0.3 × 0.2
2Θ range for data collection	4.74 to 60°
Index ranges	-11 ≤ h ≤ 12, -14 ≤ k ≤ 14, -16 ≤ l ≤ 16
Reflections collected	11139
Independent reflections	3094[R(int) = 0.0274]
Data/restraints/parameters	3094/0/145
Goodness-of-fit on F^2	1.053
Final R indexes [I>=2σ (I)]	R_1 = 0.0465, wR_2 = 0.1252
Final R indexes [all data]	R_1 = 0.0534, wR_2 = 0.1317
Largest diff. peak/hole / e Å^{-3}	0.41/-0.20

Table 2 Fractional Atomic Coordinates (×10⁴) and Equivalent Isotropic Displacement Parameters (Å²×10³) for 12srv020. U_{eq} is defined as 1/3 of of the trace of the orthogonalised U_{IJ} tensor.

Atom	*x*	*y*	*z*	U(eq)
O1	4140.9(9)	2532.4(7)	1001.4(8)	22.64(19)
O2	7086.7(10)	299.5(8)	2190.2(7)	24.5(2)
N1	4833.1(11)	1269.7(8)	1151.3(8)	19.6(2)
C1	6419.7(12)	1259.9(10)	1665.2(9)	17.9(2)
C2	3871.6(13)	307.3(10)	1527.8(10)	21.0(2)
C3	3791.8(14)	751.3(12)	2716.6(10)	24.7(2)
C4	3259.1(14)	1961.1(12)	2679.8(10)	24.8(2)
C5	2801.3(13)	2536.7(11)	1464.5(10)	21.3(2)
C6	1550.5(13)	1706.3(12)	618.2(10)	24.8(2)
C7	2243.7(13)	353.0(11)	610(1)	23.4(2)
C8	7307.4(12)	2403.6(10)	1462.9(9)	17.5(2)
C9	8619.6(13)	2788.5(11)	2374.9(10)	21.4(2)
C10	9515.8(14)	3817.8(11)	2207.5(10)	24.1(2)
C11	9122.8(14)	4439.0(11)	1120.4(10)	24.7(2)
C12	7834.1(14)	4041.6(11)	200(1)	23.9(2)
C13	6912.5(13)	3032.2(11)	372.1(9)	20.7(2)

Table 3 Anisotropic Displacement Parameters (Å²×10³) for 12srv020. The Anisotropic displacement factor exponent takes the form: -2π²[h²a*²U_{11}+...+2hka×b×U_{12}]

Atom	U_{11}	U_{22}	U_{33}	U_{23}	U_{13}	U_{12}
O1	19.5(4)	17.5(4)	32.4(4)	6.3(3)	10.2(3)	3.9(3)
O2	23.3(4)	22.0(4)	27.7(4)	6.6(3)	7.2(3)	4.5(3)
N1	18.9(4)	15.1(4)	25.3(4)	2.5(3)	7.6(4)	0.8(3)
C1	19.5(5)	18.2(5)	16.9(4)	0.1(3)	7.0(4)	0.8(3)
C2	20.3(5)	17.7(5)	25.2(5)	1.1(4)	7.6(4)	-3.1(4)
C3	21.9(5)	30.6(6)	20.7(5)	2.5(4)	5.3(4)	-6.8(4)
C4	22.2(5)	32.2(6)	20.0(5)	-6.9(4)	6.3(4)	-5.6(4)
C5	17.8(5)	21.4(5)	25.0(5)	-3.3(4)	6.8(4)	0.5(4)
C6	18.8(5)	30.2(6)	23.7(5)	-4.6(4)	4.1(4)	-1.0(4)
C7	21.5(5)	23.6(5)	24.0(5)	-5.6(4)	5.8(4)	-4.1(4)
C8	17.0(5)	18.6(5)	18.2(4)	0.6(3)	7.3(4)	0.8(3)
C9	18.3(5)	26.1(5)	19.6(5)	0.2(4)	5.4(4)	-0.1(4)
C10	18.9(5)	28.4(6)	25.2(5)	-4.3(4)	7.2(4)	-4.2(4)
C11	25.3(6)	23.5(5)	30.0(6)	-2.8(4)	15.6(5)	-5.1(4)
C12	28.9(6)	23.9(5)	21.7(5)	2.5(4)	12.1(4)	-2.3(4)
C13	21.5(5)	22.6(5)	18.0(4)	0.4(4)	6.0(4)	-1.8(4)

Table 4 Bond Lengths for 12srv020.

Atom	Atom	Length/Å	Atom	Atom	Length/Å
O1	N1	1.4383(11)	C4	C5	1.4988(16)
O1	C5	1.4775(13)	C5	C6	1.5252(16)
O2	C1	1.2295(13)	C6	C7	1.5383(16)
N1	C1	1.3729(14)	C8	C9	1.3940(15)
N1	C2	1.4810(13)	C8	C13	1.3960(14)
C1	C8	1.4927(14)	C9	C10	1.3912(16)
C2	C3	1.5102(16)	C10	C11	1.3886(16)
C2	C7	1.5364(16)	C11	C12	1.3903(17)
C3	C4	1.3397(18)	C12	C13	1.3918(15)

Table 5 Bond Angles for 12srv020.

Atom	Atom	Atom	Angle/°	Atom	Atom	Atom	Angle/°
N1	O1	C5	109.37(7)	O1	C5	C6	106.09(9)
O1	N1	C2	112.20(8)	C4	C5	C6	109.74(9)
C1	N1	O1	114.56(8)	C5	C6	C7	107.44(9)
C1	N1	C2	119.33(9)	C2	C7	C6	109.00(9)
O2	C1	N1	120.77(10)	C9	C8	C1	118.15(9)
O2	C1	C8	121.50(10)	C9	C8	C13	119.99(10)
N1	C1	C8	117.48(9)	C13	C8	C1	121.73(9)
N1	C2	C3	106.31(9)	C10	C9	C8	120.04(10)
N1	C2	C7	106.64(9)	C11	C10	C9	119.83(10)
C3	C2	C7	110.03(9)	C10	C11	C12	120.36(10)
C4	C3	C2	112.09(10)	C11	C12	C13	120.01(10)
C3	C4	C5	113.16(10)	C12	C13	C8	119.74(10)
O1	C5	C4	110.23(9)				

Table 6 Hydrogen Atom Coordinates (Å×10⁴) and Isotropic Displacement Parameters (Å²×10³) for 12srv020.

Atom	*x*	*y*	*z*	U(eq)
H2	4335	-575	1580	25
H3	4085	233	3409	30
H4	3180	2409	3355	30
H5	2410	3436	1481	26
H6A	1241	2081	-187	30
H6B	618	1659	886	30
H7A	1563	-301	804	28
H7B	2316	158	-186	28
H9	8902	2348	3111	26
H10	10394	4095	2835	29
H11	9738	5139	1005	30
H12	7582	4459	-547	29
H13	6018	2772	-250	25

Experimental

Single crystals of $C_{13}H_{13}NO_2$ **[12srv020]** were **[]**. A suitable crystal was selected and **[]** on a **Bruker SMART CCD 6000** diffractometer. The crystal was kept at 120 K during data collection. Using Olex2 [1], the structure was solved with the XS [2] structure solution program using Direct Methods and refined with the XL [3] refinement package using Least Squares minimisation.

7. O. V. Dolomanov, L. J. Bourhis, R. J. Gildea, J. A. K. Howard and H. Puschmann, OLEX2: a complete structure solution, refinement and analysis program. J. Appl. Cryst. (2009). 42, 339-341.
8. SHELXS-97 (Sheldrick, 1990)
9. XL, G.M. Sheldrick, Acta Cryst. (2008). A64, 112-122

Crystal structure determination of [12srv020]

Crystal Data. $C_{13}H_{13}NO_2$, M =215.24, monoclinic, a = 9.0358(9) Å, b = 10.3716(13) Å, c = 11.8962(14) Å, β = 108.091(10)°, V = 1059.7(2) Å^3, T = 120, space group $P2_1/c$ (no. 14), Z = 4, μ(MoKα) = 0.091, 11139 reflections measured, 3094 unique (R_{int} = 0.0274) which were used in all calculations. The final wR_2 was 0.1317 (all data) and R_1 was 0.0465 (>2sigma(I)).

This report has been created with Olex2, compiled on 2011.11.01 svn.r2039. Please let us know if there are any errors or if you would like to have additional featrues.

2-Oxa-3-azabicyclo[2.2.2]oct-5-en-3-yl)-2-phenyl-ethanone **178**

12srv025

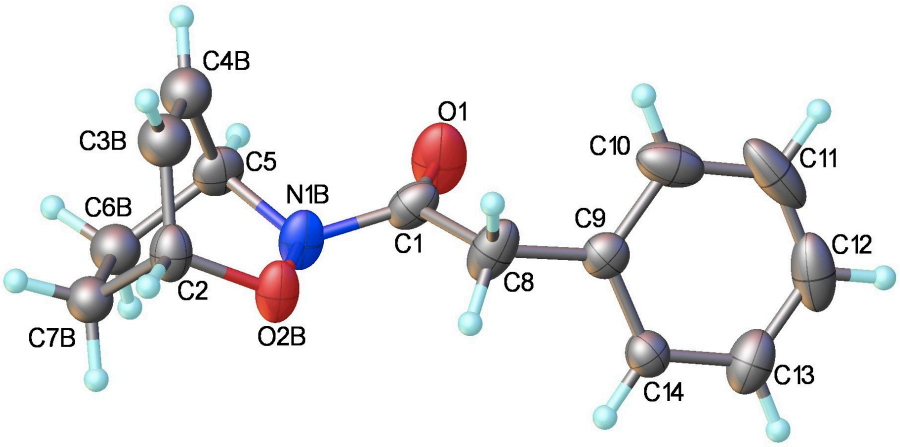

Table 1 Crystal data and structure refinement for 12srv025

Identification code	12srv025
Empirical formula	$C_{14}H_{15}NO_2$
Formula weight	229.27
Temperature/K	120
Crystal system	monoclinic
Space group	$P2_1/c$
a/Å	13.7130(10)
b/Å	5.8495(5)
c/Å	14.8249(12)
α/°	90.00
β/°	100.428(13)
γ/°	90.00
Volume/Å^3	1169.53(16)
Z	4
ρ_{calc}mg/mm^3	1.302
m/mm^{-1}	0.087
F(000)	488.0
Crystal size/mm^3	0.45 × 0.36 × 0.26
2Θ range for data collection	3.02 to 60°
Index ranges	-19 ≤ h ≤ 19, -8 ≤ k ≤ 8, -20 ≤ l ≤ 20
Reflections collected	20862
Independent reflections	3411[R(int) = 0.0390]
Data/restraints/parameters	3411/14/156
Goodness-of-fit on F^2	1.080
Final R indexes [I>=2σ (I)]	R_1 = 0.0668, wR_2 = 0.1720
Final R indexes [all data]	R_1 = 0.0806, wR_2 = 0.1847
Largest diff. peak/hole / e Å^{-3}	0.50/-0.34

Table 2 Fractional Atomic Coordinates (×10⁴) and Equivalent Isotropic Displacement Parameters (Å²×10³) for 12srv025. U_{eq} is defined as 1/3 of of the trace of the orthogonalised U_{IJ} tensor.

Atom	*x*	*y*	*z*	U(eq)
O1	8364.1(11)	4082(3)	2979(1)	60.2(5)
O2A	7538(3)	2602(5)	722(3)	41.2(8)
N1A	8145(5)	2751(6)	1608(4)	39.9(10)
O2B	7416(4)	1673(7)	803(4)	41.2(8)
N1B	8071(6)	1885(9)	1672(6)	39.9(10)
C1	7826.9(11)	3761(3)	2238.6(11)	37.5(4)
C2	8032.8(12)	1100(3)	123.2(11)	39.6(4)
C3A	8286(3)	-1116(6)	597(3)	41.3(8)
C4A	8841(3)	-1002(6)	1459(3)	43.1(8)
C3B	8818(4)	2755(9)	87(4)	49.7(15)
C4B	9408(4)	2817(8)	929(3)	44.0(11)
C5	9099.3(11)	1390(3)	1670.5(12)	39.0(4)
C6A	9691(3)	2527(7)	1028(2)	42.8(9)
C7A	9026(3)	2375(8)	98(3)	44.5(11)
C6B	9086(4)	-1090(6)	1268(3)	41.8(10)
C7B	8427(3)	-1324(6)	336(3)	36.7(8)
C8	6814.0(13)	4855(4)	1960.0(12)	47.8(5)
C9	6434.0(11)	5899(3)	2755.6(11)	33.5(3)
C10	6780.8(15)	7987(3)	3130.8(16)	50.8(5)
C11	6405(2)	8883(4)	3877.5(17)	65.1(8)
C12	5696.9(18)	7713(4)	4236.9(14)	59.6(7)
C13	5348.0(15)	5687(4)	3861.9(13)	47.9(5)
C14	5711.7(12)	4777(3)	3129.1(11)	33.9(3)

Table 3 Anisotropic Displacement Parameters (Å²×10³) for 12srv025. The Anisotropic displacement factor exponent takes the form: -2π²[h²a*²U₁₁+...+2hka×b×U₁₂]

Atom	U_{11}	U_{22}	U_{33}	U_{23}	U_{13}	U_{12}
O1	40.5(7)	89.7(12)	42.3(7)	-17.7(7)	-13.7(6)	16.3(7)
O2A	32.0(12)	60(2)	27.3(9)	-7.0(18)	-5.6(8)	16.3(18)
N1A	30.2(11)	58(3)	27.7(11)	-4(2)	-5.9(8)	14(2)
O2B	32.0(12)	60(2)	27.3(9)	-7.0(18)	-5.6(8)	16.3(18)
N1B	30.2(11)	58(3)	27.7(11)	-4(2)	-5.9(8)	14(2)
C1	24.8(7)	57.2(10)	29.0(7)	3.7(7)	0.9(5)	-0.7(7)
C2	39.2(8)	47(1)	31.2(7)	-3.4(7)	2.8(6)	12.0(7)
C5	24.3(7)	47.6(10)	41.6(8)	1.7(7)	-3.4(6)	4.8(6)
C8	28.7(8)	83.3(15)	29.9(8)	-0.7(9)	1.1(6)	9.7(9)
C9	28.7(7)	38.9(8)	30.2(7)	2.2(6)	-1.7(5)	2.1(6)
C10	43.6(10)	38.7(9)	61.3(12)	9.0(9)	-13.9(8)	-7.4(8)
C11	75.1(15)	33.9(9)	68.6(14)	-18.7(9)	-34.5(12)	16.8(10)
C12	62.0(13)	69.3(15)	40.9(10)	-16.5(10)	-8.2(9)	33.1(12)
C13	43.2(9)	65.8(13)	35.1(9)	5.4(8)	8.6(7)	16.5(9)
C14	33.6(7)	32.6(7)	34.2(8)	0.1(6)	2.5(6)	3.2(6)

Table 4 Bond Lengths for 12srv025.

Atom	Atom	Length/Å	Atom	Atom	Length/Å
O1	C1	1.221(2)	C4A	C5	1.464(3)
O2A	N1A	1.425(8)	C3B	C4B	1.361(6)
O2A	C2	1.496(5)	C4B	C5	1.500(4)
N1A	C1	1.249(7)	C5	C6A	1.513(3)
N1A	C5	1.520(6)	C5	C6B	1.567(4)
O2B	N1B	1.436(10)	C6A	C7A	1.512(5)
O2B	C2	1.467(6)	C6B	C7B	1.514(5)
N1B	C1	1.458(8)	C8	C9	1.503(2)
N1B	C5	1.440(9)	C9	C10	1.390(3)
C1	C8	1.517(2)	C9	C14	1.385(2)
C2	C3A	1.485(3)	C10	C11	1.404(4)
C2	C3B	1.456(4)	C11	C12	1.372(4)
C2	C7A	1.559(3)	C12	C13	1.359(3)
C2	C7B	1.530(3)	C13	C14	1.381(2)
C3A	C4A	1.365(5)			

Table 5 Bond Angles for 12srv025.

Atom	Atom	Atom	Angle/°	Atom	Atom	Atom	Angle/°
N1A	O2A	C2	109.3(4)	C4B	C3B	C2	107.7(4)
O2A	N1A	C5	112.1(5)	C3B	C4B	C5	117.2(4)
C1	N1A	O2A	119.6(5)	N1A	C5	C6B	120.7(3)
C1	N1A	C5	128.0(5)	N1B	C5	N1A	20.3(3)
N1B	O2B	C2	106.9(5)	N1B	C5	C4A	89.6(3)
O2B	N1B	C1	114.2(5)	N1B	C5	C4B	107.2(3)
O2B	N1B	C5	115.8(6)	N1B	C5	C6A	123.3(3)
C5	N1B	C1	118.7(5)	N1B	C5	C6B	104.1(3)
O1	C1	N1A	120.6(3)	C4A	C5	N1A	108.4(3)
O1	C1	N1B	118.0(3)	C4A	C5	C4B	117.7(3)
O1	C1	C8	123.63(17)	C4A	C5	C6A	115.0(3)
N1A	C1	N1B	20.7(4)	C4A	C5	C6B	17.8(2)
N1A	C1	C8	115.0(3)	C4B	C5	N1A	91.0(3)
N1B	C1	C8	117.1(3)	C4B	C5	C6A	16.2(2)
O2A	C2	C7A	103.0(3)	C4B	C5	C6B	102.8(3)
O2A	C2	C7B	127.1(2)	C6A	C5	N1A	106.6(3)
O2B	C2	O2A	22.84(19)	C6A	C5	C6B	97.9(3)
O2B	C2	C3A	89.4(3)	C7A	C6A	C5	104.1(3)
O2B	C2	C7A	121.5(3)	C6A	C7A	C2	113.1(3)
O2B	C2	C7B	107.2(3)	C7B	C6B	C5	113.2(3)
C3A	C2	O2A	108.9(2)	C6B	C7B	C2	103.6(3)
C3A	C2	C7A	107.4(2)	C9	C8	C1	112.84(14)
C3A	C2	C7B	18.17(18)	C10	C9	C8	121.94(18)
C3B	C2	O2A	92.8(3)	C14	C9	C8	119.74(16)
C3B	C2	O2B	113.3(3)	C14	C9	C10	118.32(17)
C3B	C2	C3A	119.1(3)	C9	C10	C11	119.7(2)
C3B	C2	C7A	13.1(3)	C12	C11	C10	120.44(19)
C3B	C2	C7B	112.8(3)	C13	C12	C11	119.8(2)

C7B	C2	C7A	99.8(3)	C12	C13	C14	120.5(2)
C4A	C3A	C2	116.3(3)	C13	C14	C9	121.19(17)
C3A	C4A	C5	108.6(3)				

Table 6 Hydrogen Atom Coordinates (Å×10⁴) and Isotropic Displacement Parameters (Å²×10³) for 12srv025.

Atom	*x*	*y*	*z*	U(eq)
H2	7624	900	-502	47
H3A	8075	-2539	320	50
H4A	9034	-2258	1858	52
H3B	8901	3618	-437	60
H4B	9989	3737	1036	53
H5	9539	1575	2282	47
H6AA	10326	1710	1040	51
H6AB	9838	4137	1210	51
H7AA	9393	1562	-322	53
H7AB	8884	3943	-141	53
H6BA	9768	-1536	1209	50
H6BB	8852	-2173	1696	50
H7BA	7876	-2408	355	44
H7BB	8804	-1843	-136	44
H8A	6853	6055	1497	57
H8B	6337	3683	1671	57
H10	7270	8805	2884	61
H11	6643	10307	4136	78
H12	5451	8319	4747	71
H13	4850	4890	4106	57
H14	5462	3355	2877	41

Experimental

Single crystals of $C_{14}H_{15}NO_2$ **[12srv025]** were **[]**. A suitable crystal was selected and **[]** on a **Bruker SMART CCD 6000** diffractometer. The crystal was kept at 120 K during data collection. Using Olex2 [1], the structure was solved with the XS [2] structure solution program using Direct Methods and refined with the XL [3] refinement package using Least Squares minimisation.

10. O. V. Dolomanov, L. J. Bourhis, R. J. Gildea, J. A. K. Howard and H. Puschmann, OLEX2: a complete structure solution, refinement and analysis program. J. Appl. Cryst. (2009). 42, 339-341.
11. SHELXS-97 (Sheldrick, 1990)
12. XL, G.M. Sheldrick, Acta Cryst. (2008). A64, 112-122

Crystal structure determination of [12srv025]

Crystal Data. $C_{14}H_{15}NO_2$, M =229.27, monoclinic, a = 13.7130(10) Å, b = 5.8495(5) Å, c = 14.8249(12) Å, β = 100.428(13)°, V = 1169.53(16) Å³, T = 120, space group $P2_1/c$ (no. 14), Z = 4, μ(MoKα) = 0.087, 20862 reflections measured, 3411 unique (R_{int} = 0.0390) which were used in all calculations. The final wR_2 was 0.1847 (all data) and R_1 was 0.0668 (>2sigma(I)).

This report has been created with Olex2, compiled on 2011.11.01 svn.r2039. Please let us know if there are any errors or if you would like to have additional featrues.

(4,5-Dimethyl-3,6-dihydro-2*H*-1,2-oxazin-2-yl)(pyridin-2-yl)methanone **185**

13srv073

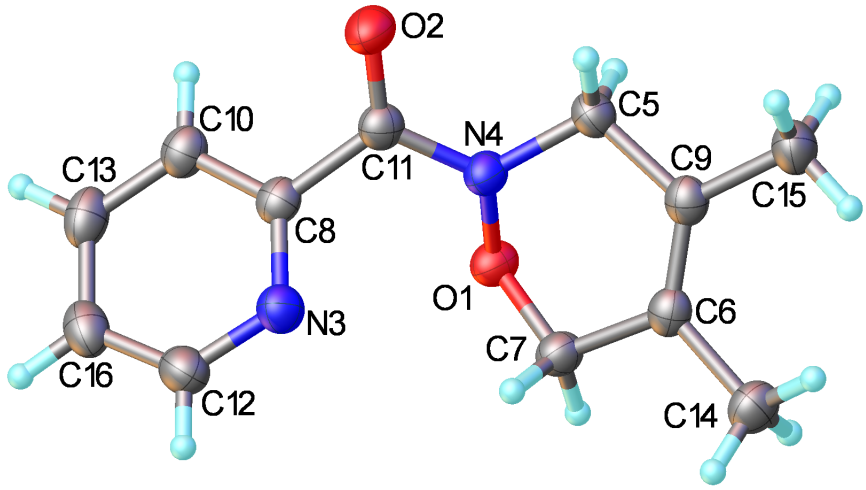

Table 1 Crystal data and structure refinement for 13srv073

Identification code	13srv073
Empirical formula	$C_{12}H_{14}N_2O_2$
Formula weight	218.25
Temperature/K	156
Crystal system	triclinic
Space group	P-1
a/Å	7.7458(6)
b/Å	8.3388(6)
c/Å	9.2703(7)
α/°	77.293(3)
β/°	68.194(3)
γ/°	84.734(3)
Volume/Å^3	542.28(7)
Z	2
ρ_{calc}mg/mm^3	1.337
m/mm^{-1}	0.093
F(000)	232.0
Crystal size/mm^3	0.33 × 0.17 × 0.04
2Θ range for data collection	4.8 to 50.0°
Index ranges	-9 ≤ h ≤ 9, -9 ≤ k ≤ 9, -11 ≤ l ≤ 10
Reflections collected	4329
Independent reflections	1896[R(int) = 0.0275]
Data/restraints/parameters	1896/0/149
Goodness-of-fit on F^2	0.950
Final R indexes [I>=2σ (I)]	R_1 = 0.0399, wR_2 = 0.0924
Final R indexes [all data]	R_1 = 0.0607, wR_2 = 0.1010
Largest diff. peak/hole / e Å^{-3}	0.22/-0.18

Table 2 Fractional Atomic Coordinates (×10⁴) and Equivalent Isotropic Displacement Parameters (Å²×10³) for 13srv073. U_{eq} is defined as 1/3 of of the trace of the orthogonalised U_{IJ} tensor.

Atom	*x*	*y*	*z*	U(eq)
O1	5721.6(16)	4635.5(13)	3353.3(14)	32.7(3)
O2	3336.0(17)	8336.1(14)	3805.4(16)	41.3(4)
N3	7881(2)	7541.4(17)	1686.1(18)	35.5(4)
N4	4369.4(19)	5855.8(17)	3245.0(17)	30.7(4)
C5	2580(2)	5174(2)	3578(2)	32.4(4)
C6	4477(2)	3328(2)	1831(2)	30.9(4)
C7	6171(2)	3850(2)	2029(2)	32.9(4)
C8	6594(2)	7855.5(19)	3037(2)	30.0(4)
C9	2801(2)	3918(2)	2569(2)	31.8(4)
C10	6957(3)	8710(2)	4013(2)	34.6(5)
C11	4631(2)	7362(2)	3428(2)	31.1(4)
C12	9590(3)	8109(2)	1303(2)	39.5(5)
C13	8738(3)	9263(2)	3596(2)	40.2(5)
C14	4903(3)	2104(2)	766(2)	40.5(5)
C15	998(3)	3434(2)	2540(2)	41.8(5)
C16	10078(3)	8963(2)	2208(2)	40.9(5)

Table 3 Anisotropic Displacement Parameters (Å²×10³) for 13srv073. The Anisotropic displacement factor exponent takes the form: -2π²[h²a*²U_{11}+...+2hka×b×U_{12}]

Atom	U_{11}	U_{22}	U_{33}	U_{23}	U_{13}	U_{12}
O1	33.7(7)	34.3(7)	34.6(7)	-11.1(5)	-16.3(6)	4.4(6)
O2	37.2(8)	38.2(7)	53.4(9)	-18.2(6)	-18.3(7)	5.6(6)
N3	33.7(9)	39.0(9)	36.2(10)	-9.7(7)	-13.9(7)	-1.2(7)
N4	29.4(8)	31.1(8)	35.1(9)	-10.2(6)	-14.1(7)	1.7(6)
C5	28(1)	34.9(10)	34.9(11)	-7.7(8)	-11.3(8)	-2.0(8)
C6	36.2(10)	29.6(9)	27.8(10)	-4.1(7)	-12.7(8)	-3.7(8)
C7	33.5(10)	33.9(10)	33.1(11)	-11.2(8)	-12.0(8)	2.0(8)
C8	34.7(10)	26.1(9)	31.3(11)	-4.7(7)	-15.0(9)	1.1(8)
C9	35(1)	31.5(10)	29.2(10)	-3.4(7)	-12.6(8)	-4.9(8)
C10	41.9(11)	31.6(10)	33.3(11)	-5.9(8)	-17.1(9)	-1.6(8)
C11	33.1(10)	34.3(10)	29.1(11)	-8.1(8)	-13.9(8)	0.0(8)
C12	33.4(11)	40.0(11)	42.8(12)	-8.9(9)	-10.6(9)	-0.6(9)
C13	50.5(12)	32.6(10)	49.1(13)	-7.9(9)	-31.0(11)	-2.1(9)
C14	45.6(12)	41.9(11)	38.4(12)	-13.7(9)	-17(1)	-0.4(9)
C15	38.5(11)	43.2(11)	46.2(13)	-12.2(9)	-14.6(10)	-7.9(9)
C16	36.0(11)	34.8(10)	54.5(14)	-3.8(9)	-21.8(10)	-3.4(9)

Table 4 Bond Lengths for 13srv073.

Atom	Atom	Length/Å	Atom	Atom	Length/Å
O1	N4	1.4072(16)	C6	C9	1.329(2)
O1	C7	1.432(2)	C6	C14	1.504(2)
O2	C11	1.226(2)	C8	C10	1.384(2)
N3	C8	1.342(2)	C8	C11	1.500(2)
N3	C12	1.339(2)	C9	C15	1.500(2)
N4	C5	1.445(2)	C10	C13	1.381(2)
N4	C11	1.347(2)	C12	C16	1.379(3)
C5	C9	1.510(2)	C13	C16	1.377(3)
C6	C7	1.505(2)			

Table 5 Bond Angles for 13srv073.

Atom	Atom	Atom	Angle/°	Atom	Atom	Atom	Angle/°
N4	O1	C7	107.56(11)	C10	C8	C11	118.84(16)
C12	N3	C8	116.26(15)	C6	C9	C5	120.18(16)
O1	N4	C5	112.57(12)	C6	C9	C15	126.10(17)
C11	N4	O1	117.80(13)	C15	C9	C5	113.71(15)
C11	N4	C5	124.88(14)	C13	C10	C8	118.88(18)
N4	C5	C9	109.87(14)	O2	C11	N4	121.62(16)
C9	C6	C7	120.85(16)	O2	C11	C8	120.84(15)
C9	C6	C14	125.83(17)	N4	C11	C8	117.40(15)
C14	C6	C7	113.32(15)	N3	C12	C16	124.16(19)
O1	C7	C6	112.89(14)	C16	C13	C10	118.56(18)
N3	C8	C10	123.49(16)	C13	C16	C12	118.65(18)
N3	C8	C11	117.49(15)				

Table 6 Hydrogen Atom Coordinates (Å×10⁴) and Isotropic Displacement Parameters (Å²×10³) for 13srv073.

Atom	*x*	*y*	*z*	U(eq)
H5A	1724	6064	3349	39
H5B	2038	4649	4714	39
H7A	6962	2871	2172	39
H7B	6899	4615	1051	39
H10	5998	8913	4954	41
H12	10525	7910	348	47
H13	9032	9838	4251	48
H14A	6005	2455	-180	63(4)
H14B	3841	2040	449	63(4)
H14C	5140	1021	1336	63(4)
H15A	208	2905	3611	62(4)
H15B	1245	2664	1823	62(4)
H15C	362	4415	2166	62(4)
H16	11314	9336	1881	49

Experimental

Single crystals of $C_{12}H_{14}N_2O_2$ **[13srv073]** were **[]**. A suitable crystal was selected and **[]** on a **Bruker SMART CCD 6000** diffractometer. The crystal was kept at 156 K during data collection. Using Olex2 [1], the structure was solved with the XS [2] structure solution program using Direct Methods and refined with the ShelXLMP-2012 [3] refinement package using Least Squares minimisation.

13. O. V. Dolomanov, L. J. Bourhis, R. J. Gildea, J. A. K. Howard and H. Puschmann, OLEX2: a complete structure solution, refinement and analysis program. J. Appl. Cryst. (2009). 42, 339-341.
14. XS, G.M. Sheldrick, Acta Cryst. (2008). A64, 112-122
15. SHELXL-2012, G.M. Sheldrick, Acta Cryst. (2008). A64, 112-122

Crystal structure determination of **[13srv073]**

Crystal Data for $C_{12}H_{14}N_2O_2$ (M =218.25): triclinic, space group P-1 (no. 2), a = 7.7458(6) Å, b = 8.3388(6) Å, c = 9.2703(7) Å, α = 77.293(3)°, β = 68.194(3)°, γ = 84.734(3)°, V = 542.28(7) Å^3, Z = 2, T = 156 K, μ(MoKα) = 0.093 mm^{-1}, *Dcalc* = 1.337 g/mm^3, 4329 reflections measured (4.832 ≤ 2Θ ≤ 49.996), 1896 unique (R_{int} = 0.0275) which were used in all calculations. The final R_1 was 0.0399 (I > 2σ(I)) and wR_2 was 0.1010 (all data).

This report has been created with Olex2, compiled on Mar 21 2013 11:16:32. Please let us know if there are any errors or if you would like to have additional featrues.

Phenyl-2-oxa-3-azabicyclo[2.2.2]oct-5-ene-3-carboxylate **182**

12srv073

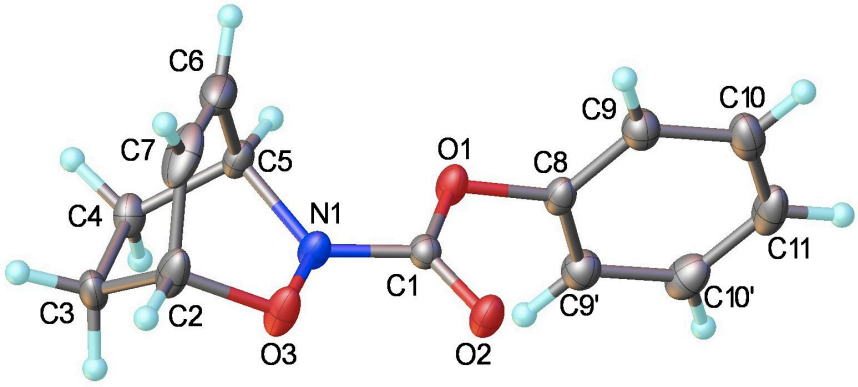

Table 1 Crystal data and structure refinement for 12srv073

Identification code	12srv073
Empirical formula	$C_{13}H_{13}NO_3$
Formula weight	231.24
Temperature/K	120
Crystal system	orthorhombic
Space group	Pnma
a/Å	7.6572(6)
b/Å	9.1842(8)
c/Å	15.6746(12)
α/°	90.00
β/°	90.00
γ/°	90.00
Volume/Å^3	1102.32(15)
Z	4
ρ_{calc}mg/mm^3	1.393
m/mm^{-1}	0.100
F(000)	488.0
Crystal size/mm^3	0.58 × 0.57 × 0.21
2Θ range for data collection	5.14 to 59.92°
Index ranges	-10 ≤ h ≤ 10, -12 ≤ k ≤ 12, -22 ≤ l ≤ 22
Reflections collected	14382
Independent reflections	1692[R(int) = 0.0265]
Data/restraints/parameters	1692/14/116
Goodness-of-fit on F^2	1.081
Final R indexes [I>=2σ (I)]	R_1 = 0.0415, wR_2 = 0.1110
Final R indexes [all data]	R_1 = 0.0465, wR_2 = 0.1149
Largest diff. peak/hole / e Å^{-3}	0.33/-0.28

Table 2 Fractional Atomic Coordinates (×10⁴) and Equivalent Isotropic Displacement Parameters (Å²×10³) for 12srv073. U_{eq} is defined as 1/3 of of the trace of the orthogonalised U_{IJ} tensor.

Atom	*x*	*y*	*z*	U(eq)
O1	2898.6(12)	2500	5431.6(6)	23.3(2)
O2	4319.4(12)	2500	4151.8(6)	25.9(2)
O3	1346.1(16)	2719(7)	3330.4(8)	30.7(13)
N1	1373.2(18)	2816.8(16)	4240.2(9)	21.2(5)
C1	2982.1(16)	2500	4558.2(8)	18.6(2)
C2	-473.9(18)	2500	3053.1(9)	31.4(3)
C3	-1555(5)	3804(6)	3380(3)	26.8(7)
C4	-1562(4)	3743(4)	4353(2)	23.1(6)
C5	-340.0(16)	2500	4643.6(8)	21.5(3)
C6	-1017(4)	1115(5)	4294(3)	33.3(8)
C7	-1091(5)	1131(6)	3442(4)	42.0(12)
C8	4525.2(16)	2500	5853.0(8)	21.0(3)
C9	5275.1(13)	1185.0(12)	6071.4(6)	26.8(2)
C10	6844.6(14)	1191.4(13)	6523.6(7)	32.2(3)
C11	7621(2)	2500	6749.4(9)	33.0(3)

Table 3 Anisotropic Displacement Parameters (Å²×10³) for 12srv073. The Anisotropic displacement factor exponent takes the form: -2π²[h²a*²U₁₁+...+2hka×b×U₁₂]

Atom	U_{11}	U_{22}	U_{33}	U_{23}	U_{13}	U_{12}
O1	15.7(4)	36.2(5)	18.1(4)	0	-1.7(3)	0
O2	17.1(4)	39.1(6)	21.5(4)	0	0.6(3)	0
O3	17.7(5)	61(4)	13.9(4)	-2.4(8)	-0.7(4)	-0.7(8)
N1	16.3(6)	33.2(14)	14.1(5)	0.0(5)	-0.4(4)	-0.9(5)
C1	17.5(5)	19.7(5)	18.6(5)	0	-1.7(4)	0
C2	17.8(6)	57.8(10)	18.7(6)	0	-3.7(5)	0
C3	18.7(18)	36.6(14)	25.1(12)	9.1(9)	-1.8(13)	7.2(14)
C4	19.4(15)	26.7(13)	23.2(10)	-4.6(8)	-2.6(12)	5.0(13)
C5	14.7(5)	30.8(6)	18.9(5)	0	0.6(4)	0
C6	21.5(17)	27.4(13)	51.0(18)	4.8(11)	-2.7(16)	-0.8(14)
C7	21(2)	44.2(18)	60(2)	-26.5(15)	-8.7(17)	-3.8(16)
C8	16.1(5)	31.3(7)	15.6(5)	0	-0.5(4)	0
C9	25.0(5)	30.1(5)	25.4(4)	0.2(4)	-1.1(3)	1.7(4)
C10	27.4(5)	44.0(6)	25.0(5)	4.7(4)	-2.0(4)	9.1(4)
C11	20.5(6)	58.2(10)	20.4(6)	0	-3.6(5)	0

Table 4 Bond Lengths for 12srv073.

Atom	Atom	Length/Å	Atom	Atom	Length/Å
O1	C1	1.3706(15)	C3	C4	1.526(6)
O1	C8	1.4098(15)	C4	C5	1.545(4)
O2	C1	1.2060(15)	C5	N1[1]	1.4850(18)
O3	N1	1.4290(18)	C5	C4[1]	1.545(4)
O3	C2	1.474(2)	C5	C6[1]	1.479(5)
N1	C1	1.3604(17)	C5	C6	1.479(5)
N1	C5	1.4850(18)	C6	C7	1.336(8)
C1	N1[1]	1.3604(17)	C8	C9[1]	1.3804(12)
C2	O3[1]	1.474(2)	C8	C9	1.3804(12)
C2	C3	1.543(4)	C9	C10	1.3952(14)
C2	C3[1]	1.543(4)	C10	C11	1.3868(14)
C2	C7[1]	1.475(5)	C11	C10[1]	1.3868(14)
C2	C7	1.475(5)			

[1]+X,1/2-Y,+Z

Table 5 Bond Angles for 12srv073.

Atom	Atom	Atom	Angle/°	Atom	Atom	Atom	Angle/°
C1	O1	C8	115.26(10)	C4	C3	C2	107.8(3)
N1	O3	C2	108.46(11)	C3	C4	C5	108.6(2)
O3	N1	C5	113.57(13)	N1	C5	N1[1]	22.60(12)
C1	N1	O3	111.43(13)	N1	C5	C4	105.34(14)
C1	N1	C5	127.02(12)	N1[1]	C5	C4	123.65(15)
O2	C1	O1	124.56(11)	N1[1]	C5	C4[1]	105.34(14)
O2	C1	N1	125.13(12)	N1	C5	C4[1]	123.65(15)
O2	C1	N1[1]	125.13(12)	C4[1]	C5	C4	95.3(3)
N1	C1	O1	108.89(11)	C6	C5	N1	108.67(17)
N1[1]	C1	O1	108.89(11)	C6[1]	C5	N1	89.03(15)
N1[1]	C1	N1	24.70(13)	C6[1]	C5	N1[1]	108.67(17)
O3	C2	O3[1]	15.7(5)	C6	C5	N1[1]	89.03(15)
O3	C2	C3[1]	121.0(3)	C6[1]	C5	C4	16.81(15)
O3[1]	C2	C3[1]	107.7(3)	C6	C5	C4[1]	16.81(15)
O3[1]	C2	C3	121.0(3)	C6[1]	C5	C4[1]	108.29(16)
O3	C2	C3	107.7(3)	C6	C5	C4	108.29(16)
O3	C2	C7	107.3(3)	C6	C5	C6[1]	118.6(4)
O3[1]	C2	C7	93.7(3)	C7	C6	C5	112.1(4)
O3	C2	C7[1]	93.7(3)	C6	C7	C2	114.1(4)
O3[1]	C2	C7[1]	107.3(3)	C9[1]	C8	O1	118.93(6)
C3[1]	C2	C3	101.8(4)	C9	C8	O1	118.93(6)
C7[1]	C2	C3	14.0(3)	C9	C8	C9[1]	122.07(12)
C7	C2	C3	110.61(16)	C8	C9	C10	118.73(10)
C7[1]	C2	C3[1]	110.61(16)	C11	C10	C9	120.17(10)
C7	C2	C3[1]	14.0(3)	C10	C11	C10[1]	120.14(13)
C7	C2	C7[1]	116.9(5)				

[1]+X,1/2-Y,+Z

Table 6 Hydrogen Atom Coordinates (Å×10⁴) and Isotropic Displacement Parameters (Å²×10³) for 12srv073.

Atom	*x*	*y*	*z*	U(eq)
H2	-539	2500	2417	38
H3A	-2760	3740	3154	32
H3B	-1030	4725	3174	32
H4A	-1147	4686	4582	28
H4B	-2764	3569	4562	28
H5	-156	2500	5262	25(4)
H6	-1350	319	4645	40
H7	-1528	327	3127	50
H9	4734	293	5916	32
H10	7382	297	6677	39
H11	8687	2500	7060	40

Experimental

Single crystals of $C_{13}H_{13}NO_3$ **[12srv073]** were **[]**. A suitable crystal was selected and **[]** on a **Bruker SMART CCD 6000** diffractometer. The crystal was kept at 120 K during data collection. Using Olex2 [1], the structure was solved with the XS [2] structure solution program using Direct Methods and refined with the XL [3] refinement package using Least Squares minimisation.

16. O. V. Dolomanov, L. J. Bourhis, R. J. Gildea, J. A. K. Howard and H. Puschmann, OLEX2: a complete structure solution, refinement and analysis program. J. Appl. Cryst. (2009). 42, 339-341.
17. XS, G.M. Sheldrick, Acta Cryst. (2008). A64, 112-122
18. XL, G.M. Sheldrick, Acta Cryst. (2008). A64, 112-122

Crystal structure determination of [12srv073]

Crystal Data. $C_{13}H_{13}NO_3$, M =231.24, orthorhombic, a = 7.6572(6) Å, b = 9.1842(8) Å, c = 15.6746(12) Å, V = 1102.32(15) Å³, T = 120, space group Pnma (no. 62), Z = 4, μ(MoKα) = 0.100, 14382 reflections measured, 1692 unique (R_{int} = 0.0265) which were used in all calculations. The final wR_2 was 0.1149 (all data) and R_1 was 0.0415 (>2sigma(I)).

This report has been created with Olex2, compiled on 2011.11.01 svn.r2039. Please let us know if there are any errors or if you would like to have additional featrues.

N-Phenyl-2-oxa-3-azabicyclo[2.2.2]oct-5-ene-3-carboxamide **183**

12srv065

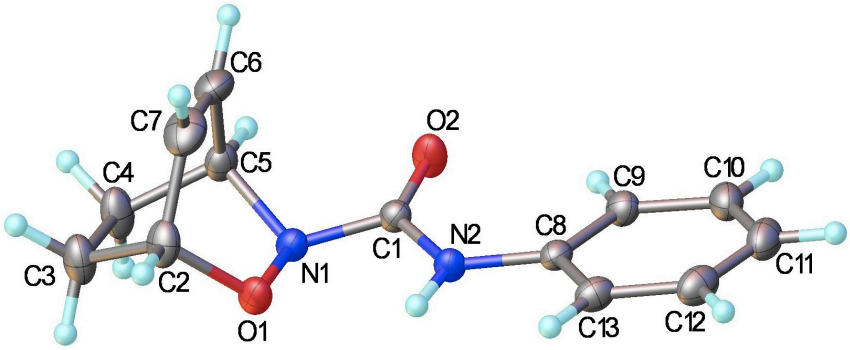

Table 1 Crystal data and structure refinement for 12srv065

Identification code	12srv065
Empirical formula	$C_{13}H_{14}N_2O_2$
Formula weight	230.26
Temperature/K	120
Crystal system	orthorhombic
Space group	$Pna2_1$
a/Å	10.0933(6)
b/Å	8.9883(5)
c/Å	12.7337(8)
α/°	90.00
β/°	90.00
γ/°	90.00
Volume/Å^3	1155.22(12)
Z	4
ρ_{calc}mg/mm^3	1.324
m/mm^{-1}	0.091
F(000)	488.0
Crystal size/mm^3	0.6 × 0.5 × 0.4
2Θ range for data collection	5.54 to 59.98°
Index ranges	-14 ≤ h ≤ 14, -12 ≤ k ≤ 12, -17 ≤ l ≤ 17
Reflections collected	20058
Independent reflections	1741[R(int) = 0.0251]
Data/restraints/parameters	1741/1/157
Goodness-of-fit on F^2	1.053
Final R indexes [I>=2σ (I)]	R_1 = 0.0321, wR_2 = 0.0853
Final R indexes [all data]	R_1 = 0.0333, wR_2 = 0.0869
Largest diff. peak/hole / e Å^{-3}	0.20/-0.28
Flack parameter	-10(10)

Table 2 Fractional Atomic Coordinates (×10⁴) and Equivalent Isotropic Displacement Parameters (Å²×10³) for 12srv065. U_{eq} is defined as 1/3 of of the trace of the orthogonalised U_{IJ} tensor.

Atom	*x*	*y*	*z*	U(eq)
O1	5919.8(9)	667.1(11)	1719(1)	25.2(2)
O2	2866.7(10)	2050.1(12)	2560.1(10)	29.7(2)
N1	4515(1)	937.6(12)	1646.4(10)	20.2(2)
N2	5005.6(10)	2817.8(12)	2854.4(10)	20.5(2)
C1	4061.7(12)	1948.7(14)	2407.9(10)	19.8(2)
C2	6186.4(15)	-936.3(16)	1815.9(13)	29.1(3)
C3	5770.4(16)	-1647.9(19)	781.2(14)	33.5(3)
C4	4290.9(16)	-1311(2)	621.8(14)	33.9(3)
C5	3762.4(13)	-483.2(15)	1583.1(12)	24.8(3)
C6	4071.5(18)	-1348.5(17)	2564.1(14)	33.5(3)
C7	5377(2)	-1558.4(19)	2694.8(14)	38.3(4)
C8	4776.4(13)	3992.0(14)	3571.5(10)	20.1(2)
C9	3526.9(13)	4603.0(15)	3763.6(11)	23.4(3)
C10	3402.1(16)	5749.4(16)	4493.8(12)	28.4(3)
C11	4486.9(18)	6288.4(17)	5040.2(13)	32.1(3)
C12	5729.1(17)	5677.6(18)	4845.7(13)	31.0(3)
C13	5880.2(14)	4544.4(16)	4114.5(12)	25.1(3)

Table 3 Anisotropic Displacement Parameters (Å²×10³) for 12srv065. The Anisotropic displacement factor exponent takes the form: -2π²[h²a*²U₁₁+...+2hka×b×U₁₂]

Atom	U_{11}	U_{22}	U_{33}	U_{23}	U_{13}	U_{12}
O1	15.5(4)	23.0(4)	37.0(5)	-4.0(4)	3.9(4)	1.7(3)
O2	15.4(4)	28.9(5)	44.9(6)	-10.6(5)	2.6(4)	0.3(4)
N1	15.5(4)	19.3(4)	25.9(5)	-1.1(4)	1.0(4)	0.4(3)
N2	14.9(4)	20.6(5)	25.9(5)	-3.0(4)	1.4(4)	-0.7(4)
C1	16.7(5)	18.5(5)	24.1(5)	-0.1(4)	0.5(4)	0.3(4)
C2	25.4(6)	26.1(6)	36.0(7)	-6.2(6)	-6.4(6)	8.9(5)
C3	27.8(6)	33.7(8)	38.9(8)	-14.2(6)	-1.2(6)	5.7(6)
C4	26.8(6)	36.8(8)	38.0(8)	-17.7(7)	-4.2(6)	3.2(6)
C5	20.8(5)	22.3(5)	31.2(7)	-5.9(5)	-0.3(5)	-2.5(4)
C6	42.3(9)	22.1(6)	36.1(8)	3.2(6)	7.1(6)	-5.1(6)
C7	52.4(10)	27.6(7)	34.9(8)	6.4(6)	-6.4(7)	7.6(7)
C8	22.0(6)	17.7(5)	20.5(5)	1.3(4)	0.9(4)	-1.6(4)
C9	22.9(6)	20.5(5)	26.8(6)	0.0(5)	1.1(5)	1.5(4)
C10	34.1(7)	23.1(6)	28.0(6)	-1.4(5)	4.4(6)	2.8(5)
C11	45.6(9)	24.9(7)	25.8(6)	-3.5(5)	-0.4(6)	-1.9(6)
C12	37.0(8)	27.8(7)	28.2(7)	0.2(5)	-6.6(6)	-7.5(6)
C13	24.4(6)	24.5(6)	26.6(6)	2.6(5)	-3.6(5)	-4.2(5)

Table 4 Bond Lengths for 12srv065.

Atom	Atom	Length/Å	Atom	Atom	Length/Å
O1	N1	1.4415(13)	C4	C5	1.529(2)
O1	C2	1.4713(17)	C5	C6	1.504(2)
O2	C1	1.2251(15)	C6	C7	1.342(3)
N1	C1	1.4056(17)	C8	C9	1.3972(17)
N1	C5	1.4881(17)	C8	C13	1.4020(18)
N2	C1	1.3568(16)	C9	C10	1.3936(19)
N2	C8	1.4147(17)	C10	C11	1.385(2)
C2	C3	1.524(2)	C11	C12	1.391(2)
C2	C7	1.494(3)	C12	C13	1.388(2)
C3	C4	1.537(2)			

Table 5 Bond Angles for 12srv065.

Atom	Atom	Atom	Angle/°	Atom	Atom	Atom	Angle/°
N1	O1	C2	110.52(9)	N1	C5	C4	106.45(12)
O1	N1	C5	111.15(10)	N1	C5	C6	107.03(12)
C1	N1	O1	112.64(10)	C6	C5	C4	109.92(12)
C1	N1	C5	115.22(11)	C7	C6	C5	112.30(14)
C1	N2	C8	125.81(10)	C6	C7	C2	113.05(14)
O2	C1	N1	118.54(12)	C9	C8	N2	123.63(12)
O2	C1	N2	125.60(12)	C9	C8	C13	119.46(13)
N2	C1	N1	115.64(10)	C13	C8	N2	116.91(12)
O1	C2	C3	106.75(13)	C10	C9	C8	119.27(13)
O1	C2	C7	109.23(12)	C11	C10	C9	121.50(14)
C7	C2	C3	109.88(13)	C10	C11	C12	119.02(14)
C2	C3	C4	107.42(13)	C13	C12	C11	120.53(14)
C5	C4	C3	109.22(13)	C12	C13	C8	120.21(14)

Table 6 Hydrogen Bonds for 12srv065.

D	H	A	d(D-H)/Å	d(H-A)/Å	d(D-A)/Å	D-H-A/°
N2	H2	O2[1]	0.897(19)	2.056(19)	2.9144(14)	159.6(18)

[1]1/2+X,1/2-Y,+Z

Table 7 Hydrogen Atom Coordinates (Å×10⁴) and Isotropic Displacement Parameters (Å²×10³) for 12srv065.

Atom	*x*	*y*	*z*	U(eq)
H2	5860(18)	2620(20)	2716(16)	25
H2A	7150	-1112	1948	35
H3A	5919	-2736	806	40
H3B	6295	-1230	194	40
H4A	4169	-694	-15	41
H4B	3795	-2252	525	41
H5	2789	-294	1519	30

H6	3417	-1706	3037	40
H7	5749	-2052	3285	46
H9	2771	4241	3400	28
H10	2554	6171	4620	34
H11	4384	7064	5541	39
H12	6480	6039	5216	37
H13	6734	4142	3982	30

Experimental

Single crystals of $C_{13}H_{14}N_2O_2$ **[12srv065]** were **[]**. A suitable crystal was selected and **[]** on a **Bruker SMART CCD 6000** diffractometer. The crystal was kept at 120 K during data collection. Using Olex2 [1], the structure was solved with the XS [2] structure solution program using Direct Methods and refined with the XL [3] refinement package using Least Squares minimisation.

19. O. V. Dolomanov, L. J. Bourhis, R. J. Gildea, J. A. K. Howard and H. Puschmann, OLEX2: a complete structure solution, refinement and analysis program. J. Appl. Cryst. (2009). 42, 339-341.
20. XS, G.M. Sheldrick, Acta Cryst. (2008). A64, 112-122
21. XL, G.M. Sheldrick, Acta Cryst. (2008). A64, 112-122

Crystal structure determination of [12srv065]

Crystal Data. $C_{13}H_{14}N_2O_2$, M =230.26, orthorhombic, a = 10.0933(6) Å, b = 8.9883(5) Å, c = 12.7337(8) Å, V = 1155.22(12) Å^3, T = 120, space group $Pna2_1$ (no. 33), Z = 4, μ(MoKα) = 0.091, 20058 reflections measured, 1741 unique (R_{int} = 0.0251) which were used in all calculations. The final wR_2 was 0.0869 (all data) and R_1 was 0.0321 (>2sigma(I)).

This report has been created with Olex2, compiled on 2011.11.01 svn.r2039. Please let us know if there are any errors or if you would like to have additional featrues.

Phenyl 2-oxa-3-azabicyclo[2.2.1]hept-5-ene-3-carboxylate **197**

12srv083

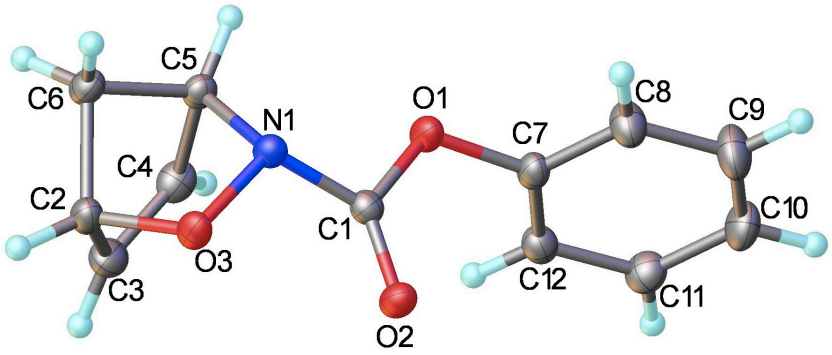

Table 1 Crystal data and structure refinement for 12srv083

Identification code	12srv083
Empirical formula	$C_{12}H_{11}NO_3$
Formula weight	217.22
Temperature/K	120
Crystal system	monoclinic
Space group	$P2_1/c$
a/Å	5.8418(5)
b/Å	8.6844(7)
c/Å	20.7247(19)
α/°	90.00
β/°	91.658(15)
γ/°	90.00
Volume/Å^3	1050.98(16)
Z	4
ρ_{calc}mg/mm^3	1.373
m/mm^{-1}	0.100
F(000)	456.0
Crystal size/mm^3	0.42 × 0.42 × 0.24
2Θ range for data collection	3.94 to 59.96°
Index ranges	-8 ≤ h ≤ 8, -12 ≤ k ≤ 12, -29 ≤ l ≤ 29
Reflections collected	12722
Independent reflections	3069[R(int) = 0.0420]
Data/restraints/parameters	3069/0/145
Goodness-of-fit on F^2	1.072
Final R indexes [I>=2σ (I)]	R_1 = 0.0493, wR_2 = 0.1396
Final R indexes [all data]	R_1 = 0.0619, wR_2 = 0.1506
Largest diff. peak/hole / e Å^{-3}	0.41/-0.22

Table 2 Fractional Atomic Coordinates (×10⁴) and Equivalent Isotropic Displacement Parameters (Å²×10³) for 12srv083. U_{eq} is defined as 1/3 of of the trace of the orthogonalised U_{IJ} tensor.

Atom	*x*	*y*	*z*	U(eq)
O1	3837.2(16)	4015.4(10)	5899.2(4)	22.5(2)
O2	2296.1(16)	1687.1(10)	6134.2(4)	23.0(2)
O3	-21.7(15)	1707.2(10)	5016.2(4)	21.5(2)
N1	1169.3(17)	3079.8(12)	5223.2(5)	18.3(2)
C1	2462.3(19)	2777.3(13)	5782.2(6)	17.7(2)
C2	686(2)	1493.3(14)	4339.5(6)	22.4(3)
C3	3211(2)	1123.9(16)	4373.9(6)	26.6(3)
C4	4287(2)	2422.6(16)	4549.0(6)	23.9(3)
C5	2447(2)	3618.9(14)	4639.9(6)	19.4(2)
C6	686(2)	3174.9(14)	4112.0(6)	21.6(3)
C7	5174(2)	4004.1(14)	6477.2(6)	20.5(3)
C8	4511(2)	4964.6(16)	6969.2(7)	28.3(3)
C9	5914(3)	5066.4(19)	7522.3(7)	35.3(4)
C10	7914(3)	4215.5(18)	7571.6(7)	30.9(3)
C11	8532(2)	3250.8(16)	7072.6(7)	26.4(3)
C12	7156(2)	3145.7(14)	6516.1(6)	22.6(3)

Table 3 Anisotropic Displacement Parameters (Å²×10³) for 12srv083. The Anisotropic displacement factor exponent takes the form: -2π²[h²a*²U₁₁+...+2hka×b×U₁₂]

Atom	U_{11}	U_{22}	U_{33}	U_{23}	U_{13}	U_{12}
O1	27.5(5)	19.6(4)	20.1(4)	1.5(3)	-6.2(3)	-6.8(3)
O2	26.7(5)	20.4(4)	21.6(4)	3.7(3)	-3.8(3)	-4.6(3)
O3	22.4(4)	21.2(4)	20.6(4)	1.2(3)	-3.3(3)	-8.7(3)
N1	18.7(5)	17.0(5)	19.0(5)	1.0(4)	-1.3(4)	-3.2(3)
C1	17.0(5)	17.6(5)	18.5(5)	-1.0(4)	0.7(4)	-0.7(4)
C2	29.3(6)	20.1(5)	17.8(6)	0.0(4)	-2.8(5)	-5.1(5)
C3	32.2(7)	24.0(6)	23.6(6)	-1.4(5)	1.4(5)	5.8(5)
C4	20.0(5)	30.0(6)	22.0(6)	1.9(5)	2.5(4)	1.5(5)
C5	21.7(6)	19.4(5)	17.1(5)	2.4(4)	0.7(4)	-3.7(4)
C6	23.1(6)	21.7(6)	19.9(6)	3.2(4)	-3.8(4)	-2.2(4)
C7	22.7(6)	20.6(5)	18.0(5)	0.0(4)	-2.6(4)	-5.1(4)
C8	27.4(7)	31.2(7)	25.9(7)	-7.4(5)	-3.3(5)	4.1(5)
C9	36.4(8)	43.3(9)	25.8(7)	-14.0(6)	-3.8(6)	4.2(6)
C10	31.9(7)	38.5(8)	21.9(6)	-2.2(5)	-7.5(5)	-0.8(6)
C11	22.8(6)	29.0(7)	27.2(7)	1.5(5)	-3.1(5)	-0.2(5)
C12	25.0(6)	22.0(6)	21.0(6)	-1.5(4)	1.5(5)	-2.3(5)

Table 4 Bond Lengths for 12srv083.

Atom	Atom	Length/Å	Atom	Atom	Length/Å
O1	C1	1.3597(14)	C3	C4	1.3363(19)
O1	C7	1.4110(14)	C4	C5	1.5107(17)
O2	C1	1.2009(15)	C5	C6	1.5295(16)
O3	N1	1.4394(13)	C7	C8	1.3815(18)
O3	C2	1.4851(15)	C7	C12	1.3773(18)
N1	C1	1.3897(15)	C8	C9	1.392(2)
N1	C5	1.5132(15)	C9	C10	1.384(2)
C2	C3	1.5095(19)	C10	C11	1.387(2)
C2	C6	1.5346(17)	C11	C12	1.3897(18)

Table 5 Bond Angles for 12srv083.

Atom	Atom	Atom	Angle/°	Atom	Atom	Atom	Angle/°
C1	O1	C7	117.10(9)	N1	C5	C6	98.99(9)
N1	O3	C2	103.87(8)	C4	C5	N1	104.83(9)
O3	N1	C5	105.28(8)	C4	C5	C6	101.76(10)
C1	N1	O3	109.77(9)	C5	C6	C2	91.50(9)
C1	N1	C5	117.11(9)	C8	C7	O1	117.53(11)
O1	C1	N1	107.65(9)	C12	C7	O1	119.81(11)
O2	C1	O1	124.95(11)	C12	C7	C8	122.48(12)
O2	C1	N1	127.15(11)	C7	C8	C9	118.35(13)
O3	C2	C3	106.27(10)	C10	C9	C8	120.17(13)
O3	C2	C6	100.00(10)	C9	C10	C11	120.32(13)
C3	C2	C6	102.01(10)	C10	C11	C12	120.12(13)
C4	C3	C2	106.56(11)	C7	C12	C11	118.56(12)
C3	C4	C5	106.46(11)				

Table 6 Hydrogen Atom Coordinates (Å×10⁴) and Isotropic Displacement Parameters (Å²×10³) for 12srv083.

Atom	*x*	*y*	*z*	U(eq)
H2	-285	773	4073	27
H3	3900	157	4288	32
H4	5893	2565	4605	29
H5	2961	4717	4644	23
H6A	1253	3306	3670	26
H6B	-811	3694	4156	26
H8	3131	5541	6931	34
H9	5496	5722	7867	42
H10	8869	4293	7949	37
H11	9899	2661	7111	32
H12	7573	2496	6170	27

Experimental

Single crystals of $C_{12}H_{11}NO_3$ **[12srv083]** were **[]**. A suitable crystal was selected and **[]** on a **Bruker SMART CCD 6000** diffractometer. The crystal was kept at 120 K during data collection. Using Olex2 [1], the structure was solved with the XS [2] structure solution program using Direct Methods and refined with the XL [3] refinement package using Least Squares minimisation.

22. O. V. Dolomanov, L. J. Bourhis, R. J. Gildea, J. A. K. Howard and H. Puschmann, OLEX2: a complete structure solution, refinement and analysis program. J. Appl. Cryst. (2009). 42, 339-341.
23. XS, G.M. Sheldrick, Acta Cryst. (2008). A64, 112-122
24. XL, G.M. Sheldrick, Acta Cryst. (2008). A64, 112-122

Crystal structure determination of [12srv083]

Crystal Data. $C_{12}H_{11}NO_3$, M =217.22, monoclinic, a = 5.8418(5) Å, b = 8.6844(7) Å, c = 20.7247(19) Å, β = 91.658(15)°, V = 1050.98(16) Å^3, T = 120, space group $P2_1/c$ (no. 14), Z = 4, μ(MoKα) = 0.100, 12722 reflections measured, 3069 unique (R_{int} = 0.0420) which were used in all calculations. The final wR_2 was 0.1506 (all data) and R_1 was 0.0493 (>2sigma(I)).

This report has been created with Olex2, compiled on 2011.11.01 svn.r2039. Please let us know if there are any errors or if you would like to have additional featrues.

4,5-Dimethyl-*N*-phenyl-3,6-dihydro-2*H*-1,2-oxazine-2-carbox-amide **195**
12srv066

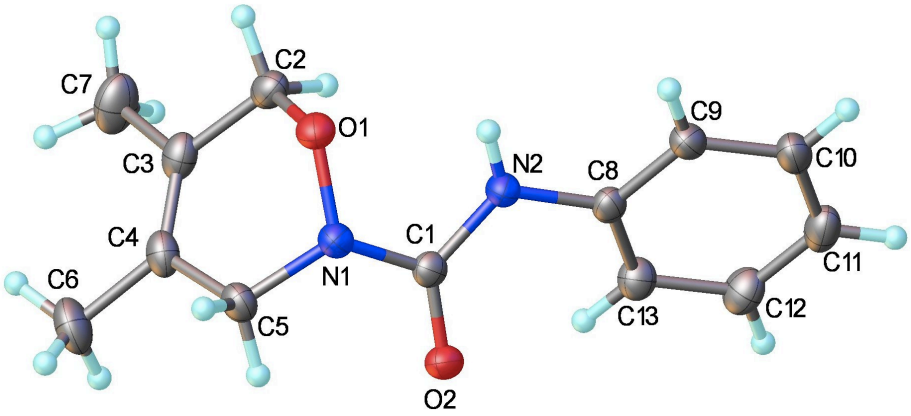

Table 1 Crystal data and structure refinement for 12srv066

Identification code	12srv066
Empirical formula	$C_{13}H_{16}N_2O_2$
Formula weight	232.28
Temperature/K	120
Crystal system	orthorhombic
Space group	Pbca
a/Å	13.5078(8)
b/Å	9.1660(5)
c/Å	19.8312(13)
α/°	90.00
β/°	90.00
γ/°	90.00
Volume/Å^3	2455.4(3)
Z	8
ρ_{calc}mg/mm^3	1.257
m/mm^{-1}	0.086
F(000)	992.0
Crystal size/mm^3	0.85 × 0.8 × 0.4
2Θ range for data collection	4.1 to 60.02°
Index ranges	-18 ≤ h ≤ 19, -12 ≤ k ≤ 12, -27 ≤ l ≤ 27
Reflections collected	27298
Independent reflections	3576[R(int) = 0.0318]
Data/restraints/parameters	3576/0/161
Goodness-of-fit on F^2	1.021
Final R indexes [I>=2σ (I)]	R_1 = 0.0426, wR_2 = 0.1151
Final R indexes [all data]	R_1 = 0.0528, wR_2 = 0.1258
Largest diff. peak/hole / e Å^{-3}	0.34/-0.18

Table 2 Fractional Atomic Coordinates (×10⁴) and Equivalent Isotropic Displacement Parameters (Å²×10³) for 12srv066. U_{eq} is defined as 1/3 of of the trace of the orthogonalised U_{IJ} tensor.

Atom	*x*	*y*	*z*	U(eq)
O1	6455.8(6)	4001.6(8)	4465.1(4)	27.45(18)
O2	6640.6(5)	458.3(8)	3812.6(4)	26.36(17)
N1	6384.1(6)	2471.9(9)	4450.1(4)	25.02(19)
N2	7451.6(6)	2587.7(10)	3542.1(4)	24.17(18)
C1	6812.7(7)	1758.9(10)	3910.9(5)	21.80(19)
C2	5683.7(8)	4633.9(11)	4056.6(6)	29.1(2)
C3	4680.7(8)	4000.3(12)	4195.5(5)	29.8(2)
C4	4581.6(8)	2772.3(13)	4544.9(5)	29.1(2)
C5	5484.6(8)	1935.7(12)	4764.5(5)	28.3(2)
C6	3613.3(9)	2070.6(17)	4733.6(7)	43.2(3)
C7	3841.2(10)	4844.8(18)	3888.2(7)	45.6(3)
C8	8069.1(7)	2031.9(11)	3026.2(5)	23.4(2)
C9	9003.8(8)	2665.9(11)	2949.5(6)	28.5(2)
C10	9646.8(8)	2154.8(12)	2456.4(6)	33.6(2)
C11	9370.1(9)	1013.7(13)	2039.2(6)	34.8(3)
C12	8437.7(9)	398.5(13)	2111.3(6)	33.9(2)
C13	7778.1(8)	911.3(12)	2597.0(5)	28.3(2)

Table 3 Anisotropic Displacement Parameters (Å²×10³) for 12srv066. The Anisotropic displacement factor exponent takes the form: -2π²[h²a*²U_{11}+...+2hka×b×U_{12}]

Atom	U_{11}	U_{22}	U_{33}	U_{23}	U_{13}	U_{12}
O1	27.7(4)	22.7(4)	31.9(4)	-3.7(3)	2.4(3)	-2.4(3)
O2	24.8(4)	20.3(3)	34.0(4)	1.2(3)	1.7(3)	0.0(3)
N1	23.1(4)	22.3(4)	29.6(4)	0.5(3)	3.7(3)	-0.8(3)
N2	22.8(4)	20.7(4)	29.0(4)	-1.9(3)	4.3(3)	-1.5(3)
C1	18.3(4)	22.5(4)	24.6(4)	1.4(3)	-1.4(3)	2.0(3)
C2	34.5(5)	24.3(5)	28.4(5)	0.6(4)	6.3(4)	4.7(4)
C3	27.7(5)	36.7(6)	24.9(5)	-2.5(4)	2.1(4)	7.9(4)
C4	22.7(5)	38.1(6)	26.5(5)	-2.5(4)	5.2(4)	0.6(4)
C5	27.0(5)	29.3(5)	28.7(5)	4.2(4)	7.1(4)	-0.2(4)
C6	26.8(6)	58.8(8)	43.9(7)	-0.8(6)	10.4(5)	-5.5(5)
C7	38.8(7)	59.5(8)	38.5(7)	4.9(6)	-0.9(5)	20.3(6)
C8	21.8(4)	22.7(4)	25.7(4)	3.4(3)	2.1(3)	4.1(3)
C9	24.9(5)	24.1(5)	36.5(5)	1.7(4)	5.3(4)	-0.5(4)
C10	27.5(5)	31.2(5)	41.9(6)	6.9(5)	11.1(4)	3.3(4)
C11	36.0(6)	36.5(6)	31.9(5)	3.8(4)	9.8(4)	11.2(5)
C12	37.4(6)	35.9(6)	28.5(5)	-4.6(4)	0.9(4)	6.2(5)
C13	25.8(5)	31.8(5)	27.2(5)	-1.0(4)	-0.5(4)	2.0(4)

Table 4 Bond Lengths for 12srv066.

Atom	Atom	Length/Å	Atom	Atom	Length/Å
O1	N1	1.4057(11)	C3	C7	1.5022(16)
O1	C2	1.4421(14)	C4	C5	1.5051(15)
O2	C1	1.2301(12)	C4	C6	1.5048(16)
N1	C1	1.3805(13)	C8	C9	1.3981(14)
N1	C5	1.4515(13)	C8	C13	1.3907(14)
N2	C1	1.3626(13)	C9	C10	1.3892(15)
N2	C8	1.4150(13)	C10	C11	1.3851(18)
C2	C3	1.4997(16)	C11	C12	1.3873(18)
C3	C4	1.3285(16)	C12	C13	1.3937(15)

Table 5 Bond Angles for 12srv066.

Atom	Atom	Atom	Angle/°	Atom	Atom	Atom	Angle/°
N1	O1	C2	109.83(8)	C3	C4	C5	120.06(9)
O1	N1	C5	112.73(8)	C3	C4	C6	125.40(11)
C1	N1	O1	117.37(8)	C6	C4	C5	114.50(10)
C1	N1	C5	121.57(9)	N1	C5	C4	112.43(9)
C1	N2	C8	124.11(8)	C9	C8	N2	117.48(9)
O2	C1	N1	120.15(9)	C13	C8	N2	122.80(9)
O2	C1	N2	125.10(9)	C13	C8	C9	119.71(9)
N2	C1	N1	114.67(8)	C10	C9	C8	120.07(10)
O1	C2	C3	113.23(9)	C11	C10	C9	120.42(11)
C2	C3	C7	114.07(10)	C10	C11	C12	119.37(10)
C4	C3	C2	120.99(10)	C11	C12	C13	120.96(11)
C4	C3	C7	124.90(11)	C8	C13	C12	119.43(10)

Table 6 Hydrogen Bonds for 12srv066.

D	H	A	d(D-H)/Å	d(H-A)/Å	d(D-A)/Å	D-H-A/°
N2	H2N	O2[1]	0.825(15)	2.168(15)	2.9520(11)	158.8(13)

[1]3/2-X,1/2+Y,+Z

Table 7 Hydrogen Atom Coordinates (Å×10⁴) and Isotropic Displacement Parameters (Å²×10³) for 12srv066.

Atom	*x*	*y*	*z*	U(eq)
H2N	7563(11)	3428(16)	3671(7)	29(3)
H2A	5847	4483	3575	35
H2B	5662	5699	4139	35
H5A	5552	2008	5261	34
H5B	5397	893	4649	34
H6A	3081	2795	4704	64(3)
H6B	3654	1698	5196	64(3)
H6C	3474	1263	4424	64(3)
H7A1	3772	4575	3412	49(4)
H7A2	3978	5892	3923	49(4)

H7A3	3226	4618	4128	49(4)
H7B1	3488	5539	4178	49(4)
H7B2	3987	5375	3471	49(4)
H7B3	3321	4197	3718	49(4)
H9	9199	3447	3235	34
H10	10280	2591	2405	40
H11	9814	656	1707	42
H12	8246	-384	1825	41
H13	7135	499	2635	34

Experimental

Single crystals of $C_{13}H_{16}N_2O_2$ **[12srv066]** were **[]**. A suitable crystal was selected and **[]** on a **Bruker SMART CCD 6000** diffractometer. The crystal was kept at 120 K during data collection. Using Olex2 [1], the structure was solved with the XS [2] structure solution program using Direct Methods and refined with the XL [3] refinement package using Least Squares minimisation.

25. O. V. Dolomanov, L. J. Bourhis, R. J. Gildea, J. A. K. Howard and H. Puschmann, OLEX2: a complete structure solution, refinement and analysis program. J. Appl. Cryst. (2009). 42, 339-341.
26. XS, G.M. Sheldrick, Acta Cryst. (2008). A64, 112-122
27. XL, G.M. Sheldrick, Acta Cryst. (2008). A64, 112-122

Crystal structure determination of [12srv066]

Crystal Data. $C_{13}H_{16}N_2O_2$, M =232.28, orthorhombic, a = 13.5078(8) Å, b = 9.1660(5) Å, c = 19.8312(13) Å, V = 2455.4(3) Å^3, T = 120, space group Pbca (no. 61), Z = 8, μ(MoKα) = 0.086, 27298 reflections measured, 3576 unique (R_{int} = 0.0318) which were used in all calculations. The final wR_2 was 0.1258 (all data) and R_1 was 0.0426 (>2sigma(I)).

This report has been created with Olex2, compiled on 2011.11.01 svn.r2039. Please let us know if there are any errors or if you would like to have additional featrues.

N-((*R*)-1-Phenylethyl)-2-oxa-3-azabicyclo[2.2.2]oct-5-ene-3-carboxamide **184**
12srv114

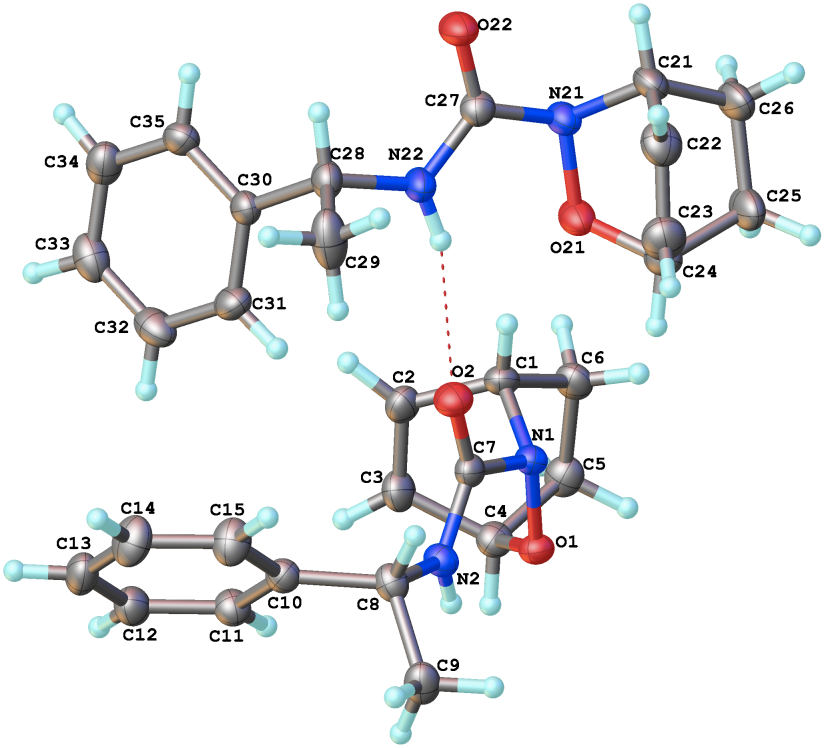

Table 1 Crystal data and structure refinement for 12srv114

Identification code	12srv114
Empirical formula	$C_{15}H_{18}N_2O_2$
Formula weight	258.31
Temperature/K	120
Crystal system	tetragonal
Space group	$P4_12_12$
a/Å	10.2990(2)
b/Å	10.2990(2)
c/Å	51.7187(14)
α/°	90.00
β/°	90.00
γ/°	90.00
Volume/Å^3	5485.8(2)
Z	16
ρ_{calc}mg/mm^3	1.251

m/mm^{-1}	0.084
F(000)	2208.0
Crystal size/mm^3	0.45 × 0.4 × 0.03
2Θ range for data collection	3.14 to 59°
Index ranges	-14 ≤ h ≤ 14, -12 ≤ k ≤ 13, -70 ≤ l ≤ 71
Reflections collected	86666
Independent reflections	7584[R(int) = 0.0443]
Data/restraints/parameters	7584/0/487
Goodness-of-fit on F^2	1.028
Final R indexes [I>=2σ (I)]	R_1 = 0.0444, wR_2 = 0.1054
Final R indexes [all data]	R_1 = 0.0548, wR_2 = 0.1113
Largest diff. peak/hole / e Å^{-3}	0.26/-0.19
Flack parameter	0.1(8)

Table 2 Fractional Atomic Coordinates (×10^4) and Equivalent Isotropic Displacement Parameters (Å^2×10^3) for 12srv114. U_{eq} is defined as 1/3 of of the trace of the orthogonalised U_{IJ} tensor.

Atom	*x*	*y*	*z*	U(eq)
O1	7058.2(10)	7835(1)	4229.99(19)	24.2(2)
O2	4441.8(10)	6073.6(11)	4483.4(2)	29.9(2)
N1	5700.4(11)	7592.6(12)	4279.8(2)	23.0(2)
N2	6640.0(13)	5955.5(12)	4531.9(2)	24.4(2)
C1	4980.7(15)	7545.3(15)	4028.1(3)	26.5(3)
C2	5517.9(16)	6410.3(16)	3879.0(3)	29.8(3)
C3	6801.2(17)	6487.7(16)	3846.6(3)	31.9(3)
C4	7371.6(15)	7711.5(15)	3952.8(3)	27.6(3)
C5	6738.9(17)	8879.7(17)	3823.3(3)	32.2(3)
C6	5282.7(16)	8821.7(16)	3887.6(3)	31.0(3)
C7	5546.2(14)	6458.1(14)	4434.6(3)	23.9(3)
C8	6596.5(15)	4930.2(15)	4726.2(3)	26.3(3)
C9	7715.3(18)	5122.6(16)	4917.0(3)	32.3(3)
C10	6619.8(14)	3569.3(14)	4613.3(3)	25.4(3)
C11	7400.2(16)	3241.7(15)	4403.2(3)	28.9(3)
C12	7461.3(17)	1957.5(16)	4319.2(3)	32.8(3)
C13	6758.6(18)	994.9(16)	4442.3(3)	35.8(4)
C14	5970(2)	1320.5(17)	4648.3(3)	40.8(4)
C15	5901.6(19)	2599.6(17)	4732.0(3)	36.5(4)
O21	2160.6(10)	7915.5(11)	4346.2(2)	32.0(2)
O22	-639.7(10)	6016.7(11)	4371.2(2)	34.7(3)
N21	789.6(12)	7680.0(13)	4322.5(2)	27.5(3)

N22	1514.3(13)	5557.9(13)	4396.1(3)	29.9(3)
C21	50.3(16)	8604.2(15)	4489.5(3)	32.0(3)
C22	448.2(18)	8325.3(18)	4764.5(3)	38.2(4)
C23	1740.7(19)	8386.6(19)	4797.7(3)	41.3(4)
C24	2442.4(16)	8812.8(16)	4559.4(3)	34.0(3)
C25	1934.2(19)	10124.3(17)	4471.0(5)	43.8(4)
C26	500.2(19)	9967.4(17)	4412.0(4)	42.1(4)
C27	504.6(14)	6358.3(15)	4371.6(3)	26.7(3)
C28	1315.8(16)	4161.4(14)	4432.6(3)	29.9(3)
C29	1700(3)	3769(2)	4706.2(4)	49.5(5)
C30	2019.2(15)	3382.2(14)	4228.7(3)	25.4(3)
C31	3369.4(16)	3288.1(16)	4225.7(3)	32.8(3)
C32	3984.0(18)	2526.9(17)	4040.5(4)	37.9(4)
C33	3271.0(18)	1874.7(16)	3855.6(3)	36.9(4)
C34	1939.0(19)	1979.8(17)	3854.9(3)	35.3(4)
C35	1317.2(16)	2731.1(15)	4040.2(3)	29.7(3)

Table 3 Anisotropic Displacement Parameters ($Å^2 \times 10^3$) for 12srv114. The Anisotropic displacement factor exponent takes the form: $-2\pi^2[h^2a^{*2}U_{11}+...+2hka \times b \times U_{12}]$

Atom	U_{11}	U_{22}	U_{33}	U_{23}	U_{13}	U_{12}
O1	19.9(5)	26.3(5)	26.5(5)	1.2(4)	-1.5(4)	-1.4(4)
O2	23.2(5)	31.4(6)	35.1(5)	1.2(4)	1.8(4)	-2.7(4)
N1	19.3(5)	23.1(6)	26.7(5)	-0.3(4)	-1.2(4)	1.0(5)
N2	22.9(6)	23.7(6)	26.6(5)	3.9(5)	1.4(5)	1.2(5)
C1	21.2(7)	28.3(7)	30.0(7)	-1.8(6)	-5.1(5)	1.6(6)
C2	33.4(8)	28.2(7)	27.8(7)	-4.9(6)	-5.3(6)	0.2(7)
C3	36.3(8)	28.0(8)	31.5(7)	-6.3(6)	2.8(6)	2.9(7)
C4	25.6(7)	29.6(8)	27.6(6)	-1.1(5)	3.1(6)	0.2(6)
C5	38.5(9)	31.2(8)	27.0(7)	3.9(6)	-2.3(6)	-1.7(7)
C6	33.5(8)	28.3(8)	31.2(7)	3.7(6)	-6.8(6)	4.9(6)
C7	24.1(7)	22.3(7)	25.2(6)	-4.7(5)	0.0(5)	0.9(5)
C8	30.4(8)	23.6(7)	24.9(6)	2.4(5)	3.9(6)	2.2(6)
C9	42.5(10)	28.0(8)	26.3(7)	0.1(6)	-4.8(6)	3.5(7)
C10	26.6(7)	24.7(7)	25.0(6)	2.0(5)	-1.6(5)	0.7(6)
C11	27.4(7)	28.5(8)	30.8(7)	0.5(6)	3.0(6)	-0.4(6)
C12	34.1(8)	31.3(8)	32.9(7)	-5.0(6)	-1.2(6)	3.4(7)
C13	44.1(10)	23.7(7)	39.7(8)	-2.9(6)	-9.2(7)	0.2(7)
C14	54.5(11)	29.3(8)	38.4(8)	5.0(7)	3.3(8)	-10.2(8)
C15	45.2(10)	31.5(8)	32.8(7)	1.0(6)	8.5(7)	-5.1(7)
O21	23.2(5)	26.4(5)	46.5(6)	1.4(5)	5.3(5)	-1.6(4)
O22	22.9(5)	30.5(6)	50.8(7)	1.8(5)	-1.1(5)	-0.9(5)
N21	22.1(6)	24.6(6)	35.8(6)	2.6(5)	2.1(5)	1.2(5)
N22	24.2(6)	21.5(6)	44.0(7)	-2.4(5)	-0.1(5)	-0.1(5)
C21	23.1(7)	26.2(8)	46.7(9)	0.1(7)	-0.9(6)	6.0(6)
C22	38.0(9)	38.9(9)	37.8(8)	-3.6(7)	9.9(7)	2.0(7)

C23	46.2(10)	42.7(10)	35.1(8)	-0.5(7)	-6.8(7)	2.2(8)
C24	26.2(8)	28.3(8)	47.5(9)	2.0(7)	-6.3(7)	0.7(7)
C25	37.8(9)	21.3(8)	72.3(13)	3.5(8)	-2.8(9)	1.4(7)
C26	35.9(9)	23.7(8)	66.8(12)	5.7(8)	-10.0(9)	5.9(7)
C27	25.8(7)	26.2(7)	28.0(6)	-0.1(5)	2.8(5)	-1.2(6)
C28	31.7(8)	20.6(7)	37.4(8)	-2.0(6)	1.9(6)	0.1(6)
C29	83.5(17)	31.0(9)	34.0(9)	-3.7(7)	2.5(9)	9.5(10)
C30	26.1(7)	18.7(6)	31.5(7)	0.8(5)	-2.2(5)	1.3(5)
C31	26.6(7)	27.7(8)	44.1(8)	-0.1(6)	-5.7(7)	-3.8(6)
C32	27.0(8)	32.7(8)	54(1)	7.4(7)	7.4(7)	3.8(7)
C33	45.9(10)	27.5(8)	37.4(8)	2.7(6)	11.0(7)	4.7(7)
C34	46.2(10)	28.4(8)	31.4(7)	-0.9(6)	-6.7(7)	1.7(7)
C35	26.6(8)	26.4(7)	35.9(7)	2.6(6)	-6.1(6)	2.4(6)

Table 4 Bond Lengths for 12srv114.

Atom	Atom	Length/Å	Atom	Atom	Length/Å
O1	N1	1.4437(15)	O21	N21	1.4380(16)
O1	C4	1.4748(17)	O21	C24	1.468(2)
O2	C7	1.2305(18)	O22	C27	1.2300(18)
N1	C1	1.4989(18)	N21	C21	1.494(2)
N1	C7	1.4252(18)	N21	C27	1.4155(19)
N2	C7	1.3380(19)	N22	C27	1.333(2)
N2	C8	1.4584(19)	N22	C28	1.465(2)
C1	C2	1.506(2)	C21	C22	1.508(2)
C1	C6	1.534(2)	C21	C26	1.532(2)
C2	C3	1.335(2)	C22	C23	1.344(3)
C3	C4	1.495(2)	C23	C24	1.494(3)
C4	C5	1.523(2)	C24	C25	1.519(2)
C5	C6	1.537(2)	C25	C26	1.517(3)
C8	C9	1.530(2)	C28	C29	1.524(2)
C8	C10	1.519(2)	C28	C30	1.511(2)
C10	C11	1.393(2)	C30	C31	1.394(2)
C10	C15	1.386(2)	C30	C35	1.386(2)
C11	C12	1.393(2)	C31	C32	1.390(2)
C12	C13	1.383(2)	C32	C33	1.380(3)
C13	C14	1.381(3)	C33	C34	1.376(3)
C14	C15	1.388(2)	C34	C35	1.388(2)

Table 5 Bond Angles for 12srv114.

Atom	Atom	Atom	Angle/°	Atom	Atom	Atom	Angle/°
N1	O1	C4	111.75(10)	N21	O21	C24	111.38(11)
O1	N1	C1	109.24(10)	O21	N21	C21	110.10(11)
C7	N1	O1	110.49(10)	C27	N21	O21	110.52(11)

C7	N1	C1	113.96(11)	C27	N21	C21	113.79(12)
C7	N2	C8	120.89(13)	C27	N22	C28	120.70(14)
N1	C1	C2	106.76(12)	N21	C21	C22	106.59(13)
N1	C1	C6	106.46(12)	N21	C21	C26	106.18(14)
C2	C1	C6	110.38(13)	C22	C21	C26	109.82(15)
C3	C2	C1	112.44(14)	C23	C22	C21	112.37(16)
C2	C3	C4	113.16(14)	C22	C23	C24	112.82(16)
O1	C4	C3	110.11(12)	O21	C24	C23	109.81(13)
O1	C4	C5	105.41(12)	O21	C24	C25	105.40(14)
C3	C4	C5	109.64(13)	C23	C24	C25	110.05(16)
C4	C5	C6	106.94(13)	C26	C25	C24	107.53(15)
C1	C6	C5	109.49(13)	C25	C26	C21	109.86(14)
O2	C7	N1	118.81(13)	O22	C27	N21	118.26(13)
O2	C7	N2	125.21(14)	O22	C27	N22	124.80(15)
N2	C7	N1	115.76(12)	N22	C27	N21	116.74(13)
N2	C8	C9	109.12(13)	N22	C28	C29	110.10(14)
N2	C8	C10	113.75(11)	N22	C28	C30	111.38(13)
C10	C8	C9	110.83(12)	C30	C28	C29	112.53(14)
C11	C10	C8	122.18(13)	C31	C30	C28	121.54(14)
C15	C10	C8	119.09(13)	C35	C30	C28	119.85(14)
C15	C10	C11	118.61(14)	C35	C30	C31	118.61(14)
C10	C11	C12	119.93(15)	C32	C31	C30	120.07(15)
C13	C12	C11	120.89(15)	C33	C32	C31	120.63(17)
C14	C13	C12	119.27(16)	C34	C33	C32	119.60(16)
C13	C14	C15	120.04(16)	C33	C34	C35	120.13(16)
C10	C15	C14	121.23(16)	C30	C35	C34	120.94(16)

Table 6 Hydrogen Bonds for 12srv114.

D	H	A	d(D-H)/Å	d(H-A)/Å	d(D-A)/Å	D-H-A/°
N2	H2	O22[1]	0.84(2)	2.15(2)	2.9231(17)	153.4(17)
N22	H22	O2	0.86(2)	2.26(2)	3.0946(18)	163.5(18)

[1]1+X,+Y,+Z

Table 7 Hydrogen Atom Coordinates (Å×10⁴) and Isotropic Displacement Parameters (Å²×10³) for 12srv114.

Atom	*x*	*y*	*z*	U(eq)
H1	4103(18)	7482(17)	4078(3)	25(4)
H6A	5033(19)	9553(19)	3993(4)	32(5)
H2	7351(19)	6232(18)	4477(3)	28(5)
H2A	4980(20)	5690(20)	3822(4)	52(6)
H3	7290(20)	5850(20)	3774(4)	50(6)
H4	8302(18)	7716(18)	3949(3)	26(4)
H5A	6882(18)	8850(19)	3642(4)	33(5)
H5B	7124(19)	9702(19)	3884(4)	33(5)

H6B	4754(17)	8883(18)	3726(3)	29(4)
H8	5776(17)	5047(16)	4824(3)	22(4)
H9A	7660(20)	4504(19)	5055(4)	38(5)
H9B	7708(17)	6024(18)	4982(3)	29(4)
H9C	8560(20)	5006(19)	4832(4)	37(5)
H11	7845(18)	3902(19)	4312(3)	29(4)
H12	8000(20)	1764(19)	4170(4)	37(5)
H13	6770(20)	130(20)	4385(4)	44(5)
H14	5480(20)	650(20)	4738(5)	61(7)
H15	5330(20)	2840(20)	4875(4)	46(6)
H23	2170(20)	8240(20)	4955(5)	60(7)
H24	3380(20)	8757(19)	4569(3)	36(5)
H21	-874(18)	8441(17)	4455(3)	29(4)
H26A	290(20)	10120(20)	4232(4)	51(6)
H22	2280(20)	5868(19)	4415(3)	33(5)
H22A	-160(30)	8050(20)	4885(5)	60(7)
H25A	2460(20)	10440(20)	4321(4)	54(6)
H25B	2100(30)	10790(30)	4615(5)	70(8)
H26B	-60(30)	10580(30)	4524(5)	78(8)
H28	403(19)	4030(19)	4408(4)	33(5)
H29A	2670(30)	3910(20)	4730(4)	55(6)
H29B	1240(30)	4270(30)	4820(5)	65(7)
H29C	1560(20)	2840(30)	4742(5)	67(7)
H31	3830(19)	3741(19)	4352(4)	36(5)
H32	4880(20)	2460(20)	4036(4)	38(5)
H33	3680(20)	1290(20)	3725(4)	51(6)
H34	1430(20)	1590(20)	3724(4)	46(6)
H35	402(19)	2791(18)	4039(3)	31(5)